

Averages of b -hadron, c -hadron, and τ -lepton Properties

Heavy Flavor Averaging Group (HFAG):

D. Asner¹, Sw. Banerjee², R. Bernhard³, S. Blyth⁴, A. Bozek⁵, C. Bozzi⁶,
D. G. Cassel⁷, G. Cavoto⁸, G. Cibinetto⁶, J. Coleman⁹, W. Dungel¹⁰,
T. J. Gershon¹¹, L. Gibbons⁷, B. Golob¹², R. Harr¹³, K. Hayasaka¹⁴,
H. Hayashii¹⁵, C.-J. Lin¹⁶, D. Lopes Pegna¹⁷, R. Louvot¹⁸, A. Lusiani¹⁹,
V. Lüth²⁰, B. Meadows²¹, S. Nishida²², D. Pedrini²³, M. Purohit²⁴,
M. Rama²⁵, M. Roney², O. Schneider¹⁸, C. Schwanda¹⁰, A. J. Schwartz²¹,
B. Shwartz²⁶, J. G. Smith²⁷, R. Tesarek²⁸, D. Tonelli²⁸, K. Trabelsi²²,
P. Urquijo²⁹, and R. Van Kooten³⁰

¹*Pacific Northwest National Laboratory, USA*

²*University of Victoria, Canada*

³*University of Zürich, Switzerland*

⁴*National United University, Taiwan*

⁵*University of Krakow, Poland*

⁶*INFN Ferrara, Italy*

⁷*Cornell University, USA*

⁸*INFN Rome, Italy*

⁹*University of Liverpool, UK*

¹⁰*Austrian Academy of Sciences, Austria*

¹¹*University of Warwick, UK*

¹²*University of Ljubljana, Slovenia*

¹³*Wayne State University, USA*

¹⁴*Nagoya University, Japan*

¹⁵*Nara Womana's University, Japan*

¹⁶*Lawrence Berkeley National Laboratory, USA*

¹⁷*Princeton University, USA*

¹⁸*Ecole Polytechnique Fédérale de Lausanne (EPFL), Switzerland*

¹⁹*INFN Pisa, Italy*

²⁰*SLAC National Accelerator Laboratory, USA*

²¹*University of Cincinnati, USA*

²²*KEK, Tsukuba, Japan*

²³*INFN Milano-Bicocca, Italy*

²⁴*University of South Carolina, USA*

²⁵*INFN Frascati, Italy*

²⁶*Budker Institute of Nuclear Physics, Russia*

²⁷*University of Colorado, USA*

²⁸*Fermilab, USA*

²⁹*Syracuse University, USA*

³⁰*Indiana University, USA*

6 September 2011
(original version: 8 October 2010)

Abstract

This article reports world averages for measurements of b -hadron, c -hadron, and τ lepton properties obtained by the Heavy Flavor Averaging Group (HFAG) using results available at least through the end of 2009. Some of the world averages presented use data available through the spring of 2010. For the averaging, common input parameters used in the various analyses are adjusted (rescaled) to common values, and known correlations are taken into account. The averages include branching fractions, lifetimes, neutral meson mixing parameters, CP violation parameters, and parameters of semileptonic decays.

Contents

1	Introduction	6
2	Methodology	7
3	<i>b</i>-hadron production fractions, lifetimes and mixing parameters	15
3.1	<i>b</i> -hadron production fractions	15
3.1.1	<i>b</i> -hadron production fractions in $\Upsilon(4S)$ decays	15
3.1.2	<i>b</i> -hadron production fractions in $\Upsilon(5S)$ decays	17
3.1.3	<i>b</i> -hadron production fractions at high energy	19
3.2	<i>b</i> -hadron lifetimes	22
3.2.1	Lifetime measurements, uncertainties and correlations	23
3.2.2	Inclusive <i>b</i> -hadron lifetimes	24
3.2.3	B^0 and B^+ lifetimes and their ratio	26
3.2.4	B_s^0 lifetime	27
3.2.5	B_c^+ lifetime	31
3.2.6	Λ_b^0 and <i>b</i> -baryon lifetimes	31
3.2.7	Summary and comparison with theoretical predictions	33
3.3	Neutral <i>B</i> -meson mixing	34
3.3.1	B^0 mixing parameters	35
3.3.2	B_s^0 mixing parameters	41
4	Measurements related to Unitarity Triangle angles	53
4.1	Introduction	53
4.2	Notations	55
4.2.1	<i>CP</i> asymmetries	55
4.2.2	Time-dependent <i>CP</i> asymmetries in decays to <i>CP</i> eigenstates	55
4.2.3	Time-dependent <i>CP</i> asymmetries in decays to vector-vector final states	56
4.2.4	Time-dependent asymmetries: self-conjugate multiparticle final states	57
4.2.5	Time-dependent <i>CP</i> asymmetries in decays to non- <i>CP</i> eigenstates	60
4.2.6	Time-dependent <i>CP</i> asymmetries in the B_s System	65
4.2.7	Asymmetries in $B \rightarrow D^{(*)}K^{(*)}$ decays	66
4.3	Common inputs and error treatment	68
4.4	Time-dependent asymmetries in $b \rightarrow c\bar{c}s$ transitions	70
4.4.1	Time-dependent <i>CP</i> asymmetries in $b \rightarrow c\bar{c}s$ decays to <i>CP</i> eigenstates	70
4.4.2	Time-dependent transversity analysis of $B^0 \rightarrow J/\psi K^{*0}$	71
4.4.3	Time-dependent <i>CP</i> asymmetries in $B^0 \rightarrow D^{*+}D^{*-}K_s^0$ decays	72
4.4.4	Time-dependent analysis of $B_s^0 \rightarrow J/\psi\phi$	72
4.5	Time-dependent <i>CP</i> asymmetries in colour-suppressed $b \rightarrow c\bar{u}d$ transitions	74
4.6	Time-dependent <i>CP</i> asymmetries in charmless $b \rightarrow q\bar{q}s$ transitions	76
4.6.1	Time-dependent <i>CP</i> asymmetries: $b \rightarrow q\bar{q}s$ decays to <i>CP</i> eigenstates	76
4.6.2	Time-dependent Dalitz plot analyses: $B^0 \rightarrow K^+K^-K^0$ and $B^0 \rightarrow \pi^+\pi^-K_s^0$	79
4.6.3	Time-dependent analyses of $B^0 \rightarrow \phi K_s^0\pi^0$	80
4.7	Time-dependent <i>CP</i> asymmetries in $b \rightarrow c\bar{c}d$ transitions	85
4.8	Time-dependent <i>CP</i> asymmetries in $b \rightarrow q\bar{q}d$ transitions	90
4.9	Time-dependent asymmetries in $b \rightarrow s\gamma$ transitions	91

4.10	Time-dependent asymmetries in $b \rightarrow d\gamma$ transitions	92
4.11	Time-dependent CP asymmetries in $b \rightarrow u\bar{u}d$ transitions	94
4.12	Time-dependent CP asymmetries in $b \rightarrow c\bar{u}d/u\bar{c}d$ transitions	100
4.13	Time-dependent CP asymmetries in $b \rightarrow c\bar{u}s/u\bar{c}s$ transitions	101
4.14	Rates and asymmetries in $B^\mp \rightarrow D^{(*)}K^{(*)\mp}$ decays	103
4.14.1	D decays to CP eigenstates	103
4.14.2	D decays to suppressed final states	103
4.14.3	D decays to multiparticle self-conjugate final states	104
5	Semileptonic B decays	110
5.1	Exclusive CKM-favored decays	110
5.1.1	$\bar{B} \rightarrow D\ell^-\bar{\nu}_\ell$	110
5.1.2	$\bar{B} \rightarrow D^*\ell^-\bar{\nu}_\ell$	112
5.1.3	$\bar{B} \rightarrow D^{(*)}\pi\ell^-\bar{\nu}_\ell$	116
5.1.4	$\bar{B} \rightarrow D^{**}\ell^-\bar{\nu}_\ell$	116
5.2	Inclusive CKM-favored decays	119
5.2.1	Inclusive Semileptonic Branching Fraction	119
5.2.2	Determination of $ V_{cb} $	120
5.2.3	Global Fit in the Kinetic Scheme	122
5.3	Exclusive CKM-suppressed decays	123
5.4	Inclusive CKM-suppressed decays	125
5.4.1	BLNP	128
5.4.2	DGE	129
5.4.3	GGOU	130
5.4.4	ADFR	132
5.4.5	BLL	132
5.4.6	Summary	133
6	B decays to charmed hadrons	135
7	B decays to charmless final states	170
7.1	Mesonic charmless decays	170
7.2	Radiative and leptonic decays	177
7.3	$B \rightarrow X_s\gamma$	178
7.4	Baryonic decays	181
7.5	B_s decays	184
7.6	Charge asymmetries	184
7.7	Polarization measurements	189
8	D decays	191
8.1	D^0 - \bar{D}^0 Mixing and CP Violation	191
8.1.1	Introduction	191
8.1.2	Input Observables	192
8.1.3	Fit results	193
8.1.4	Conclusions	195
8.2	Excited $D_{(s)}$ Mesons	201
8.3	Semileptonic Decays	208

8.3.1	Introduction	208
8.3.2	$D \rightarrow P\ell\nu$ Decays	208
8.3.3	Simple Pole	208
8.3.4	z Expansion	209
8.3.5	$D \rightarrow V\ell\nu$ Decays	211
8.3.6	S -Wave Component	213
8.3.7	Model-independent Form Factor Measurement	213
8.4	CP Asymmetries	217
8.5	T -violating Asymmetries	221
8.6	World Average for the D_s^+ Decay Constant f_{D_s}	222
8.7	Two-body Hadronic D^0 Decays and Final State Radiation	227
8.7.1	Branching Fraction Corrections	227
8.7.2	Average Branching Fractions	230
9	τ lepton Properties	235
9.1	Mass of the τ lepton	235
9.2	τ Branching Fractions:	235
9.3	Tests of Lepton Universality	245
9.4	Measurement of $ V_{us} $	250
9.5	Search for lepton flavor violation in τ decays	251
10	Summary	253
11	Acknowledgments	253

1 Introduction

Flavor dynamics is an important element in understanding the nature of particle physics. The accurate knowledge of properties of heavy flavor hadrons, especially b hadrons, plays an essential role for determining the elements of the Cabibbo-Kobayashi-Maskawa (CKM) weak-mixing matrix [1, 2]. Since the Belle and *BABAR* $e^+e^- B$ factory experiments began collecting data, the size of available B meson samples has dramatically increased, and the accuracies of measurements have greatly improved. The CDF and DØ experiments at the Fermilab Tevatron have also provided important results on B and D meson decays, most notably the discovery of B_s^0 - \bar{B}_s^0 mixing, and confirmation of D^0 - \bar{D}^0 mixing.

The Heavy Flavor Averaging Group (HFAG) was formed in 2002 to continue the activities of the LEP Heavy Flavor Steering group [3]. This group was responsible for calculating averages of measurements of b -flavor related quantities. HFAG has evolved since its inception and currently consists of seven subgroups:

- the “ B Lifetime and Oscillations” subgroup provides averages for b -hadron lifetimes, b -hadron fractions in $\Upsilon(4S)$ decay and $p\bar{p}$ collisions, and various parameters governing B^0 - \bar{B}^0 and B_s^0 - \bar{B}_s^0 mixing;
- the “Unitarity Triangle Parameters” subgroup provides averages for time-dependent CP asymmetry parameters and resulting determinations of the angles of the CKM unitarity triangle;
- the “Semileptonic B Decays” subgroup provides averages for inclusive and exclusive B -decay branching fractions, and subsequent determinations of the CKM matrix elements $|V_{cb}|$ and $|V_{ub}|$;
- the “ B to Charm Decays” subgroup provides averages of branching fractions for B decays to final states involving open charm or charmonium mesons;
- the “Rare Decays” subgroup provides averages of branching fractions and CP asymmetries for charmless, radiative, leptonic, and baryonic B meson decays;
- the “Charm Physics” subgroup provides averages of branching fractions for D meson hadronic and semileptonic decays, properties of excited D^{**} and $D_{s,J}$ mesons, averages of D^0 - \bar{D}^0 mixing and CP and T violation parameters, and an average value for the D_s decay constant f_{D_s} .
- the “Tau Physics” subgroup provides documentation and averages for the τ lepton mass and branching fractions, and documents upper limits for τ lepton-flavor-violating decays.

The “Lifetime and Oscillations” and “Semileptonic” subgroups continue the activities of the LEP working groups with some reorganization, i.e., merging four groups into two. The “Unitarity Triangle,” “ B to Charm Decays,” and “Rare Decays” subgroups were formed to provide averages for new results obtained from the B factory experiments (and now also from the Fermilab Tevatron experiments). The “Charm” and “Tau” subgroups were formed more recently in response to the wealth of new data concerning D and τ decays. All subgroups include representatives from Belle and *BABAR* and, when relevant, CLEO, CDF, and DØ.

This article is an update of the “End of 2007” HFAG preprint [4]. Here we report world averages using results available at least through the end of 2009. Averages reported in Chapters 3 and 8 incorporate results available through the spring of 2010. In general, we use all publicly available results that have written documentation. These include preliminary results presented at conferences or workshops. However, we do not use preliminary results that remain unpublished for an extended period of time, or for which no publication is planned. Close contacts have been established between representatives from the experiments and members of subgroups that perform averaging to ensure that the data are prepared in a form suitable for combinations.

In the case of obtaining a world average for which $\chi^2/\text{dof} > 1$, where dof is the number of degrees of freedom in the average calculation, we do not scale the resulting error, as is presently done by the Particle Data Group [5]. Rather, we examine the systematics of each measurement to better understand them. Unless we find possible systematic discrepancies between the measurements, we do not apply any additional correction to the calculated error. We provide the confidence level of the fit as an indicator for the consistency of the measurements included in the average. In case some special treatment was necessary to calculate an average, or if an approximation used in the average calculation may not be good enough (*e.g.*, assuming Gaussian errors when the likelihood function indicates non-Gaussian behavior), we include a warning message.

Chapter 2 describes the methodology used for calculating averages. In the averaging procedure, common input parameters used in the various analyses are adjusted (rescaled) to common values, and, where possible, known correlations are taken into account. Chapters 3–9 present world average values from each of the subgroups listed above. A brief summary of the averages presented is given in Chapter 10. A complete listing of the averages and plots are also available on the HFAG web site:

<http://www.slac.stanford.edu/xorg/hfag> and

<http://belle.kek.jp/mirror/hfag> (KEK mirror site).

2 Methodology

The general averaging problem that HFAG faces is to combine information provided by different measurements of the same parameter to obtain our best estimate of the parameter’s value and uncertainty. The methodology described here focuses on the problems of combining measurements performed with different systematic assumptions and with potentially-correlated systematic uncertainties. Our methodology relies on the close involvement of the people performing the measurements in the averaging process.

Consider two hypothetical measurements of a parameter x , which might be summarized as

$$\begin{aligned} x &= x_1 \pm \delta x_1 \pm \Delta x_{1,1} \pm \Delta x_{2,1} \dots \\ x &= x_2 \pm \delta x_2 \pm \Delta x_{1,2} \pm \Delta x_{2,2} \dots , \end{aligned}$$

where the δx_k are statistical uncertainties, and the $\Delta x_{i,k}$ are contributions to the systematic uncertainty. One popular approach is to combine statistical and systematic uncertainties in

quadrature

$$x = x_1 \pm (\delta x_1 \oplus \Delta x_{1,1} \oplus \Delta x_{2,1} \oplus \dots)$$

$$x = x_2 \pm (\delta x_2 \oplus \Delta x_{1,2} \oplus \Delta x_{2,2} \oplus \dots)$$

and then perform a weighted average of x_1 and x_2 , using their combined uncertainties, as if they were independent. This approach suffers from two potential problems that we attempt to address. First, the values of the x_k may have been obtained using different systematic assumptions. For example, different values of the B^0 lifetime may have been assumed in separate measurements of the oscillation frequency Δm_d . The second potential problem is that some contributions of the systematic uncertainty may be correlated between experiments. For example, separate measurements of Δm_d may both depend on an assumed Monte-Carlo branching fraction used to model a common background.

The problems mentioned above are related since, ideally, any quantity y_i that x_k depends on has a corresponding contribution $\Delta x_{i,k}$ to the systematic error which reflects the uncertainty Δy_i on y_i itself. We assume that this is the case and use the values of y_i and Δy_i assumed by each measurement explicitly in our averaging (we refer to these values as $y_{i,k}$ and $\Delta y_{i,k}$ below). Furthermore, since we do not lump all the systematics together, we require that each measurement used in an average have a consistent definition of the various contributions to the systematic uncertainty. Different analyses often use different decompositions of their systematic uncertainties, so achieving consistent definitions for any potentially correlated contributions requires close coordination between HFAG and the experiments. In some cases, a group of systematic uncertainties must be lumped to obtain a coarser description that is consistent between measurements. Systematic uncertainties that are uncorrelated with any other sources of uncertainty appearing in an average are lumped with the statistical error, so that the only systematic uncertainties treated explicitly are those that are correlated with at least one other measurement via a consistently-defined external parameter y_i . When asymmetric statistical or systematic uncertainties are quoted, we symmetrize them since our combination method implicitly assumes parabolic likelihoods for each measurement.

The fact that a measurement of x is sensitive to the value of y_i indicates that, in principle, the data used to measure x could equally-well be used for a simultaneous measurement of x and y_i , as illustrated by the large contour in Fig. 1(a) for a hypothetical measurement. However, we often have an external constraint Δy_i on the value of y_i (represented by the horizontal band in Fig. 1(a)) that is more precise than the constraint $\sigma(y_i)$ from our data alone. Ideally, in such cases we would perform a simultaneous fit to x and y_i , including the external constraint, obtaining the filled (x, y) contour and corresponding dashed one-dimensional estimate of x shown in Fig. 1(a). Throughout, we assume that the external constraint Δy_i on y_i is Gaussian.

In practice, the added technical complexity of a constrained fit with extra free parameters is not justified by the small increase in sensitivity, as long as the external constraints Δy_i are sufficiently precise when compared with the sensitivities $\sigma(y_i)$ to each y_i of the data alone. Instead, the usual procedure adopted by the experiments is to perform a baseline fit with all y_i fixed to nominal values $y_{i,0}$, obtaining $x = x_0 \pm \delta x$. This baseline fit neglects the uncertainty due to Δy_i , but this error can be mostly recovered by repeating the fit separately for each external parameter y_i with its value fixed at $y_i = y_{i,0} + \Delta y_i$ to obtain $x = \tilde{x}_{i,0} \pm \delta \tilde{x}$, as illustrated in Fig. 1(b). The absolute shift, $|\tilde{x}_{i,0} - x_0|$, in the central value of x is what the experiments usually quote as their systematic uncertainty Δx_i on x due to the unknown value of y_i . Our procedure requires that we know not only the magnitude of this shift but also its sign. In the

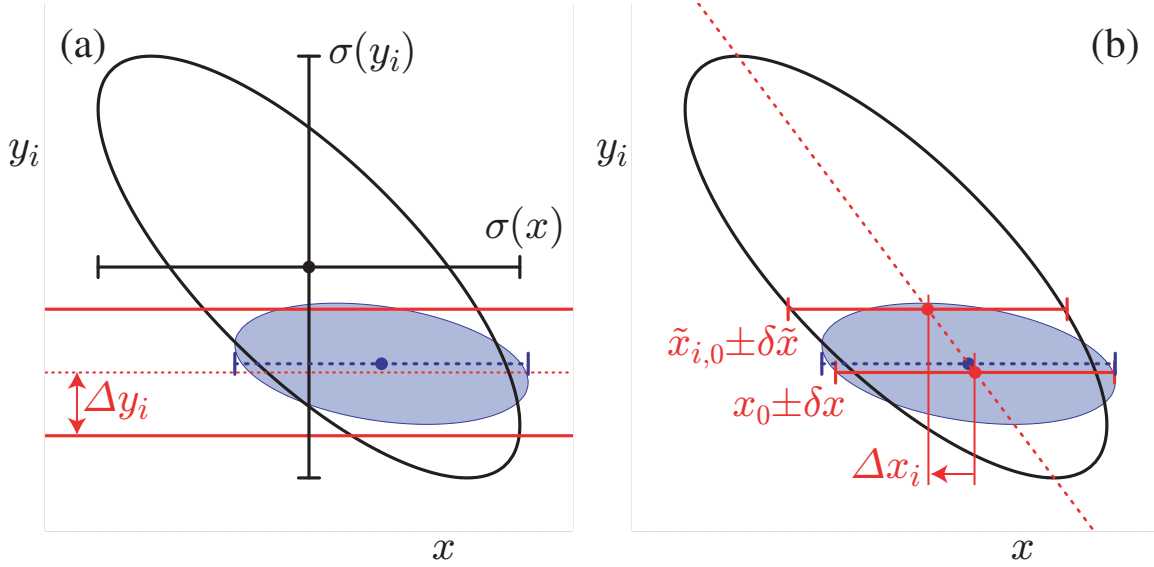


Figure 1: The left-hand plot (a) compares the 68% confidence-level contours of a hypothetical measurement's unconstrained (large ellipse) and constrained (filled ellipse) likelihoods, using the Gaussian constraint on y_i represented by the horizontal band. The solid error bars represent the statistical uncertainties $\sigma(x)$ and $\sigma(y_i)$ of the unconstrained likelihood. The dashed error bar shows the statistical error on x from a constrained simultaneous fit to x and y_i . The right-hand plot (b) illustrates the method described in the text of performing fits to x with y_i fixed at different values. The dashed diagonal line between these fit results has the slope $\rho(x, y_i)\sigma(y_i)/\sigma(x)$ in the limit of a parabolic unconstrained likelihood. The result of the constrained simultaneous fit from (a) is shown as a dashed error bar on x .

limit that the unconstrained data is represented by a parabolic likelihood, the signed shift is given by

$$\Delta x_i = \rho(x, y_i) \frac{\sigma(x)}{\sigma(y_i)} \Delta y_i, \quad (1)$$

where $\sigma(x)$ and $\rho(x, y_i)$ are the statistical uncertainty on x and the correlation between x and y_i in the unconstrained data. While our procedure is not equivalent to the constrained fit with extra parameters, it yields (in the limit of a parabolic unconstrained likelihood) a central value x_0 that agrees to $\mathcal{O}(\Delta y_i/\sigma(y_i))^2$ and an uncertainty $\delta x \oplus \Delta x_i$ that agrees to $\mathcal{O}(\Delta y_i/\sigma(y_i))^4$.

In order to combine two or more measurements that share systematics due to the same external parameters y_i , we would ideally perform a constrained simultaneous fit of all data samples to obtain values of x and each y_i , being careful to only apply the constraint on each y_i once. This is not practical since we generally do not have sufficient information to reconstruct the unconstrained likelihoods corresponding to each measurement. Instead, we perform the two-step approximate procedure described below.

Figs. 2(a,b) illustrate two statistically-independent measurements, $x_1 \pm (\delta x_1 \oplus \Delta x_{i,1})$ and $x_2 \pm (\delta x_2 \oplus \Delta x_{i,2})$, of the same hypothetical quantity x (for simplicity, we only show the contribution of a single correlated systematic due to an external parameter y_i). As our knowledge of the external parameters y_i evolves, it is natural that the different measurements of x will assume different nominal values and ranges for each y_i . The first step of our procedure is to adjust the values of each measurement to reflect the current best knowledge of the values y'_i and ranges $\Delta y'_i$ of the external parameters y_i , as illustrated in Figs. 2(c,b). We adjust the central values x_k and correlated systematic uncertainties $\Delta x_{i,k}$ linearly for each measurement (indexed by k) and each external parameter (indexed by i):

$$x'_k = x_k + \sum_i \frac{\Delta x_{i,k}}{\Delta y_{i,k}} (y'_i - y_{i,k}) \quad (2)$$

$$\Delta x'_{i,k} = \Delta x_{i,k} \cdot \frac{\Delta y'_i}{\Delta y_{i,k}}. \quad (3)$$

This procedure is exact in the limit that the unconstrained likelihoods of each measurement is parabolic.

The second step of our procedure is to combine the adjusted measurements, $x'_k \pm (\delta x_k \oplus \Delta x'_{k,1} \oplus \Delta x'_{k,2} \oplus \dots)$ using the chi-square

$$\chi^2_{\text{comb}}(x, y_1, y_2, \dots) \equiv \sum_k \frac{1}{\delta x_k^2} \left[x'_k - \left(x + \sum_i (y_i - y'_i) \frac{\Delta x'_{i,k}}{\Delta y'_i} \right) \right]^2 + \sum_i \left(\frac{y_i - y'_i}{\Delta y'_i} \right)^2, \quad (4)$$

and then minimize this χ^2 to obtain the best values of x and y_i and their uncertainties, as illustrated in Fig. 3. Although this method determines new values for the y_i , we do not report them since the $\Delta x_{i,k}$ reported by each experiment are generally not intended for this purpose (for example, they may represent a conservative upper limit rather than a true reflection of a 68% confidence level).

For comparison, the exact method we would perform if we had the unconstrained likelihoods $\mathcal{L}_k(x, y_1, y_2, \dots)$ available for each measurement is to minimize the simultaneous constrained likelihood

$$\mathcal{L}_{\text{comb}}(x, y_1, y_2, \dots) \equiv \prod_k \mathcal{L}_k(x, y_1, y_2, \dots) \prod_i \mathcal{L}_i(y_i), \quad (5)$$

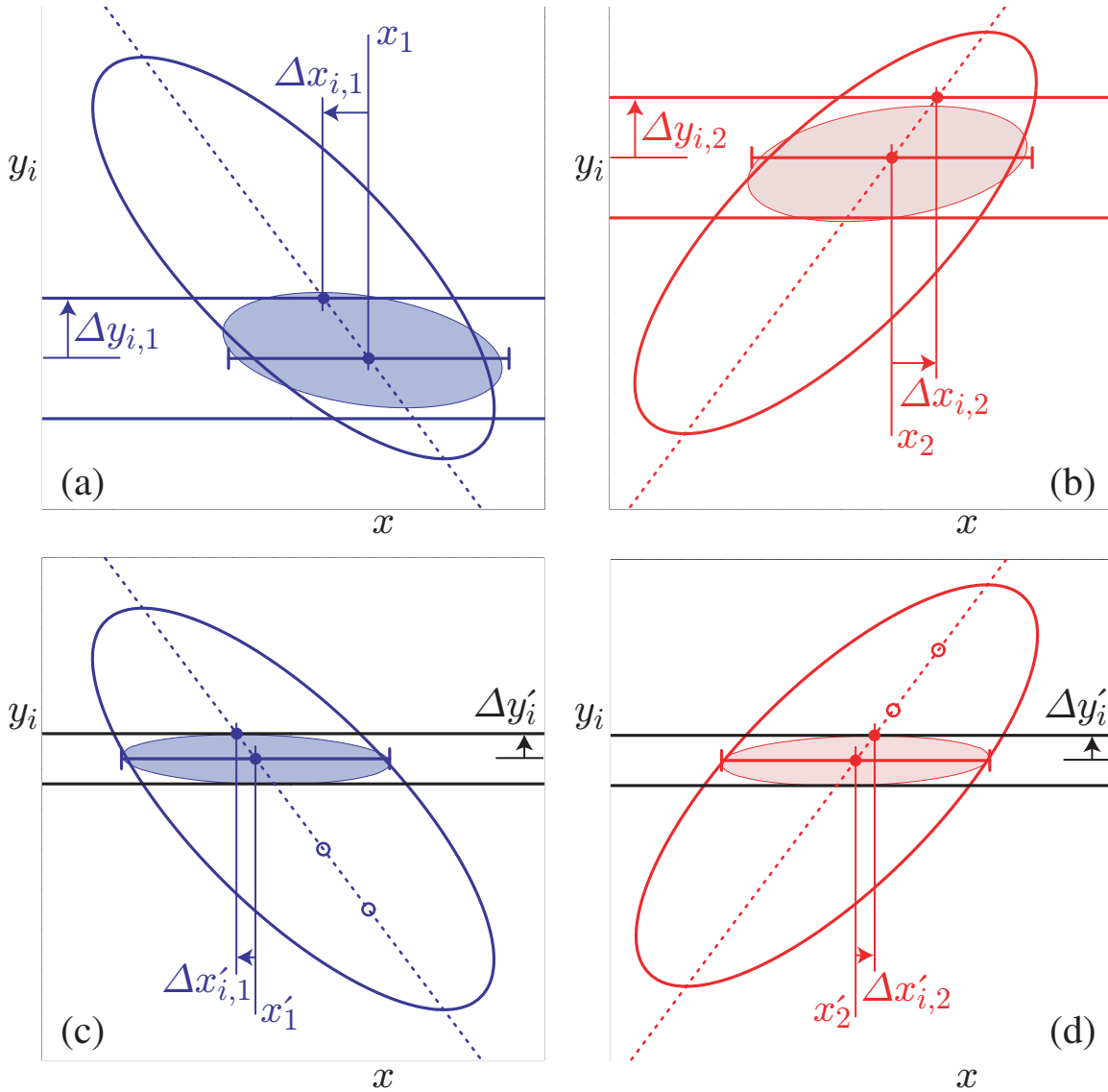


Figure 2: The upper plots (a) and (b) show examples of two individual measurements to be combined. The large ellipses represent their unconstrained likelihoods, and the filled ellipses represent their constrained likelihoods. Horizontal bands indicate the different assumptions about the value and uncertainty of y_i used by each measurement. The error bars show the results of the approximate method described in the text for obtaining x by performing fits with y_i fixed to different values. The lower plots (c) and (d) illustrate the adjustments to accommodate updated and consistent knowledge of y_i as described in the text. Open circles mark the central values of the unadjusted fits to x with y fixed; these determine the dashed line used to obtain the adjusted values.

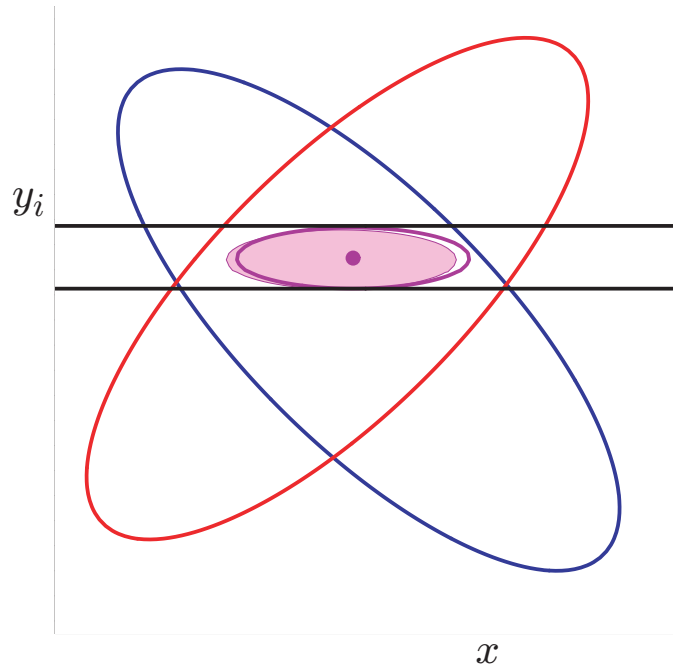


Figure 3: An illustration of the combination of two hypothetical measurements of x using the method described in the text. The ellipses represent the unconstrained likelihoods of each measurement, and the horizontal band represents the latest knowledge about y_i that is used to adjust the individual measurements. The filled small ellipse shows the result of the exact method using $\mathcal{L}_{\text{comb}}$, and the hollow small ellipse and dot show the result of the approximate method using χ_{comb}^2 .

with an independent Gaussian external constraint on each y_i

$$\mathcal{L}_i(y_i) \equiv \exp \left[-\frac{1}{2} \left(\frac{y_i - y'_i}{\Delta y'_i} \right)^2 \right]. \quad (6)$$

The results of this exact method are illustrated by the filled ellipses in Figs. 3(a,b) and agree with our method in the limit that each \mathcal{L}_k is parabolic and that each $\Delta y'_i \ll \sigma(y_i)$. In the case of a non-parabolic unconstrained likelihood, experiments would have to provide a description of \mathcal{L}_k itself to allow an improved combination. In the case of $\sigma(y_i) \simeq \Delta y'_i$, experiments are advised to perform a simultaneous measurement of both x and y so that their data will improve the world knowledge about y .

The algorithm described above is used as a default in the averages reported in the following sections. For some cases, somewhat simplified or more complex algorithms are used and noted in the corresponding sections. Some examples for extensions of the standard method for extracting averages are given here. These include the case where measurement errors depend on the measured value, i.e. are relative errors, unknown correlation coefficients and the breakdown of error sources.

For measurements with Gaussian errors, the usual estimator for the average of a set of measurements is obtained by minimizing the following χ^2 :

$$\chi^2(t) = \sum_i^N \frac{(y_i - t)^2}{\sigma_i^2}, \quad (7)$$

where y_i is the measured value for input i and σ_i^2 is the variance of the distribution from which y_i was drawn. The value \hat{t} of t at minimum χ^2 is our estimator for the average. (This discussion is given for independent measurements for the sake of simplicity; the generalization to correlated measurements is straightforward, and has been used when averaging results.) The true σ_i are unknown but typically the error as assigned by the experiment σ_i^{raw} is used as an estimator for it. Caution is advised, however, in the case where σ_i^{raw} depends on the value measured for y_i . Examples of this include an uncertainty in any multiplicative factor (like an acceptance) that enters the determination of y_i , i.e. the \sqrt{N} dependence of Poisson statistics, where $y_i \propto N$ and $\sigma_i \propto \sqrt{N}$. Failing to account for this type of dependence when averaging leads to a biased average. Biases in the average can be avoided (or at least reduced) by minimizing the following χ^2 :

$$\chi^2(t) = \sum_i^N \frac{(y_i - t)^2}{\sigma_i^2(\hat{t})}. \quad (8)$$

In the above $\sigma_i(\hat{t})$ is the uncertainty assigned to input i that includes the assumed dependence of the stated error on the value measured. As an example, consider a pure acceptance error, for which $\sigma_i(\hat{t}) = (\hat{t}/y_i) \times \sigma_i^{\text{raw}}$. It is easily verified that solving Eq. 8 leads to the correct behavior, namely

$$\hat{t} = \frac{\sum_i^N y_i^3 / (\sigma_i^{\text{raw}})^2}{\sum_i^N y_i^2 / (\sigma_i^{\text{raw}})^2},$$

i.e. weighting by the inverse square of the fractional uncertainty, $\sigma_i^{\text{raw}}/y_i$. It is sometimes difficult to assess the dependence of σ_i^{raw} on \hat{t} from the errors quoted by experiments.

Another issue that needs careful treatment is the question of correlation among different measurements, e.g. due to using the same theory for calculating acceptances. A common practice is to set the correlation coefficient to unity to indicate full correlation. However, this is not a “conservative” thing to do, and can in fact lead to a significantly underestimated uncertainty on the average. In the absence of better information, the most conservative choice of correlation coefficient between two measurements i and j is the one that maximizes the uncertainty on \hat{t} due to that pair of measurements:

$$\sigma_{\hat{t}(i,j)}^2 = \frac{\sigma_i^2 \sigma_j^2 (1 - \rho_{ij}^2)}{\sigma_i^2 + \sigma_j^2 - 2 \rho_{ij} \sigma_i \sigma_j}, \quad (9)$$

namely

$$\rho_{ij} = \min \left(\frac{\sigma_i}{\sigma_j}, \frac{\sigma_j}{\sigma_i} \right), \quad (10)$$

which corresponds to setting $\sigma_{\hat{t}(i,j)}^2 = \min(\sigma_i^2, \sigma_j^2)$. Setting $\rho_{ij} = 1$ when $\sigma_i \neq \sigma_j$ can lead to a significant underestimate of the uncertainty on \hat{t} , as can be seen from Eq. 9.

Finally, we carefully consider the various sources of error contributing to the overall uncertainty of an average. The overall covariance matrix is constructed from a number of individual sources, e.g. $\mathbf{V} = \mathbf{V}_{\text{stat}} + \mathbf{V}_{\text{sys}} + \mathbf{V}_{\text{th}}$. The variance on the average \hat{t} can be written

$$\sigma_{\hat{t}}^2 = \frac{\sum_{i,j} (\mathbf{V}^{-1} [\mathbf{V}_{\text{stat}} + \mathbf{V}_{\text{sys}} + \mathbf{V}_{\text{th}}] \mathbf{V}^{-1})_{ij}}{\left(\sum_{i,j} V_{ij}^{-1} \right)^2} = \sigma_{\text{stat}}^2 + \sigma_{\text{sys}}^2 + \sigma_{\text{th}}^2. \quad (11)$$

Written in this form, one can readily determine the contribution of each source of uncertainty to the overall uncertainty on the average. This breakdown of the uncertainties is used in the following sections.

Following the prescription described above, the central values and errors are rescaled to a common set of input parameters in the averaging procedures according to the dependency on any of these input parameters. We try to use the most up-to-date values for these common inputs and the same values among the HFAG subgroups. For the parameters whose averages are produced by HFAG, we use the values in the current update cycle. For other external parameters, we use the most recent PDG values available (usually Ref. [5]). The parameters and values used are listed in each subgroup section.

3 b -hadron production fractions, lifetimes and mixing parameters

Quantities such as b -hadron production fractions, b -hadron lifetimes, and neutral B -meson oscillation frequencies have been studied in the nineties at LEP and SLC (e^+e^- colliders at $\sqrt{s} = m_Z$) as well as at the first version of the Tevatron ($p\bar{p}$ collider at $\sqrt{s} = 1.8$ TeV). Since then precise measurements of the B^0 and B^+ lifetimes, as well as of the B^0 oscillation frequency, have also been performed at the asymmetric B factories, KEKB and PEP-II (e^+e^- colliders at $\sqrt{s} = m_{\Upsilon(4S)}$) while measurements related to the other b -hadrons, in particular B_s^0 , B_c^+ and A_b^0 , are being performed at the upgraded Tevatron ($\sqrt{s} = 1.96$ TeV). In most cases, these basic quantities, although interesting by themselves, became necessary ingredients for the more complicated and refined analyses at the asymmetric B factories and at the Tevatron, in particular the time-dependent CP asymmetry measurements. It is therefore important that the best experimental values of these quantities continue to be kept up-to-date and improved.

In several cases, the averages presented in this chapter are needed and used as input for the results given in the subsequent chapters. Within this chapter, some averages need the knowledge of other averages in a circular way. This coupling, which appears through the b -hadron fractions whenever inclusive or semi-exclusive measurements have to be considered, has been reduced significantly in the last several years with increasingly precise exclusive measurements becoming available.

In addition to b -hadron fractions, lifetimes and mixing parameters, this chapter also deals with the CP -violating phase β_s , which is the phase difference between the B_s^0 mixing amplitude and the $b \rightarrow c\bar{c}s$ decay amplitude. The angle β , which is the equivalent of β_s for the B^0 system, is discussed in Chapter 4.

3.1 b -hadron production fractions

We consider here the relative fractions of the different b -hadron species found in an unbiased sample of weakly-decaying b hadrons produced under some specific conditions. The knowledge of these fractions is useful to characterize the signal composition in inclusive b -hadron analyses, or to predict the background composition in exclusive analyses. Many analyses in B physics need these fractions as input. We distinguish here the following three conditions: $\Upsilon(4S)$ decays, $\Upsilon(5S)$ decays, and high-energy collisions (including Z^0 decays).

3.1.1 b -hadron production fractions in $\Upsilon(4S)$ decays

Only pairs of the two lightest (charged and neutral) B mesons can be produced in $\Upsilon(4S)$ decays, and it is enough to determine the following branching fractions:

$$f^{+-} = \Gamma(\Upsilon(4S) \rightarrow B^+B^-)/\Gamma_{\text{tot}}(\Upsilon(4S)), \quad (12)$$

$$f^{00} = \Gamma(\Upsilon(4S) \rightarrow B^0\bar{B}^0)/\Gamma_{\text{tot}}(\Upsilon(4S)). \quad (13)$$

In practice, most analyses measure their ratio

$$R^{+-/00} = f^{+-}/f^{00} = \Gamma(\Upsilon(4S) \rightarrow B^+B^-)/\Gamma(\Upsilon(4S) \rightarrow B^0\bar{B}^0), \quad (14)$$

Table 1: Published measurements of the B^+/B^0 production ratio in $\Upsilon(4S)$ decays, together with their average (see text). Systematic uncertainties due to the imperfect knowledge of $\tau(B^+)/\tau(B^0)$ are included. The latest *BABAR* result[6] supersedes the earlier *BABAR* measurements [7, 8].

Experiment and year	Ref.	Decay modes or method	Published value of $R^{+-/00} = f^{+-}/f^{00}$	Assumed value of $\tau(B^+)/\tau(B^0)$
CLEO, 2001	[9]	$J/\psi K^{(*)}$	$1.04 \pm 0.07 \pm 0.04$	1.066 ± 0.024
<i>BABAR</i> , 2002	[7]	$(c\bar{c})K^{(*)}$	$1.10 \pm 0.06 \pm 0.05$	1.062 ± 0.029
CLEO, 2002	[10]	$D^* \ell \nu$	$1.058 \pm 0.084 \pm 0.136$	1.074 ± 0.028
Belle, 2003	[11]	dilepton events	$1.01 \pm 0.03 \pm 0.09$	1.083 ± 0.017
<i>BABAR</i> , 2004	[8]	$J/\psi K$	$1.006 \pm 0.036 \pm 0.031$	1.083 ± 0.017
<i>BABAR</i> , 2005	[6]	$(c\bar{c})K^{(*)}$	$1.06 \pm 0.02 \pm 0.03$	1.086 ± 0.017
Average			1.052 ± 0.028 (tot)	1.081 ± 0.006

which is easier to access experimentally. Since an inclusive (but separate) reconstruction of B^+ and B^0 is difficult, specific exclusive decay modes, $B^+ \rightarrow x^+$ and $B^0 \rightarrow x^0$, are usually considered to perform a measurement of $R^{+-/00}$, whenever they can be related by isospin symmetry (for example $B^+ \rightarrow J/\psi K^+$ and $B^0 \rightarrow J/\psi K^0$). Under the assumption that $\Gamma(B^+ \rightarrow x^+) = \Gamma(B^0 \rightarrow x^0)$, *i.e.* that isospin invariance holds in these B decays, the ratio of the number of reconstructed $B^+ \rightarrow x^+$ and $B^0 \rightarrow x^0$ mesons is proportional to

$$\frac{f^{+-} \mathcal{B}(B^+ \rightarrow x^+)}{f^{00} \mathcal{B}(B^0 \rightarrow x^0)} = \frac{f^{+-} \Gamma(B^+ \rightarrow x^+) \tau(B^+)}{f^{00} \Gamma(B^0 \rightarrow x^0) \tau(B^0)} = \frac{f^{+-}}{f^{00}} \frac{\tau(B^+)}{\tau(B^0)}, \quad (15)$$

where $\tau(B^+)$ and $\tau(B^0)$ are the B^+ and B^0 lifetimes respectively. Hence the primary quantity measured in these analyses is $R^{+-/00} \tau(B^+)/\tau(B^0)$, and the extraction of $R^{+-/00}$ with this method therefore requires the knowledge of the $\tau(B^+)/\tau(B^0)$ lifetime ratio.

The published measurements of $R^{+-/00}$ are listed in Table 1 together with the corresponding assumed values of $\tau(B^+)/\tau(B^0)$. All measurements are based on the above-mentioned method, except the one from Belle, which is a by-product of the B^0 mixing frequency analysis using dilepton events (but note that it also assumes isospin invariance, namely $\Gamma(B^+ \rightarrow \ell^+ X) = \Gamma(B^0 \rightarrow \ell^+ X)$). The latter is therefore treated in a slightly different manner in the following procedure used to combine these measurements:

- each published value of $R^{+-/00}$ from CLEO and *BABAR* is first converted back to the original measurement of $R^{+-/00} \tau(B^+)/\tau(B^0)$, using the value of the lifetime ratio assumed in the corresponding analysis;
- a simple weighted average of these original measurements of $R^{+-/00} \tau(B^+)/\tau(B^0)$ from CLEO and *BABAR* (which do not depend on the assumed value of the lifetime ratio) is then computed, assuming no statistical or systematic correlations between them;
- the weighted average of $R^{+-/00} \tau(B^+)/\tau(B^0)$ is converted into a value of $R^{+-/00}$, using the latest average of the lifetime ratios, $\tau(B^+)/\tau(B^0) = 1.081 \pm 0.006$ (see Sec. 3.2.3);

- the Belle measurement of $R^{+-/00}$ is adjusted to the current values of $\tau(B^0) = 1.518 \pm 0.007$ ps and $\tau(B^+)/\tau(B^0) = 1.081 \pm 0.006$ (see Sec. 3.2.3), using the quoted systematic uncertainties due to these parameters;
- the combined value of $R^{+-/00}$ from CLEO and *BABAR* is averaged with the adjusted value of $R^{+-/00}$ from Belle, assuming a 100% correlation of the systematic uncertainty due to the limited knowledge on $\tau(B^+)/\tau(B^0)$; no other correlation is considered.

The resulting global average,

$$R^{+-/00} = \frac{f^{+-}}{f^{00}} = 1.052 \pm 0.028, \quad (16)$$

is consistent with an equal production of charged and neutral B mesons, although only at the 1.9σ level.

On the other hand, the *BABAR* collaboration has performed a direct measurement of the f^{00} fraction using a novel method, which does not rely on isospin symmetry nor requires the knowledge of $\tau(B^+)/\tau(B^0)$. Its analysis, based on a comparison between the number of events where a single $B^0 \rightarrow D^{*-}\ell^+\nu$ decay could be reconstructed and the number of events where two such decays could be reconstructed, yields [12]

$$f^{00} = 0.487 \pm 0.010 \text{ (stat)} \pm 0.008 \text{ (syst)}. \quad (17)$$

The two results of Eqs. (16) and (17) are of very different natures and completely independent of each other. Their product is equal to $f^{+-} = 0.512 \pm 0.019$, while another combination of them gives $f^{+-} + f^{00} = 0.999 \pm 0.030$, compatible with unity. Assuming¹ $f^{+-} + f^{00} = 1$, also consistent with CLEO's observation that the fraction of $\Upsilon(4S)$ decays to $B\bar{B}$ pairs is larger than 0.96 at 95% CL [14], the results of Eqs. (16) and (17) can be averaged (first converting Eq. (16) into a value of $f^{00} = 1/(R^{+-/00} + 1)$) to yield the following more precise estimates:

$$f^{00} = 0.487 \pm 0.006, \quad f^{+-} = 1 - f^{00} = 0.513 \pm 0.006, \quad \frac{f^{+-}}{f^{00}} = 1.052 \pm 0.025. \quad (18)$$

The latter ratio differs from one by 2.1σ .

3.1.2 b -hadron production fractions in $\Upsilon(5S)$ decays

Hadronic events produced in e^+e^- collisions at the $\Upsilon(5S)$ energy can be classified into three categories: light-quark (u, d, s, c) continuum events, $b\bar{b}$ continuum events, and $\Upsilon(5S)$ events. The latter two cannot be distinguished and will be called $b\bar{b}$ events in the following. These $b\bar{b}$ events, which also include $b\bar{b}\gamma$ events because of possible initial-state radiation, can hadronize in different final states. We define $f_{u,d}^{\Upsilon(5S)}$ as the fraction of $b\bar{b}$ events with a pair of non-strange bottom mesons (final states $B\bar{B}, B\bar{B}^*, B^*\bar{B}, B^*\bar{B}^*, B\bar{B}\pi, B\bar{B}^*\pi, B^*\bar{B}\pi, B^*\bar{B}^*\pi$, and $B\bar{B}\pi\pi$, where B denotes a B^0 or B^+ meson and \bar{B} denotes a \bar{B}^0 or B^- meson), $f_s^{\Upsilon(5S)}$ as the fraction of

¹A few non- $B\bar{B}$ decay modes of the $\Upsilon(4S)$ ($\Upsilon(1S)\pi^+\pi^-$, $\Upsilon(2S)\pi^+\pi^-$, $\Upsilon(1S)\eta$) have been observed with branching fractions of the order of 10^{-4} [13], corresponding to a partial width several times larger than that in the e^+e^- channel. However, this can still be neglected and the assumption $f^{+-} + f^{00} = 1$ remains valid in the present context of the determination of f^{+-} and f^{00} .

Table 2: Published measurements of $f_s^{\Upsilon(5S)}$. All values have been obtained assuming $f_{\mathcal{B}}^{\Upsilon(5S)} = 0$. They are quoted as in the original publication, except for the most recent measurement which is quoted as $1 - f_{u,d}^{\Upsilon(5S)}$, with $f_{u,d}^{\Upsilon(5S)}$ from Ref. [15]. The last line gives our average of $f_s^{\Upsilon(5S)}$ assuming $f_{\mathcal{B}}^{\Upsilon(5S)} = 0$.

Experiment, year, dataset	Decay mode or method	Value of $f_s^{\Upsilon(5S)}$
CLEO, 2006, 0.42 fb ⁻¹ [16]	$\Upsilon(5S) \rightarrow D_s X$	$0.168 \pm 0.026^{+0.067}_{-0.034}$
	$\Upsilon(5S) \rightarrow \phi X$	$0.246 \pm 0.029^{+0.110}_{-0.053}$
	$\Upsilon(5S) \rightarrow B\bar{B}X$	$0.411 \pm 0.100 \pm 0.092$
	CLEO average of above 3	$0.21^{+0.06}_{-0.03}$
Belle, 2006, 1.86 fb ⁻¹ [17]	$\Upsilon(5S) \rightarrow D_s X$	$0.179 \pm 0.014 \pm 0.041$
	$\Upsilon(5S) \rightarrow D^0 X$	$0.181 \pm 0.036 \pm 0.075$
	Belle average of above 2	$0.180 \pm 0.013 \pm 0.032$
Belle, 2010, 23.6 fb ⁻¹ [15]	$\Upsilon(5S) \rightarrow B\bar{B}X$	$0.263 \pm 0.032 \pm 0.051$
Average of all above after adjustments to inputs of Table 3		0.215 ± 0.031

Table 3: External inputs on which the $f_s^{\Upsilon(5S)}$ averages are based.

Branching fraction	Value	Explanation and reference
$\mathcal{B}(B \rightarrow D_s X) \times \mathcal{B}(D_s \rightarrow \phi\pi)$	0.00374 ± 0.00014	derived from [5]
$\mathcal{B}(B_s^0 \rightarrow D_s X)$	0.92 ± 0.11	model-dependent estimate [18]
$\mathcal{B}(D_s \rightarrow \phi\pi)$	0.045 ± 0.004	[5]
$\mathcal{B}(B \rightarrow D^0 X) \times \mathcal{B}(D^0 \rightarrow K\pi)$	0.0243 ± 0.0011	derived from [5]
$\mathcal{B}(B_s^0 \rightarrow D^0 X)$	0.08 ± 0.07	model-dependent estimate [17, 18]
$\mathcal{B}(D^0 \rightarrow K\pi)$	0.0389 ± 0.0005	[5]
$\mathcal{B}(B \rightarrow \phi X)$	0.0343 ± 0.0012	world average [5, 16]
$\mathcal{B}(B_s^0 \rightarrow \phi X)$	0.161 ± 0.024	model-dependent estimate [16]

$b\bar{b}$ events with a pair of strange bottom mesons (final states $B_s^0\bar{B}_s^0$, $B_s^0\bar{B}_s^{0*}$, $B_s^{0*}\bar{B}_s^0$, and $B_s^{0*}\bar{B}_s^{0*}$), and $f_{\mathcal{B}}^{\Upsilon(5S)}$ as the fraction of $b\bar{b}$ events without bottom meson in the final state. Note that the excited bottom-meson states decay via $B^* \rightarrow B\gamma$ and $B_s^{0*} \rightarrow B_s^0\gamma$. These fractions satisfy

$$f_{u,d}^{\Upsilon(5S)} + f_s^{\Upsilon(5S)} + f_{\mathcal{B}}^{\Upsilon(5S)} = 1. \quad (19)$$

The CLEO and Belle collaborations have published in 2006 measurements of several inclusive $\Upsilon(5S)$ branching fractions, $\mathcal{B}(\Upsilon(5S) \rightarrow D_s X)$, $\mathcal{B}(\Upsilon(5S) \rightarrow \phi X)$ and $\mathcal{B}(\Upsilon(5S) \rightarrow D^0 X)$, from which they extracted the model-dependent estimates of $f_s^{\Upsilon(5S)}$ reported in Table 2. This extraction was performed under the implicit assumption $f_{\mathcal{B}}^{\Upsilon(5S)} = 0$, using the relation

$$\frac{1}{2}\mathcal{B}(\Upsilon(5S) \rightarrow D_s X) = f_s^{\Upsilon(5S)} \times \mathcal{B}(B_s^0 \rightarrow D_s X) + \left(1 - f_s^{\Upsilon(5S)} - f_{\mathcal{B}}^{\Upsilon(5S)}\right) \times \mathcal{B}(B \rightarrow D_s X), \quad (20)$$

and similar relations for $\mathcal{B}(\Upsilon(5S) \rightarrow D^0 X)$ and $\mathcal{B}(\Upsilon(5S) \rightarrow \phi X)$. We list also in Table 2 the

values of $f_s^{\Upsilon(5S)}$ derived from measurements of $f_{u,d}^{\Upsilon(5S)} = \mathcal{B}(\Upsilon(5S) \rightarrow B\bar{B}X)$ [16, 15], as well as our average value of $f_s^{\Upsilon(5S)}$, all obtained under the assumption $f_{\mathcal{B}}^{\Upsilon(5S)} = 0$.

Since the observation of $\Upsilon(5S)$ decays to final states without bottom hadrons [19], the assumption $f_{\mathcal{B}}^{\Upsilon(5S)} = 0$ is no longer valid. We therefore perform a χ^2 fit of the original measurements of the $\Upsilon(5S)$ branching fractions of Refs. [16, 17, 15], using the inputs of Table 3 and the constraints of Eqs. (19) and (20), to simultaneously extract $f_{u,d}^{\Upsilon(5S)}$, $f_s^{\Upsilon(5S)}$ and $f_{\mathcal{B}}^{\Upsilon(5S)}$. Taking all known correlations into account, the best fit values are

$$f_{u,d}^{\Upsilon(5S)} = 0.763 \pm 0.046, \quad (21)$$

$$f_s^{\Upsilon(5S)} = 0.202 \pm 0.036, \quad (22)$$

$$f_{\mathcal{B}}^{\Upsilon(5S)} = 0.035 \pm 0.057. \quad (23)$$

The $\Upsilon(5S)$ resonance has been observed to decay to $\Upsilon(1S)\pi^+\pi^-$, $\Upsilon(2S)\pi^+\pi^-$, $\Upsilon(3S)\pi^+\pi^-$ and $\Upsilon(1S)K^+K^-$ final states [19]. The sum of these measured branching fractions, adding also the contribution of the $\Upsilon(1S)\pi^0\pi^0$, $\Upsilon(2S)\pi^0\pi^0$, $\Upsilon(3S)\pi^0\pi^0$ and $\Upsilon(1S)K^0\bar{K}^0$ final states assuming isospin conservation, amounts to

$$\mathcal{B}(\Upsilon(5S) \rightarrow \Upsilon(nS)hh) = 0.028 \pm 0.003, \quad \text{for } n = 1, 2, 3 \text{ and } h = \pi, K,$$

which represents a lower bound for $f_{\mathcal{B}}^{\Upsilon(5S)}$. Our central value of Eq. (23) is indeed larger than this bound.

The production of B_s^0 mesons at the $\Upsilon(5S)$ is observed to be dominated by the $B_s^{0*}\bar{B}_s^{0*}$ channel, with $\sigma(e^+e^- \rightarrow B_s^{0*}\bar{B}_s^{0*})/\sigma(e^+e^- \rightarrow B_s^{0(*)}\bar{B}_s^{0(*)}) = (90.1_{-4.0}^{+3.8} \pm 0.2)\%$ [20]. The proportion of the various production channels for non-strange B mesons have also been recently measured [15].

3.1.3 b -hadron production fractions at high energy

At high energy, all species of weakly-decaying b hadrons can be produced, either directly or in strong and electromagnetic decays of excited b hadrons. It is often assumed that the fractions of these different species are the same in unbiased samples of high- p_T b jets originating from Z^0 decays or from $p\bar{p}$ collisions at the Tevatron. This hypothesis is plausible considering that, in both cases, the last step of the jet hadronization is a non-perturbative QCD process occurring at the scale of Λ_{QCD} . On the other hand, there is no strong argument to claim that these fractions should be strictly equal, so this assumption should be checked experimentally. Although the available data is not sufficient at this time to perform a significant check, it is expected that more data from Tevatron Run II may improve this situation and allow one to confirm or disprove this assumption with reasonable confidence. Meanwhile, the attitude adopted here is that these fractions are assumed to be equal at all high-energy colliders until demonstrated otherwise by experiment.² However, as explained below, the measurements performed at LEP and at the Tevatron show discrepancies. Therefore we present three sets of averages: one set including only measurements performed at LEP, a second set including only measurements performed at the Tevatron, and a third set including measurements performed at both LEP and Tevatron.

²It is likely that the b -hadron fractions in low- p_T jets at a hadronic machine be different; in particular, beam-remnant effects may enhance the b -baryon production.

Contrary to what happens in the charm sector where the fractions of D^+ and D^0 are different, the relative amount of B^+ and B^0 is not affected by the electromagnetic decays of excited B^{+*} and B^{0*} states and strong decays of excited B^{+**} and B^{0**} states. Decays of the type $B_s^{0**} \rightarrow B^{(*)}K$ also contribute to the B^+ and B^0 rates, but with the same magnitude if mass effects can be neglected. We therefore assume equal production of B^+ and B^0 . We also neglect the production of weakly-decaying states made of several heavy quarks (like B_c^+ and other heavy baryons) which is known to be very small. Hence, for the purpose of determining the b -hadron fractions, we use the constraints

$$f_u = f_d \quad \text{and} \quad f_u + f_d + f_s + f_{\text{baryon}} = 1, \quad (24)$$

where f_u , f_d , f_s and f_{baryon} are the unbiased fractions of B^+ , B^0 , B_s^0 and b baryons, respectively.

The LEP experiments have measured $f_s \times \mathcal{B}(B_s^0 \rightarrow D_s^- \ell^+ \nu_\ell X)$ [21], $\mathcal{B}(b \rightarrow \Lambda_b^0) \times \mathcal{B}(\Lambda_b^0 \rightarrow \Lambda_c^+ \ell^- \bar{\nu}_\ell X)$ [22, 23] and $\mathcal{B}(b \rightarrow \Xi_b^-) \times \mathcal{B}(\Xi_b^- \rightarrow \Xi^- \ell^- \bar{\nu}_\ell X)$ [24, 25]³ from partially reconstructed final states including a lepton, f_{baryon} from protons identified in b events [27], and the production rate of charged b hadrons [28]. The various b -hadron fractions have also been measured at CDF using lepton-charm final states [29, 30, 31]⁴ and double semileptonic decays with $K^* \mu \mu$ and $\phi \mu \mu$ final states [32]. Recent measurements of heavy flavor baryon production at the Tevatron are included in the determination of f_{baryon} [33, 34, 35]⁵ using the constraint

$$\begin{aligned} f_{\text{baryon}} &= f_{\Lambda_b} + f_{\Xi_b^0} + f_{\Xi_b^-} + f_{\Omega_b^-} \\ &= f_{\Lambda_b} \left(1 + 2 \frac{f_{\Xi_b^-}}{f_{\Lambda_b}} + \frac{f_{\Omega_b^-}}{f_{\Lambda_b}} \right), \end{aligned} \quad (25)$$

where isospin invariance is assumed in the production of Ξ_b^0 and Ξ_b^- . Other b baryons are expected to decay strongly or electromagnetically to those baryons listed. For the production measurements, both CDF and DØ reconstruct their b baryons exclusively to final states which include a J/ψ and a hyperon ($\Lambda_b \rightarrow J/\psi \Lambda$, $\Xi_b^- \rightarrow J/\psi \Xi^-$ and $\Omega_b^- \rightarrow J/\psi \Omega^-$). We assume that the partial decay width of a b baryon to a J/ψ and the corresponding hyperon is equal to the partial width of any other b baryon to a J/ψ and the corresponding hyperon.

All these published results have been combined following the procedure and assumptions described in [3], to yield $f_u = f_d = 0.405 \pm 0.012$, $f_s = 0.100 \pm 0.017$ and $f_{\text{baryon}} = 0.089 \pm 0.022$ under the constraints of Eq. (24). Following the PDG prescription, we have scaled the combined uncertainties on these fractions by 1.4 to account for slight discrepancies in the input data. Repeating the combinations, we obtain $f_u = f_d = 0.407 \pm 0.009$, $f_s = 0.087 \pm 0.014$ and $f_{\text{baryon}} = 0.099 \pm 0.016$ when using the LEP data only, and $f_u = f_d = 0.322 \pm 0.032$, $f_s = 0.094 \pm 0.016$ $f_{\text{baryon}} = 0.262 \pm 0.073$ when using the Tevatron data only. When the Tevatron and LEP data are separated, we find no need to scale the uncertainties of either combination. For these combinations other external inputs are used, *e.g.* the branching ratios of B mesons to final states with a D , D^* or D^{**} in semileptonic decays, which are needed to evaluate the fraction of semileptonic B_s^0 decays with a D_s^- in the final state.

³The DELPHI result of Ref. [25] is considered to supersede an older one [26].

⁴CDF updated their measurement of f_{baryon}/f_d [29] to account for a measured p_T dependence between exclusively reconstructed Λ_b and B^0 [31].

⁵DØ reports $f_{\Omega_b^-}/f_{\Xi_b^-}$. We use the CDF+DØ average of $f_{\Xi_b^-}/f_{\Lambda_b}$ to obtain $f_{\Omega_b^-}/f_{\Lambda_b}$ and then combine with the CDF result.

Table 4: Time-integrated mixing probability $\bar{\chi}$ (defined in Eq. (26)), and fractions of the different b -hadron species in an unbiased sample of weakly-decaying b hadrons, obtained from both direct and mixing measurements. The last column includes measurements performed at both LEP and Tevatron.

Quantity		in Z decays	at Tevatron	combined
Mixing probability	$\bar{\chi}$	0.1259 ± 0.0042	0.147 ± 0.011	0.1284 ± 0.0069
B^+ or B^0 fraction	$f_u = f_d$	0.403 ± 0.009	0.339 ± 0.031	0.404 ± 0.012
B_s^0 fraction	f_s	0.103 ± 0.009	0.111 ± 0.014	0.109 ± 0.012
b -baryon fraction	f_{baryon}	0.090 ± 0.015	0.211 ± 0.069	0.083 ± 0.020
Correlation between f_s and $f_u = f_d$		-0.523	$+0.426$	-0.475
Correlation between f_{baryon} and $f_u = f_d$		-0.870	-0.984	-0.854
Correlation between f_{baryon} and f_s		$+0.035$	-0.582	-0.053

Time-integrated mixing analyses performed with lepton pairs from $b\bar{b}$ events produced at high-energy colliders measure the quantity

$$\bar{\chi} = f'_d \chi_d + f'_s \chi_s, \quad (26)$$

where f'_d and f'_s are the fractions of B^0 and B_s^0 hadrons in a sample of semileptonic b -hadron decays, and where χ_d and χ_s are the B^0 and B_s^0 time-integrated mixing probabilities. Assuming that all b hadrons have the same semileptonic decay width implies $f'_i = f_i R_i$, where $R_i = \tau_i/\tau_b$ is the ratio of the lifetime τ_i of species i to the average b -hadron lifetime $\tau_b = \sum_i f_i \tau_i$. Hence measurements of the mixing probabilities $\bar{\chi}$, χ_d and χ_s can be used to improve our knowledge of f_u , f_d , f_s and f_{baryon} . In practice, the above relations yield another determination of f_s obtained from f_{baryon} and mixing information,

$$f_s = \frac{1}{R_s} \frac{(1+r)\bar{\chi} - (1 - f_{\text{baryon}} R_{\text{baryon}})\chi_d}{(1+r)\chi_s - \chi_d}, \quad (27)$$

where $r = R_u/R_d = \tau(B^+)/\tau(B^0)$.

The published measurements of $\bar{\chi}$ performed by the LEP experiments have been combined by the LEP Electroweak Working Group to yield $\bar{\chi} = 0.1259 \pm 0.0042$ [36]. This can be compared with the Tevatron average, $\bar{\chi} = 0.147 \pm 0.011$, obtained from a CDF measurement with Run I data [37] and from a recent $D\bar{O}$ measurement with Run II data [38]. The two averages deviate from each other by 1.8σ ; this could be an indication that the production fractions of b hadrons at the Z peak or at the Tevatron are not the same. Although this discrepancy is not very significant it should be carefully monitored in the future. We choose to combine these two results in a simple weighted average, assuming no correlations, and, following the PDG prescription, we multiply the combined uncertainty by 1.8 to account for the discrepancy. Our world average is then $\bar{\chi} = 0.1284 \pm 0.0069$.

Introducing the $\bar{\chi}$ average in Eq. (27), together with our world average $\chi_d = 0.1864 \pm 0.0022$ (see Eq. (59) of Sec. 3.3.1), the assumption $\chi_s = 1/2$ (justified by Eq. (122) in Sec. 3.3.2), the best knowledge of the lifetimes (see Sec. 3.2) and the estimate of f_{baryon} given above, yields $f_s = 0.120 \pm 0.019$ (or $f_s = 0.116 \pm 0.012$ using only LEP data, or $f_s = 0.172 \pm 0.031$ using only Tevatron data), an estimate dominated by the mixing information. Taking into account all

known correlations (including the one introduced by f_{baryon}), this result is then combined with the set of fractions obtained from direct measurements (given above), to yield the improved estimates of Table 4, still under the constraints of Eq. (24).⁶ As can be seen, our knowledge on the mixing parameters substantially reduces the uncertainty on f_s , and this even in the case of the world averages where a rather strong deweighting was introduced in the computation of $\bar{\chi}$. It should be noted that the results are correlated, as indicated in Table 4.

3.2 b -hadron lifetimes

In the spectator model the decay of b -flavored hadrons H_b is governed entirely by the flavor changing $b \rightarrow Wq$ transition ($q = c, u$). For this very reason, lifetimes of all b -flavored hadrons are the same in the spectator approximation regardless of the (spectator) quark content of the H_b . In the early 1990's experiments became sophisticated enough to start seeing the differences of the lifetimes among various H_b species. The first theoretical calculations of the spectator quark effects on H_b lifetime emerged only few years earlier.

Currently, most of such calculations are performed in the framework of the Heavy Quark Expansion, HQE. In the HQE, under certain assumptions (most important of which is that of quark-hadron duality), the decay rate of an H_b to an inclusive final state f is expressed as the sum of a series of expectation values of operators of increasing dimension, multiplied by the correspondingly higher powers of Λ_{QCD}/m_b :

$$\Gamma_{H_b \rightarrow f} = |CKM|^2 \sum_n c_n^{(f)} \left(\frac{\Lambda_{\text{QCD}}}{m_b} \right)^n \langle H_b | O_n | H_b \rangle, \quad (28)$$

where $|CKM|^2$ is the relevant combination of the CKM matrix elements. Coefficients $c_n^{(f)}$ of this expansion, known as Operator Product Expansion [39], can be calculated perturbatively. Hence, the HQE predicts $\Gamma_{H_b \rightarrow f}$ in the form of an expansion in both Λ_{QCD}/m_b and $\alpha_s(m_b)$. The precision of current experiments makes it mandatory to go to the next-to-leading order in QCD, *i.e.* to include correction of the order of $\alpha_s(m_b)$ to the $c_n^{(f)}$'s. All non-perturbative physics is shifted into the expectation values $\langle H_b | O_n | H_b \rangle$ of operators O_n . These can be calculated using lattice QCD or QCD sum rules, or can be related to other observables via the HQE [40]. One may reasonably expect that powers of Λ_{QCD}/m_b provide enough suppression that only the first few terms of the sum in Eq. (28) matter.

Theoretical predictions are usually made for the ratios of the lifetimes (with $\tau(B^0)$ chosen as the common denominator) rather than for the individual lifetimes, for this allows several uncertainties to cancel. The precision of the current HQE calculations (see Refs. [41, 42, 43] for the latest updates) is in some instances already surpassed by the measurements, *e.g.* in the case of $\tau(B^+)/\tau(B^0)$. Also, HQE calculations are not assumption-free. More accurate predictions are a matter of progress in the evaluation of the non-perturbative hadronic matrix elements and verifying the assumptions that the calculations are based upon. However, the HQE, even in its present shape, draws a number of important conclusions, which are in agreement with experimental observations:

⁶The combined value of f_{baryon} is smaller than the results from either LEP or Tevatron separately. This seemingly surprising result arises from the smaller uncertainties on the other fractions and the application of the unitarity constraint of Eq. (24).

- The heavier the mass of the heavy quark the smaller is the variation in the lifetimes among different hadrons containing this quark, which is to say that as $m_b \rightarrow \infty$ we retrieve the spectator picture in which the lifetimes of all H_b 's are the same. This is well illustrated by the fact that lifetimes are rather similar in the b sector, while they differ by large factors in the c sector ($m_c < m_b$).
- The non-perturbative corrections arise only at the order of $\Lambda_{\text{QCD}}^2/m_b^2$, which translates into differences among H_b lifetimes of only a few percent.
- It is only the difference between meson and baryon lifetimes that appears at the $\Lambda_{\text{QCD}}^2/m_b^2$ level. The splitting of the meson lifetimes occurs at the $\Lambda_{\text{QCD}}^3/m_b^3$ level, yet it is enhanced by a phase space factor $16\pi^2$ with respect to the leading free b decay.

To ensure that certain sources of systematic uncertainty cancel, lifetime analyses are sometimes designed to measure a ratio of lifetimes. However, because of the differences in decay topologies, abundance (or lack thereof) of decays of a certain kind, *etc.*, measurements of the individual lifetimes are more common. In the following section we review the most common types of the lifetime measurements. This discussion is followed by the presentation of the averaging of the various lifetime measurements, each with a brief description of its particularities.

3.2.1 Lifetime measurements, uncertainties and correlations

In most cases lifetime of an H_b is estimated from a flight distance and a $\beta\gamma$ factor which is used to convert the geometrical distance into the proper decay time. Methods of accessing lifetime information can roughly be divided in the following five categories:

1. ***Inclusive (flavor-blind) measurements.*** These measurements are aimed at extracting the lifetime from a mixture of b -hadron decays, without distinguishing the decaying species. Often the knowledge of the mixture composition is limited, which makes these measurements experiment-specific. Also, these measurements have to rely on Monte Carlo for estimating the $\beta\gamma$ factor, because the decaying hadrons are not fully reconstructed. On the bright side, these usually are the largest statistics b -hadron lifetime measurements that are accessible to a given experiment, and can, therefore, serve as an important performance benchmark.
2. ***Measurements in semileptonic decays of a specific H_b .*** W from $b \rightarrow Wc$ produces $\ell\nu_\ell$ pair ($\ell = e, \mu$) in about 21% of the cases. Electron or muon from such decays is usually a well-detected signature, which provides for clean and efficient trigger. c quark from $b \rightarrow Wc$ transition and the other quark(s) making up the decaying H_b combine into a charm hadron, which is reconstructed in one or more exclusive decay channels. Knowing what this charmed hadron is allows one to separate, at least statistically, different H_b species. The advantage of these measurements is in statistics, which usually is superior to that of the exclusively reconstructed H_b decays. Some of the main disadvantages are related to the difficulty of estimating lepton+charm sample composition and Monte Carlo reliance for the $\beta\gamma$ factor estimate.
3. ***Measurements in exclusively reconstructed hadronic decays.*** These have the advantage of complete reconstruction of decaying H_b , which allows one to infer the decaying

species as well as to perform precise measurement of the $\beta\gamma$ factor. Both lead to generally smaller systematic uncertainties than in the above two categories. The downsides are smaller branching ratios, larger combinatoric backgrounds, especially in $H_b \rightarrow H_c\pi(\pi\pi)$ and multi-body H_c decays, or in a hadron collider environment with non-trivial underlying event. $H_b \rightarrow J/\psi H_s$ are relatively clean and easy to trigger on $J/\psi \rightarrow \ell^+\ell^-$, but their branching fraction is only about 1%.

4. *Measurements at asymmetric B factories.*

In the $\Upsilon(4S) \rightarrow B\bar{B}$ decay, the B mesons (B^+ or B^0) are essentially at rest in the $\Upsilon(4S)$ frame. This makes direct lifetime measurements impossible in experiments at symmetric colliders producing $\Upsilon(4S)$ at rest. At asymmetric B factories the $\Upsilon(4S)$ meson is boosted resulting in B and \bar{B} moving nearly parallel to each other with the same boost. The lifetime is inferred from the distance Δz separating the B and \bar{B} decay vertices along the beam axis and from the $\Upsilon(4S)$ boost known from the beam energies. This boost is equal to $\beta\gamma \approx 0.55$ (0.43) in the *BABAR* (*Belle*) experiment, resulting in an average B decay length of approximately 250 (190) μm .

In order to determine the charge of the B mesons in each event, one of the them is fully reconstructed in a semileptonic or hadronic decay mode. The other B is typically not fully reconstructed, only the position of its decay vertex is determined from the remaining tracks in the event. These measurements benefit from large statistics, but suffer from poor proper time resolution, comparable to the B lifetime itself. This resolution is dominated by the uncertainty on the decay vertices, which is typically 50 (100) μm for a fully (partially) reconstructed B meson. With very large future statistics, the resolution and purity could be improved (and hence the systematics reduced) by fully reconstructing both B mesons in the event.

5. *Direct measurement of lifetime ratios.* This method has so far been only applied in the measurement of $\tau(B^+)/\tau(B^0)$. The ratio of the lifetimes is extracted from the dependence of the observed relative number of B^+ and B^0 candidates (both reconstructed in semileptonic decays) on the proper decay time.

In some of the latest analyses, measurements of two (*e.g.* $\tau(B^+)$ and $\tau(B^+)/\tau(B^0)$) or three (*e.g.* $\tau(B^+)$, $\tau(B^+)/\tau(B^0)$, and Δm_d) quantities are combined. This introduces correlations among measurements. Another source of correlations among the measurements are the systematic effects, which could be common to an experiment or to an analysis technique across the experiments. When calculating the averages, such correlations are taken into account per general procedure, described in Ref. [44].

3.2.2 Inclusive b -hadron lifetimes

The inclusive b hadron lifetime is defined as $\tau_b = \sum_i f_i \tau_i$ where τ_i are the individual species lifetimes and f_i are the fractions of the various species present in an unbiased sample of weakly-decaying b hadrons produced at a high-energy collider.⁷ This quantity is certainly less fundamental than the lifetimes of the individual species, the latter being much more useful in

⁷In principle such a quantity could be slightly different in Z decays and at the Tevatron, in case the fractions of b -hadron species are not exactly the same; see the discussion in Sec. 3.1.3.

Table 5: Measurements of average b -hadron lifetimes.

Experiment	Method	Data set	τ_b (ps)	Ref.
ALEPH	Dipole	91	$1.511 \pm 0.022 \pm 0.078$	[45]
DELPHI	All track i.p. (2D)	91–92	$1.542 \pm 0.021 \pm 0.045$	[46] ^a
DELPHI	Sec. vtx	91–93	$1.582 \pm 0.011 \pm 0.027$	[47] ^a
DELPHI	Sec. vtx	94–95	$1.570 \pm 0.005 \pm 0.008$	[48]
L3	Sec. vtx + i.p.	91–94	$1.556 \pm 0.010 \pm 0.017$	[49] ^b
OPAL	Sec. vtx	91–94	$1.611 \pm 0.010 \pm 0.027$	[50]
SLD	Sec. vtx	93	$1.564 \pm 0.030 \pm 0.036$	[51]
Average set 1 (b vertex)			1.572 ± 0.009	
ALEPH	Lepton i.p. (3D)	91–93	$1.533 \pm 0.013 \pm 0.022$	[52]
L3	Lepton i.p. (2D)	91–94	$1.544 \pm 0.016 \pm 0.021$	[49] ^b
OPAL	Lepton i.p. (2D)	90–91	$1.523 \pm 0.034 \pm 0.038$	[53]
Average set 2 ($b \rightarrow \ell$)			1.537 ± 0.020	
CDF1	J/ψ vtx	92–95	$1.533 \pm 0.015^{+0.035}_{-0.031}$	[54]
Average of all above			1.568 ± 0.009	

^a The combined DELPHI result quoted in [47] is $1.575 \pm 0.010 \pm 0.026$ ps.

^b The combined L3 result quoted in [49] is $1.549 \pm 0.009 \pm 0.015$ ps.

comparisons of the measurements with the theoretical predictions. Nonetheless, we perform the averaging of the inclusive lifetime measurements for completeness as well as for the reason that they might be of interest as “technical numbers.”

In practice, an unbiased measurement of the inclusive lifetime is difficult to achieve, because it would imply an efficiency which is guaranteed to be the same across species. So most of the measurements are biased. In an attempt to group analyses which are expected to select the same mixture of b hadrons, the available results (given in Table 5) are divided into the following three sets:

1. measurements at LEP and SLD that accept any b -hadron decay, based on topological reconstruction (secondary vertex or track impact parameters);
2. measurements at LEP based on the identification of a lepton from a b decay; and
3. measurements at the Tevatron based on inclusive $H_b \rightarrow J/\psi X$ reconstruction, where the J/ψ is fully reconstructed.

The measurements of the first set are generally considered as estimates of τ_b , although the efficiency to reconstruct a secondary vertex most probably depends, in an analysis-specific way, on the number of tracks coming from the vertex, thereby depending on the type of the H_b . Even though these efficiency variations can in principle be accounted for using Monte Carlo simulations (which inevitably contain assumptions on branching fractions), the H_b mixture in that case can remain somewhat ill-defined and could be slightly different among analyses in this set.

On the contrary, the mixtures corresponding to the other two sets of measurements are better defined in the limit where the reconstruction and selection efficiency of a lepton or a J/ψ

from an H_b does not depend on the decaying hadron type. These mixtures are given by the production fractions and the inclusive branching fractions for each H_b species to give a lepton or a J/ψ . In particular, under the assumption that all b hadrons have the same semileptonic decay width, the analyses of the second set should measure $\tau(b \rightarrow \ell) = (\sum_i f_i \tau_i^2) / (\sum_i f_i \tau_i)$ which is necessarily larger than τ_b if lifetime differences exist. Given the present knowledge on τ_i and f_i , $\tau(b \rightarrow \ell) - \tau_b$ is expected to be of the order of 0.01 ps.

Measurements by SLC and LEP experiments are subject to a number of common systematic uncertainties, such as those due to (lack of knowledge of) b and c fragmentation, b and c decay models, $\mathcal{B}(B \rightarrow \ell)$, $\mathcal{B}(B \rightarrow c \rightarrow \ell)$, $\mathcal{B}(c \rightarrow \ell)$, τ_c , and H_b decay multiplicity. In the averaging, these systematic uncertainties are assumed to be 100% correlated. The averages for the sets defined above (also given in Table 5) are

$$\tau(b \text{ vertex}) = 1.572 \pm 0.009 \text{ ps}, \quad (29)$$

$$\tau(b \rightarrow \ell) = 1.537 \pm 0.020 \text{ ps}, \quad (30)$$

$$\tau(b \rightarrow J/\psi) = 1.533_{-0.034}^{+0.038} \text{ ps}, \quad (31)$$

whereas an average of all measurements, ignoring mixture differences, yields 1.568 ± 0.009 ps.

3.2.3 B^0 and B^+ lifetimes and their ratio

After a number of years of dominating these averages the LEP experiments yielded the scene to the asymmetric B factories and the Tevatron experiments. The B factories have been very successful in utilizing their potential – in only a few years of running, *BABAR* and, to a greater extent, *Belle*, have struck a balance between the statistical and the systematic uncertainties, with both being close to (or even better than) the impressive 1%. In the meanwhile, CDF and $D\bar{O}$ have emerged as significant contributors to the field as the Tevatron Run II data flowed in. Both appear to enjoy relatively small systematic effects, and while current statistical uncertainties of their measurements are factors of 2 to 4 larger than those of their B -factory counterparts, both Tevatron experiments stand to increase their samples by almost an order of magnitude.

At present time we are in an interesting position of having three sets of measurements (from LEP/SLC, B factories and the Tevatron) that originate from different environments, obtained using substantially different techniques and are precise enough for incisive comparison.

The averaging of $\tau(B^+)$, $\tau(B^0)$ and $\tau(B^+)/\tau(B^0)$ measurements is summarized in Tables 6, 7, and 8. For $\tau(B^+)/\tau(B^0)$ we averaged only the measurements of this quantity provided by experiments rather than using all available knowledge, which would have included, for example, $\tau(B^+)$ and $\tau(B^0)$ measurements which did not contribute to any of the ratio measurements.

The following sources of correlated (within experiment/machine) systematic uncertainties have been considered:

- for SLC/LEP measurements – D^{**} branching ratio uncertainties [3], momentum estimation of b mesons from Z^0 decays (b -quark fragmentation parameter $\langle X_E \rangle = 0.702 \pm 0.008$ [3]), B_s^0 and b baryon lifetimes (see Secs. 3.2.4 and 3.2.6), and b -hadron fractions at high energy (see Table 4);
- for *BABAR* measurements – alignment, z scale, PEP-II boost, sample composition (where applicable);

Table 6: Measurements of the B^0 lifetime.

Experiment	Method	Data set	$\tau(B^0)$ (ps)	Ref.
ALEPH	$D^{(*)}\ell$	91–95	$1.518 \pm 0.053 \pm 0.034$	[55]
ALEPH	Exclusive	91–94	$1.25_{-0.13}^{+0.15} \pm 0.05$	[56]
ALEPH	Partial rec. $\pi^+\pi^-$	91–94	$1.49_{-0.15-0.06}^{+0.17+0.08}$	[56]
DELPHI	$D^{(*)}\ell$	91–93	$1.61_{-0.13}^{+0.14} \pm 0.08$	[57]
DELPHI	Charge sec. vtx	91–93	$1.63 \pm 0.14 \pm 0.13$	[58]
DELPHI	Inclusive $D^*\ell$	91–93	$1.532 \pm 0.041 \pm 0.040$	[59]
DELPHI	Charge sec. vtx	94–95	$1.531 \pm 0.021 \pm 0.031$	[48]
L3	Charge sec. vtx	94–95	$1.52 \pm 0.06 \pm 0.04$	[60]
OPAL	$D^{(*)}\ell$	91–93	$1.53 \pm 0.12 \pm 0.08$	[61]
OPAL	Charge sec. vtx	93–95	$1.523 \pm 0.057 \pm 0.053$	[62]
OPAL	Inclusive $D^*\ell$	91–00	$1.541 \pm 0.028 \pm 0.023$	[63]
SLD	Charge sec. vtx ℓ	93–95	$1.56_{-0.13}^{+0.14} \pm 0.10$	[64] ^a
SLD	Charge sec. vtx	93–95	$1.66 \pm 0.08 \pm 0.08$	[64] ^a
CDF1	$D^{(*)}\ell$	92–95	$1.474 \pm 0.039_{-0.051}^{+0.052}$	[65]
CDF1	Excl. $J/\psi K^{*0}$	92–95	$1.497 \pm 0.073 \pm 0.032$	[66]
CDF2	Incl. $D^{(*)}\ell$	02–04	$1.473 \pm 0.036 \pm 0.054$	[67] ^p
CDF2	Excl. $D^-(3)\pi$	02–04	$1.511 \pm 0.023 \pm 0.013$	[68] ^p
CDF2	Excl. $J/\psi K_S, J/\psi K^{*0}$	02–09	$1.507 \pm 0.010 \pm 0.008$	[69] ^p
DØ	Excl. $J/\psi K^{*0}$	03–07	$1.414 \pm 0.018 \pm 0.034$	[70]
DØ	Excl. $J/\psi K_S$	02–06	$1.501_{-0.074}^{+0.078} \pm 0.050$	[71]
BABAR	Exclusive	99–00	$1.546 \pm 0.032 \pm 0.022$	[72]
BABAR	Inclusive $D^*\ell$	99–01	$1.529 \pm 0.012 \pm 0.029$	[73]
BABAR	Exclusive $D^*\ell$	99–02	$1.523_{-0.023}^{+0.024} \pm 0.022$	[74]
BABAR	Incl. $D^*\pi, D^*\rho$	99–01	$1.533 \pm 0.034 \pm 0.038$	[75]
BABAR	Inclusive $D^*\ell$	99–04	$1.504 \pm 0.013_{-0.013}^{+0.018}$	[76]
Belle	Exclusive	00–03	$1.534 \pm 0.008 \pm 0.010$	[77]
Average			1.518 ± 0.007	

^a The combined SLD result quoted in [64] is $1.64 \pm 0.08 \pm 0.08$ ps.

^p Preliminary.

- for DØ and CDF Run II measurements – alignment (separately within each experiment).

The resultant averages are:

$$\tau(B^0) = 1.518 \pm 0.007 \text{ ps}, \quad (32)$$

$$\tau(B^+) = 1.641 \pm 0.008 \text{ ps}, \quad (33)$$

$$\tau(B^+)/\tau(B^0) = 1.081 \pm 0.006. \quad (34)$$

3.2.4 B_s^0 lifetime

Similar to the kaon system, neutral B mesons contain short- and long-lived components, since the light (L) and heavy (H) eigenstates, B_L and B_H , differ not only in their masses, but also in

Table 7: Measurements of the B^+ lifetime.

Experiment	Method	Data set	$\tau(B^+)$ (ps)	Ref.
ALEPH	$D^{(*)}\ell$	91–95	$1.648 \pm 0.049 \pm 0.035$	[55]
ALEPH	Exclusive	91–94	$1.58_{-0.18-0.03}^{+0.21+0.04}$	[56]
DELPHI	$D^{(*)}\ell$	91–93	$1.61 \pm 0.16 \pm 0.12$	[57] ^a
DELPHI	Charge sec. vtx	91–93	$1.72 \pm 0.08 \pm 0.06$	[58] ^a
DELPHI	Charge sec. vtx	94–95	$1.624 \pm 0.014 \pm 0.018$	[48]
L3	Charge sec. vtx	94–95	$1.66 \pm 0.06 \pm 0.03$	[60]
OPAL	$D^{(*)}\ell$	91–93	$1.52 \pm 0.14 \pm 0.09$	[61]
OPAL	Charge sec. vtx	93–95	$1.643 \pm 0.037 \pm 0.025$	[62]
SLD	Charge sec. vtx ℓ	93–95	$1.61_{-0.12}^{+0.13} \pm 0.07$	[64] ^b
SLD	Charge sec. vtx	93–95	$1.67 \pm 0.07 \pm 0.06$	[64] ^b
CDF1	$D^{(*)}\ell$	92–95	$1.637 \pm 0.058_{-0.043}^{+0.045}$	[65]
CDF1	Excl. $J/\psi K$	92–95	$1.636 \pm 0.058 \pm 0.025$	[66]
CDF2	Excl. $J/\psi K$	02–09	$1.639 \pm 0.009 \pm 0.009$	[69] ^p
CDF2	Incl. $D^0\ell$	02–04	$1.653 \pm 0.029_{-0.031}^{+0.033}$	[67] ^p
CDF2	Excl. $D^0\pi$	02–06	$1.662 \pm 0.023 \pm 0.015$	[78] ^p
BABAR	Exclusive	99–00	$1.673 \pm 0.032 \pm 0.023$	[72]
Belle	Exclusive	00–03	$1.635 \pm 0.011 \pm 0.011$	[77]
Average			1.641 ± 0.008	

^a The combined DELPHI result quoted in [58] is 1.70 ± 0.09 ps.

^b The combined SLD result quoted in [64] is $1.66 \pm 0.06 \pm 0.05$ ps.

^p Preliminary.

their widths with $\Delta\Gamma = \Gamma_L - \Gamma_H$. In the case of the B_s^0 system, $\Delta\Gamma_s$ can be particularly large. The current theoretical prediction in the Standard Model for the fractional width difference is $\Delta\Gamma_s = 0.096 \pm 0.039$ [80, 81], where $\Gamma_s = (\Gamma_L + \Gamma_H)/2$. Specific measurements of $\Delta\Gamma_s$ and Γ_s are explained in Sec. 3.3.2, but the result for Γ_s is quoted here.

Neglecting CP violation in $B_s^0 - \bar{B}_s^0$ mixing, which is expected to be small [80, 81], the B_s^0 mass eigenstates are also CP eigenstates. In the Standard Model assuming no CP violation in the B_s^0 system, Γ_L is the width of the CP -even state and Γ_H the width of the CP -odd state. Final states can be decomposed into CP -even and CP -odd components, each with a different lifetime.

In view of a possibly substantial width difference, and the fact that various decay channels will have different proportions of the B_L and B_H eigenstates, the straight average of all available B_s^0 lifetime measurements is rather ill-defined. Therefore, the B_s^0 lifetime measurements are broken down into four categories and averaged separately.

- **Flavor-specific decays**, such as semileptonic $B_s \rightarrow D_s\ell\nu$ or $B_s \rightarrow D_s\pi$, will have equal fractions of B_L and B_H at time zero, where $\tau_L = 1/\Gamma_L$ is expected to be the shorter-lived component and $\tau_H = 1/\Gamma_H$ expected to be the longer-lived component. A superposition of two exponentials thus results with decay widths $\Gamma_s \pm \Delta\Gamma_s/2$. Fitting to a single

Table 8: Measurements of the ratio $\tau(B^+)/\tau(B^0)$.

Experiment	Method	Data set	Ratio $\tau(B^+)/\tau(B^0)$	Ref.
ALEPH	$D^{(*)}\ell$	91–95	$1.085 \pm 0.059 \pm 0.018$	[55]
ALEPH	Exclusive	91–94	$1.27^{+0.23+0.03}_{-0.19-0.02}$	[56]
DELPHI	$D^{(*)}\ell$	91–93	$1.00^{+0.17}_{-0.15} \pm 0.10$	[57]
DELPHI	Charge sec. vtx	91–93	$1.06^{+0.13}_{-0.11} \pm 0.10$	[58]
DELPHI	Charge sec. vtx	94–95	$1.060 \pm 0.021 \pm 0.024$	[48]
L3	Charge sec. vtx	94–95	$1.09 \pm 0.07 \pm 0.03$	[60]
OPAL	$D^{(*)}\ell$	91–93	$0.99 \pm 0.14^{+0.05}_{-0.04}$	[61]
OPAL	Charge sec. vtx	93–95	$1.079 \pm 0.064 \pm 0.041$	[62]
SLD	Charge sec. vtx ℓ	93–95	$1.03^{+0.16}_{-0.14} \pm 0.09$	[64] ^a
SLD	Charge sec. vtx	93–95	$1.01^{+0.09}_{-0.08} \pm 0.05$	[64] ^a
CDF1	$D^{(*)}\ell$	92–95	$1.110 \pm 0.056^{+0.033}_{-0.030}$	[65]
CDF1	Excl. $J/\psi K$	92–95	$1.093 \pm 0.066 \pm 0.028$	[66]
CDF2	Excl. $J/\psi K^{(*)}$	02–09	$1.088 \pm 0.009 \pm 0.004$	[69] ^p
CDF2	Incl. $D\ell$	02–04	$1.123 \pm 0.040^{+0.041}_{-0.039}$	[67] ^p
CDF2	Excl. $D\pi$	02–04	$1.10 \pm 0.02 \pm 0.01$	[68] ^p
DØ	$D^{*+}\mu D^0\mu$ ratio	02–04	$1.080 \pm 0.016 \pm 0.014$	[79]
BABAR	Exclusive	99–00	$1.082 \pm 0.026 \pm 0.012$	[72]
Belle	Exclusive	00–03	$1.066 \pm 0.008 \pm 0.008$	[77]
Average			1.081 ± 0.006	

^a The combined SLD result quoted in [64] is $1.01 \pm 0.07 \pm 0.06$.

^p Preliminary.

exponential one obtains a measure of the flavor-specific lifetime [82]:

$$\tau(B_s^0)_{\text{fs}} = \frac{1}{\Gamma_s} \frac{1 + \left(\frac{\Delta\Gamma_s}{2\Gamma_s}\right)^2}{1 - \left(\frac{\Delta\Gamma_s}{2\Gamma_s}\right)^2}. \quad (35)$$

As given in Table 9, the flavor-specific B_s^0 lifetime world average is:

$$\tau(B_s^0)_{\text{fs}} = 1.455 \pm 0.030 \text{ ps}. \quad (36)$$

This world average will be used later in Sec. 3.3.2 in combination with other measurements to find $\bar{\tau}(B_s^0) = 1/\Gamma_s$ and $\Delta\Gamma_s$.

The following correlated systematic errors were considered: average B lifetime used in backgrounds, B_s^0 decay multiplicity, and branching ratios used to determine backgrounds (*e.g.* $\mathcal{B}(B \rightarrow D_s D)$). A knowledge of the multiplicity of B_s^0 decays is important for measurements that partially reconstruct the final state such as $B \rightarrow D_s X$ (where X is not a lepton). The boost deduced from Monte Carlo simulation depends on the multiplicity used. Since this is not well known, the multiplicity in the simulation is varied and this range of values observed is taken to be a systematic. Similarly not all the branching ratios

Table 9: Measurements of the B_s^0 lifetime obtained from simple exponential fits, without attempting to separate the CP -even and CP -odd components.

Experiment	Method	Data set	$\tau(B_s^0)$ (ps)	Ref.
ALEPH	$D_s\ell$	91–95	$1.54_{-0.13}^{+0.14} \pm 0.04$	[83]
CDF1	$D_s\ell$	92–96	$1.36 \pm 0.09_{-0.05}^{+0.06}$	[84]
DELPHI	$D_s\ell$	91–95	$1.42_{-0.13}^{+0.14} \pm 0.03$	[85]
OPAL	$D_s\ell$	90–95	$1.50_{-0.15}^{+0.16} \pm 0.04$	[86]
DØ	$D_s\mu$	02–04	$1.398 \pm 0.044_{-0.025}^{+0.028}$	[87]
CDF2	$D_s\pi(X)$	02–06	$1.518 \pm 0.041 \pm 0.027$	[88] ^p
CDF2	$D_s\ell$	02–04	$1.381 \pm 0.055_{-0.046}^{+0.052}$	[89] ^p
Average of flavor-specific measurements			1.455 ± 0.030	
ALEPH	$D_s h$	91–95	$1.47 \pm 0.14 \pm 0.08$	[90]
DELPHI	$D_s h$	91–95	$1.53_{-0.15}^{+0.16} \pm 0.07$	[91]
OPAL	D_s incl.	90–95	$1.72_{-0.19-0.17}^{+0.20+0.18}$	[92]
Average of all above D_s measurements			1.458 ± 0.030	
CDF1	$J/\psi\phi$	92–95	$1.34_{-0.19}^{+0.23} \pm 0.05$	[54]
CDF2	$J/\psi\phi$	02–06	$1.494 \pm 0.054 \pm 0.009$	[93] ^p
DØ	$J/\psi\phi$	02–04	$1.444_{-0.090}^{+0.098} \pm 0.02$	[94]
Average of $J/\psi\phi$ measurements			1.477 ± 0.046	

^p Preliminary.

for the potential background processes are measured. Where they are available, the PDG values are used for the error estimate. Where no measurements are available estimates can usually be made by using measured branching ratios of related processes and using some reasonable extrapolation.

- **$B_s^0 \rightarrow D_s^+ X$ decays.** Included in Table 9 are measurements of lifetimes using samples of B_s^0 decays to D_s plus hadrons, and hence into a less known mixture of CP -states. A lifetime weighted this way can still be a useful input for analyses examining such an inclusive sample. These are separated in Table 9 and combined with the semileptonic lifetime to obtain:

$$\tau(B_s^0)_{D_s X} = 1.458 \pm 0.030 \text{ ps} . \quad (37)$$

- **Fully exclusive $B_s^0 \rightarrow J/\psi\phi$ decays** are expected to be dominated by the CP -even state and its lifetime. First measurements of the CP mix for this decay mode are outlined in Sec. 3.3.2. CDF and DØ measurements based on simple exponential fits of the $B_s^0 \rightarrow J/\psi\phi$ lifetime distribution are combined into an average given in Table 9. There are no correlations between the measurements for this fully exclusive channel, and the world average for this specific decay is:

$$\tau(B_s^0)_{J/\psi\phi} = 1.477 \pm 0.046 \text{ ps} . \quad (38)$$

A caveat is that different experimental acceptances will likely lead to different admixtures of the CP -even and CP -odd states, and fits to a single exponential may result in inherently different measurements of these quantities.

- **Decays to (almost) pure CP -even eigenstates**, such as $B_s^0 \rightarrow K^+K^-$ and $B_s^0 \rightarrow D_s^{(*)+}D_s^{(*)+}$ decays which are expected to be CP even to within 5%, and hence allow the measurement of the lifetime of the “light” mass eigenstate $\tau_L = 1/\Gamma_L$. ALEPH has measured $1.27 \pm 0.33 \pm 0.08$ ps with $B_s^0 \rightarrow D_s^{(*)+}D_s^{(*)+}$ decays [95], while CDF has measured $1.53 \pm 0.18 \pm 0.02$ ps with $B_s^0 \rightarrow K^+K^-$ in Run II [96]. The average of these two measurements is:

$$\tau_L = 1/\Gamma_L = \tau(B_s^0 \rightarrow CP \text{ even}) = 1.47 \pm 0.16 \text{ ps}. \quad (39)$$

Finally, as will be shown in Sec. 3.3.2, measurements of $\Delta\Gamma_s$, including separation into CP -even and CP -odd components, give⁸

$$\bar{\tau}(B_s^0) = 1/\Gamma_s = 1.506 \pm 0.032 \text{ ps}, \quad (40)$$

and when combined with the flavor-specific lifetime measurements:

$$\bar{\tau}(B_s^0) = 1/\Gamma_s = 1.477_{-0.022}^{+0.021} \text{ ps}. \quad (41)$$

3.2.5 B_c^+ lifetime

There are currently three measurements of the lifetime of the B_c^+ meson from CDF [98, 99] and DØ [100] using the semileptonic decay mode $B_c^+ \rightarrow J/\psi\ell$ and fitting simultaneously to the mass and lifetime using the vertex formed with the leptons from the decay of the J/ψ and the third lepton. Correction factors to estimate the boost due to the missing neutrino are used. In the analysis of the CDF Run I data [98], a mass value of $6.40 \pm 0.39 \pm 0.13 \text{ GeV}/c^2$ is found by fitting to the tri-lepton invariant mass spectrum. In the CDF and DØ Run II results [99, 100], the B_c^+ mass is assumed to be $6285.7 \pm 5.3 \pm 1.2 \text{ MeV}/c^2$, taken from a CDF result [101]. These mass measurements are consistent within uncertainties, and also consistent with the most recent precision determination from CDF of $6275.6 \pm 2.9 \pm 2.5 \text{ MeV}/c^2$ [102]. Correlated systematic errors include the impact of the uncertainty of the B_c^+ p_T spectrum on the correction factors, the level of feed-down from $\psi(2S)$, MC modeling of the decay model varying from phase space to the ISGW model, and mass variations. Values of the B_c^+ lifetime are given in Table 10 and the world average is determined to be:

$$\tau(B_c^+) = 0.461 \pm 0.036 \text{ ps}. \quad (42)$$

3.2.6 Λ_b^0 and b -baryon lifetimes

The first measurements of b -baryon lifetimes originate from two classes of partially reconstructed decays. In the first class, decays with an exclusively reconstructed Λ_c^+ baryon and a lepton of opposite charge are used. These products are more likely to occur in the decay of Λ_b^0 baryons. In the second class, more inclusive final states with a baryon (p , \bar{p} , Λ , or $\bar{\Lambda}$) and a lepton have been used, and these final states can generally arise from any b baryon. With the large b -hadron samples available at the Tevatron, the most precise measurements of b -baryons now come from fully reconstructed exclusive decays.

⁸A recent CDF result, $1/\Gamma_s = 1.530 \pm 0.025 \pm 0.012$ [97], has not yet been included in this average.

Table 10: Measurements of the B_c^+ lifetime.

Experiment	Method	Data set	$\tau(B_c^+)$ (ps)	Ref.
CDF1	$J/\psi\ell$	92–95	$0.46_{-0.16}^{+0.18} \pm 0.03$	[98]
CDF2	$J/\psi\ell$	02–06	$0.475_{-0.049}^{+0.053} \pm 0.018$	[99] ^p
DØ	$J/\psi\mu$	02–06	$0.448_{-0.036}^{+0.038} \pm 0.032$	[100]
Average			0.461 ± 0.036	

^p Preliminary.

The following sources of correlated systematic uncertainties have been considered: experimental time resolution within a given experiment, b -quark fragmentation distribution into weakly decaying b baryons, Λ_b^0 polarization, decay model, and evaluation of the b -baryon purity in the selected event samples. In computing the averages the central values of the masses are scaled to $M(\Lambda_b^0) = 5620 \pm 2$ MeV/ c^2 [103] and $M(b\text{-baryon}) = 5670 \pm 100$ MeV/ c^2 .

For the semi-inclusive lifetime measurements, the meaning of decay model systematic uncertainties and the correlation of these uncertainties between measurements are not always clear. Uncertainties related to the decay model are dominated by assumptions on the fraction of n -body semileptonic decays. To be conservative it is assumed that these are 100% correlated whenever given as an error. DELPHI varies the fraction of 4-body decays from 0.0 to 0.3. In computing the average, the DELPHI result is corrected to a value of 0.2 ± 0.2 for this fraction.

Furthermore, in computing the average, the semileptonic decay results from LEP are corrected for a polarization of $-0.45_{-0.17}^{+0.19}$ [3] and a Λ_b^0 fragmentation parameter $\langle X_E \rangle = 0.70 \pm 0.03$ [104].

Inputs to the averages are given in Table 11. Note that the CDF $\Lambda_b \rightarrow J/\psi\Lambda$ lifetime result [69] is 3.3σ larger than the world average computed excluding this result. It is nonetheless combined with the rest without adjustment of input errors. The world average lifetime of b baryons is then:

$$\langle \tau(b\text{-baryon}) \rangle = 1.382 \pm 0.029 \text{ ps} . \quad (43)$$

Keeping only $\Lambda_c^\pm \ell^\mp$, $\Lambda \ell^- \ell^+$, and fully exclusive final states, as representative of the Λ_b^0 baryon, the following lifetime is obtained:

$$\tau(\Lambda_b^0) = 1.425 \pm 0.032 \text{ ps} . \quad (44)$$

Averaging the measurements based on the $\Xi^\mp \ell^\mp$ [24, 25, 26] and $J/\psi \Xi^\mp$ [35] final states gives a lifetime value for a sample of events containing Ξ_b^0 and Ξ_b^- baryons:

$$\langle \tau(\Xi_b) \rangle = 1.49_{-0.18}^{+0.19} \text{ ps} . \quad (45)$$

Recent (and first) measurements of fully reconstructed $\Xi_b^- \rightarrow J/\psi \Xi^-$ and $\Omega_b^- \rightarrow J/\psi \Omega^-$ baryons yield [35]

$$\tau(\Xi_b^-) = 1.56_{-0.25}^{+0.27} \text{ ps} , \quad (46)$$

$$\tau(\Omega_b^-) = 1.13_{-0.40}^{+0.53} \text{ ps} . \quad (47)$$

Table 11: Measurements of the b -baryon lifetimes.

Experiment	Method	Data set	Lifetime (ps)	Ref.
ALEPH	$\Lambda_c^+ \ell$	91–95	$1.18_{-0.12}^{+0.13} \pm 0.03$	[23] ^a
ALEPH	$\Lambda \ell^- \ell^+$	91–95	$1.30_{-0.21}^{+0.26} \pm 0.04$	[23] ^a
CDF1	$\Lambda_c^+ \ell$	91–95	$1.32 \pm 0.15 \pm 0.07$	[105]
CDF2	$\Lambda_c^+ \pi$	02–06	$1.401 \pm 0.046 \pm 0.035$	[106]
CDF2	$J/\psi \Lambda$	02–09	$1.537 \pm 0.045 \pm 0.014$	[69] ^p
DØ	$J/\psi \Lambda$	02–06	$1.218_{-0.115}^{+0.130} \pm 0.042$	[71] ^b
DØ	$\Lambda_c^+ \mu$	02–06	$1.290_{-0.110-0.091}^{+0.119+0.087}$	[107] ^b
DELPHI	$\Lambda_c^+ \ell$	91–94	$1.11_{-0.18}^{+0.19} \pm 0.05$	[108] ^c
OPAL	$\Lambda_c^+ \ell, \Lambda \ell^- \ell^+$	90–95	$1.29_{-0.22}^{+0.24} \pm 0.06$	[86]
Average of above 9:		Λ_b^0 lifetime =	1.425 ± 0.032	
ALEPH	$\Lambda \ell$	91–95	$1.20 \pm 0.08 \pm 0.06$	[23]
DELPHI	$\Lambda \ell \pi$ vtx	91–94	$1.16 \pm 0.20 \pm 0.08$	[108] ^c
DELPHI	$\Lambda \mu$ i.p.	91–94	$1.10_{-0.17}^{+0.19} \pm 0.09$	[109] ^c
DELPHI	$p \ell$	91–94	$1.19 \pm 0.14 \pm 0.07$	[108] ^c
OPAL	$\Lambda \ell$ i.p.	90–94	$1.21_{-0.13}^{+0.15} \pm 0.10$	[110] ^d
OPAL	$\Lambda \ell$ vtx	90–94	$1.15 \pm 0.12 \pm 0.06$	[110] ^d
Average of above 15: mean b -baryon lifetime =			1.382 ± 0.029	
CDF2	$J/\psi \Xi^-$	02–09	$1.56_{-0.25}^{+0.27} \pm 0.02$	[35]
Average of above 1:		Ξ_b^- lifetime =	$1.56_{-0.25}^{+0.27}$	
ALEPH	$\Xi \ell$	90–95	$1.35_{-0.28-0.17}^{+0.37+0.15}$	[24]
DELPHI	$\Xi \ell$	91–93	$1.5_{-0.4}^{+0.7} \pm 0.3$	[26] ^e
DELPHI	$\Xi \ell$	92–95	$1.45_{-0.43}^{+0.55} \pm 0.13$	[25] ^e
Average of above 4: mean Ξ_b^- lifetime =			$1.49_{-0.18}^{+0.19}$	
CDF2	$J/\psi \Omega^-$	02–09	$1.13_{-0.40}^{+0.53} \pm 0.02$	[35]
Average of above 1:		Ω_b^- lifetime =	$1.13_{-0.40}^{+0.53}$	

^a The combined ALEPH result quoted in [23] is 1.21 ± 0.11 ps.

^b The combined DØ result quoted in [107] is $1.251_{-0.096}^{+0.102}$ ps.

^c The combined DELPHI result quoted in [108] is $1.14 \pm 0.08 \pm 0.04$ ps.

^d The combined OPAL result quoted in [110] is $1.16 \pm 0.11 \pm 0.06$ ps.

^e The combined DELPHI result quoted in [25] is $1.48_{-0.31}^{+0.40} \pm 0.12$ ps.

^p Preliminary.

3.2.7 Summary and comparison with theoretical predictions

Averages of lifetimes of specific b -hadron species are collected in Table 12. As described in Sec. 3.2, Heavy Quark Effective Theory can be employed to explain the hierarchy of $\tau(B_c^+) \ll \tau(A_b^0) < \bar{\tau}(B_s^0) \approx \tau(B^0) < \tau(B^+)$, and used to predict the ratios between lifetimes. Typical predictions are compared to the measured lifetime ratios in Table 13. A recent prediction of the ratio between the B^+ and B^0 lifetimes, is 1.06 ± 0.02 [42], in good agreement with experiment.

The total widths of the B_s^0 and B^0 mesons are expected to be very close and differ by at most 1% [111, 43]. However, the experimental ratio $\bar{\tau}(B_s^0)/\tau(B^0)$, where $\bar{\tau}(B_s^0) = 1/\Gamma_s$ is obtained from $\Delta\Gamma_s$ and flavour-specific lifetime measurements, appears to be smaller than 1 by

Table 12: Summary of lifetimes of different b -hadron species.

b -hadron species	Measured lifetime
B^+	1.641 ± 0.008 ps
B^0	1.518 ± 0.007 ps
B_s^0 (\rightarrow flavor specific)	1.455 ± 0.030 ps
B_s^0 ($\rightarrow J/\psi\phi$)	1.477 ± 0.046 ps
B_s^0 ($1/\Gamma_s$)	$1.477^{+0.021}_{-0.022}$ ps
B_c^+	0.461 ± 0.036 ps
Λ_b^0	1.425 ± 0.032 ps
Ξ_b mixture	$1.49^{+0.19}_{-0.18}$ ps
b -baryon mixture	1.382 ± 0.029 ps
b -hadron mixture	1.568 ± 0.009 ps

Table 13: Measured ratios of b -hadron lifetimes relative to the B^0 lifetime and ranges predicted by theory [42, 43].

Lifetime ratio	Measured value	Predicted range
$\tau(B^+)/\tau(B^0)$	1.081 ± 0.006	1.04 – 1.08
$\bar{\tau}(B_s^0)/\tau(B^0)^a$	0.973 ± 0.015	0.99 – 1.01
$\tau(\Lambda_b^0)/\tau(B^0)$	0.939 ± 0.022	0.86 – 0.95
$\tau(b\text{-baryon})/\tau(B^0)$	0.910 ± 0.020	0.86 – 0.95

^a Using $\bar{\tau}(B_s^0) = 1/\Gamma_s = 2/(\Gamma_L + \Gamma_H)$.

$(2.7 \pm 1.5)\%$, at deviation with respect to the prediction.

The ratio $\tau(\Lambda_b^0)/\tau(B^0)$ has particularly been the source of theoretical scrutiny since earlier calculations [39, 112] predicted a value greater than 0.90, almost two sigma higher than the world average at the time. Many predictions cluster around a most likely central value of 0.94 [113]. More recent calculations of this ratio that include higher-order effects predict a lower ratio between the Λ_b^0 and B^0 lifetimes [42, 43] and reduce this difference. References [42, 43] present probability density functions of their predictions with variation of theoretical inputs, and the indicated ranges in Table 13 are the RMS of the distributions from the most probable values. Note that in contrast to the B mesons, complete NLO QCD corrections and fully reliable lattice determinations of the matrix elements for Λ_b^0 are not yet available. Again, the CDF measurement of the Λ_b lifetime in the exclusive decay mode $J/\psi\Lambda$ [69] is significantly higher than the world average before inclusion, with a ratio to the $\tau(B^0)$ world average of $\tau(\Lambda_b^0)/\tau(B^0) = 1.012 \pm 0.031$, resulting in continued interest in lifetimes of b baryons.

3.3 Neutral B -meson mixing

The $B^0 - \bar{B}^0$ and $B_s^0 - \bar{B}_s^0$ systems both exhibit the phenomenon of particle-antiparticle mixing. For each of them, there are two mass eigenstates which are linear combinations of the two flavour states, B and \bar{B} . The heaviest (lightest) of these mass states is denoted B_H (B_L), with

mass m_H (m_L) and total decay width Γ_H (Γ_L). We define

$$\Delta m = m_H - m_L, \quad x = \Delta m/\Gamma, \quad (48)$$

$$\Delta\Gamma = \Gamma_L - \Gamma_H, \quad y = \Delta\Gamma/(2\Gamma), \quad (49)$$

where $\Gamma = (\Gamma_H + \Gamma_L)/2 = 1/\bar{\tau}(B)$ is the average decay width. Δm is positive by definition, and $\Delta\Gamma$ is expected to be positive within the Standard Model.⁹

There are four different time-dependent probabilities describing the case of a neutral B meson produced as a flavour state and decaying to a flavour-specific final state. If CPT is conserved (which will be assumed throughout), they can be written as

$$\begin{cases} \mathcal{P}(B \rightarrow B) &= \frac{e^{-\Gamma t}}{2} \left[\cosh\left(\frac{\Delta\Gamma}{2}t\right) + \cos(\Delta mt) \right] \\ \mathcal{P}(B \rightarrow \bar{B}) &= \frac{e^{-\Gamma t}}{2} \left[\cosh\left(\frac{\Delta\Gamma}{2}t\right) - \cos(\Delta mt) \right] \left| \frac{q}{p} \right|^2 \\ \mathcal{P}(\bar{B} \rightarrow B) &= \frac{e^{-\Gamma t}}{2} \left[\cosh\left(\frac{\Delta\Gamma}{2}t\right) - \cos(\Delta mt) \right] \left| \frac{p}{q} \right|^2 \\ \mathcal{P}(\bar{B} \rightarrow \bar{B}) &= \frac{e^{-\Gamma t}}{2} \left[\cosh\left(\frac{\Delta\Gamma}{2}t\right) + \cos(\Delta mt) \right] \end{cases}, \quad (50)$$

where t is the proper time of the system (*i.e.* the time interval between the production and the decay in the rest frame of the B meson). At the B factories, only the proper-time difference Δt between the decays of the two neutral B mesons from the $\Upsilon(4S)$ can be determined, but, because the two B mesons evolve coherently (keeping opposite flavours as long as none of them has decayed), the above formulae remain valid if t is replaced with Δt and the production flavour is replaced by the flavour at the time of the decay of the accompanying B meson in a flavour-specific state. As can be seen in the above expressions, the mixing probabilities depend on three mixing observables: Δm , $\Delta\Gamma$, and $|q/p|^2$ which signals CP violation in the mixing if $|q/p|^2 \neq 1$.

In the next sections we review in turn the experimental knowledge on these three parameters, separately for the B^0 meson (Δm_d , $\Delta\Gamma_d$, $|q/p|_d$) and the B_s^0 meson (Δm_s , $\Delta\Gamma_s$, $|q/p|_s$).

3.3.1 B^0 mixing parameters

CP violation parameter $|q/p|_d$

Evidence for CP violation in B^0 mixing has been searched for, both with flavor-specific and inclusive B^0 decays, in samples where the initial flavor state is tagged. In the case of semileptonic (or other flavor-specific) decays, where the final state tag is also available, the following asymmetry

$$\mathcal{A}_{\text{SL}}^d = \frac{N(\bar{B}^0(t) \rightarrow \ell^+ \nu_\ell X) - N(B^0(t) \rightarrow \ell^- \bar{\nu}_\ell X)}{N(\bar{B}^0(t) \rightarrow \ell^+ \nu_\ell X) + N(B^0(t) \rightarrow \ell^- \bar{\nu}_\ell X)} = \frac{|p/q|_d^2 - |q/p|_d^2}{|p/q|_d^2 + |q/p|_d^2} \quad (51)$$

has been measured, either in time-integrated analyses at CLEO [114, 115, 116], CDF [117, 118] and DØ [38], or in time-dependent analyses at OPAL [119], ALEPH [120], BABAR [121, 122,

⁹For reason of symmetry in Eqs. (48) and (49), $\Delta\Gamma$ is sometimes defined with the opposite sign. The definition adopted here, *i.e.* Eq. (49), is the one used by most experimentalists and many phenomenologists in B physics.

123, 124] and Belle [125]. In the inclusive case, also investigated and published at ALEPH [120] and OPAL [62], no final state tag is used, and the asymmetry [126]

$$\frac{N(B^0(t) \rightarrow \text{all}) - N(\overline{B}^0(t) \rightarrow \text{all})}{N(B^0(t) \rightarrow \text{all}) + N(\overline{B}^0(t) \rightarrow \text{all})} \simeq \mathcal{A}_{\text{SL}}^d \left[\frac{\Delta m_d}{2\Gamma_d} \sin(\Delta m_d t) - \sin^2 \left(\frac{\Delta m_d t}{2} \right) \right] \quad (52)$$

must be measured as a function of the proper time to extract information on CP violation. In all cases asymmetries compatible with zero have been found, with a precision limited by the available statistics.

A simple average of all measurements performed at B factories [115, 116, 121, 123, 124, 125] yields

$$\mathcal{A}_{\text{SL}}^d = -0.0047 \pm 0.0046 \quad (53)$$

or, equivalently through Eq. (51),

$$|q/p|_d = 1.0024 \pm 0.0023. \quad (54)$$

Analyses performed at higher energy, either at LEP or at the Tevatron, can't separate the contributions from the B^0 and B_s^0 mesons. Under the assumption of no CP violation in B_s^0 mixing, a number of these analyses [38, 119, 120, 62] quote a measurement of $\mathcal{A}_{\text{SL}}^d$ or $|q/p|_d$ for the B^0 meson. Combining these results, as well as that of a preliminary CDF analysis [118]¹⁰, with the above B factory averages leads to

$$\left. \begin{array}{l} \mathcal{A}_{\text{SL}}^d = -0.0058 \pm 0.0034 \\ |q/p|_d = 1.0030 \pm 0.0017 \end{array} \right\} \text{ if } \mathcal{A}_{\text{SL}}^s = 0, |q/p|_s = 1. \quad (55)$$

These results¹¹, summarized in Table 14, are compatible with no CP violation in the B^0 mixing, an assumption we make for the rest of this section. Note that as described in Sec. 3.3.2, a recent update [127] of the $D\bar{O}$ dimuon analysis gives a measurement of the semileptonic charge asymmetry at the Tevatron that deviates from the Standard Model by more than 3σ , but without a separation of the asymmetry due to B^0 or B_s^0 mesons; however, the world average value of $\mathcal{A}_{\text{SL}}^d$ measured at the B factories is used to extract $\mathcal{A}_{\text{SL}}^s$.

Mass and decay width differences Δm_d and $\Delta\Gamma_d$

Many time-dependent B^0 - \overline{B}^0 oscillation analyses have been performed by the ALEPH, BABAR, Belle, CDF, $D\bar{O}$, DELPHI, L3 and OPAL collaborations. The corresponding measurements of Δm_d are summarized in Table 15, where only the most recent results are listed (*i.e.* measurements superseded by more recent ones have been omitted). Although a variety of different techniques have been used, the individual Δm_d results obtained at high-energy colliders have remarkably similar precision. Their average is compatible with the recent and more precise measurements from the asymmetric B factories. The systematic uncertainties are not negligible; they are often dominated by sample composition, mistag probability, or b -hadron lifetime contributions. Before being combined, the measurements are adjusted on the

¹⁰A low-statistics analysis published by CDF using the Run I data[117] has not been included.

¹¹Early analyses and (perhaps hence) the PDG use the complex parameter $\epsilon_B = (p - q)/(p + q)$; if CP violation in the mixing is small, $\mathcal{A}_{\text{SL}}^d \cong 4\text{Re}(\epsilon_B)/(1 + |\epsilon_B|^2)$ and our current averages are $\text{Re}(\epsilon_B)/(1 + |\epsilon_B|^2) = -0.0012 \pm 0.0011$ (B factory measurements only) and -0.0015 ± 0.0008 (all measurements).

Table 14: Measurements of CP violation in B^0 mixing and their average in terms of both $\mathcal{A}_{\text{SL}}^d$ and $|q/p|_d$. The individual results are listed as quoted in the original publications, or converted¹¹ to an $\mathcal{A}_{\text{SL}}^d$ value. When two errors are quoted, the first one is statistical and the second one systematic. The second group of measurements, performed at high-energy colliders, assume no CP violation in B_s^0 mixing, *i.e.* $|q/p|_s = 1$.

Exp. & Ref.	Method	Measured $\mathcal{A}_{\text{SL}}^d$	Measured $ q/p _d$
CLEO [115]	partial hadronic rec.	+0.017 ±0.070 ±0.014	
CLEO [116]	dileptons	+0.013 ±0.050 ±0.005	
CLEO [116]	average of above two	+0.014 ±0.041 ±0.006	
BABAR [121]	full hadronic rec.		1.029 ±0.013 ±0.011
BABAR [123]	dileptons		0.9992 ±0.0027±0.0019
BABAR [124] ^p	part. rec. $D^*\ell\nu$	-0.0130 ±0.0068±0.0040	1.0065 ±0.0034±0.0020
Belle [125]	dileptons	-0.0011 ±0.0079±0.0085	1.0005 ±0.0040±0.0043
Average of 7 above		-0.0047 ± 0.0046 (tot)	1.0024 ± 0.0023 (tot)
OPAL [119]	leptons	+0.008 ±0.028 ±0.012	
OPAL [62]	inclusive (Eq. (52))	+0.005 ±0.055 ±0.013	
ALEPH [120]	leptons	-0.037 ±0.032 ±0.007	
ALEPH [120]	inclusive (Eq. (52))	+0.016 ±0.034 ±0.009	
ALEPH [120]	average of above two	-0.013 ± 0.026 (tot)	
DØ [38]	dimuons	-0.0092 ±0.0044±0.0032	
CDF2 [118] ^p	dimuons	+0.0136 ±0.0151±0.0115	
Average of 14 above		-0.0058 ± 0.0034 (tot)	1.0030 ± 0.0017 (tot)

^p Preliminary.

basis of a common set of input values, including the averages of the b -hadron fractions and lifetimes given in this report (see Secs. 3.1 and 3.2). Some measurements are statistically correlated. Systematic correlations arise both from common physics sources (fractions, lifetimes, branching ratios of b hadrons), and from purely experimental or algorithmic effects (efficiency, resolution, flavour tagging, background description). Combining all published measurements listed in Table 15 and accounting for all identified correlations as described in Ref. [3] yields $\Delta m_d = 0.508 \pm 0.003 \pm 0.003 \text{ ps}^{-1}$.

On the other hand, ARGUS and CLEO have published measurements of the time-integrated mixing probability χ_d [144, 114, 115], which average to $\chi_d = 0.182 \pm 0.015$. Following Ref. [115], the width difference $\Delta\Gamma_d$ could in principle be extracted from the measured value of $\Gamma_d = 1/\tau(B^0)$ and the above averages for Δm_d and χ_d (provided that $\Delta\Gamma_d$ has a negligible impact on the $\Delta m_d \tau(B^0)$ analyses that have assumed $\Delta\Gamma_d = 0$), using the relation

$$\chi_d = \frac{x_d^2 + y_d^2}{2(x_d^2 + 1)} \quad \text{with} \quad x_d = \frac{\Delta m_d}{\Gamma_d} \quad \text{and} \quad y_d = \frac{\Delta\Gamma_d}{2\Gamma_d}. \quad (56)$$

However, direct time-dependent studies provide much stronger constraints: $|\Delta\Gamma_d|/\Gamma_d < 18\%$ at 95% CL from DELPHI [130], and $-6.8\% < \text{sign}(\text{Re}\lambda_{CP})\Delta\Gamma_d/\Gamma_d < 8.4\%$ at 90% CL from BABAR [121], where $\lambda_{CP} = (q/p)_d(\bar{A}_{CP}/A_{CP})$ is defined for a CP -even final state (the sensitivity to the overall sign of $\text{sign}(\text{Re}\lambda_{CP})\Delta\Gamma_d/\Gamma_d$ comes from the use of B^0 decays to CP final states).

Table 15: Time-dependent measurements included in the Δm_d average. The results obtained from multi-dimensional fits involving also the B^0 (and B^+) lifetimes as free parameter(s) [74, 76, 77] have been converted into one-dimensional measurements of Δm_d . All the measurements have then been adjusted to a common set of physics parameters before being combined. The CDF results from Run II are preliminary.

Experiment and Ref.	Method		Δm_d in ps^{-1}	Δm_d in ps^{-1}
	rec.	tag	before adjustment	after adjustment
ALEPH [128]	ℓ	Q_{jet}	$0.404 \pm 0.045 \pm 0.027$	
ALEPH [128]	ℓ	ℓ	$0.452 \pm 0.039 \pm 0.044$	
ALEPH [128]	above two combined		$0.422 \pm 0.032 \pm 0.026$	$0.442 \pm 0.032 \begin{smallmatrix} +0.020 \\ -0.019 \end{smallmatrix}$
ALEPH [128]	D^*	ℓ, Q_{jet}	$0.482 \pm 0.044 \pm 0.024$	$0.482 \pm 0.044 \pm 0.024$
DELPHI [129]	ℓ	Q_{jet}	$0.493 \pm 0.042 \pm 0.027$	$0.503 \pm 0.042 \pm 0.024$
DELPHI [129]	$\pi^* \ell$	Q_{jet}	$0.499 \pm 0.053 \pm 0.015$	$0.501 \pm 0.053 \pm 0.015$
DELPHI [129]	ℓ	ℓ	$0.480 \pm 0.040 \pm 0.051$	$0.497 \pm 0.040 \begin{smallmatrix} +0.042 \\ -0.041 \end{smallmatrix}$
DELPHI [129]	D^*	Q_{jet}	$0.523 \pm 0.072 \pm 0.043$	$0.518 \pm 0.072 \pm 0.043$
DELPHI [130]	vtx	comb	$0.531 \pm 0.025 \pm 0.007$	$0.527 \pm 0.025 \pm 0.006$
L3 [131]	ℓ	ℓ	$0.458 \pm 0.046 \pm 0.032$	$0.466 \pm 0.046 \pm 0.028$
L3 [131]	ℓ	Q_{jet}	$0.427 \pm 0.044 \pm 0.044$	$0.439 \pm 0.044 \pm 0.042$
L3 [131]	ℓ	$\ell(\text{IP})$	$0.462 \pm 0.063 \pm 0.053$	$0.473 \pm 0.063 \begin{smallmatrix} +0.045 \\ -0.044 \end{smallmatrix}$
OPAL [132]	ℓ	ℓ	$0.430 \pm 0.043 \begin{smallmatrix} +0.028 \\ -0.030 \end{smallmatrix}$	$0.467 \pm 0.043 \begin{smallmatrix} +0.017 \\ -0.016 \end{smallmatrix}$
OPAL [119]	ℓ	Q_{jet}	$0.444 \pm 0.029 \begin{smallmatrix} +0.020 \\ -0.017 \end{smallmatrix}$	$0.476 \pm 0.029 \begin{smallmatrix} +0.014 \\ -0.013 \end{smallmatrix}$
OPAL [133]	$D^* \ell$	Q_{jet}	$0.539 \pm 0.060 \pm 0.024$	$0.544 \pm 0.060 \pm 0.023$
OPAL [133]	D^*	ℓ	$0.567 \pm 0.089 \begin{smallmatrix} +0.029 \\ -0.023 \end{smallmatrix}$	$0.572 \pm 0.089 \begin{smallmatrix} +0.028 \\ -0.022 \end{smallmatrix}$
OPAL [63]	$\pi^* \ell$	Q_{jet}	$0.497 \pm 0.024 \pm 0.025$	$0.496 \pm 0.024 \pm 0.025$
CDF1 [134]	$D \ell$	SST	$0.471 \begin{smallmatrix} +0.078 \\ -0.068 \end{smallmatrix} \begin{smallmatrix} +0.033 \\ -0.034 \end{smallmatrix}$	$0.470 \begin{smallmatrix} +0.078 \\ -0.068 \end{smallmatrix} \begin{smallmatrix} +0.033 \\ -0.034 \end{smallmatrix}$
CDF1 [135]	μ	μ	$0.503 \pm 0.064 \pm 0.071$	$0.515 \pm 0.064 \pm 0.070$
CDF1 [136]	ℓ	ℓ, Q_{jet}	$0.500 \pm 0.052 \pm 0.043$	$0.547 \pm 0.052 \pm 0.036$
CDF1 [137]	$D^* \ell$	ℓ	$0.516 \pm 0.099 \begin{smallmatrix} +0.029 \\ -0.035 \end{smallmatrix}$	$0.523 \pm 0.099 \begin{smallmatrix} +0.028 \\ -0.035 \end{smallmatrix}$
CDF2 [138]	$D^{(*)} \ell$	OST	$0.509 \pm 0.010 \pm 0.016$	$0.509 \pm 0.010 \pm 0.016$
CDF2 [139]	B^0	comb	$0.536 \pm 0.028 \pm 0.006$	$0.536 \pm 0.028 \pm 0.006$
DØ [140]	$D^{(*)} \mu$	OST	$0.506 \pm 0.020 \pm 0.016$	$0.506 \pm 0.020 \pm 0.016$
BABAR [141]	B^0	ℓ, K, NN	$0.516 \pm 0.016 \pm 0.010$	$0.521 \pm 0.016 \pm 0.008$
BABAR [142]	ℓ	ℓ	$0.493 \pm 0.012 \pm 0.009$	$0.486 \pm 0.012 \pm 0.006$
BABAR [76]	$D^* \ell \nu(\text{part})$	ℓ	$0.511 \pm 0.007 \pm 0.007$	$0.512 \pm 0.007 \pm 0.007$
BABAR [74]	$D^* \ell \nu$	ℓ, K, NN	$0.492 \pm 0.018 \pm 0.014$	$0.493 \pm 0.018 \pm 0.013$
Belle [143]	$D^* \pi(\text{part})$	ℓ	$0.509 \pm 0.017 \pm 0.020$	$0.514 \pm 0.017 \pm 0.019$
Belle [11]	ℓ	ℓ	$0.503 \pm 0.008 \pm 0.010$	$0.505 \pm 0.008 \pm 0.008$
Belle [77]	$B^0, D^* \ell \nu$	comb	$0.511 \pm 0.005 \pm 0.006$	$0.513 \pm 0.005 \pm 0.006$
World average (all above measurements included):				$0.508 \pm 0.003 \pm 0.003$
– ALEPH, DELPHI, L3, OPAL and CDF1 only:				$0.496 \pm 0.010 \pm 0.009$
– Above measurements of BABAR and Belle only:				$0.508 \pm 0.003 \pm 0.003$

Table 16: Simultaneous measurements of Δm_d and $\tau(B^0)$, and their average. The Belle analysis also measures $\tau(B^+)$ at the same time, but it is converted here into a two-dimensional measurement of Δm_d and $\tau(B^0)$, for an assumed value of $\tau(B^+)$. The first quoted error on the measurements is statistical and the second one systematic; in the case of adjusted measurements, the latter includes a contribution obtained from the variation of $\tau(B^+)$ or $\tau(B^+)/\tau(B^0)$ in the indicated range. Units are ps^{-1} for Δm_d and ps for lifetimes. The three different values of $\rho(\Delta m_d, \tau(B^0))$ correspond to the statistical, systematic and total correlation coefficients between the adjusted measurements of Δm_d and $\tau(B^0)$.

Exp. & Ref.	Measured Δm_d	Measured $\tau(B^0)$	Measured $\tau(B^+)$	Assumed $\tau(B^+)$
<i>BABAR</i> [74]	$0.492 \pm 0.018 \pm 0.013$	$1.523 \pm 0.024 \pm 0.022$	—	$(1.083 \pm 0.017)\tau(B^0)$
<i>BABAR</i> [76]	$0.511 \pm 0.007 \begin{smallmatrix} +0.007 \\ -0.006 \end{smallmatrix}$	$1.504 \pm 0.013 \begin{smallmatrix} +0.018 \\ -0.013 \end{smallmatrix}$	—	1.671 ± 0.018
Belle [77]	$0.511 \pm 0.005 \pm 0.006$	$1.534 \pm 0.008 \pm 0.010$	$1.635 \pm 0.011 \pm 0.011$	—
	Adjusted Δm_d	Adjusted $\tau(B^0)$	$\rho(\Delta m_d, B^0)$	Assumed $\tau(B^+)$
<i>BABAR</i> [74]	$0.492 \pm 0.018 \pm 0.013$	$1.523 \pm 0.024 \pm 0.022$	$-0.22 \ +0.71 \ +0.16$	$(1.081 \pm 0.006)\tau(B^0)$
<i>BABAR</i> [76]	$0.512 \pm 0.007 \pm 0.007$	$1.506 \pm 0.013 \pm 0.018$	$+0.01 \ -0.85 \ -0.48$	1.641 ± 0.008
Belle [77]	$0.511 \pm 0.005 \pm 0.006$	$1.535 \pm 0.008 \pm 0.011$	$-0.27 \ -0.14 \ -0.19$	1.641 ± 0.008
Average	$0.509 \pm 0.004 \pm 0.004$	$1.527 \pm 0.006 \pm 0.008$	$-0.19 \ -0.26 \ -0.23$	1.641 ± 0.008

Combining these two results after adjustment to $1/\Gamma_d = \tau(B^0) = 1.518 \pm 0.007$ ps yields

$$\text{sign}(\text{Re}\lambda_{CP})\Delta\Gamma_d/\Gamma_d = 0.011 \pm 0.037. \quad (57)$$

The sign of $\text{Re}\lambda_{CP}$ is not measured, but expected to be positive from the global fits of the Unitarity Triangle within the Standard Model.

Assuming $\Delta\Gamma_d = 0$ and using $1/\Gamma_d = \tau(B^0) = 1.518 \pm 0.007$ ps, the Δm_d and χ_d results are combined through Eq. (56) to yield the world average

$$\Delta m_d = 0.508 \pm 0.004 \text{ ps}^{-1}, \quad (58)$$

or, equivalently,

$$x_d = 0.771 \pm 0.007 \quad \text{and} \quad \chi_d = 0.1864 \pm 0.0022. \quad (59)$$

Figure 4 compares the Δm_d values obtained by the different experiments.

The B^0 mixing averages given in Eqs. (58) and (59) and the b -hadron fractions of Table 4 have been obtained in a fully consistent way, taking into account the fact that the fractions are computed using the χ_d value of Eq. (59) and that many individual measurements of Δm_d at high energy depend on the assumed values for the b -hadron fractions. Furthermore, this set of averages is consistent with the lifetime averages of Sec. 3.2.

It should be noted that the most recent (and precise) analyses at the asymmetric B factories measure Δm_d as a result of a multi-dimensional fit. Two *BABAR* analyses [74, 76], based on fully and partially reconstructed $B^0 \rightarrow D^* \ell \nu$ decays respectively, extract simultaneously Δm_d and $\tau(B^0)$ while the latest Belle analysis [77], based on fully reconstructed hadronic B^0 decays and $B^0 \rightarrow D^* \ell \nu$ decays, extracts simultaneously Δm_d , $\tau(B^0)$ and $\tau(B^+)$. The measurements of Δm_d and $\tau(B^0)$ of these three analyses are displayed in Table 16 and in Fig. 5. Their

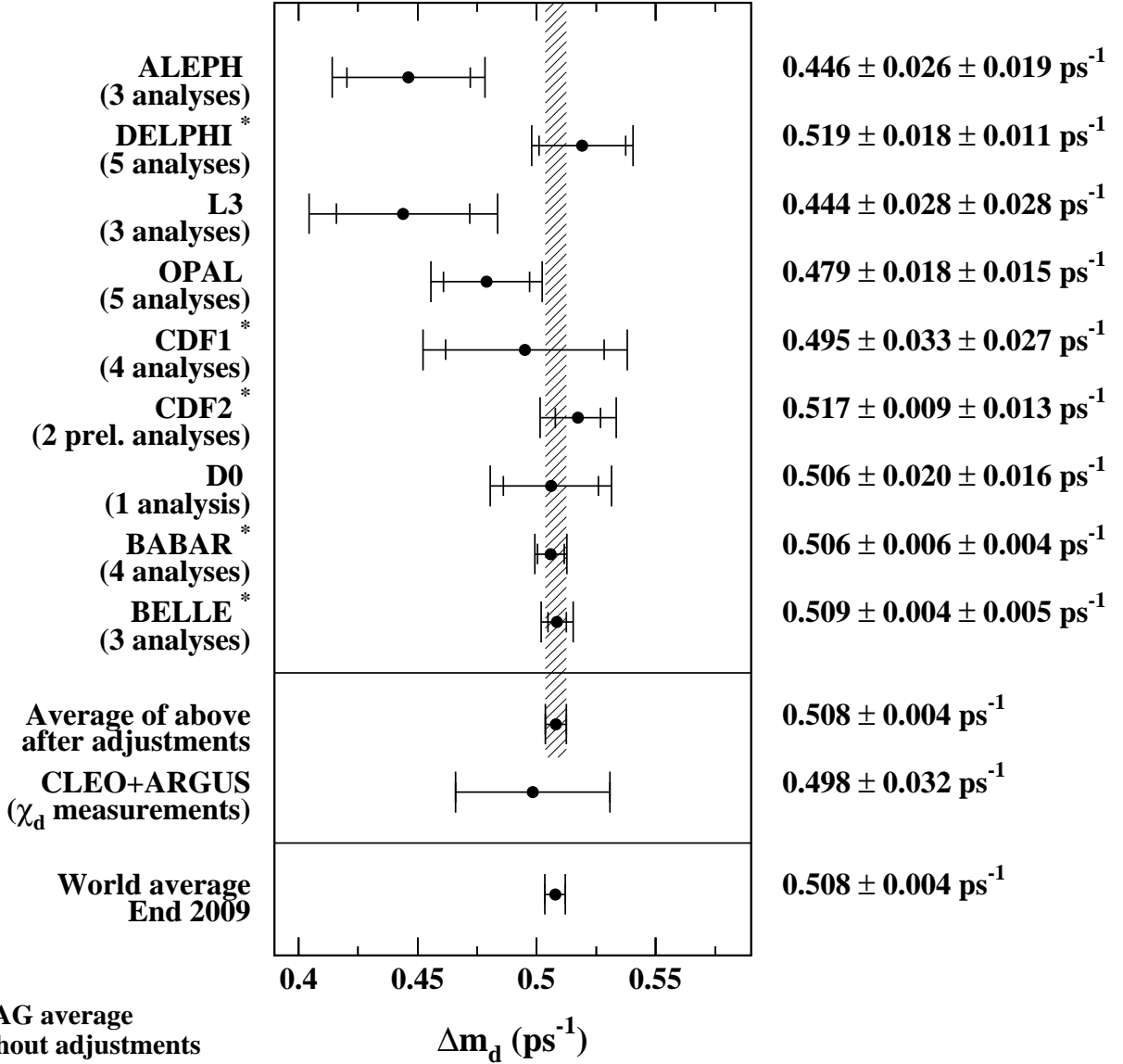


Figure 4: The $B^0-\bar{B}^0$ oscillation frequency Δm_d as measured by the different experiments. The averages quoted for ALEPH, L3 and OPAL are taken from the original publications, while the ones for DELPHI, CDF, BABAR, and Belle have been computed from the individual results listed in Table 15 without performing any adjustments. The time-integrated measurements of χ_d from the symmetric B factory experiments ARGUS and CLEO have been converted to a Δm_d value using $\tau(B^0) = 1.518 \pm 0.007 \text{ ps}$. The two global averages have been obtained after adjustments of all the individual Δm_d results of Table 15 (see text).

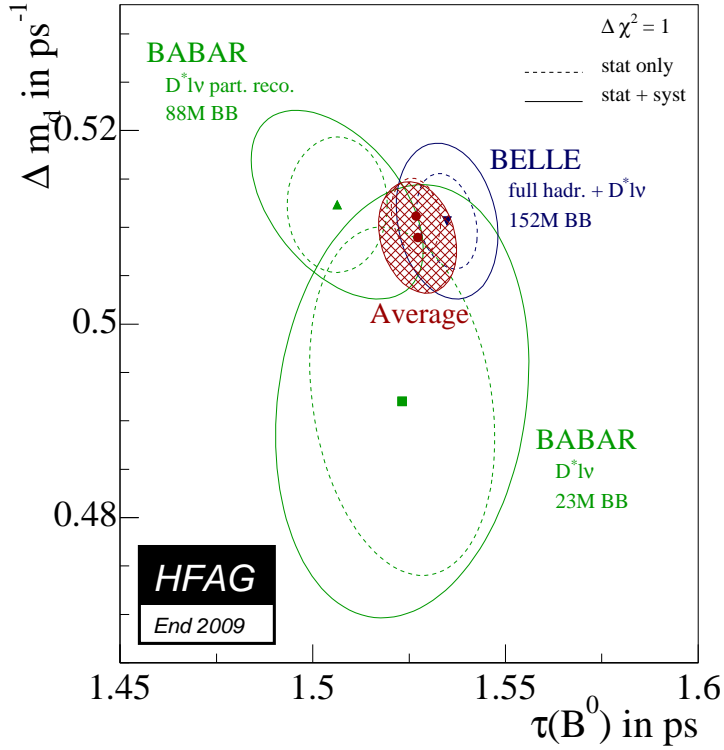


Figure 5: Simultaneous measurements of Δm_d and $\tau(B^0)$ [74, 76, 77], after adjustment to a common set of parameters (see text). Statistical and total uncertainties are represented as dashed and solid contours respectively. The average of the three measurements is indicated by a hatched ellipse.

two-dimensional average, taking into account all statistical and systematic correlations, and expressed at $\tau(B^+) = 1.641 \pm 0.008$ ps, is

$$\left. \begin{aligned} \Delta m_d &= 0.509 \pm 0.006 \text{ ps}^{-1} \\ \tau(B^0) &= 1.527 \pm 0.010 \text{ ps} \end{aligned} \right\} \text{ with a total correlation of } -0.23. \quad (60)$$

3.3.2 B_s^0 mixing parameters

CP violation parameter $|q/p|_s$

Constraints on a combination of $|q/p|_d$ and $|q/p|_s$ (or equivalently $\mathcal{A}_{\text{SL}}^d$ and $\mathcal{A}_{\text{SL}}^s$) have been explicitly quoted by the Tevatron experiments, using inclusive semileptonic decays of b hadrons:

$$\frac{1}{4} (f'_d \chi_d \mathcal{A}_{\text{SL}}^d + f'_s \chi_s \mathcal{A}_{\text{SL}}^s) = +0.0015 \pm 0.0038(\text{stat}) \pm 0.0020(\text{syst}) \quad \text{CDF1 [117]}, (61)$$

$$\mathcal{A}_{\text{SL}}^b = \frac{f'_d Z_d \mathcal{A}_{\text{SL}}^d + f'_s Z_s \mathcal{A}_{\text{SL}}^s}{f'_d Z_d + f'_s Z_s} = +0.0080 \pm 0.0090(\text{stat}) \pm 0.0068(\text{syst}) \quad \text{CDF2 [118]}, (62)$$

$$\mathcal{A}_{\text{SL}}^b = -0.00957 \pm 0.00251(\text{stat}) \pm 0.00146(\text{syst}) \quad \text{D}\emptyset [127], (63)$$

where¹² $Z_q = 1/(1 - y_q^2) - 1/(1 + x_q^2) = 2\chi_q/(1 - y_q^2)$, $q = d, s$. The D \emptyset result of Eq. (63),

¹²In Ref. [145], the D \emptyset result [38] was reinterpreted by replacing χ_s/χ_d with Z_s/Z_d . For simplicity, and

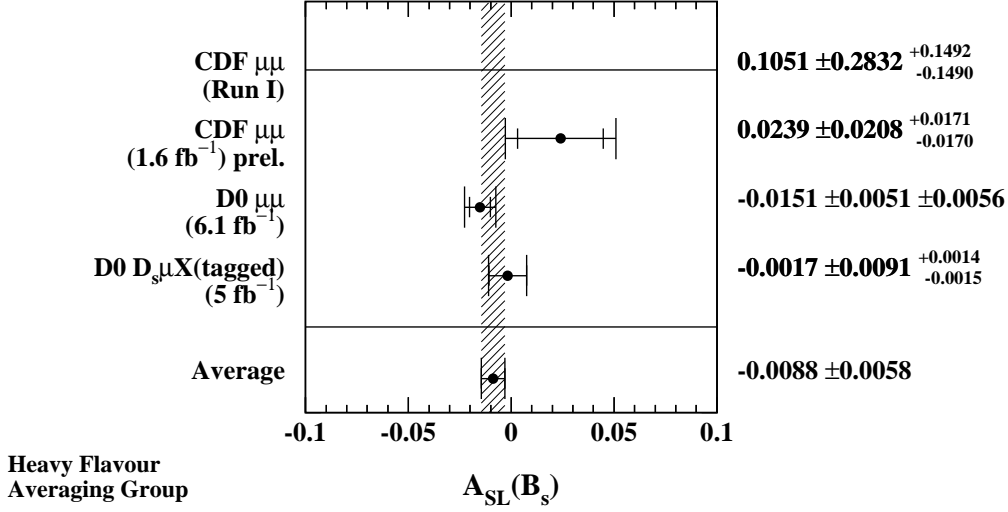


Figure 6: Measurements of $\mathcal{A}_{\text{SL}}^s$, derived from CDF [117, 118] and DØ [38, 146] analyses and adjusted to the latest averages of $\mathcal{A}_{\text{SL}}^d$, b -hadron fractions and mixing parameters. The combined value of $\mathcal{A}_{\text{SL}}^s$ is also shown.

obtained by measuring the charge asymmetry of like-sign dimuons, differs by 3.2 standard deviations from the Standard Model prediction of

$$\mathcal{A}_{\text{SL}}^b(\text{SM}) = (-2.3^{+0.5}_{-0.6}) \times 10^{-4} \quad [80]. \quad (64)$$

In addition a first direct determination of $\mathcal{A}_{\text{SL}}^s$ and hence $|q/p|_s$ has been obtained by DØ by measuring the charge asymmetry of tagged $B_s^0 \rightarrow D_s \mu X$ decays:

$$\mathcal{A}_{\text{SL}}^s = -0.0017 \pm 0.0091(\text{stat})^{+0.0014}_{-0.0015}(\text{syst}) \quad \text{DØ [146]}. \quad (65)$$

Given the average $\mathcal{A}_{\text{SL}}^d = -0.0047 \pm 0.0046$ of Eq. (53), obtained from results at B factories, as well as other averages presented in this chapter for the quantities appearing in Eqs. (61), (62), and (63), these four results are turned into measurements of $\mathcal{A}_{\text{SL}}^s$ (displayed in Fig. 6). The DØ result for $\mathcal{A}_{\text{SL}}^b$ yields

$$\mathcal{A}_{\text{SL}}^s = -0.00146 \pm 0.0075 \quad \text{DØ [127]}, \quad (66)$$

with an increased uncertainty due to uncertainties in f'_d , f'_s , Z_d , and Z_s , and does not represent evidence of CP violation exclusively in the B_s^0 system. The four results of Fig. 6 are combined to yield

$$\mathcal{A}_{\text{SL}}^s = -0.0088 \pm 0.0043(\text{stat}) \pm 0.0039(\text{syst}) = -0.0088 \pm 0.0058 \quad (67)$$

or, equivalently through Eq. (51),

$$|q/p|_s = 1.0044 \pm 0.0022(\text{stat}) \pm 0.0019(\text{syst}) = 1.0044 \pm 0.0029. \quad (68)$$

since this has anyway a negligible numerical effect on our combined result of Eq. (67), we follow the same interpretation and set $\chi_q = Z_q/2$ in Eqs. (61) and (63). We also set $f'_q = f_q$.

Table 17: Experimental constraints on $\Delta\Gamma_s/\Gamma_s$ from lifetime and $B_s \rightarrow J/\psi\phi$ analyses, assuming no (or very small SM) CP violation. The upper limits, which have been obtained by the working group, are quoted at the 95% CL.

Experiment	Method	$\Delta\Gamma_s/\Gamma_s$	Ref.
L3	lifetime of inclusive b -sample	< 0.67	[60]
DELPHI	$\bar{B}_s \rightarrow D_s^+ \ell^- \bar{\nu}_\ell X$, lifetime	< 0.46	[85]
DELPHI	$\bar{B}_s \rightarrow D_s^+$ hadron, lifetime	< 0.69	[91]
CDF1	$B_s^0 \rightarrow J/\psi\phi$, lifetime	$0.33^{+0.45}_{-0.42}$	[54]
		$\Delta\Gamma_s$	
CDF2	$B_s^0 \rightarrow J/\psi\phi$, time-dependent angular analysis	$0.02 \pm 0.05 \pm 0.01 \text{ ps}^{-1}$	[148]
DØ	$B_s^0 \rightarrow J/\psi\phi$, time-dependent angular analysis	$0.14 \pm 0.07 \text{ ps}^{-1}$	[149]

The quoted systematic errors include experimental systematics as well as the correlated dependence on external parameters. These results are compatible with no CP violation in B_s^0 mixing, an assumption made in almost all of the results described below.

Decay width difference $\Delta\Gamma_s$

Definitions and an introduction to $\Delta\Gamma_s$ can also be found in Sec. 3.2.4. Neglecting CP violation, the mass eigenstates are also CP eigenstates, with the short-lived state being CP -even and the long-lived one being CP -odd. Information on $\Delta\Gamma_s$ can be obtained by studying the proper time distribution of untagged data samples enriched in B_s^0 mesons [82]. In the case of an inclusive B_s^0 selection [60] or a semileptonic B_s^0 decay selection [85, 84, 87], both the short- and long-lived components are present, and the proper time distribution is a superposition of two exponentials with decay constants $\Gamma_s \pm \Delta\Gamma_s/2$. In principle, this provides sensitivity to both Γ_s and $(\Delta\Gamma_s/\Gamma_s)^2$. Ignoring $\Delta\Gamma_s$ and fitting for a single exponential leads to an estimate of Γ_s with a relative bias proportional to $(\Delta\Gamma_s/\Gamma_s)^2$. An alternative approach, which is directly sensitive to first order in $\Delta\Gamma_s/\Gamma_s$, is to determine the lifetime of B_s^0 candidates decaying to CP eigenstates; measurements exist for $B_s^0 \rightarrow J/\psi\phi$ [54, 93, 94] and $B_s^0 \rightarrow D_s^{(*)+} D_s^{(*)-}$, discussed later, which are mostly CP -even states [147]. However, later, more sophisticated, time-dependent angular analyses of $B_s^0 \rightarrow J/\psi\phi$ allow the simultaneous extraction of $\Delta\Gamma_s$ and the CP -even and CP -odd amplitudes [148, 149]. Flavor tagging the B_s^0 (or \bar{B}_s^0) that subsequently decays to $J/\psi\phi$ allows for a more effective extraction of the weak mixing phase as discussed later. Both the CDF and DØ flavor-tagged $B_s^0 \rightarrow J/\psi\phi$ analyses [148, 149] present results first assuming the very small SM value of mixing-induced CP violation in the B_s^0 system (effectively zero compared to current experimental resolution) used in the averaging of $\Delta\Gamma_s$, and then also allowing for large CP violation, used for determining an average weak mixing phase in the next subsection.

Measurements quoting $\Delta\Gamma_s/\Gamma_s$ results from lifetime analyses and $\Delta\Gamma_s$ results from $B_s^0 \rightarrow J/\psi\phi$ analyses under the hypothesis of no (or very small SM) CP violation are listed in Table 17. There is significant correlation between $\Delta\Gamma_s$ and $1/\Gamma_s$. In order to combine these measurements, the two-dimensional log-likelihood for each measurement in the $(1/\Gamma_s, \Delta\Gamma_s)$ plane is summed and the total normalized with respect to its minimum. The one-sigma contour (corresponding to 0.5 units of log-likelihood greater than the minimum) and 95% CL contour are found. Only

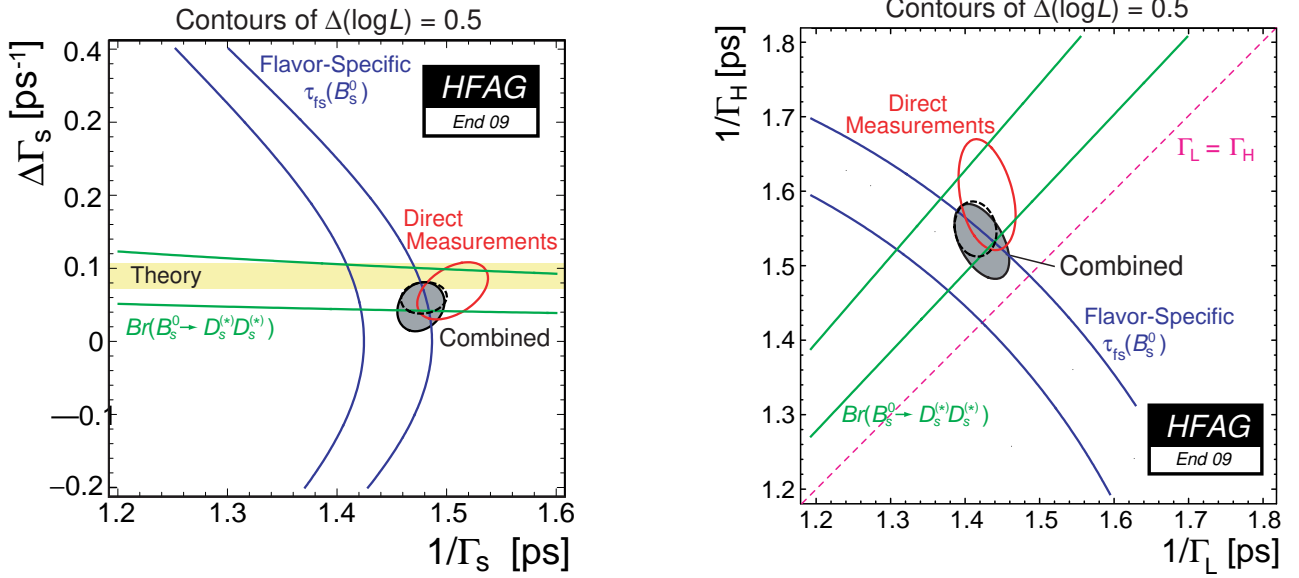


Figure 7: $\Delta\Gamma_s$ combination results with one-sigma contours ($\Delta \log \mathcal{L} = 0.5$) shown for (a) $\Delta\Gamma_s$ versus $\bar{\tau}(B_s^0) = 1/\Gamma_s$ and (b) $\tau_H = 1/\Gamma_H$ versus $\tau_L = 1/\Gamma_L$. The red contours labeled “Direct” are the result of the combination of last two measurements of Table 17, the blue bands are the one-sigma contours due to the world average of flavor-specific B_s^0 lifetime measurements, and the solid and dashed-outlined shaded regions result using the combination constraints described in the text. In (b), the diagonal dashed line indicates $\Gamma_L = \Gamma_H$, *i.e.*, where $\Delta\Gamma_s = 0$.

the $\Delta\Gamma_s$ inputs from CDF2 and DØ as indicated in Table 17 were used in the combinations below (adding the other ones would not change the results). CDF has very recently made a preliminary update [97] to their $B_s^0 \rightarrow J/\psi\phi$ analysis to an integrated luminosity of 5.2 fb^{-1} , and assuming no CP violation, find

$$\Delta\Gamma_s = 0.075 \pm 0.035 \pm 0.01 \text{ ps}^{-1}, \quad (69)$$

$$\bar{\tau}(B_s^0) = 1/\Gamma_s = 1.530 \pm 0.025 \pm 0.012 \text{ ps}. \quad (70)$$

However, this new update has yet to be included in the following combinations.

Results of the combination are shown as the one-sigma contour labeled “Direct” in both plots of Fig. 7. Transformation of variables from $(1/\Gamma_s, \Delta\Gamma_s)$ space to other pairs of variables such as $(1/\Gamma_s, \Delta\Gamma_s/\Gamma_s)$ and $(\tau_L = 1/\Gamma_L, \tau_H = 1/\Gamma_H)$ are also made. The resulting one-sigma contour for the latter is shown in Fig. 7(b).

Numerical results of the combination of the CDF2 and DØ inputs of Table 17 are:

$$\Delta\Gamma_s/\Gamma_s \in [-0.011, +0.224] \text{ at } 95\% \text{ CL}, \quad (71)$$

$$\Delta\Gamma_s/\Gamma_s = +0.105 \pm +0.060, \quad (72)$$

$$\Delta\Gamma_s \in [-0.006, +0.146] \text{ ps}^{-1} \text{ at } 95\% \text{ CL}, \quad (73)$$

$$\Delta\Gamma_s = +0.070 \pm 0.039 \text{ ps}^{-1}, \quad (74)$$

$$\bar{\tau}(B_s^0) = 1/\Gamma_s = 1.506 \pm 0.032 \text{ ps}, \quad (75)$$

$$1/\Gamma_L = \tau_{\text{short}} = 1.431_{-0.037}^{+0.038} \text{ ps}, \quad (76)$$

$$1/\Gamma_H = \tau_{\text{long}} = 1.590_{+0.071}^{+0.075} \text{ ps}. \quad (77)$$

Flavor-specific lifetime measurements are of an equal mix of CP -even and CP -odd states at time zero, and if a single exponential function is used in the likelihood lifetime fit of such a sample [82],

$$\tau(B_s^0)_{\text{fs}} = \frac{1}{\Gamma_s} \frac{1 + \left(\frac{\Delta\Gamma_s}{2\Gamma_s}\right)^2}{1 - \left(\frac{\Delta\Gamma_s}{2\Gamma_s}\right)^2}. \quad (78)$$

Using the world average flavor-specific lifetime of Eq. (36) in Sec. 3.2.4 the one-sigma blue bands shown in Fig. 7 are obtained. Higher-order corrections were checked to be negligible in the combination.

When the flavor-specific lifetime measurements are combined with the CDF2 and DØ measurements of Table 17, the solid-outline shaded regions of Fig. 7 are obtained, with numerical results:

$$\Delta\Gamma_s/\Gamma_s \in [-0.028, +0.167] \text{ at 95\% CL}, \quad (79)$$

$$\Delta\Gamma_s/\Gamma_s = +0.072_{-0.051}^{+0.049}, \quad (80)$$

$$\Delta\Gamma_s \in [-0.019, +0.112] \text{ ps}^{-1} \text{ at 95\% CL}, \quad (81)$$

$$\Delta\Gamma_s = +0.049_{-0.034}^{+0.033} \text{ ps}^{-1}, \quad (82)$$

$$\bar{\tau}(B_s^0) = 1/\Gamma_s = 1.477_{-0.022}^{+0.021} \text{ ps}, \quad (83)$$

$$1/\Gamma_L = \tau_{\text{short}} = 1.425_{-0.035}^{+0.037} \text{ ps}, \quad (84)$$

$$1/\Gamma_H = \tau_{\text{long}} = 1.532 \pm 0.049 \text{ ps}. \quad (85)$$

These results can be compared with the theoretical prediction of $\Delta\Gamma_s = 0.096 \pm 0.039 \text{ ps}^{-1}$ (or $\Delta\Gamma_s = 0.088 \pm 0.017 \text{ ps}^{-1}$ if there is no new physics in Δm_s) [80, 81].

Measurements of $\mathcal{B}(B_s^0 \rightarrow D_s^{(*)+} D_s^{(*)-})$ can also be sensitive to $\Delta\Gamma_s$. The decay $B_s^0 \rightarrow D_s^+ D_s^-$ is into a final state that is purely CP even. Under various theoretical assumptions [147, 150], the inclusive decay into this plus the excited states $B_s^0 \rightarrow D_s^{(*)+} D_s^{(*)-}$ is also CP even to within 5%, and $B_s^0 \rightarrow D_s^{(*)+} D_s^{(*)-}$ saturates $\Gamma_s^{CP \text{ even}}$. Under these assumptions, for no CP violation, we have:

$$\Delta\Gamma_s/\Gamma_s \approx \frac{2\mathcal{B}(B_s^0 \rightarrow D_s^{(*)+} D_s^{(*)-})}{1 - \mathcal{B}(B_s^0 \rightarrow D_s^{(*)+} D_s^{(*)-})}. \quad (86)$$

However, there are concerns [151] that the assumptions needed for the above are overly restrictive and that the inclusive branching ratio may be CP even to only 30%. In the application of the constraint as a Gaussian penalty function, the theoretical uncertainty is dealt with in two ways: the fraction of the CP -odd component of the decay [150] is taken to be a uniform distribution ranging from 0 to 0.05 and convoluted in the Gaussian, and the fractional uncertainty on the average measured value is increased in quadrature by 30%.

Measurements for the branching fraction for this decay channel are shown in Table 18. Using their average value of 0.049 ± 0.014 with Eq. (86) yields

$$\Delta\Gamma_s/\Gamma_s = +0.103 \pm 0.032, \quad (87)$$

consistent with the value given in Eq. (80).

As described in Sec. 3.2.4 and Eq. (39), the average of the lifetime measurements with $B_s^0 \rightarrow K^+ K^-$ and $B_s^0 \rightarrow D_s^{(*)+} D_s^{(*)-}$ decays can be used to measure the lifetime of the CP -even (or

Table 18: Measurements of $\mathcal{B}(B_s^0 \rightarrow D_s^{(*)+} D_s^{(*)-})$.

Experiment	Method	Value	Ref.
ALEPH	ϕ - ϕ correlations	$0.115 \pm 0.050^{+0.095}_{-0.045}$	[95] ^a
DØ	$D_s \rightarrow \phi\pi$, $D_s \rightarrow \phi\mu\nu$	$0.035 \pm 0.010 \pm 0.011$	[152]
Belle	full reco. in 6 excl. D_s modes	$0.069^{+0.015}_{-0.013} \pm 0.019$	[153]
Average of above 3		0.049 ± 0.014	

^a The value quoted in this table is half of $\mathcal{B}(B_s^0(\text{short}) \rightarrow D_s^{(*)+} D_s^{(*)-})$ given in Ref. [95]. Before averaging, it has been adjusted the latest values of f_s at LEP and $\mathcal{B}(D_s^+ \rightarrow \phi X)$.

“light” mass) eigenstate $\tau(B_s^0 \rightarrow CP\text{-even}) = \tau_L = 1/\Gamma_L = 1.47 \pm 0.16$ ps. These decays are assumed to be 100% CP even, with a 5% theoretical uncertainty on this assumption added in quadrature for the combination.

When the constraint due this CP -even lifetime and the $\mathcal{B}(B_s^0 \rightarrow D_s^{(*)+} D_s^{(*)-})$ branching fraction are added to the previous ones, the dashed-outline shaded regions of Fig. 7 are obtained, with numerical results:

$$\Delta\Gamma_s/\Gamma_s \in [+0.025, +0.150] \text{ at } 95\% \text{ CL}, \quad (88)$$

$$\Delta\Gamma_s/\Gamma_s = +0.089 \pm 0.032, \quad (89)$$

$$\Delta\Gamma_s \in [+0.017, +0.101] \text{ ps}^{-1} \text{ at } 95\% \text{ CL}, \quad (90)$$

$$\Delta\Gamma_s = +0.060 \pm 0.021 \text{ ps}^{-1}, \quad (91)$$

$$\bar{\tau}(B_s^0) = 1/\Gamma_s = 1.477^{+0.021}_{-0.022} \text{ ps}, \quad (92)$$

$$1/\Gamma_L = \tau_{\text{short}} = 1.416 \pm 0.027 \text{ ps}, \quad (93)$$

$$1/\Gamma_H = \tau_{\text{long}} = 1.548^{+0.036}_{-0.037} \text{ ps}. \quad (94)$$

CDF has also measured the exclusive branching fraction $\mathcal{B}(B_s^0 \rightarrow D_s^+ D_s^-) = (9.4^{+4.4}_{-4.2}) \times 10^{-3}$ [154], and they use this to set a lower bound of $\Delta\Gamma_s^{CP}/\Gamma_s \geq 0.012$ at 95% CL (since on its own it does not saturate the CP -even states).

Weak phase in B_s^0 mixing

In general there will be a CP -violating weak phase difference:

$$\phi_s = \arg[-M_{12}/\Gamma_{12}], \quad (95)$$

where M_{12} and Γ_{12} are the off-diagonal elements of the mass and decay matrices of the B_s^0 - \bar{B}_s^0 system. This is related to the observed $\Delta\Gamma_s$ through the relation:

$$\Delta\Gamma_s = 2|\Gamma_{12}| \cos \phi_s. \quad (96)$$

The SM prediction for this phase is tiny, $\phi_s^{\text{SM}} = 0.004$ [80]; however, new physics in B_s^0 mixing could change this observed phase to

$$\phi_s = \phi_s^{\text{SM}} + \phi_s^{\text{NP}}. \quad (97)$$

The relative phase between the B_s^0 mixing amplitude and that of specific $b \rightarrow c\bar{c}s$ quark transitions such as for B_s^0 or $\bar{B}_s^0 \rightarrow J/\psi\phi$ in the SM is [80, 155]:

$$2\beta_s^{SM} = 2 \arg[-(V_{ts}V_{tb}^*) / (V_{cs}V_{cb}^*)] = 0.037 \pm 0.002 \approx 0.04. \quad (98)$$

This angle is analogous to the β angle in the usual CKM unitarity triangle aside from the negative sign (resulting in a positive angle in the SM). The same additional contribution due to new physics would show up in this observed phase [80], i.e.:

$$2\beta_s = 2\beta_s^{SM} - \phi_s^{NP}. \quad (99)$$

The current experimental precision does not allow these small CP -violating phases ϕ_s^{SM} and β_s^{SM} to be resolved, and for large new physics effect, we can approximate $\phi_s \approx -2\beta_s \approx \phi_s^{NP}$, i.e., a significantly large observed phase would indicate new physics.

For non-zero $|\Gamma_{12}|$, analysis of the time-dependent decay $B_s^0 \rightarrow J/\psi\phi$ can measure the weak phase. Including information on the B_s^0 flavor at production time via flavor tagging improves precision and also resolves the sign ambiguity on the weak phase angle for a given $\Delta\Gamma_s$. Both CDF [148] and DØ [149] have performed such analyses and measure the same observed phase that we denote $\phi_s^{J/\psi\phi} = -2\beta_s^{J/\psi\phi}$ to reflect the different conventions of the experiments.

Under the assumption of non-zero $\phi_s^{J/\psi\phi}$, in addition to the result listed in Table 17, the DØ collaboration [149] has also made simultaneous fits allowing $\phi_s^{J/\psi\phi}$ to float while weakly constraining the strong phases, δ_i to find:

$$\Delta\Gamma_s = +0.19 \pm 0.07_{-0.01}^{+0.02} \text{ ps}^{-1}, \quad (100)$$

$$\bar{\tau}(B_s^0) = 1/\Gamma_s = 1.52 \pm 0.06 \text{ ps}, \quad (101)$$

$$\phi_s^{J/\psi\phi} = -0.57_{-0.30-0.02}^{+0.24+0.07}. \quad (102)$$

If the SM value of $\phi_s^{J/\psi\phi} = -0.04$ is assumed, a probability of 6.6% to obtain a value of $\phi_s^{J/\psi\phi}$ lower than -0.57 is found.

The CDF analysis [148] reports confidence regions in the two-dimensional space of $2\beta_s^{J/\psi\phi}$ and $\Delta\Gamma_s$. They present a Feldman-Cousins confidence interval of $2\beta_s^{J/\psi\phi}$ where $\Delta\Gamma_s$ is treated as a nuisance parameter:

$$2\beta_s^{J/\psi\phi} = -\phi_s^{J/\psi\phi} \in [0.56, 2.58] \text{ at } 68\% \text{ CL}. \quad (103)$$

Only a confidence range is quoted and a point estimate is not given since biases were observed in the analysis. Assuming the SM predictions for $2\beta_s$ and $\Delta\Gamma_s$, they find that the probability of a deviation as large as the level of the observed data is 7%. Note that CDF has very recently made a preliminary update [97] to their $B_s^0 \rightarrow J/\psi\phi$ analysis to an integrated luminosity of 5.2 fb^{-1} indicating a best-fit confidence interval of:

$$2\beta_s^{J/\psi\phi} = -\phi_s^{J/\psi\phi} \in [0.04, 1.04] \cup [2.16, 3.10] \text{ at } 68\% \text{ CL}, \quad (104)$$

where the probability of a larger deviation from the SM prediction is 44% or 0.8σ . However, this new result has not yet been used in the combinations below.

Given the consistency of these two measurements of the weak phase, as well as their deviations from the SM, there is interest in combining the results and using in global fits, e.g.,

see Ref. [156]. To allow a combination on equal footing, the DØ collaboration has redone their fits [157] allowing strong phase values, δ_i , to float as in the CDF analysis. Ensemble studies to test confidence level coverage were performed by both collaborations and used to adjust likelihood values to correspond to the usual Gaussian confidence levels. Two-dimensional likelihoods were combined [158, 159] with the result shown in Fig. 8(a). After the combination, consistency of the best fit values for $\phi_s^{J/\psi\phi} = -2\beta_s^{J/\psi\phi}$ with SM predictions is at the level of 2.3σ , with numerical results for the two solutions given below. Despite possible biases in the CDF input, point estimates are still presented and the confidence level regions are straight projections onto the $\Delta\Gamma_s$ or phase angle axes.

$$\Delta\Gamma_s = +0.150_{-0.056}^{+0.055} \text{ ps}^{-1} \text{ or } -0.150_{-0.055}^{+0.056} \text{ ps}^{-1}, \quad (105)$$

$$\in [+0.060, +0.297] \cup [-0.297, -0.060] \text{ ps}^{-1} \text{ at } 90\% \text{ CL}, \quad (106)$$

$$\phi_s^{J/\psi\phi} = -2\beta_s^{J/\psi\phi} = -0.83_{-0.36}^{+0.30} \text{ or } -2.31_{-0.30}^{+0.36}, \quad (107)$$

$$\in [-1.50, -0.32] \cup [-2.82, -1.64] \text{ at } 90\% \text{ CL}. \quad (108)$$

A comparison between the above sum of the CDF and DØ likelihoods and the world average B_s^0 semileptonic asymmetry of Eq. (67) through [160]:

$$\mathcal{A}_{\text{SL}}^s = \frac{|\Gamma_s^{12}|}{|M_s^{12}|} \sin \phi_s = \frac{\Delta\Gamma_s}{\Delta m_s} \tan \phi_s \quad (109)$$

is also made and shown in Fig. 8(a). Consistency between the two is observed, and the value of $\mathcal{A}_{\text{SL}}^s$ is applied as a constraint resulting in the confidence level regions shown in Fig. 8(b) including the region delineated by new physics traced by the relation of Eq. (96). Numerical results for the two solutions are:

$$\Delta\Gamma_s = +0.150_{-0.049}^{+0.045} \text{ ps}^{-1} \text{ or } -0.150_{-0.049}^{+0.042} \text{ ps}^{-1}, \quad (110)$$

$$\in [+0.075, +0.228] \cup [-0.220, -0.071] \text{ ps}^{-1} \text{ at } 90\% \text{ CL}, \quad (111)$$

$$\phi_s^{J/\psi\phi} = -2\beta_s^{J/\psi\phi} = -0.82_{-0.21}^{+0.16} \text{ or } -2.36_{-0.14}^{+0.20}, \quad (112)$$

$$\in [-1.20, -0.45] \cup [-2.72, -1.99] \text{ at } 90\% \text{ CL}. \quad (113)$$

with a consistency of the best fit values with SM predictions of $2\beta_s$ at the level of 2.8σ .

Finally, additional constraints are added due to the flavor-specific B_s^0 lifetime world average of Eq. (36) through Eq. (78), the CP -event lifetime of Eq. (39), and the world average of the branching fraction $\mathcal{B}(B_s^0 \rightarrow D_s^{(*)+} D_s^{(*)-})$ through [150]:

$$2\mathcal{B}(B_s^0 \rightarrow D_s^{(*)+} D_s^{(*)-}) \simeq \Delta\Gamma_s^{\text{CP}} \left[\frac{\frac{1}{1-2x_f} + \cos \phi_s}{2\Gamma_L} + \frac{\frac{1}{1-2x_f} - \cos \phi_s}{2\Gamma_H} \right]. \quad (114)$$

Here x_f is the fraction of the CP -odd component of the decay. To apply this as a constraint, we expand the above expression to second order,

$$2\mathcal{B}(B_s^0 \rightarrow D_s^{(*)+} D_s^{(*)-}) \simeq \frac{\Delta\Gamma_s}{\Gamma_s \cos \phi_s} \left[\frac{1}{1-2x_f} - \frac{\Delta\Gamma_s \cos \phi_s}{2\Gamma_s} \right], \quad (115)$$

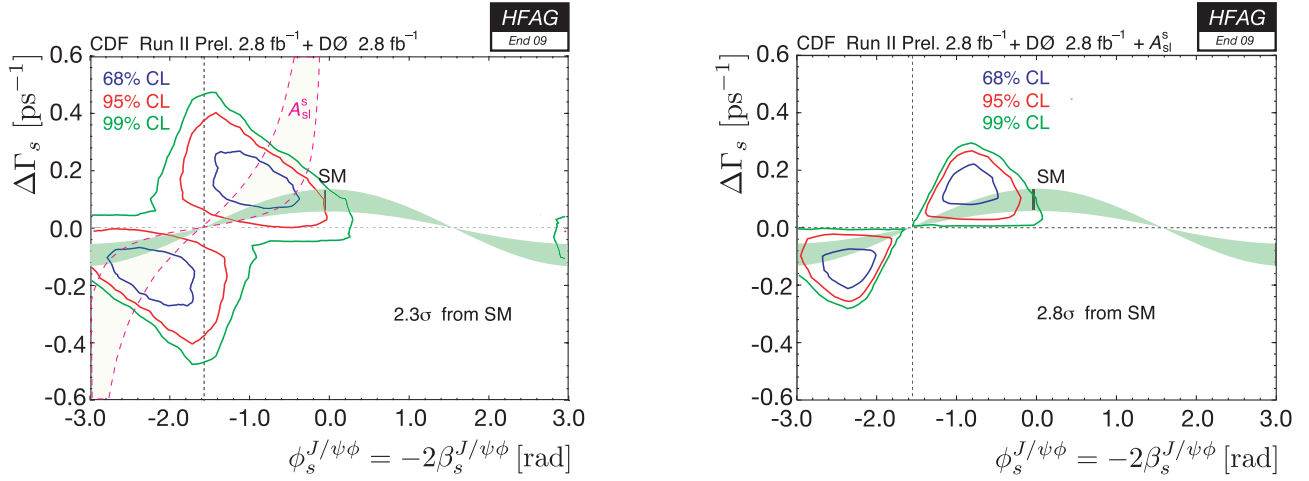


Figure 8: (a) Confidence regions in B_s^0 width difference $\Delta\Gamma_s$ and weak phase angle $\phi_s^{J/\psi\phi} = -2\beta_s^{J/\psi\phi}$ from combined CDF and DØ likelihoods determined in flavor-tagged $B_s^0 \rightarrow J/\psi\phi$ time-dependent angular analyses [148, 157] compared to the SM value of $-2\beta_s^{SM}$ and to the world-average value of the B_s^0 semileptonic asymmetry, \mathcal{A}_{SL}^s (overlaid); (b) after adding the constraint due to the world-average value of \mathcal{A}_{SL}^s . The region allowed in new physics models given by $\Delta\Gamma_s = 2|\Gamma_{12}|\cos\phi_s$ is also shown (light green band).

and use the world average of the branching ratio of Table 18. Numerical results following these final constraints are:

$$\Delta\Gamma_s = +0.054_{-0.015}^{+0.026} \text{ ps}^{-1} \text{ or } -0.054_{-0.026}^{+0.016} \text{ ps}^{-1}, \quad (116)$$

$$\in [+0.025, +0.097] \cup [-0.099, -0.024] \text{ ps}^{-1} \text{ at } 90\% \text{ CL}, \quad (117)$$

$$\phi_s^{J/\psi\phi} = -2\beta_s^{J/\psi\phi} = -0.75_{-0.21}^{+0.32} \text{ or } -2.38_{-0.34}^{+0.25}, \quad (118)$$

$$\in [-1.19, -0.21] \cup [-2.94, -1.93] \text{ at } 90\% \text{ CL}. \quad (119)$$

with a consistency of the best fit values with SM predictions of $2\beta_s$ at the level of 2.7σ .

Mass difference Δm_s

B_s^0 oscillations have been observed for the first time in 2006 by the CDF collaboration [161], based on samples of flavour-tagged hadronic and semileptonic B_s^0 decays (in flavour-specific final states), partially or fully reconstructed in 1 fb^{-1} of data collected during Tevatron's Run II. From the proper-time dependence of these B_s^0 candidates, CDF observe B_s^0 oscillations with a significance of at least 5σ and measure $\Delta m_s = 17.77 \pm 0.10 \pm 0.07 \text{ ps}^{-1}$ [161]. More recently, the DØ collaboration has obtained with 2.4 fb^{-1} an independent $\sim 3\sigma$ preliminary evidence for B_s^0 oscillations; combining all their results [162] they obtain $\Delta m_s = 18.53 \pm 0.93 \pm 0.30 \text{ ps}^{-1}$ [163]. To a good approximation, both the CDF and DØ results have Gaussian errors, and the world average value of Δm_s can be obtained as a simple weighted average:

$$\Delta m_s = 17.78 \pm 0.12 \text{ ps}^{-1}. \quad (120)$$

Multiplying this result with the mean B_s^0 lifetime of Eq. (83), $1/\Gamma_s = 1.477_{-0.022}^{+0.021} \text{ ps}$, yields

$$x_s = \frac{\Delta m_s}{\Gamma_s} = 26.3 \pm 0.4. \quad (121)$$

With $2y_s = \Delta\Gamma_s/\Gamma_s = +0.072_{-0.051}^{+0.049}$ (see Eq. (80)) and under the assumption of no CP violation in B_s^0 mixing, this corresponds to

$$\chi_s = \frac{x_s^2 + y_s^2}{2(x_s^2 + 1)} = 0.49928 \pm 0.00002. \quad (122)$$

The ratio of the B^0 and B_s^0 oscillation frequencies, obtained from Eqs. (58) and (120),

$$\frac{\Delta m_d}{\Delta m_s} = 0.0286 \pm 0.0003, \quad (123)$$

can be used to extract the following ratio of CKM matrix elements,

$$\left| \frac{V_{td}}{V_{ts}} \right| = \xi \sqrt{\frac{\Delta m_d m(B_s^0)}{\Delta m_s m(B^0)}} = 0.2062 \pm 0.0011_{-0.0060}^{+0.0080}, \quad (124)$$

where the first quoted error is from experimental uncertainties (with the masses $m(B_s^0)$ and $m(B^0)$ taken from [5]), and where the second quoted error is from theoretical uncertainties in the estimation of the SU(3) flavor-symmetry breaking factor $\xi = 1.210_{-0.035}^{+0.047}$ obtained from lattice QCD calculations [164].

B_s^0 mesons were known to mix since many years. Indeed the time-integrated measurements of $\bar{\chi}$ (see Sec. 3.1.3), when compared to our knowledge of χ_d and the b -hadron fractions, indicated that B_s^0 mixing was large, with a value of χ_s close to its maximal possible value of $1/2$. However, the time dependence of this mixing could not be observed until recently, mainly because of lack of proper-time resolution to resolve the small period of the B_s^0 oscillations.

The statistical significance \mathcal{S} of a B_s^0 oscillation signal can be approximated as [165]

$$\mathcal{S} \approx \sqrt{\frac{N}{2}} f_{\text{sig}} (1 - 2w) \exp(-(\Delta m_s \sigma_t)^2 / 2), \quad (125)$$

where N is the number of selected and tagged B_s^0 candidates, f_{sig} is the fraction of B_s^0 signal in the selected and tagged sample, w is the total mistag probability, and σ_t is the resolution on proper time. As can be seen, the quantity \mathcal{S} decreases very quickly as Δm_s increases: this dependence is controlled by σ_t , which is therefore the most critical parameter for Δm_s analyses. The method widely used for B_s^0 oscillation searches consists of measuring a B_s^0 oscillation amplitude \mathcal{A} at several different test values of Δm_s , using a maximum likelihood fit based on the functions of Eq. (50) where the cosine terms have been multiplied by \mathcal{A} . One expects $\mathcal{A} = 1$ at the true value of Δm_s and $\mathcal{A} = 0$ at a test value of Δm_s (far) below the true value. To a good approximation, the statistical uncertainty on \mathcal{A} is Gaussian and equal to $1/\mathcal{S}$ [165]. In any analysis, a particular value of Δm_s can be excluded at 95% CL if $\mathcal{A} + 1.645 \sigma_{\mathcal{A}} < 1$, where $\sigma_{\mathcal{A}}$ is the total uncertainty on \mathcal{A} . Because of the proper time resolution, the quantity $\sigma_{\mathcal{A}}(\Delta m_s)$ is an increasing function of Δm_s (see Eq. (125) which merely models $1/\sigma_{\mathcal{A}}(\Delta m_s)$ in an analysis limited by the available statistics). Therefore, if the true value of Δm_s were infinitely large, one expects to be able to exclude all values of Δm_s up to Δm_s^{sens} , where Δm_s^{sens} , called here the sensitivity of the analysis, is defined by $1.645 \sigma_{\mathcal{A}}(\Delta m_s^{\text{sens}}) = 1$.

Figure 9 shows the measured B_s^0 amplitude as a function of Δm_s , as obtained by CDF (top) and DØ (middle) using Run II data. The recent DØ evidence of a B_s^0 oscillation signal is consistent with the 2006 observation by CDF. A large number of B_s^0 oscillation searches,

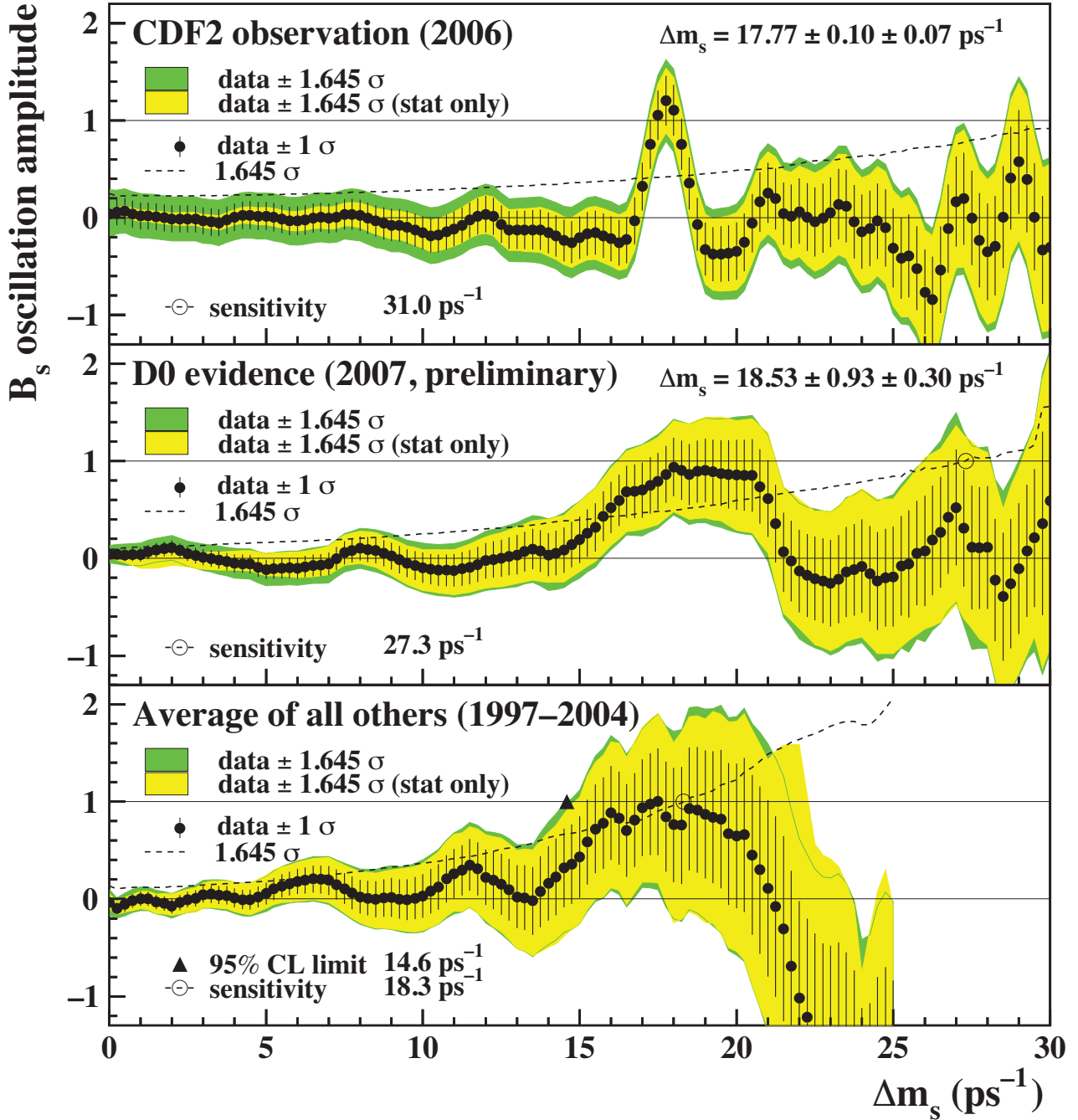


Figure 9: B_s^0 oscillation amplitude as a function of Δm_s , and measured value of Δm_s (when available). Top: CDF result based on Run II data, published in 2006 [161]. Middle: Average of the latest $D\bar{0}$ amplitude measurements released as preliminary results in 2007 [162], and corresponding measurement of Δm_s [163]. Bottom: Average of all ALEPH [166], DELPHI [85, 91, 130, 167], OPAL [168, 169], SLD [170, 171], and CDF Run I [172] results published between 1997 and 2004. Statistical uncertainties dominate. Neighboring points are statistically correlated.

already based on the amplitude method, had been performed previously by ALEPH [166], CDF (Run I) [172], DELPHI [85, 91, 130, 167], OPAL [168, 169] and SLD [170, 171, 173] (we omit references to searches that have been superseded by more recent ones). All the results published by these experiments (between 1997 and 2004) have been combined by averaging the measured amplitudes \mathcal{A} at each test value of Δm_s . The individual results have been adjusted to common physics inputs, and all known correlations have been accounted for; in the case of the inclusive (lepton) analyses, performed at LEP and SLC, the sensitivities (*i.e.* the statistical uncertainties on \mathcal{A}), which depend directly through Eq. (125) on the assumed fraction $f_{\text{sig}} \sim f_s$ of B_s^0 mesons in an unbiased sample of weakly-decaying b hadrons, have also been rescaled to the LEP average $f_s = 0.103 \pm 0.009$. The resulting average amplitude spectrum, completely dominated by the $e^+e^- \rightarrow Z$ experiments, is displayed as the bottom plot of Fig. 9. Although no significant signal is seen, it is interesting to note the hint in the region 15–20 ps^{-1} , consistent with the recent results from the Tevatron.

4 Measurements related to Unitarity Triangle angles

The charge of the “ $CP(t)$ and Unitarity Triangle angles” group is to provide averages of measurements from time-dependent asymmetry analyses, and other quantities that are related to the angles of the Unitarity Triangle (UT). In cases where considerable theoretical input is required to extract the fundamental quantities, no attempt is made to do so at this stage. However, straightforward interpretations of the averages are given, where possible.

In Sec. 4.1 a brief introduction to the relevant phenomenology is given. In Sec. 4.2 an attempt is made to clarify the various different notations in use. In Sec. 4.3 the common inputs to which experimental results are rescaled in the averaging procedure are listed. We also briefly introduce the treatment of experimental errors. In the remainder of this section, the experimental results and their averages are given, divided into subsections based on the underlying quark-level decays.

4.1 Introduction

The Standard Model Cabibbo-Kobayashi-Maskawa (CKM) quark mixing matrix V must be unitary. A 3×3 unitary matrix has four free parameters,¹³ and these are conventionally written by the product of three (complex) rotation matrices [174], where the rotations are characterized by the Euler angles θ_{12} , θ_{13} and θ_{23} , which are the mixing angles between the generations, and one overall phase δ ,

$$V = \begin{pmatrix} V_{ud} & V_{us} & V_{ub} \\ V_{cd} & V_{cs} & V_{cb} \\ V_{td} & V_{ts} & V_{tb} \end{pmatrix} = \begin{pmatrix} c_{12}c_{13} & s_{12}c_{13} & s_{13}e^{-i\delta} \\ -s_{12}c_{23} - c_{12}s_{23}s_{13}e^{i\delta} & c_{12}c_{23} - s_{12}s_{23}s_{13}e^{i\delta} & s_{23}c_{13} \\ s_{12}s_{23} - c_{12}c_{23}s_{13}e^{i\delta} & -c_{12}s_{23} - s_{12}c_{23}s_{13}e^{i\delta} & c_{23}c_{13} \end{pmatrix} \quad (126)$$

where $c_{ij} = \cos \theta_{ij}$, $s_{ij} = \sin \theta_{ij}$ for $i < j = 1, 2, 3$.

Following the observation of a hierarchy between the different matrix elements, the Wolfenstein parameterization [175] is an expansion of V in terms of the four real parameters λ (the expansion parameter), A , ρ and η . Defining to all orders in λ [176]

$$\begin{aligned} s_{12} &\equiv \lambda, \\ s_{23} &\equiv A\lambda^2, \\ s_{13}e^{-i\delta} &\equiv A\lambda^3(\rho - i\eta), \end{aligned} \quad (127)$$

and inserting these into the representation of Eq. (126), unitarity of the CKM matrix is achieved to all orders. A Taylor expansion of V leads to the familiar approximation

$$V = \begin{pmatrix} 1 - \lambda^2/2 & \lambda & A\lambda^3(\rho - i\eta) \\ -\lambda & 1 - \lambda^2/2 & A\lambda^2 \\ A\lambda^3(1 - \rho - i\eta) & -A\lambda^2 & 1 \end{pmatrix} + \mathcal{O}(\lambda^4). \quad (128)$$

At order λ^5 , the obtained CKM matrix in this extended Wolfenstein parametrization is:

$$V = \begin{pmatrix} 1 - \frac{1}{2}\lambda^2 - \frac{1}{8}\lambda^4 & \lambda & A\lambda^3(\rho - i\eta) \\ -\lambda + \frac{1}{2}A^2\lambda^5[1 - 2(\rho + i\eta)] & 1 - \frac{1}{2}\lambda^2 - \frac{1}{8}\lambda^4(1 + 4A^2) & A\lambda^2 \\ A\lambda^3[1 - (1 - \frac{1}{2}\lambda^2)(\rho + i\eta)] & -A\lambda^2 + \frac{1}{2}A\lambda^4[1 - 2(\rho + i\eta)] & 1 - \frac{1}{2}A^2\lambda^4 \end{pmatrix} + \mathcal{O}(\lambda^6). \quad (129)$$

¹³ In the general case there are nine free parameters, but five of these are absorbed into unobservable quark phases.

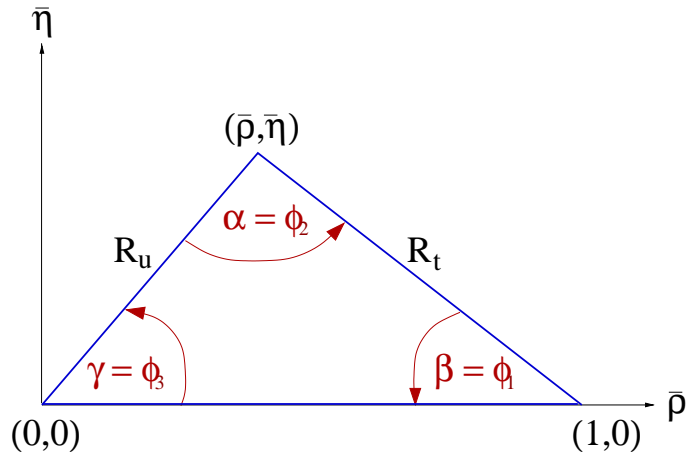


Figure 10: The Unitarity Triangle.

The non-zero imaginary part of the CKM matrix, which is the origin of CP violation in the Standard Model, is encapsulated in a non-zero value of η .

The unitarity relation $V^\dagger V = 1$ results in a total of nine expressions, that can be written as $\sum_{i=u,c,t} V_{ij}^* V_{ik} = \delta_{jk}$, where δ_{jk} is the Kronecker symbol. Of the off-diagonal expressions ($j \neq k$), three can be transformed into the other three leaving six relations, in which three complex numbers sum to zero, which therefore can be expressed as triangles in the complex plane. More details about unitarity triangles can be found in [177, 178, 179, 180].

One of these relations,

$$V_{ud}V_{ub}^* + V_{cd}V_{cb}^* + V_{td}V_{tb}^* = 0, \quad (130)$$

is of particular importance to the B system, being specifically related to flavour changing neutral current $b \rightarrow d$ transitions. The three terms in Eq. (130) are of the same order ($\mathcal{O}(\lambda^3)$), and this relation is commonly known as the Unitarity Triangle. For presentational purposes, it is convenient to rescale the triangle by $(V_{cd}V_{cb}^*)^{-1}$, as shown in Fig. 10.

Two popular naming conventions for the UT angles exist in the literature:

$$\alpha \equiv \phi_2 = \arg \left[-\frac{V_{td}V_{tb}^*}{V_{ud}V_{ub}^*} \right], \quad \beta \equiv \phi_1 = \arg \left[-\frac{V_{cd}V_{cb}^*}{V_{td}V_{tb}^*} \right], \quad \gamma \equiv \phi_3 = \arg \left[-\frac{V_{ud}V_{ub}^*}{V_{cd}V_{cb}^*} \right]. \quad (131)$$

In this document the (α, β, γ) set is used.¹⁴ The sides R_u and R_t of the Unitarity Triangle (the third side being normalized to unity) are given by

$$R_u = \left| \frac{V_{ud}V_{ub}^*}{V_{cd}V_{cb}^*} \right| = \sqrt{\bar{\rho}^2 + \bar{\eta}^2}, \quad R_t = \left| \frac{V_{td}V_{tb}^*}{V_{cd}V_{cb}^*} \right| = \sqrt{(1 - \bar{\rho})^2 + \bar{\eta}^2}. \quad (132)$$

where $\bar{\rho}$ and $\bar{\eta}$ define the apex of the Unitarity Triangle [176]

$$\bar{\rho} + i\bar{\eta} \equiv -\frac{V_{ud}V_{ub}^*}{V_{cd}V_{cb}^*} \equiv 1 + \frac{V_{td}V_{tb}^*}{V_{cd}V_{cb}^*} = \frac{\sqrt{1 - \lambda^2}(\rho + i\eta)}{\sqrt{1 - A^2\lambda^4} + \sqrt{1 - \lambda^2}A^2\lambda^4(\rho + i\eta)} \quad (133)$$

¹⁴ The relevant unitarity triangle for the B_s^0 system is obtained by replacing $d \leftrightarrow s$ in Eq. 130. Definitions of the set of angles $(\alpha_s, \beta_s, \gamma_s)$ can be obtained using equivalent relations to those of Eq. 131, for example $\beta_s = \arg[-(V_{cs}V_{cb}^*)/(V_{ts}V_{tb}^*)]$. This definition gives a value of β_s that is negative in the Standard Model, so that the sign is often flipped in the literature.

The exact relation between (ρ, η) and $(\bar{\rho}, \bar{\eta})$ is

$$\rho + i\eta = \frac{\sqrt{1 - A^2\lambda^4}(\bar{\rho} + i\bar{\eta})}{\sqrt{1 - \lambda^2}[1 - A^2\lambda^4(\bar{\rho} + i\bar{\eta})]}. \quad (134)$$

By expanding in powers of λ , several useful approximate expressions can be obtained, including

$$\bar{\rho} = \rho(1 - \frac{1}{2}\lambda^2) + \mathcal{O}(\lambda^4), \quad \bar{\eta} = \eta(1 - \frac{1}{2}\lambda^2) + \mathcal{O}(\lambda^4), \quad V_{td} = A\lambda^3(1 - \bar{\rho} - i\bar{\eta}) + \mathcal{O}(\lambda^6). \quad (135)$$

4.2 Notations

Several different notations for CP violation parameters are commonly used. This section reviews those found in the experimental literature, in the hope of reducing the potential for confusion, and to define the frame that is used for the averages.

In some cases, when B mesons decay into multibody final states via broad resonances (ρ , K^* , *etc.*), the experimental analyses ignore the effects of interference between the overlapping structures. This is referred to as the quasi-two-body (Q2B) approximation in the following.

4.2.1 CP asymmetries

The CP asymmetry is defined as the difference between the rate involving a b quark and that involving a \bar{b} quark, divided by the sum. For example, the partial rate (or charge) asymmetry for a charged B decay would be given as

$$\mathcal{A}_f \equiv \frac{\Gamma(B^- \rightarrow f) - \Gamma(B^+ \rightarrow \bar{f})}{\Gamma(B^- \rightarrow f) + \Gamma(B^+ \rightarrow \bar{f})}. \quad (136)$$

4.2.2 Time-dependent CP asymmetries in decays to CP eigenstates

If the amplitudes for B^0 and \bar{B}^0 to decay to a final state f , which is a CP eigenstate with eigenvalue η_f , are given by A_f and \bar{A}_f , respectively, then the decay distributions for neutral B mesons, with known flavour at time $\Delta t = 0$, are given by

$$\Gamma_{\bar{B}^0 \rightarrow f}(\Delta t) = \frac{e^{-|\Delta t|/\tau(B^0)}}{4\tau(B^0)} \left[1 + \frac{2 \operatorname{Im}(\lambda_f)}{1 + |\lambda_f|^2} \sin(\Delta m \Delta t) - \frac{1 - |\lambda_f|^2}{1 + |\lambda_f|^2} \cos(\Delta m \Delta t) \right], \quad (137)$$

$$\Gamma_{B^0 \rightarrow f}(\Delta t) = \frac{e^{-|\Delta t|/\tau(B^0)}}{4\tau(B^0)} \left[1 - \frac{2 \operatorname{Im}(\lambda_f)}{1 + |\lambda_f|^2} \sin(\Delta m \Delta t) + \frac{1 - |\lambda_f|^2}{1 + |\lambda_f|^2} \cos(\Delta m \Delta t) \right]. \quad (138)$$

Here $\lambda_f = \frac{q \bar{A}_f}{p A_f}$ contains terms related to B^0 - \bar{B}^0 mixing and to the decay amplitude (the eigenstates of the effective Hamiltonian in the $B^0\bar{B}^0$ system are $|B_{\pm}\rangle = p|B^0\rangle \pm q|\bar{B}^0\rangle$). This formulation assumes CPT invariance, and neglects possible lifetime differences (between the eigenstates of the effective Hamiltonian; see Section 3.3 where the mass difference Δm is also defined) in the neutral B meson system. The case where non-zero lifetime differences are taken into account is discussed in Section 4.2.6. The time-dependent CP asymmetry, again defined as

the difference between the rate involving a b quark and that involving a \bar{b} quark, is then given by

$$\mathcal{A}_f(\Delta t) \equiv \frac{\Gamma_{\bar{B}^0 \rightarrow f}(\Delta t) - \Gamma_{B^0 \rightarrow f}(\Delta t)}{\Gamma_{\bar{B}^0 \rightarrow f}(\Delta t) + \Gamma_{B^0 \rightarrow f}(\Delta t)} = \frac{2 \operatorname{Im}(\lambda_f)}{1 + |\lambda_f|^2} \sin(\Delta m \Delta t) - \frac{1 - |\lambda_f|^2}{1 + |\lambda_f|^2} \cos(\Delta m \Delta t). \quad (139)$$

While the coefficient of the $\sin(\Delta m \Delta t)$ term in Eq. (139) is everywhere¹⁵ denoted S_f :

$$S_f \equiv \frac{2 \operatorname{Im}(\lambda_f)}{1 + |\lambda_f|^2}, \quad (140)$$

different notations are in use for the coefficient of the $\cos(\Delta m \Delta t)$ term:

$$C_f \equiv -A_f \equiv \frac{1 - |\lambda_f|^2}{1 + |\lambda_f|^2}. \quad (141)$$

The C notation is used by the *BABAR* collaboration (see *e.g.* [181]), and also in this document. The A notation is used by the Belle collaboration (see *e.g.* [182]).

Neglecting effects due to CP violation in mixing (by taking $|q/p| = 1$), if the decay amplitude contains terms with a single weak (*i.e.*, CP violating) phase then $|\lambda_f| = 1$ and one finds $S_f = -\eta_f \sin(\phi_{\text{mix}} + \phi_{\text{dec}})$, $C_f = 0$, where $\phi_{\text{mix}} = \arg(q/p)$ and $\phi_{\text{dec}} = \arg(\bar{A}_f/A_f)$. Note that the B^0 - \bar{B}^0 mixing phase $\phi_{\text{mix}} \approx 2\beta$ in the Standard Model (in the usual phase convention) [183, 184].

If amplitudes with different weak phases contribute to the decay, no clean interpretation of S_f is possible. If the decay amplitudes have in addition different CP conserving strong phases, then $|\lambda_f| \neq 1$ and no clean interpretation is possible. The coefficient of the cosine term becomes non-zero, indicating direct CP violation. The sign of A_f as defined above is consistent with that of \mathcal{A}_f in Eq. (136).

Frequently, we are interested in combining measurements governed by similar or identical short-distance physics, but with different final states (*e.g.*, $B^0 \rightarrow J/\psi K_S^0$ and $B^0 \rightarrow J/\psi K_L^0$). In this case, we remove the dependence on the CP eigenvalue of the final state by quoting $-\eta S_f$. In cases where the final state is not a CP eigenstate but has an effective CP content (see below), the reported $-\eta S$ is corrected by the effective CP .

4.2.3 Time-dependent CP asymmetries in decays to vector-vector final states

Consider B decays to states consisting of two spin-1 particles, such as $J/\psi K^{*0} (\rightarrow K_S^0 \pi^0)$, $D^{*+} D^{*-}$ and $\rho^+ \rho^-$, which are eigenstates of charge conjugation but not of parity.¹⁶ In fact, for such a system, there are three possible final states; in the helicity basis these can be written h_{-1}, h_0, h_{+1} . The h_0 state is an eigenstate of parity, and hence of CP ; however, CP transforms $h_{+1} \leftrightarrow h_{-1}$ (up to an unobservable phase). In the transversity basis, these states are transformed into $h_{\parallel} = (h_{+1} + h_{-1})/2$ and $h_{\perp} = (h_{+1} - h_{-1})/2$. In this basis all three states are CP eigenstates, and h_{\perp} has the opposite CP to the others.

The amplitudes to these states are usually given by $A_{0,\perp,\parallel}$ (here we use a normalization such that $|A_0|^2 + |A_{\perp}|^2 + |A_{\parallel}|^2 = 1$). Then the effective CP of the vector-vector state is known

¹⁵ Occasionally one also finds Eq. (139) written as $\mathcal{A}_f(\Delta t) = \mathcal{A}_f^{\text{mix}} \sin(\Delta m \Delta t) + \mathcal{A}_f^{\text{dir}} \cos(\Delta m \Delta t)$, or similar.

¹⁶ This is not true of all vector-vector final states, *e.g.*, $D^{*\pm} \rho^{\mp}$ is clearly not an eigenstate of charge conjugation.

if $|A_{\perp}|^2$ is measured. An alternative strategy is to measure just the longitudinally polarized component, $|A_0|^2$ (sometimes denoted by f_{long}), which allows a limit to be set on the effective CP since $|A_{\perp}|^2 \leq |A_{\perp}|^2 + |A_{\parallel}|^2 = 1 - |A_0|^2$. The most complete treatment for neutral B decays to vector-vector final states is time-dependent angular analysis (also known as time-dependent transversity analysis). In such an analysis, the interference between the CP -even and CP -odd states provides additional sensitivity to the weak and strong phases involved.

In most analyses of time-dependent CP asymmetries in decays to vector-vector final states carried out to date, an assumption has been made that each helicity (or transversity) amplitude has the same weak phase. This is a good approximation for decays that are dominated by amplitudes with a single weak phase, such as $B^0 \rightarrow J/\psi K^{*0}$, and is a reasonable approximation in any mode for which only very limited statistics are available. However, for modes that have contributions from amplitudes with different weak phases, the relative size of these contributions can be different for each helicity (or transversity) amplitude, and therefore the time-dependent CP asymmetry parameters can also differ. The most generic analysis, suitable for modes with sufficient statistics, would allow for this effect; an intermediate analysis can allow different parameters for the CP -even and CP -odd components. Such an analysis has been carried out by *BABAR* for the decay $B^0 \rightarrow D^{*+}D^{*-}$ [185].

4.2.4 Time-dependent asymmetries: self-conjugate multiparticle final states

Amplitudes for neutral B decays into self-conjugate multiparticle final states such as $\pi^+\pi^-\pi^0$, $K^+K^-K_s^0$, $\pi^+\pi^-K_s^0$, $J/\psi\pi^+\pi^-$ or $D\pi^0$ with $D \rightarrow K_s^0\pi^+\pi^-$ may be written in terms of CP -even and CP -odd amplitudes. As above, the interference between these terms provides additional sensitivity to the weak and strong phases involved in the decay, and the time-dependence depends on both the sine and cosine of the weak phase difference. In order to perform unbinned maximum likelihood fits, and thereby extract as much information as possible from the distributions, it is necessary to select a model for the multiparticle decay, and therefore the results acquire some model dependence (binned, model independent methods are also possible, though are not as statistically powerful). The number of observables depends on the final state (and on the model used); the key feature is that as long as there are regions where both CP -even and CP -odd amplitudes contribute, the interference terms will be sensitive to the cosine of the weak phase difference. Therefore, these measurements allow distinction between multiple solutions for, *e.g.*, the four values of β from the measurement of $\sin(2\beta)$.

We now consider the various notations which have been used in experimental studies of time-dependent asymmetries in decays to self-conjugate multiparticle final states.

$$B^0 \rightarrow D^{(*)}h^0 \text{ with } D \rightarrow K_s^0\pi^+\pi^-$$

The states $D\pi^0$, $D^*\pi^0$, $D\eta$, $D^*\eta$, $D\omega$ are collectively denoted $D^{(*)}h^0$. When the D decay model is fixed, fits to the time-dependent decay distributions can be performed to extract the weak phase difference. However, it is experimentally advantageous to use the sine and cosine of this phase as fit parameters, since these behave as essentially independent parameters, with low correlations and (potentially) rather different uncertainties. A parameter representing direct CP violation in the B decay can also be floated. For consistency with other analyses, this could be chosen to be C_f , but could equally well be $|\lambda_f|$, or other possibilities.

Belle performed an analysis of these channels with $\sin(2\phi_1)$ and $\cos(2\phi_1)$ as free parameters [186]. *BABAR* have performed an analysis floating also $|\lambda_f|$ [187] (and, of course, replacing

$\phi_1 \Leftrightarrow \beta$).

$B^0 \rightarrow D^{*+}D^{*-}K_S^0$

The hadronic structure of the $B^0 \rightarrow D^{*+}D^{*-}K_S^0$ decay is not sufficiently well understood to perform a full time-dependent Dalitz plot analysis. Instead, following Browder *et al.* [188], BABAR [189] divide the Dalitz plane in two: $m(D^{*+}K_S^0)^2 > m(D^{*-}K_S^0)^2$ ($\eta_y = +1$) and $m(D^{*+}K_S^0)^2 < m(D^{*-}K_S^0)^2$ ($\eta_y = -1$); and then fit to a decay time distribution with asymmetry given by

$$\mathcal{A}_f(\Delta t) = \eta_y \frac{J_c}{J_0} \cos(\Delta m \Delta t) - \left[\frac{2J_{s1}}{J_0} \sin(2\beta) + \eta_y \frac{2J_{s2}}{J_0} \cos(2\beta) \right] \sin(\Delta m \Delta t). \quad (142)$$

A similar analysis has also been carried out by Belle [190]. The measured values are $\frac{J_c}{J_0}$, $\frac{2J_{s1}}{J_0} \sin(2\beta)$ and $\frac{2J_{s2}}{J_0} \cos(2\beta)$, where the parameters J_0 , J_c , J_{s1} and J_{s2} are the integrals over the half Dalitz plane $m(D^{*+}K_S^0)^2 < m(D^{*-}K_S^0)^2$ of the functions $|a|^2 + |\bar{a}|^2$, $|a|^2 - |\bar{a}|^2$, $\text{Re}(\bar{a}a^*)$ and $\text{Im}(\bar{a}a^*)$ respectively, where a and \bar{a} are the decay amplitudes of $B^0 \rightarrow D^{*+}D^{*-}K_S^0$ and $\bar{B}^0 \rightarrow D^{*+}D^{*-}K_S^0$ respectively. The parameter J_{s2} (and hence J_{s2}/J_0) is predicted to be positive; with this assumption is it possible to determine the sign of $\cos(2\beta)$.

$B^0 \rightarrow K^+K^-K^0$

Studies of $B^0 \rightarrow K^+K^-K^0$ [191, 192, 193] and of the related decay $B^+ \rightarrow K^+K^-K^+$ [194, 195], show that the decay is dominated by components from the intermediate K^+K^- resonances $\phi(1020)$, $f_0(980)$, a poorly understood scalar structure that peaks near $m(K^+K^-) \sim 1550$ MeV/ c^2 and is denoted $X_0(1550)$, as well as a large nonresonant contribution. There is also a contribution from χ_{c0} .

The full time-dependent Dalitz plot analysis allows the complex amplitudes of each contributing term to be determined from data, including CP violation effects (*i.e.* allowing the complex amplitude for the B^0 decay to be independent from that for \bar{B}^0 decay), although one amplitude must be fixed to give a reference point. There are several choices for parametrization of the complex amplitudes (*e.g.* real and imaginary part, or magnitude and phase). Similarly, there are various approaches to include CP violation effects. Note that positive definite parameters such as magnitudes are disfavoured in certain circumstances (they inevitably lead to biases for small values). In order to compare results between analyses, it is useful for each experiment to present results in terms of the parameters that can be measured in a Q2B analysis (such as \mathcal{A}_f , S_f , C_f , $\sin(2\beta^{\text{eff}})$, $\cos(2\beta^{\text{eff}})$, *etc.*)

In the BABAR analysis of $B^0 \rightarrow K^+K^-K^0$ [191, 192], the complex amplitude for each resonant contribution is written as

$$\mathcal{A}_f = c_f(1 + b_f)e^{i(\phi_f + \delta_f)}, \quad \bar{\mathcal{A}}_f = c_f(1 - b_f)e^{i(\phi_f - \delta_f)}, \quad (143)$$

where b_f and δ_f introduce CP violation in the magnitude and phase respectively. [The weak phase in B^0 - \bar{B}^0 mixing (2β) also appears in the full formula for the time-dependent decay distribution.] The Q2B direct CP violation parameter is directly related to b_f

$$\mathcal{A}_f = \frac{-2b_f}{1 + b_f^2} \approx C_f, \quad (144)$$

and the mixing-induced CP violation parameter can be used to obtain $\sin(2\beta^{\text{eff}})$

$$-\eta_f S_f \approx \frac{1 - b_f^2}{1 + b_f^2} \sin(2\beta_f^{\text{eff}}), \quad (145)$$

where the approximations are exact in the case that $|q/p| = 1$.

BABAR [191, 192] present results for c_f , ϕ_f , \mathcal{A}_f and β^{eff} for each resonant contribution, as well as averaged values of \mathcal{A}_f and β^{eff} for the entire $K^+K^-K^0$ Dalitz plot. *Belle* [193] present results for the resonant contributions only.

$B^0 \rightarrow \pi^+\pi^-K_S^0$

Studies of $B^0 \rightarrow \pi^+\pi^-K_S^0$ [196, 197] and of the related decay $B^+ \rightarrow \pi^+\pi^-K^+$ [194, 198, 199, 200] show that the decay is dominated by components from intermediate resonances in the $K\pi$ ($K^*(892)$, $K_0^*(1430)$) and $\pi\pi$ ($\rho(770)$, $f_0(980)$, $f_2(1270)$) spectra, together with a poorly understood scalar structure that peaks near $m(\pi\pi) \sim 1300$ MeV/ c^2 and is denoted $f_X(1300)$ (that could be identified as either the $f_0(1370)$ or $f_0(1500)$), and a large nonresonant component. There is also a contribution from the χ_{c0} state.

The full time-dependent Dalitz plot analysis allows the complex amplitudes of each contributing term to be determined from data, including CP violation effects. In the *BABAR* analysis [196], the magnitude and phase of each component (for both B^0 and \bar{B}^0 decays) are measured relative to $B^0 \rightarrow f_0(980)K_S^0$, using the following parameterisation

$$A_f = |A_f| e^{i \arg(A_f)}, \quad \bar{A}_f = |\bar{A}_f| e^{i \arg(\bar{A}_f)}. \quad (146)$$

In the *Belle* analysis [197], the $B^0 \rightarrow K^{*+}\pi^-$ amplitude is chosen as the reference, and the amplitudes are parameterised as

$$A_f = a_f(1 + c_f)e^{i(b_f+d_f)}, \quad \bar{A}_f = a_f(1 - c_f)e^{i(b_f-d_f)}. \quad (147)$$

In both cases, the results are translated into quasi-two-body parameters such as $2\beta_f^{\text{eff}}$, S_f , C_f for each CP eigenstate f , and direct CP asymmetries for each flavour-specific state. Relative phase differences between resonant terms are also extracted.

$B^0 \rightarrow \pi^+\pi^-\pi^0$

The $B^0 \rightarrow \pi^+\pi^-\pi^0$ decay is dominated by intermediate ρ resonances. Though it is possible, as above, to determine directly the complex amplitudes for each component, an alternative approach [201, 202], has been used by both *BABAR* [203] and *Belle* [204, 205]. The amplitudes for B^0 and \bar{B}^0 to $\pi^+\pi^-\pi^0$ are written

$$A_{3\pi} = f_+A_+ + f_-A_- + f_0A_0, \quad \bar{A}_{3\pi} = f_+\bar{A}_+ + f_-\bar{A}_- + f_0\bar{A}_0 \quad (148)$$

respectively. A_+ , A_- and A_0 represent the complex decay amplitudes for $B^0 \rightarrow \rho^+\pi^-$, $B^0 \rightarrow \rho^-\pi^+$ and $B^0 \rightarrow \rho^0\pi^0$ while \bar{A}_+ , \bar{A}_- and \bar{A}_0 represent those for $\bar{B}^0 \rightarrow \rho^+\pi^-$, $\bar{B}^0 \rightarrow \rho^-\pi^+$ and $\bar{B}^0 \rightarrow \rho^0\pi^0$ respectively. f_+ , f_- and f_0 incorporate kinematical and dynamical factors and depend on the Dalitz plot coordinates. The full time-dependent decay distribution can then be written in terms of 27 free parameters, one for each coefficient of the form factor bilinears, as listed in Table 19. These parameters are often referred to as “the U s and I s”, and can be

expressed in terms of A_+ , A_- , A_0 , \bar{A}_+ , \bar{A}_- and \bar{A}_0 . If the full set of parameters is determined, together with their correlations, other parameters, such as weak and strong phases, direct CP violation parameters, *etc.*, can be subsequently extracted. Note that one of the parameters (typically U_+^+) is often fixed to unity to provide a reference point; this does not affect the analysis.

Parameter	Description
U_+^+	Coefficient of $ f_+ ^2$
U_0^+	Coefficient of $ f_0 ^2$
U_-^+	Coefficient of $ f_- ^2$
U_0^-	Coefficient of $ f_0 ^2 \cos(\Delta m \Delta t)$
U_-^-	Coefficient of $ f_- ^2 \cos(\Delta m \Delta t)$
U_+^-	Coefficient of $ f_+ ^2 \cos(\Delta m \Delta t)$
I_0	Coefficient of $ f_0 ^2 \sin(\Delta m \Delta t)$
I_-	Coefficient of $ f_- ^2 \sin(\Delta m \Delta t)$
I_+	Coefficient of $ f_+ ^2 \sin(\Delta m \Delta t)$
$U_{+-}^{+,Im}$	Coefficient of $\text{Im}[f_+ f_-^*]$
$U_{+-}^{+,Re}$	Coefficient of $\text{Re}[f_+ f_-^*]$
$U_{+-}^{-,Im}$	Coefficient of $\text{Im}[f_+ f_-^*] \cos(\Delta m \Delta t)$
$U_{+-}^{-,Re}$	Coefficient of $\text{Re}[f_+ f_-^*] \cos(\Delta m \Delta t)$
I_{+-}^{Im}	Coefficient of $\text{Im}[f_+ f_-^*] \sin(\Delta m \Delta t)$
I_{+-}^{Re}	Coefficient of $\text{Re}[f_+ f_-^*] \sin(\Delta m \Delta t)$
$U_{+0}^{+,Im}$	Coefficient of $\text{Im}[f_+ f_0^*]$
$U_{+0}^{+,Re}$	Coefficient of $\text{Re}[f_+ f_0^*]$
$U_{+0}^{-,Im}$	Coefficient of $\text{Im}[f_+ f_0^*] \cos(\Delta m \Delta t)$
$U_{+0}^{-,Re}$	Coefficient of $\text{Re}[f_+ f_0^*] \cos(\Delta m \Delta t)$
I_{+0}^{Im}	Coefficient of $\text{Im}[f_+ f_0^*] \sin(\Delta m \Delta t)$
I_{+0}^{Re}	Coefficient of $\text{Re}[f_+ f_0^*] \sin(\Delta m \Delta t)$
$U_{-0}^{+,Im}$	Coefficient of $\text{Im}[f_- f_0^*]$
$U_{-0}^{+,Re}$	Coefficient of $\text{Re}[f_- f_0^*]$
$U_{-0}^{-,Im}$	Coefficient of $\text{Im}[f_- f_0^*] \cos(\Delta m \Delta t)$
$U_{-0}^{-,Re}$	Coefficient of $\text{Re}[f_- f_0^*] \cos(\Delta m \Delta t)$
I_{-0}^{Im}	Coefficient of $\text{Im}[f_- f_0^*] \sin(\Delta m \Delta t)$
I_{-0}^{Re}	Coefficient of $\text{Re}[f_- f_0^*] \sin(\Delta m \Delta t)$

Table 19: Definitions of the U and I coefficients. Modified from [203].

4.2.5 Time-dependent CP asymmetries in decays to non- CP eigenstates

Consider a non- CP eigenstate f , and its conjugate \bar{f} . For neutral B decays to these final states, there are four amplitudes to consider: those for B^0 to decay to f and \bar{f} (A_f and $A_{\bar{f}}$, respectively), and the equivalents for \bar{B}^0 (\bar{A}_f and $\bar{A}_{\bar{f}}$). If CP is conserved in the decay, then $A_f = \bar{A}_{\bar{f}}$ and $A_{\bar{f}} = \bar{A}_f$.

The time-dependent decay distributions can be written in many different ways. Here, we follow Sec. 4.2.2 and define $\lambda_f = \frac{q \bar{A}_f}{p A_f}$ and $\lambda_{\bar{f}} = \frac{q \bar{A}_{\bar{f}}}{p A_{\bar{f}}}$. The time-dependent CP asymmetries then follow Eq. (139):

$$\mathcal{A}_f(\Delta t) \equiv \frac{\Gamma_{\bar{B}^0 \rightarrow f}(\Delta t) - \Gamma_{B^0 \rightarrow f}(\Delta t)}{\Gamma_{\bar{B}^0 \rightarrow f}(\Delta t) + \Gamma_{B^0 \rightarrow f}(\Delta t)} = S_f \sin(\Delta m \Delta t) - C_f \cos(\Delta m \Delta t), \quad (149)$$

$$\mathcal{A}_{\bar{f}}(\Delta t) \equiv \frac{\Gamma_{\bar{B}^0 \rightarrow \bar{f}}(\Delta t) - \Gamma_{B^0 \rightarrow \bar{f}}(\Delta t)}{\Gamma_{\bar{B}^0 \rightarrow \bar{f}}(\Delta t) + \Gamma_{B^0 \rightarrow \bar{f}}(\Delta t)} = S_{\bar{f}} \sin(\Delta m \Delta t) - C_{\bar{f}} \cos(\Delta m \Delta t), \quad (150)$$

with the definitions of the parameters C_f , S_f , $C_{\bar{f}}$ and $S_{\bar{f}}$, following Eqs. (140) and (141).

The time-dependent decay rates are given by

$$\Gamma_{\bar{B}^0 \rightarrow f}(\Delta t) = \frac{e^{-|\Delta t|/\tau(B^0)}}{8\tau(B^0)} (1 + \langle \mathcal{A}_{f\bar{f}} \rangle) \{1 + S_f \sin(\Delta m \Delta t) - C_f \cos(\Delta m \Delta t)\}, \quad (151)$$

$$\Gamma_{B^0 \rightarrow f}(\Delta t) = \frac{e^{-|\Delta t|/\tau(B^0)}}{8\tau(B^0)} (1 + \langle \mathcal{A}_{f\bar{f}} \rangle) \{1 - S_f \sin(\Delta m \Delta t) + C_f \cos(\Delta m \Delta t)\}, \quad (152)$$

$$\Gamma_{\bar{B}^0 \rightarrow \bar{f}}(\Delta t) = \frac{e^{-|\Delta t|/\tau(B^0)}}{8\tau(B^0)} (1 - \langle \mathcal{A}_{f\bar{f}} \rangle) \{1 + S_{\bar{f}} \sin(\Delta m \Delta t) - C_{\bar{f}} \cos(\Delta m \Delta t)\}, \quad (153)$$

$$\Gamma_{B^0 \rightarrow \bar{f}}(\Delta t) = \frac{e^{-|\Delta t|/\tau(B^0)}}{8\tau(B^0)} (1 - \langle \mathcal{A}_{f\bar{f}} \rangle) \{1 - S_{\bar{f}} \sin(\Delta m \Delta t) + C_{\bar{f}} \cos(\Delta m \Delta t)\}, \quad (154)$$

where the time-independent parameter $\langle \mathcal{A}_{f\bar{f}} \rangle$ represents an overall asymmetry in the production of the f and \bar{f} final states,¹⁷

$$\langle \mathcal{A}_{f\bar{f}} \rangle = \frac{(|A_f|^2 + |\bar{A}_f|^2) - (|A_{\bar{f}}|^2 + |\bar{A}_{\bar{f}}|^2)}{(|A_f|^2 + |\bar{A}_f|^2) + (|A_{\bar{f}}|^2 + |\bar{A}_{\bar{f}}|^2)}. \quad (155)$$

Assuming $|q/p| = 1$, the parameters C_f and $C_{\bar{f}}$ can also be written in terms of the decay amplitudes as follows:

$$C_f = \frac{|A_f|^2 - |\bar{A}_f|^2}{|A_f|^2 + |\bar{A}_f|^2} \quad \text{and} \quad C_{\bar{f}} = \frac{|A_{\bar{f}}|^2 - |\bar{A}_{\bar{f}}|^2}{|A_{\bar{f}}|^2 + |\bar{A}_{\bar{f}}|^2}, \quad (156)$$

giving asymmetries in the decay amplitudes of B^0 and \bar{B}^0 to the final states f and \bar{f} respectively. In this notation, the direct CP invariance conditions are $\langle \mathcal{A}_{f\bar{f}} \rangle = 0$ and $C_f = -C_{\bar{f}}$. Note that C_f and $C_{\bar{f}}$ are typically non-zero; *e.g.*, for a flavour-specific final state, $\bar{A}_f = A_{\bar{f}} = 0$ ($A_f = \bar{A}_{\bar{f}} = 0$), they take the values $C_f = -C_{\bar{f}} = 1$ ($C_f = -C_{\bar{f}} = -1$).

The coefficients of the sine terms contain information about the weak phase. In the case that each decay amplitude contains only a single weak phase (*i.e.*, no direct CP violation), these terms can be written

$$S_f = \frac{-2 |A_f| |\bar{A}_f| \sin(\phi_{\text{mix}} + \phi_{\text{dec}} - \delta_f)}{|A_f|^2 + |\bar{A}_f|^2} \quad \text{and} \quad S_{\bar{f}} = \frac{-2 |A_{\bar{f}}| |\bar{A}_{\bar{f}}| \sin(\phi_{\text{mix}} + \phi_{\text{dec}} + \delta_f)}{|A_{\bar{f}}|^2 + |\bar{A}_{\bar{f}}|^2}, \quad (157)$$

¹⁷ This parameter is often denoted \mathcal{A}_f (or \mathcal{A}_{CP}), but here we avoid this notation to prevent confusion with the time-dependent CP asymmetry.

where δ_f is the strong phase difference between the decay amplitudes. If there is no CP violation, the condition $S_f = -S_{\bar{f}}$ holds. If decay amplitudes with different weak and strong phases contribute, no clean interpretation of S_f and $S_{\bar{f}}$ is possible.

Since two of the CP invariance conditions are $C_f = -C_{\bar{f}}$ and $S_f = -S_{\bar{f}}$, there is motivation for a rotation of the parameters:

$$S_{f\bar{f}} = \frac{S_f + S_{\bar{f}}}{2}, \quad \Delta S_{f\bar{f}} = \frac{S_f - S_{\bar{f}}}{2}, \quad C_{f\bar{f}} = \frac{C_f + C_{\bar{f}}}{2}, \quad \Delta C_{f\bar{f}} = \frac{C_f - C_{\bar{f}}}{2}. \quad (158)$$

With these parameters, the CP invariance conditions become $S_{f\bar{f}} = 0$ and $C_{f\bar{f}} = 0$. The parameter $\Delta C_{f\bar{f}}$ gives a measure of the ‘‘flavour-specificity’’ of the decay: $\Delta C_{f\bar{f}} = \pm 1$ corresponds to a completely flavour-specific decay, in which no interference between decays with and without mixing can occur, while $\Delta C_{f\bar{f}} = 0$ results in maximum sensitivity to mixing-induced CP violation. The parameter $\Delta S_{f\bar{f}}$ is related to the strong phase difference between the decay amplitudes of B^0 to f and to \bar{f} . We note that the observables of Eq. (158) exhibit experimental correlations (typically of $\sim 20\%$, depending on the tagging purity, and other effects) between $S_{f\bar{f}}$ and $\Delta S_{f\bar{f}}$, and between $C_{f\bar{f}}$ and $\Delta C_{f\bar{f}}$. On the other hand, the final state specific observables of Eq. (149) tend to have low correlations.

Alternatively, if we recall that the CP invariance conditions at the decay amplitude level are $A_f = \bar{A}_{\bar{f}}$ and $A_{\bar{f}} = \bar{A}_f$, we are led to consider the parameters [206]

$$\mathcal{A}_{f\bar{f}} = \frac{|\bar{A}_{\bar{f}}|^2 - |A_f|^2}{|\bar{A}_{\bar{f}}|^2 + |A_f|^2} \quad \text{and} \quad \mathcal{A}_{\bar{f}f} = \frac{|\bar{A}_f|^2 - |A_{\bar{f}}|^2}{|\bar{A}_f|^2 + |A_{\bar{f}}|^2}. \quad (159)$$

These are sometimes considered more physically intuitive parameters since they characterize direct CP violation in decays with particular topologies. For example, in the case of $B^0 \rightarrow \rho^\pm \pi^\mp$ (choosing $f = \rho^+ \pi^-$ and $\bar{f} = \rho^- \pi^+$), $\mathcal{A}_{f\bar{f}}$ (also denoted $\mathcal{A}_{\rho\pi}^{+-}$) parameterizes direct CP violation in decays in which the produced ρ meson does not contain the spectator quark, while $\mathcal{A}_{\bar{f}f}$ (also denoted $\mathcal{A}_{\rho\pi}^{-+}$) parameterizes direct CP violation in decays in which it does. Note that we have again followed the sign convention that the asymmetry is the difference between the rate involving a b quark and that involving a \bar{b} quark, *cf.* Eq. (136). Of course, these parameters are not independent of the other sets of parameters given above, and can be written

$$\mathcal{A}_{f\bar{f}} = -\frac{\langle \mathcal{A}_{f\bar{f}} \rangle + C_{f\bar{f}} + \langle \mathcal{A}_{f\bar{f}} \rangle \Delta C_{f\bar{f}}}{1 + \Delta C_{f\bar{f}} + \langle \mathcal{A}_{f\bar{f}} \rangle C_{f\bar{f}}} \quad \text{and} \quad \mathcal{A}_{\bar{f}f} = \frac{-\langle \mathcal{A}_{f\bar{f}} \rangle + C_{f\bar{f}} + \langle \mathcal{A}_{f\bar{f}} \rangle \Delta C_{f\bar{f}}}{-1 + \Delta C_{f\bar{f}} + \langle \mathcal{A}_{f\bar{f}} \rangle C_{f\bar{f}}}. \quad (160)$$

They usually exhibit strong correlations.

We now consider the various notations which have been used in experimental studies of time-dependent CP asymmetries in decays to non- CP eigenstates.

$B^0 \rightarrow D^{*\pm} D^\mp$

The above set of parameters ($\langle \mathcal{A}_{f\bar{f}} \rangle$, C_f , S_f , $C_{\bar{f}}$, $S_{\bar{f}}$), has been used by both *BABAR* [185] and *Belle* [207] in the $D^{*\pm} D^\mp$ system ($f = D^{*+} D^-$, $\bar{f} = D^{*-} D^+$). However, slightly different names for the parameters are used: *BABAR* uses (\mathcal{A} , C_{+-} , S_{+-} , C_{-+} , S_{-+}); *Belle* uses (\mathcal{A} , C_+ , S_+ , C_- , S_-). In this document, we follow the notation used by *BABAR*.

$B^0 \rightarrow \rho^\pm \pi^\mp$

In the $\rho^\pm\pi^\mp$ system, the $(\langle\mathcal{A}_{f\bar{f}}\rangle, C_{f\bar{f}}, S_{f\bar{f}}, \Delta C_{f\bar{f}}, \Delta S_{f\bar{f}})$ set of parameters has been used originally by *BABAR* [208] and Belle [209], in the Q2B approximation; the exact names¹⁸ used in this case are $(\mathcal{A}_{CP}^{\rho\pi}, C_{\rho\pi}, S_{\rho\pi}, \Delta C_{\rho\pi}, \Delta S_{\rho\pi})$, and these names are also used in this document.

Since $\rho^\pm\pi^\mp$ is reconstructed in the final state $\pi^+\pi^-\pi^0$, the interference between the ρ resonances can provide additional information about the phases (see Sec. 4.2.4). Both *BABAR* [203] and Belle [204, 205] have performed time-dependent Dalitz plot analyses, from which the weak phase α is directly extracted. In such an analysis, the measured Q2B parameters are also naturally corrected for interference effects. See Sec. 4.2.4.

$B^0 \rightarrow D^\pm\pi^\mp, D^{*\pm}\pi^\mp, D^\pm\rho^\mp$

Time-dependent CP analyses have also been performed for the final states $D^\pm\pi^\mp, D^{*\pm}\pi^\mp$ and $D^\pm\rho^\mp$. In these theoretically clean cases, no penguin contributions are possible, so there is no direct CP violation. Furthermore, due to the smallness of the ratio of the magnitudes of the suppressed ($b \rightarrow u$) and favoured ($b \rightarrow c$) amplitudes (denoted R_f), to a very good approximation, $C_f = -C_{\bar{f}} = 1$ (using $f = D^{(*)-}h^+, \bar{f} = D^{(*)+}h^-$ $h = \pi, \rho$), and the coefficients of the sine terms are given by

$$S_f = -2R_f \sin(\phi_{\text{mix}} + \phi_{\text{dec}} - \delta_f) \quad \text{and} \quad S_{\bar{f}} = -2R_f \sin(\phi_{\text{mix}} + \phi_{\text{dec}} + \delta_f). \quad (161)$$

Thus weak phase information can be cleanly obtained from measurements of S_f and $S_{\bar{f}}$, although external information on at least one of R_f or δ_f is necessary. (Note that $\phi_{\text{mix}} + \phi_{\text{dec}} = 2\beta + \gamma$ for all the decay modes in question, while R_f and δ_f depend on the decay mode.)

Again, different notations have been used in the literature. *BABAR* [210, 211] defines the time-dependent probability function by

$$f^\pm(\eta, \Delta t) = \frac{e^{-|\Delta t|/\tau}}{4\tau} [1 \mp S_\zeta \sin(\Delta m \Delta t) \mp \eta C_\zeta \cos(\Delta m \Delta t)], \quad (162)$$

where the upper (lower) sign corresponds to the tagging meson being a B^0 (\bar{B}^0). [Note here that a tagging B^0 (\bar{B}^0) corresponds to $-S_\zeta$ ($+S_\zeta$).] The parameters η and ζ take the values $+1$ and -1 (-1 and -1) when the final state is, *e.g.*, $D^-\pi^+$ ($D^+\pi^-$). However, in the fit, the substitutions $C_\zeta = 1$ and $S_\zeta = a \mp \eta b_i - \eta c_i$ are made.¹⁹ [Note that, neglecting b terms, $S_+ = a - c$ and $S_- = a + c$, so that $a = (S_+ + S_-)/2$, $c = (S_- - S_+)/2$, in analogy to the parameters of Eq. (158).] The subscript i denotes the tagging category. These are motivated by the possibility of CP violation on the tag side [212], which is absent for semileptonic B decays (mostly lepton tags). The parameter a is not affected by tag side CP violation. The parameter b only depends on tag side CP violation parameters and is not directly useful for determining UT angles. A clean interpretation of the c parameter is only possible for lepton-tagged events, so the *BABAR* measurements report c measured with those events only.

The parameters used by Belle in the analysis using partially reconstructed B decays [213], are similar to the S_ζ parameters defined above. However, in the Belle convention, a tagging B^0 corresponds to a $+$ sign in front of the sine coefficient; furthermore the correspondence between the super/subscript and the final state is opposite, so that S_\pm (*BABAR*) = $-S^\mp$ (Belle). In this analysis, only lepton tags are used, so there is no effect from tag side CP violation. In the

¹⁸ *BABAR* has used the notations $\mathcal{A}_{CP}^{\rho\pi}$ [208] and $\mathcal{A}_{\rho\pi}$ [203] in place of $\mathcal{A}_{CP}^{\rho\pi}$.

¹⁹ The subscript i denotes tagging category.

Table 20: Conversion between the various notations used for CP violation parameters in the $D^\pm\pi^\mp$, $D^{*\pm}\pi^\mp$ and $D^\pm\rho^\mp$ systems. The b_i terms used by *BABAR* have been neglected. Recall that $(\alpha, \beta, \gamma) = (\phi_2, \phi_1, \phi_3)$.

	<i>BABAR</i>	Belle partial rec.	Belle full rec.
$S_{D^+\pi^-}$	$-S_- = -(a + c_i)$	N/A	$2R_{D\pi} \sin(2\phi_1 + \phi_3 + \delta_{D\pi})$
$S_{D^-\pi^+}$	$-S_+ = -(a - c_i)$	N/A	$2R_{D\pi} \sin(2\phi_1 + \phi_3 - \delta_{D\pi})$
$S_{D^{*+}\pi^-}$	$-S_- = -(a + c_i)$	S^+	$-2R_{D^*\pi} \sin(2\phi_1 + \phi_3 + \delta_{D^*\pi})$
$S_{D^{*-}\pi^+}$	$-S_+ = -(a - c_i)$	S^-	$-2R_{D^*\pi} \sin(2\phi_1 + \phi_3 - \delta_{D^*\pi})$
$S_{D^+\rho^-}$	$-S_- = -(a + c_i)$	N/A	N/A
$S_{D^-\rho^+}$	$-S_+ = -(a - c_i)$	N/A	N/A

Table 21: Translations used to convert the parameters measured by Belle to the parameters used for averaging in this document. The angular momentum factor L is -1 for $D^*\pi$ and $+1$ for $D\pi$. Recall that $(\alpha, \beta, \gamma) = (\phi_2, \phi_1, \phi_3)$.

	$D^*\pi$ partial rec.	$D^{(*)}\pi$ full rec.
a	$-(S^+ + S^-)$	$\frac{1}{2}(-1)^{L+1} (2R_{D^{(*)}\pi} \sin(2\phi_1 + \phi_3 + \delta_{D^{(*)}\pi}) + 2R_{D^{(*)}\pi} \sin(2\phi_1 + \phi_3 - \delta_{D^{(*)}\pi}))$
c	$-(S^+ - S^-)$	$\frac{1}{2}(-1)^{L+1} (2R_{D^{(*)}\pi} \sin(2\phi_1 + \phi_3 + \delta_{D^{(*)}\pi}) - 2R_{D^{(*)}\pi} \sin(2\phi_1 + \phi_3 - \delta_{D^{(*)}\pi}))$

Belle analysis using fully reconstructed B decays [214], this effect is measured and taken into account using $D^*l\nu$ decays; in neither Belle analysis are the a , b and c parameters used. In the latter case, the measured parameters are $2R_{D^{(*)}\pi} \sin(2\phi_1 + \phi_3 \pm \delta_{D^{(*)}\pi})$; the definition is such that S^\pm (Belle) = $-2R_{D^*\pi} \sin(2\phi_1 + \phi_3 \pm \delta_{D^*\pi})$. However, the definition includes an angular momentum factor $(-1)^L$ [215], and so for the results in the $D\pi$ system, there is an additional factor of -1 in the conversion.

Explicitly, the conversion then reads as given in Table 20, where we have neglected the b_i terms used by *BABAR* (which are zero in the absence of tag side CP violation). For the averages in this document, we use the a and c parameters, and give the explicit translations used in Table 21. It is to be fervently hoped that the experiments will converge on a common notation in future.

Time-dependent asymmetries in radiative B decays

As a special case of decays to non- CP eigenstates, let us consider radiative B decays. Here, the emitted photon has a distinct helicity, which is in principle observable, but in practice is not usually measured. Thus the measured time-dependent decay rates are given by [216, 217]

$$\begin{aligned} \Gamma_{\bar{B}^0 \rightarrow X\gamma}(\Delta t) &= \Gamma_{\bar{B}^0 \rightarrow X\gamma_L}(\Delta t) + \Gamma_{\bar{B}^0 \rightarrow X\gamma_R}(\Delta t) \\ &= \frac{e^{-|\Delta t|/\tau(B^0)}}{4\tau(B^0)} \{1 + (S_L + S_R) \sin(\Delta m\Delta t) - (C_L + C_R) \cos(\Delta m\Delta t)\}, \end{aligned} \quad (163)$$

$$\begin{aligned} \Gamma_{B^0 \rightarrow X\gamma}(\Delta t) &= \Gamma_{B^0 \rightarrow X\gamma_L}(\Delta t) + \Gamma_{B^0 \rightarrow X\gamma_R}(\Delta t) \\ &= \frac{e^{-|\Delta t|/\tau(B^0)}}{4\tau(B^0)} \{1 - (S_L + S_R) \sin(\Delta m\Delta t) + (C_L + C_R) \cos(\Delta m\Delta t)\}, \end{aligned} \quad (164)$$

where in place of the subscripts f and \bar{f} we have used L and R to indicate the photon helicity. In order for interference between decays with and without B^0 - \bar{B}^0 mixing to occur, the X system must not be flavour-specific, *e.g.*, in case of $B^0 \rightarrow K^{*0}\gamma$, the final state must be $K_s^0\pi^0\gamma$. The sign of the sine term depends on the C eigenvalue of the X system. At leading order, the photons from $b \rightarrow q\gamma$ ($\bar{b} \rightarrow \bar{q}\gamma$) are predominantly left (right) polarized, with corrections of order of m_q/m_b , thus interference effects are suppressed. Higher order effects can lead to corrections of order Λ_{QCD}/m_b [218, 219], though explicit calculations indicate such corrections are small for exclusive final states [220, 221]. The predicted smallness of the S terms in the Standard Model results in sensitivity to new physics contributions.

4.2.6 Time-dependent CP asymmetries in the B_s System

A complete analysis of the time-dependent decay rates of neutral B mesons must also take into account the lifetime difference between the eigenstates of the effective Hamiltonian, denoted by $\Delta\Gamma$. This is particularly important in the B_s system, since non-negligible values of $\Delta\Gamma_s$ are expected (see Section 3.3 for the latest experimental constraints). Neglecting CP violation in mixing, the relevant replacements for Eqs. 137 & 138 are [150]

$$\Gamma_{\bar{B}_s \rightarrow f}(\Delta t) = \mathcal{N} \frac{e^{-|\Delta t|/\tau(B_s^0)}}{4\tau(B_s^0)} \left[\cosh\left(\frac{\Delta\Gamma\Delta t}{2}\right) + \frac{2\text{Im}(\lambda_f)}{1+|\lambda_f|^2} \sin(\Delta m\Delta t) - \frac{1-|\lambda_f|^2}{1+|\lambda_f|^2} \cos(\Delta m\Delta t) - \frac{2\text{Re}(\lambda_f)}{1+|\lambda_f|^2} \sinh\left(\frac{\Delta\Gamma\Delta t}{2}\right) \right], \quad (165)$$

and

$$\Gamma_{B_s^0 \rightarrow f}(\Delta t) = \mathcal{N} \frac{e^{-|\Delta t|/\tau(B_s^0)}}{4\tau(B_s^0)} \left[\cosh\left(\frac{\Delta\Gamma\Delta t}{2}\right) - \frac{2\text{Im}(\lambda_f)}{1+|\lambda_f|^2} \sin(\Delta m\Delta t) + \frac{1-|\lambda_f|^2}{1+|\lambda_f|^2} \cos(\Delta m\Delta t) - \frac{2\text{Re}(\lambda_f)}{1+|\lambda_f|^2} \sinh\left(\frac{\Delta\Gamma\Delta t}{2}\right) \right]. \quad (166)$$

To be consistent with our earlier notation,²⁰ we write here the coefficient of the sinh term as

$$A_f^{\Delta\Gamma} = -\frac{2\text{Re}(\lambda_f)}{1+|\lambda_f|^2}. \quad (167)$$

A complete, tagged, time-dependent analysis of CP asymmetries in B_s decays to a CP eigenstate f can thus obtain the parameters S_f , C_f and $A_f^{\Delta\Gamma}$. Note that

$$(S_f)^2 + (C_f)^2 + (A_f^{\Delta\Gamma})^2 = 1. \quad (168)$$

Since these parameters have sensitivity to both $\text{Im}(\lambda_f)$ and $\text{Re}(\lambda_f)$, alternative choices of parametrization, including those directly involving CP violating phases (such as β_s), are possible. These can also be adopted for vector-vector final states.

The *untagged* time-dependent decay rate is given by

$$\Gamma_{\bar{B}_s \rightarrow f}(\Delta t) + \Gamma_{B_s^0 \rightarrow f}(\Delta t) = \mathcal{N} \frac{e^{-|\Delta t|/\tau(B_s^0)}}{2\tau(B_s^0)} \left[\cosh\left(\frac{\Delta\Gamma\Delta t}{2}\right) - \frac{2\text{Re}(\lambda_f)}{1+|\lambda_f|^2} \sinh\left(\frac{\Delta\Gamma\Delta t}{2}\right) \right]. \quad (169)$$

²⁰ As ever, alternative and conflicting notations appear in the literature. One popular alternative notation for this parameter is $\mathcal{A}_{\Delta\Gamma}$. Particular care must be taken over the signs.

With the requirement $\int_{-\infty}^{+\infty} \Gamma_{\bar{B}_s \rightarrow f}(\Delta t) + \Gamma_{B_s^0 \rightarrow f}(\Delta t) d(\Delta t) = 1$, the normalization factor \mathcal{N} is fixed to $1 - (\frac{\Delta\Gamma}{2\Gamma})^2$. Note that an untagged time-dependent analysis can probe λ_f , through $\text{Re}(\lambda_f)$, when $\Delta\Gamma \neq 0$. The tagged analysis is, of course, more sensitive.

Other expressions can be similarly modified to take into account non-zero lifetime differences. Note that when the final state contains a mixture of CP -even and CP -odd states (as, for example, for vector-vector or multibody self-conjugate states), that $\text{Re}(\lambda_f)$ contains terms proportional to both the sine and cosine of the weak phase difference, albeit with rather different sensitivities.

4.2.7 Asymmetries in $B \rightarrow D^{(*)}K^{(*)}$ decays

CP asymmetries in $B \rightarrow D^{(*)}K^{(*)}$ decays are sensitive to γ . The neutral $D^{(*)}$ meson produced is an admixture of $D^{(*)0}$ (produced by a $b \rightarrow c$ transition) and $\bar{D}^{(*)0}$ (produced by a colour-suppressed $b \rightarrow u$ transition) states. If the final state is chosen so that both $D^{(*)0}$ and $\bar{D}^{(*)0}$ can contribute, the two amplitudes interfere, and the resulting observables are sensitive to γ , the relative weak phase between the two B decay amplitudes [222]. Various methods have been proposed to exploit this interference, including those where the neutral D meson is reconstructed as a CP eigenstate (GLW) [223, 224], in a suppressed final state (ADS) [225, 226], or in a self-conjugate three-body final state, such as $K_S^0\pi^+\pi^-$ (Dalitz) [227, 228]. It should be emphasised that while each method differs in the choice of D decay, they are all sensitive to the same parameters of the B decay, and can be considered as variations of the same technique.

Consider the case of $B^\mp \rightarrow DK^\mp$, with D decaying to a final state f , which is accessible to both D^0 and \bar{D}^0 . We can write the decay rates for B^- and B^+ (Γ_\mp), the charge averaged rate ($\Gamma = (\Gamma_- + \Gamma_+)/2$) and the charge asymmetry ($\mathcal{A} = (\Gamma_- - \Gamma_+)/(\Gamma_- + \Gamma_+)$, see Eq. (136)) as

$$\Gamma_\mp \propto r_B^2 + r_D^2 + 2r_B r_D \cos(\delta_B + \delta_D \mp \gamma), \quad (170)$$

$$\Gamma \propto r_B^2 + r_D^2 + 2r_B r_D \cos(\delta_B + \delta_D) \cos(\gamma), \quad (171)$$

$$\mathcal{A} = \frac{2r_B r_D \sin(\delta_B + \delta_D) \sin(\gamma)}{r_B^2 + r_D^2 + 2r_B r_D \cos(\delta_B + \delta_D) \cos(\gamma)}, \quad (172)$$

where the ratio of B decay amplitudes²¹ is usually defined to be less than one,

$$r_B = \frac{|A(B^- \rightarrow \bar{D}^0 K^-)|}{|A(B^- \rightarrow D^0 K^-)|}, \quad (173)$$

and the ratio of D decay amplitudes is correspondingly defined by

$$r_D = \frac{|A(D^0 \rightarrow f)|}{|A(\bar{D}^0 \rightarrow f)|}. \quad (174)$$

The strong phase differences between the B and D decay amplitudes are given by δ_B and δ_D , respectively. The values of r_D and δ_D depend on the final state f : for the GLW analysis, $r_D = 1$ and δ_D is trivial (either zero or π), in the Dalitz plot analysis r_D and δ_D vary across the Dalitz

²¹ Note that here we use the notation r_B to denote the ratio of B decay amplitudes, whereas in Sec. 4.2.5 we used, *e.g.*, $R_{D\pi}$, for a rather similar quantity. The reason is that here we need to be concerned also with D decay amplitudes, and so it is convenient to use the subscript to denote the decaying particle. Hopefully, using r in place of R will help reduce potential confusion.

plot, and depend on the D decay model used, for the ADS analysis, the values of r_D and δ_D are not trivial.

Note that, for given values of r_B and r_D , the maximum size of \mathcal{A} (at $\sin(\delta_B + \delta_D) = 1$) is $2r_B r_D \sin(\gamma) / (r_B^2 + r_D^2)$. Thus even for D decay modes with small r_D , large asymmetries, and hence sensitivity to γ , may occur for B decay modes with similar values of r_B . For this reason, the ADS analysis of the decay $B^\mp \rightarrow D\pi^\mp$ is also of interest.

In the GLW analysis, the measured quantities are the partial rate asymmetry, and the charge averaged rate, which are measured both for CP -even and CP -odd D decays. The former is defined as

$$R_{CP} = \frac{2\Gamma(B^- \rightarrow D_{CP}K^-)}{\Gamma(B^- \rightarrow D^0K^-)}. \quad (175)$$

It is experimentally convenient to measure R_{CP} using a double ratio,

$$R_{CP} = \frac{\Gamma(B^- \rightarrow D_{CP}K^-) / \Gamma(B^- \rightarrow D^0K^-)}{\Gamma(B^- \rightarrow D_{CP}\pi^-) / \Gamma(B^- \rightarrow D^0\pi^-)} \quad (176)$$

that is normalized both to the rate for the favoured $D^0 \rightarrow K^-\pi^+$ decay, and to the equivalent quantities for $B^- \rightarrow D\pi^-$ decays (charge conjugate modes are implicitly included in Eq. (175) and (176)). In this way the constant of proportionality drops out of Eq. (171). Eq. (176) is exact in the limit that the contribution of the $b \rightarrow u$ decay amplitude to $B^- \rightarrow D\pi^-$ vanishes and when the flavour-specific rates $\Gamma(B^- \rightarrow D^0h^-)$ ($h = \pi, K$) are determined using appropriately flavour-specific D decays. The direct CP asymmetry is defined as

$$A_{CP} = \frac{\Gamma(B^- \rightarrow D_{CP}K^-) - \Gamma(B^+ \rightarrow D_{CP}K^+)}{\Gamma(B^- \rightarrow D_{CP}K^-) + \Gamma(B^+ \rightarrow D_{CP}K^+)}. \quad (177)$$

For the ADS analysis, using a suppressed $D \rightarrow f$ decay, the measured quantities are again the partial rate asymmetry, and the charge averaged rate. In this case it is sufficient to measure the rate in a single ratio (normalized to the favoured $D \rightarrow \bar{f}$ decay) since detection systematics cancel naturally; the observed quantity is then

$$R_{\text{ADS}} = \frac{\Gamma(B^- \rightarrow [f]_D K^-)}{\Gamma(B^- \rightarrow [\bar{f}]_D K^-)}, \quad (178)$$

where inclusion of charge conjugate modes is implied. The direct CP asymmetry is defined as

$$R_{\text{ADS}} = \frac{\Gamma(B^- \rightarrow [f]_D K^-) - \Gamma(B^+ \rightarrow [f]_D K^+)}{\Gamma(B^- \rightarrow [f]_D K^-) + \Gamma(B^+ \rightarrow [f]_D K^+)}. \quad (179)$$

In the ADS analysis, there are an additional two unknowns (r_D and δ_D) compared to the GLW case. However, the value of r_D can be measured using decays of D mesons of known flavour.

In the Dalitz plot analysis, once a model is assumed for the D decay, which gives the values of r_D and δ_D across the Dalitz plot, it is possible to perform a simultaneous fit to the B^+ and B^- samples and directly extract γ , r_B and δ_B . However, the uncertainties on the phases depend approximately inversely on r_B . Furthermore, r_B is positive definite (and small), and therefore tends to be overestimated, which can lead to an underestimation of the uncertainty. Some statistical treatment is necessary to correct for this bias. An alternative approach is to extract from the data the ‘‘Cartesian’’ variables

$$(x_\pm, y_\pm) = (\text{Re}(r_B e^{i(\delta_B \pm \gamma)}), \text{Im}(r_B e^{i(\delta_B \pm \gamma)})) = (r_B \cos(\delta_B \pm \gamma), r_B \sin(\delta_B \pm \gamma)). \quad (180)$$

These are (a) approximately statistically uncorrelated and (b) almost Gaussian. The pairs of variables (x_{\pm}, y_{\pm}) can be extracted from independent fits of the B^{\pm} data samples. Use of these variables makes the combination of results much simpler.

However, if the Dalitz plot is effectively dominated by one CP state, there will be additional sensitivity to γ in the numbers of events in the B^{\pm} data samples. This can be taken into account in various ways. One possibility is to extract GLW-like variables in addition to the (x_{\pm}, y_{\pm}) parameters. An alternative proceeds by defining $z_{\pm} = x_{\pm} + iy_{\pm}$ and $x_0 = -\int \text{Re}[f(s_1, s_2)f^*(s_2, s_1)] ds_1 ds_2$, where s_1, s_2 are the coordinates of invariant mass squared that define the Dalitz plot and f is the complex amplitude for D decay as a function of the Dalitz plot coordinates.²² The fitted parameters $(\rho^{\pm}, \theta^{\pm})$ are then defined by

$$\rho^{\pm} e^{i\theta^{\pm}} = z_{\pm} - x_0. \quad (181)$$

Note that the yields of B^{\pm} decays are proportional to $1 + (\rho^{\pm})^2 - (x_0)^2$. This choice of variables has been used by *BABAR* in the analysis of $B^{\mp} \rightarrow DK^{\mp}$ with $D \rightarrow \pi^+\pi^-\pi^0$ [232]; for this D decay, $x_0 = 0.850$.

The relations between the measured quantities and the underlying parameters are summarized in Table 22. Note carefully that the hadronic factors r_B and δ_B are different, in general, for each B decay mode.

Table 22: Summary of relations between measured and physical parameters in GLW, ADS and Dalitz analyses of $B \rightarrow D^{(*)}K^{(*)}$.

GLW analysis	
$R_{CP\pm}$	$1 + r_B^2 \pm 2r_B \cos(\delta_B) \cos(\gamma)$
$A_{CP\pm}$	$\pm 2r_B \sin(\delta_B) \sin(\gamma) / R_{CP\pm}$
ADS analysis	
R_{ADS}	$r_B^2 + r_D^2 + 2r_B r_D \cos(\delta_B + \delta_D) \cos(\gamma)$
A_{ADS}	$2r_B r_D \sin(\delta_B + \delta_D) \sin(\gamma) / R_{\text{ADS}}$
Dalitz analysis ($D \rightarrow K_s^0 \pi^+ \pi^-$)	
x_{\pm}	$r_B \cos(\delta_B \pm \gamma)$
y_{\pm}	$r_B \sin(\delta_B \pm \gamma)$
Dalitz analysis ($D \rightarrow \pi^+ \pi^- \pi^0$)	
ρ^{\pm}	$ z_{\pm} - x_0 $
θ^{\pm}	$\tan^{-1}(\text{Im}(z_{\pm}) / (\text{Re}(z_{\pm}) - x_0))$

4.3 Common inputs and error treatment

The common inputs used for rescaling are listed in Table 23. The B^0 lifetime ($\tau(B^0)$) and mixing parameter (Δm_d) averages are provided by the HFAG Lifetimes and Oscillations subgroup (Sec. 3). The fraction of the perpendicularly polarized component ($|A_{\perp}|^2$) in $B \rightarrow J/\psi K^*(892)$ decays, which determines the CP composition, is averaged from results by *BABAR* [233] and *Belle* [234]. See also HFAG B to Charm Decay Parameters subgroup (Sec. 6).

²² The x_0 parameter is closely related to the c_i parameters of the model dependent Dalitz plot analysis [227, 229, 230], and the coherence factor of inclusive ADS-type analyses [231], integrated over the entire Dalitz plot.

At present, we only rescale to a common set of input parameters for modes with reasonably small statistical errors ($b \rightarrow c\bar{c}s$ transitions). Correlated systematic errors are taken into account in these modes as well. For all other modes, the effect of such a procedure is currently negligible.

Table 23: Common inputs used in calculating the averages.

$\tau(B^0)$ (ps)	1.530 ± 0.008
Δm_d (ps^{-1})	0.507 ± 0.004
$ A_\perp ^2(J/\psi K^*)$	0.219 ± 0.009

As explained in Sec. 1, we do not apply a rescaling factor on the error of an average that has $\chi^2/\text{dof} > 1$ (unlike the procedure currently used by the PDG [5]). We provide a confidence level of the fit so that one can know the consistency of the measurements included in the average, and attach comments in case some care needs to be taken in the interpretation. Note that, in general, results obtained from data samples with low statistics will exhibit some non-Gaussian behaviour. We average measurements with asymmetric errors using the PDG [5] prescription. In cases where several measurements are correlated (*e.g.* S_f and C_f in measurements of time-dependent CP violation in B decays to a particular CP eigenstate) we take these into account in the averaging procedure if the uncertainties are sufficiently Gaussian. For measurements where one error is given, it represents the total error, where statistical and systematic uncertainties have been added in quadrature. If two errors are given, the first is statistical and the second systematic. If more than two errors are given, the origin of the additional uncertainty will be explained in the text.

4.4 Time-dependent asymmetries in $b \rightarrow c\bar{c}s$ transitions

4.4.1 Time-dependent CP asymmetries in $b \rightarrow c\bar{c}s$ decays to CP eigenstates

In the Standard Model, the time-dependent parameters for $b \rightarrow c\bar{c}s$ transitions are predicted to be: $S_{b \rightarrow c\bar{c}s} = -\eta \sin(2\beta)$, $C_{b \rightarrow c\bar{c}s} = 0$ to very good accuracy. The averages for $-\eta S_{b \rightarrow c\bar{c}s}$ and $C_{b \rightarrow c\bar{c}s}$ are provided in Table 24. The averages for $-\eta S_{b \rightarrow c\bar{c}s}$ are shown in Fig. 11.

Both *BABAR* and Belle have used the $\eta = -1$ modes $J/\psi K_S^0$, $\psi(2S)K_S^0$, $\chi_{c1}K_S^0$ and $\eta_c K_S^0$, as well as $J/\psi K_L^0$, which has $\eta = +1$ and $J/\psi K^{*0}(892)$, which is found to have η close to $+1$ based on the measurement of $|A_\perp|$ (see Sec. 4.3). ALEPH, OPAL and CDF used only the $J/\psi K_S^0$ final state. In the latest result from Belle [235], only $J/\psi K_S^0$ and $J/\psi K_L^0$ are used, while results from $\psi(2S)K_S^0$ have been presented separately [236]. *BABAR* have also determined the CP -violation parameters of the $B^0 \rightarrow \chi_{c0}K_S^0$ decay from the time-dependent Dalitz plot analysis of $B^0 \rightarrow \pi^+\pi^-K_S^0$ (see subsection 4.6.2) [196]. A breakdown of results in each charmonium-kaon final state is given in Table 25.

Table 24: $S_{b \rightarrow c\bar{c}s}$ and $C_{b \rightarrow c\bar{c}s}$.

Experiment		$N(B\bar{B})$	$-\eta S_{b \rightarrow c\bar{c}s}$	$C_{b \rightarrow c\bar{c}s}$
<i>BABAR</i>	[237]	465M	$0.687 \pm 0.028 \pm 0.012$	$0.024 \pm 0.020 \pm 0.016$
<i>BABAR</i> $\chi_{c0}K_S^0$	[196]	383M	$0.690 \pm 0.520 \pm 0.040 \pm 0.070$	$-0.290^{+0.530}_{-0.440} \pm 0.030 \pm 0.050$
<i>BABAR</i> $J/\psi K_S^0$ (*)	[238]	88M	$1.560 \pm 0.420 \pm 0.210$	–
Belle $J/\psi K^0$	[235]	535M	$0.642 \pm 0.031 \pm 0.017$	$-0.018 \pm 0.021 \pm 0.014$
Belle $\psi(2S)K_S^0$	[236]	657M	$0.718 \pm 0.090 \pm 0.031$	$-0.039 \pm 0.069 \pm 0.0$
B factory average			0.672 ± 0.023	0.004 ± 0.019
Confidence level			0.30	0.51
ALEPH	[239]	–	$0.84^{+0.82}_{-1.04} \pm 0.16$	–
OPAL	[240]	–	$3.2^{+1.8}_{-2.0} \pm 0.5$	–
CDF	[241]	–	$0.79^{+0.41}_{-0.44}$	–
Average			0.673 ± 0.023	0.004 ± 0.019

* This result uses "hadronic and previously unused muonic decays of the J/ψ ". We neglect a small possible correlation of this result with the main *BABAR* result [237] that could be caused by reprocessing of the data.

It should be noted that, while the uncertainty in the average for $-\eta S_{b \rightarrow c\bar{c}s}$ is still limited by statistics, that for $C_{b \rightarrow c\bar{c}s}$ is close to being dominated by systematics. This occurs due to the possible effect of tag side interference on the $C_{b \rightarrow c\bar{c}s}$ measurement, an effect which is correlated between the different experiments. Understanding of this effect may continue to improve in future, allowing the uncertainty to reduce.

From the average for $-\eta S_{b \rightarrow c\bar{c}s}$ above, we obtain the following solutions for β (in $[0, \pi]$):

$$\beta = (21.1 \pm 0.9)^\circ \quad \text{or} \quad \beta = (68.9 \pm 0.9)^\circ \quad (182)$$

In radians, these values are $\beta = (0.368 \pm 0.016)$, $\beta = (1.203 \pm 0.016)$.

This result gives a precise constraint on the $(\bar{\rho}, \bar{\eta})$ plane, as shown in Fig. 11. The measurement is in remarkable agreement with other constraints from CP conserving quantities, and with CP violation in the kaon system, in the form of the parameter ϵ_K . Such comparisons have been performed by various phenomenological groups, such as CKMfitter [206] and UTFit [242].

Table 25: Breakdown of B factory results on $S_{b \rightarrow c\bar{c}s}$ and $C_{b \rightarrow c\bar{c}s}$.

Mode		$N(B\bar{B})$	$-\eta S_{b \rightarrow c\bar{c}s}$	$C_{b \rightarrow c\bar{c}s}$
<i>BABAR</i>				
$J/\psi K_S^0$	[237]	465M	$0.657 \pm 0.036 \pm 0.012$	$0.026 \pm 0.025 \pm 0.016$
$J/\psi K_L^0$	[237]	465M	$0.694 \pm 0.061 \pm 0.031$	$-0.033 \pm 0.050 \pm 0.027$
$\mathbf{J/\psi K^0}$	[237]	465M	$0.666 \pm 0.031 \pm 0.013$	$0.016 \pm 0.023 \pm 0.018$
$\psi(2S)K_S^0$	[237]	465M	$0.897 \pm 0.100 \pm 0.036$	$0.089 \pm 0.076 \pm 0.020$
$\chi_{c1}K_S^0$	[237]	465M	$0.614 \pm 0.160 \pm 0.040$	$0.129 \pm 0.109 \pm 0.025$
$\eta_c K_S^0$	[237]	465M	$0.925 \pm 0.160 \pm 0.057$	$0.080 \pm 0.124 \pm 0.029$
$J/\psi K^{*0}(892)$	[237]	465M	$0.601 \pm 0.239 \pm 0.087$	$0.025 \pm 0.083 \pm 0.054$
All	[237]	465M	$0.687 \pm 0.028 \pm 0.012$	$0.024 \pm 0.020 \pm 0.016$
<i>Belle</i>				
$J/\psi K_S^0$	[235]	535M	$0.643 \pm 0.038_{\text{stat}}$	$0.001 \pm 0.028_{\text{stat}}$
$J/\psi K_L^0$	[235]	535M	$0.641 \pm 0.057_{\text{stat}}$	$-0.045 \pm 0.033_{\text{stat}}$
$\mathbf{J/\psi K^0}$	[235]	535M	$0.642 \pm 0.031 \pm 0.017$	$-0.018 \pm 0.021 \pm 0.014$
$\psi(2S)K_S^0$	[236]	657M	$0.718 \pm 0.090 \pm 0.033$	$-0.039 \pm 0.069 \pm 0.049$
All	[236]	–	$0.650 \pm 0.029 \pm 0.015$	–
$\mathbf{J/\psi K^0}$ average			0.655 ± 0.0244	-0.003 ± 0.020
$\mathbf{\psi(2S) K^0}$ average			0.798 ± 0.071	0.032 ± 0.060

4.4.2 Time-dependent transversity analysis of $B^0 \rightarrow J/\psi K^{*0}$

B meson decays to the vector-vector final state $J/\psi K^{*0}$ are also mediated by the $b \rightarrow c\bar{c}s$ transition. When a final state which is not flavour-specific ($K^{*0} \rightarrow K_S^0 \pi^0$) is used, a time-dependent transversity analysis can be performed allowing sensitivity to both $\sin(2\beta)$ and $\cos(2\beta)$ [243]. Such analyses have been performed by both B factory experiments. In principle, the strong phases between the transversity amplitudes are not uniquely determined by such an analysis, leading to a discrete ambiguity in the sign of $\cos(2\beta)$. The *BABAR* collaboration resolves this ambiguity using the known variation [244] of the P-wave phase (fast) relative to the S-wave phase (slow) with the invariant mass of the $K\pi$ system in the vicinity of the $K^*(892)$ resonance. The result is in agreement with the prediction from s quark helicity conservation, and corresponds to Solution II defined by Suzuki [245]. We use this phase convention for the averages given in Table 26.

 Table 26: Averages from $B^0 \rightarrow J/\psi K^{*0}$ transversity analyses.

Experiment		$N(B\bar{B})$	$\sin 2\beta$	$\cos 2\beta$	Correlation
<i>BABAR</i>	[246]	88M	$-0.10 \pm 0.57 \pm 0.14$	$3.32_{-0.96}^{+0.76} \pm 0.27$	-0.37
<i>Belle</i>	[234]	275M	$0.24 \pm 0.31 \pm 0.05$	$0.56 \pm 0.79 \pm 0.11$	0.22
Average			0.16 ± 0.28	1.64 ± 0.62	uncorrelated averages
Confidence level			0.61 (0.5σ)	0.03 (2.2σ)	

At present the results are dominated by large and non-Gaussian statistical errors, and

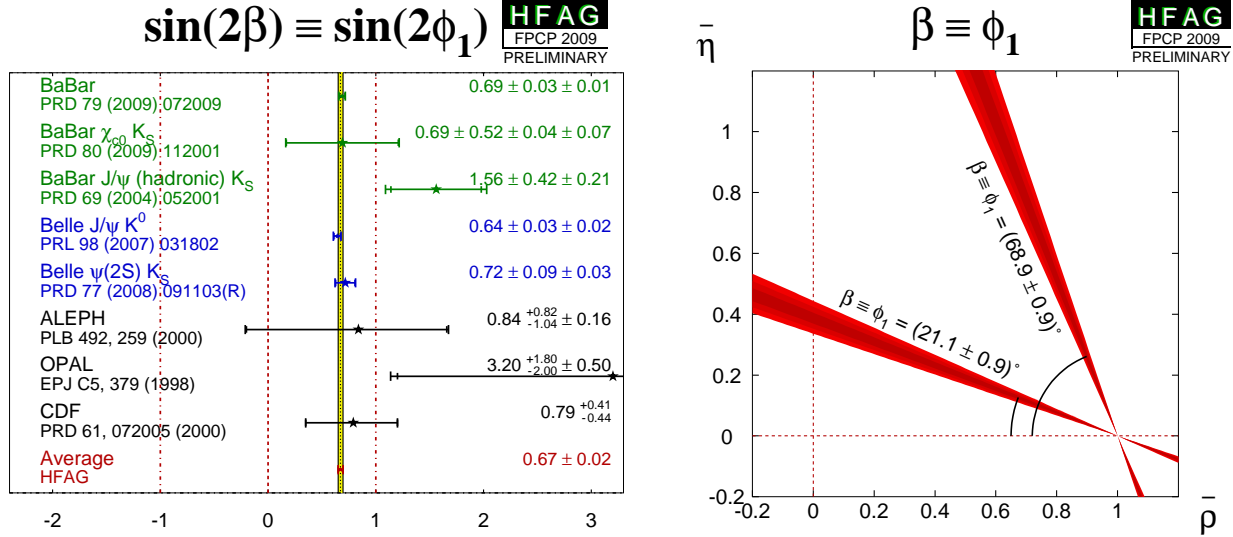


Figure 11: (Left) Average of measurements of $S_{b \to c \bar{c} s}$. (Right) Constraints on the $(\bar{\rho}, \bar{\eta})$ plane, obtained from the average of $-\eta S_{b \to c \bar{c} s}$ and Eq. 182.

exhibit significant correlations. We perform uncorrelated averages, the interpretation of which has to be done with the greatest care. Nonetheless, it is clear that $\cos(2\beta) > 0$ is preferred by the experimental data in $J/\psi K^*$. [BABAR [246] find a confidence level for $\cos(2\beta) > 0$ of 89%.]

4.4.3 Time-dependent CP asymmetries in $B^0 \rightarrow D^{*+} D^{*-} K_s^0$ decays

Both BABAR [189] and Belle [190] have performed time-dependent analyses of the $B^0 \rightarrow D^{*+} D^{*-} K_s^0$ decay, to obtain information on the sign of $\cos(2\beta)$. More information can be found in Sec. 4.2.4. The results are shown in Table 27, and Fig. 12.

Table 27: Results from time-dependent analysis of $B^0 \rightarrow D^{*+} D^{*-} K_s^0$.

Experiment	$N(B\bar{B})$	$\frac{J_c}{J_0}$	$\frac{2J_{s1}}{J_0} \sin(2\beta)$	$\frac{2J_{s2}}{J_0} \cos(2\beta)$
BABAR [189]	230M	$0.76 \pm 0.18 \pm 0.07$	$0.10 \pm 0.24 \pm 0.06$	$0.38 \pm 0.24 \pm 0.05$
Belle [190]	449M	$0.60^{+0.25}_{-0.28} \pm 0.08$	$-0.17 \pm 0.42 \pm 0.09$	$-0.23^{+0.43}_{-0.41} \pm 0.13$
Average		0.71 ± 0.16	0.03 ± 0.21	0.24 ± 0.22
Confidence level		$0.63 (0.5\sigma)$	$0.59 (0.5\sigma)$	$0.23 (1.2\sigma)$

From the above result and the assumption that $J_{s2} > 0$, BABAR infer that $\cos(2\beta) > 0$ at the 94% confidence level [189].

4.4.4 Time-dependent analysis of $B_s^0 \rightarrow J/\psi \phi$

As described in Sec. 4.2.6, time-dependent analysis of $B_s^0 \rightarrow J/\psi \phi$ probes the CP violating phase of $B_s^0 - \bar{B}_s^0$ oscillations, ϕ_s . Within the Standard Model, this parameter is predicted to be

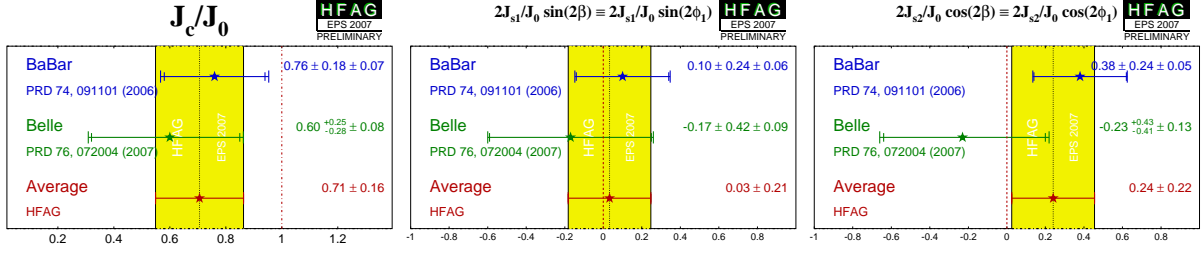


Figure 12: Averages of (left) (J_c/J_0) , (middle) $(2J_{s1}/J_0) \sin(2\beta)$ and (right) $(2J_{s2}/J_0) \cos(2\beta)$ from time-dependent analyses of $B^0 \rightarrow D^{*+} D^{*-} K_S^0$ decays.

small.²³

Both CDF [247, 248] and DØ [249, 248] have performed full tagged, time-dependent angular analyses of $B_s^0 \rightarrow J/\psi\phi$ decays. Both experiments perform analyses that take into account the correlations between the average B_s^0 lifetime $\tau(B_s^0)$, $\Delta\Gamma_s$, ϕ_s , the magnitude of the perpendicularly polarized component A_\perp , the difference in the fractions of the two CP -even components $|A_0|^2 - |A_\parallel|^2$, and the strong phases associated with the two CP -even components δ_0 and δ_\parallel . Both experiments find that the likelihood function has a highly non-Gaussian shape, so that central values and uncertainties are not presented. The combination of results is performed by the experiments themselves [248], and the results are summarised by the HFAG Lifetimes and Oscillations group, see Sec. 3.

²³ We make the approximation $\phi_s = 2\beta_s$, where $\phi_s \equiv \arg[-M_{12}/\Gamma_{12}]$ and $2\beta_s \equiv 2\arg[-(V_{ts}V_{tb}^*)/(V_{cs}V_{cb}^*)]$ (see Section 4.1). This is a reasonable approximation since, although the equality does not hold in the Standard Model [80], both are much smaller than the current experimental resolution, whereas new physics contributions add a phase ϕ_{NP} to ϕ_s and subtract the same phase from $2\beta_s$, so that the approximation remains valid.

4.5 Time-dependent CP asymmetries in colour-suppressed $b \rightarrow c\bar{u}d$ transitions

Decays of B mesons to final states such as $D\pi^0$ are governed by $b \rightarrow c\bar{u}d$ transitions. If the final state is a CP eigenstate, *e.g.* $D_{CP}\pi^0$, the usual time-dependence formulae are recovered, with the sine coefficient sensitive to $\sin(2\beta)$. Since there is no penguin contribution to these decays, there is even less associated theoretical uncertainty than for $b \rightarrow c\bar{c}s$ decays like $B \rightarrow J/\psi K_s^0$. Such measurements therefore allow to test the Standard Model prediction that the CP violation parameters in $b \rightarrow c\bar{u}d$ transitions are the same as those in $b \rightarrow c\bar{c}s$ [250].

Note that there is an additional contribution from CKM suppressed $b \rightarrow u\bar{c}d$ decays. The effect of this contribution is small, and can be taken into account in the analysis [251, 252].

Results of such an analysis are available from *BABAR* [253]. The decays $B^0 \rightarrow D\pi^0$, $B^0 \rightarrow D\eta$, $B^0 \rightarrow D\omega$, $B^0 \rightarrow D^*\pi^0$ and $B^0 \rightarrow D^*\eta$ are used. The daughter decay $D^* \rightarrow D\pi^0$ is used. The CP -even D decay to K^+K^- is used for all decay modes, with the CP -odd D decay to $K_s^0\omega$ also used in $B^0 \rightarrow D^{(*)}\pi^0$ and the additional CP -odd D decay to $K_s^0\pi^0$ also used in $B^0 \rightarrow D\omega$. Results are presented separately for CP -even and CP -odd $D^{(*)}$ decays (denoted $D_+^{(*)}h^0$ and $D_-^{(*)}h^0$ respectively), and for both combined, with the different CP factors accounted for (denoted $D_{CP}^{(*)}h^0$). The results are summarized in Table 28.

Table 28: Results from analyses of $B^0 \rightarrow D^{(*)}h^0$, $D \rightarrow CP$ eigenstates decays.

Experiment	$N(B\bar{B})$	S_{CP}	C_{CP}	Correlation	
		$D_+^{(*)}h^0$			
<i>BABAR</i>	[253]	383M	$-0.65 \pm 0.26 \pm 0.06$	$-0.33 \pm 0.19 \pm 0.04$	0.04
		$D_-^{(*)}h^0$			
<i>BABAR</i>	[253]	383M	$-0.46 \pm 0.46 \pm 0.13$	$-0.03 \pm 0.28 \pm 0.07$	-0.14
		$D_{CP}^{(*)}h^0$			
<i>BABAR</i>	[253]	383M	$-0.56 \pm 0.23 \pm 0.05$	$-0.23 \pm 0.16 \pm 0.04$	-0.02

When multibody D decays, such as $D \rightarrow K_s^0\pi^+\pi^-$ are used, a time-dependent analysis of the Dalitz plot of the neutral D decay allows a direct determination of the weak phase: 2β . (Equivalently, both $\sin(2\beta)$ and $\cos(2\beta)$ can be measured.) This information allows to resolve the ambiguity in the measurement of 2β from $\sin(2\beta)$ [254].

Results of such analyses are available from both Belle [186] and *BABAR* [187]. The decays $B \rightarrow D\pi^0$, $B \rightarrow D\eta$, $B \rightarrow D\omega$, $B \rightarrow D^*\pi^0$ and $B \rightarrow D^*\eta$ are used. [This collection of states is denoted by $D^{(*)}h^0$.] The daughter decays are $D^* \rightarrow D\pi^0$ and $D \rightarrow K_s^0\pi^+\pi^-$. The results are shown in Table 29, and Fig. 13. Note that *BABAR* quote uncertainties due to the D decay model separately from other systematic errors, while Belle do not.

Again, it is clear that the data prefer $\cos(2\beta) > 0$. Indeed, Belle [186] determine the sign of $\cos(2\phi_1)$ to be positive at 98.3% confidence level, while *BABAR* [187] favour the solution of β with $\cos(2\beta) > 0$ at 87% confidence level. Note, however, that the Belle measurement has strongly non-Gaussian behaviour. Therefore, we perform uncorrelated averages, from which any interpretation has to be done with the greatest care.

Table 29: Averages from $B^0 \rightarrow D^{(*)}h^0$, $D \rightarrow K_S\pi^+\pi^-$ analyses.

Experiment	$N(B\bar{B})$	$\sin 2\beta$	$\cos 2\beta$	$ \lambda $
BABAR [187]	383M	$0.29 \pm 0.34 \pm 0.03 \pm 0.05$	$0.42 \pm 0.49 \pm 0.09 \pm 0.13$	$1.01 \pm 0.08 \pm 0.02$
Belle [186]	386M	$0.78 \pm 0.44 \pm 0.22$	$1.87^{+0.40+0.22}_{-0.53-0.32}$	–
Average		0.45 ± 0.28	1.01 ± 0.40	1.01 ± 0.08
Confidence level		0.59 (0.5σ)	0.12 (1.6σ)	–

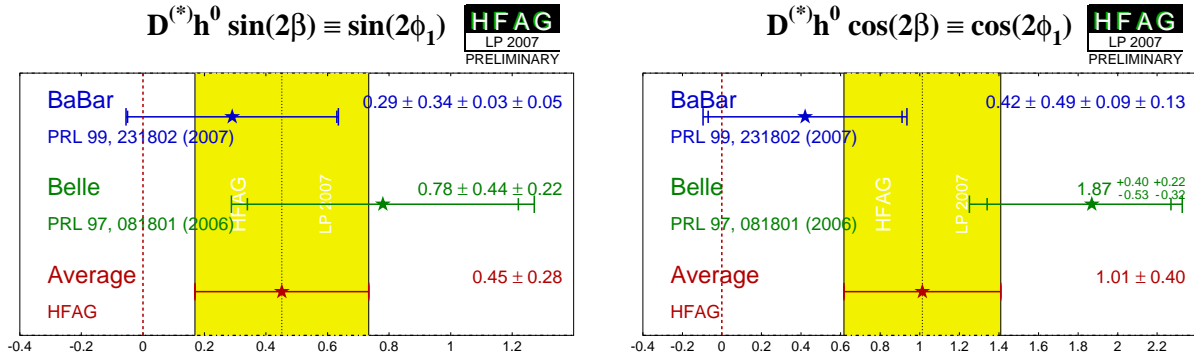


Figure 13: Averages of (left) $\sin(2\beta)$ and (right) $\cos(2\beta)$ measured in colour-suppressed $b \rightarrow c\bar{u}d$ transitions.

4.6 Time-dependent CP asymmetries in charmless $b \rightarrow q\bar{q}s$ transitions

The flavour changing neutral current $b \rightarrow s$ penguin can be mediated by any up-type quark in the loop, and hence the amplitude can be written as

$$\begin{aligned} A_{b \rightarrow s} &= F_u V_{ub} V_{us}^* + F_c V_{cb} V_{cs}^* + F_t V_{tb} V_{ts}^* \\ &= (F_u - F_c) V_{ub} V_{us}^* + (F_t - F_c) V_{tb} V_{ts}^* \\ &= \mathcal{O}(\lambda^4) + \mathcal{O}(\lambda^2) \end{aligned} \quad (183)$$

using the unitarity of the CKM matrix. Therefore, in the Standard Model, this amplitude is dominated by $V_{tb} V_{ts}^*$, and to within a few degrees ($\delta\beta \lesssim 2^\circ$ for $\beta \approx 20^\circ$) the time-dependent parameters can be written²⁴ $S_{b \rightarrow q\bar{q}s} \approx -\eta \sin(2\beta)$, $C_{b \rightarrow q\bar{q}s} \approx 0$, assuming $b \rightarrow s$ penguin contributions only ($q = u, d, s$).

Due to the large virtual mass scales occurring in the penguin loops, additional diagrams from physics beyond the Standard Model, with heavy particles in the loops, may contribute. In general, these contributions will affect the values of $S_{b \rightarrow q\bar{q}s}$ and $C_{b \rightarrow q\bar{q}s}$. A discrepancy between the values of $S_{b \rightarrow c\bar{c}s}$ and $S_{b \rightarrow q\bar{q}s}$ can therefore provide a clean indication of new physics [250, 255, 256, 257].

However, there is an additional consideration to take into account. The above argument assumes only the $b \rightarrow s$ penguin contributes to the $b \rightarrow q\bar{q}s$ transition. For $q = s$ this is a good assumption, which neglects only rescattering effects. However, for $q = u$ there is a colour-suppressed $b \rightarrow u$ tree diagram (of order $\mathcal{O}(\lambda^4)$), which has a different weak (and possibly strong) phase. In the case $q = d$, any light neutral meson that is formed from $d\bar{d}$ also has a $u\bar{u}$ component, and so again there is “tree pollution”. The B^0 decays to $\pi^0 K_s^0$, $\rho^0 K_s^0$ and ωK_s^0 belong to this category. The mesons ϕ , f_0 and η' are expected to have predominant $s\bar{s}$ parts, which reduces the relative size of the possible tree pollution. If the inclusive decay $B^0 \rightarrow K^+ K^- K^0$ (excluding ϕK^0) is dominated by a nonresonant three-body transition, an OZI-rule suppressed tree-level diagram can occur through insertion of an $s\bar{s}$ pair. The corresponding penguin-type transition proceeds via insertion of a $u\bar{u}$ pair, which is expected to be favored over the $s\bar{s}$ insertion by fragmentation models. Neglecting rescattering, the final state $K^0 \bar{K}^0 K^0$ (reconstructed as $K_s^0 K_s^0 K_s^0$) has no tree pollution [258]. Various estimates, using different theoretical approaches, of the values of $\Delta S = S_{b \rightarrow q\bar{q}s} - S_{b \rightarrow c\bar{c}s}$ exist in the literature [259, 260, 261, 262, 263, 264, 265, 266, 267, 268, 269, 270, 271, 272]. In general, there is agreement that the modes ϕK^0 , $\eta' K^0$ and $K^0 \bar{K}^0 K^0$ are the cleanest, with values of $|\Delta S|$ at or below the few percent level (ΔS is usually positive).

4.6.1 Time-dependent CP asymmetries: $b \rightarrow q\bar{q}s$ decays to CP eigenstates

The averages for $-\eta S_{b \rightarrow q\bar{q}s}$ and $C_{b \rightarrow q\bar{q}s}$ can be found in Table 30, and are shown in Figs. 14, 15 and 16. Results from both *BABAR* and *Belle* are averaged for the modes ϕK^0 , $\eta' K^0$, $f_0 K^0$ and $K^+ K^- K^0$ (K^0 indicates that both K_s^0 and K_L^0 are used, although *Belle* use neither $f_0 K_L^0$

²⁴ The presence of a small ($\mathcal{O}(\lambda^2)$) weak phase in the dominant amplitude of the s penguin decays introduces a phase shift given by $S_{b \rightarrow q\bar{q}s} = -\eta \sin(2\beta) \cdot (1 + \Delta)$. Using the CKMfitter results for the Wolfenstein parameters [206], one finds: $\Delta \simeq 0.033$, which corresponds to a shift of 2β of $+2.1$ degrees. Nonperturbative contributions can alter this result.

nor $K^+K^-K_L^0$, $K_S^0K_S^0K_S^0$, $\pi^0K_S^0$,²⁵ $\rho^0K_S^0$ and ωK_S^0 . *BABAR* also has presented results with the final states $\pi^0\pi^0K_S^0$,²⁶ $f_2K_S^0$, $f_XK_S^0$, $\pi^+\pi^-K_S^0$ nonresonant and $\phi K_S^0\pi^0$. Results for f_0K^0 , $K^+K^-K^0$, $\rho^0K_S^0$, $f_2K_S^0$, $f_XK_S^0$ and $\pi^+\pi^-K_S^0$ nonresonant are taken from time-dependent Dalitz plot analyses of $B^0 \rightarrow K^+K^-K^0$ and $B^0 \rightarrow \pi^+\pi^-K_S^0$ (see subsection 4.6.2). The results presented in Table 30 for f_0K^0 are for both experiments combinations of the results determined in the $K^+K^-K^0$ and $\pi^+\pi^-K_S^0$ final states.

Of these final states, ϕK_S^0 , $\eta'K_S^0$, $\pi^0K_S^0$, $\rho^0K_S^0$, ωK_S^0 and $f_0K_L^0$ have CP eigenvalue $\eta = -1$, while ϕK_L^0 , $\eta'K_L^0$, $K_S^0K_S^0K_S^0$, $f_0K_S^0$, $f_2K_S^0$, $f_XK_S^0$,²⁷ $\pi^0\pi^0K_S^0$ and $\pi^+\pi^-K_S^0$ nonresonant have $\eta = +1$.

The final state $K^+K^-K^0$ (contributions from ϕK^0 are implicitly excluded) is not a CP eigenstate. However, it can be treated as a quasi-two-body decay, with the CP composition determined using either an isospin argument (used by Belle to determine a CP -even fraction of $0.93 \pm 0.09 \pm 0.05$ [277]) or a moments analysis (previously used by *BABAR* to find a CP -even fractions of $0.89 \pm 0.08 \pm 0.06$ in $K^+K^-K_S^0$ [280]). Note that uncertainty in the CP composition of the final state leads to a third source of uncertainty on the Belle results for $-\eta S_{K^+K^-K^0}$. *BABAR* results for $K^+K^-K^0$ are determined from the inclusive “high-mass” ($m_{K^+K^-} > 1.1 \text{ GeV}/c^2$) region in their $B^0 \rightarrow K^+K^-K^0$ time-dependent Dalitz plot analysis [192] (this approach automatically corrects for the CP composition of the final state). Belle have also performed a time-dependent Dalitz plot analysis of $B^0 \rightarrow K^+K^-K^0$ [193], but the results presented in Table 30 are from their previous analysis [277].

The final state $\phi K_S^0\pi^0$ is also not a CP -eigenstate but its CP -composition can be determined from an angular analysis. Since the angular parameters are common to the $B^0 \rightarrow \phi K_S^0\pi^0$ and $B^0 \rightarrow \phi K^+\pi^-$ decays (because only $K\pi$ resonance contribute), *BABAR* perform a simultaneous analysis of the two final states [279] (see subsection 4.6.3).

It must be noted that Q2B parameters extracted from Dalitz plot analyses are constrained to lie within the physical boundary ($S_{CP}^2 + C_{CP}^2 < 1$) and consequently the obtained errors are highly non-Gaussian when the central value is close to the boundary. This is particularly evident in the *BABAR* results for $B^0 \rightarrow f_0K^0$ with $f_0 \rightarrow \pi^+\pi^-$ [196]. These results must be treated with extreme caution.

As explained above, each of the modes listed in Table 30 has different uncertainties within the Standard Model, and so each may have a different value of $-\eta S_{b \rightarrow q\bar{q}s}$. Therefore, there is no strong motivation to make a combined average over the different modes. We refer to such an average as a “naïve s -penguin average.” It is naïve not only because of the neglect of the theoretical uncertainty, but also since possible correlations of systematic effects between different modes are neglected. In spite of these caveats, there remains substantial interest in the value of this quantity, and therefore it is given here: $\langle -\eta S_{b \rightarrow q\bar{q}s} \rangle = 0.62 \pm 0.04$, with confidence level 0.18 (1.3σ). This value is in agreement with the average $-\eta S_{b \rightarrow c\bar{c}s}$ given in Sec. 4.4.1. (The average for $C_{b \rightarrow q\bar{q}s}$ is $\langle C_{b \rightarrow q\bar{q}s} \rangle = -0.05 \pm 0.03$ with confidence level 0.78 (0.3σ .) We emphasise again that we do not advocate the use of these averages, and that the values should be treated with *extreme caution*, if at all.

From Table 30 it may be noted that the average for $-\eta S_{b \rightarrow q\bar{q}s}$ in $\eta'K^0$ (0.59 ± 0.07), is now

²⁵ Belle [273] include the $\pi^0K_L^0$ final state in order to improve the constraint on the direct CP violation parameter; these events cannot be used for time-dependent analysis.

²⁶ We do not include a preliminary result from Belle [274], which remains unpublished after more than two years.

²⁷ The f_X is assumed to be spin even.

Table 30: Averages of $-\eta S_{b \rightarrow q\bar{q}s}$ and $C_{b \rightarrow q\bar{q}s}$.

Experiment	$N(B\bar{B})$	$-\eta S_{b \rightarrow q\bar{q}s}$	$C_{b \rightarrow q\bar{q}s}$	Correlation
ϕK^0				
BABAR	[192] 465M	$0.26 \pm 0.26 \pm 0.03$	$-0.14 \pm 0.19 \pm 0.02$	–
Belle	[193] 657M	$0.67^{+0.22}_{-0.32}$	$-0.31^{+0.21}_{-0.23} \pm 0.04 \pm 0.09$	–
Average		$0.44^{+0.17}_{-0.18}$	-0.23 ± 0.15	uncorrelated averages
$\eta' K^0$				
BABAR	[275] 467M	$0.57 \pm 0.08 \pm 0.02$	$-0.08 \pm 0.06 \pm 0.02$	0.03
Belle	[235] 535M	$0.64 \pm 0.10 \pm 0.04$	$0.01 \pm 0.07 \pm 0.05$	0.09
Average		0.59 ± 0.07	-0.05 ± 0.05	0.04
Confidence level		$0.63 (0.5\sigma)$		
$K_s^0 K_s^0 K_s^0$				
BABAR	[276] 465M	$0.90^{+0.18}_{-0.20} {}^{+0.03}_{-0.04}$	$-0.16 \pm 0.17 \pm 0.03$	0.10
Belle	[235] 535M	$0.30 \pm 0.32 \pm 0.08$	$-0.31 \pm 0.20 \pm 0.07$	–
Average		0.74 ± 0.17	-0.23 ± 0.13	0.06
Confidence level		$0.26 (1.1\sigma)$		
$\pi^0 K^0$				
BABAR	[275] 467M	$0.55 \pm 0.20 \pm 0.03$	$0.13 \pm 0.13 \pm 0.03$	0.06
Belle	[273] 657M	$0.67 \pm 0.31 \pm 0.08$	$-0.14 \pm 0.13 \pm 0.06$	–0.04
Average		0.57 ± 0.17	0.01 ± 0.10	0.02
Confidence level		$0.37 (0.9\sigma)$		
$\rho^0 K_s^0$				
BABAR	[196] 383M	$0.35^{+0.26}_{-0.31} \pm 0.06 \pm 0.03$	$-0.05 \pm 0.26 \pm 0.10 \pm 0.03$	–
Belle	[197] 657M	$0.64^{+0.19}_{-0.25} \pm 0.09 \pm 0.10$	$-0.03^{+0.24}_{-0.23} \pm 0.11 \pm 0.10$	–
Average		$0.54^{+0.18}_{-0.21}$	-0.06 ± 0.20	uncorrelated averages
ωK_s^0				
BABAR	[275] 467M	$0.55^{+0.26}_{-0.29} \pm 0.02$	$-0.52^{+0.22}_{-0.20} \pm 0.03$	0.03
Belle	[277] 535M	$0.11 \pm 0.46 \pm 0.07$	$0.09 \pm 0.29 \pm 0.06$	–0.04
Average		0.45 ± 0.24	-0.32 ± 0.17	0.01
Confidence level		$0.18 (1.3\sigma)$		
$f_0 K^0$				
BABAR	[192, 196] 0M	$0.60^{+0.16}_{-0.18}$	0.05 ± 0.16	–
Belle	[193, 197] 0M	$0.60^{+0.16}_{-0.19}$	0.05 ± 0.18	–
Average		$0.60^{+0.11}_{-0.13}$	0.05 ± 0.12	uncorrelated averages
$f_2 K_s^0$				
BABAR	[196] 383M	$0.48 \pm 0.52 \pm 0.06 \pm 0.10$	$0.28^{+0.35}_{-0.40} \pm 0.08 \pm 0.07$	–
$f_X K_s^0$				
BABAR	[196] 383M	$0.20 \pm 0.52 \pm 0.07 \pm 0.07$	$0.13^{+0.33}_{-0.35} \pm 0.04 \pm 0.09$	–

more than 5σ away from zero, so that CP violation in this mode is well established. Amongst other modes, CP violation effects in both $f_0 K^0$ and $K^+ K^- K^0$ appear to be established – BABAR have claimed 5.1σ observation of CP violation in $B^0 \rightarrow K^+ K^- K^0$ [191] and 4.3σ evidence of CP violation in $B^0 \rightarrow f_0 K_s^0$ with $f_0 \rightarrow \pi^+ \pi^-$ [196]. Due to possible non-Gaussian errors in

Table 31: Averages of $-\eta S_{b \rightarrow q\bar{q}s}$ and $C_{b \rightarrow q\bar{q}s}$ (continued).

Experiment	$N(B\bar{B})$	$-\eta S_{b \rightarrow q\bar{q}s}$	$C_{b \rightarrow q\bar{q}s}$	Correlation
		$\pi^0 \pi^0 K_s^0$		
<i>BABAR</i> [278]	227M	$-0.72 \pm 0.71 \pm 0.08$	$0.23 \pm 0.52 \pm 0.13$	-0.02
		$\phi K_s^0 \pi^0$		
<i>BABAR</i> [279]	465M	$0.97^{+0.03}_{-0.52}$	$-0.20 \pm 0.14 \pm 0.06$	-
		$\pi^+ \pi^- K_s^0$ nonresonant		
<i>BABAR</i> [196]	383M	$0.01 \pm 0.31 \pm 0.05 \pm 0.09$	$0.01 \pm 0.25 \pm 0.06 \pm 0.05$	-
		$K^+ K^- K^0$		
<i>BABAR</i> [192]	465M	$0.86 \pm 0.08 \pm 0.03$	$-0.05 \pm 0.09 \pm 0.04$	-
<i>Belle</i> [277]	535M	$0.68 \pm 0.15 \pm 0.03^{+0.21}_{-0.13}$	$0.09 \pm 0.10 \pm 0.05$	-
Average		0.82 ± 0.07	0.01 ± 0.07	uncorrelated averages

these results it may be prudent to defer any strong conclusions on the numerical significance of the averages. The average for $-\eta S_{b \rightarrow q\bar{q}s}$ in $K_s^0 K_s^0 K_s^0$ also appears to have significance greater than 4σ . There is no evidence (above 2σ) for direct CP violation in any $b \rightarrow q\bar{q}s$ mode.

4.6.2 Time-dependent Dalitz plot analyses: $B^0 \rightarrow K^+ K^- K^0$ and $B^0 \rightarrow \pi^+ \pi^- K_s^0$

As mentioned in Sec. 4.2.4 and above, both *BABAR* and *Belle* have performed time-dependent Dalitz plot analysis of $B^0 \rightarrow K^+ K^- K^0$ and $B^0 \rightarrow \pi^+ \pi^- K_s^0$ decays. The results are summarized in Tabs. 32 and 33. Averages for the $B^0 \rightarrow f_0 K_s^0$ decay, which contributes to both Dalitz plots, are shown in Fig. 17. Results are presented in terms of the effective weak phase (from mixing and decay) difference β^{eff} and the direct CP violation parameter \mathcal{A} ($\mathcal{A} = -C$) for each of the resonant contributions. Note that Dalitz plot analyses, including all those included in these averages, often suffer from ambiguous solutions – we quote the results corresponding to those presented as solution 1 in all cases. Results on flavour specific amplitudes that may contribute to these Dalitz plots (such as $K^{*+} \pi^-$) are averaged by the HFAG Rare Decays subgroup (Sec. 7).

 Table 32: Results from time-dependent Dalitz plot analysis of the $B^0 \rightarrow K^+ K^- K^0$ decay.

Experiment	$N(B\bar{B})$	$K^+ K^- K^0$ (whole Dalitz plot)	
		β^{eff}	\mathcal{A}
<i>BABAR</i> [192]	465M	$(25.3 \pm 3.9 \pm 0.9)^\circ$	$0.03 \pm 0.07 \pm 0.02$

Experiment	$N(B\bar{B})$	β^{eff}	ϕK^0	\mathcal{A}	β^{eff}	$f_0 K^0$	\mathcal{A}	$K^+ K^- K^0$ ($m_{K+K^-} > 1.1 \text{GeV}/c^2$)
								β^{eff}
<i>BABAR</i> [192]	465M	$(7.7 \pm 7.7 \pm 0.9)^\circ$	$0.14 \pm 0.19 \pm 0.02$		$(8.5 \pm 7.5 \pm 1.8)^\circ$	$0.01 \pm 0.26 \pm 0.07$		$(29.5 \pm 4.5 \pm 1.5)^\circ$
<i>Belle</i> [193]	657M	$(21.2^{+9.8}_{-10.4} \pm 2.0 \pm 2.0)^\circ$	$0.31^{+0.23}_{-0.23} \pm 0.04 \pm 0.09$		$(28.2^{+9.9}_{-9.8} \pm 2.0 \pm 2.0)^\circ$	$-0.02 \pm 0.34 \pm 0.08 \pm 0.09$		$0.05 \pm 0.09 \pm 0.04$
Average		$(12.9 \pm 5.6)^\circ$	0.23 ± 0.15		$(16.3 \pm 6.0)^\circ$	0.06 ± 0.19		
Confidence level					0.58 (0.6σ)			

From the results in Tab. 33, *BABAR* infer that the trigonometric reflection at $\pi/2 - \beta^{\text{eff}}$ in $B^0 \rightarrow K^+ K^- K^0$, which is inconsistent with the Standard Model expectation, is disfavoured at 4.8σ .

Table 33: Results from time-dependent Dalitz plot analysis of the $B^0 \rightarrow \pi^+\pi^-K_s^0$ decay.

Experiment	$N(B\bar{B})$	β^{eff}	$\rho^0 K_s^0$	\mathcal{A}	β^{eff}	$f_0 K_s^0$	\mathcal{A}
BABAR [196]	383M	$(10.2 \pm 8.9 \pm 3.0 \pm 1.9)^\circ$	$0.05 \pm 0.26 \pm 0.10 \pm 0.03$		$(36.0 \pm 9.8 \pm 2.1 \pm 2.1)^\circ$	$-0.08 \pm 0.19 \pm 0.03 \pm 0.04$	
Belle [197]	657M	$(20.0_{-8.5}^{+8.6} \pm 3.2 \pm 3.5)^\circ$	$0.03_{-0.24}^{+0.23} \pm 0.11 \pm 0.10$		$(12.7_{-6.5}^{+6.9} \pm 2.8 \pm 3.3)^\circ$	$-0.06 \pm 0.17 \pm 0.07 \pm 0.09$	
Average		16.4 ± 6.8	0.06 ± 0.20		20.6 ± 6.2		-0.07 ± 0.14
Confidence level		$0.39 (0.9\sigma)$					

Experiment	$N(B\bar{B})$	β^{eff}	$f_2 K_s^0$	\mathcal{A}	β^{eff}	$f_X K_s^0$	\mathcal{A}
BABAR [196]	383M	$(14.9 \pm 17.9 \pm 3.1 \pm 5.2)^\circ$	$-0.28_{-0.35}^{+0.40} \pm 0.08 \pm 0.07$		$(5.8 \pm 15.2 \pm 2.2 \pm 2.3)^\circ$	$-0.13_{-0.33}^{+0.35} \pm 0.04 \pm 0.09$	

Experiment	$N(B\bar{B})$	$B^0 \rightarrow \pi^+\pi^-K_s^0$ nonresonant	$\chi_{c0} K_s^0$	\mathcal{A}	
BABAR [196]	383M	β^{eff} $(0.4 \pm 8.8 \pm 1.9 \pm 3.8)^\circ$	$-0.01 \pm 0.25 \pm 0.06 \pm 0.05$	β^{eff} $(23.2 \pm 22.4 \pm 2.3 \pm 4.2)^\circ$	$0.29_{-0.53}^{+0.44} \pm 0.03 \pm 0.05$

4.6.3 Time-dependent analyses of $B^0 \rightarrow \phi K_s^0 \pi^0$

The final state in the decay $B^0 \rightarrow \phi K_s^0 \pi^0$ is a mixture of CP -even and CP -odd amplitudes. However, since only ϕK^{*0} resonant states contribute (in particular, $\phi K^{*0}(892)$, $\phi K_0^{*0}(1430)$ and $\phi K_2^{*0}(1430)$ are seen), the composition can be determined from the analysis of $B \rightarrow \phi K^+ \pi^-$, assuming only that the ratio of branching fractions $\mathcal{B}(K^{*0} \rightarrow K_s^0 \pi^0)/\mathcal{B}(K^{*0} \rightarrow K^+ \pi^-)$ is the same for each excited kaon state.

BABAR [279] have performed a simultaneous analysis of $B^0 \rightarrow \phi K_s^0 \pi^0$ and $B^0 \rightarrow \phi K^+ \pi^-$ that is time-dependent for the former mode and time-integrated for the latter. Such an analysis allows, in principle, all parameters of the $B^0 \rightarrow \phi K^{*0}$ system to be determined, including mixing-induced CP violation effects. The latter is determined to be $\Delta\phi_{00} = 0.28 \pm 0.42 \pm 0.04$, where $\Delta\phi_{00}$ is half the weak phase difference between B^0 and \bar{B}^0 decays to $\phi K_0^{*0}(1430)$. As discussed above, this can also be presented in terms of the quasi-two-body parameter $\sin(2\beta_{00}^{\text{eff}}) = \sin(2\beta + 2\Delta\phi_{00}) = 0.97_{-0.52}^{+0.03}$. The highly asymmetric uncertainty arises due to the conversion from the phase to the sine of the phase, and the proximity of the physical boundary.

Similar $\sin(2\beta^{\text{eff}})$ parameters can be defined for each of the helicity amplitudes for both $\phi K^{*0}(892)$ and $\phi K_2^{*0}(1430)$. However, the relative phases between these decays are constrained due to the nature of the simultaneous analysis of $B^0 \rightarrow \phi K_s^0 \pi^0$ and $B^0 \rightarrow \phi K^+ \pi^-$, and therefore these measurements are highly correlated. Instead of quoting all these results, BaBar provide an illustration of their measurements with the following differences:

$$\sin(2\beta - 2\Delta\delta_{01}) - \sin(2\beta) = -0.42_{-0.34}^{+0.26} \quad (184)$$

$$\sin(2\beta - 2\Delta\phi_{\parallel 1}) - \sin(2\beta) = -0.32_{-0.30}^{+0.22} \quad (185)$$

$$\sin(2\beta - 2\Delta\phi_{\perp 1}) - \sin(2\beta) = -0.30_{-0.32}^{+0.23} \quad (186)$$

$$\sin(2\beta - 2\Delta\phi_{\perp 1}) - \sin(2\beta - 2\Delta\phi_{\parallel 1}) = 0.02 \pm 0.23 \quad (187)$$

$$\sin(2\beta - 2\Delta\delta_{02}) - \sin(2\beta) = -0.10_{-0.29}^{+0.18} \quad (188)$$

where the first subscript indicates the helicity amplitude and the second indicates the spin of the kaon resonance. For the complete definitions of the $\Delta\delta$ and $\Delta\phi$ parameters, please refer to the BABAR paper [279].

Direct CP violation parameters for each of the contributing helicity amplitudes can also be measured. Again, these are determined from a simultaneous fit of $B^0 \rightarrow \phi K_S^0 \pi^0$ and $B^0 \rightarrow \phi K^+ \pi^-$, with the precision being dominated by the statistics of the latter mode. Direct CP violation measurements are tabulated by HFAG - Rare Decays (Sec. 7).

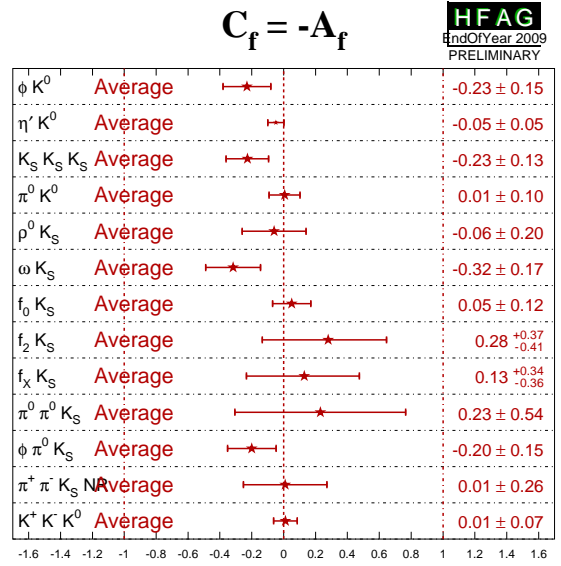
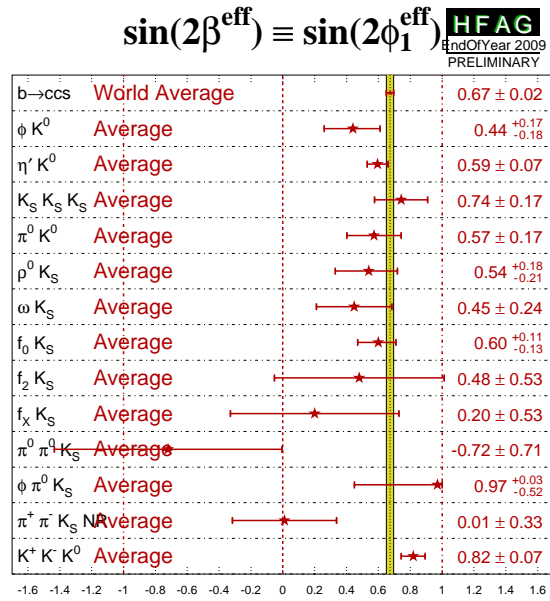
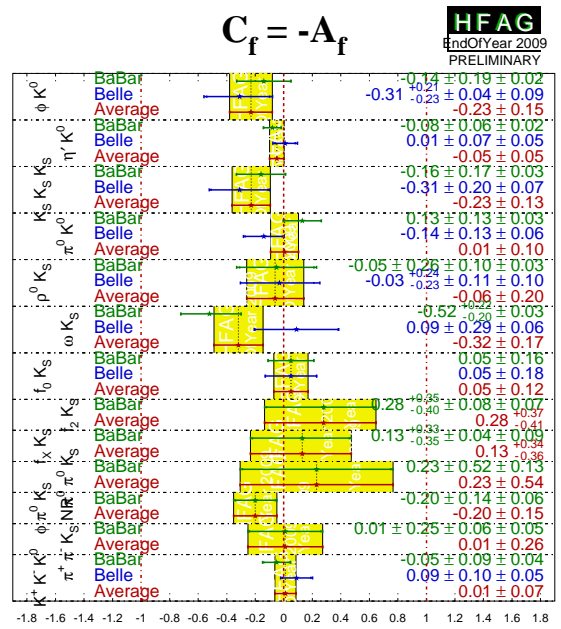
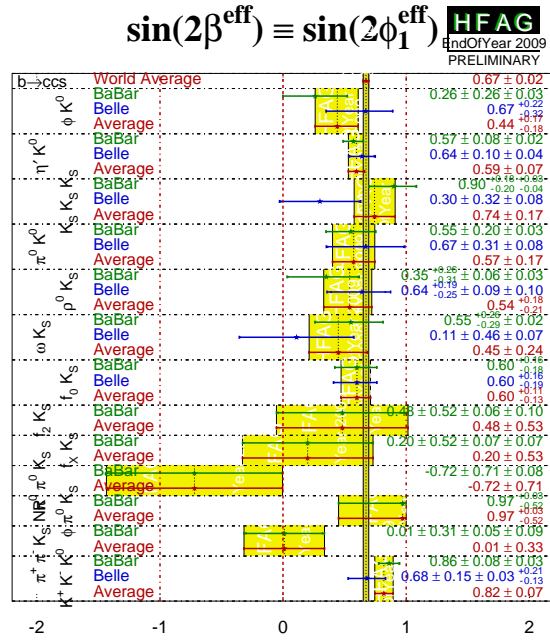


Figure 14: (Top) Averages of (left) $-\eta S_{b \rightarrow q\bar{q}s}$ and (right) $C_{b \rightarrow q\bar{q}s}$. The $-\eta S_{b \rightarrow q\bar{q}s}$ figure compares the results to the world average for $-\eta S_{b \rightarrow c\bar{c}s}$ (see Section 4.4.1). (Bottom) Same, but only averages for each mode are shown. More figures are available from the HFAG web pages.

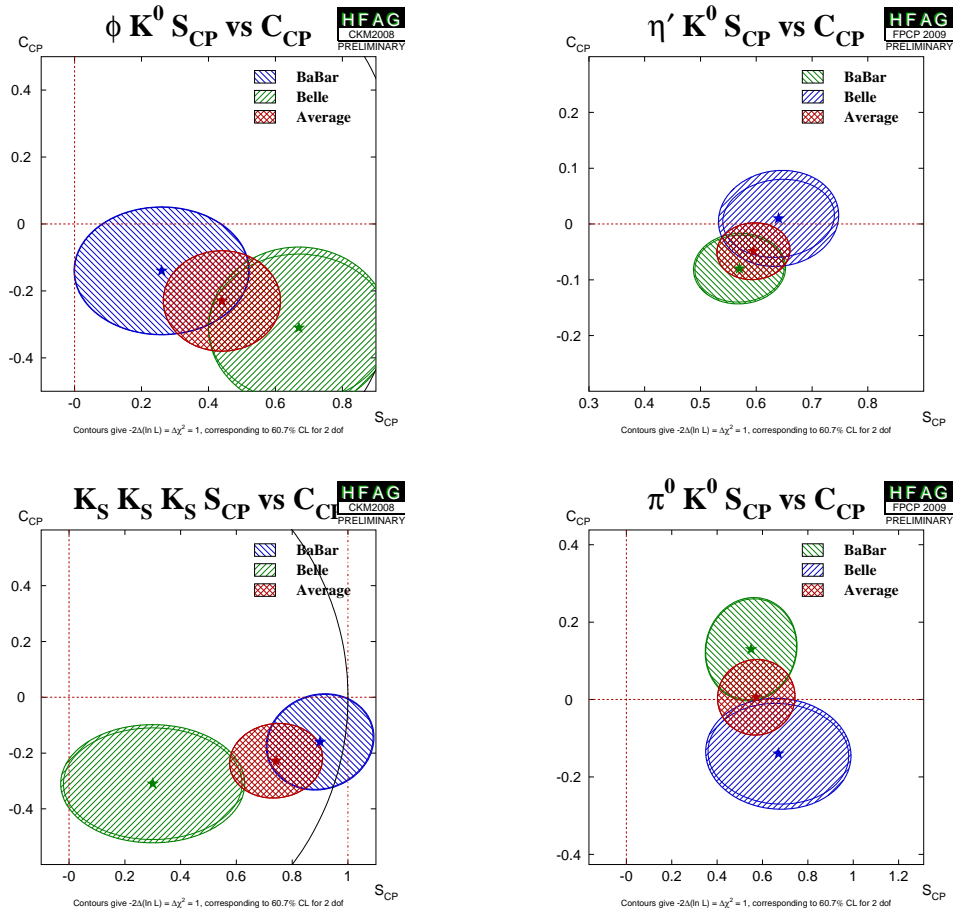


Figure 15: Averages of four $b \rightarrow q\bar{q}s$ dominated channels, for which correlated averages are performed, in the S_{CP} vs. C_{CP} plane, where S_{CP} has been corrected by the CP eigenvalue to give $\sin(2\beta^{\text{eff}})$. (Top left) $B^0 \rightarrow \phi K^0$, (top right) $B^0 \rightarrow \eta' K^0$, (bottom left) $B^0 \rightarrow K_S^0 K_S^0 K_S^0$, (bottom right) $B^0 \rightarrow \pi^0 K^0$. More figures are available from the HFAG web pages.

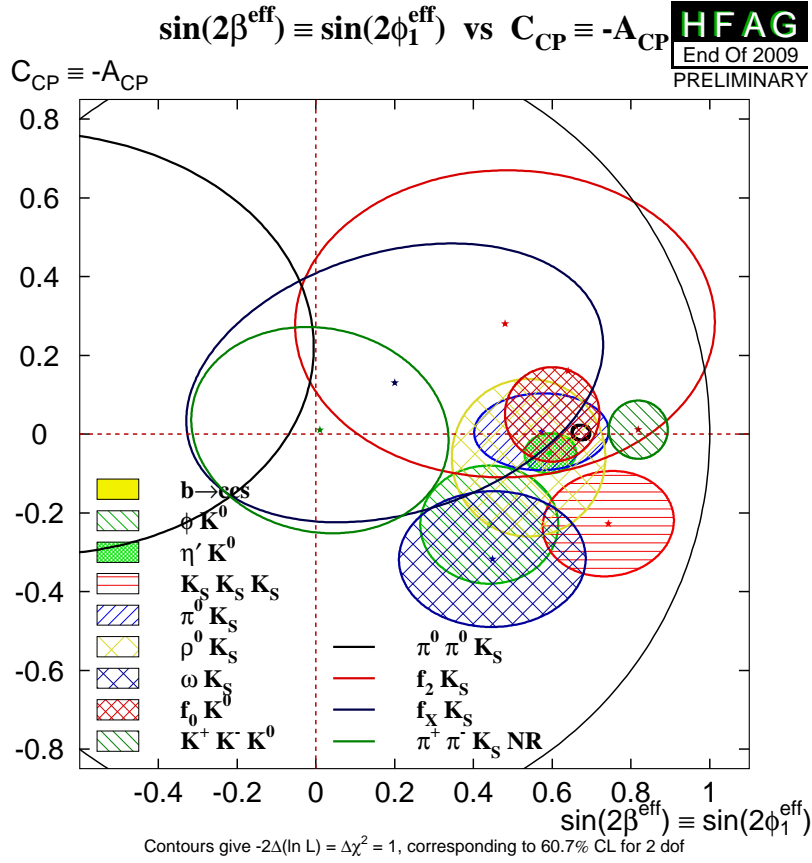


Figure 16: Compilation of constraints in the $-\eta S_{b \rightarrow q\bar{q}s}$ vs. $C_{b \rightarrow q\bar{q}s}$ plane.

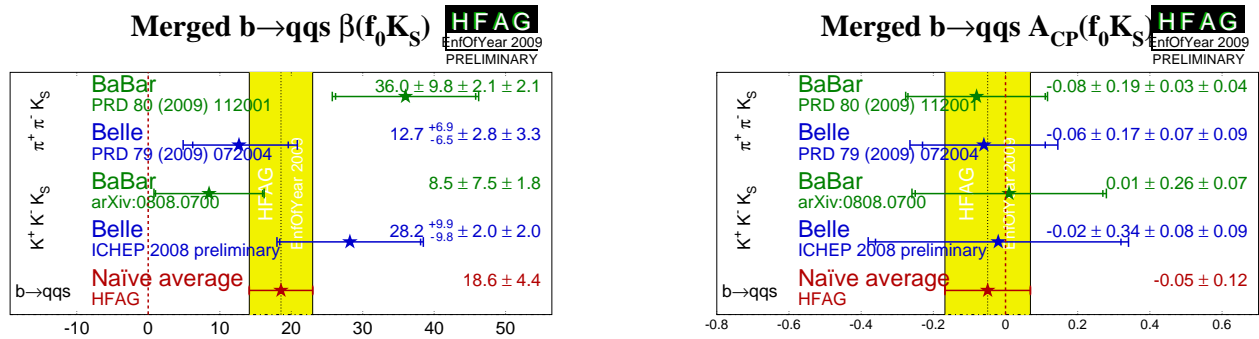


Figure 17: (Top) Averages of (left) $\beta^{\text{eff}} \equiv \phi_1^{\text{eff}}$ and (right) A_{CP} for the $B^0 \rightarrow f_0 K_S^0$ decay including measurements from Dalitz plot analyses of both $B^0 \rightarrow K^+ K^- K_S^0$ and $B^0 \rightarrow \pi^+ \pi^- K_S^0$.

4.7 Time-dependent CP asymmetries in $b \rightarrow c\bar{c}d$ transitions

The transition $b \rightarrow c\bar{c}d$ can occur via either a $b \rightarrow c$ tree or a $b \rightarrow d$ penguin amplitude. Similarly to Eq. (183), the amplitude for the $b \rightarrow d$ penguin can be written

$$\begin{aligned} A_{b \rightarrow d} &= F_u V_{ub} V_{ud}^* + F_c V_{cb} V_{cd}^* + F_t V_{tb} V_{td}^* \\ &= (F_u - F_c) V_{ub} V_{ud}^* + (F_t - F_c) V_{tb} V_{td}^* \\ &= \mathcal{O}(\lambda^3) + \mathcal{O}(\lambda^3). \end{aligned} \quad (189)$$

From this it can be seen that the $b \rightarrow d$ penguin amplitude contains terms with different weak phases at the same order of CKM suppression.

In the above, we have followed Eq. (183) by eliminating the F_c term using unitarity. However, we could equally well write

$$\begin{aligned} A_{b \rightarrow d} &= (F_u - F_t) V_{ub} V_{ud}^* + (F_c - F_t) V_{cb} V_{cd}^*, \\ &= (F_c - F_u) V_{cb} V_{cd}^* + (F_t - F_u) V_{tb} V_{td}^*. \end{aligned} \quad (190)$$

Since the $b \rightarrow c\bar{c}d$ tree amplitude has the weak phase of $V_{cb} V_{cd}^*$, either of the above expressions allow the penguin to be decomposed into parts with weak phases the same and different to the tree amplitude (the relative weak phase can be chosen to be either β or γ). However, if the tree amplitude dominates, there is little sensitivity to any phase other than that from $B^0 - \bar{B}^0$ mixing.

The $b \rightarrow c\bar{c}d$ transitions can be investigated with studies of various different final states. Results are available from both *BABAR* and Belle using the final states $J/\psi \pi^0$, $D^+ D^-$, $D^{*+} D^{*-}$ and $D^{*\pm} D^\mp$, the averages of these results are given in Table 34. The results using the CP eigenstate ($\eta = +1$) modes $J/\psi \pi^0$ and $D^+ D^-$ are shown in Fig. 18 and Fig. 19 respectively, with two-dimensional constraints shown in Fig. 20.

The vector-vector mode $D^{*+} D^{*-}$ is found to be dominated by the CP -even longitudinally polarized component; *BABAR* measures a CP -odd fraction of $0.158 \pm 0.028 \pm 0.006$ [185] while Belle measures a CP -odd fraction of $0.125 \pm 0.043 \pm 0.023$ [281]. These values, listed as R_\perp , are included in the averages which ensures the correlations to be taken into account.²⁸ *BABAR* have also performed an additional fit in which the CP -even and CP -odd components are allowed to have different CP violation parameters S and C . These results are included in Table 34. Results using $D^{*+} D^{*-}$ are shown in Fig. 21.

For the non- CP eigenstate mode $D^{*\pm} D^\mp$ *BABAR* uses fully reconstructed events while Belle combines both fully and partially reconstructed samples. At present we perform uncorrelated averages of the parameters in the $D^{*\pm} D^\mp$ system.

In the absence of the penguin contribution (tree dominance), the time-dependent parameters would be given by $S_{b \rightarrow c\bar{c}d} = -\eta \sin(2\beta)$, $C_{b \rightarrow c\bar{c}d} = 0$, $S_{+-} = \sin(2\beta + \delta)$, $S_{-+} = \sin(2\beta - \delta)$, $C_{+-} = -C_{-+}$ and $\mathcal{A} = 0$, where δ is the strong phase difference between the $D^{*+} D^-$ and $D^{*-} D^+$ decay amplitudes. In the presence of the penguin contribution, there is no clean interpretation in terms of CKM parameters, however direct CP violation may be observed as any of $C_{b \rightarrow c\bar{c}d} \neq 0$, $C_{+-} \neq -C_{-+}$ or $A_{+-} \neq 0$.

The averages for the $b \rightarrow c\bar{c}d$ modes are shown in Figs. 22 and 23. Results are consistent with tree dominance, and with the Standard Model, though the Belle results in $B^0 \rightarrow D^+ D^-$ [284]

²⁸ Note that the *BABAR* value given in Table 34 differs from that given above, since that in the table is not corrected for efficiency.

Table 34: Averages for the $b \rightarrow c\bar{c}d$ modes, $B^0 \rightarrow J/\psi\pi^0$, D^+D^- , $D^{*+}D^{*-}$ and $D^{*\pm}D^\mp$.

Experiment	$N(B\bar{B})$	S_{CP}	C_{CP}	Correlation		
$J/\psi\pi^0$						
BABAR [282]	466M	$-1.23 \pm 0.21 \pm 0.04$	$-0.20 \pm 0.19 \pm 0.03$	0.20		
Belle [283]	535M	$-0.65 \pm 0.21 \pm 0.05$	$-0.08 \pm 0.16 \pm 0.05$	-0.10		
Average		-0.93 ± 0.15	-0.10 ± 0.13	0.04		
Confidence level		0.15 (1.4 σ)				
D^+D^-						
BABAR [185]	467M	$-0.65 \pm 0.36 \pm 0.05$	$-0.07 \pm 0.23 \pm 0.03$	-0.01		
Belle [284]	535M	$-1.13 \pm 0.37 \pm 0.09$	$-0.91 \pm 0.23 \pm 0.06$	-0.04		
Average		-0.89 ± 0.26	-0.48 ± 0.17	-0.02		
Confidence level		0.025 (2.2 σ)				
Experiment	$N(B\bar{B})$	S_{CP}	C_{CP}	R_\perp		
$D^{*+}D^{*-}$						
BABAR [185]	467M	$-0.71 \pm 0.16 \pm 0.03$	$0.05 \pm 0.09 \pm 0.02$	0.17 ± 0.03		
Belle [281]	657M	$-0.96 \pm 0.25^{+0.12}_{-0.16}$	$-0.15 \pm 0.13 \pm 0.04$	$0.12 \pm 0.04 \pm 0.02$		
Average		-0.77 ± 0.14	-0.02 ± 0.08	0.16 ± 0.02		
Confidence level		0.41 (0.8 σ)				
Experiment	$N(B\bar{B})$	S_{CP+}	C_{CP+}	S_{CP-}	C_{CP-}	R_\perp
$D^{*+}D^{*-}$						
BABAR [185]	467M	$-0.76 \pm 0.16 \pm 0.04$	$0.02 \pm 0.12 \pm 0.02$	$-1.81 \pm 0.71 \pm 0.16$	$0.41 \pm 0.50 \pm 0.08$	0.15 ± 0.03
Experiment	$N(B\bar{B})$	S_{+-}	C_{+-}	S_{-+}	C_{-+}	\mathcal{A}
$D^{*\pm}D^\mp$						
BABAR [185]	467M	$-0.63 \pm 0.21 \pm 0.03$	$0.08 \pm 0.17 \pm 0.04$	$-0.74 \pm 0.23 \pm 0.05$	$0.00 \pm 0.17 \pm 0.03$	$0.01 \pm 0.05 \pm 0.01$
Belle [207]	152M	$-0.55 \pm 0.39 \pm 0.12$	$-0.37 \pm 0.22 \pm 0.06$	$-0.96 \pm 0.43 \pm 0.12$	$0.23 \pm 0.25 \pm 0.06$	$0.07 \pm 0.08 \pm 0.04$
Average		-0.61 ± 0.19	-0.09 ± 0.14	-0.79 ± 0.21	0.07 ± 0.14	0.02 ± 0.04
Confidence level		0.86 (0.2 σ)	0.12 (1.6 σ)	0.66 (0.4 σ)	0.46 (0.7 σ)	0.54 (0.6 σ)

show an indication of direct CP violation, and hence a non-zero penguin contribution. The average of $S_{b \rightarrow c\bar{c}d}$ in both $J/\psi\pi^0$ and $D^{*+}D^{*-}$ final states is more than 5σ from zero, corresponding to observations of CP violation in these decay channels., That in the D^+D^- final state is more than 3σ from zero; however, due to the large uncertainty and possible non-Gaussian effects, any strong conclusion should be deferred.

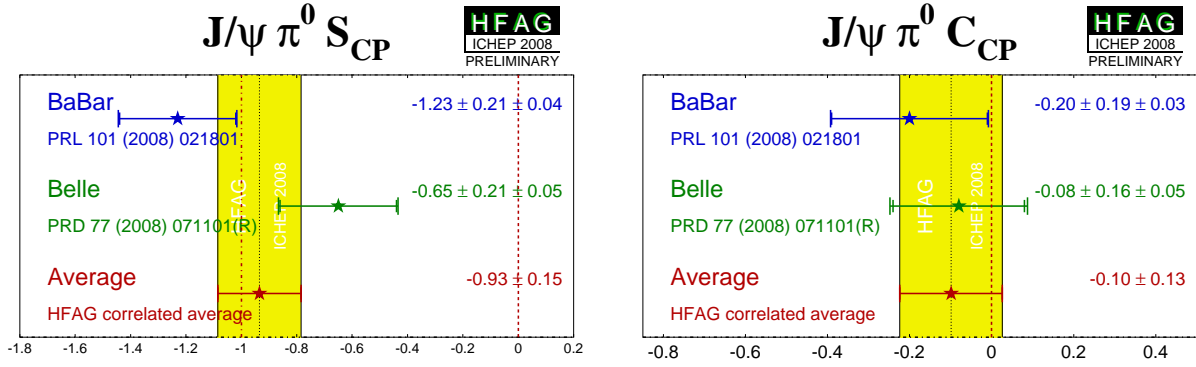


Figure 18: Averages of (left) $S_{b \rightarrow c\bar{c}d}$ and (right) $C_{b \rightarrow c\bar{c}d}$ for the mode $B^0 \rightarrow J/\psi\pi^0$.

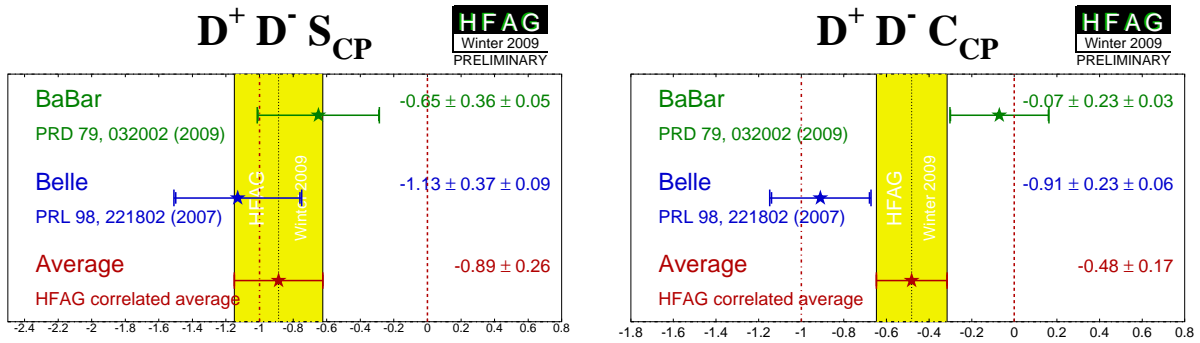


Figure 19: Averages of (left) $S_{b \rightarrow c\bar{c}d}$ and (right) $C_{b \rightarrow c\bar{c}d}$ for the mode $B^0 \rightarrow D^+D^-$.

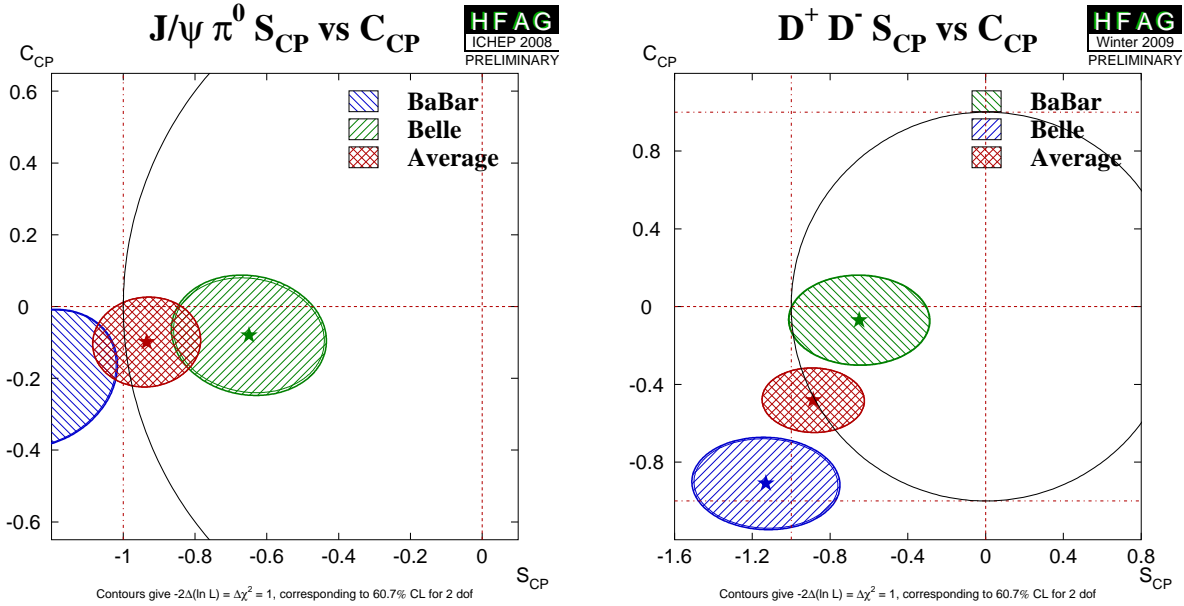


Figure 20: Averages of two $b \rightarrow c\bar{c}d$ dominated channels, for which correlated averages are performed, in the S_{CP} vs. C_{CP} plane. (Left) $B^0 \rightarrow J/\psi\pi^0$ and (right) $B^0 \rightarrow D^+D^-$.

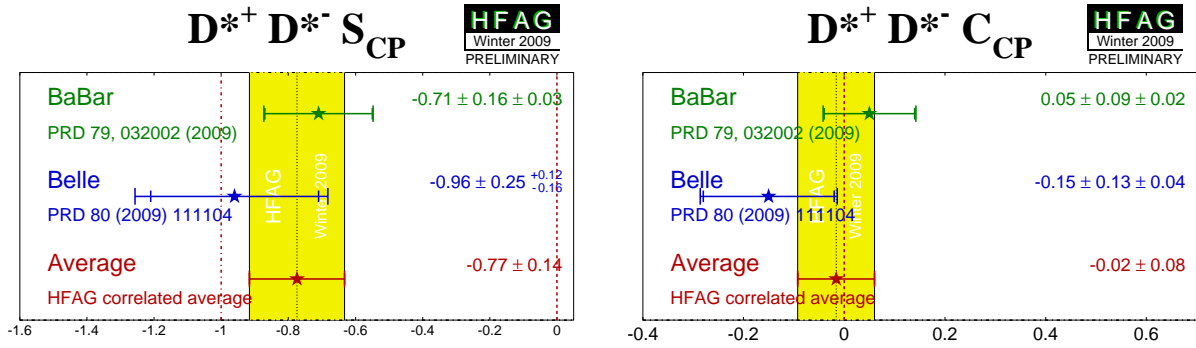


Figure 21: Averages of (left) $S_{b \rightarrow c\bar{c}d}$ and (right) $C_{b \rightarrow c\bar{c}d}$ for the mode $B^0 \rightarrow D^{*+} D^{*-}$.

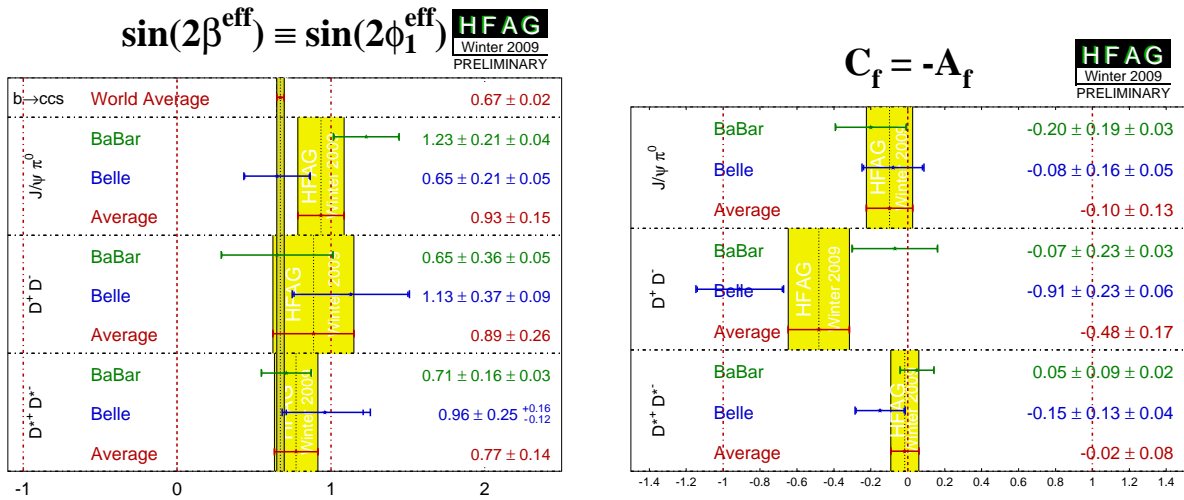


Figure 22: Averages of (left) $-\eta S_{b \rightarrow c\bar{c}d}$ and (right) $C_{b \rightarrow c\bar{c}d}$. The $-\eta S_{b \rightarrow q\bar{q}s}$ figure compares the results to the world average for $-\eta S_{b \rightarrow c\bar{c}s}$ (see Section 4.4.1).

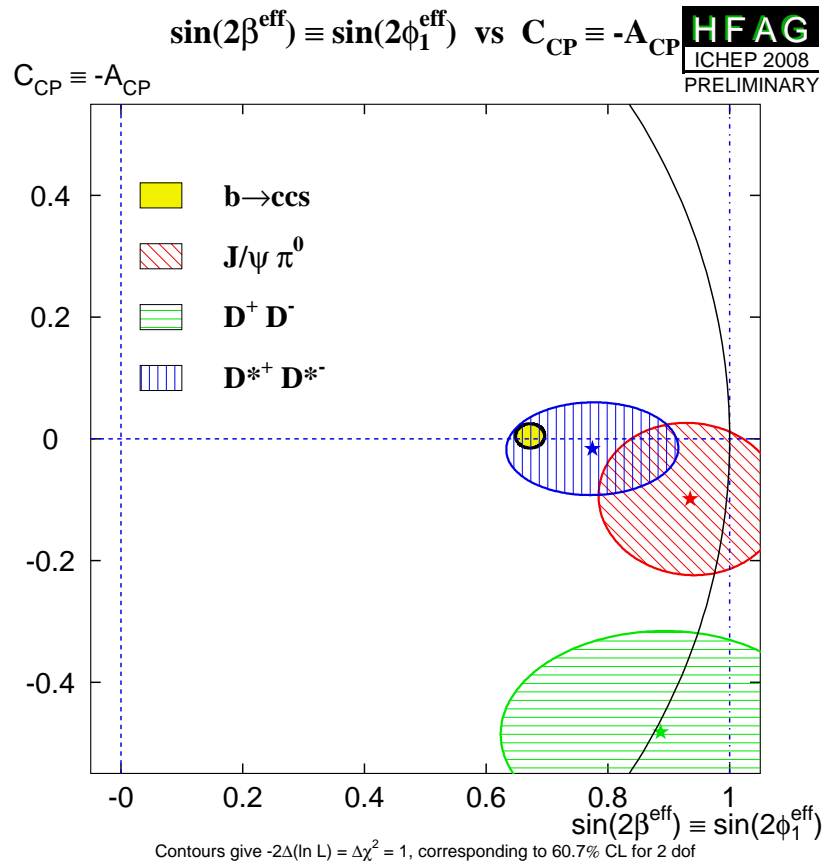


Figure 23: Compilation of constraints in the $-\eta S_{b \rightarrow c\bar{c}d}$ vs. $C_{b \rightarrow c\bar{c}d}$ plane.

4.8 Time-dependent CP asymmetries in $b \rightarrow q\bar{q}d$ transitions

Decays such as $B^0 \rightarrow K_S^0 K_S^0$ are pure $b \rightarrow q\bar{q}d$ penguin transitions. As shown in Eq. 189, this diagram has different contributing weak phases, and therefore the observables are sensitive to the difference (which can be chosen to be either β or γ). Note that if the contribution with the top quark in the loop dominates, the weak phase from the decay amplitudes should cancel that from mixing, so that no CP violation (neither mixing-induced nor direct) occurs. Non-zero contributions from loops with intermediate up and charm quarks can result in both types of effect (as usual, a strong phase difference is required for direct CP violation to occur).

Both *BABAR* [285] and Belle [286] have performed time-dependent analyses of $B^0 \rightarrow K_S^0 K_S^0$. The results are shown in Table 35 and Fig. 24.

Table 35: Results for $B^0 \rightarrow K_S^0 K_S^0$.

Experiment	$N(B\bar{B})$	S_{CP}	C_{CP}	Correlation
<i>BABAR</i> [285]	350M	$-1.28^{+0.80+0.11}_{-0.73-0.16}$	$-0.40 \pm 0.41 \pm 0.06$	-0.32
Belle [286]	657M	$-0.38^{+0.69}_{-0.77} \pm 0.09$	$0.38 \pm 0.38 \pm 0.05$	0.48
Average		-1.08 ± 0.49	-0.06 ± 0.26	0.14
Confidence level		0.29 (1.1 σ)		

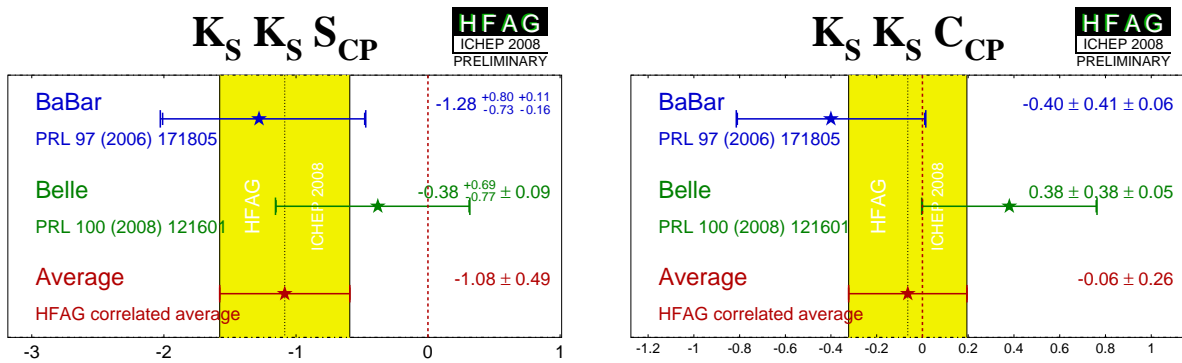


Figure 24: Averages of (left) $S_{b \rightarrow q\bar{q}d}$ and (right) $C_{b \rightarrow q\bar{q}d}$ for the mode $B^0 \rightarrow K_S^0 K_S^0$.

4.9 Time-dependent asymmetries in $b \rightarrow s\gamma$ transitions

The radiative decays $b \rightarrow s\gamma$ produce photons which are highly polarized in the Standard Model. The decays $B^0 \rightarrow F\gamma$ and $\bar{B}^0 \rightarrow F\gamma$ produce photons with opposite helicities, and since the polarization is, in principle, observable, these final states cannot interfere. The finite mass of the s quark introduces small corrections to the limit of maximum polarization, but any large mixing induced CP violation would be a signal for new physics. Since a single weak phase dominates the $b \rightarrow s\gamma$ transition in the Standard Model, the cosine term is also expected to be small.

Atwood *et al.* [217] have shown that an inclusive analysis with respect to $K_s^0\pi^0\gamma$ can be performed, since the properties of the decay amplitudes are independent of the angular momentum of the $K_s^0\pi^0$ system. However, if non-dipole operators contribute significantly to the amplitudes, then the Standard Model mixing-induced CP violation could be larger than the naïve expectation $S \simeq -2(m_s/m_b)\sin(2\beta)$ [218, 219]. In this case, the CP parameters may vary over the $K_s^0\pi^0\gamma$ Dalitz plot, for example as a function of the $K_s^0\pi^0$ invariant mass. Explicit calculations indicate such corrections are small for exclusive final states [220, 221].

With the above in mind, we quote two averages: one for $K^*(892)$ candidates only, and the other one for the inclusive $K_s^0\pi^0\gamma$ decay (including the $K^*(892)$). If the Standard Model dipole operator is dominant, both should give the same quantities (the latter naturally with smaller statistical error). If not, care needs to be taken in interpretation of the inclusive parameters, while the results on the $K^*(892)$ resonance remain relatively clean. Results from *BABAR* [287] and Belle [288] are used for both averages; both experiments use the invariant mass range $0.60 \text{ GeV}/c^2 < M_{K_s^0\pi^0} < 1.80 \text{ GeV}/c^2$ in the inclusive analysis. In addition to the $K_s^0\pi^0\gamma$ decay, *BABAR* have presented results using $K_s^0\eta\gamma$ [289], and Belle have presented results using $K_s^0\rho\gamma$ [290].

Table 36: Averages for $b \rightarrow s\gamma$ modes.

Experiment	$N(B\bar{B})$	$S_{CP}(b \rightarrow s\gamma)$	$C_{CP}(b \rightarrow s\gamma)$	Correlation
$K^*(892)\gamma$				
<i>BABAR</i> [287]	467M	$-0.03 \pm 0.29 \pm 0.03$	$-0.14 \pm 0.16 \pm 0.03$	0.05
Belle [288]	535M	$-0.32^{+0.36}_{-0.33} \pm 0.05$	$0.20 \pm 0.24 \pm 0.05$	0.08
Average		-0.16 ± 0.22	-0.04 ± 0.14	0.06
Confidence level		0.40 (0.9 σ)		
$K_s^0\pi^0\gamma$ (including $K^*(892)\gamma$)				
<i>BABAR</i> [287]	467M	$-0.17 \pm 0.26 \pm 0.03$	$-0.19 \pm 0.14 \pm 0.03$	0.04
Belle [288]	535M	$-0.10 \pm 0.31 \pm 0.07$	$0.20 \pm 0.20 \pm 0.06$	0.08
Average		-0.15 ± 0.20	-0.07 ± 0.12	0.05
Confidence level		0.30 (1.0 σ)		
$K_s^0\eta\gamma$				
<i>BABAR</i> [289]	465M	$-0.18^{+0.49}_{-0.46} \pm 0.12$	$-0.32^{+0.40}_{-0.39} \pm 0.07$	-0.17
$K_s^0\rho^0\gamma$				
Belle [290]	657M	$0.11 \pm 0.33^{+0.05}_{-0.09}$	$-0.05 \pm 0.18 \pm 0.06$	0.04

The results are shown in Table 36, and in Figs. 25 and 26. No significant CP violation results are seen; the results are consistent with the Standard Model and with other measurements in

the $b \rightarrow s\gamma$ system (see Sec. 7).

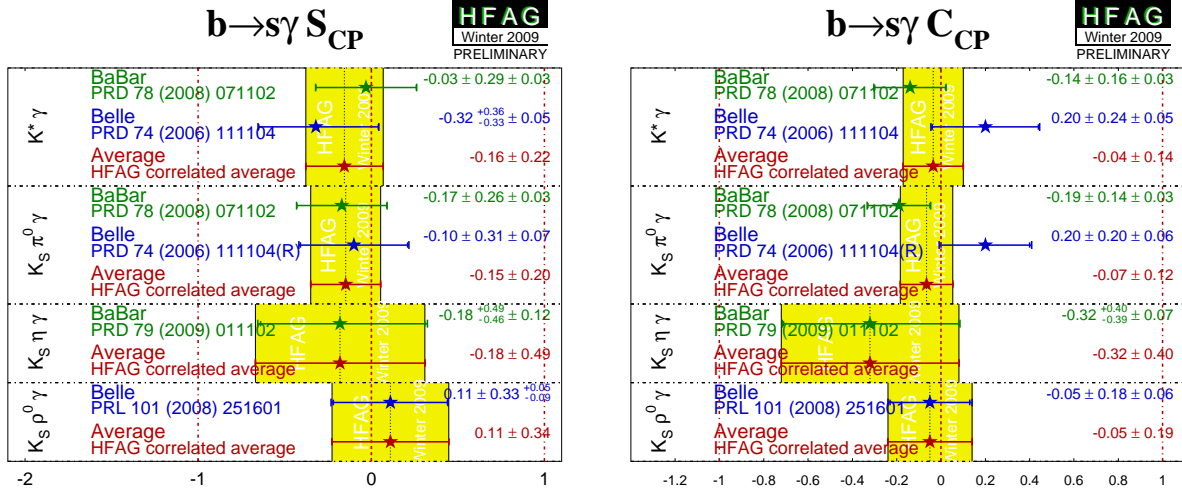


Figure 25: Averages of (left) $S_{b \rightarrow s\gamma}$ and (right) $C_{b \rightarrow s\gamma}$. Recall that the data for $K^*\gamma$ is a subset of that for $K_S^0\pi^0\gamma$.

4.10 Time-dependent asymmetries in $b \rightarrow d\gamma$ transitions

The formalism for the radiative decays $b \rightarrow d\gamma$ is much the same as that for $b \rightarrow s\gamma$ discussed above. Assuming dominance of the top quark in the loop, the weak phase in decay should cancel with that from mixing, so that the mixing-induced CP violation parameter S_{CP} should be very small. Corrections due to the finite light quark mass are smaller compared to $b \rightarrow s\gamma$, since $m_d < m_s$, and although QCD corrections may still play a role, they cannot significantly affect the prediction $S_{b \rightarrow d\gamma} \simeq 0$. Large direct CP violation effects could, however, be seen through a non-zero value of $C_{b \rightarrow d\gamma}$, since the top loop is not the only contribution.

Results using the mode $B^0 \rightarrow \rho^0\gamma$ are available from Belle and are shown in Table 37.

Table 37: Averages for $B^0 \rightarrow \rho^0\gamma$.

Experiment	$N(BB)$	S_{CP}	C_{CP}	Correlation
Belle [291]	657M	$-0.83 \pm 0.65 \pm 0.18$	$0.44 \pm 0.49 \pm 0.14$	-0.08

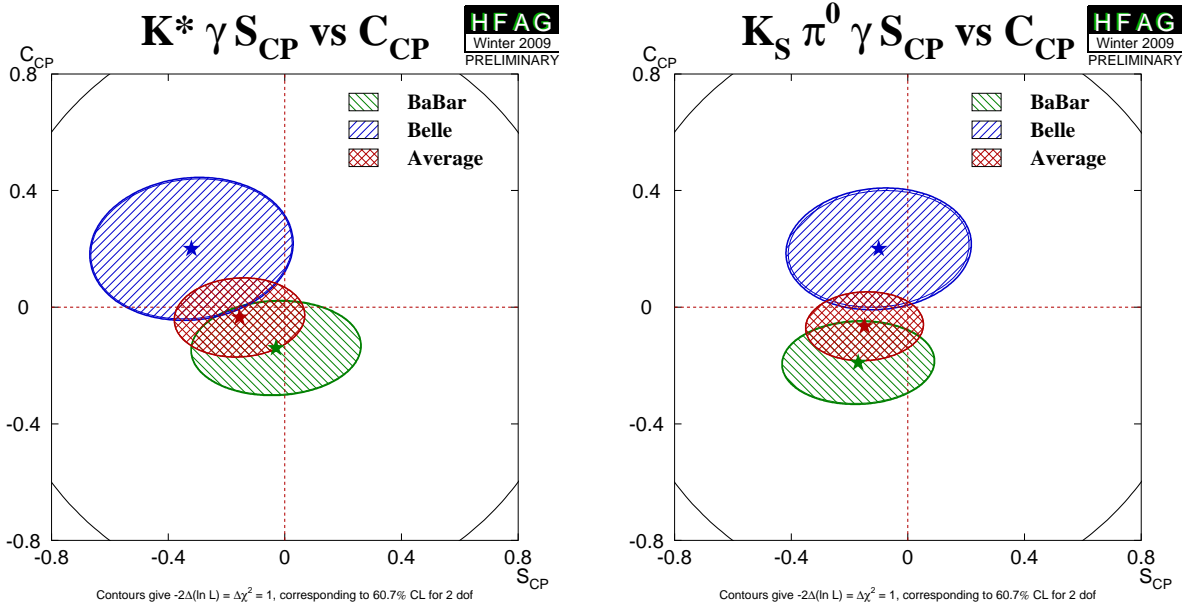


Figure 26: Averages of $b \rightarrow s\gamma$ dominated channels, for which correlated averages are performed, in the S_{CP} vs. C_{CP} plane. (Left) $B^0 \rightarrow K^*\gamma$ and (right) $B^0 \rightarrow K_S^0\pi^0\gamma$ (including $K^*\gamma$).

4.11 Time-dependent CP asymmetries in $b \rightarrow u\bar{u}d$ transitions

The $b \rightarrow u\bar{u}d$ transition can be mediated by either a $b \rightarrow u$ tree amplitude or a $b \rightarrow d$ penguin amplitude. These transitions can be investigated using the time dependence of B^0 decays to final states containing light mesons. Results are available from both *BABAR* and Belle for the CP eigenstate ($\eta = +1$) $\pi^+\pi^-$ final state and for the vector-vector final state $\rho^+\rho^-$, which is found to be dominated by the CP -even longitudinally polarized component (*BABAR* measure $f_{\text{long}} = 0.992 \pm 0.024^{+0.026}_{-0.013}$ [292] while Belle measure $f_{\text{long}} = 0.941^{+0.034}_{-0.040} \pm 0.030$ [293]). *BABAR* have also performed a time-dependent analysis of the vector-vector final state $\rho^0\rho^0$ [294], in which they measure $f_{\text{long}} = 0.70 \pm 0.14 \pm 0.05$; Belle measures a smaller branching fraction than *BABAR* for $B^0 \rightarrow \rho^0\rho^0$ [295] with corresponding signal yields too small to perform time-dependent or angular analyses. *BABAR* have furthermore performed a time-dependent analysis of the $B^0 \rightarrow a_1^\pm\pi^\mp$ decay [296]; further experimental input for the extraction of α from this channel is reported in a later publication [297].

Results, and averages, of time-dependent CP -violation parameters in $b \rightarrow u\bar{u}d$ transitions are listed in Table 38. The averages for $\pi^+\pi^-$ are shown in Fig. 27, and those for $\rho^+\rho^-$ are shown in Fig. 28, with the averages in the S_{CP} vs. C_{CP} plane shown in Fig. 29.

Table 38: Averages for $b \rightarrow u\bar{u}d$ modes.

Experiment	$N(B\bar{B})$	S_{CP}	C_{CP}	Correlation		
$\pi^+\pi^-$						
<i>BABAR</i> [298]	467M	$-0.68 \pm 0.10 \pm 0.03$	$-0.25 \pm 0.08 \pm 0.02$	-0.06		
Belle [299]	535M	$-0.61 \pm 0.10 \pm 0.04$	$-0.55 \pm 0.08 \pm 0.05$	-0.15		
Average		-0.65 ± 0.07	-0.38 ± 0.06	-0.08		
Confidence level		0.055 (1.9σ)				
$\rho^+\rho^-$						
<i>BABAR</i> [292]	387M	$-0.17 \pm 0.20^{+0.05}_{-0.06}$	$0.01 \pm 0.15 \pm 0.06$	-0.04		
Belle [300]	535M	$0.19 \pm 0.30 \pm 0.07$	$-0.16 \pm 0.21 \pm 0.07$	0.10		
Average		-0.05 ± 0.17	-0.06 ± 0.13	0.01		
Confidence level		0.50 (0.7σ)				
$\rho^0\rho^0$						
<i>BABAR</i> [294]	465M	$0.30 \pm 0.70 \pm 0.20$	$0.20 \pm 0.80 \pm 0.30$	-0.04		
Experiment	$N(B\bar{B})$	A_{CP}	C	S	ΔC	ΔS
$a_1^\pm\pi^\mp$						
<i>BABAR</i> [296]	384M	$-0.07 \pm 0.07 \pm 0.02$	$-0.10 \pm 0.15 \pm 0.09$	$0.37 \pm 0.21 \pm 0.07$	$0.26 \pm 0.15 \pm 0.07$	$-0.14 \pm 0.21 \pm 0.06$

If the penguin contribution is negligible, the time-dependent parameters for $B^0 \rightarrow \pi^+\pi^-$ and $B^0 \rightarrow \rho^+\rho^-$ are given by $S_{b \rightarrow u\bar{u}d} = \eta \sin(2\alpha)$ and $C_{b \rightarrow u\bar{u}d} = 0$. In the presence of the penguin contribution, direct CP violation may arise, and there is no straightforward interpretation of $S_{b \rightarrow u\bar{u}d}$ and $C_{b \rightarrow u\bar{u}d}$. An isospin analysis [301] can be used to disentangle the contributions and extract α .

For the non- CP eigenstate $\rho^\pm\pi^\mp$, both *BABAR* [203] and Belle [204, 205] have performed time-dependent Dalitz plot (DP) analyses of the $\pi^+\pi^-\pi^0$ final state [201]; such analyses allow direct measurements of the phases. Both experiments have measured the U and I parameters

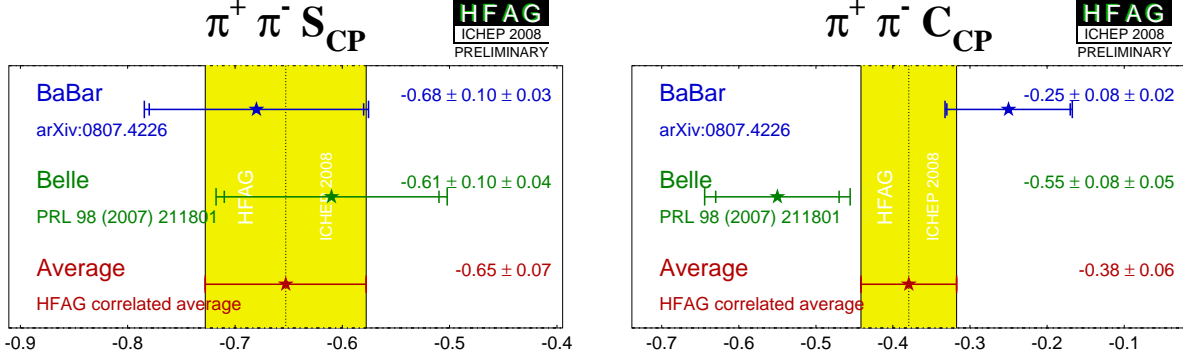


Figure 27: Averages of (left) $S_{b \rightarrow u\bar{u}d}$ and (right) $C_{b \rightarrow u\bar{u}d}$ for the mode $B^0 \rightarrow \pi^+ \pi^-$.

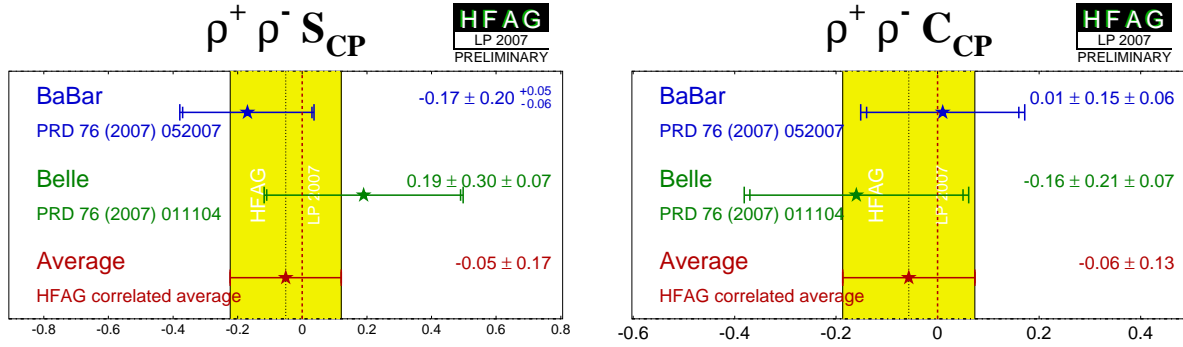


Figure 28: Averages of (left) $S_{b \rightarrow u\bar{u}d}$ and (right) $C_{b \rightarrow u\bar{u}d}$ for the mode $B^0 \rightarrow \rho^+ \rho^-$.

discussed in Sec. 4.2.4 and defined in Table 19. We have performed a full correlated average of these parameters, the results of which are summarized in Fig. 30.

Both experiments have also extracted the Q2B parameters. We have performed a full correlated average of these parameters, which is equivalent to determining the values from the averaged U and I parameters. The results are shown in Table. 39. Averages of the $B^0 \rightarrow \rho^0 \pi^0$ Q2B parameters are shown in Figs. 31 and 32.

With the notation described in Sec. 4.2 (Eq. (158)), the time-dependent parameters for the Q2B $B^0 \rightarrow \rho^\pm \pi^\mp$ analysis are, neglecting penguin contributions, given by

$$S_{\rho\pi} = \sqrt{1 - \left(\frac{\Delta C}{2}\right)^2} \sin(2\alpha) \cos(\delta), \quad \Delta S_{\rho\pi} = \sqrt{1 - \left(\frac{\Delta C}{2}\right)^2} \cos(2\alpha) \sin(\delta) \quad (191)$$

and $C_{\rho\pi} = \mathcal{A}_{CP}^{\rho\pi} = 0$, where $\delta = \arg(A_{-+} A_{+-}^*)$ is the strong phase difference between the $\rho^- \pi^+$ and $\rho^+ \pi^-$ decay amplitudes. In the presence of the penguin contribution, there is no straightforward interpretation of the Q2B observables in the $B^0 \rightarrow \rho^\pm \pi^\mp$ system in terms of CKM parameters. However direct CP violation may arise, resulting in either or both of $C_{\rho\pi} \neq 0$ and $\mathcal{A}_{CP}^{\rho\pi} \neq 0$. Equivalently, direct CP violation may be seen by either of the decay-type-specific observables $\mathcal{A}_{\rho\pi}^{+-}$ and $\mathcal{A}_{\rho\pi}^{-+}$, defined in Eq. (159), deviating from zero. Results and averages for these parameters are also given in Table 39. Averages of the direct CP violation effect in

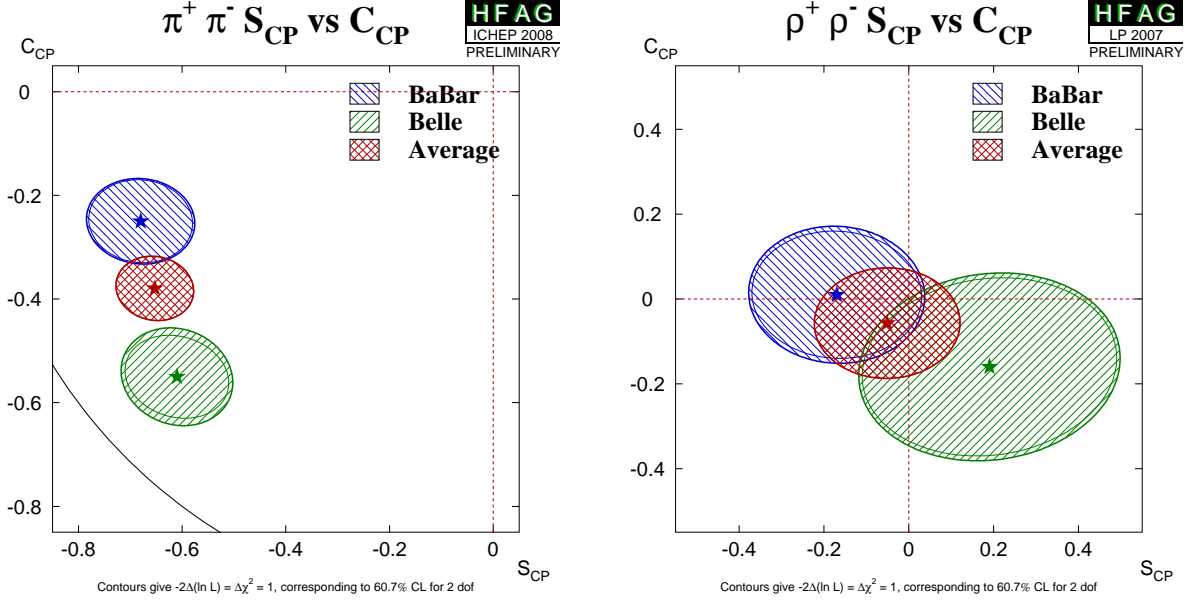


Figure 29: Averages of $b \rightarrow u\bar{u}d$ dominated channels, for which correlated averages are performed, in the S_{CP} vs. C_{CP} plane. (Left) $B^0 \rightarrow \pi^+\pi^-$ and (right) $B^0 \rightarrow \rho^+\rho^-$.

$B^0 \rightarrow \rho^\pm\pi^\mp$ are shown in Fig. 33, both in $\mathcal{A}_{CP}^{\rho\pi}$ vs. $C_{\rho\pi}$ space and in $\mathcal{A}_{\rho\pi}^{-+}$ vs. $\mathcal{A}_{\rho\pi}^{+-}$ space.

Some difference is seen between the *BABAR* and Belle measurements in the $\pi^+\pi^-$ system. The confidence level of the average is 0.034, which corresponds to a 2.1σ discrepancy. Since there is no evidence of systematic problems in either analysis, we do not rescale the errors of the averages. The averages for $S_{b \rightarrow u\bar{u}d}$ and $C_{b \rightarrow u\bar{u}d}$ in $B^0 \rightarrow \pi^+\pi^-$ are both more than 5σ away from zero, suggesting that both mixing-induced and direct CP violation are well-established in this channel. Nonetheless, due to the possible discrepancy mentioned above, a slightly cautious interpretation should be made with regard to the significance of direct CP violation.

In $B^0 \rightarrow \rho^\pm\pi^\mp$, however, both experiments see an indication of direct CP violation in the $\mathcal{A}_{CP}^{\rho\pi}$ parameter (as seen in Fig. 33). The average is more than 3σ from zero, providing evidence of direct CP violation in this channel.

Constraints on α

The precision of the measured CP violation parameters in $b \rightarrow u\bar{u}d$ transitions allows constraints to be set on the UT angle α . Constraints have been obtained with various methods:

- Both *BABAR* [302] and Belle [299] have performed isospin analyses in the $\pi\pi$ system. Belle exclude $9^\circ < \phi_2 < 81^\circ$ at the 95.4% C.L. while *BABAR* give a confidence level interpretation for α , exclude the range $23^\circ < \alpha < 67^\circ$ at the 90% C.L. In both cases, only solutions in 0° – 180° are considered.
- Both experiments have also performed isospin analyses in the $\rho\rho$ system. The most recent result from *BABAR* is given in an update of the measurements of the $B^+ \rightarrow \rho^+\rho^0$ decay [303], and sets the constraint $\alpha = (92.4^{+6.0}_{-6.5})^\circ$. The most recent result from Belle is given in an update of the search for the $B^0 \rightarrow \rho^0\rho^0$ decay and sets the constraint $\phi_2 = (91.7 \pm 14.9)^\circ$ [295].

Table 39: Averages of quasi-two-body parameters extracted from time-dependent Dalitz plot analysis of $B^0 \rightarrow \pi^+\pi^-\pi^0$.

Experiment	$N(B\bar{B})$	$\mathcal{A}_{CP}^{\rho\pi}$	$C_{\rho\pi}$	$S_{\rho\pi}$	$\Delta C_{\rho\pi}$	$\Delta S_{\rho\pi}$
<i>BABAR</i> [203]	375M	$-0.14 \pm 0.05 \pm 0.02$	$0.15 \pm 0.09 \pm 0.05$	$-0.03 \pm 0.11 \pm 0.04$	$0.39 \pm 0.09 \pm 0.09$	$-0.01 \pm 0.14 \pm 0.06$
Belle [204, 205]	449M	$-0.12 \pm 0.05 \pm 0.04$	$-0.13 \pm 0.09 \pm 0.05$	$0.06 \pm 0.13 \pm 0.05$	$0.36 \pm 0.10 \pm 0.05$	$-0.08 \pm 0.13 \pm 0.05$
Average		-0.13 ± 0.04	0.01 ± 0.07	0.01 ± 0.09	0.37 ± 0.08	-0.04 ± 0.10
Confidence level				$0.52 (0.6\sigma)$		

Experiment	$N(B\bar{B})$	$\mathcal{A}_{\rho\pi}^{-+}$	$\mathcal{A}_{\rho\pi}^{+-}$	Correlation
<i>BABAR</i> [203]	375M	$-0.37^{+0.16}_{-0.10} \pm 0.09$	$0.03 \pm 0.07 \pm 0.04$	0.62
Belle [204, 205]	449M	$0.08 \pm 0.16 \pm 0.11$	$0.21 \pm 0.08 \pm 0.04$	0.47
Average		-0.18 ± 0.12	0.11 ± 0.06	0.40
Confidence level			$0.14 (1.5\sigma)$	

Experiment	$N(B\bar{B})$	$C_{\rho^0\pi^0}$	$S_{\rho^0\pi^0}$	Correlation
<i>BABAR</i> [203]	375M	$-0.10 \pm 0.40 \pm 0.53$	$0.04 \pm 0.44 \pm 0.18$	0.35
Belle [204, 205]	449M	$0.49 \pm 0.36 \pm 0.28$	$0.17 \pm 0.57 \pm 0.35$	0.08
Average		0.30 ± 0.38	0.12 ± 0.38	0.12
Confidence level			$0.76 (0.3\sigma)$	

- Each experiment has obtained a value of α from combining its results in the different $b \rightarrow u\bar{u}d$ modes (with some input also from HFAG). These values have appeared in talks, but not in publications, and are not listed here.
- The CKMfitter [206] and UTFit [242] groups use the measurements from Belle and *BABAR* given above with other branching fractions and CP asymmetries in $B \rightarrow \pi\pi$, $\rho\pi$ and $\rho\rho$ modes, to perform isospin analyses for each system, and to make combined constraints on α .

Note that methods based on isospin symmetry make extensive use of measurements of branching fractions and direct CP asymmetries, as averaged by the HFAG Rare Decays subgroup (Sec. 7). Note also that each method suffers from discrete ambiguities in the solutions. The model assumption in the $B^0 \rightarrow \pi^+\pi^-\pi^0$ analysis allows to resolve some of the multiple solutions, and results in a single preferred value for α in $[0, \pi]$. All the above measurements correspond to the choice that is in agreement with the global CKM fit.

At present we make no attempt to provide an HFAG average for α . More details on procedures to calculate a best fit value for α can be found in Refs. [206, 242].

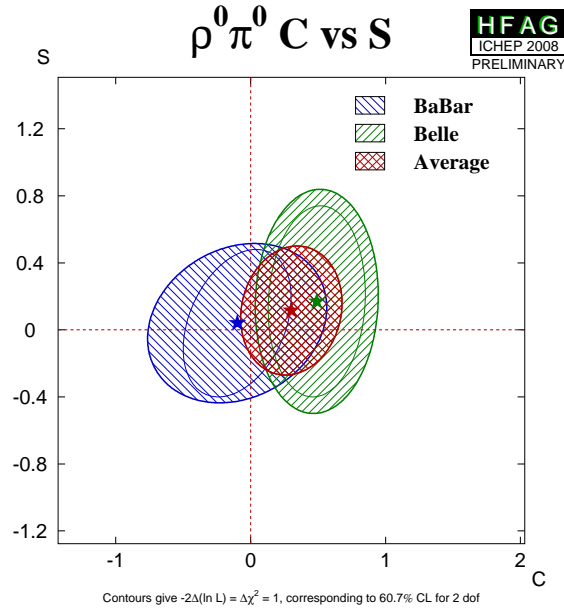


Figure 32: Averages of $b \rightarrow u\bar{u}d$ dominated channels, for the mode $B^0 \rightarrow \rho^0\pi^0$ in the S_{CP} vs. C_{CP} plane.

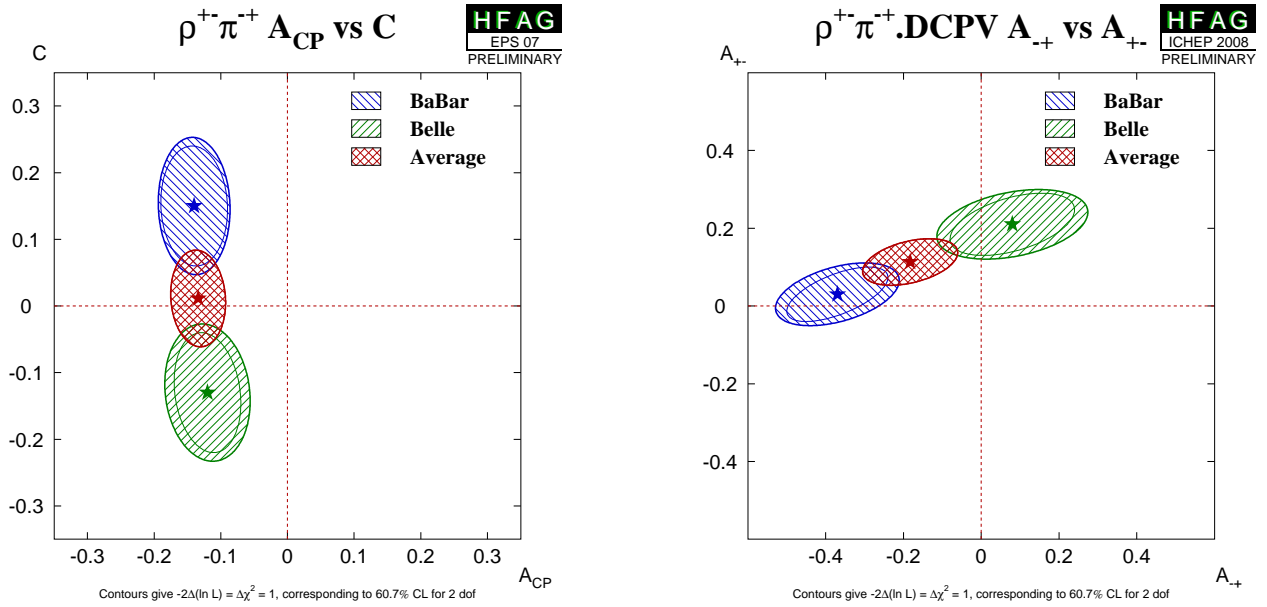


Figure 33: Direct CP violation in $B^0 \rightarrow \rho^\pm\pi^\mp$. (Left) $\mathcal{A}_{CP}^{\rho\pi}$ vs. $C_{\rho\pi}$ space, (right) $\mathcal{A}_{\rho\pi}^{-+}$ vs. $\mathcal{A}_{\rho\pi}^{+-}$ space.

4.12 Time-dependent CP asymmetries in $b \rightarrow c\bar{u}d/u\bar{c}d$ transitions

Non- CP eigenstates such as $D^\pm\pi^\mp$, $D^{*\pm}\pi^\mp$ and $D^\pm\rho^\mp$ can be produced in decays of B^0 mesons either via Cabibbo favoured ($b \rightarrow c$) or doubly Cabibbo suppressed ($b \rightarrow u$) tree amplitudes. Since no penguin contribution is possible, these modes are theoretically clean. The ratio of the magnitudes of the suppressed and favoured amplitudes, R , is sufficiently small (predicted to be about 0.02), that terms of $\mathcal{O}(R^2)$ can be neglected, and the sine terms give sensitivity to the combination of UT angles $2\beta + \gamma$.

As described in Sec. 4.2.5, the averages are given in terms of parameters a and c . CP violation would appear as $a \neq 0$. Results are available from both *BABAR* and Belle in the modes $D^\pm\pi^\mp$ and $D^{*\pm}\pi^\mp$; for the latter mode both experiments have used both full and partial reconstruction techniques. Results are also available from *BABAR* using $D^\pm\rho^\mp$. These results, and their averages, are listed in Table 40, and are shown in Fig. 34. The constraints in c vs. a space for the $D\pi$ and $D^*\pi$ modes are shown in Fig. 35. It is notable that the average value of a from $D^*\pi$ is more than 3σ from zero, providing evidence of CP violation in this channel.

Table 40: Averages for $b \rightarrow c\bar{u}d/u\bar{c}d$ modes.

Experiment		$N(BB)$	a	c
$D^\pm\pi^\mp$				
<i>BABAR</i> (full rec.)	[210]	232M	$-0.010 \pm 0.023 \pm 0.007$	$-0.033 \pm 0.042 \pm 0.012$
Belle (full rec.)	[214]	386M	$-0.050 \pm 0.021 \pm 0.012$	$-0.019 \pm 0.021 \pm 0.012$
Average			-0.030 ± 0.017	-0.022 ± 0.021
Confidence level			0.24 (1.2 σ)	0.78 (0.3 σ)
$D^{*\pm}\pi^\mp$				
<i>BABAR</i> (full rec.)	[210]	232M	$-0.040 \pm 0.023 \pm 0.010$	$0.049 \pm 0.042 \pm 0.015$
<i>BABAR</i> (partial rec.)	[211]	232M	$-0.034 \pm 0.014 \pm 0.009$	$-0.019 \pm 0.022 \pm 0.013$
Belle (full rec.)	[214]	386M	$-0.039 \pm 0.020 \pm 0.013$	$-0.011 \pm 0.020 \pm 0.013$
Belle (partial rec.)	[213]	657M	$-0.047 \pm 0.014 \pm 0.012$	$-0.009 \pm 0.014 \pm 0.012$
Average			-0.040 ± 0.010	-0.007 ± 0.012
Confidence level			0.96 (0.0 σ)	0.61 (0.5 σ)
$D^\pm\rho^\mp$				
<i>BABAR</i> (full rec.)	[210]	232M	$-0.024 \pm 0.031 \pm 0.009$	$-0.098 \pm 0.055 \pm 0.018$

For each of $D\pi$, $D^*\pi$ and $D\rho$, there are two measurements (a and c , or S^+ and S^-) which depend on three unknowns (R , δ and $2\beta + \gamma$), of which two are different for each decay mode. Therefore, there is not enough information to solve directly for $2\beta + \gamma$. However, for each choice of R and $2\beta + \gamma$, one can find the value of δ that allows a and c to be closest to their measured values, and calculate the distance in terms of numbers of standard deviations. (We currently neglect experimental correlations in this analysis.) These values of $N(\sigma)_{\min}$ can then be plotted as a function of R and $2\beta + \gamma$ (and can trivially be converted to confidence levels). These plots are given for the $D\pi$ and $D^*\pi$ modes in Figure 35; the uncertainties in the $D\rho$ mode are currently too large to give any meaningful constraint.

The constraints can be tightened if one is willing to use theoretical input on the values of R and/or δ . One popular choice is the use of SU(3) symmetry to obtain R by relating

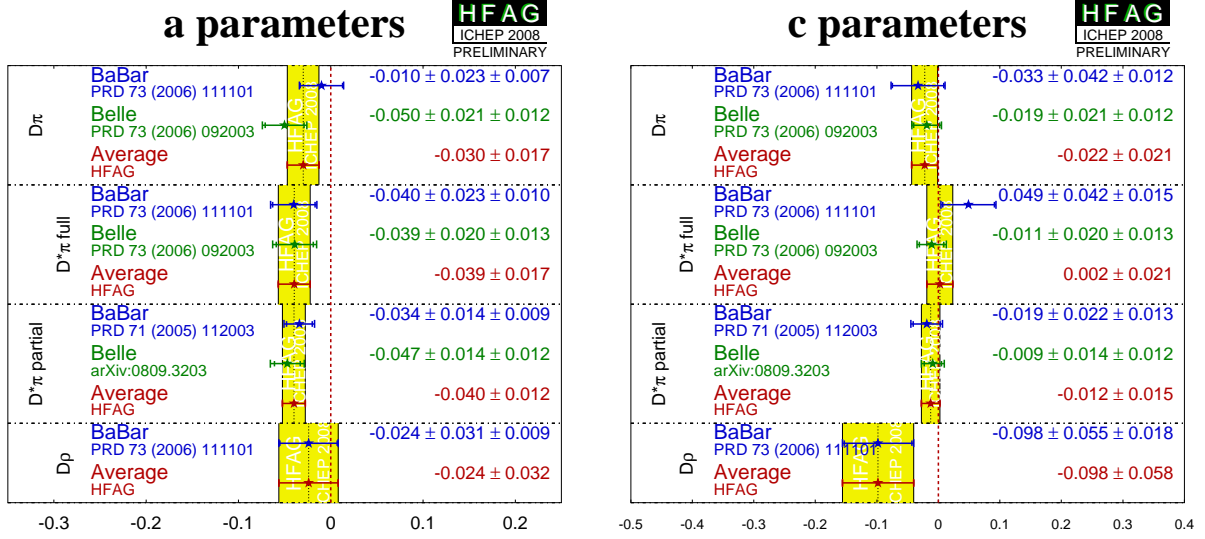


Figure 34: Averages for $b \rightarrow c\bar{u}d/u\bar{c}d$ modes.

the suppressed decay mode to B decays involving D_s mesons. More details can be found in Refs. [206, 242].

4.13 Time-dependent CP asymmetries in $b \rightarrow c\bar{u}s/u\bar{c}s$ transitions

Time-dependent analyses of transitions such as $B^0 \rightarrow D^\pm K_s^0 \pi^\mp$ can be used to probe $\sin(2\beta+\gamma)$ in a similar way to that discussed above (Sec. 4.12). Since the final state contains three particles, a Dalitz plot analysis is necessary to maximise the sensitivity. *BABAR* [306] have carried out such an analysis. They obtain $2\beta+\gamma = (83 \pm 53 \pm 20)^\circ$ (with an ambiguity $2\beta+\gamma \leftrightarrow 2\beta+\gamma+\pi$) assuming the ratio of the $b \rightarrow u$ and $b \rightarrow c$ amplitude to be constant across the Dalitz plot at 0.3.

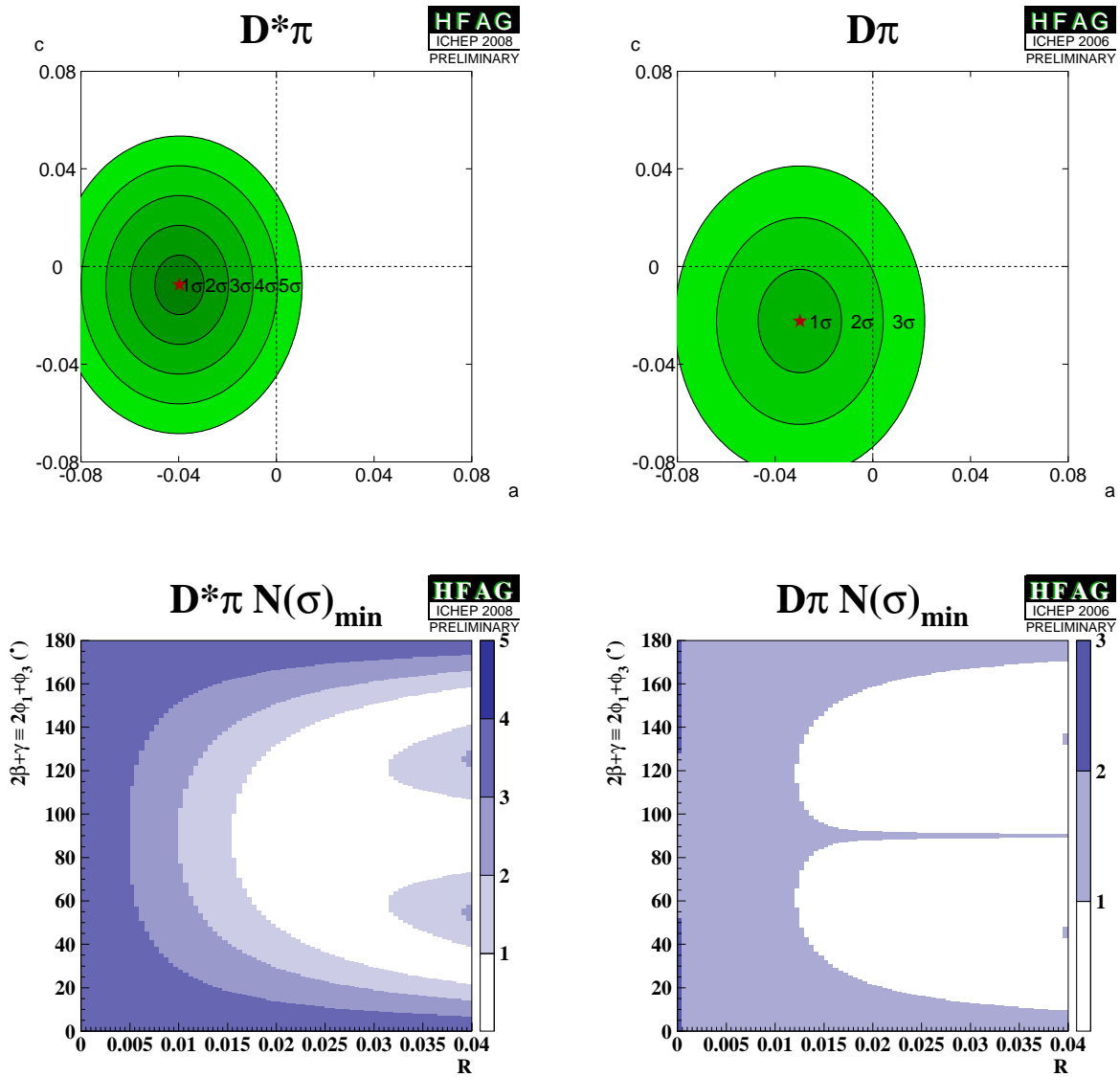


Figure 35: Results from $b \rightarrow c\bar{u}d/u\bar{c}d$ modes. (Top) Constraints in c vs. a space. (Bottom) Constraints in $2\beta + \gamma$ vs. R space. (Left) $D^*\pi$ and (right) $D\pi$ modes.

4.14 Rates and asymmetries in $B^\mp \rightarrow D^{(*)}K^{(*)\mp}$ decays

As explained in Sec. 4.2.7, rates and asymmetries in $B^\mp \rightarrow D^{(*)}K^{(*)\mp}$ decays are sensitive to γ . Various methods using different $D^{(*)}$ final states exist.

4.14.1 D decays to CP eigenstates

Results are available from both *BABAR* and Belle on GLW analyses in the decay modes $B^\mp \rightarrow DK^\mp$, $B^\mp \rightarrow D^*K^\mp$ and $B^\mp \rightarrow DK^{*\mp}$.²⁹ Both experiments use the CP -even D decay final states K^+K^- and $\pi^+\pi^-$ in all three modes; both experiments generally use the CP -odd decay modes $K_s^0\pi^0$, $K_s^0\omega$ and $K_s^0\phi$, though care is taken to avoid statistical overlap with the $K_s^0K^+K^-$ sample used for Dalitz plot analysis (see Sec. 4.14.3), and asymmetric systematic errors are assigned due to CP -even pollution under the $K_s^0\omega$ and $K_s^0\phi$ signals. Both experiments also use the $D^* \rightarrow D\pi^0$ decay, which gives $CP(D^*) = CP(D)$; *BABAR* in addition use the $D^* \rightarrow D\gamma$ decays, which gives $CP(D^*) = -CP(D)$. In addition, results from CDF, using 1 fb^{-1} , are available in the decay mode $B^\mp \rightarrow DK^\mp$, for CP -even final states (K^+K^- and $\pi^+\pi^-$) only. The results and averages are given in Table 41 and shown in Fig. 36.

Table 41: Averages from GLW analyses of $b \rightarrow c\bar{u}s/u\bar{c}s$ modes.

Experiment	$N(B\bar{B})$	A_{CP+}	A_{CP-}	R_{CP+}	R_{CP-}
$D_{CP}K^-$					
<i>BABAR</i> [308]	382M	$0.27 \pm 0.09 \pm 0.04$	$-0.09 \pm 0.09 \pm 0.02$	$1.06 \pm 0.10 \pm 0.05$	$1.03 \pm 0.10 \pm 0.05$
Belle [309]	275M	$0.06 \pm 0.14 \pm 0.05$	$-0.12 \pm 0.14 \pm 0.05$	$1.13 \pm 0.16 \pm 0.08$	$1.17 \pm 0.14 \pm 0.14$
CDF [310]	–	$0.39 \pm 0.17 \pm 0.04$	–	$1.30 \pm 0.24 \pm 0.12$	–
Average		0.24 ± 0.07	-0.10 ± 0.08	1.10 ± 0.09	1.06 ± 0.10
Confidence level		0.32 (1.0σ)	0.86 (0.2σ)	0.70 (0.4σ)	0.54 (0.6σ)
$D_{CP}^*K^-$					
<i>BABAR</i> [311]	383M	$-0.11 \pm 0.09 \pm 0.01$	$0.06 \pm 0.10 \pm 0.02$	$1.31 \pm 0.13 \pm 0.03$	$1.09 \pm 0.12 \pm 0.04$
Belle [309]	275M	$-0.20 \pm 0.22 \pm 0.04$	$0.13 \pm 0.30 \pm 0.08$	$1.41 \pm 0.25 \pm 0.06$	$1.15 \pm 0.31 \pm 0.12$
Average		-0.12 ± 0.08	0.07 ± 0.10	1.33 ± 0.12	1.10 ± 0.12
Confidence level		0.71 (0.4σ)	0.83 (0.2σ)	0.73 (0.4σ)	0.87 (0.2σ)
$D_{CP}K^{*-}$					
<i>BABAR</i> [312]	379M	$0.09 \pm 0.13 \pm 0.06$	$-0.23 \pm 0.21 \pm 0.07$	$2.17 \pm 0.35 \pm 0.09$	$1.03 \pm 0.27 \pm 0.13$

4.14.2 D decays to suppressed final states

For ADS analysis, both *BABAR* and Belle have studied the modes $B^\mp \rightarrow DK^\mp$ and $B^\mp \rightarrow D\pi^\mp$. *BABAR* has also analyzed the $B^\mp \rightarrow D^*K^\mp$ and $B^\mp \rightarrow DK^{*\mp}$ modes. There is an effective shift of π in the strong phase difference between the cases that the D^* is reconstructed as $D\pi^0$ and $D\gamma$ [313], therefore these modes are studied separately. $K^{*\mp}$ is reconstructed as $K_s^0\pi^\mp$. In all cases the suppressed decay $D \rightarrow K^+\pi^-$ has been used. *BABAR* also has results using $B^\mp \rightarrow DK^\mp$ with $D \rightarrow K^+\pi^-\pi^0$. The results and averages are given in Table 42 and shown

²⁹ We do not include a preliminary result from Belle [307], which remains unpublished after more than two years.

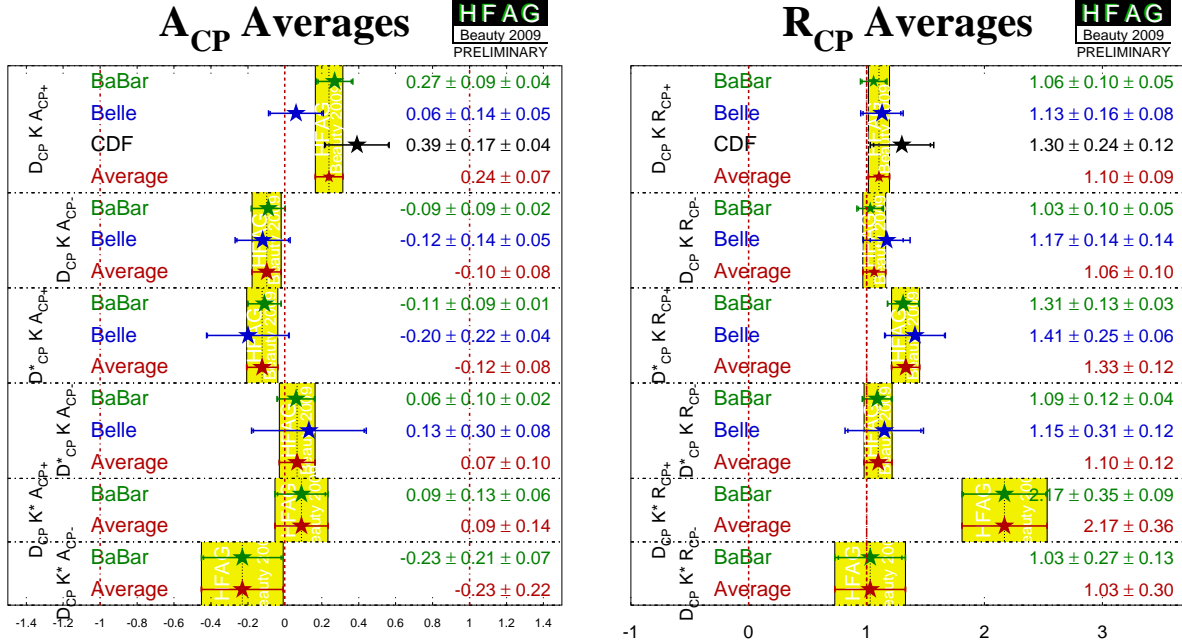


Figure 36: Averages of A_{CP} and R_{CP} from GLW analyses.

in Fig. 37. Note that although no clear signals for these modes have yet been seen, the central values are given.

BABAR [317] have also presented results on a similar analysis with self-tagging neutral B decays: $B^0 \rightarrow DK^{*0}$ with $D \rightarrow K^-\pi^+$, $D \rightarrow K^-\pi^+\pi^0$ and $D \rightarrow K^-\pi^+\pi^+\pi^-$ (all with $K^{*0} \rightarrow K^+\pi^-$). Effects due to the natural width of the K^{*0} are handled using the parametrization suggested by Gronau [318].

The following 95% C.L. limits are set:

$$R_{\text{ADS}}(K\pi) < 0.244 \quad R_{\text{ADS}}(K\pi\pi^0) < 0.181 \quad R_{\text{ADS}}(K\pi\pi\pi) < 0.391. \quad (192)$$

Combining the results and using additional input from CLEOc [319, 320] a limit on the ratio between the $b \rightarrow u$ and $b \rightarrow c$ amplitudes of $r_s \in [0.07, 0.41]$ at 95% C.L. limit is set.

Belle [321] have also presented results that set constraints on r_s .

4.14.3 D decays to multiparticle self-conjugate final states

For the Dalitz plot analysis, both *BABAR* [322] and Belle [323, 324] have studied the modes $B^\mp \rightarrow DK^\mp$, $B^\mp \rightarrow D^*K^\mp$ and $B^\mp \rightarrow DK^{*\mp}$. For $B^\mp \rightarrow D^*K^\mp$, both experiments have used both D^* decay modes, $D^* \rightarrow D\pi^0$ and $D^* \rightarrow D\gamma$, taking the effective shift in the strong phase difference into account. In all cases the decay $D \rightarrow K_s^0\pi^+\pi^-$ has been used. *BABAR* also used the decay $D \rightarrow K_s^0K^+K^-$. *BABAR* has also performed an analysis of $B^\mp \rightarrow DK^\mp$ with $D \rightarrow \pi^+\pi^-\pi^0$ [232]. Results and averages are given in Table 43. The third error on each measurement is due to D decay model uncertainty.

The parameters measured in the analyses are explained in Sec. 4.2.7. Both *BABAR* and Belle have measured the ‘‘Cartesian’’ (x_\pm, y_\pm) variables, and perform frequentist statistical

Table 42: Averages from ADS analyses of $b \rightarrow c\bar{u}s/u\bar{c}s$ and $b \rightarrow c\bar{u}d/u\bar{c}d$ modes.

Experiment		$N(B\bar{B})$	A_{ADS}	R_{ADS}
$DK^-, D \rightarrow K^+\pi^-$				
<i>BABAR</i>	[314]	426M	$-0.70 \pm 0.35^{+0.09}_{-0.14}$	$0.0136 \pm 0.0055 \pm 0.0027$
<i>Belle</i>	[315]	657M	$-0.13^{+0.97}_{-0.88} \pm 0.26$	$0.0080^{+0.0063}_{-0.0057} {}^{+0.0020}_{-0.0028}$
Average			-0.62 ± 0.34	0.0110 ± 0.0045
Confidence level			0.57 (0.6 σ)	0.53 (0.6 σ)
$D^*K^-, D^* \rightarrow D\pi^0, D \rightarrow K^+\pi^-$				
<i>BABAR</i>	[314]	426M	$0.77 \pm 0.35 \pm 0.12$	$0.018 \pm 0.009 \pm 0.004$
$D^*K^-, D^* \rightarrow D\gamma, D \rightarrow K^+\pi^-$				
<i>BABAR</i>	[314]	426M	$0.36 \pm 0.94^{+0.25}_{-0.41}$	$0.013 \pm 0.014 \pm 0.007$
$DK^{*-}, D \rightarrow K^+\pi^-, K^{*-} \rightarrow K_s^0\pi^-$				
<i>BABAR</i>	[312]	379M	$-0.34 \pm 0.43 \pm 0.16$	$0.066 \pm 0.031 \pm 0.010$
$DK^-, D \rightarrow K^+\pi^-\pi^0$				
<i>BABAR</i>	[316]	226M	–	$0.012 \pm 0.012 \pm 0.009$
$D\pi^-, D \rightarrow K^+\pi^-$				
<i>BABAR</i>	[314]	426M	–	$0.0033 \pm 0.0006 \pm 0.0003$
<i>Belle</i>	[315]	657M	$-0.023 \pm 0.218 \pm 0.071$	$0.0034^{+0.0006}_{-0.0005} {}^{+0.0001}_{-0.0002}$
Average			–	0.0034 ± 0.0004
Confidence level			–	0.91 (0.1 σ)
$D^*\pi^-, D^* \rightarrow D\pi^0, D \rightarrow K^+\pi^-$				
<i>BABAR</i>	[314]	426M	–	$0.0032 \pm 0.0009 \pm 0.0009$
$D^*\pi^-, D^* \rightarrow D\gamma, D \rightarrow K^+\pi^-$				
<i>BABAR</i>	[314]	426M	–	$0.0027 \pm 0.0014 \pm 0.0022$

procedures, to convert these into measurements of γ , r_B and δ_B . In the $B^\mp \rightarrow DK^\mp$ with $D \rightarrow \pi^+\pi^-\pi^0$ analysis, the parameters (ρ^\pm, θ^\pm) are used instead.

Both experiments reconstruct $K^{*\mp}$ as $K_s^0\pi^\mp$, but the treatment of possible nonresonant $K_s^0\pi^\mp$ differs: Belle assign an additional model uncertainty, while *BABAR* use a reparametrization suggested by Gronau [318]. The parameters r_B and δ_B are replaced with effective parameters κr_s and δ_s ; no attempt is made to extract the true hadronic parameters of the $B^\mp \rightarrow DK^{*\mp}$ decay.

We perform averages using the following procedure, which is based on a set of (more or less) reasonable, though imperfect, assumptions.

- It is assumed that effects due to the different D decay models used by the two experiments are negligible. Therefore, we do not rescale the results to a common model.
- It is further assumed that the model uncertainty is 100% correlated between experiments, and therefore this source of error is not used in the averaging procedure. (This approximation is significantly less valid now that the *BABAR* results include $D \rightarrow K_s^0K^+K^-$ decays in addition to $D \rightarrow K_s^0\pi^+\pi^-$.)

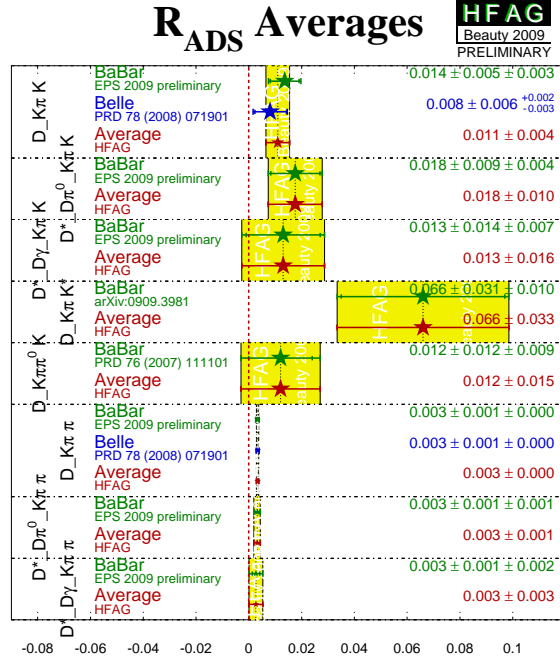


Figure 37: Averages of R_{ADS} .

- We include in the average the effect of correlations within each experiments set of measurements.
- At present it is unclear how to assign an average model uncertainty. We have not attempted to do so. Our average includes only statistical and systematic error. An unknown amount of model uncertainty should be added to the final error.
- We follow the suggestion of Gronau [318] in making the DK^* averages. Explicitly, we assume that the selection of $K^{*\pm} \rightarrow K_s^0 \pi^\pm$ is the same in both experiments (so that κ , r_s and δ_s are the same), and drop the additional source of model uncertainty assigned by Belle due to possible nonresonant decays.
- We do not consider common systematic errors, other than the D decay model.

Constraints on γ

The measurements of (x_\pm, y_\pm) can be used to obtain constraints on γ , as well as the hadronic parameters r_B and δ_B . Both *BABAR* [322] and Belle [323, 324] have done so using a frequentist procedure (there are some differences in the details of the techniques used).

- *BABAR* obtain $\gamma = (76 \pm 22 \pm 5 \pm 5)^\circ$ from DK^\pm , D^*K^\pm and $DK^{*\pm}$
- Belle obtain $\phi_3 = (78_{-12}^{+11} \pm 4 \pm 9)^\circ$ from DK^\pm and D^*K^\pm
- The experiments also obtain values for the hadronic parameters as detailed in Tab. 44.
- Improved constraints can be achieved combining the information from $B^\pm \rightarrow DK^\pm$ analysis with different D decay modes. The experiments have not yet published such results, and none are listed here.

Table 43: Averages from Dalitz plot analyses of $b \rightarrow c\bar{u}s/u\bar{c}s$ modes. Note that the uncertainties assigned to the averages do not include model errors.

Experiment	$N(B\bar{B})$	x_+	y_+	x_-	y_-
$DK^{\mp}, D \rightarrow K_s^0\pi^+\pi^-$					
BABAR [322]	383M	$-0.067 \pm 0.043 \pm 0.014 \pm 0.011$	$-0.015 \pm 0.055 \pm 0.006 \pm 0.008$	$0.090 \pm 0.043 \pm 0.015 \pm 0.011$	$0.053 \pm 0.056 \pm 0.007 \pm 0.015$
Belle [323]	657M	$-0.107 \pm 0.043 \pm 0.011 \pm 0.055$	$-0.067 \pm 0.059 \pm 0.018 \pm 0.063$	$0.105 \pm 0.047 \pm 0.011 \pm 0.064$	$0.177 \pm 0.060 \pm 0.018 \pm 0.054$
Average		-0.087 ± 0.032	-0.037 ± 0.041	0.104 ± 0.033	0.111 ± 0.042
Confidence level 0.54 (0.6σ)					
$D^*K^-, D^* \rightarrow D\pi^0$ or $D\gamma, D \rightarrow K_s^0\pi^+\pi^-$					
BABAR [322]	383M	$0.137 \pm 0.068 \pm 0.014 \pm 0.005$	$0.080 \pm 0.102 \pm 0.010 \pm 0.012$	$-0.111 \pm 0.069 \pm 0.014 \pm 0.004$	$-0.051 \pm 0.080 \pm 0.009 \pm 0.010$
Belle [323]	657M	$0.083 \pm 0.092 \pm 0.081$	$0.157 \pm 0.109 \pm 0.063$	$-0.036 \pm 0.127 \pm 0.090$	$-0.249 \pm 0.118 \pm 0.049$
Average		0.117 ± 0.055	0.117 ± 0.075	-0.082 ± 0.061	-0.119 ± 0.066
Confidence level 0.59 (0.5σ)					
$DK^{*\mp}, D \rightarrow K_s^0\pi^+\pi^-$					
BABAR [322]	383M	$-0.113 \pm 0.107 \pm 0.028 \pm 0.018$	$0.125 \pm 0.139 \pm 0.051 \pm 0.010$	$0.115 \pm 0.138 \pm 0.039 \pm 0.014$	$0.226 \pm 0.142 \pm 0.058 \pm 0.011$
Belle [324]	386M	$-0.105^{+0.177}_{-0.167} \pm 0.006 \pm 0.088$	$-0.004^{+0.164}_{-0.156} \pm 0.013 \pm 0.095$	$-0.784^{+0.249}_{-0.295} \pm 0.029 \pm 0.097$	$-0.281^{+0.440}_{-0.335} \pm 0.046 \pm 0.086$
Average		-0.117 ± 0.092	0.067 ± 0.108	-0.097 ± 0.127	0.161 ± 0.143
Confidence level 0.008 (2.7σ)					

Experiment	$N(B\bar{B})$	ρ^+	θ^+	ρ^-	θ^-
$DK^{\mp}, D \rightarrow \pi^+\pi^-\pi^0$					
BABAR [232]	324M	$0.75 \pm 0.11 \pm 0.04$	$147 \pm 23 \pm 1$	$0.72 \pm 0.11 \pm 0.04$	$173 \pm 42 \pm 2$

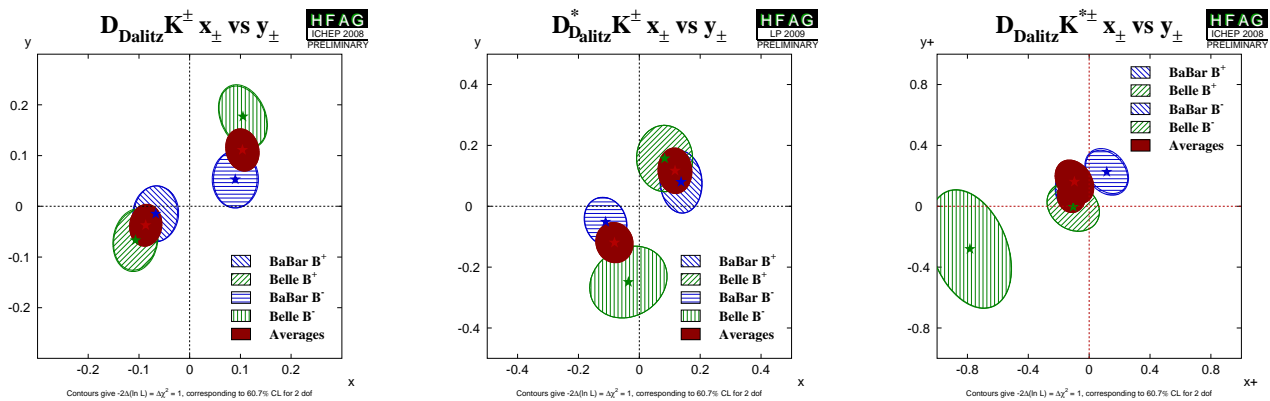


Figure 38: Contours in the (x_{\pm}, y_{\pm}) from $B^{\mp} \rightarrow D^{(*)}K^{(*)\pm}$. (Left) $B^{\mp} \rightarrow DK^{\mp}$, (middle) $B^{\mp} \rightarrow D^*K^{\mp}$, (right) $B^{\mp} \rightarrow DK^{*\mp}$. Note that the uncertainties assigned to the averages given in these plots do not include model errors.

- The CKMfitter [206] and UFit [242] groups use the measurements from Belle and BABAR given above to make combined constraints on γ .
- In the BABAR analysis of $B^{\mp} \rightarrow DK^{\mp}$ with $D \rightarrow \pi^+\pi^-\pi^0$ [232], a constraint of $-30^\circ < \gamma < 76^\circ$ is obtained at the 68% confidence level.

At present we make no attempt to provide an HFAG average for γ , nor indeed for the hadronic parameters. More details on procedures to calculate a best fit value for γ can be found in Refs. [206, 242].

BABAR [325] have also performed a similar Dalitz plot analysis to that described above using the self-tagging neutral B decay $B^0 \rightarrow DK^{*0}$ (with $K^{*0} \rightarrow K^+\pi^-$). Effects due to the natural width of the K^{*0} are handled using the parametrization suggested by Gronau [318].

BABAR extract the three-dimensional likelihood for the parameters (γ, δ_S, r_S) and, combining

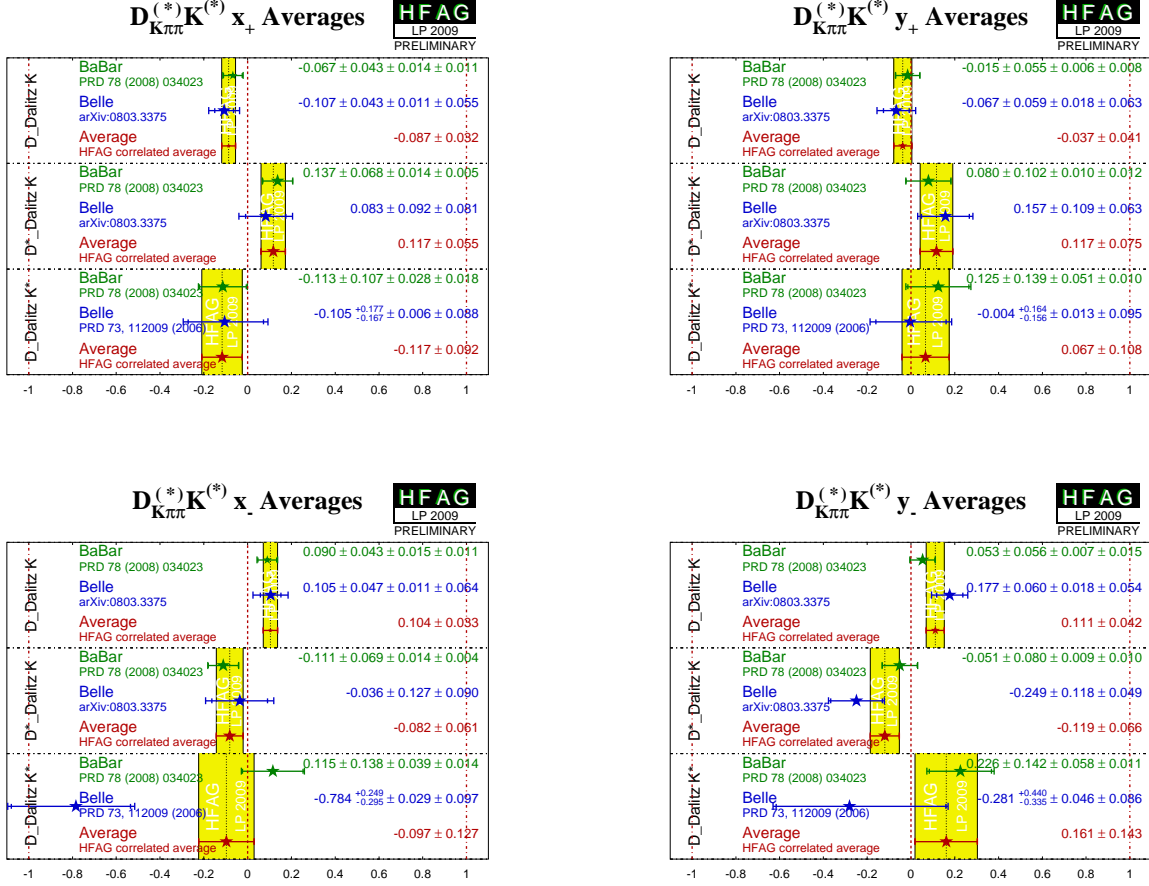


Figure 39: Averages of (x_{\pm}, y_{\pm}) from $B^{\pm} \rightarrow D^{(*)}K^{(*)\pm}$. (Top left) x_+ , (top right) y_+ , (bottom left) x_- , (bottom right) y_- . Note that the uncertainties assigned to the averages given in these plots do not include model errors.

with a separately measured PDF for r_S (using a Bayesian technique), obtain bounds on each of the three parameters.

$$\gamma = (162 \pm 56)^{\circ} \quad \delta_S = (62 \pm 57)^{\circ} \quad r_S < 0.55, \quad (193)$$

where the limit on r_S is at 95% probability. Note that there is an ambiguity in the solutions $(\gamma, \delta_S \leftrightarrow \gamma + \pi, \delta_S + \pi)$.

	r_B	δ_B
	In DK^\pm	
<i>BABAR</i>	0.086 ± 0.035	$\delta_B(DK^\pm) = (109_{-31}^{+28})^\circ$
<i>Belle</i>	$0.160_{-0.038}^{+0.040} \pm 0.011_{-0.010}^{+0.05}$	$(138_{-16}^{+13} \pm 4 \pm 23)^\circ$
	In D^*K^\pm	
<i>BABAR</i>	0.135 ± 0.051	$(297_{-28}^{+30})^\circ$
<i>Belle</i>	$0.196_{-0.069}^{+0.072} \pm 0.012_{-0.012}^{+0.062}$	$(342_{-21}^{+19} \pm 3 \pm 23)^\circ$
	In $DK^{*\pm}$	
<i>BABAR</i>	$\kappa r_S = 0.163_{-0.105}^{+0.088}$	$\delta_S = (104_{-41}^{+43})^\circ$
<i>Belle</i>	$0.56_{-0.16}^{+0.22} \pm 0.04 \pm 0.08$	$(243_{-23}^{+20} \pm 3 \pm 50)^\circ$

Table 44: Summary of constraints on hadronic parameters in $B^\pm \rightarrow D^{(*)}K^{(*)\pm}$ decays. Note the alternative parametrisation of the hadronic parameters used by *BABAR* in the $DK^{*\pm}$ mode.

5 Semileptonic B decays

Measurements of semileptonic B -meson decays are an important tool to study the magnitude of the CKM matrix elements $|V_{cb}|$ and $|V_{ub}|$, the Heavy Quark parameters (e.g. b and c -quark masses), QCD form factors, QCD dynamics, new physics, etc.

In the following, we provide averages of exclusive and inclusive branching fractions, the product of $|V_{cb}|$ and the form factor normalization $\mathcal{F}(1)$ and $\mathcal{G}(1)$ for $\overline{B} \rightarrow D^* \ell^- \overline{\nu}_\ell$ and $\overline{B} \rightarrow D \ell^- \overline{\nu}_\ell$ decays, respectively, and $|V_{ub}|$ as determined from inclusive and exclusive measurements of $B \rightarrow X_u \ell \nu_\ell$ decays. We will compute Heavy Quark parameters and extract QCD form factors for $\overline{B} \rightarrow D^* \ell^- \overline{\nu}_\ell$ decays. Throughout this section, charge conjugate states are implicitly included, unless otherwise indicated.

Brief descriptions of all parameters and analyses (published or preliminary) relevant for the determination of the combined results are given. The descriptions are based on the information available on the web page at

<http://www.slac.stanford.edu/xorg/hfag/semi/EndOfYear09>

A description of the technique employed for calculating averages was presented in the previous update [4]. Asymmetric errors have been introduced in the current averages for $\overline{B} \rightarrow X_u \ell \overline{\nu}$ decays to take into account theoretical asymmetric errors.

5.1 Exclusive CKM-favored decays

Averages are provided for the branching fractions $\mathcal{B}(\overline{B} \rightarrow D \ell^- \overline{\nu}_\ell)$ and $\mathcal{B}(\overline{B} \rightarrow D^* \ell^- \overline{\nu}_\ell)$. We then provide averages for the inclusive branching fractions $\mathcal{B}(\overline{B} \rightarrow D^{(*)} \pi \ell^- \overline{\nu}_\ell)$ and for B semileptonic decays into orbitally-excited P -wave charm mesons (D^{**}). As the D^{**} branching fraction is poorly known, we report the averages for the products $\mathcal{B}(B^- \rightarrow D^{**} (D^{(*)} \pi) \ell^- \overline{\nu}_\ell) \times \mathcal{B}(D^{**} \rightarrow D^{(*)} \pi)$. In addition, averages are provided for $\mathcal{F}(1)|V_{cb}|$ vs ρ^2 , where $\mathcal{F}(1)$ and ρ^2 are the normalization and slope of the form factor at zero recoil in $\overline{B} \rightarrow D^* \ell^- \overline{\nu}_\ell$ decays, and for the corresponding quantities $\mathcal{G}(1)|V_{cb}|$ vs ρ^2 in $\overline{B} \rightarrow D \ell^- \overline{\nu}_\ell$ decays.

5.1.1 $\overline{B} \rightarrow D \ell^- \overline{\nu}_\ell$

The average branching fraction $\mathcal{B}(\overline{B} \rightarrow D \ell^- \overline{\nu}_\ell)$ is determined by the combination of the results provided in Table 45 and 46, for $\overline{B}^0 \rightarrow D^+ \ell^- \overline{\nu}_\ell$ and $B^- \rightarrow D^0 \ell^- \overline{\nu}_\ell$, respectively. The measurements included in the average are scaled to a consistent set of input parameters and their errors [326]. Therefore some of the (older) measurements are subject to considerable adjustments. The branching fractions are obtained from the integral over the measured differential decay rates, apart for the *BABAR* results, for which the semileptonic B signal yields are extracted from a fit to the missing mass squared in a sample of fully reconstructed $B\overline{B}$ events.

Figure 40 illustrates the measurements and the resulting average.

Recent measurement [332, 333] assume isospin conservation for the $\overline{B} \rightarrow D \ell^- \overline{\nu}_\ell$ decays and are averaged independently from the previous determinations of the $\mathcal{B}(\overline{B} \rightarrow D \ell^- \overline{\nu}_\ell)$ average branching fraction. Figure 41 and table 47 illustrates the measurements and the resulting average.

The average for $\mathcal{G}(1)|V_{cb}|$ is determined by the two-dimensional combination of the results provided in Table 48. Figure 42 (a) provides a one-dimensional projection for illustrative purposes, (b) illustrates the average $\mathcal{G}(1)|V_{cb}|$ and the measurements included in the average.

Table 45: Average of the branching fraction $\mathcal{B}(\bar{B}^0 \rightarrow D^+ \ell^- \bar{\nu})$ and individual results.

Experiment	$\mathcal{B}(\bar{B}^0 \rightarrow D^+ \ell^- \bar{\nu})[\%]$ (rescaled)	$\mathcal{B}(\bar{B}^0 \rightarrow D^+ \ell^- \bar{\nu})[\%]$ (published)
ALEPH [327]	$2.25 \pm 0.18_{\text{stat}} \pm 0.36_{\text{syst}}$	$2.35 \pm 0.18_{\text{stat}} \pm 0.44_{\text{syst}}$
CLEO [328]	$2.12 \pm 0.13_{\text{stat}} \pm 0.15_{\text{syst}}$	$2.20 \pm 0.13_{\text{stat}} \pm 0.18_{\text{syst}}$
Belle [329]	$2.10 \pm 0.12_{\text{stat}} \pm 0.39_{\text{syst}}$	$2.13 \pm 0.12_{\text{stat}} \pm 0.41_{\text{syst}}$
BABAR [330]	$2.20 \pm 0.11_{\text{stat}} \pm 0.12_{\text{syst}}$	$2.22 \pm 0.11_{\text{stat}} \pm 0.12_{\text{syst}}$
Average	2.17 ± 0.12	$\chi^2/\text{dof} = 0.2/3$ (CL=98%)

Table 46: Average of the branching fraction $\mathcal{B}(B^- \rightarrow D^0 \ell^- \bar{\nu}_\ell)$ and individual results.

Experiment	$\mathcal{B}(B^- \rightarrow D^0 \ell^- \bar{\nu}_\ell)[\%]$ (rescaled)	$\mathcal{B}(B^- \rightarrow D^0 \ell^- \bar{\nu}_\ell)[\%]$ (published)
CLEO-2 [328]	$2.19 \pm 0.13_{\text{stat}} \pm 0.17_{\text{syst}}$	$2.21 \pm 0.13_{\text{stat}} \pm 0.19_{\text{syst}}$
CLEO [331]	$1.66 \pm 0.6_{\text{stat}} \pm 0.21_{\text{syst}}$	$1.60 \pm 0.6_{\text{stat}} \pm 0.3_{\text{syst}}$
BABAR [330]	$2.27 \pm 0.09_{\text{stat}} \pm 0.09_{\text{syst}}$	$2.33 \pm 0.09_{\text{stat}} \pm 0.09_{\text{syst}}$
Average	2.23 ± 0.11	$\chi^2/\text{dof} = 0.95/2$ (CL=62%)

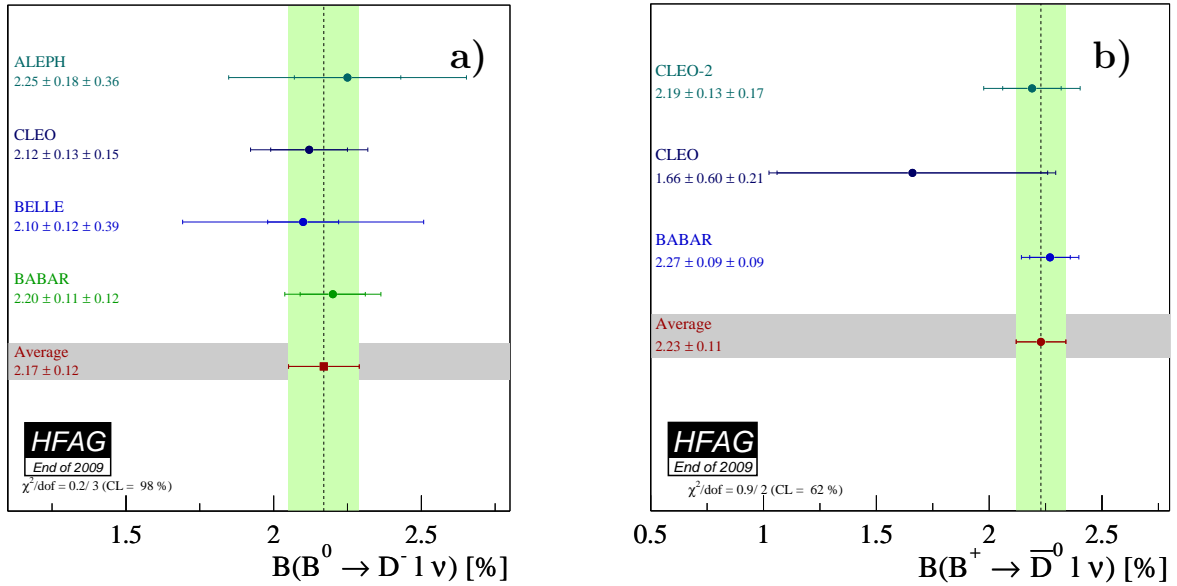


Figure 40: Average branching fraction of exclusive semileptonic B decays (a) $\bar{B}^0 \rightarrow D^+ \ell^- \bar{\nu}_\ell$ and (b) $B^- \rightarrow D^0 \ell^- \bar{\nu}_\ell$ and individual results.

For a determination of $|V_{cb}|$, the form factor at zero recoil $G(1)$ needs to be computed. Using an unquenched lattice calculation [334], corrected by a factor of 1.007 for QED effects, we obtain

$$|V_{cb}| = (39.2 \pm 1.4_{\text{exp}} \pm 0.9_{\text{theo}}) \times 10^{-3},$$

Table 47: Average of the branching fraction $\mathcal{B}(B^- \rightarrow D^0 \ell^- \bar{\nu}_\ell)$ and individual results.

Experiment	$\mathcal{B}(B^- \rightarrow D^0 \ell^- \bar{\nu}_\ell)[\%]$ (rescaled)	$\mathcal{B}(B^- \rightarrow D^0 \ell^- \bar{\nu}_\ell)[\%]$ (published)
BABAR [332]	$2.34 \pm 0.03_{\text{stat}} \pm 0.12_{\text{syst}}$	$2.34 \pm 0.03_{\text{stat}} \pm 0.13_{\text{syst}}$
BABAR [333]	$2.30 \pm 0.06_{\text{stat}} \pm 0.08_{\text{syst}}$	$2.30 \pm 0.06_{\text{stat}} \pm 0.08_{\text{syst}}$
Average	2.31 ± 0.09	$\chi^2/\text{dof} = 0.11$ (CL=71%)

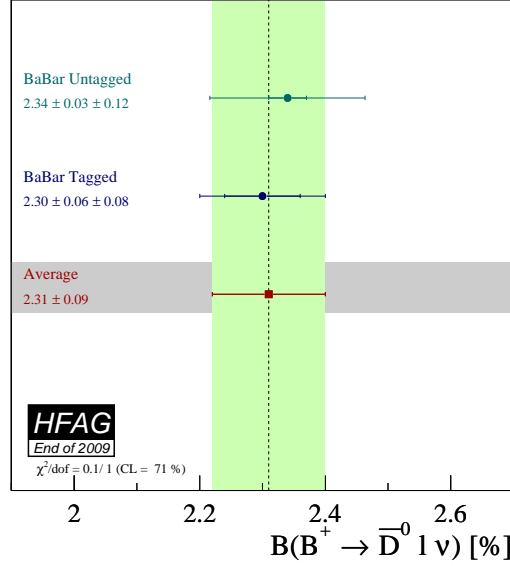


Figure 41: Average branching fraction of exclusive semileptonic B decays $\bar{B} \rightarrow D \ell^- \bar{\nu}_\ell$ and individual results assuming isospin conservation.

where the third error is due to the theoretical uncertainty in $\mathcal{G}(1)$. As an alternative, we use a quenched lattice calculation based on the Step Scaling Method (SSM) [335], and obtain

$$|V_{cb}| = (40.9 \pm 1.5_{\text{exp}} \pm 0.7_{\text{theo}}) \times 10^{-3}.$$

5.1.2 $\bar{B} \rightarrow D^* \ell^- \bar{\nu}_\ell$

The average branching fraction $\mathcal{B}(\bar{B} \rightarrow D^* \ell^- \bar{\nu}_\ell)$ is determined by the combination of the results provided in Table 49 and 50, for $\bar{B}^0 \rightarrow D^{*+} \ell^- \bar{\nu}_\ell$ and $B^- \rightarrow D^{*0} \ell^- \bar{\nu}_\ell$, respectively. Advances have also been made in the determination of $|V_{cb}|$ from exclusive $\bar{B} \rightarrow D^* \ell^- \bar{\nu}_\ell$ decays with substantially improved measurements of the form factor ratios R_1 and R_2 .

For the $\mathcal{B}(B^- \rightarrow D^{*0} \ell^- \bar{\nu}_\ell)$, the average is performed as for the $\bar{B} \rightarrow D \ell^- \bar{\nu}_\ell$ modes, by scaling the different measurements to a common set of input parameters. For the $\mathcal{B}(\bar{B}^0 \rightarrow D^{*+} \ell^- \bar{\nu}_\ell)$, the average is performed with a new method that combines all the information available from the different experiments regarding the measurements of $|V_{cb}|$, the slope parameter ρ^2 and the other form-factor parameters R_1 and R_2 . A global χ^2 is built incorporating all the inputs provided

Table 48: Average of $G(1)|V_{cb}|$ determined in the decay $\bar{B}^0 \rightarrow D^+ \ell^- \bar{\nu}$ and individual results. The fit for the average has $\chi^2/\text{dof} = 0.3/4$. The total correlation between the average $G(1)|V_{cb}|$ and ρ^2 is 0.93.

Experiment	$G(1) V_{cb} [10^{-3}]$ (rescaled) $G(1) V_{cb} [10^{-3}]$ (published)	ρ^2 (rescaled) ρ^2 (published)
ALEPH [327]	$38.3 \pm 11.8_{\text{stat}} \pm 6.2_{\text{syst}}$ $31.1 \pm 9.9_{\text{stat}} \pm 8.6_{\text{syst}}$	$0.92 \pm 0.98_{\text{stat}} \pm 0.36_{\text{syst}}$ $0.70 \pm 0.98_{\text{stat}} \pm 0.50_{\text{syst}}$
CLEO [328]	$44.7 \pm 5.9_{\text{stat}} \pm 3.45_{\text{syst}}$ $44.8 \pm 6.1_{\text{stat}} \pm 3.7_{\text{syst}}$	$1.27 \pm 0.25_{\text{stat}} \pm 0.14_{\text{syst}}$ $1.30 \pm 0.27_{\text{stat}} \pm 0.14_{\text{syst}}$
Belle [329]	$40.85 \pm 4.4_{\text{stat}} \pm 5.14_{\text{syst}}$ $41.1 \pm 4.4_{\text{stat}} \pm 5.1_{\text{syst}}$	$1.12 \pm 0.22_{\text{stat}} \pm 0.14_{\text{syst}}$ $1.12 \pm 0.22_{\text{stat}} \pm 0.14_{\text{syst}}$
BABAR [332]	$43.1 \pm 0.8_{\text{stat}} \pm 2.1_{\text{syst}}$ $43.1 \pm 0.8_{\text{stat}} \pm 2.3_{\text{syst}}$	$1.20 \pm 0.04_{\text{stat}} \pm 0.06_{\text{syst}}$ $1.20 \pm 0.04_{\text{stat}} \pm 0.07_{\text{syst}}$
BABAR [333]	$42.3 \pm 1.9_{\text{stat}} \pm 1.0_{\text{syst}}$ $42.3 \pm 1.9_{\text{stat}} \pm 1.0_{\text{syst}}$	$1.20 \pm 0.09_{\text{stat}} \pm 0.04_{\text{syst}}$ $1.20 \pm 0.09_{\text{stat}} \pm 0.04_{\text{syst}}$
Average	42.3 ± 1.5	1.18 ± 0.06

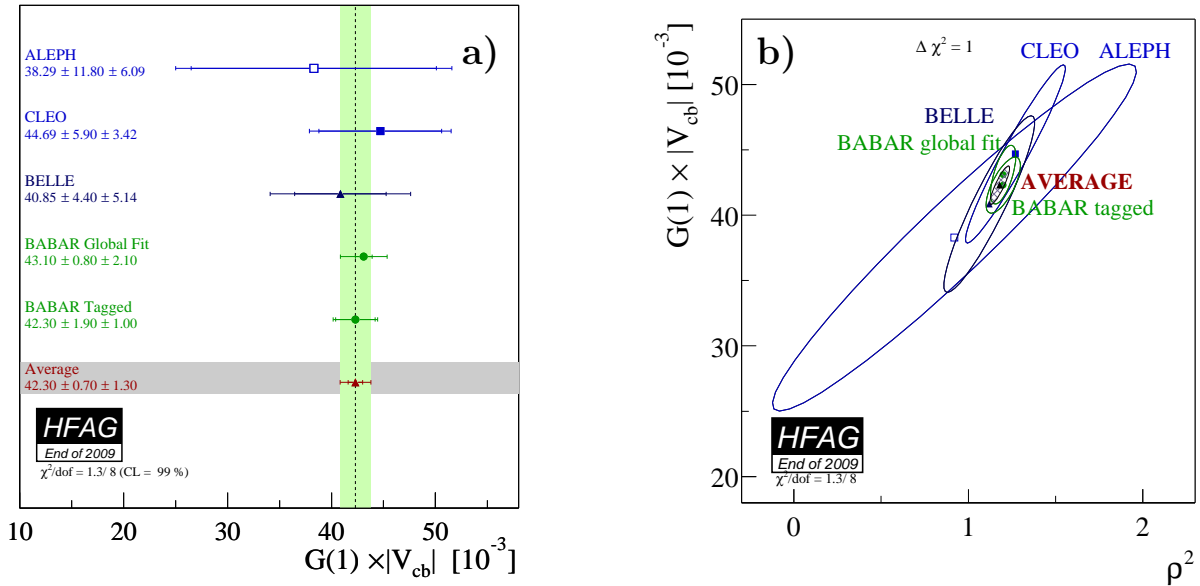


Figure 42: (a) Illustration of $G(1)|V_{cb}|$ vs. ρ^2 . The error ellipses correspond to $\Delta\chi^2 = 1$. (b) Illustration of the average $G(1)|V_{cb}|$ and rescaled measurements of exclusive $\bar{B} \rightarrow D\ell\bar{\nu}_\ell$ decays determined in a two-dimensional fit.

by each experiment. The dependence of the $\mathcal{F}(1)|V_{cb}| - \rho^2$ only measurements on the global values of R_1 and R_2 is explicitly included through a Taylor expansion in $\Delta R_{1,2} = R_{1,2} - R_{1,2}^{\text{nom}}$ where $R_{1,2}^{\text{nom}}$ are some nominal values for the form-factor parameters. Statistical correlations between measurements from the same experiment are taken into account. The form-factor

Table 49: Average branching fraction $\mathcal{B}(\overline{B}^0 \rightarrow D^{*+}\ell^-\overline{\nu})$ and individual results, where “excl” and “partial reco” refer to full and partial reconstruction of the $\overline{B}^0 \rightarrow D^{*+}\ell^-\overline{\nu}$ decay, respectively.

Experiment	$\mathcal{B}(\overline{B}^0 \rightarrow D^{*+}\ell^-\overline{\nu})[\%]$ (rescaled)	$\mathcal{B}(\overline{B}^0 \rightarrow D^{*+}\ell^-\overline{\nu})[\%]$ (published)
ALEPH (excl) [327]	$5.29 \pm 0.24_{\text{stat}} \pm 0.19_{\text{syst}}$	$5.53 \pm 0.26_{\text{stat}} \pm 0.52_{\text{syst}}$
OPAL (excl) [336]	$5.10 \pm 0.19_{\text{stat}} \pm 0.37_{\text{syst}}$	$5.11 \pm 0.20_{\text{stat}} \pm 0.49_{\text{syst}}$
OPAL (partial reco) [336]	$5.52 \pm 0.26_{\text{stat}} \pm 0.42_{\text{syst}}$	$5.92 \pm 0.28_{\text{stat}} \pm 0.68_{\text{syst}}$
DELPHI (partial reco) [337]	$4.93 \pm 0.15_{\text{stat}} \pm 0.17_{\text{syst}}$	$4.70 \pm 0.14_{\text{stat}} \begin{smallmatrix} +0.36 \\ -0.31 \end{smallmatrix}_{\text{syst}}$
Belle (excl) [338]	$4.40 \pm 0.03_{\text{stat}} \pm 0.25_{\text{syst}}$	$4.42 \pm 0.03_{\text{stat}} \pm 0.25_{\text{syst}}$
CLEO (excl) [339]	$5.65 \pm 0.18_{\text{stat}} \pm 0.19_{\text{syst}}$	$6.09 \pm 0.19_{\text{stat}} \pm 0.40_{\text{syst}}$
DELPHI (excl) [340]	$5.41 \pm 0.18_{\text{stat}} \pm 0.33_{\text{syst}}$	$5.90 \pm 0.20_{\text{stat}} \pm 0.50_{\text{syst}}$
BABAR (excl) [341]	$4.59 \pm 0.04_{\text{stat}} \pm 0.24_{\text{syst}}$	$4.69 \pm 0.04_{\text{stat}} \pm 0.34_{\text{syst}}$
BABAR (tagged) [330]	$5.40 \pm 0.16_{\text{stat}} \pm 0.25_{\text{syst}}$	$5.49 \pm 0.16_{\text{stat}} \pm 0.25_{\text{syst}}$
Average	5.05 ± 0.12	$\chi^2/\text{dof} = 16.6/9$ (CL=5.5%)

Table 50: Average of the branching fraction $\mathcal{B}(B^- \rightarrow D^{*0}\ell^-\overline{\nu})$ and individual results.

Experiment	$\mathcal{B}(B^- \rightarrow D^{*0}\ell^-\overline{\nu})[\%]$ (rescaled)	$\mathcal{B}(B^- \rightarrow D^{*0}\ell^-\overline{\nu})[\%]$ (published)
ARGUS [342]	$6.07 \pm 1.40_{\text{stat}} \pm 1.0_{\text{syst}}$	$6.6 \pm 1.6_{\text{stat}} \pm 1.5_{\text{syst}}$
CLEO [339]	$6.58 \pm 0.2_{\text{stat}} \pm 0.39_{\text{syst}}$	$6.50 \pm 0.20_{\text{stat}} \pm 0.43_{\text{syst}}$
BABAR [330]	$5.71 \pm 0.15_{\text{stat}} \pm 0.30_{\text{syst}}$	$5.80 \pm 0.15_{\text{stat}} \pm 0.30_{\text{syst}}$
BABAR [343]	$5.32 \pm 0.08_{\text{stat}} \pm 0.40_{\text{syst}}$	$5.56 \pm 0.08_{\text{stat}} \pm 0.41_{\text{syst}}$
BABAR [332]	$5.40 \pm 0.02_{\text{stat}} \pm 0.21_{\text{syst}}$	$5.40 \pm 0.02_{\text{stat}} \pm 0.21_{\text{syst}}$
Belle [344]	$4.83 \pm 0.04_{\text{stat}} \pm 0.56_{\text{syst}}$	$4.84 \pm 0.04_{\text{stat}} \pm 0.56_{\text{syst}}$
Average	5.63 ± 0.18	$\chi^2/\text{dof} = 12.7/5$ (CL=2.5%)

parametrization derived by Caprini, Lellouch and Neubert [345] is used.

The χ^2 minimization gives values for the form-factor parameters equal to $R_1 = 1.410 \pm 0.049$ and $R_2 = 0.844 \pm 0.027$. The errors contain both the common and the experiment dependent systematic uncertainties.

The values extracted from the fit for $\mathcal{F}(1)|V_{cb}|$ and the form-factor parameters are used to obtain the $\mathcal{B}(\overline{B}^0 \rightarrow D^{*+}\ell^-\overline{\nu}_\ell)$ branching fractions by computing the integral over the measured differential decay rates. The $\mathcal{B}(\overline{B}^0 \rightarrow D^{*+}\ell^-\overline{\nu}_\ell)$ average is computed from these inputs, apart for the BABAR results [330], for which the semileptonic B signal yields are extracted from a fit to the missing mass squared in a sample of fully reconstructed $B\overline{B}$ events. This measurement is rescaled to the common set of input parameters, and then averaged with the other ones, neglecting at this stage remaining correlations. Figure 43 illustrates the measurements and the resulting average for the $\mathcal{B}(\overline{B} \rightarrow D^*\ell^-\overline{\nu}_\ell)$.

The average for $F(1)|V_{cb}|$ is determined by the two-dimensional combination of the results provided by the global χ^2 minimization described above: the corresponding values are reported

in Table 51. This allows the correlation between $F(1)|V_{cb}|$ and ρ^2 to be maintained. Figure 44(a) illustrates the average $F(1)|V_{cb}|$ and the measurements included in the average. Figure 44(b) provides a one-dimensional projection for illustrative purposes. The largest systematic errors correlated between measurements are owing to uncertainties on: R_b , the ratio of production cross-sections $\sigma_{b\bar{b}}/\sigma_{\text{had}}$, the B^0 fraction at $\sqrt{s} = m_{Z^0}$, the branching fractions $\mathcal{B}(D^0 \rightarrow K^-\pi^+)$ and $\mathcal{B}(D^0 \rightarrow K^-\pi^+\pi^0)$, the correlated background from D^{**} , and the D^* form factor ratios R_1 and R_2 . Together these uncertainties account for about two thirds of the systematic error. In all the measurements the total systematic errors are reduced with respect to the published values because the values and uncertainties assumed for parameters on which these measurements depend, for example R_1 and R_2 , have since been better determined. The $\chi^2/\text{dof} = 38.7/23$ corresponds to a 2.1% confidence level, suggesting some caution in interpreting the errors on the average.

Table 51: Average of $F(1)|V_{cb}|$ determined in the decay $\bar{B}^0 \rightarrow D^{*+}\ell^-\bar{\nu}$ and individual results, where “excl” and “partial reco” refer to full and partial reconstruction of the $\bar{B}^0 \rightarrow D^{*+}\ell^-\bar{\nu}$ decay, respectively. The fit for the average has $\chi^2/\text{dof} = 38.7/23$ (CL=2.1%). The total correlation between the average $F(1)|V_{cb}|$ and ρ^2 is 0.23.

Experiment	$F(1) V_{cb} [10^{-3}]$ (rescaled) $F(1) V_{cb} [10^{-3}]$ (published)	ρ^2 (rescaled) ρ^2 (published)
ALEPH (excl) [327]	$31.0 \pm 1.7_{\text{stat}} \pm 1.3_{\text{syst}}$ $31.9 \pm 1.8_{\text{stat}} \pm 1.9_{\text{syst}}$	$0.51 \pm 0.19_{\text{stat}} \pm 0.09_{\text{syst}}$ $0.37 \pm 0.26_{\text{stat}} \pm 0.14_{\text{syst}}$
OPAL (excl) [336]	$36.6 \pm 1.6_{\text{stat}} \pm 1.5_{\text{syst}}$ $36.8 \pm 1.6_{\text{stat}} \pm 2.0_{\text{syst}}$	$1.24 \pm 0.20_{\text{stat}} \pm 0.14_{\text{syst}}$ $1.31 \pm 0.21_{\text{stat}} \pm 0.16_{\text{syst}}$
OPAL (partial reco) [336]	$37.2 \pm 1.2_{\text{stat}} \pm 2.4_{\text{syst}}$ $37.5 \pm 1.2_{\text{stat}} \pm 2.5_{\text{syst}}$	$1.16 \pm 0.13_{\text{stat}} \pm 0.27_{\text{syst}}$ $1.12 \pm 0.14_{\text{stat}} \pm 0.29_{\text{syst}}$
DELPHI (partial reco) [337]	$35.4 \pm 1.4_{\text{stat}} \pm 2.3_{\text{syst}}$ $35.5 \pm 1.4_{\text{stat}} \begin{smallmatrix} +2.3 \\ -2.4 \end{smallmatrix}_{\text{syst}}$	$1.19 \pm 0.13_{\text{stat}} \pm 0.25_{\text{syst}}$ $1.34 \pm 0.14_{\text{stat}} \begin{smallmatrix} +0.24 \\ -0.22 \end{smallmatrix}_{\text{syst}}$
Belle (excl) [338]	$34.3 \pm 0.3_{\text{stat}} \pm 1.0_{\text{syst}}$ $34.4 \pm 0.3_{\text{stat}} \pm 1.1_{\text{syst}}$	$1.29 \pm 0.04_{\text{stat}} \pm 0.03_{\text{syst}}$ $1.29 \pm 0.04_{\text{stat}} \pm 0.03_{\text{syst}}$
CLEO (excl) [339]	$39.9 \pm 1.3_{\text{stat}} \pm 1.7_{\text{syst}}$ $43.1 \pm 1.3_{\text{stat}} \pm 1.8_{\text{syst}}$	$1.37 \pm 0.08_{\text{stat}} \pm 0.18_{\text{syst}}$ $1.61 \pm 0.09_{\text{stat}} \pm 0.21_{\text{syst}}$
DELPHI (excl) [340]	$36.1 \pm 1.8_{\text{stat}} \pm 1.9_{\text{syst}}$ $39.2 \pm 1.8_{\text{stat}} \pm 2.3_{\text{syst}}$	$1.09 \pm 0.14_{\text{stat}} \pm 0.15_{\text{syst}}$ $1.32 \pm 0.15_{\text{stat}} \pm 0.33_{\text{syst}}$
BABAR (excl) [341]	$34.0 \pm 0.3_{\text{stat}} \pm 1.1_{\text{syst}}$ $34.7 \pm 0.3_{\text{stat}} \pm 1.1_{\text{syst}}$	$1.18 \pm 0.05_{\text{stat}} \pm 0.03_{\text{syst}}$ $1.18 \pm 0.05_{\text{stat}} \pm 0.03_{\text{syst}}$
BABAR (D^{*0}) [343]	$35.1 \pm 0.8_{\text{stat}} \pm 1.4_{\text{syst}}$ $35.9 \pm 0.6_{\text{stat}} \pm 1.4_{\text{syst}}$	$1.14 \pm 0.06_{\text{stat}} \pm 0.08_{\text{syst}}$ $1.16 \pm 0.06_{\text{stat}} \pm 0.08_{\text{syst}}$
BABAR (Global) [332]	$35.7 \pm 0.2_{\text{stat}} \pm 1.2_{\text{syst}}$ $35.7 \pm 0.2_{\text{stat}} \pm 1.2_{\text{syst}}$	$1.20 \pm 0.02_{\text{stat}} \pm 0.07_{\text{syst}}$ $1.21 \pm 0.02_{\text{stat}} \pm 0.07_{\text{syst}}$
Average	36.04 ± 0.52	1.24 ± 0.04

For a determination of $|V_{cb}|$, the form factor at zero recoil $F(1)$ needs to be computed. A possible choice is $F(1) = 0.921^{+0.013}_{-0.020}$ [346], which, taking into account the QED correction(+0.7%),

gives in

$$|V_{cb}| = (38.9 \pm 0.6_{\text{exp}} \pm 1.0_{\text{theo}}) \times 10^{-3},$$

where the errors are from experiment and theory, respectively.

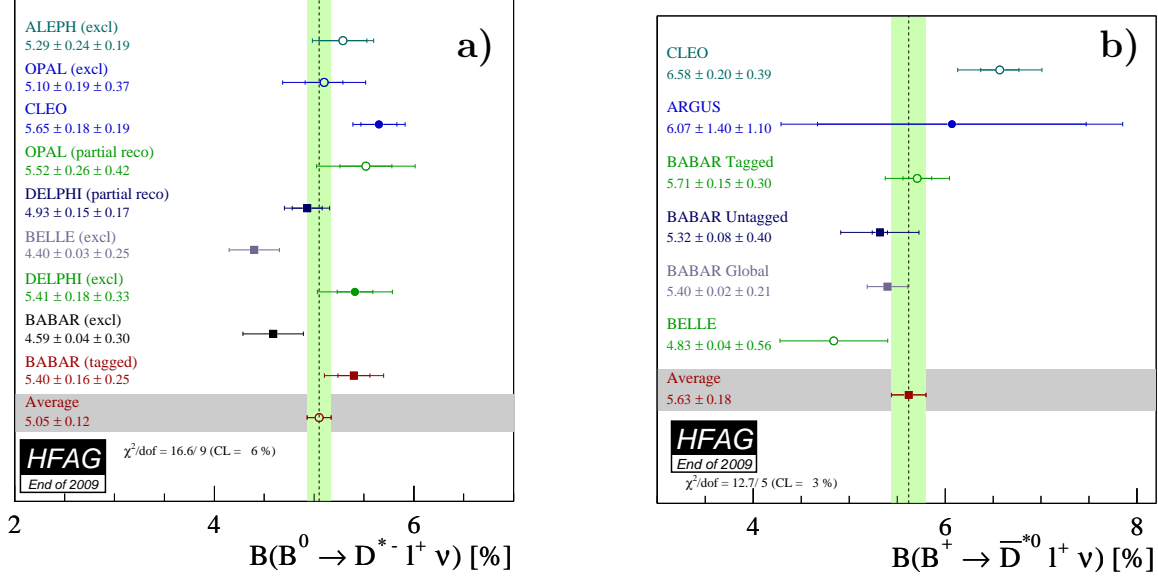


Figure 43: Average branching fraction of exclusive semileptonic B decays (a) $\overline{B}^0 \rightarrow D^{*+} \ell^- \bar{\nu}_\ell$ and (b) $B^+ \rightarrow \overline{D}^{*0} \ell^+ \nu$ and individual results. At LEP, the measurements of $\overline{B}^0 \rightarrow D^{*+} \ell^- \bar{\nu}_\ell$ decays have been done both with inclusive (“partial reco”) and exclusive (“excl”) analyses based on a partial and full reconstruction of the $\overline{B}^0 \rightarrow D^{*+} \ell^- \bar{\nu}_\ell$ decay, respectively.

5.1.3 $\overline{B} \rightarrow D^{(*)} \pi \ell^- \bar{\nu}_\ell$

The average inclusive branching fractions for $\overline{B} \rightarrow D^{(*)} \pi \ell^- \bar{\nu}_\ell$ decays, where no constrain is applied to the hadronic $D^{(*)} \pi$ system, are determined by the combination of the results provided in Table 52 - 55 for $\overline{B}^0 \rightarrow D^0 \pi^+ \ell^- \bar{\nu}_\ell$, $\overline{B}^0 \rightarrow D^{*0} \pi^+ \ell^- \bar{\nu}_\ell$, $B^- \rightarrow D^+ \pi^- \ell^- \bar{\nu}_\ell$, and $B^- \rightarrow D^{*+} \pi^- \ell^- \bar{\nu}_\ell$. The measurements included in the average are scaled to a consistent set of input parameters and their errors [326].

For both the *BABAR* and Belle results, the B semileptonic signal yields are extracted from a fit to the missing mass squared in a sample of fully reconstructed $B\overline{B}$ events.

Figure 45 illustrates the measurements and the resulting average.

5.1.4 $\overline{B} \rightarrow D^{**} \ell^- \bar{\nu}_\ell$

The D^{**} mesons contain one charm quark and one light quark with relative angular momentum $L = 1$. According to Heavy Quark Symmetry (HQS) [348], they form one doublet of states with angular momentum $j \equiv s_q + L = 3/2$ [$D_1(2420), D_2^*(2460)$] and another doublet with $j = 1/2$ [$D_0^*(2400), D_1'(2430)$], where s_q is the light quark spin. Parity and angular momentum conservation constrain the decays allowed for each state. The D_1 and D_2^* states decay through

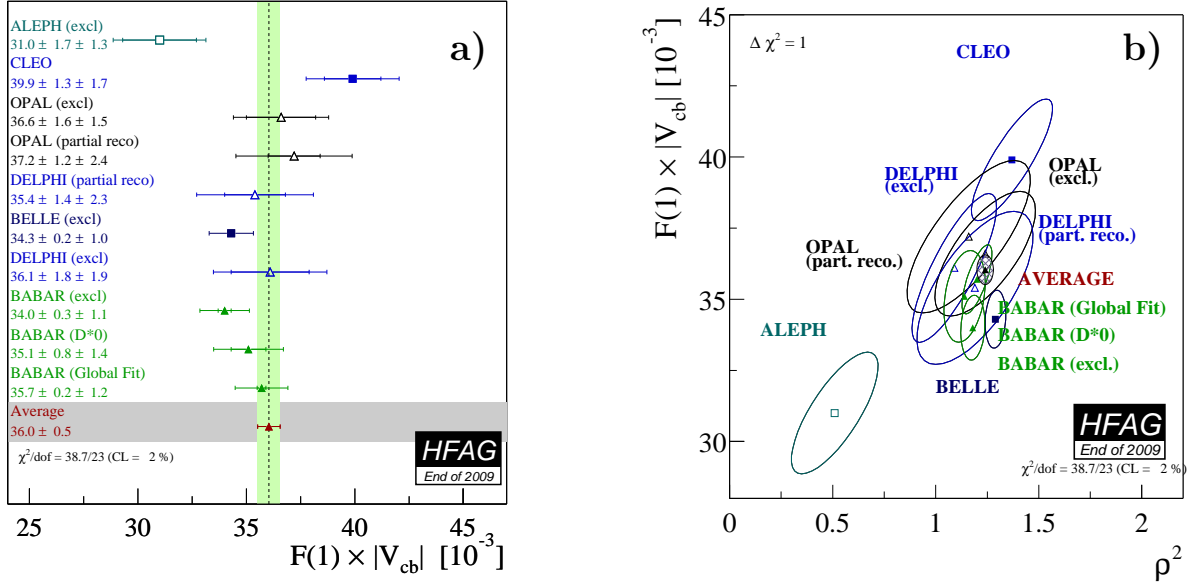


Figure 44: (a) Illustration of $F(1)|V_{cb}|$ vs. ρ^2 . The error ellipses correspond to $\Delta\chi^2 = 1$ (CL=39%). (b) Illustration of the average $F(1)|V_{cb}|$ and rescaled measurements of exclusive $\bar{B}^0 \rightarrow D^{*+}\ell^-\bar{\nu}_\ell$ decays determined in a two-dimensional fit, where “excl” and “partial reco” refer to full and partial reconstruction.

Table 52: Average of the branching fraction $\bar{B}^0 \rightarrow D^0\pi^+\ell^-\bar{\nu}_\ell$ and individual results.

Experiment	$\mathcal{B}(\bar{B}^0 \rightarrow D^0\pi^+\ell^-\bar{\nu}_\ell)$ [%] (rescaled)	$\mathcal{B}(\bar{B}^0 \rightarrow D^0\pi^+\ell^-\bar{\nu}_\ell)$ [%] (published)
Belle [347]	$0.43 \pm 0.07_{\text{stat}} \pm 0.05_{\text{syst}}$	$0.42 \pm 0.07_{\text{stat}} \pm 0.06_{\text{syst}}$
BABAR [330]	$0.42 \pm 0.08_{\text{stat}} \pm 0.03_{\text{syst}}$	$0.43 \pm 0.08_{\text{stat}} \pm 0.03_{\text{syst}}$
Average	0.43 ± 0.06	$\chi^2/\text{dof} = 0.005$ (CL=95%)

Table 53: Average of the branching fraction $\bar{B}^0 \rightarrow D^{*0}\pi^+\ell^-\bar{\nu}_\ell$ and individual results.

Experiment	$\mathcal{B}(\bar{B}^0 \rightarrow D^{*0}\pi^+\ell^-\bar{\nu}_\ell)$ [%] (rescaled)	$\mathcal{B}(\bar{B}^0 \rightarrow D^{*0}\pi^+\ell^-\bar{\nu}_\ell)$ [%] (published)
Belle [347]	$0.57 \pm 0.21_{\text{stat}} \pm 0.07_{\text{syst}}$	$0.56 \pm 0.21_{\text{stat}} \pm 0.08_{\text{syst}}$
BABAR [330]	$0.48 \pm 0.08_{\text{stat}} \pm 0.04_{\text{syst}}$	$0.48 \pm 0.08_{\text{stat}} \pm 0.04_{\text{syst}}$
Average	0.49 ± 0.08	$\chi^2/\text{dof} = 0.15$ (CL=69%)

a D-wave to $D^*\pi$ and $D^{(*)}\pi$, respectively, and have small decay widths, while the D_0^* and D_1' states decay through an S-wave to $D\pi$ and $D^*\pi$ and are very broad. For the narrow states, the average are determined by the combination of the results provided in Table 56 and 57 for $\mathcal{B}(B^- \rightarrow D_1^0(D^{*+}\pi^-)\ell^-\bar{\nu}_\ell) \times \mathcal{B}(D_1^0 \rightarrow D^{*+}\pi^-)$ and $\mathcal{B}(B^- \rightarrow D_2^0(D^{*+}\pi^-)\ell^-\bar{\nu}_\ell) \times \mathcal{B}(D_2^0 \rightarrow D^{*+}\pi^-)$. For the broad states, the average are determined by the combination of the results

Table 54: Average of the branching fraction $B^- \rightarrow D^+ \pi^- \ell^- \bar{\nu}_\ell$ and individual results.

Experiment	$\mathcal{B}(B^- \rightarrow D^+ \pi^- \ell^- \bar{\nu}_\ell)[\%]$ (rescaled)	$\mathcal{B}(B^- \rightarrow D^+ \pi^- \ell^- \bar{\nu}_\ell)[\%]$ (published)
Belle [347]	$0.42 \pm 0.04_{\text{stat}} \pm 0.05_{\text{syst}}$	$0.40 \pm 0.04_{\text{stat}} \pm 0.06_{\text{syst}}$
BABAR [330]	$0.42 \pm 0.06_{\text{stat}} \pm 0.03_{\text{syst}}$	$0.42 \pm 0.06_{\text{stat}} \pm 0.03_{\text{syst}}$
Average	0.42 ± 0.05	$\chi^2/\text{dof} = 0.001$ (CL=99%)

Table 55: Average of the branching fraction $B^- \rightarrow D^{*+} \pi^- \ell^- \bar{\nu}_\ell$ and individual results.

Experiment	$\mathcal{B}(B^- \rightarrow D^{*+} \pi^- \ell^- \bar{\nu}_\ell)[\%]$ (rescaled)	$\mathcal{B}(B^- \rightarrow D^{*+} \pi^- \ell^- \bar{\nu}_\ell)[\%]$ (published)
Belle [347]	$0.67 \pm 0.08_{\text{stat}} \pm 0.07_{\text{syst}}$	$0.64 \pm 0.08_{\text{stat}} \pm 0.09_{\text{syst}}$
BABAR [330]	$0.59 \pm 0.05_{\text{stat}} \pm 0.04_{\text{syst}}$	$0.59 \pm 0.05_{\text{stat}} \pm 0.04_{\text{syst}}$
Average	0.61 ± 0.05	$\chi^2/\text{dof} = 0.5$ (CL=52%)

provided in Table 58 and 59 for $\mathcal{B}(B^- \rightarrow D_1^0(D^{*+} \pi^-) \ell^- \bar{\nu}_\ell) \times \mathcal{B}(D_1^0 \rightarrow D^{*+} \pi^-)$ and $\mathcal{B}(B^- \rightarrow D_0^{*0}(D^+ \pi^-) \ell^- \bar{\nu}_\ell) \times \mathcal{B}(D_0^{*0} \rightarrow D^+ \pi^-)$. The measurements included in the average are scaled to a consistent set of input parameters and their errors [326].

For both the B-factory and the LEP and Tevatron results, the B semileptonic signal yields are extracted from a fit to the invariant mass distribution of the $D^{(*)+} \pi^-$ system. Apart for the CLEO and BELLE results, the other measurements are for the final state $\bar{B} \rightarrow D_2(D^{*+} \pi^-) X \ell^- \bar{\nu}_\ell$. We assume that no particle is left in the X system. Figure 46 and 47 illustrate the measurements and the resulting average.

Table 56: Average of the branching fraction $\mathcal{B}(B^- \rightarrow D_1^0(D^{*+} \pi^-) \ell^- \bar{\nu}_\ell) \times \mathcal{B}(D_1^0 \rightarrow D^{*+} \pi^-)$ and individual results.

Experiment	$\mathcal{B}(B^- \rightarrow D_1^0(D^{*+} \pi^-) \ell^- \bar{\nu}_\ell)[\%]$ (rescaled)	$\mathcal{B}(B^- \rightarrow D_1^0(D^{*+} \pi^-) \ell^- \bar{\nu}_\ell)[\%]$ (published)
ALEPH [349]	$0.45 \pm 0.10_{\text{stat}} \pm 0.07_{\text{syst}}$	$0.47 \pm 0.098_{\text{stat}} \pm 0.074_{\text{syst}}$
OPAL [350]	$0.59 \pm 0.21_{\text{stat}} \pm 0.10_{\text{syst}}$	$0.698 \pm 0.21_{\text{stat}} \pm 0.10_{\text{syst}}$
CLEO [351]	$0.35 \pm 0.08_{\text{stat}} \pm 0.06_{\text{syst}}$	$0.373 \pm 0.085_{\text{stat}} \pm 0.057_{\text{syst}}$
D0 [352]	$0.22 \pm 0.02_{\text{stat}} \pm 0.04_{\text{syst}}$	$0.219 \pm 0.018_{\text{stat}} \pm 0.035_{\text{syst}}$
Belle [347]	$0.44 \pm 0.07_{\text{stat}} \pm 0.06_{\text{syst}}$	$0.42 \pm 0.07_{\text{stat}} \pm 0.07_{\text{syst}}$
BABAR [353]	$0.28 \pm 0.03_{\text{stat}} \pm 0.03_{\text{syst}}$	$0.29 \pm 0.03_{\text{stat}} \pm 0.03_{\text{syst}}$
BABAR [354]	$0.29 \pm 0.02_{\text{stat}} \pm 0.02_{\text{syst}}$	$0.30 \pm 0.02_{\text{stat}} \pm 0.02_{\text{syst}}$
Average	0.28 ± 0.02	$\chi^2/\text{dof} = 13/6$ (CL=4.5%)

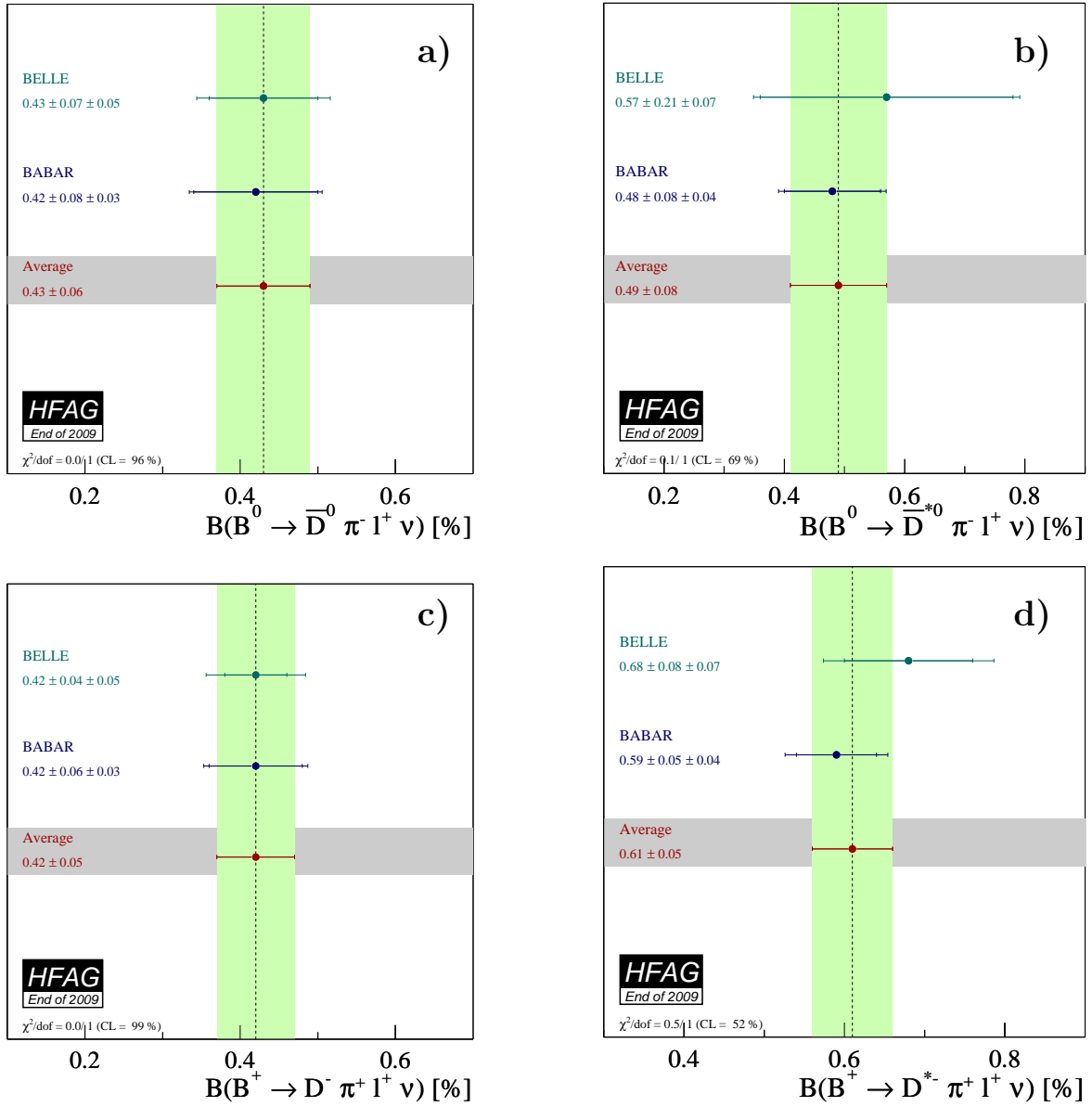


Figure 45: Average branching fraction of exclusive semileptonic B decays (a) $\overline{B}^0 \rightarrow D^0 \pi^+ \ell^- \overline{\nu}_\ell$, (b) $\overline{B}^0 \rightarrow D^{*0} \pi^+ \ell^- \overline{\nu}_\ell$, (c) $B^- \rightarrow D^+ \pi^- \ell^- \overline{\nu}_\ell$, and (d) $B^- \rightarrow D^{*+} \pi^- \ell^- \overline{\nu}_\ell$. The corresponding individual results are also shown.

5.2 Inclusive CKM-favored decays

5.2.1 Inclusive Semileptonic Branching Fraction

In our previous update [4], the branching fraction of inclusive semileptonic B decays $B \rightarrow X \ell \nu_\ell$, where B refers to both charged and neutral B mesons, was averaged for a lepton momentum threshold of 0.6 GeV/ c , as measured in the rest frame of the B meson. A value of $(10.23 \pm 0.15)\%$ was found with a χ^2/dof of the combination of 4.2/5. Since no new measurements have become available, we do not update this average and just refer to our previous update [4].

Table 57: Average of the branching fraction $\mathcal{B}(B^- \rightarrow D_2^0(D^{*+}\pi^-)\ell^-\bar{\nu}_\ell) \times \mathcal{B}(D_2^0 \rightarrow D^{*+}\pi^-)$ and individual results.

Experiment	$\mathcal{B}(B^- \rightarrow D_2^0(D^{*+}\pi^-)\ell^-\bar{\nu}_\ell)[\%]$ (rescaled)	$\mathcal{B}(B^- \rightarrow D_2^0(D^{*+}\pi^-)\ell^-\bar{\nu}_\ell)[\%]$ (published)
CLEO [351]	$0.055 \pm 0.07_{\text{stat}} \pm 0.01_{\text{syst}}$	$0.059 \pm 0.066_{\text{stat}} \pm 0.011_{\text{syst}}$
D0 [352]	$0.09 \pm 0.02_{\text{stat}} \pm 0.02_{\text{syst}}$	$0.088 \pm 0.018_{\text{stat}} \pm 0.020_{\text{syst}}$
Belle [347]	$0.19 \pm 0.06_{\text{stat}} \pm 0.03_{\text{syst}}$	$0.18 \pm 0.06_{\text{stat}} \pm 0.03_{\text{syst}}$
BABAR [353]	$0.067 \pm 0.009_{\text{stat}} \pm 0.016_{\text{syst}}$	$0.068 \pm 0.009_{\text{stat}} \pm 0.016_{\text{syst}}$
BABAR [354]	$0.089 \pm 0.013_{\text{stat}} \pm 0.007_{\text{syst}}$	$0.087 \pm 0.013_{\text{stat}} \pm 0.007_{\text{syst}}$
Average	0.082 ± 0.011	$\chi^2/\text{dof} = 3.7/4$ (CL=44%)

Table 58: Average of the branching fraction $\mathcal{B}(B^- \rightarrow D_1^{\prime 0}(D^{*+}\pi^-)\ell^-\bar{\nu}_\ell) \times \mathcal{B}(D_1^{\prime 0} \rightarrow D^{*+}\pi^-)$ and individual results.

Experiment	$\mathcal{B}(B^- \rightarrow D_1^{\prime 0}(D^{*+}\pi^-)\ell^-\bar{\nu}_\ell)[\%]$ (rescaled)	$\mathcal{B}(B^- \rightarrow D_1^{\prime 0}(D^{*+}\pi^-)\ell^-\bar{\nu}_\ell)[\%]$ (published)
DELPHI [355]	$0.73 \pm 0.17_{\text{stat}} \pm 0.18_{\text{syst}}$	$0.83 \pm 0.17_{\text{stat}} \pm 0.18_{\text{syst}}$
Belle [347]	$-0.03 \pm 0.06_{\text{stat}} \pm 0.01_{\text{syst}}$	$-0.03 \pm 0.06_{\text{stat}} \pm 0.01_{\text{syst}}$
BABAR [353]	$0.26 \pm 0.04_{\text{stat}} \pm 0.04_{\text{syst}}$	$0.27 \pm 0.04_{\text{stat}} \pm 0.05_{\text{syst}}$
Average	0.13 ± 0.04	$\chi^2/\text{dof} = 18/2$ (CL=0.01%)

Table 59: Average of the branching fraction $\mathcal{B}(B^- \rightarrow D_0^{*0}(D^+\pi^-)\ell^-\bar{\nu}_\ell) \times \mathcal{B}(D_0^{*0} \rightarrow D^+\pi^-)$ and individual results.

Experiment	$\mathcal{B}(B^- \rightarrow D_0^{*0}(D^+\pi^-)\ell^-\bar{\nu}_\ell)[\%]$ (rescaled)	$\mathcal{B}(B^- \rightarrow D_0^{*0}(D^+\pi^-)\ell^-\bar{\nu}_\ell)[\%]$ (published)
Belle [347]	$0.25 \pm 0.04_{\text{stat}} \pm 0.06_{\text{syst}}$	$0.24 \pm 0.04_{\text{stat}} \pm 0.06_{\text{syst}}$
BABAR [353]	$0.26 \pm 0.05_{\text{stat}} \pm 0.04_{\text{syst}}$	$0.26 \pm 0.05_{\text{stat}} \pm 0.04_{\text{syst}}$
Average	0.25 ± 0.05	$\chi^2/\text{dof} = 0.2$ (CL=92%)

This partial branching fraction corresponds to an inclusive semileptonic branching fraction of $(10.74 \pm 0.16)\%$.

For the same reason, we do not update our averages of the ratio $\mathcal{B}(B^+ \rightarrow X^0\ell^+\nu_\ell)/\mathcal{B}(B^0 \rightarrow X^-\ell^+\nu_\ell)$, of $\mathcal{B}(B^+ \rightarrow X^0\ell^+\nu_\ell)$, and of $\mathcal{B}(B^0 \rightarrow X^-\ell^+\nu_\ell)$. For these averages the reader is referred to our previous update [4].

5.2.2 Determination of $|V_{cb}|$

The magnitude of the CKM matrix element $|V_{cb}|$ can be determined from inclusive semileptonic B decays $B \rightarrow X_c\ell\nu_\ell$ using calculations based on the Heavy Quark Effective Theory and the Operator Production Expansion [356, 357]. However, these expressions depend also on non-

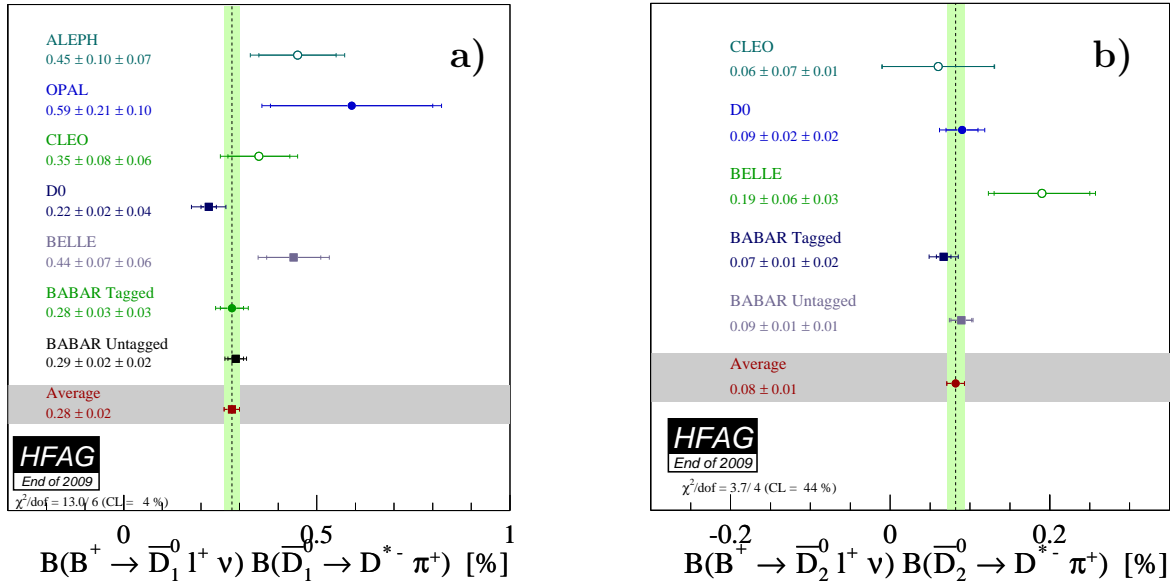


Figure 46: Average of the product of branching fraction (a) $\mathcal{B}(B^+ \rightarrow \bar{D}_1^0(D^{*+}\pi^-)\ell^+\bar{\nu}_\ell) \times \mathcal{B}(D_1^0 \rightarrow D^{*+}\pi^-)$ and (b) $\mathcal{B}(B^+ \rightarrow \bar{D}_2^0(D^{*+}\pi^-)\ell^+\bar{\nu}_\ell) \times \mathcal{B}(D_2^0 \rightarrow D^{*+}\pi^-)$ The corresponding individual results are also shown.

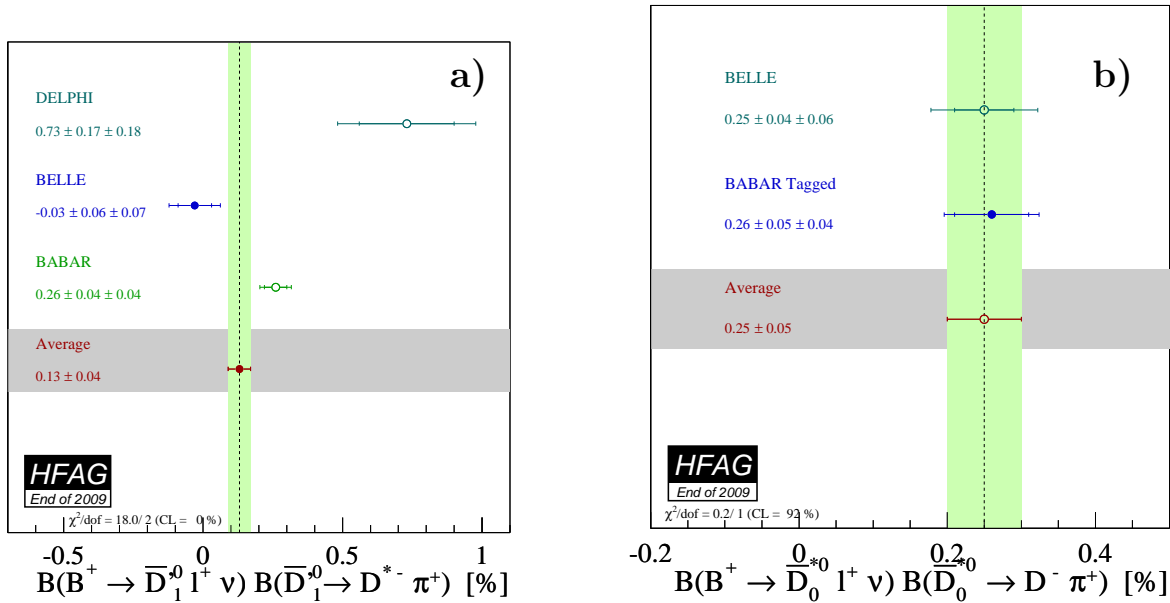


Figure 47: Average of the product of branching fraction (a) $\mathcal{B}(B^- \rightarrow D_1^0(D^{*+}\pi^-)\ell^+\bar{\nu}_\ell) \times \mathcal{B}(D_1^0 \rightarrow D^{*+}\pi^-)$ and (b) $\mathcal{B}(B^- \rightarrow D_0^{*0}(D^{*+}\pi^-)\ell^+\bar{\nu}_\ell) \times \mathcal{B}(D_0^{*0} \rightarrow D^+\pi^-)$ The corresponding individual results are also shown.

perturbative parameters such as the b -quark mass m_b which can be determined from inclusive observables in B decays. In practice, $|V_{cb}|$ and these parameters are determined simultaneously from a global fit to measured moments of the inclusive lepton and hadronic mass spectrum

in semileptonic decays, and of the inclusive photon spectrum in radiative B meson penguin decays. The moments are measured as a function of the minimum lepton or photon energy.

Two independent sets of theoretical expressions, referred to as kinetic [356, 358, 359] and 1S schemes [357] are available for this kind of analysis. The HFAG fit presented here is done in the kinetic scheme and follows closely the approach of Ref. [360]. The fit is based on the experimental data given in Table 60. The only external input is the average lifetime τ_B of neutral and charged B mesons, taken to be (1.582 ± 0.007) ps (Sect. 3).

Table 60: Experimental inputs used in the global fit analysis. n is the order of the moment, c is the threshold value in GeV. In total, there are 29 measurements from BaBar, 25 measurements from Belle and 12 from other experiments.

Experiment	Hadron moments $\langle M_X^n \rangle$	Lepton moments $\langle E_\ell^n \rangle$	Photons moment $\langle E_\gamma^n \rangle$
BaBar	$n = 2, c = 0.9, 1.1, 1.3, 1.5$	$n = 0, c = 0.6, 1.2, 1.5$	$n = 1, c = 1.9, 2.0$
	$n = 4, c = 0.8, 1.0, 1.2, 1.4$	$n = 1, c = 0.6, 0.8, 1.0, 1.2, 1.5$	$n = 2, c = 1.9$ [361, 362]
	$n = 6, c = 0.9, 1.3$ [363]	$n = 2, c = 0.6, 1.0, 1.5$ $n = 3, c = 0.8, 1.2$ [363, 364]	
Belle	$n = 2, c = 0.7, 1.1, 1.3, 1.5$	$n = 0, c = 0.6, 1.0, 1.4$	$n = 1, c = 1.8, 1.9$
	$n = 4, c = 0.7, 0.9, 1.3$ [365]	$n = 1, c = 0.6, 0.8, 1.0, 1.2, 1.4$ $n = 2, c = 0.6, 1.0, 1.4$ $n = 3, c = 0.8, 1.0, 1.2$ [367]	$n = 2, c = 1.8, 2.0$ [366]
CDF	$n = 2, c = 0.7$ $n = 4, c = 0.7$ [368]		
CLEO	$n = 2, c = 1.0, 1.5$ $n = 4, c = 1.0, 1.5$ [370]		$n = 1, c = 2.0$ [369]
DELPHI	$n = 2, c = 0.0$	$n = 1, c = 0.0$	
	$n = 4, c = 0.0$ [371]	$n = 2, c = 0.0$ $n = 3, c = 0.0$ [371]	

5.2.3 Global Fit in the Kinetic Scheme

This fit relies on the calculations of the spectral moments in $B \rightarrow X_c \ell \nu_\ell$ decays in the kinetic mass scheme [358]. Compared to the original publication, the expressions have been updated by the authors. For the moments in $B \rightarrow X_s \gamma$, the (biased) OPE prediction and the bias correction have been calculated [359]. All these expressions depend on the following set of parameters: the b - and c -quark masses m_b^{kin} and m_c^{kin} , μ_π^2 and μ_G^2 at $\mathcal{O}(1/m_b^2)$ and ρ_D^3 and ρ_{LS}^3 at $\mathcal{O}(1/m_b^3)$ ³⁰. In our analysis, we determine these six parameters together with the semileptonic branching fraction (over the full lepton energy range) $\mathcal{B}(B \rightarrow X_c \ell \nu_\ell)$. The total number of parameters in the fit is thus seven. The conversion from $\mathcal{B}(B \rightarrow X_c \ell \nu_\ell)$ to $|V_{cb}|$ is done using the expression in Ref. [356].

The results of the fit in the kinetic scheme to the $X_c \ell \nu_\ell$ and $X_s \gamma$ data (Table 60) are given in Table 61. For the semileptonic branching fraction we obtain $\mathcal{B}(B \rightarrow X_c \ell \nu_\ell) = (10.55 \pm 0.14)\%$. The χ^2 of the fit is 29.7 for (66–7) degrees of freedom. The predictions of the $B \rightarrow X_s \gamma$ moments

³⁰All non-perturbative parameters in the kinetic scheme are defined at the scale $\mu = 1$ GeV.

are not entirely OPE-based and involve some amount of modeling. Therefore, we have also performed a fit to the $X_c \ell \nu_\ell$ data only, Table 62. The comparison of the $\Delta\chi^2 = 1$ ellipses of these two fits in the $(m_b^{\text{kin}}, \mu_\pi^2)$ and $(m_b^{\text{kin}}, |V_{cb}|)$ planes is shown in Fig. 48.

Table 61: Result of the kinetic scheme fit to all moments in Table 60. The $\sigma(\text{fit})$ error contains the experimental and theoretical uncertainties in the moments. The $\sigma(\tau_B)$ and $\sigma(\text{th})$ errors on $|V_{cb}|$ are due to the uncertainty in the average B meson lifetime and the limited accuracy of the expression for $|V_{cb}|$ [356], respectively. In the lower part of the table, the correlation matrix of the parameters is given.

	$ V_{cb} $ (10^{-3})	m_b^{kin} (GeV)	m_c^{kin} (GeV)	μ_π^2 (GeV^2)	ρ_D^3 (GeV^3)	μ_G^2 (GeV^2)	ρ_{LS}^3 (GeV^3)
value	41.85	4.591	1.152	0.454	0.193	0.262	-0.177
$\sigma(\text{fit})$	0.42	0.031	0.046	0.038	0.020	0.044	0.085
$\sigma(\tau_B)$	0.09						
$\sigma(\text{th})$	0.59						
$ V_{cb} $	1.000	-0.169	-0.024	0.118	0.297	-0.248	0.109
m_b^{kin}		1.000	0.926	-0.405	-0.126	-0.021	-0.266
m_c^{kin}			1.000	-0.464	-0.051	-0.307	-0.056
μ_π^2				1.000	0.392	-0.010	-0.077
ρ_D^3					1.000	-0.236	-0.318
μ_G^2						1.000	-0.203
ρ_{LS}^3							1.000

Table 62: Kinetic fit results for $B \rightarrow X_c \ell \nu_\ell$ and $B \rightarrow X_s \gamma$, and for $B \rightarrow X_c \ell \nu_\ell$ only.

Data	χ^2/dof	$ V_{cb} $ (10^{-3})	m_b^{kin} (GeV)	μ_π^2 (GeV^2)
All moments ($X_c \ell \nu_\ell$ and $X_s \gamma$)	29.7/(66 - 7)	41.85 ± 0.73	4.591 ± 0.031	0.454 ± 0.038
$X_c \ell \nu_\ell$ only	24.2/(55 - 7)	41.68 ± 0.74	4.646 ± 0.047	0.439 ± 0.042

5.3 Exclusive CKM-suppressed decays

In this section, we list results on exclusive charmless semileptonic branching fractions and determinations of $|V_{ub}|$ based on $\bar{B} \rightarrow \pi \ell \bar{\nu}$ decays. The measurements are based on two different event selections: tagged events, in which case the second B meson in the event is fully reconstructed in either a hadronic decay (“ B_{reco} ”) or in a CKM-favored semileptonic decay (“SL”); and untagged events, in which case the selection infers the momentum of the undetected neutrino based on measurements of the total momentum sum of detected particles and knowledge of the initial state. We present averages for $\bar{B} \rightarrow \rho \ell \bar{\nu}$ and $\bar{B} \rightarrow \omega \ell \bar{\nu}$. Moreover, the average for the branching fraction $\bar{B} \rightarrow \eta \ell \bar{\nu}$ is presented for the first time.

The results for the full and partial branching fraction for $\bar{B} \rightarrow \pi \ell \bar{\nu}$ are given in Table 63 and shown in Figure 49 (a).

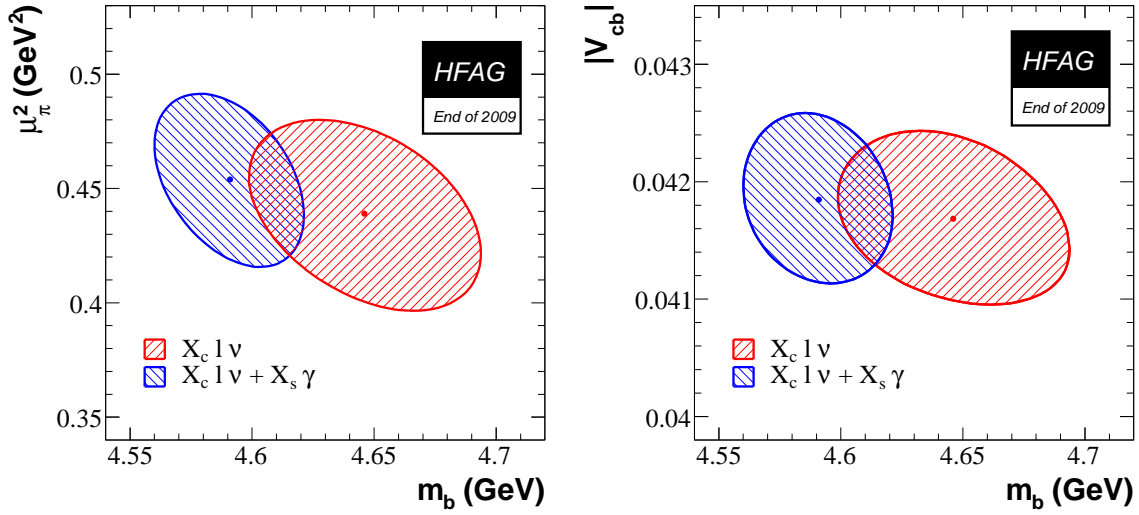


Figure 48: $\Delta\chi^2 = 1$ contours for the fit in the kinetic mass scheme.

When averaging these results, systematic uncertainties due to external inputs, e.g., form factor shapes and background estimates from the modeling of $\bar{B} \rightarrow X_c \ell \bar{\nu}$ and $\bar{B} \rightarrow X_u \ell \bar{\nu}$ decays, are treated as fully correlated (in the sense of Eq. 10). Uncertainties due to experimental reconstruction effects are treated as fully correlated among measurements from a given experiment. Varying the assumed dependence of the quoted errors on the measured value for error sources where the dependence was not obvious had no significant impact.

Table 63: Summary of exclusive determinations of $\mathcal{B}(\bar{B} \rightarrow \pi \ell \bar{\nu})$. The errors quoted correspond to statistical and systematic uncertainties, respectively. Measured branching fractions for $B \rightarrow \pi^0 l \nu$ have been multiplied by $2 \times \tau_{B^0}/\tau_{B^+}$ in accordance with isospin symmetry. The labels “ B_{reco} ” and “SL” tags refer to the type of B decay tag used in a measurement, and “untagged” refers to an untagged measurement.

	$\mathcal{B}[10^{-4}]$	$\mathcal{B}(q^2 > 16 \text{ GeV}^2/c^2)[10^{-4}]$	$\mathcal{B}(q^2 < 16 \text{ GeV}^2/c^2)[10^{-4}]$
CLEO π^+, π^0 [372]	$1.38 \pm 0.15 \pm 0.11$	$0.41 \pm 0.08 \pm 0.04$	$0.97 \pm 0.13 \pm 0.09$
BABAR π^+ [373]	$1.45 \pm 0.07 \pm 0.11$	$0.38 \pm 0.04 \pm 0.05$	$1.08 \pm 0.06 \pm 0.09$
BELLE SL π^+ [374]	$1.38 \pm 0.19 \pm 0.15$	$0.36 \pm 0.10 \pm 0.04$	$1.02 \pm 0.16 \pm 0.11$
BELLE SL π^0 [374]	$1.43 \pm 0.26 \pm 0.15$	$0.37 \pm 0.15 \pm 0.04$	$1.05 \pm 0.23 \pm 0.11$
BABAR SL π^+ [375]	$1.39 \pm 0.21 \pm 0.08$	$0.46 \pm 0.13 \pm 0.03$	$0.92 \pm 0.16 \pm 0.05$
BABAR SL π^0 [375]	$1.80 \pm 0.28 \pm 0.15$	$0.45 \pm 0.17 \pm 0.06$	$1.38 \pm 0.23 \pm 0.11$
BABAR $B_{reco} \pi^+$ [376]	$1.07 \pm 0.27 \pm 0.19$	$0.65 \pm 0.20 \pm 0.13$	$0.42 \pm 0.18 \pm 0.06$
BABAR $B_{reco} \pi^0$ [376]	$1.54 \pm 0.41 \pm 0.30$	$0.49 \pm 0.23 \pm 0.12$	$1.05 \pm 0.36 \pm 0.19$
BELLE $B_{reco} \pi^+$ [377]	$1.12 \pm 0.18 \pm 0.05$	$0.26 \pm 0.08 \pm 0.01$	$0.85 \pm 0.16 \pm 0.04$
BELLE $B_{reco} \pi^0$ [377]	$1.24 \pm 0.23 \pm 0.05$	$0.41 \pm 0.11 \pm 0.02$	$0.85 \pm 0.16 \pm 0.04$
Average	$1.36 \pm 0.05 \pm 0.05$	$0.37 \pm 0.02 \pm 0.02$	$0.94 \pm 0.05 \pm 0.04$

The determination of $|V_{ub}|$ from the $\bar{B} \rightarrow \pi \ell \bar{\nu}$ decays is shown in Table 64, and uses our

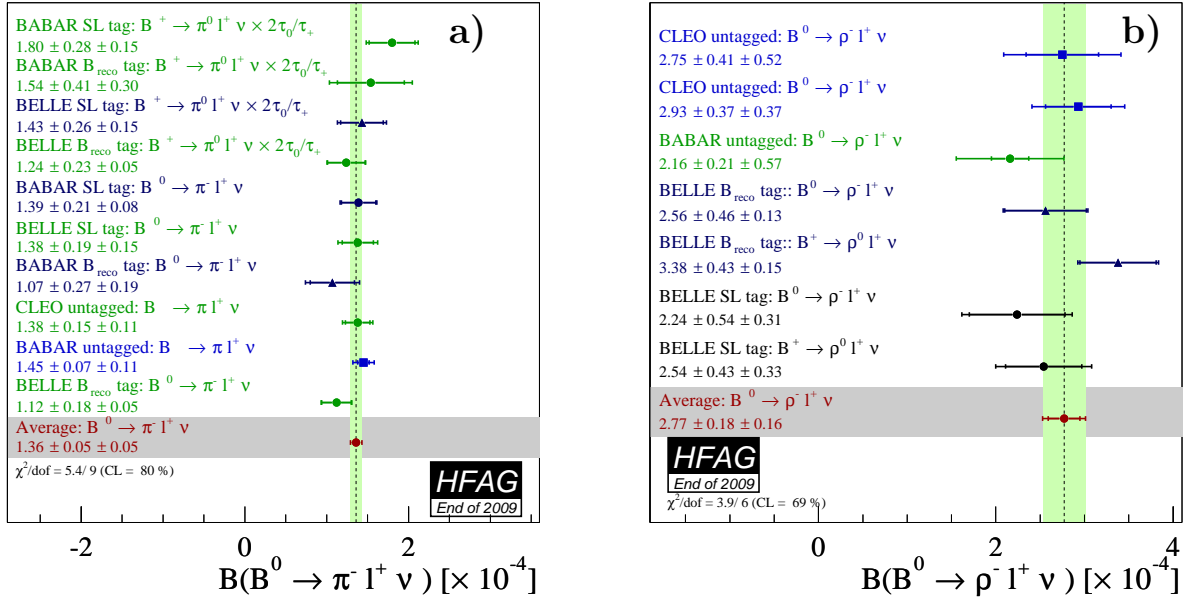


Figure 49: (a) Summary of exclusive determinations of $\mathcal{B}(\bar{B} \rightarrow \pi \ell \bar{\nu})$ and their average. Measured branching fractions for $B \rightarrow \pi^0 l \nu$ have been multiplied by $2 \times \tau_{B^0}/\tau_{B^+}$ in accordance with isospin symmetry. The labels “ B_{reco} ” and “SL” refer to type of B decay tag used in a measurement. “untagged” refers to an untagged measurement. (b) Summary of exclusive determinations of $\mathcal{B}(\bar{B} \rightarrow \rho \ell \bar{\nu})$ and their average.

average for the branching fraction given in Table 63. Two theoretical approaches are used: Lattice QCD (quenched and unquenched) and QCD sum rules. Lattice calculations of the Form Factors (FF) are limited to small hadron momenta, i.e. large q^2 , while calculations based on light cone sum rules are restricted to small q^2 .

The branching fractions for $\bar{B} \rightarrow \rho \ell \bar{\nu}$ decays is computed based on the measurements in Table 5.3 and is shown in Figure 49 (b). The determination of $|V_{ub}|$ from these other channels looks less promising than for $\bar{B} \rightarrow \pi \ell \bar{\nu}$ and at the moment it is not extracted.

We also report the branching fraction average for $\bar{B} \rightarrow \omega \ell \bar{\nu}$ and $\bar{B} \rightarrow \eta \ell \bar{\nu}$. The measurements for $\bar{B} \rightarrow \omega \ell \bar{\nu}$ are reported in Table and shown in Figure 50, while the ones for $\bar{B} \rightarrow \eta \ell \bar{\nu}$ are reported in Table and shown in Figure 50.

Branching fractions for other $\bar{B} \rightarrow X_u \ell \bar{\nu}$ decays are given in Table 68.

5.4 Inclusive CKM-suppressed decays

The large background from $B \rightarrow X_c \ell^+ \nu_\ell$ decays is the chief experimental limitation in determinations of $|V_{ub}|$. Cuts designed to reject this background limit the acceptance for $B \rightarrow X_u \ell^+ \nu_\ell$ decays. The calculation of partial rates for these restricted acceptances is more complicated and requires substantial theoretical machinery. In this update, we use several theoretical calculations to extract $|V_{ub}|$. We do not advocate the use of one method over another. The authors for the different calculations have provided codes to compute the partial rates in limited regions of phase space covered by the measurements. A recent result by Belle [387], superceding the previous three measurements of [388], selects a big portion of the phase space by using

Table 64: Determinations of $|V_{ub}|$ based on the average total and partial $\bar{B} \rightarrow \pi \ell \bar{\nu}$ decay branching fraction stated in Table 63. The first uncertainty is experimental, and the second is from theory. The full or partial branching fractions are used as indicated. Acronyms for the calculations refer to either the method (LCSR) or the collaboration working on it (HPQCD, FNAL, APE).

Method	$ V_{ub} [10^{-3}]$
LCSR, full q^2 [378]	$3.45 \pm 0.11^{+0.67}_{-0.42}$
LCSR, $q^2 < 16 \text{ GeV}^2/c^2$ [378]	$3.34 \pm 0.12^{+0.55}_{-0.37}$
HPQCD, full q^2 [379]	$3.05 \pm 0.10^{+0.73}_{-0.43}$
HPQCD, $q^2 > 16 \text{ GeV}^2/c^2$ [379]	$3.40 \pm 0.20^{+0.59}_{-0.39}$
FNAL, full q^2 [334]	$3.73 \pm 0.12^{+0.88}_{-0.52}$
FNAL, $q^2 > 16 \text{ GeV}^2/c^2$ [334]	$3.62 \pm 0.22^{+0.63}_{-0.41}$
APE, full q^2 [380]	$3.59 \pm 0.11^{+1.11}_{-0.57}$
APE, $q^2 > 16 \text{ GeV}^2/c^2$ [380]	$3.72 \pm 0.21^{+1.43}_{-0.66}$

Table 65: Summary of exclusive determinations of $\mathcal{B}(\bar{B} \rightarrow \rho \ell \bar{\nu})$. The errors quoted correspond to statistical and systematic uncertainties, respectively.

	$\mathcal{B}[10^{-4}]$
CLEO ρ^+ [381]	$2.75 \pm 0.41 \pm 0.52$
CLEO ρ^+ [372]	$2.93 \pm 0.37 \pm 0.37$
BABAR ρ^+ [382]	$2.16 \pm 0.21 \pm 0.57$
BELLE ρ^+ [377]	$2.56 \pm 0.46 \pm 0.13$
BELLE ρ^0 [377]	$3.38 \pm 0.43 \pm 0.15$
BELLE ρ^+ [374]	$2.24 \pm 0.54 \pm 0.31$
BELLE ρ^0 [374]	$2.54 \pm 0.43 \pm 0.33$
Average	$2.77 \pm 0.18 \pm 0.16$

Table 66: Summary of exclusive determinations of $\mathcal{B}(\bar{B} \rightarrow \omega \ell \bar{\nu})$. The errors quoted correspond to statistical and systematic uncertainties, respectively.

	$\mathcal{B}[10^{-4}]$
BELLE ω [377]	$1.19 \pm 0.32 \pm 0.06$
BABAR ω [383]	$1.14 \pm 0.16 \pm 0.08$
Average	1.15 ± 0.16

a multivariate technique to reject background, with a consequent reduction of the theoretical uncertainties.

For the averages we performed, the systematic errors associated with the modeling of $B \rightarrow X_c \ell^+ \nu_\ell$ and $B \rightarrow X_u \ell^+ \nu_\ell$ decays and the theoretical uncertainties are taken as fully correlated among all measurements. Reconstruction-related uncertainties are taken as fully correlated within a given experiment. We use all three results published by *BABAR* in [389],

Table 67: Summary of exclusive determinations of $\mathcal{B}(\bar{B} \rightarrow \eta \ell \bar{\nu})$. The errors quoted correspond to statistical and systematic uncertainties, respectively.

$\mathcal{B}[10^{-4}]$	
CLEO η [384]	$0.45 \pm 0.23 \pm 0.11$
BABAR η [383]	$0.31 \pm 0.06 \pm 0.08$
BABAR η [375]	$0.64 \pm 0.20 \pm 0.04$
Average	0.38 ± 0.09

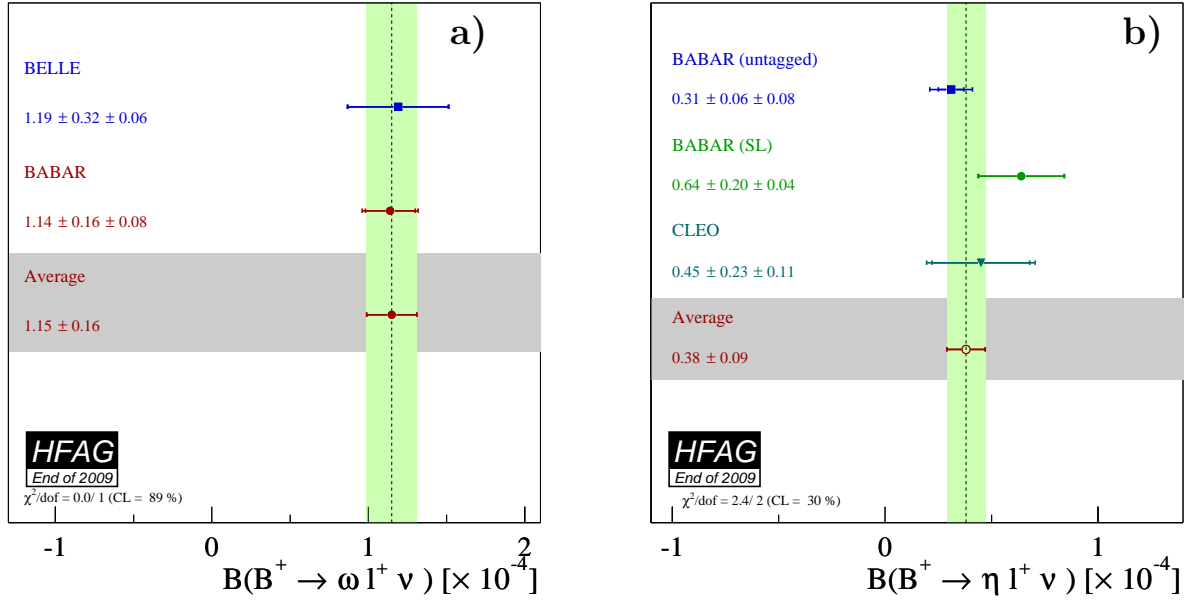


Figure 50: (a) Summary of exclusive determinations of $\mathcal{B}(\bar{B} \rightarrow \omega \ell \bar{\nu})$ and their average. (b) Summary of exclusive determinations of $\mathcal{B}(\bar{B} \rightarrow \eta \ell \bar{\nu})$ and their average.

Table 68: Summary of other branching fractions to $\mathcal{B}(\bar{B} \rightarrow X \ell \bar{\nu})$ decays not included in the averages. The errors quoted correspond to statistical and systematic uncertainties, respectively. Where a third uncertainty is quoted, it corresponds to uncertainties from form factor shapes.

Experiment	Mode	$\mathcal{B}[10^{-4}]$
CLEO [385]	$B^+ \rightarrow \eta \ell \bar{\nu}$	$0.84 \pm 0.31 \pm 0.16 \pm 0.09$
BABAR [386]	$B^+ \rightarrow \eta \ell \bar{\nu}$	$0.84 \pm 0.27 \pm 0.21$
CLEO [384]	$B^+ \rightarrow \eta' \ell \bar{\nu}$	$2.66 \pm 0.80 \pm 0.56$
BABAR [386]	$B^+ \rightarrow \eta' \ell \bar{\nu}$	$0.33 \pm 0.60 \pm 0.30$
BABAR [375]	$B^+ \rightarrow \eta' \ell \bar{\nu}$	< 0.47 @90 CL

since the statistical correlations are given. To make use of the theoretical calculations of Ref. [390], we restrict the kinematic range in M_X and q^2 , thereby reducing the size of the data sample significantly, but also the theoretical uncertainty, as stated by the authors [390]. The

dependence of the quoted error on the measured value for each source of error is taken into account in the calculation of the averages. Measurements of partial branching fractions for $B \rightarrow X_u \ell^+ \nu_\ell$ transitions from $\Upsilon(4S)$ decays, together with the corresponding accepted region, are given in Table 69. The signal yields for all the measurements shown in Table 69 are not rescaled to common input values of the B meson lifetime [326] and the semileptonic width [5].

It has been first suggested by Neubert [391] and later detailed by Leibovich, Low, and Rothstein (LLR) [392] and Lange, Neubert and Paz (LNP) [393], that the uncertainty of the leading shape functions can be eliminated by comparing inclusive rates for $B \rightarrow X_u \ell^+ \nu_\ell$ decays with the inclusive photon spectrum in $B \rightarrow X_s \gamma$, based on the assumption that the shape functions for transitions to light quarks, u or s , are the same to first order. However, shape function uncertainties are only eliminated at the leading order and they still enter via the signal models used for the determination of efficiency. For completeness, we provide a comparison of the results using calculations with reduced dependence on the shape function, as just introduced, with our averages using different theoretical approaches. Results are presented by *BABAR* in Ref.[394] using the LLR prescription. More recently, V.B.Golubev, V.G.Luth and Yu.I.Skovpen (Ref. [395]) extracted $|V_{ub}|$ from the endpoint spectrum of $B \rightarrow X_u \ell^+ \nu_\ell$ from *BABAR* [396], using several theoretical approaches with reduced dependence on the shape function. In both cases, the photon energy spectrum in the rest frame of the B -meson by *BABAR* [397] has been used.

Table 69: Summary of inclusive determinations of partial branching fractions for $B \rightarrow X_u \ell^+ \nu_\ell$ decays. The errors quoted on $\Delta\mathcal{B}$ correspond to statistical and systematic uncertainties. The statistical correlations between the analysis are given where applicable. The s_h^{\max} variable is described in Refs. [398, 399].

Measurement	Accepted region	$\Delta\mathcal{B}[10^{-4}]$	Notes
CLEO [400]	$E_e > 2.1 \text{ GeV}$	$3.3 \pm 0.2 \pm 0.7$	
<i>BABAR</i> [399]	$E_e > 2.0 \text{ GeV}, s_h^{\max} < 3.5 \text{ GeV}^2$	$4.4 \pm 0.4 \pm 0.4$	
<i>BABAR</i> [396]	$E_e > 2.0 \text{ GeV}$	$5.7 \pm 0.4 \pm 0.5$	
BELLE [401]	$E_e > 1.9 \text{ GeV}$	$8.5 \pm 0.4 \pm 1.5$	
<i>BABAR</i> [389]	$M_X < 1.7 \text{ GeV}/c^2, q^2 > 8 \text{ GeV}^2/c^2$	$7.7 \pm 0.7 \pm 0.7$	65% correlation with <i>BABAR</i> M_X analysis
BELLE [402]	$M_X < 1.7 \text{ GeV}/c^2, q^2 > 8 \text{ GeV}^2/c^2$	$7.4 \pm 0.9 \pm 1.3$	
<i>BABAR</i> [389]	$P_+ < 0.66 \text{ GeV}$	$9.4 \pm 0.9 \pm 0.8$	38% correlation with <i>BABAR</i> ($M_X - q^2$) analysis
<i>BABAR</i> [389]	$M_X < 1.55 \text{ GeV}/c^2$	$11.7 \pm 0.9 \pm 0.7$	67% correlation with <i>BABAR</i> P_+ analysis
BELLE [387]	$p_\ell^* > 1 \text{ GeV}/c$	$19.6 \pm 1.7 \pm 1.6$	

5.4.1 BLNP

Bosch, Lange, Neubert and Paz (BLNP) [403, 404, 405, 406] provide theoretical expressions for the triple differential decay rate for $B \rightarrow X_u \ell^+ \nu_\ell$ events, incorporating all known contributions, whilst smoothly interpolating between the “shape-function region” of large hadronic energy and small invariant mass, and the “OPE region” in which all hadronic kinematical variables scale

with the b -quark mass. BLNP assign uncertainties to the b -quark mass which enters through the leading shape function, to sub-leading shape function forms, to possible weak annihilation contribution, and to matching scales. The extracted values of $|V_{ub}|$ for each measurement along with their average are given in Table 70 and illustrated in Figure 51. The total uncertainty is ${}^{+6.2\%}_{-6.6\%}$ and is due to: statistics (${}^{+2.4\%}_{-2.6\%}$), detector (${}^{+1.9\%}_{-1.9\%}$), $B \rightarrow X_c \ell^+ \nu_\ell$ model (${}^{+0.9\%}_{-0.9\%}$), $B \rightarrow X_u \ell^+ \nu_\ell$ model (${}^{+1.7\%}_{-1.6\%}$), heavy quark parameters (${}^{+3.3\%}_{-3.8\%}$), SF functional form (${}^{+0.5\%}_{-0.5\%}$), sub-leading shape functions (${}^{+0.8\%}_{-0.8\%}$), BLNP theory: matching scales μ, μ_i, μ_h (${}^{+3.5\%}_{-3.5\%}$), and weak annihilation (${}^{+1.3\%}_{-1.2\%}$). The error on the HQE parameters (b -quark mass and μ_π^2) and the uncertainty assigned for the matching scales are the dominant contribution to the total uncertainty.

Table 70: Summary of input parameters used by the different theory calculations, corresponding inclusive determinations of $|V_{ub}|$ and their average. The errors quoted on $|V_{ub}|$ correspond to experimental and theoretical uncertainties, respectively.

	BLNP	DGE	GGOU	ADFR	BLL
Input parameters					
scheme	SF	\overline{MS}	kinetic	\overline{MS}	1S
Ref.	see Sect. 5.2.3	Ref. [5]	see Sect. 5.2.3	Ref. [5]	Ref. [4]
m_b (GeV)	4.620 ${}^{+0.039}_{-0.032}$	4.222 ± 0.051	4.591 ± 0.031	4.222 ± 0.051	4.70 ± 0.03
μ_π^2 (GeV 2)	0.288 ${}^{+0.054}_{-0.074}$	-	0.454 ± 0.038	-	-
Ref.	V_{ub} values				
E_e [400]	4.01 ± 0.47 ${}^{+0.34}_{-0.34}$	3.71 ± 0.43 ${}^{+0.30}_{-0.26}$	3.82 ± 0.45 ${}^{+0.22}_{-0.39}$	3.47 ± 0.41 ${}^{+0.21}_{-0.22}$	-
M_X, q^2 [402]	4.40 ± 0.46 ${}^{+0.31}_{-0.19}$	4.31 ± 0.45 ${}^{+0.24}_{-0.23}$	4.25 ± 0.45 ${}^{+0.25}_{-0.33}$	3.94 ± 0.41 ${}^{+0.23}_{-0.24}$	4.67 ± 0.49 ${}^{+0.34}_{-0.34}$
E_e [401]	4.82 ± 0.45 ${}^{+0.32}_{-0.29}$	4.67 ± 0.43 ${}^{+0.26}_{-0.25}$	4.66 ± 0.43 ${}^{+0.19}_{-0.30}$	4.53 ± 0.42 ${}^{+0.27}_{-0.27}$	-
E_e [396]	4.36 ± 0.25 ${}^{+0.31}_{-0.30}$	4.16 ± 0.28 ${}^{+0.28}_{-0.25}$	4.18 ± 0.24 ${}^{+0.20}_{-0.33}$	3.98 ± 0.27 ${}^{+0.24}_{-0.25}$	-
E_e, s_h^{\max} [399]	4.49 ± 0.30 ${}^{+0.39}_{-0.37}$	4.16 ± 0.28 ${}^{+0.30}_{-0.30}$	-	3.87 ± 0.26 ${}^{+0.24}_{-0.24}$	-
p_ℓ^* [387]	4.46 ± 0.27 ${}^{+0.24}_{-0.21}$	4.54 ± 0.27 ${}^{+0.15}_{-0.15}$	4.48 ± 0.27 ${}^{+0.11}_{-0.15}$	4.55 ± 0.30 ${}^{+0.27}_{-0.27}$	-
M_X [389]	4.20 ± 0.20 ${}^{+0.29}_{-0.27}$	4.41 ± 0.21 ${}^{+0.23}_{-0.20}$	4.12 ± 0.20 ${}^{+0.25}_{-0.28}$	4.01 ± 0.19 ${}^{+0.25}_{-0.26}$	-
M_X, q^2 [389]	4.49 ± 0.29 ${}^{+0.32}_{-0.29}$	4.37 ± 0.29 ${}^{+0.24}_{-0.23}$	4.34 ± 0.28 ${}^{+0.26}_{-0.34}$	4.12 ± 0.26 ${}^{+0.24}_{-0.25}$	4.88 ± 0.32 ${}^{+0.36}_{-0.36}$
P_+ [389]	3.83 ± 0.25 ${}^{+0.27}_{-0.25}$	3.86 ± 0.25 ${}^{+0.35}_{-0.28}$	3.57 ± 0.23 ${}^{+0.28}_{-0.27}$	3.53 ± 0.23 ${}^{+0.23}_{-0.23}$	-
M_X, q^2 [388]	-	-	-	-	4.97 ± 0.39 ${}^{+0.37}_{-0.37}$
Average	4.32 ± 0.16 ${}^{+0.22}_{-0.23}$	4.46 ± 0.16 ${}^{+0.18}_{-0.17}$	4.34 ± 0.16 ${}^{+0.15}_{-0.22}$	4.16 ± 0.14 ${}^{+0.25}_{-0.22}$	4.87 ± 0.24 ${}^{+0.38}_{-0.38}$

5.4.2 DGE

J.R. Andersen and E. Gardi (Dressed Gluon Exponentiation, DGE) [407] provide a framework where the on-shell b -quark calculation, converted into hadronic variables, is directly used as an approximation to the meson decay spectrum without the use of a leading-power non-perturbative function (or, in other words, a shape function). The on-shell mass of the b -quark within the B -meson (m_b) is required as input. The extracted values of $|V_{ub}|$ for each measurement along with their average are given in Table 70 and illustrated in Figure 52. The total error is ${}^{+5.4\%}_{-5.2\%}$, whose breakdown is: statistics (${}^{+2.4\%}_{-2.3\%}$), detector (${}^{+1.8\%}_{-1.8\%}$), $B \rightarrow X_c \ell^+ \nu_\ell$ model (${}^{+0.8\%}_{-0.9\%}$), $B \rightarrow X_u \ell^+ \nu_\ell$ model (${}^{+1.7\%}_{-1.6\%}$), strong coupling α_s (${}^{+0.5\%}_{-0.5\%}$), m_b (${}^{+3.8\%}_{-3.6\%}$), weak annihilation

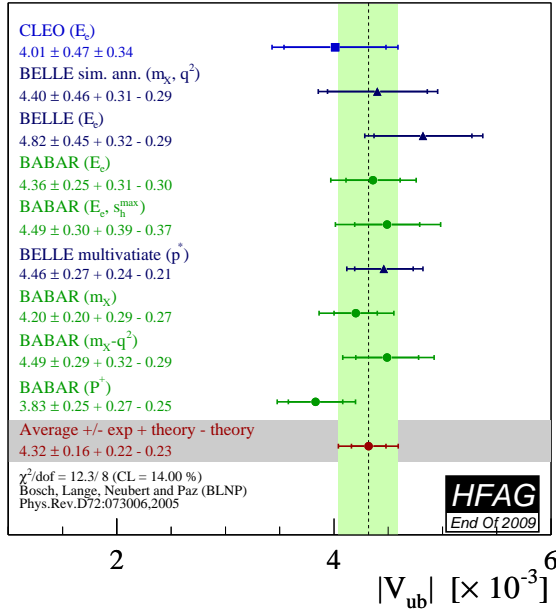


Figure 51: Measurements of $|V_{ub}|$ from inclusive semileptonic decays and their average based on the BLNP prescription. “ E_e ”, “ M_X ”, “ (M_X, q^2) ” and “ (E_e, s_h^{max}) ” indicate the distributions and cuts used for the measurement of the partial decay rates.

($+1.3\%$), DGE theory: matching scales ($+0.7\%$). The largest contribution to the total error is due to the effect of the uncertainty on m_b

5.4.3 GGOU

Gambino, Giordano, Ossola and Uraltsev (GGOU) [408] compute the triple differential decay rates of $B \rightarrow X_u \ell^+ \nu_\ell$, including all perturbative and non-perturbative effects through $O(\alpha_s^2 \beta_0)$ and $O(1/m_b^3)$. The Fermi motion is parameterized in terms of a single light-cone function for each structure function and for any value of q^2 , accounting for all subleading effects. The calculations are performed in the kinetic scheme, a framework characterized by a Wilsonian treatment with a hard cutoff $\mu \sim 1$ GeV. At present, GGOU have not included calculations for the “ (E_e, s_h^{max}) ” analysis, but this addition is planned. The extracted values of $|V_{ub}|$ for each measurement along with their average are given in Table 70 and illustrated in Figure 53. The total error is $+4.9\%$ -6.3% whose breakdown is: statistics ($+2.3\%$), detector ($+1.9\%$), $B \rightarrow X_c \ell^+ \nu_\ell$ model ($+1.2\%$), $B \rightarrow X_u \ell^+ \nu_\ell$ model ($+1.6\%$), α_s , m_b and other non-perturbative parameters ($+2.5\%$), higher order perturbative and non-perturbative corrections ($+1.5\%$), modelling of the q^2 tail and choice of the scale q^{2*} ($+1.7\%$), weak annihilations matrix element ($+0\%$), functional form of the distribution functions ($+0.5\%$). The leading uncertainties on $|V_{ub}|$ are both from theory, and are due to perturbative and non-perturbative parameters and the modelling of the q^2 tail and choice of the scale q^{2*} .

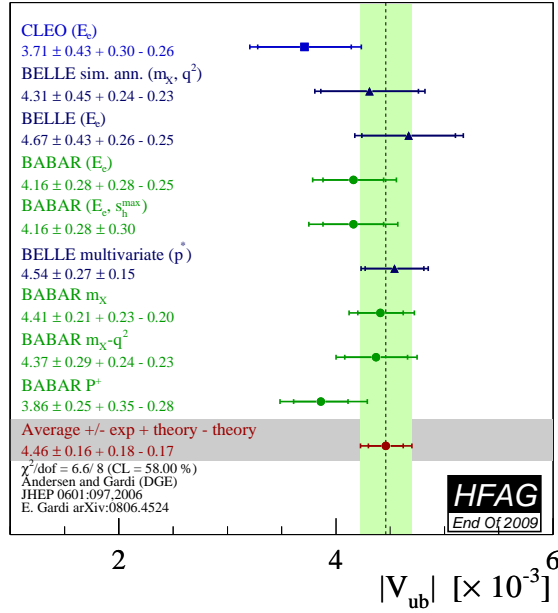


Figure 52: Measurements of $|V_{ub}|$ from inclusive semileptonic decays and their average based on the DGE prescription. “ E_e ”, “ M_X ”, “ (M_X, q^2) ” and “ (E_e, s_h^{max}) ” indicate the analysis type.

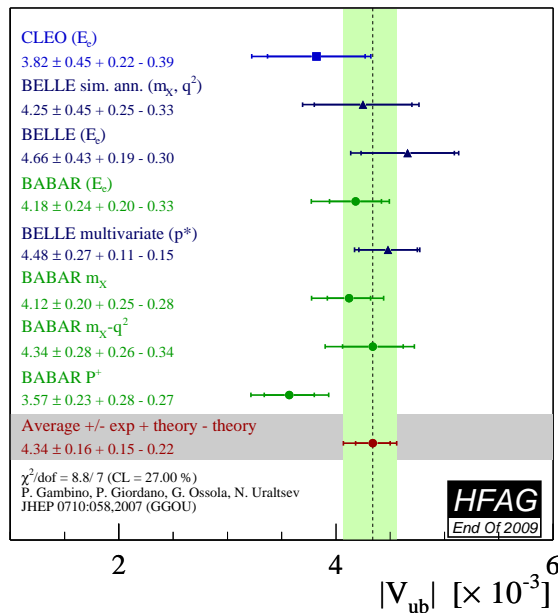


Figure 53: Measurements of $|V_{ub}|$ from inclusive semileptonic decays and their average based on the GGOU prescription. “ E_e ”, “ M_X ”, “ (M_X, q^2) ” and “ (E_e, s_h^{max}) ” indicate the analysis type.

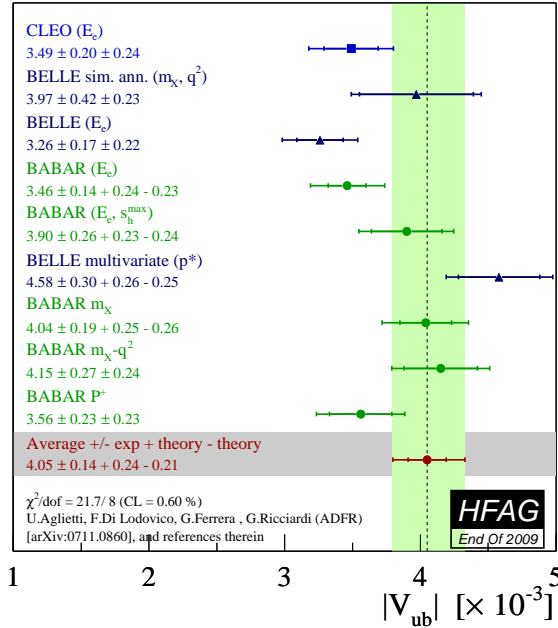


Figure 54: Measurements of $|V_{ub}|$ from inclusive semileptonic decays and their average based on the ADFR prescription. “ E_e ”, “ M_X ”, “ (M_X, q^2) ” and “ (E_e, s_h^{max}) ” indicate the analysis type.

5.4.4 ADFR

Aglietti, Di Lodovico, Ferrera and Ricciardi (ADFR) [409] use an approach to extract $|V_{ub}|$, which makes use of the ratio of the $B \rightarrow X_c \ell^+ \nu_\ell$ and $B \rightarrow X_u \ell^+ \nu_\ell$ widths. The normalized triple differential decay rate for $B \rightarrow X_u \ell^+ \nu_\ell$ [410, 411, 412, 413] is calculated with a model based on (i) soft-gluon resummation to next-to-next-leading order and (ii) an effective QCD coupling without Landau pole. This coupling is constructed by means of an extrapolation to low energy of the high-energy behaviour of the standard coupling. More technically, an analyticity principle is used. Following a recommendation by the ADFR authors, we lowered the cut on the electron energy for the endpoint analyses from 2.3 GeV to 2.1 GeV and recomputed the $|V_{ub}|$ values accordingly.

The extracted values of $|V_{ub}|$ for each measurement along with their average are given in Table 70 and illustrated in Figure 54. The total error is $^{+6.8\%}_{-6.9\%}$ whose breakdown is: statistics ($^{+1.9\%}_{-1.9\%}$), detector ($^{+2.0\%}_{-2.0\%}$), $B \rightarrow X_c \ell^+ \nu_\ell$ model ($^{+1.2\%}_{-1.2\%}$), $B \rightarrow X_u \ell^+ \nu_\ell$ model ($^{+1.3\%}_{-1.3\%}$), α_s ($^{+1.0\%}_{-1.6\%}$), $|V_{cb}|$ ($^{+1.7\%}_{-1.7\%}$), m_b ($^{+0.7\%}_{-0.8\%}$), m_c ($^{+4.5\%}_{-4.4\%}$), semileptonic branching fraction ($^{+0.9\%}_{-1.0\%}$), theory model ($^{+3.2\%}_{-3.2\%}$). The leading uncertainties, both from theory, are due to the m_c mass and the theory model.

5.4.5 BLL

Bauer, Ligeti, and Luke (BLL) [390] give a HQET-based prescription that advocates combined cuts on the dilepton invariant mass, q^2 , and hadronic mass, m_X , to minimise the overall uncertainty on $|V_{ub}|$. In their reckoning a cut on m_X only, although most efficient at preserving phase space ($\sim 80\%$), makes the calculation of the partial rate untenable due to uncalculable corrections to the b -quark distribution function or shape function. These corrections are sup-

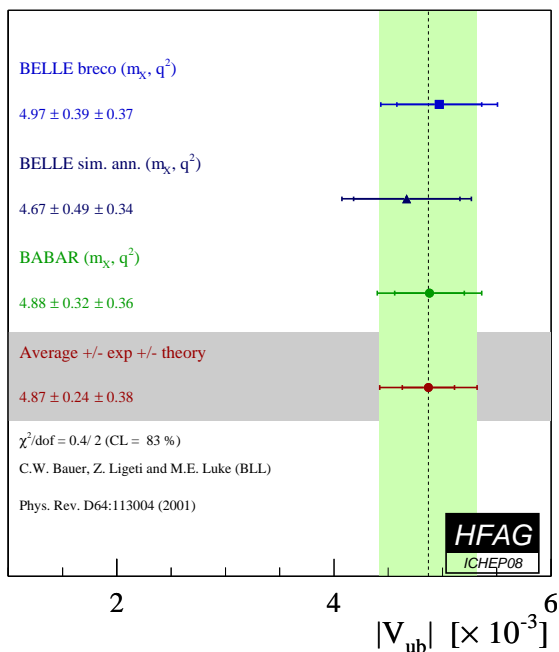


Figure 55: Measurements of $|V_{ub}|$ from inclusive semileptonic decays and their average in the BLL prescription. “(M_X, q^2)” indicates the analysis type.

pressed if events in the low q^2 region are removed. The cut combination used in measurements is $M_x < 1.7 \text{ GeV}/c^2$ and $q^2 > 8 \text{ GeV}^2/c^2$. The extracted values of $|V_{ub}|$ for each measurement along with their average are given in Table 70 and illustrated in Figure 55. The total error is $^{+9.0\%}_{-9.0\%}$ whose breakdown is: statistics ($^{+3.2\%}_{-3.2\%}$), detector ($^{+3.8\%}_{-3.8\%}$), $B \rightarrow X_c \ell^+ \nu_\ell$ model ($^{+1.3\%}_{-1.3\%}$), $B \rightarrow X_u \ell^+ \nu_\ell$ model ($^{+2.1\%}_{-2.1\%}$), spectral fraction (m_b) ($^{+3.0\%}_{-3.0\%}$), perturbative : strong coupling α_s ($^{+3.0\%}_{-3.0\%}$), residual shape function ($^{+4.5\%}_{-4.5\%}$), third order terms in the OPE ($^{+4.0\%}_{-4.0\%}$). The leading uncertainties, both from theory, are due to residual shape function effects and third order terms in the OPE expansion. The leading experimental uncertainty is due to statistics.

5.4.6 Summary

A summary of the averages presented in several different frameworks and results by V.B.Golubev, V.G.Luth and Yu.I.Skovpen [395], based on prescriptions by LLR [392] and LNP [393] to reduce the leading shape function uncertainties are presented in Table 71. It is difficult to quote a preferred value: the experimental and theoretical uncertainties play out differently among the schemes, and the theoretical assumptions underlying the theory calculations are different.

Table 71: Summary of inclusive determinations of $|V_{ub}|$. The errors quoted on $|V_{ub}|$ correspond to experimental and theoretical uncertainties, except for the last two measurements where the errors are due to the *BABAR* endpoint analysis, the *BABAR* $b \rightarrow s\gamma$ analysis [394], the theoretical errors and V_{ts} for the last averages.

Framework	$ V_{ub} [10^{-3}]$
BLNP	$4.32 \pm 0.16^{+0.22}_{-0.23}$
DGE	$4.46 \pm 0.16^{+0.18}_{-0.17}$
GGOU	$4.34 \pm 0.16^{+0.15}_{-0.22}$
ADFR	$4.16 \pm 0.14^{+0.25}_{-0.22}$
BLL (m_X/q^2 only)	$4.87 \pm 0.24 \pm 0.38$
LLR (<i>BABAR</i>) [394]	$4.43 \pm 0.45 \pm 0.29$
LLR (<i>BABAR</i>) [395]	$4.28 \pm 0.29 \pm 0.29 \pm 0.26 \pm 0.28$
LNP (<i>BABAR</i>) [395]	$4.40 \pm 0.30 \pm 0.41 \pm 0.23$

6 B decays to charmed hadrons

This section reports the updated contribution to the HFAG report from the “ $B \rightarrow$ charm” group³¹. The mandate of the group is to compile measurements and perform averages of all available quantities related to B decays to charmed particles, excluding CP related quantities. To date the group has analyzed a total of 492 measurements reported in 148 papers, principally branching fractions. The group aims to organize and present the copious information on B decays to charmed particles obtained from a combined sample of about two billion B mesons from the BABAR, Belle and CDF Collaborations.

This huge sample of B mesons allows to measure decays to states with open or hidden charm content with unprecedented precision. Branching fractions for rare B -meson decays or decay chains of a few 10^{-7} are being measured with statistical uncertainties typically below 30%, and new decay chains can be accessed with branching fractions down to 10^{-8} . Results for more common decay chains, with branching fractions around 10^{-4} , are becoming precision measurements, with uncertainties typically at the 3% level. Some decays have been observed for the first time, for example $B^0 \rightarrow J/\psi\eta$ or $\overline{B}^0 \rightarrow \Lambda_c^+ \overline{p} K^- \pi^+$, with a branching fraction of $(9.6 \pm 1.8) \times 10^{-6}$ and $(4.3 \pm 1.4) \times 10^{-5}$, respectively.

The large sample of B mesons allows to greatly improve our understanding of recently discovered new states with either hidden or open charm content, such as the $X(3872)$, the $Y(3940)$, the $Z(4430)^-$, the D_{sJ}^{*-} (2317) and D_{sJ}^- (2460) mesons. Measurements with many different final states for these particles are reported, allowing to shed more light on their nature. The $D^0 \overline{D}^{*0}$ (2007) decay of the $X(3872)$ has been observed for the first time, as well as the decay into $\psi(2S)\gamma$. Using the branching fraction products $\mathcal{B}(B^- \rightarrow X(3872)K^-) \times \mathcal{B}(X(3872) \rightarrow f)$, a hierarchy can be established between the decay modes f : these branching fraction products are found to be $(1.67 \pm 0.59) \times 10^{-4}$, $(0.12 \pm 0.02) \times 10^{-4}$, and $(0.022 \pm 0.005) \times 10^{-4}$, for $D^0 \overline{D}^{*0}$ (2007), $J/\psi\pi^+\pi^-$ and $J/\psi\gamma$, respectively. This is an important piece of information to discriminate between various interpretations for the $X(3872)$ state.

The measurements are classified according to the decaying particle: Charged B, Neutral B or Miscellaneous; the decay products and the type of quantity: branching fraction, product of branching fractions, ratio of branching fractions or other quantities. For the decay product classification the below precedence order is used to ensure that each measurement appears in only one category.

- new particles
- strange D mesons
- baryons
- J/ψ
- charmonium other than J/ψ
- multiple D , D^* or D^{**} mesons
- a single D^* or D^{**} meson
- a single D meson
- other particles

³¹The HFAG/BtoCharm group was formed in the spring of 2005; it performs its work using an XML database backed web application.

Within each table the measurements are color coded according to the publication status and age. Table 72 provides a key to the color scheme and categories used. When viewing the tables with most pdf viewers every number, label and average provides hyperlinks to the corresponding reference and individual quantity web pages on the HFAG/BtoCharm group website <http://hfag.phys.ntu.edu.tw>. The links provided in the captions of the table lead to the corresponding compilation pages. Both the individual and compilation webpages provide a graphical view of the results, in a variety of formats.

Tables 73 to 114 provide either limits at 90% confidence level or measurements with statistical and systematic uncertainties and in some cases a third error corresponding to correlated systematics. For details on the meanings of the uncertainties and access to the references click on the numbers to visit the corresponding web pages. Where there are multiple determinations of the same quantity by one experiment the table footnotes act to distinguish the methods or datasets used; such cases are visually highlighted in the table by presenting the measurements on the lines beneath the quantity label. Where both limits and measured values of a quantity are available the limits are presented in the tables but are not used in the determination of the average. Where only limits are available the most stringent is presented in the Average column of the tables. Where available the PDG 2008 result is also presented.

Table 72: Key to the colors used to classify the results presented in tables 73 to 114. When viewing these tables in a pdf viewer each number, label and average provides a hyperlink to the corresponding online version provided by the charm subgroup website <http://hfag.phys.ntu.edu.tw/b2charm/>. Where an experiment has multiple determinations of a single quantity they are distinguished by the table footnotes.

Class	Definition
waiting	Results without a preprint available
pubhot	Results published during or after 2009
prehot	Preprint released during or after 2009
pub	Results published after or during 2008
pre	Preprint released after or during 2008
pubold	Results published before 2008
preold	Preprint released before 2008
error	Incomplete information to classify
superceeded	Results superceeded by more recent measurements from the same experiment
inactive	Results in the process of being entered into the database
noquo	Results without quotes

Table 73: Branching fractions of charged B modes producing new particles in units of 10^{-3} , upper limits are at 90% CL. The latest version is available at: <http://hfag.phys.ntu.edu.tw/b2charm/00101.html>

Mode	PDG 2008	Belle	<i>BABAR</i>	CDF	Average
$X(3872)K^-$	< 0.32		< 0.32		< 0.32
$D_{sJ}^-(2460)D^0$	3.10 ± 1.00		$4.3 \pm 1.6 \pm 1.3$		4.3 ± 2.1
$D_{sJ}^-(2460)D^{*0}(2007)$	12.0 ± 3.0		$11.2 \pm 2.6 \pm 2.0$		11.2 ± 3.3

Table 74: Product branching fractions of charged B modes producing new particles in units of 10^{-4} , upper limits are at 90% CL. The latest version is available at: <http://hfag.phys.ntu.edu.tw/b2charm/00101.html>

Mode	PDG 2008	Belle	BABAR	CDF	Average
$K^- X(3872)[\gamma J/\psi(1S)]$	0.033 ± 0.010	$0.0180 \pm 0.0060 \pm 0.0010$	$0.0280 \pm 0.0080 \pm 0.0010$		0.022 ± 0.005
$K^{*-}(892)X(3872)[J/\psi(1S)\gamma]$			< 0.048		< 0.048
$K^- X(3872)[J/\psi(1S)\eta]$	< 0.077		< 0.077		< 0.077
$K^- X(3872)[\psi(2S)\gamma]$			$0.095 \pm 0.027 \pm 0.006$		0.09 ± 0.03
$K^- X(3872)[\pi^+\pi^- J/\psi(1S)]$	0.11 ± 0.02	$0.13 \pm 0.02 \pm 0.01$	$0.084 \pm 0.015 \pm 0.007$		0.10 ± 0.01
$\bar{K}^0 Z^-(4430)[J/\psi(1S)\pi^-]$			< 0.130		< 0.130
$K^- Y(3940)[J/\psi(1S)\gamma]$	< 0.140		< 0.140		< 0.140
$K^- Y(4260)[J/\psi(1S)\pi^+\pi^-]$	< 0.29		$0.20 \pm 0.07 \pm 0.02$		0.20 ± 0.07
$\bar{K}^0 X^-(3872)[J/\psi(1S)\pi^-\pi^0]$	< 0.22		< 0.22		< 0.22
$K^{*-}(892)X(3872)[\psi(2S)\gamma]$			< 0.28		< 0.28
$K^- X(3872)[D^+ D^-]$	< 0.40	< 0.40			< 0.40
$\bar{K}^0 Z^-(4430)[\psi(2S)\pi^-]$			< 0.43		< 0.43
$K^- Y(3940)[J/\psi(1S)\omega(782)]$					0.49 ± 0.11
			$0.49 \pm_{0.09}^{0.10} \pm 0.05$ ¹		
			$0.49 \pm 0.10 \pm 0.05$ ²		
$K^- X(3872)[D^0 \bar{D}^0]$	1.70 ± 0.60	< 0.60			< 0.60
$K^- X(3872)[D^0 \bar{D}^0 \pi^0]$	1.00 ± 0.40	< 0.60			< 0.60
$K^- X(3872)[\bar{D}^{*0}(2007)D^0]$			$1.67 \pm 0.36 \pm 0.47$		1.67 ± 0.59
$D^0 D_{sJ}^-(2460)[D_s^- \pi^+ \pi^-]$	< 2.2	< 2.2			< 2.2
$D^0 D_{sJ}^-(2460)[D_s^- \pi^0]$	< 2.7	< 2.7			< 2.7
$D^0 D_{sJ}^-(2460)[D_s^- \gamma]$	4.8 ± 1.2	$5.6 \pm_{1.5}^{1.6} \pm 1.7$	$6.00 \pm 2.00 \pm 1.00 \pm_{1.00}^{2.00}$		$5.8 \pm_{1.9}^{1.7}$
$D^0 D_{sJ}^*(2317)^-[D_s^{*-} \gamma]$	< 7.6	< 7.6			< 7.6
$D^{*0}(2007)D_{sJ}^*(2317)^-[D_s^- \pi^0]$	9.0 ± 7.0		$9.0 \pm 6.0 \pm 2.0 \pm_{2.0}^{3.0}$		$9.0 \pm_{6.6}^{7.0}$
$D^0 D_{sJ}^*(2317)^-[D_s^- \pi^0]$	7.5 ± 2.0	$8.1 \pm_{2.7}^{3.0} \pm 2.4$	$10.00 \pm 3.00 \pm 1.00 \pm_{2.00}^{4.00}$		$8.9 \pm_{3.2}^{2.7}$
$D^0 D_{sJ}^-(2460)[D_s^{*-} \gamma]$	< 9.8	< 9.8			< 9.8
$D^{*0}(2007)D_{sJ}^-(2460)[D_s^- \gamma]$	14.0 ± 7.0		$14.0 \pm 4.0 \pm 3.0 \pm_{3.0}^{5.0}$		$14.0 \pm_{5.8}^{7.1}$
$D^0 D_{sJ}^-(2460)[D_s^{*-} \pi^0]$		$11.9 \pm_{4.9}^{6.1} \pm 3.6$	$27.0 \pm 7.0 \pm 5.0 \pm_{6.0}^{9.0}$		$15.0 \pm_{5.8}^{5.3}$
$D^{*0}(2007)D_{sJ}^-(2460)[D_s^{*-} \pi^0]$			$76 \pm 17 \pm 18 \pm_{16}^{26}$		$76 \pm_{29}^{36}$

¹ Observation of $Y(3940) \rightarrow J/\psi\omega$ in $B \rightarrow J/\psi\omega K$ at BaBar

² Observation of $Y(3940) \rightarrow J/\psi\omega$ in $B \rightarrow J/\psi\omega K$ at BABAR (383M $B\bar{B}$ pairs) ; by3940kpsiomega

Table 75: Branching fractions of charged B modes producing strange D mesons in units of 10^{-4} , upper limits are at 90% CL. The latest version is available at: <http://hfag.phys.ntu.edu.tw/b2charm/00102.html>

Mode	PDG 2008	Belle	BABAR	CDF	Average
$D_s^- \phi(1020)$	< 0.019		< 0.019		< 0.019
$D_s^+ K^- K^-$			$0.110 \pm 0.040 \pm 0.020 \pm 0.003$		0.11 ± 0.04
$D_s^{*-} \phi(1020)$	< 0.120		< 0.120		< 0.120
$D_s^{*+} K^- K^-$			< 0.150		< 0.150
$D_s^- \pi^0$	0.16 ± 0.06		$0.15 \pm_{0.04}^{0.05} \pm 0.01 \pm 0.02$		0.15 ± 0.05
$D_s^{*-} K^+ \pi^+$	< 9.9	$1.47 \pm_{0.14}^{0.15} \pm_{0.19}^{0.19} \pm 0.13$			1.47 ± 0.27
$D_s^{*+} K^- \pi^-$	< 9.9		$1.67 \pm 0.16 \pm 0.35 \pm 0.05$		1.67 ± 0.39
$D_s^+ K^- \pi^-$	< 7.0	$1.77 \pm 0.12 \pm 0.16 \pm 0.23$	$2.02 \pm 0.13 \pm 0.38 \pm 0.06$		1.86 ± 0.24
$D_s^- K^+ \pi^+$	< 7.0	$1.94 \pm_{0.08}^{0.09} \pm_{0.20}^{0.20} \pm 0.17$			1.94 ± 0.28
$D_s^- D^0$	103 ± 17	$85.2 \pm_{3.8}^{3.9}$	$133 \pm 18 \pm 32$		$85.7 \pm_{3.9}^{3.8}$
$D_s^{*-} D^0$	78 ± 16		$93 \pm 18 \pm 19$		93 ± 26
$D_s^- D^{*0}(2007)$	84 ± 17		$121 \pm 23 \pm 20$		121 ± 30
$D_s^{*-} D^{*0}(2007)$	175 ± 23		$170 \pm 26 \pm 24$		170 ± 35

Table 76: Product branching fractions of charged B modes producing strange D mesons in units of 10^{-4} , upper limits are at 90% CL. The latest version is available at: <http://hfag.phys.ntu.edu.tw/b2charm/00102.html>

Mode	PDG 2008	Belle	BABAR	CDF	Average
$D^0 D_{s1}^- (2536) [\bar{D}^{*0} (2007) K^-]$	2.20 ± 0.70		$2.16 \pm 0.52 \pm 0.45$		2.16 ± 0.69
$D^0 D_{s1}^- (2536) [D^{*-} (2010) \bar{K}^0]$	2.3 ± 1.1		$2.30 \pm 0.98 \pm 0.43$		2.3 ± 1.1
$D^{*0} (2007) D_s^- [\phi(1020) \pi^-]$			$2.95 \pm 0.65 \pm 0.36$		2.95 ± 0.74
$D_s^{*-} D^0 [D_s^- \rightarrow \phi(1020) \pi^-]$			$3.13 \pm 1.19 \pm 0.58$		3.1 ± 1.3
$D^0 D_s^- [\phi(1020) \pi^-]$			$4.00 \pm 0.61 \pm 0.61$		4.00 ± 0.86
$\bar{D}^{*0} (2007) D_{s1}^- (2536) [\bar{D}^{*0} (2007) K^-]$	5.5 ± 1.6		$5.5 \pm 1.2 \pm 1.0$		5.5 ± 1.6
$D_s^{*-} D^{*0} (2007) [D_s^- \rightarrow \phi(1020) \pi^-]$			$8.6 \pm 1.5 \pm 1.1$		8.6 ± 1.9
$D^{*0} (2007) D_{s1}^- (2536) [D^{*-} (2010) \bar{K}^0]$	3.9 ± 2.6		< 10.7		< 10.7

Table 77: Branching fractions of charged B modes producing baryons in units of 10^{-5} , upper limits are at 90% CL. The latest version is available at: <http://hfag.phys.ntu.edu.tw/b2charm/00103.html>

Mode	PDG 2008	Belle	BABAR	CDF	Average
$J/\psi(1S)\Sigma^0\bar{p}$	< 1.10	< 1.10			< 1.10
$J/\psi(1S)\Lambda\bar{p}$	1.18 ± 0.31	$1.16 \pm 0.28 \pm_{0.23}^{0.18}$	$1.16 \pm_{0.53}^{0.74} \pm_{0.18}^{0.42}$		1.16 ± 0.31
$D^- p\bar{p}$		< 1.50			< 1.50
$D^{*-}(2010)p\bar{p}$		< 1.50			< 1.50
$\Sigma_c^{*0}\bar{p}$	< 2.7	< 4.6			< 4.6
$\Sigma_c^0\bar{p}$	3.7 ± 1.3	< 9.3			< 9.3
$\Lambda_c^+ \bar{p}\pi^-$	21.0 ± 6.0	$18.7 \pm_{4.0}^{4.3} \pm 2.8 \pm 4.9$	$33.8 \pm 1.2 \pm 1.2 \pm 8.8$		24.4 ± 5.5
$\Lambda_c^+ \Lambda_c^- K^-$	70 ± 40	$65.0 \pm_{9.0}^{10.0} \pm 11.0 \pm 34.0$	$114 \pm 15 \pm 17 \pm 60$		77 ± 32

Table 78: Product branching fractions of charged B modes producing baryons in units of 10^{-5} , upper limits are at 90% CL. The latest version is available at: <http://hfag.phys.ntu.edu.tw/b2charm/00103.html>

Mode	PDG 2008	Belle	BABAR	CDF	Average
$K^- \eta_c(1S)[\Lambda\bar{\Lambda}]$		$0.095 \pm_{0.022}^{0.025} \pm_{0.011}^{0.008}$			0.10 ± 0.03
$K^- \eta_c(1S)[p\bar{p}]$		$0.14 \pm 0.01 \pm_{0.02}^{0.02}$	$0.18 \pm_{0.02}^{0.03} \pm 0.02$		0.15 ± 0.02
$K^- J/\psi(1S)[\Lambda\bar{\Lambda}]$		$0.20 \pm_{0.03}^{0.03} \pm 0.03$			0.20 ± 0.05
$K^- J/\psi(1S)[p\bar{p}]$		$0.22 \pm 0.01 \pm 0.01$	$0.22 \pm 0.02 \pm 0.01$		0.22 ± 0.01
$\Lambda_c^- \Xi_c^0[\Xi^- \pi^+]$	5.6 ± 2.6	$4.80 \pm_{0.90}^{1.00} \pm 1.10 \pm 1.20$	$2.08 \pm 0.65 \pm 0.29 \pm 0.54$		2.57 ± 0.81

Table 79: Ratios of branching fractions of charged B modes producing baryons in units of 10^{-1} , upper limits are at 90% CL. The latest version is available at: <http://hfag.phys.ntu.edu.tw/b2charm/00103.html>

Mode	PDG 2008	Belle	BABAR	CDF	Average
$\frac{\mathcal{B}(B^- \rightarrow \Sigma_c^0(2800)\bar{p})}{\mathcal{B}(B^- \rightarrow \Lambda_c^+ \bar{p}\pi^-)}$			$1.17 \pm 0.23 \pm 0.24$		1.17 ± 0.33
$\frac{\mathcal{B}(B^- \rightarrow \Sigma_c^0(2455)\bar{p})}{\mathcal{B}(B^- \rightarrow \Lambda_c^+ \bar{p}\pi^-)}$			$1.23 \pm 0.12 \pm 0.08$		1.23 ± 0.14
$\frac{\mathcal{B}(B^- \rightarrow \Lambda_c^+ \bar{p}\pi^-)}{\mathcal{B}(\bar{B}^0 \rightarrow \Lambda_c^+ \bar{p})}$			$154.0 \pm 18.0 \pm 3.0$		154 ± 18

Table 80: Branching fractions of charged B modes producing $J/\psi(1S)$ in units of 10^{-4} , upper limits are at 90% CL. The latest version is available at: <http://hfag.phys.ntu.edu.tw/b2charm/00104.html>

Mode	PDG 2008	Belle	BABAR	CDF	Average
$\pi^- \pi^0 J/\psi(1S)$	< 0.073		< 0.073		$< \mathbf{0.073}$
$J/\psi(1S)D^0\pi^-$	< 0.25	< 0.25	< 0.52		< 0.25
$J/\psi(1S)\phi(1020)K^-$	0.52 ± 0.17		$0.44 \pm 0.14 \pm 0.05 \pm 0.01$		0.44 ± 0.15
$J/\psi(1S)\pi^-$	0.49 ± 0.06	$0.38 \pm 0.06 \pm 0.03$	$0.54 \pm 0.04 \pm 0.02$		0.48 ± 0.04
$\rho^-(770)J/\psi(1S)$	0.50 ± 0.08		$0.50 \pm 0.07 \pm 0.03$		$\mathbf{0.50 \pm 0.08}$
$J/\psi(1S)\eta K^-$	1.08 ± 0.33		$1.08 \pm 0.23 \pm 0.24 \pm 0.03$		1.08 ± 0.33
$J/\psi(1S)D^-$	< 1.20		< 1.20		< 1.20
$J/\psi(1S)\omega(782)K^-$			$3.50 \pm 0.20 \pm 0.40$ ¹		$\mathbf{3.50 \pm 0.45}$
			$3.50 \pm 0.20 \pm 0.40$ ²		
$J/\psi(1S)K^-$	10.07 ± 0.35				10.26 ± 0.37
		$10.10 \pm 0.20 \pm 0.70 \pm 0.20$	$10.61 \pm 0.15 \pm 0.44 \pm 0.18$ ³		
			$10.10 \pm 0.90 \pm 0.60$ ⁴		
			$8.10 \pm 1.30 \pm 0.70$ ⁵		
$J/\psi(1S)K^-\pi^+\pi^-$	10.7 ± 1.9		$11.60 \pm 0.70 \pm 0.90$	$6.9 \pm 1.8 \pm 1.2$	10.6 ± 1.0
$J/\psi(1S)K^{*-}(892)$	14.10 ± 0.80	$12.80 \pm 0.70 \pm 1.40 \pm 0.20$	$14.54 \pm 0.47 \pm 0.94 \pm 0.25$	$15.8 \pm 4.7 \pm 2.7$	14.03 ± 0.88
$J/\psi(1S)K_1^-(1270)$	18.0 ± 5.2	$18.0 \pm 3.4 \pm 3.0 \pm 2.5$			18.0 ± 5.2

¹ Observation of $Y(3940) \rightarrow J/\psi\omega$ in $B \rightarrow J/\psi\omega K$ at BaBar

² Observation of $Y(3940) \rightarrow J/\psi\omega$ in $B \rightarrow J/\psi\omega K$ at BABAR (383M $B\bar{B}$ pairs) ; bjpsiomegak

³ MEASUREMENT OF BRANCHING FRACTIONS AND CHARGE ASYMMETRIES FOR EXCLUSIVE B DECAYS TO CHARMONIUM (124M $B\bar{B}$ pairs) ; $B^- \rightarrow J/\psi K^-$ with J/ψ to leptons

⁴ MEASUREMENT OF THE $B^+ \rightarrow p\bar{p}K^+$ BRANCHING FRACTION AND STUDY OF THE DECAY DYNAMICS (232M $B\bar{B}$ pairs) ; $B^- \rightarrow J/\psi K^-$ with $J/\psi \rightarrow p\bar{p}$

⁵ Measurements of the absolute branching fractions of $B^\pm \rightarrow K^\pm X_{c\bar{c}}$ (231.8M $B\bar{B}$ pairs) ; $B^- \rightarrow J/\psi K^-$ (inclusive)

Table 81: Product branching fractions of charged B modes producing $J/\psi(1S)$ in units of 10^{-4} , upper limits are at 90% CL. The latest version is available at: <http://hfag.phys.ntu.edu.tw/b2charm/00104.html>

Mode	PDG 2008	Belle	BABAR	CDF	Average
$K^- h_c(1P)[J/\psi(1S)\pi^+\pi^-]$	< 0.034		< 0.034		< 0.034

Table 82: Ratios of branching fractions of charged B modes producing $J/\psi(1S)$ in units of 10^0 , upper limits are at 90% CL. The latest version is available at: <http://hfag.phys.ntu.edu.tw/b2charm/00104.html>

Mode	PDG 2008	Belle	BABAR	CDF	Average
$\frac{\mathcal{B}(B^- \rightarrow J/\psi(1S)\pi^-)}{\mathcal{B}(B^- \rightarrow J/\psi(1S)K^-)}$			$0.054 \pm 0.004 \pm 0.001$	$0.0500 \pm_{0.0170}^{0.0190} \pm 0.0010$ ¹ $0.049 \pm 0.008 \pm 0.002$ ²	0.052 ± 0.004
$\frac{\mathcal{B}(B^- \rightarrow J/\psi(1S)K_1^-(1400))}{\mathcal{B}(B^- \rightarrow J/\psi(1S)K_1^-(1270))}$		< 0.30			< 0.30
$\frac{\mathcal{B}(B^- \rightarrow \chi_{c0}(1P)K^-)}{\mathcal{B}(B^- \rightarrow J/\psi(1S)K^-)}$		$0.60 \pm_{0.18}^{0.21} \pm 0.05 \pm 0.08$			$0.60 \pm_{0.20}^{0.23}$
$\frac{\mathcal{B}(B^- \rightarrow \eta_c(1S)K^-)}{\mathcal{B}(B^- \rightarrow J/\psi(1S)K^-)}$			$1.28 \pm 0.10 \pm 0.38$ ³ $1.06 \pm 0.23 \pm 0.04$ ⁴		1.12 ± 0.20
$\frac{\mathcal{B}(B^- \rightarrow J/\psi(1S)K^{*-}(892))}{\mathcal{B}(B^- \rightarrow J/\psi(1S)K^-)}$			$1.37 \pm 0.05 \pm 0.08$	$1.92 \pm 0.60 \pm 0.17$	1.38 ± 0.09
$\frac{\mathcal{B}(B^- \rightarrow J/\psi(1S)K_1^-(1270))}{\mathcal{B}(B^- \rightarrow J/\psi(1S)K^-)}$		$1.80 \pm 0.34 \pm 0.34$			1.80 ± 0.48

¹ Measurement of the Branching Fraction $B(B^+ \rightarrow J/\psi\pi^+)$ and Search for $B^{c+} \rightarrow J/\psi\pi^+$

¹ Measurement of the Branching Fraction $B(B^+ \rightarrow J/\psi\pi^+)$ and Search for $B^{c+} \rightarrow J/\psi\pi^+$

² Measurement of the Ratio of Branching Fractions $B(B - J/\psi\pi)/B(B - J/\psi K)$; $Br(B - J/\psi\pi)/Br(B - J/\psi K)$

³ Branching Fraction Measurements of $B \rightarrow \eta_c K$ Decays (86.1M $B\bar{B}$ pairs) ; Ratio $B^- \rightarrow \eta_c K^-$ to $B^- \rightarrow J/\psi K^-$ with $\eta_c \rightarrow K\bar{K}\pi$

⁴ Measurements of the absolute branching fractions of $B^\pm \rightarrow K^\pm X_{c\bar{c}}$ (231.8M $B\bar{B}$ pairs) ; Ratio $B^- \rightarrow \eta_c K^-$ to $B^- \rightarrow J/\psi K^-$ (inclusive analysis)

Table 83: Branching fractions of charged B modes producing charmonium other than $J/\psi(1S)$ in units of 10^{-4} , upper limits are at 90% CL. The latest version is available at: <http://hfag.phys.ntu.edu.tw/b2charm/00105.html>

Mode	PDG 2008	Belle	BABAR	CDF	Average
$h_c(1P)K^-$	< 0.38	< 0.038			< 0.038
$\chi_{c2}(1P)K^-$	< 0.29		< 0.180		< 0.180
$\chi_{c1}(1P)\pi^-$	0.22 ± 0.05	$0.22 \pm 0.04 \pm 0.03$			0.22 ± 0.05
$\chi_{c0}(1P)\pi^-$			< 0.61		< 0.61
$\chi_{c2}(1P)K^{*-}(892)$	< 0.120		< 1.20		< 1.20
$\chi_{c0}(1P)K^-$	1.40 ± 0.20	$6.00 \pm_{1.80}^{2.10} \pm 0.70 \pm 0.90$	2.70 ± 0.70 ³ $1.84 \pm 0.32 \pm 0.14 \pm 0.28$ ¹ $1.34 \pm 0.45 \pm 0.15 \pm 0.14$ ⁴ < 1.80 ^{2a}		1.88 ± 0.30
$\chi_{c0}(1P)K^{*+}(892)$	< 29		< 2.1		< 2.1
$\chi_{c1}(1P)K^{*-}(892)$	3.60 ± 0.90	$4.10 \pm 0.60 \pm 0.90$	$2.60 \pm 0.50 \pm 0.40$		2.99 ± 0.55
$\eta_c(2S)K^-$	3.4 ± 1.8		$3.40 \pm 1.80 \pm 0.30$		3.4 ± 1.8
$\psi(3770)K^-$	4.9 ± 1.3	$4.80 \pm 1.10 \pm 0.70$	$3.50 \pm 2.50 \pm 0.30$		4.5 ± 1.2
$\chi_{c1}(1P)K^-$	4.90 ± 0.50	$4.50 \pm 0.20 \pm 0.70$	$4.50 \pm 0.10 \pm 0.30$ ⁵ $8.00 \pm 1.40 \pm 0.70$ ^{2c}	$15.5 \pm 5.4 \pm 2.0$	4.64 ± 0.28
$\psi(2S)K^-$	6.48 ± 0.35	6.90 ± 0.60	$6.17 \pm 0.32 \pm 0.38 \pm 0.23$ ⁶ $4.90 \pm 1.60 \pm 0.40$ ^{2b} $5.92 \pm 0.85 \pm 0.86 \pm 0.22$	$5.50 \pm 1.00 \pm 0.60$	6.32 ± 0.37
$\psi(2S)K^{*-}(892)$	6.7 ± 1.4	$8.13 \pm 0.77 \pm 0.89$	$5.92 \pm 0.85 \pm 0.86 \pm 0.22$		7.07 ± 0.85
$\eta_c(1S)K^-$	9.1 ± 1.3	$12.50 \pm 1.40 \pm_{1.20}^{1.00} \pm 3.80$	$12.90 \pm 0.90 \pm 1.30 \pm 3.60$ ⁷ $13.8 \pm_{1.5}^{2.3} \pm 1.5 \pm 4.2$ ⁸ 8.7 ± 1.5 ^{2d}		9.8 ± 1.3
$\eta_c(1S)K^{*-}(892)$	12.0 ± 7.0		$12.1 \pm_{3.5}^{4.3} \pm_{2.8}^{3.4} \pm_{2.8}^{5.4}$		$12.1 \pm_{5.3}^{7.7}$
$\chi_{c0}(1P)K^{*-}(892)$	< 29		< 29		< 29

¹ Dalitz plot analysis of the decay $B^\pm \rightarrow K^\pm K^\pm K^\mp$ (226M $B\bar{B}$ pairs) ; $B^\pm \rightarrow K^\pm \chi_{c0}$, with $chi_{c0} \rightarrow K^+ K^-$ (Dalitz analysis)

² Measurements of the absolute branching fractions of $B^\pm \rightarrow K^\pm X_{c\bar{c}}$ (231.8M $B\bar{B}$ pairs) ; ^{2a} $B^- \rightarrow \chi_{c0} K^-$ (inclusive) ; ^{2b} $B^- \rightarrow \psi(2S)K^-$ (inclusive) ; ^{2c} $B^- \rightarrow \chi_{c1} K^-$ (inclusive) ; ^{2d} $B^- \rightarrow \eta_c K^-$ (inclusive)

³ MEASUREMENT OF THE BRANCHING FRACTION FOR $B^\pm \rightarrow \chi_{c0} K^\pm$. (88.9M $B\bar{B}$ pairs) ; $B^- \rightarrow \chi_{c0} K^-$ with $\chi_{c0} \rightarrow K^+ K^-, \pi^+ \pi^-$

⁴ Dalitz-plot analysis of the decays $B^\pm \rightarrow K^\pm \pi^\mp \pi^\pm$ (226M $B\bar{B}$ pairs) ; $B^- \rightarrow \chi_{c0} K^-$ with $\chi_{c0} \rightarrow \pi^+ \pi^-$ (Dalitz analysis)

⁵ Search for $X(3872) \rightarrow \psi(2S)\gamma$ in $B^\pm \rightarrow X(3872)K^\pm$ decays, and a study of $B \rightarrow \bar{c}c\gamma K$

⁶ Search for $X(3872) \rightarrow \psi(2S)\gamma$ in $B^\pm \rightarrow X(3872)K^\pm$ decays, and a study of $B \rightarrow \bar{c}c\gamma K$

⁷ MEASUREMENT OF BRANCHING FRACTIONS AND CHARGE ASYMMETRIES FOR EXCLUSIVE B DECAYS TO CHARMONIUM (124M $B\bar{B}$ pairs) ; $B^- \rightarrow \psi(2S)K^-$ with $\psi(2S)$ to leptons

⁸ Branching Fraction Measurements of $B \rightarrow \eta_c K$ Decays (86.1M $B\bar{B}$ pairs) ; $B^- \rightarrow \eta_c K^-$ with $\eta_c \rightarrow K\bar{K}\pi$

⁹ MEASUREMENT OF THE $B^+ \rightarrow p\bar{p}K^+$ BRANCHING FRACTION AND STUDY OF THE DECAY DYNAMICS (232M $B\bar{B}$ pairs) ; $B^- \rightarrow \eta_c K^-$ with $\eta_c \rightarrow p\bar{p}$

Table 84: Product branching fractions of charged B modes producing charmonium other than $J/\psi(1S)$ in units of 10^{-4} , upper limits are at 90% CL. The latest version is available at: <http://hfag.phys.ntu.edu.tw/b2charm/00105.html>

Mode	PDG 2008	Belle	BABAR	CDF	Average
$K^- h_c(1P)[\eta_c(1S)\gamma]$			< 0.48		< 0.48
$K^- \psi(3770)[D^+ D^-]$	0.94 ± 0.35		$0.84 \pm 0.32 \pm 0.21$		0.84 ± 0.38
$K^- \psi(3770)[D^0 \bar{D}^0]$	1.60 ± 0.40		$1.41 \pm 0.30 \pm 0.22$		1.41 ± 0.37

Table 85: Ratios of branching fractions of charged B modes producing charmonium other than $J/\psi(1S)$ in units of 10^{-1} , upper limits are at 90% CL. The latest version is available at: <http://hfag.phys.ntu.edu.tw/b2charm/00105.html>

Mode	PDG 2008	Belle	BABAR	CDF	Average
$\frac{\mathcal{B}(B^- \rightarrow \chi_{c1}(1P)\pi^-)}{\mathcal{B}(B^- \rightarrow \chi_{c1}(1P)K^-)}$		$0.43 \pm 0.08 \pm 0.03$			0.43 ± 0.09
$\frac{\mathcal{B}(B^- \rightarrow h_c(1P)K^-) \times \mathcal{B}(h_c(1P) \rightarrow \eta_c(1S)\gamma)}{\mathcal{B}(B^- \rightarrow \eta_c(1S)K^-)}$			< 0.58		< 0.58
$\frac{\mathcal{B}(B^- \rightarrow \chi_{c1}(1P)K^{*-}(892))}{\mathcal{B}(B^- \rightarrow \chi_{c1}(1P)K^-)}$			$5.1 \pm 1.7 \pm 1.6$		5.1 ± 2.3
$\frac{\mathcal{B}(B^- \rightarrow \psi(2S)K^{*-}(892))}{\mathcal{B}(B^- \rightarrow \psi(2S)K^-)}$			$9.60 \pm 1.50 \pm 0.90$		9.6 ± 1.7

Table 86: Branching fractions of charged B modes producing multiple D , D^* or D^{**} mesons in units of 10^{-3} , upper limits are at 90% CL. The latest version is available at: <http://hfag.phys.ntu.edu.tw/b2charm/00106.html>

Mode	PDG 2008	Belle	BABAR	CDF	Average
$D^0\bar{D}^0\pi^0K^-$		$0.11 \pm 0.03 \pm_{0.03}^{0.02}$			0.11 ± 0.04
$D^0D^{*-}(2010)$	0.39 ± 0.05	$0.46 \pm 0.07 \pm 0.06$	$0.36 \pm 0.05 \pm 0.04$		0.39 ± 0.05
D^-D^0	0.42 ± 0.06				0.41 ± 0.04
		$0.38 \pm 0.03 \pm 0.04$ ¹	$0.38 \pm 0.06 \pm 0.04 \pm 0.03$		
		$0.56 \pm 0.08 \pm 0.06$ ²			
$D^+D^-K^-$	< 0.40	< 0.90	< 0.40		< 0.40
$D^+D^{*-}(2010)K^-$	< 0.70		< 0.70		< 0.70
$D^{*0}(2007)D^{*-}(2010)$	0.81 ± 0.17		$0.81 \pm 0.12 \pm 0.11 \pm 0.06$		0.81 ± 0.17
$D^0\bar{D}^0K^-$	2.10 ± 0.26	$1.17 \pm 0.21 \pm 0.15$	$1.90 \pm 0.30 \pm 0.30$		1.37 ± 0.22
$D^{*+}(2010)D^-K^-$	1.50 ± 0.40		$1.50 \pm 0.30 \pm 0.20$		1.50 ± 0.36
$D^{*-}(2010)D^{*+}(2010)K^-$	< 1.80		< 1.80		< 1.80
$D^0D^-\bar{K}^0$	< 2.8		< 2.8		< 2.8
$D^{*0}(2007)\bar{D}^0K^-$	< 3.8		< 3.8		< 3.8
$D^0\bar{D}^{*0}(2007)K^-$	4.70 ± 1.00		$4.70 \pm 0.70 \pm 0.70$		4.70 ± 0.99
$D^0D^{*-}(2010)\bar{K}^0$	5.2 ± 1.2		$5.20 \pm_{0.90}^{1.00} \pm 0.70$		$5.2 \pm_{1.1}^{1.2}$
$\bar{D}^{*0}(2007)D^{*0}(2007)K^-$	5.3 ± 1.6		$5.30 \pm_{1.00}^{1.10} \pm 1.20$		5.3 ± 1.6
$D^{*0}(2007)D^-\bar{K}^0$	< 6.1		< 6.1		< 6.1
$D^{*0}(2007)D^{*-}(2010)\bar{K}^0$	7.8 ± 2.6		$7.8 \pm_{2.1}^{2.3} \pm 1.4$		$7.8 \pm_{2.5}^{2.7}$

¹ Measurement of $B^+ \rightarrow D^+ D^0 \bar{D}^0$ branching fraction and charge asymmetry and search for $B^0 \rightarrow D^0 D^0 \bar{D}^0$ ($656.7M B\bar{B}$ pairs)

² Observation of $B^0 \rightarrow D^+ D^-$, $B^- \rightarrow D^0 D^-$ and $B^- \rightarrow D^0 D^{*-}$ decays ($152M B\bar{B}$ pairs)

Table 87: Product branching fractions of charged B modes producing multiple D , D^* or D^{**} mesons in units of 10^{-4} , upper limits are at 90% CL. The latest version is available at: <http://hfag.phys.ntu.edu.tw/b2charm/00106.html>

Mode	PDG 2008	Belle	BABAR	CDF	Average
$\pi^- D_1^0(2420)[D^{*0}(2007)\pi^-\pi^+]$	< 0.060	< 0.060			< 0.060
$\pi^- D_2^{*0}(2460)[D^{*0}(2007)\pi^-\pi^+]$	< 0.22	< 0.22			< 0.22
$\pi^- D_2^{*0}(2460)[D^{*+}(2010)\pi^-]$	1.80 ± 0.50	$1.80 \pm 0.30 \pm 0.30 \pm 0.20$	$1.80 \pm 0.30 \pm 0.50$		1.80 ± 0.36
$\pi^- D_1^0(2420)[D^0\pi^-\pi^+]$	1.90 ± 0.60	$1.85 \pm 0.29 \pm 0.35 \pm_{0.46}^{0.00}$			$1.85 \pm_{0.65}^{0.45}$
$\pi^- D_2^{*0}(2460)[D^+\pi^-]$	3.40 ± 0.80	$3.40 \pm 0.30 \pm 0.60 \pm 0.40$	$3.50 \pm 0.20 \pm 0.20 \pm 0.40$		3.47 ± 0.42
$\pi^- D_1^0(H)[D^{*+}(2010)\pi^-]$		$5.00 \pm 0.40 \pm 1.00 \pm 0.40$			5.0 ± 1.1
$\pi^- D_1^0(2420)[D^{*+}(2010)\pi^-]$	6.8 ± 1.5	$6.80 \pm 0.70 \pm 1.30 \pm 0.30$	$5.90 \pm 0.30 \pm 1.10$		6.23 ± 0.91
$\pi^- D_0^{*0}[D^+\pi^-]$	6.1 ± 1.9	$6.10 \pm 0.60 \pm 0.90 \pm 1.60$	$6.80 \pm 0.30 \pm 0.40 \pm 2.00$		6.4 ± 1.4

149

Table 88: Ratios of branching fractions of charged B modes producing multiple D , D^* or D^{**} mesons in units of 10^0 , upper limits are at 90% CL. The latest version is available at: <http://hfag.phys.ntu.edu.tw/b2charm/00106.html>

Mode	PDG 2008	Belle	BABAR	CDF	Average
$\frac{\mathcal{B}(B^- \rightarrow D^0 K^-)}{\mathcal{B}(B^- \rightarrow D^0 \pi^-)}$	0.084 ± 0.003	$0.077 \pm 0.005 \pm 0.006$	$0.083 \pm 0.003 \pm 0.002$	$0.065 \pm 0.007 \pm 0.004$	0.079 ± 0.003
$\frac{\mathcal{B}(B^- \rightarrow D^{*0}(2007)K^-)}{\mathcal{B}(B^- \rightarrow D^{*0}(2007)\pi^-)}$		$0.078 \pm 0.019 \pm 0.009$	$0.081 \pm 0.004 \pm_{0.003}^{0.004}$		0.081 ± 0.005
$\frac{\mathcal{B}(B^- \rightarrow D_2^{*0}(2460)\pi^-)}{\mathcal{B}(B^- \rightarrow D_1^0(2420)\pi^-)}$			$0.80 \pm 0.07 \pm 0.16$		0.80 ± 0.17
$\frac{\mathcal{B}(B^- \rightarrow D^{*0}(2007)\pi^-)}{\mathcal{B}(B^- \rightarrow D^0\pi^-)}$			$1.14 \pm 0.07 \pm 0.04$		1.14 ± 0.08
$\frac{\mathcal{B}(B^- \rightarrow D^{*+}\pi^-)}{\mathcal{B}(B^- \rightarrow D^0\pi^-)}$			$1.22 \pm 0.13 \pm 0.23$		1.22 ± 0.26
$\frac{\mathcal{B}(B^- \rightarrow D^0\pi^-)}{\mathcal{B}(\bar{B}^0 \rightarrow D^+\pi^-)}$				$1.97 \pm 0.10 \pm 0.21$	1.97 ± 0.23

Table 89: Branching fractions of charged B modes producing a single D^* or D^{**} meson in units of 10^{-4} , upper limits are at 90% CL. The latest version is available at: <http://hfag.phys.ntu.edu.tw/b2charm/00107.html>

Mode	PDG 2008	Belle	BABAR	CDF	Average
$D^{*-}(2010)\pi^0$	< 1.70	< 0.030			$< \mathbf{0.030}$
$D^{*-}(2010)\bar{K}^0$	< 0.090		< 0.090		< 0.090
$D^{*+}(2010)\pi^0$		< 0.36			$< \mathbf{0.36}$
$D^{*0}(2007)K^-$	4.16 ± 0.33	$3.59 \pm 0.87 \pm 0.41 \pm 0.31$			3.6 ± 1.0
$D^{*0}(2007)K^{*-}(892)$	8.1 ± 1.4		$8.30 \pm 1.10 \pm 0.96 \pm 0.27$		8.3 ± 1.5
$D^{*0}(2007)K^-K^0$	< 10.6	< 10.6			< 10.6
$D^{*+}(2010)\pi^-\pi^-$	13.5 ± 2.2	$12.50 \pm 0.80 \pm 2.20$	$12.20 \pm 0.50 \pm 1.80$		12.3 ± 1.5
$D^{*0}(2007)K^-K^{*0}(892)$	15.0 ± 4.0	$15.3 \pm 3.1 \pm 2.9$			15.3 ± 4.2
$D^{*+}(2010)\pi^-\pi^+\pi^-\pi^-$	26.0 ± 4.0	$25.6 \pm 2.6 \pm 3.3$			25.6 ± 4.2
$D^{*0}(2007)\pi^-$	51.9 ± 2.6				$\mathbf{52.8 \pm 2.8}$
			$55.20 \pm 1.70 \pm 4.20 \pm 0.20$ ¹		
			$51.3 \pm 2.2 \pm 2.8$ ²		
$D^{**0}\pi^-$	59 ± 13		$55.0 \pm 5.2 \pm 10.4$		$\mathbf{55 \pm 12}$
$D^{*0}(2007)\pi^-\pi^+\pi^-\pi^+\pi^-$		$56.7 \pm 9.1 \pm 8.5$			57 ± 12
$D^{*0}(2007)\pi^-\pi^+\pi^-$	103 ± 12	$105.5 \pm 4.7 \pm 12.9$			106 ± 14

¹ Branching fraction measurements and isospin analyses for $\bar{B} \rightarrow D^{(*)}\pi^-$ decays (65M $B\bar{B}$ pairs) ; $B^- \rightarrow D^{*0}\pi^-$

² Measurement of the Absolute Branching Fractions $B \rightarrow D^{(**)}\pi$ with a Missing Mass method (231M $B\bar{B}$ pairs) ; $B^- \rightarrow D^{*0}\pi^-$

Table 90: Branching fractions of charged B modes producing a single D meson in units of 10^{-3} , upper limits are at 90% CL. The latest version is available at: <http://hfag.phys.ntu.edu.tw/b2charm/00108.html>

Mode	PDG 2008	Belle	BABAR	CDF	Average
$D^- \bar{K}^0$	< 0.005		< 0.005		< 0.005
$D^0 K^-$	0.40 ± 0.02	$0.38 \pm 0.02 \pm 0.03 \pm 0.02$			0.38 ± 0.04
$D^0 K^{*-}(892)$	0.53 ± 0.04		$0.53 \pm 0.03 \pm 0.03$		0.53 ± 0.05
$D^0 K^- K^0$	0.55 ± 0.16	$0.55 \pm 0.14 \pm 0.08$			0.55 ± 0.16
$D^0 K^- K^{*0}(892)$	0.75 ± 0.17	$0.75 \pm 0.13 \pm 0.11$			0.75 ± 0.17
$D^+ \pi^- \pi^-$	1.02 ± 0.16	$1.02 \pm 0.04 \pm 0.15$	$1.08 \pm 0.03 \pm 0.05$		1.07 ± 0.05
$D^0 \pi^-$	4.84 ± 0.15			$4.900 \pm 0.070 \pm 0.220 \pm 0.006$ ¹	
				$4.49 \pm 0.21 \pm 0.23$ ²	
$\bar{D}^0 K^-$		< 190			< 190

¹ Branching fraction measurements and isospin analyses for $\bar{B} \rightarrow D^{(*)} \pi^-$ decays (65M $B\bar{B}$ pairs) ; $B^- \rightarrow D^0 \pi^-$

² Measurement of the Absolute Branching Fractions $B \rightarrow D^{(*,**)} \pi$ with a Missing Mass method (231M $B\bar{B}$ pairs) ; $B^- \rightarrow D^0 \pi^-$

Table 91: Branching fractions of charged B modes producing charmed particles in units of 10^{-6} , upper limits are at 90% CL. The latest version is available at: <http://hfag.phys.ntu.edu.tw/b2charm/00109.html>

Mode	PDG 2008	Belle	BABAR	CDF	Average
$K^- \omega(1650) \phi(1020)$		< 1.90			< 1.90

Table 92: Branching fractions of neutral B modes producing new particles in units of 10^{-4} , upper limits are at 90% CL. The latest version is available at: <http://hfag.phys.ntu.edu.tw/b2charm/00201.html>

Mode	PDG 2008	Belle	<i>BABAR</i>	CDF	Average
$D_{sJ}^*(2317)^+ K^-$		$0.53 \pm_{0.14}^{0.13} \pm 0.07 \pm 0.02$			0.53 ± 0.15
$X^+(3872) K^-$	< 5.0		< 5.0		< 5.0
$D_{sJ}^-(2460) D^+$	35 ± 11		$26.0 \pm 15.0 \pm 7.0$		26 ± 17
$D_{sJ}^-(2460) D^{*+}(2010)$	93 ± 22		$88 \pm 20 \pm 14$		88 ± 24

Table 93: Product branching fractions of neutral B modes producing new particles in units of 10^{-4} , upper limits are at 90% CL. The latest version is available at: <http://hfag.phys.ntu.edu.tw/b2charm/00201.html>

Mode	PDG 2008	Belle	BABAR	CDF	Average
$\bar{K}^{*0}(892)X(3872)[J/\psi(1S)\gamma]$			< 0.028		< 0.028
$K^+Z^-(4430)[J/\psi(1S)\pi^-]$			< 0.030		< 0.030
$\pi^+D_{sJ}^-(2460)[D_s^-\gamma]$		< 0.040			< 0.040
$\bar{K}^{*0}(892)X(3872)[\psi(2S)\gamma]$			< 0.044		< 0.044
$\bar{K}^0X(3872)[J/\psi(1S)\gamma]$			< 0.049		< 0.049
$K^-X^+(3872)[J/\psi(1S)\pi^+\pi^0]$	< 0.054		< 0.054		< 0.054
$\bar{K}^0X(3872)[J/\psi(1S)\pi^+\pi^-]$	< 0.060		< 0.060		< 0.060
$K^-D_{sJ}^+(2460)[D_s^+\gamma]$		< 0.086			< 0.086
$\bar{K}^0X(3872)[\psi(2S)\gamma]$			< 0.190		< 0.190
$\pi^+D_{sJ}^*(2317)^-[D_s^-\pi^0]$	< 0.25	< 0.25			< 0.25
$K^+Z^-(4430)[\psi(2S)\pi^-]$			< 0.29		< 0.29
$K^0Y(3940)[J/\psi(1S)\omega(782)]$			< 0.31		< 0.31
$K^-D_{sJ}^*(2317)^+[D_s^+\pi^0]$	0.43 ± 0.14	$0.44 \pm 0.08 \pm 0.06 \pm 0.11$			0.44 ± 0.15
$D^+D_{sJ}^-(2460)[D_s^-\pi^+\pi^-]$	< 2.00	< 2.00			< 2.00
$D^+D_{sJ}^-(2460)[D_s^-\pi^0]$	< 3.6	< 3.6			< 3.6
$\bar{K}^0X(3872)[\bar{D}^{*0}(2007)D^0]$	< 4.4		< 4.4		< 4.4
$D^+D_{sJ}^-(2460)[D_s^{*-}\gamma]$	< 6.0	< 6.0			< 6.0
$D^+D_{sJ}^-(2460)[D_s^-\gamma]$	6.6 ± 1.7	$8.2 \pm_{1.9}^{2.2} \pm 2.5$	$8.0 \pm 2.0 \pm 1.0 \pm_{2.00}^{3.00}$		$8.1 \pm_{2.5}^{2.2}$
$D^+D_{sJ}^*(2317)^-[D_s^{*-}\gamma]$	< 9.5	< 9.5			< 9.5
$D^+D_{sJ}^*(2317)^-[D_s^-\pi^0]$	9.9 ± 3.7	$8.6 \pm_{2.6}^{3.3} \pm 2.6$	$18.0 \pm 4.0 \pm 3.0 \pm_{4.0}^{6.0}$		$10.4 \pm_{3.5}^{3.2}$
$D^{*+}(2010)D_{sJ}^*(2317)^-[D_s^-\pi^0]$	15.0 ± 6.0		$15.0 \pm 4.0 \pm 2.0 \pm_{3.0}^{5.0}$		$15.0 \pm_{5.4}^{6.7}$
$D^{*+}(2010)D_{sJ}^-(2460)[D_s^-\gamma]$	23.0 ± 8.0		$23.0 \pm 3.0 \pm 3.0 \pm_{5.0}^{8.0}$		$23.0 \pm_{6.6}^{9.1}$
$D^+D_{sJ}^-(2460)[D_s^{*-}\pi^0]$		$22.7 \pm_{6.2}^{7.3} \pm 6.8$	$28.0 \pm 8.0 \pm 5.0 \pm_{6.0}^{10.0}$		$24.6 \pm_{8.2}^{7.2}$
$D^{*+}(2010)D_{sJ}^-(2460)[D_s^{*-}\pi^0]$			$55.0 \pm 12.0 \pm 10.0 \pm_{12.0}^{19.0}$		$55 \pm_{20}^{25}$

Table 94: Ratios of branching fractions of neutral B modes producing new particles in units of 10^0 , upper limits are at 90% CL. The latest version is available at: <http://hfag.phys.ntu.edu.tw/b2charm/00201.html>

Mode	PDG 2008	Belle	BABAR	CDF	Average
$\frac{\mathcal{B}(\overline{B}^0 \rightarrow X(3872)\overline{K}^0)}{\mathcal{B}(B^- \rightarrow X(3872)K^-)}$			$0.41 \pm 0.24 \pm 0.05$		0.41 ± 0.25

Table 95: Branching fractions of neutral B modes producing strange D mesons in units of 10^{-3} , upper limits are at 90% CL. The latest version is available at: <http://hfag.phys.ntu.edu.tw/b2charm/00202.html>

Mode	PDG 2008	Belle	BABAR	CDF	Average
$D_s^- a_0^+(980)$	< 0.019		< 0.019		< 0.019
$D_s^- \rho^+(770)$	< 0.024		< 0.019 ² < 0.024 ¹		< 0.019
$D_s^{*+} K^-$	0.024 ± 0.004		$0.024 \pm 0.004 \pm 0.001 \pm 0.001$		0.024 ± 0.004
$D_s^- \pi^+$	0.024 ± 0.004	$0.024 \pm_{0.008}^{0.010} \pm 0.004 \pm 0.006$	$0.025 \pm 0.004 \pm 0.001 \pm 0.001$		0.025 ± 0.004
$D_s^{*+} \pi^+$	0.026 ± 0.005		$0.026 \pm_{0.004}^{0.005} \pm 0.001 \pm 0.001$		0.026 ± 0.005
$D_s^+ K^-$	0.030 ± 0.004	$0.046 \pm_{0.011}^{0.012} \pm 0.006 \pm 0.012$	$0.029 \pm 0.004 \pm 0.001 \pm 0.002$		0.030 ± 0.004
$D_s^+ \Lambda \bar{p}$		$0.029 \pm 0.007 \pm 0.005 \pm 0.004$ ⁴ $0.036 \pm 0.009 \pm 0.006 \pm 0.009$ ³			0.031 ± 0.008
$D_s^{*+} K^{*-}(892)$	0.03 ± 0.01		$0.032 \pm_{0.010}^{0.014} \pm 0.004 \pm 0.002$		0.03 ± 0.01
$D_s^+ K^{*-}(892)$	0.035 ± 0.010		$0.035 \pm_{0.009}^{0.010} \pm 0.003 \pm 0.002$		0.04 ± 0.01
$D_s^{*-} a_0^+(980)$	< 0.036		< 0.036		< 0.036
$D_s^{*-} \rho^+(770)$	0.04 ± 0.01		$0.041 \pm_{0.012}^{0.013} \pm 0.003 \pm 0.002$		0.04 ± 0.01
$D_s^+ K_S^0 \pi^-$	< 2.5		$0.055 \pm 0.013 \pm 0.010 \pm 0.002$		0.06 ± 0.02
$D_s^{*+} K^0 \pi^-$	< 2.6		< 0.055		< 0.055
$D_s^- D_s^+$	< 0.036	< 0.200 ⁶ < 0.036 ⁵	< 0.100		< 0.036
$D_s^- D_s^{*+}$	< 0.130		< 0.130		< 0.130
$D_s^- a_2^+(1320)$	< 0.190		< 0.190		< 0.190
$D_s^{*-} a_2^+(1320)$	< 0.200		< 0.200		< 0.200
$D_s^{*+} D_s^{*-}$	< 0.24		< 0.24		< 0.24
$D_s^- D^+$	7.5 ± 1.6		$6.7 \pm 2.0 \pm 1.1$		6.7 ± 2.3
$D_s^- D^+$	7.40 ± 0.70	$7.42 \pm 0.23 \pm 1.36$ ⁶ $7.50 \pm 0.20 \pm 0.80 \pm 0.80$ ⁵	$9.0 \pm 1.8 \pm 1.4$		7.67 ± 0.82
$D_s^- D^{*+}(2010)$	8.2 ± 1.1		$5.70 \pm 1.60 \pm 0.90$ ^{7a} $10.3 \pm 1.4 \pm 1.3 \pm 2.6$ ^{8a}		6.8 ± 1.6
$D_s^{*-} D^{*+}(2010)$	17.8 ± 1.4		$18.80 \pm 0.90 \pm 1.60 \pm 0.60$ ⁹ $16.5 \pm 2.3 \pm 1.9$ ^{7b} $19.7 \pm 1.5 \pm 3.0 \pm 4.9$ ^{8b}		18.2 ± 1.6
$D_{s1}^-(2536) D^{*+}(2010)$			$92.00 \pm 24.00 \pm 1.00$		92 ± 24

¹ Measurement of the Branching Fractions of the Rare Decays $B^0 \rightarrow D_s^{(*)+} \pi^-$, $B^0 \rightarrow D_s^{(*)+} \rho^-$, and $B^0 \rightarrow D_s^{(*)-} K^{(*)+}$ (381M $B\bar{B}$ pairs)

² A search for the rare decay $\bar{B}^0 \rightarrow D_s^- \rho^+$ (90M $B\bar{B}$ pairs) ; $\bar{B}^0 \rightarrow D_s^- \rho^+$

³ Observation of B0bar to Ds+ Lambda pbar (447M $B\bar{B}$ pairs)

⁴ Observation of B0bar - Ds+ Lambda pbar decay (449M $B\bar{B}$ pairs)

⁵ Improved measurement of B0bar - Ds-D+ and search for B0bar - Ds+Ds- (449M $B\bar{B}$ pairs)

⁶ Improved measurement of $\bar{B}^0 \rightarrow D_s^- D^+$ and search for $\bar{B}^0 \rightarrow D_s^+ D_s^-$ at Belle

⁷ Study of $\bar{B} \rightarrow D^{(*)+} X^-$ and $\bar{B} \rightarrow D_s^{(*)-} X^{+0}$ decays and measurement of D_s^- and D_{sJ}^- (2460) absolute branching fractions (230M $B\bar{B}$ pairs) ; ^{7a} $\bar{B}^0 \rightarrow D_s^- D^{*+}$; ^{7b} $\bar{B}^0 \rightarrow D_s^{*-} D^{*+}$

⁸ Measurement of $\bar{B}^0 \rightarrow D_s^{(*)} D^*$ Branching Fractions and $D_s^* D^*$ Polarization with a Partial Reconstruction technique (22.7M $B\bar{B}$ pairs) ; ^{8a} $\bar{B}^0 \rightarrow D_s^- D^{*+}$; ^{8b} $\bar{B}^0 \rightarrow D_s^{*-} D^{*+}$

⁹ Measurement of the $\bar{B}^0 \rightarrow D_s^{*-} D^+$ and $D_s^+ \rightarrow \phi \pi^+$ branching fractions (123M $B\bar{B}$ pairs) ; $\bar{B}^0 \rightarrow D_s^{*-} D^{*+}$

Table 96: Product branching fractions of neutral B modes producing strange D mesons in units of 10^{-4} , upper limits are at 90% CL. The latest version is available at: <http://hfag.phys.ntu.edu.tw/b2charm/00202.html>

Mode	PDG 2008	Belle	BABAR	CDF	Average
$D^+ D_s^- [\pi^- \phi(1020) [K^+ K^-]]$		$1.47 \pm 0.05 \pm 0.21$			1.47 ± 0.22
$D^+ D_{s1}^- (2536) [K^- \bar{D}^{*0} (2007)]$	1.70 ± 0.60		$1.71 \pm 0.48 \pm 0.32$		1.71 ± 0.58
$D^+ D_{s1}^- (2536) [D^{*-} (2010) \bar{K}^0]$	2.6 ± 1.1		$2.61 \pm 1.03 \pm 0.31$		2.6 ± 1.1
$D^+ D_s^- [\phi(1020) \pi^-]$			$2.67 \pm 0.61 \pm 0.47$		2.67 ± 0.77
$D^{*+} (2010) D_{s1}^- (2536) [\bar{D}^{*0} (2007) K^+]$	3.3 ± 1.1		$3.32 \pm 0.88 \pm 0.66$		3.3 ± 1.1
$D_s^{*-} D^+ [D_s^- \rightarrow \phi(1020) \pi^-]$			$4.14 \pm 1.19 \pm 0.94$		4.1 ± 1.5
$D^{*+} (2010) D_{s1}^- (2536) [D^{*-} (2010) \bar{K}^0]$	5.0 ± 1.7		$5.00 \pm 1.51 \pm 0.67$		5.0 ± 1.7
$D^{*+} (2010) D_s^- [\phi(1020) \pi^-]$			$5.11 \pm 0.94 \pm 0.72$		5.1 ± 1.2
$D^{*-} (2010) D_{s1}^+ (2536) [D^{*+} (2010) K_S^0]$	2.50 ± 0.90	< 6.0			< 6.0
$D_s^{*-} D^{*+} (2010) [D_s^- \rightarrow \phi(1020) \pi^-]$			$12.2 \pm 2.2 \pm 2.2$		12.2 ± 3.1

Table 97: Ratios of branching fractions of neutral B modes producing strange D mesons in units of 10^0 , upper limits are at 90% CL. The latest version is available at: <http://hfag.phys.ntu.edu.tw/b2charm/00202.html>

Mode	PDG 2008	Belle	BABAR	CDF	Average
$\frac{\mathcal{B}(\bar{B}^0 \rightarrow D_s^{*-} D^+)}{\mathcal{B}(\bar{B}^0 \rightarrow D_s^- D^+)}$				$0.90 \pm 0.20 \pm 0.10$	0.90 ± 0.22
$\frac{\mathcal{B}(\bar{B}^0 \rightarrow D_s^- D^{*+} (2010))}{\mathcal{B}(\bar{B}^0 \rightarrow D_s^- D^+)}$				$1.50 \pm 0.40 \pm 0.10$	1.50 ± 0.41
$\frac{\mathcal{B}(\bar{B}^0 \rightarrow D^+ \pi^+ \pi^- \pi^-)}{\mathcal{B}(\bar{B}^0 \rightarrow D_s^- D^+)}$				$1.99 \pm 0.13 \pm 0.11 \pm 0.45$	1.99 ± 0.48
$\frac{\mathcal{B}(\bar{B}^0 \rightarrow D_s^{*-} D^{*+} (2010))}{\mathcal{B}(\bar{B}^0 \rightarrow D_s^- D^+)}$				$2.60 \pm 0.50 \pm 0.20$	2.60 ± 0.54

Table 98: Branching fractions of neutral B modes producing baryons in units of 10^{-5} , upper limits are at 90% CL. The latest version is available at: <http://hfag.phys.ntu.edu.tw/b2charm/00203.html>

Mode	PDG 2008	Belle	BABAR	CDF	Average
$J/\psi(1S)\bar{p}p$		< 0.083	< 0.190		< 0.083
$\Sigma_c^{*+}\bar{p}K^-$			$1.11 \pm 0.30 \pm 0.09 \pm 0.29$		1.11 ± 0.43
$\Lambda_c^+\bar{p}$	2.00 ± 0.40	$2.19 \pm_{0.49}^{0.56} \pm 0.32 \pm 0.57$	$1.89 \pm 0.21 \pm 0.06 \pm 0.49$		1.98 ± 0.45
Λ_c^+p	2.00 ± 0.40		-		$2.1 \pm_{0.9}^{1.2}$
$\Lambda_c^+\bar{p}K^{*0}(892)$			< 2.4		< 2.4
$\Lambda_c^+\bar{p}K^-\pi^+$			$4.33 \pm 0.82 \pm 0.33 \pm 1.13$		4.3 ± 1.4
$\Lambda_c^+\Lambda_c^-$	< 6.2	< 5.7			< 5.7
$\Sigma_c^{*0}\bar{p}\pi^+$	15.0 ± 5.0				< 3.3
		< 12.1 ¹			
		< 3.3 ²			
$D^{*0}(2007)p\bar{p}$	10.3 ± 1.3	$12.0 \pm_{2.9}^{3.3} \pm 2.1$	$10.10 \pm 1.00 \pm 0.90$		10.3 ± 1.3
$D^0p\bar{p}$	11.40 ± 0.90	$11.8 \pm 1.5 \pm 1.6$	$11.30 \pm 0.60 \pm 0.80$		11.39 ± 0.91
$\Sigma_c^{*+}\bar{p}\pi^-$		$16.3 \pm_{5.1}^{5.7} \pm 2.8 \pm 4.2$ ¹			
		$12.0 \pm 1.0 \pm 2.0 \pm 3.0$ ²			
$\Sigma_c^0\bar{p}\pi^+$		$14.0 \pm 2.0 \pm 2.0 \pm 4.0$ ²			14.0 ± 4.9
		< 15.9 ¹			
$\Sigma_c^{*+}\bar{p}\pi^-$	22.0 ± 7.0	$23.8 \pm_{5.5}^{6.3} \pm 4.1 \pm 6.2$ ¹			$21.8 \pm_{5.2}^{5.1}$
		$21.0 \pm 2.0 \pm 3.0 \pm 5.0$ ^{2a}			
$D^+p\bar{p}\pi^-$	33.8 ± 3.2		$33.8 \pm 1.4 \pm 2.9$		33.8 ± 3.2
$D^{*+}(2010)p\bar{p}\pi^-$	50.0 ± 5.0		$48.1 \pm 2.2 \pm 4.4$		48.1 ± 4.9
$\Lambda_c^+\Lambda_c^-\bar{K}^0$		$79 \pm_{23}^{29} \pm 12 \pm 41$	< 150		$79 \pm_{49}^{52}$
$\Lambda_c^+\bar{p}\pi^+\pi^-$	130 ± 40	$110 \pm_{12}^{12} \pm 19 \pm 29$			110 ± 37

¹ STUDY OF EXCLUSIVE B DECAYS TO CHARMED BARYONS AT BELLE. (31.7M $B\bar{B}$ pairs)

² Study of the charmed baryonic decays $\bar{B}^0 \rightarrow \Sigma_c^{*+}\bar{p}\pi^-$ and $\bar{B}^0 \rightarrow \Sigma_c^0\bar{p}\pi^+$ (386M $B\bar{B}$ pairs) ; ^{2a} $B_0\text{bar}$ to Sigmac(2455)++ pbar pi

Table 99: Product branching fractions of neutral B modes producing baryons in units of 10^{-5} , upper limits are at 90% CL. The latest version is available at: <http://hfag.phys.ntu.edu.tw/b2charm/00203.html>

Mode	PDG 2008	Belle	<i>BABAR</i>	CDF	Average
$A_c^- \Xi_c^+ [\Xi^- \pi^+ \pi^+]$	9.0 ± 5.0	$9.3 \pm_{2.8}^{3.7} \pm 1.9 \pm 2.4$	< 5.6		$9.3 \pm_{4.1}^{4.8}$

Table 100: Branching fractions of neutral B modes producing $J/\psi(1S)$ in units of 10^{-5} , upper limits are at 90% CL. The latest version is available at: <http://hfag.phys.ntu.edu.tw/b2charm/00204.html>

Mode	PDG 2008	Belle	BABAR	CDF	Average
$J/\psi(1S)\phi(1020)$	< 0.094	< 0.094			< 0.094
$J/\psi(1S)\gamma$	< 0.160		< 0.160		< 0.160
$J/\psi(1S)\phi(1020)$	< 0.094		< 0.90		< 0.90
$J/\psi(1S)\eta$	0.95 ± 0.19	$0.96 \pm 0.17 \pm 0.07$	< 2.7		0.96 ± 0.18
$J/\psi(1S)f_2(1270)$	< 0.46				0.98 ± 0.44
		$0.98 \pm 0.39 \pm 0.20$ ²	< 0.46		
		< 0.49 ¹			
$J/\psi(1S)D^0$	< 1.30	< 2.0	< 1.30		< 1.30
$J/\psi(1S)\pi^0$	1.76 ± 0.16	$2.30 \pm 0.50 \pm 0.20$	$1.69 \pm 0.14 \pm 0.07$		1.74 ± 0.15
$J/\psi(1S)\pi^+\pi^-$	4.60 ± 0.90				2.20 ± 0.36
		$2.20 \pm 0.30 \pm 0.20$ ¹	< 1.20		
		< 1.00 ²			
$J/\psi(1S)\rho^0(770)$	2.70 ± 0.40				2.33 ± 0.20
		$2.80 \pm 0.30 \pm 0.30$ ²	$2.70 \pm 0.30 \pm 0.20$		
		$1.90 \pm 0.20 \pm 0.20$ ¹			
$J/\psi(1S)\eta'(958)$	< 6.3		< 6.3		< 6.3
$J/\psi(1S)\eta K_S^0$	8.0 ± 4.0		$8.40 \pm 2.60 \pm 2.70 \pm 0.20$		8.4 ± 3.8
$J/\psi(1S)\phi(1020)\overline{K}^0$	9.4 ± 2.6		$10.20 \pm 3.80 \pm 1.00 \pm 0.20$		10.2 ± 3.9
$J/\psi(1S)\omega(782)\overline{K}^0$	$310,000 \pm 70,000$				31.0 ± 6.7
			$31.0 \pm 6.0 \pm 3.0$ ³		
			$30.0 \pm 6.0 \pm 3.0$ ⁴		
$J/\psi(1S)\overline{K}^0\rho^0(770)$	54 ± 30			$54.0 \pm 29.0 \pm 9.0$	54 ± 30
$J/\psi(1S)\overline{K}^{*0}(892)\pi^+\pi^-$	66 ± 22			$66 \pm 19 \pm 11$	66 ± 22
$J/\psi(1S)K^{*-}(892)\pi^+$	80 ± 40			$77 \pm 41 \pm 13$	77 ± 43
$J/\psi(1S)\overline{K}^0$	87.1 ± 3.2	$79.0 \pm 4.0 \pm 9.0 \pm 1.0$	$86.9 \pm 2.2 \pm 2.6 \pm 1.5$	$115 \pm 23 \pm 17$	86.3 ± 3.5
$J/\psi(1S)\overline{K}^0\pi^+\pi^-$	120 ± 60			$103 \pm 33 \pm 15$	103 ± 36
$J/\psi(1S)\overline{K}_1^0(1270)$	130 ± 50	$130 \pm 34 \pm 25 \pm 18$			130 ± 46
$J/\psi(1S)\overline{K}^{*0}(892)$	133.0 ± 6.0	$129.0 \pm 5.0 \pm 13.0 \pm 2.0$	$130.9 \pm 2.6 \pm 7.4 \pm 2.2$	$174 \pm 20 \pm 18$	133.2 ± 6.8

¹ Study of $B^0 \rightarrow J/\psi\pi^+\pi^-$ decays with 449 million $B\overline{B}$ pairs at Belle (449M $B\overline{B}$ pairs)

² MEASUREMENT OF BRANCHING FRACTIONS IN $B_0 \rightarrow J/\psi\pi^+\pi^-$ DECAY. (152M $B\overline{B}$ pairs)

³ Observation of $Y(3940) \rightarrow J/\psi\omega$ in $B \rightarrow J/\psi\omega K$ at BaBar

⁴ Observation of $Y(3940) \rightarrow J/\psi\omega$ in $B \rightarrow J/\psi\omega K$ at BABAR (383M $B\overline{B}$ pairs) ; bjpsiomegak0

Table 101: Ratios of branching fractions of neutral B modes producing $J/\psi(1S)$ in units of 10^0 , upper limits are at 90% CL. The latest version is available at: <http://hfag.phys.ntu.edu.tw/b2charm/00204.html>

Mode	PDG 2008	Belle	BABAR	CDF	Average
$\frac{\mathcal{B}(\overline{B}^0 \rightarrow J/\psi(1S)\overline{K}_1^0(1270))}{\mathcal{B}(B^- \rightarrow J/\psi(1S)K^-)}$		$1.30 \pm 0.34 \pm 0.28$			1.30 ± 0.44
$\frac{\mathcal{B}(\overline{B}^0 \rightarrow \eta_c(1S)\overline{K}^0)}{\mathcal{B}(\overline{B}^0 \rightarrow J/\psi(1S)\overline{K}^0)}$			$1.34 \pm 0.19 \pm 0.13 \pm 0.38$		1.34 ± 0.44
$\frac{\mathcal{B}(\overline{B}^0 \rightarrow J/\psi(1S)\overline{K}^{*0}(892))}{\mathcal{B}(\overline{B}^0 \rightarrow J/\psi(1S)\overline{K}^0)}$			$1.51 \pm 0.05 \pm 0.08$	$1.39 \pm 0.36 \pm 0.10$	1.50 ± 0.09

Table 102: Miscellaneous quantities of neutral B modes producing $J/\psi(1S)$ in units of 10^0 , upper limits are at 90% CL. The latest version is available at: <http://hfag.phys.ntu.edu.tw/b2charm/00204.html>

Mode	PDG 2008	Belle	BABAR	CDF	Average
$ \mathcal{A}_0 ^2(\overline{B}^0 \rightarrow J/\psi(1S)K^{*0}(892))$			< 0.26		< 0.26
$ \mathcal{A}_0 ^2(B^0 \rightarrow J/\psi(1S)K^{*0}(892))$			< 0.32		< 0.32

Table 103: Branching fractions of neutral B modes producing charmonium other than $J/\psi(1S)$ in units of 10^{-4} , upper limits are at 90% CL. The latest version is available at: <http://hfag.phys.ntu.edu.tw/b2charm/00205.html>

Mode	PDG 2008	Belle	BABAR	CDF	Average
$\chi_{c1}(1P)\pi^0$	0.11 ± 0.03	$0.11 \pm 0.02 \pm 0.01$			0.11 ± 0.03
$\chi_{c2}(1P)\bar{K}^0$	< 0.26		< 0.28		< 0.28
$\chi_{c2}(1P)\bar{K}^{*0}(892)$	< 0.36		$0.66 \pm 0.18 \pm 0.05$		0.66 ± 0.19
$\chi_{c0}(1P)K^{*0}(892)$	1.70 ± 0.40		$1.70 \pm 0.30 \pm 0.20$		1.70 ± 0.36
$\chi_{c1}(1P)\bar{K}^{*0}(892)$	2.00 ± 0.50	$3.10 \pm 0.30 \pm 0.70$	$2.50 \pm 0.20 \pm 0.20$		2.57 ± 0.26
$\eta_c(2S)\bar{K}^{*0}(892)$	6.10 ± 1.00		< 3.9		< 3.9
$\chi_{c1}(1P)\bar{K}^0$	3.90 ± 0.40	$3.50 \pm 0.30 \pm 0.50$	$4.20 \pm 0.30 \pm 0.30$		3.96 ± 0.34
$\eta_c(1S)\bar{K}^{*0}(892)$	6.10 ± 1.00				$6.1 \pm_{1.1}^{1.0}$
		$16.2 \pm 3.2 \pm_{3.4}^{2.4} \pm 5.0$	$5.70 \pm 0.60 \pm 0.40 \pm 0.80$ ¹ $8.0 \pm_{1.9}^{2.1} \pm 1.3 \pm_{1.9}^{3.5}$ ^{3b}		
$\psi(2S)\bar{K}^0$	6.20 ± 0.60	6.7 ± 1.1	$6.46 \pm 0.65 \pm 0.44 \pm 0.25$		6.55 ± 0.66
$\psi(2S)\bar{K}^{*0}(892)$	7.20 ± 0.80	$7.20 \pm 0.43 \pm 0.65$	$6.49 \pm 0.59 \pm 0.94 \pm 0.25$	$9.00 \pm 2.20 \pm 0.90$	7.11 ± 0.62
$\chi_{c0}(1P)\bar{K}^{*0}(892)$	1.70 ± 0.40		< 7.7		< 7.7
$\eta_c(1S)\bar{K}^0$	8.9 ± 1.6				8.7 ± 1.9
		$12.3 \pm 2.3 \pm_{1.6}^{1.2} \pm 3.8$	$11.4 \pm 1.5 \pm 1.2 \pm 3.2$ ² $6.40 \pm_{2.00}^{2.20} \pm 0.40 \pm_{1.50}^{2.80}$ ^{3a}		
$\chi_{c0}(1P)\bar{K}^0$	< 1.13		< 12.4		< 12.4

¹ Study of B-meson decays to etac K^* , etac(2S) K^* and etac gamma K^*

² Branching Fraction Measurements of $B \rightarrow \eta_c K$ Decays (86.1M $B\bar{B}$ pairs)

³ Evidence for the $B^0 \rightarrow p\bar{p}K^{*0}$ and $B^+ \rightarrow \eta_c K^{*+}$ decays and Study of the Decay Dynamics of B Meson Decays into $p\bar{p}h$ Final States. (232M $B\bar{B}$ pairs) ; ^{3a} betackzero ; ^{3b} betackstarzppbar

Table 104: Product branching fractions of neutral B modes producing charmonium other than $J/\psi(1S)$ in units of 10^{-4} , upper limits are at 90% CL. The latest version is available at: <http://hfag.phys.ntu.edu.tw/b2charm/00205.html>

Mode	PDG 2008	Belle	BABAR	CDF	Average
$\overline{K}^0\psi(3770)[D^0\overline{D}^0]$			< 1.23		< 1.23
$\overline{K}^0\psi(3770)[D^+D^-]$			< 1.88		< 1.88
$\overline{K}^{*0}(892)h_c(1P)[\eta_c(1S)\gamma]$			< 2.2		< 2.2

Table 105: Ratios of branching fractions of neutral B modes producing charmonium other than $J/\psi(1S)$ in units of 10^0 , upper limits are at 90% CL. The latest version is available at: <http://hfag.phys.ntu.edu.tw/b2charm/00205.html>

Mode	PDG 2008	Belle	BABAR	CDF	Average
$\frac{\mathcal{B}(\overline{B}^0 \rightarrow h_c(1P)\overline{K}^{*0}(892)) \times \mathcal{B}(h_c(1P) \rightarrow \eta_c(1S)\gamma)}{\mathcal{B}(B^- \rightarrow \eta_c(1S)K^-)}$			< 0.26		< 0.26
$\frac{\mathcal{B}(\overline{B}^0 \rightarrow h_c(1P)\overline{K}^{*0}(892)) \times \mathcal{B}(h_c(1P) \rightarrow \eta_c(1S)\gamma)}{\mathcal{B}(\overline{B}^0 \rightarrow \eta_c(1S)\overline{K}^{*0}(892))}$			< 0.39		< 0.39
$\frac{\mathcal{B}(\overline{B}^0 \rightarrow \eta_c(1S)\overline{K}^{*0}(892))}{\mathcal{B}(B^- \rightarrow \eta_c(1S)K^-)}$			$0.67 \pm 0.09 \pm 0.07$		0.67 ± 0.11
$\frac{\mathcal{B}(\overline{B}^0 \rightarrow \chi_{c1}(1P)\overline{K}^{*0}(892))}{\mathcal{B}(\overline{B}^0 \rightarrow \chi_{c1}(1P)\overline{K}^0)}$			$0.72 \pm 0.11 \pm 0.12$		0.72 ± 0.16
$\frac{\mathcal{B}(\overline{B}^0 \rightarrow \eta_c(1S)\overline{K}^0)}{\mathcal{B}(B^- \rightarrow \eta_c(1S)K^-)}$			$0.87 \pm 0.13 \pm 0.07$		0.87 ± 0.15
$\frac{\mathcal{B}(\overline{B}^0 \rightarrow \psi(2S)\overline{K}^{*0}(892))}{\mathcal{B}(\overline{B}^0 \rightarrow \psi(2S)\overline{K}^0)}$			$1.00 \pm 0.14 \pm 0.09$		1.00 ± 0.17
$\frac{\mathcal{B}(\overline{B}^0 \rightarrow \eta_c(1S)\overline{K}^{*0}(892))}{\mathcal{B}(\overline{B}^0 \rightarrow \eta_c(1S)\overline{K}^0)}$		$1.33 \pm 0.36 \pm_{0.33}^{0.24}$			$1.33 \pm_{0.49}^{0.43}$

Table 106: Branching fractions of neutral B modes producing multiple D , D^* or D^{**} mesons in units of 10^{-3} , upper limits are at 90% CL. The latest version is available at: <http://hfag.phys.ntu.edu.tw/b2charm/00206.html>

Mode	PDG 2008	Belle	BABAR	CDF	Average
$D^0\bar{D}^0$	< 0.043	< 0.042	< 0.060		< 0.042
$D^{*0}(2007)\bar{D}^{*0}(2007)$	< 0.090		< 0.090		< 0.090
$D^0\bar{D}^0\pi^0\bar{K}^0$		$0.17 \pm 0.07 \pm_{0.05}^{0.03}$			0.17 ± 0.08
D^+D^-	0.21 ± 0.03				0.22 ± 0.02
		$0.20 \pm 0.02 \pm 0.02$ ¹	$0.28 \pm 0.04 \pm 0.03 \pm 0.04$		
		$0.32 \pm 0.06 \pm 0.05$ ²			
$D^0\bar{D}^{*0}(2007)$	< 0.29		< 0.29		< 0.29
$D^{*-}(2010)D^+$	0.61 ± 0.15	$1.17 \pm 0.26 \pm_{0.24}^{0.20} \pm 0.08$	$0.57 \pm 0.07 \pm 0.06 \pm 0.04$		0.62 ± 0.09
$D^{*+}(2010)D^{*-}(2010)$	0.82 ± 0.09	$0.81 \pm 0.08 \pm 0.11$	$0.81 \pm 0.06 \pm 0.09 \pm 0.05$		0.81 ± 0.09
$D^0\bar{D}^0\bar{K}^0$	< 1.40		< 1.40		< 1.40
$D^+D^-\bar{K}^0$	< 1.70		< 1.70		< 1.70
$D^+\bar{D}^0K^-$	1.70 ± 0.40		$1.70 \pm 0.30 \pm 0.30$		1.70 ± 0.42
$D^{*+}(2010)\bar{D}^0K^-$	3.10 ± 0.60		$3.10 \pm_{0.30}^{0.40} \pm 0.40$		$3.10 \pm_{0.50}^{0.57}$
$D^0\bar{D}^{*0}(2007)\bar{K}^0$	< 3.7		< 3.7		< 3.7
$D^{*+}(2010)D^{*-}(2010)K_S^0$		$3.40 \pm 0.40 \pm 0.70$	$4.40 \pm 0.40 \pm 0.70 \pm 0.04$		3.90 ± 0.57
$D^+\bar{D}^{*0}(2007)K^-$	4.60 ± 1.00		$4.60 \pm 0.70 \pm 0.70$		4.60 ± 0.99
$D^{*+}(2010)D^-\bar{K}^0$	6.5 ± 1.6		$6.50 \pm 1.20 \pm 1.00$		6.5 ± 1.6
$D^{*0}(2007)\bar{D}^{*0}(2007)\bar{K}^0$	< 6.6		< 6.6		< 6.6
$D^{*-}(2010)D^{*+}(2010)\bar{K}^0$	7.8 ± 1.1		$8.8 \pm_{1.4}^{1.5} \pm 1.3$		$8.8 \pm_{1.9}^{2.0}$
$D^{*+}(2010)\bar{D}^{*0}(2007)K^-$	11.8 ± 2.0		$11.80 \pm 1.00 \pm 1.70$		11.8 ± 2.0

¹ Evidence for CP Violation in $B^0 \rightarrow D^+D^-$ Decays (535M $B\bar{B}$ pairs)

² Observation of $B^0 \rightarrow D^+D^-$, $B^- \rightarrow D^0D^-$ and $B^- \rightarrow D^0D^{*-}$ decays (152M $B\bar{B}$ pairs)

Table 107: Product branching fractions of neutral B modes producing multiple D , D^* or D^{**} mesons in units of 10^{-4} , upper limits are at 90% CL. The latest version is available at: <http://hfag.phys.ntu.edu.tw/b2charm/00206.html>

Mode	PDG 2008	Belle	BABAR	CDF	Average
$K^- D_2^{*+}(2460)[D^0 \pi^+]$			$0.18 \pm 0.04 \pm 0.03$		0.18 ± 0.05
$\pi^- D_2^{*+}(2460)[D^{*+}(2010)\pi^- \pi^+]$	< 0.24	< 0.24			< 0.24
$\pi^- D_1^+(2420)[D^{*+}(2010)\pi^- \pi^+]$	< 0.33	< 0.33			< 0.33
$\pi^- D_1^+(H)[D^{*0}(2007)\pi^+]$		< 0.70			< 0.70
$\pi^- D_1^+(2420)[D^+ \pi^- \pi^+]$	0.89 ± 0.29	$0.89 \pm 0.15 \pm 0.17 \pm_{0.26}^{0.00}$			$0.89 \pm_{0.34}^{0.23}$
$\pi^- D_0^{*+}[D^0 \pi^+]$	0.60 ± 0.30	< 1.20			< 1.20
$\pi^- D_2^{*+}(2460)[D^{*0}(2007)\pi^+]$		$2.45 \pm 0.42 \pm_{0.45}^{0.35} \pm_{0.17}^{0.39}$			$2.45 \pm_{0.64}^{0.67}$
$\pi^- D_2^{*+}(2460)[D^0 \pi^+]$	2.15 ± 0.35	$3.08 \pm 0.33 \pm 0.09 \pm_{0.02}^{0.15}$			$3.08 \pm_{0.34}^{0.37}$
$\pi^- D_1^+(2420)[D^{*0}(2007)\pi^+]$		$3.68 \pm 0.60 \pm_{0.40}^{0.71} \pm_{0.30}^{0.65}$			$3.68 \pm_{0.78}^{1.13}$
$\omega(782)D_1^0(H)[D^{*+}(2010)\pi^-]$	4.1 ± 1.6		$4.10 \pm 1.20 \pm 1.00 \pm 0.40$		4.1 ± 1.6

164

Table 108: Ratios of branching fractions of neutral B modes producing multiple D , D^* or D^{**} mesons in units of 10^0 , upper limits are at 90% CL. The latest version is available at: <http://hfag.phys.ntu.edu.tw/b2charm/00206.html>

Mode	PDG 2008	Belle	BABAR	CDF	Average
$\frac{\mathcal{B}(\overline{B}^0 \rightarrow D^+ K^-)}{\mathcal{B}(\overline{B}^0 \rightarrow D^+ \pi^-)}$		$0.068 \pm 0.015 \pm 0.007$			0.07 ± 0.02
$\frac{\mathcal{B}(\overline{B}^0 \rightarrow D^{*+}(2010)K^-)}{\mathcal{B}(\overline{B}^0 \rightarrow D^{*+}(2010)\pi^-)}$		$0.074 \pm 0.015 \pm 0.006$	$0.078 \pm 0.003 \pm 0.003$		0.077 ± 0.004
$\frac{\mathcal{B}(\overline{B}^0 \rightarrow D^{**+}\pi^-)}{\mathcal{B}(\overline{B}^0 \rightarrow D^+ \pi^-)}$			$0.77 \pm 0.22 \pm 0.29$		0.77 ± 0.36
$\frac{\mathcal{B}(\overline{B}^0 \rightarrow D^{*+}(2010)\pi^-)}{\mathcal{B}(\overline{B}^0 \rightarrow D^+ \pi^-)}$			$0.99 \pm 0.11 \pm 0.08$		0.99 ± 0.14
$\frac{\mathcal{B}(\overline{B}^0 \rightarrow D^0 \rho^0(770))}{\mathcal{B}(\overline{B}^0 \rightarrow D^0 \omega(782))}$		1.60 ± 0.80			1.60 ± 0.80
$\frac{\mathcal{B}(\overline{B}^0 \rightarrow D^+ \mu^- \overline{\nu}_\mu)}{\mathcal{B}(\overline{B}^0 \rightarrow D^+ \pi^-)}$				$9.80 \pm 1.00 \pm 0.60 \pm 1.20$	9.8 ± 1.7
$\frac{\mathcal{B}(\overline{B}^0 \rightarrow D^{*+}(2010)\mu^- \overline{\nu}_\mu)}{\mathcal{B}(\overline{B}^0 \rightarrow D^{*+}(2010)\pi^-)}$				$17.70 \pm 2.30 \pm 0.60 \pm 1.20$	17.7 ± 2.7

Table 109: Branching fractions of neutral B modes producing a single D^* or D^{**} meson in units of 10^{-4} , upper limits are at 90% CL. The latest version is available at: <http://hfag.phys.ntu.edu.tw/b2charm/00207.html>

Mode	PDG 2008	Belle	BABAR	CDF	Average
$D^{*0}(2007)\bar{K}^0$	0.36 ± 0.12	< 0.66	$0.36 \pm 0.12 \pm 0.03$		0.36 ± 0.12
$\bar{D}^{*0}(2007)\bar{K}^{*0}(892)$	< 0.40	< 0.40			< 0.40
$D^{*0}(2007)\bar{K}^{*0}(892)$	< 0.69	< 0.69			< 0.69
$D^{*0}(2007)\eta'(958)$	1.23 ± 0.35	$1.21 \pm 0.34 \pm 0.22$	< 2.6		1.21 ± 0.40
$D^{*0}(2007)\pi^0$	1.70 ± 0.40	$1.39 \pm 0.18 \pm 0.26$	$2.90 \pm 0.40 \pm 0.46 \pm 0.19$		1.69 ± 0.28
$D^{*0}(2007)\eta$	1.80 ± 0.60	$1.40 \pm 0.28 \pm 0.26$	$2.60 \pm 0.40 \pm 0.37 \pm 0.16$		1.77 ± 0.32
$f_2(1270)D^{*0}(2007)$		$1.86 \pm 0.65 \pm 0.60 \pm_{0.52}^{0.80}$			$1.9 \pm_{1.0}^{1.2}$
$D^{*+}(2010)K^-$	2.14 ± 0.16	$2.04 \pm 0.41 \pm 0.17 \pm 0.16$			2.04 ± 0.47
$D^{*0}(2007)\omega(782)$	2.70 ± 0.80	$2.29 \pm 0.39 \pm 0.40$	$4.20 \pm 0.70 \pm 0.86 \pm 0.27$		2.66 ± 0.50
$D^{*+}(2010)K^0\pi^-$	3.00 ± 0.80		$3.00 \pm 0.70 \pm 0.22 \pm 0.20$		3.00 ± 0.76
$D^{*+}(2010)K^{*-}(892)$	3.30 ± 0.60		$3.20 \pm 0.60 \pm 0.27 \pm 0.12$		3.20 ± 0.67
$D^{*0}(2007)\rho^0(770)$	< 5.1	$3.73 \pm 0.87 \pm 0.46 \pm_{0.08}^{0.18}$ ²			3.73 ± 0.99
		< 5.1 ¹			
$D^{*+}(2010)K^-K^0$	< 4.7	< 4.7			< 4.7
$D^{*0}(2007)\pi^+\pi^-$	6.2 ± 2.2	$6.2 \pm 1.2 \pm 1.8$ ¹			9.0 ± 1.4
		$10.90 \pm 0.80 \pm 1.60$ ²			
$D^{*+}(2010)K^-K^{*0}(892)$	12.9 ± 3.3	$12.9 \pm 2.2 \pm 2.5$			12.9 ± 3.3
$D^{**+}\pi^-$	21.0 ± 10.0		$23.4 \pm 6.5 \pm 8.8$		23 ± 11
$D^{*0}(2007)\pi^-\pi^+\pi^-\pi^+$	27.0 ± 5.0	$26.0 \pm 4.7 \pm 3.7$			26.0 ± 6.0
$D^{*+}(2010)\pi^-$	27.6 ± 1.3	$23.00 \pm 0.60 \pm 1.90$	$27.90 \pm 0.80 \pm 1.70 \pm 0.05$ ³		26.2 ± 1.3
			$29.9 \pm 2.3 \pm 2.4$ ⁴		
$D^{*+}(2010)\omega(782)\pi^-$	28.9 ± 3.0		$28.8 \pm 2.1 \pm 2.8 \pm 1.4$		28.8 ± 3.8
$D^{*+}(2010)\pi^-\pi^+\pi^-\pi^+\pi^-$	47.0 ± 9.0	$47.2 \pm 5.9 \pm 7.1$			47.2 ± 9.2
$D^{*+}(2010)\pi^-\pi^+\pi^-$	70.0 ± 8.0	$68.1 \pm 2.3 \pm 7.2$			68.1 ± 7.6

¹ Study of $\bar{B}^0 \rightarrow D^{(*)0}\pi^+\pi^-$ Decays (31.3M $B\bar{B}$ pairs)

² Study of $\bar{B}^0 \rightarrow D^{(*)0}\pi^+\pi^-$ decays ; Dalitz fit analysis (152M $B\bar{B}$ pairs)

³ Branching fraction measurements and isospin analyses for $\bar{B} \rightarrow D^{(*)}\pi^-$ decays (65M $B\bar{B}$ pairs) ; $\bar{B}^0 \rightarrow D^{*+}\pi^-$

⁴ Measurement of the Absolute Branching Fractions $B \rightarrow D^{(**)}\pi$ with a Missing Mass method (231M $B\bar{B}$ pairs) ; $\bar{B}^0 \rightarrow D^{*+}\pi^-$

Table 110: Branching fractions of neutral B modes producing a single D meson in units of 10^{-4} , upper limits are at 90% CL. The latest version is available at: <http://hfag.phys.ntu.edu.tw/b2charm/00208.html>

Mode	PDG 2008	Belle	BABAR	CDF	Average
$\overline{D}^0 \overline{K}^{*0}$ (892)	< 0.110	< 0.180	< 0.110		< 0.110
$\overline{D}^0 K^- \pi^+$	< 0.190		< 0.190		< 0.190
$D^0 \overline{K}^{*0}$ (892)	0.42 ± 0.06	$0.48 \pm_{0.10}^{0.11} \pm 0.05$	$0.40 \pm 0.07 \pm 0.03$		0.42 ± 0.06
$D^0 \overline{K}^0$	0.52 ± 0.07	$0.50 \pm_{0.12}^{0.13} \pm 0.06$	$0.53 \pm 0.07 \pm 0.03$		0.52 ± 0.07
$D^0 K^- \pi^+$	0.88 ± 0.17		$0.88 \pm 0.15 \pm 0.09$		0.88 ± 0.17
$D^0 \eta'$ (958)	1.25 ± 0.23	$1.14 \pm 0.20 \pm_{0.13}^{0.10}$	$1.70 \pm 0.40 \pm 0.18 \pm 0.10$		1.26 ± 0.21
$f_2(1270) D^0$	1.20 ± 0.40	$1.95 \pm 0.34 \pm 0.38 \pm_{0.02}^{0.32}$			$1.95 \pm_{0.51}^{0.60}$
$D^0 \eta$	2.02 ± 0.35	$1.77 \pm 0.16 \pm 0.21$	$2.50 \pm 0.20 \pm 0.29 \pm 0.11$		2.02 ± 0.21
$D^+ K^-$	2.00 ± 0.60	$2.04 \pm 0.45 \pm 0.21 \pm 0.27$			2.04 ± 0.57
$D^0 \omega$ (782)	2.59 ± 0.30	$2.37 \pm 0.23 \pm 0.28$	$3.00 \pm 0.30 \pm 0.38 \pm 0.13$		2.59 ± 0.29
$D^0 \pi^0$	2.61 ± 0.24	$2.25 \pm 0.14 \pm 0.35$	$2.90 \pm 0.20 \pm 0.27 \pm 0.13$		2.59 ± 0.26
$D^0 \rho^0$ (770)	3.20 ± 0.50				$2.91 \pm_{0.40}^{0.58}$
		$2.90 \pm 1.00 \pm 0.40$ ¹			
		$2.91 \pm 0.28 \pm 0.33 \pm_{0.54}^{0.98}$ ²			
$D^+ K^- K^0$	< 3.1	< 3.1			< 3.1
$D^+ K^{*-}$ (892)	4.50 ± 0.70		$4.60 \pm 0.60 \pm 0.47 \pm 0.16$		4.60 ± 0.78
$D^+ K^0 \pi^-$	4.90 ± 0.90		$4.90 \pm 0.70 \pm 0.38 \pm 0.32$		4.90 ± 0.86
$D^+ K^- K^{*0}$ (892)	8.8 ± 1.9	$8.8 \pm 1.1 \pm 1.5$			8.8 ± 1.9
$D^0 \pi^+ \pi^-$	8.40 ± 0.90				9.78 ± 0.95
		$8.00 \pm 0.60 \pm 1.50$ ¹			
		$10.70 \pm 0.60 \pm 1.00$ ²			
$D^+ \pi^-$	26.8 ± 1.3				26.5 ± 1.5
			$25.50 \pm 0.50 \pm 1.60 \pm 0.10$ ³		
			$30.3 \pm 2.3 \pm 2.3$ ⁴		

¹ Study of $\overline{B}^0 \rightarrow D^{(*)0} \pi^+ \pi^-$ Decays (31.3M $B\overline{B}$ pairs)

² Study of $\overline{B}^0 \rightarrow D^{(*)0} \pi^+ \pi^-$ decays ; Dalitz fit analysis (152M $B\overline{B}$ pairs)

³ Branching fraction measurements and isospin analyses for $\overline{B} \rightarrow D^{(*)} \pi^-$ decays (65M $B\overline{B}$ pairs) ; $\overline{B}^0 \rightarrow D^+ \pi^-$

⁴ Measurement of the Absolute Branching Fractions $B \rightarrow D^{(**)} \pi$ with a Missing Mass method (231M $B\overline{B}$ pairs) ; $\overline{B}^0 \rightarrow D^+ \pi^-$

Table 111: Product branching fractions of neutral B modes producing a single D meson in units of 10^{-5} , upper limits are at 90% CL. The latest version is available at: <http://hfag.phys.ntu.edu.tw/b2charm/00208.html>

Mode	PDG 2008	Belle	BABAR	CDF	Average
$D^0\bar{K}^{*0}(892)[K^-\pi^+]$			$3.80 \pm 0.60 \pm 0.40$		3.80 ± 0.72

Table 112: Branching fractions of miscellaneous modes producing charmed particles in units of 10^{-3} , upper limits are at 90% CL. The latest version is available at: <http://hfag.phys.ntu.edu.tw/b2charm/00300.html>

Mode	PDG 2008	Belle	BABAR	CDF	Average
$\mathcal{B}(B \rightarrow D^0\bar{D}^0\pi^0K)$		$0.13 \pm 0.03 \pm_{0.04}^{0.02}$			0.13 ± 0.04
$\mathcal{B}(\bar{\Lambda}_b^0 \rightarrow J/\psi(1S)\bar{\Lambda})$				$0.47 \pm 0.21 \pm 0.19$	0.47 ± 0.28
$\mathcal{B}(\bar{D}^0 \rightarrow D^{*0}(2007)D^-)$			$0.63 \pm 0.14 \pm 0.08 \pm 0.06$		0.63 ± 0.17
$\mathcal{B}(\bar{B}_s^0 \rightarrow J/\psi(1S)\phi(1020))$				$0.93 \pm 0.28 \pm 0.17$	0.93 ± 0.33

Table 113: Product branching fractions of miscellaneous modes producing charmed particles in units of 10^{-5} , upper limits are at 90% CL. The latest version is available at: <http://hfag.phys.ntu.edu.tw/b2charm/00300.html>

Mode	PDG 2008	Belle	BABAR	CDF	Average
$\mathcal{B}(B \rightarrow KY(3940)[\omega(782)J/\psi(1S)])$		$7.1 \pm 1.3 \pm 3.1$			7.1 ± 3.4

Table 114: Ratios of branching fractions of miscellaneous modes producing charmed particles in units of 10^0 , upper limits are at 90% CL. The latest version is available at: <http://hfag.phys.ntu.edu.tw/b2charm/00300.html>

Mode	PDG 2008	Belle	BABAR	CDF	Average
$\frac{\mathcal{B}(\overline{B}_s^0 \rightarrow D_s^+ K^-)}{\mathcal{B}(\overline{B}_s^0 \rightarrow D_s^+ \pi^-)}$				$0.107 \pm 0.019 \pm 0.008$	0.11 ± 0.02
$\frac{\mathcal{B}(\overline{B}_s^0 \rightarrow \psi(2S)\phi(1020))}{\mathcal{B}(\overline{B}_s^0 \rightarrow J/\psi(1S)\phi(1020))}$				$0.52 \pm 0.13 \pm 0.07$	0.52 ± 0.15
$\frac{\mathcal{B}(\overline{B}_s^0 \rightarrow D_s^+ \pi^+ \pi^- \pi^-)}{\mathcal{B}(\overline{B}_s^0 \rightarrow D^+ \pi^+ \pi^- \pi^-)}$				$1.05 \pm 0.10 \pm 0.22$	1.05 ± 0.24
$\frac{\mathcal{B}(\overline{B}_s^0 \rightarrow D_s^+ \pi^-)}{\mathcal{B}(\overline{B}_s^0 \rightarrow D^+ \pi^-)}$				$1.13 \pm 0.08 \pm 0.05 \pm 0.15$	1.13 ± 0.18
$\frac{\mathcal{B}(\overline{B}_s^0 \rightarrow D_s^- D_s^+)}{\mathcal{B}(\overline{B}_s^0 \rightarrow D_s^- D^+)}$				$1.67 \pm 0.41 \pm 0.12 \pm 0.46$	1.67 ± 0.63
$\frac{\mathcal{B}(\overline{\Lambda}_b^0 \rightarrow \Lambda_c^- \pi^+)}{\mathcal{B}(\overline{B}_s^0 \rightarrow D^+ \pi^-)}$				$3.30 \pm 0.30 \pm 0.40 \pm 1.10$	3.3 ± 1.2
$\frac{\mathcal{B}(\overline{\Lambda}_b^0 \rightarrow \Lambda_c^- \mu^+ \nu_\mu)}{\mathcal{B}(\overline{\Lambda}_b^0 \rightarrow \Lambda_c^- \pi^+)}$				$20.00 \pm 3.00 \pm 1.20 \pm_{2.20}^{0.90}$	$20.0 \pm_{3.9}^{3.4}$

Table 115: Miscellaneous quantities of miscellaneous modes producing charmed particles in units of 10^0 , upper limits are at 90% CL. The latest version is available at: <http://hfag.phys.ntu.edu.tw/b2charm/00300.html>

Mode	PDG 2008	Belle	BABAR	CDF	Average
$\delta_{\parallel}(B \rightarrow J/\psi(1S)K^*)$		$-2.887 \pm 0.090 \pm 0.008$	$-2.93 \pm 0.08 \pm 0.04$		-2.91 ± 0.06
$\delta_{\parallel}(B \rightarrow \psi(2S)K^*)$			$-2.80 \pm 0.40 \pm 0.10$		-2.80 ± 0.41
$\delta_{\parallel}(B \rightarrow \chi_{c1}(1P)K^*)$			$0.00 \pm 0.30 \pm 0.10$		0.00 ± 0.32
$ \mathcal{A}_{\perp} ^2(B \rightarrow \chi_{c1}(1P)K^*)$			$0.03 \pm 0.04 \pm 0.02$		0.03 ± 0.04
$ \mathcal{A}_{\parallel} ^2(B \rightarrow \chi_{c1}(1P)K^*)$			$0.20 \pm 0.07 \pm 0.04$		0.20 ± 0.08
$ \mathcal{A}_{\perp} ^2(B \rightarrow J/\psi(1S)K^*)$		$0.195 \pm 0.012 \pm 0.008$	$0.233 \pm 0.010 \pm 0.005$		0.219 ± 0.009
$ \mathcal{A}_{\parallel} ^2(B \rightarrow J/\psi(1S)K^*)$		$0.231 \pm 0.012 \pm 0.008$	$0.211 \pm 0.010 \pm 0.006$		0.219 ± 0.009
$ \mathcal{A}_{\parallel} ^2(B \rightarrow \psi(2S)K^*)$			$0.22 \pm 0.06 \pm 0.02$		0.22 ± 0.06
$ \mathcal{A}_{\perp} ^2(B \rightarrow \psi(2S)K^*)$			$0.30 \pm 0.06 \pm 0.02$		0.30 ± 0.06
$ \mathcal{A}_0 ^2(B \rightarrow \psi(2S)K^*)$			$0.48 \pm 0.05 \pm 0.02$		0.48 ± 0.05
$ \mathcal{A}_0 ^2(B \rightarrow J/\psi(1S)K^*)$		$0.574 \pm 0.012 \pm 0.009$	$0.556 \pm 0.009 \pm 0.010$		0.56 ± 0.01
$ \mathcal{A}_0 ^2(B \rightarrow \chi_{c1}(1P)K^*)$			$0.77 \pm 0.07 \pm 0.04$		0.77 ± 0.08
$\delta_{\perp}(B \rightarrow \psi(2S)K^*)$			$2.80 \pm 0.30 \pm 0.10$		2.80 ± 0.32
$\delta_{\perp}(B \rightarrow J/\psi(1S)K^*)$		$2.938 \pm 0.064 \pm 0.010$	$2.91 \pm 0.05 \pm 0.03$		2.92 ± 0.04

7 B decays to charmless final states

The aim of this section is to provide the branching fractions and the partial rate asymmetries (A_{CP}) of charmless B decays. The asymmetry is defined as $A_{CP} = \frac{N_{\bar{B}} - N_B}{N_{\bar{B}} + N_B}$, where $N_{\bar{B}}$ and N_B are respectively number of \bar{B}^0/B^- and B^0/B^+ decaying into a specific final state. Four different B decay categories are considered: charmless mesonic, baryonic, radiative and leptonic. Measurements supported with written documents are accepted in the averages; written documents could be journal papers, conference contributed papers, preprints or conference proceedings. Results from A_{CP} measurements obtained from time dependent analyses are listed and described in Sec. 4. Measurements of charmful baryonic B decays, which were included in our previous averages [4], are now shown in Section 7, which deals with B decays to charm.

So far all branching fractions assume equal production of charged and neutral B pairs. The best measurements to date show that this is still a good approximation (see Sec. 3). For branching fractions, we provide either averages or the most stringent 90% confidence level upper limits. If one or more experiments have measurements with $>4\sigma$ for a decay channel, all available central values for that channel are used in the averaging. We also give central values and errors for cases where the significance of the average value is at least 3σ , even if no single measurement is above 4σ . Since a few decay modes are sensitive to the contribution of new physics and the current experimental upper limits are not far from the Standard Model expectation, we provide the combined upper limits or averages in these cases. Their upper limits can be estimated assuming that the errors are Gaussian. For A_{CP} we provide averages in all cases.

Our averaging is performed by maximizing the likelihood, $\mathcal{L} = \prod_i \mathcal{P}_i(x)$, where \mathcal{P}_i is the probability density function (PDF) of the i th measurement, and x is the branching fraction or A_{CP} . The PDF is modeled by an asymmetric Gaussian function with the measured central value as its mean and the quadratic sum of the statistical and systematic errors as the standard deviations. The experimental uncertainties are considered to be uncorrelated with each other when the averaging is performed. No error scaling is applied when the fit χ^2 is greater than 1 since we believe that tends to overestimate the errors except in cases of extreme disagreement (we have no such cases). One exception to consider the correlated systematic errors is the inclusive $B \rightarrow X_s \gamma$ mode, which is sensitive to physics beyond the Standard Model. In this update, we have included new measurements from both Belle and BaBar to perform the average. The detail is described in Sec. 7.3.

At present, we have measurements of about 400 decay modes, reported in more than 200 papers. Because the number of references is so large, we do not include them with the tables shown here but the full set of references is available quickly from active gifs at the “Winter 2010” link on the rare web page: <http://www.slac.stanford.edu/xorg/hfag/rare/index.html>. Finally many new measurements involving scalar and tensor mesons are included for the first time.

7.1 Mesonic charmless decays

Table 116: Branching fractions (BF) of charmless mesonic B^+ decays with kaons (in units of $\times 10^6$). Upper limits are at 90% CL. Values in red (blue) are new published (preliminary) results since PDG2008 [as of March 12, 2010].

RPP#	Mode	PDG2008 Avg.	BABAR	Belle	CLEO	CDF	New avg.
207	$K^0\pi^+$	23.1 ± 1.0	$23.9 \pm 1.1 \pm 1.0$	$22.8^{+0.8}_{-0.7} \pm 1.3$	$18.8^{+3.7+2.1}_{-3.3-1.8}$		23.1 ± 1.0
208	$K^+\pi^0$	12.9 ± 0.6	$13.6 \pm 0.6 \pm 0.7$	$12.4 \pm 0.5 \pm 0.6$	$12.9^{+2.4+1.2}_{-2.2-1.1}$		12.9 ± 0.6
209	$\eta'K^+$	70.2 ± 2.5	$71.5 \pm 1.3 \pm 3.2$	$69.2 \pm 2.2 \pm 3.7$	$80^{+10}_{-9} \pm 7$		71.1 ± 2.6
210	$\eta'K^{*+}$	4.9 ± 2.0	$4.9^{+1.9}_{-1.7} \pm 0.8$	< 2.9	$11.1^{+12.7}_{-8.0}$		$4.9^{+2.1}_{-1.9}$
211	ηK^+	2.7 ± 0.9	$2.94^{+0.39}_{-0.34} \pm 0.21$	$1.9 \pm 0.3^{+0.2}_{-0.1}$	$2.2^{+2.8}_{-2.2}$		2.36 ± 0.27
212	ηK^{*+}	19.3 ± 1.6	$18.9 \pm 1.8 \pm 1.3$	$19.3^{+2.0}_{-1.9} \pm 1.5$	$26.4^{+9.6}_{-8.2} \pm 3.3$		19.3 ± 1.6
213	$\eta K_0^*(1430)^+$	18 ± 4	$15.8 \pm 2.2 \pm 2.2$				15.8 ± 3.1
214	$\eta K_2^*(1430)^+$	9.1 ± 3.0	$9.1 \pm 2.7 \pm 1.4$				9.1 ± 3.0
–	$\eta(1295)K^+\dagger$	New	< 4.0				< 4.0
–	$\eta(1405)K^+\dagger$	New	< 1.2				< 1.2
–	$\eta(1475)K^+\dagger$	New	$13.8^{+1.8+1.0}_{-1.7-0.6}$				$13.8^{+2.1}_{-1.8}$
215	ωK^+	6.7 ± 0.8	$6.3 \pm 0.5 \pm 0.3$	$8.1 \pm 0.6 \pm 0.6$	$3.2^{+2.4}_{-1.9} \pm 0.8$		6.7 ± 0.5
216	ωK^{*+}	< 3.4	< 7.4		< 87		< 7.4
–	$\omega K_0^*(1430)^+$	New	$24.0 \pm 2.6 \pm 4.4$				24.0 ± 5.1
–	$\omega K_2^*(1430)^+$	New	$21.5 \pm 3.6 \pm 2.4$				21.5 ± 4.3
217	$a_0(980)^+K^0\dagger$	< 3.9	< 3.9				< 3.9
218	$a_0(980)^0K^+\dagger$	< 2.5	< 2.5				< 2.5
219	$K^{*0}\pi^+$	10.9 ± 1.8	$10.8 \pm 0.6^{+1.2}_{-1.4}$	$9.7 \pm 0.6^{+0.8}_{-0.9}$	$7.6^{+3.5}_{-3.0} \pm 1.6$		$9.9^{+0.8}_{-0.9}$
220	$K^{*+}\pi^0$	6.9 ± 2.4	$6.9 \pm 2.0 \pm 1.3$		$7.1^{+11.4}_{-7.1} \pm 1.0$		6.9 ± 2.3
221	$K^+\pi^+\pi^-$	55 ± 7	$54.4 \pm 1.1 \pm 4.6$	$48.8 \pm 1.1 \pm 3.6$			51.0 ± 3.0
222	$K^+\pi^+\pi^- (NR)$	6^{+6}_{-4}	$9.3 \pm 1.0^{+6.8}_{-1.2}$	$16.9 \pm 1.3^{+1.7}_{-1.6}$	< 28		16.3 ± 2.0
223	$f_0(980)K^+\dagger$	$9.2^{+0.8}_{-1.1}$	$10.3 \pm 0.5^{+2.0}_{-1.3}$	$8.8 \pm 0.8^{+0.9}_{-1.8}$			9.5 ± 0.9
224	$f_2(1270)^0K^+$	$1.3^{+0.4}_{-0.5}$	$0.88 \pm 0.26^{+0.26}_{-0.21}$	$1.33 \pm 0.30^{+0.23}_{-0.34}$			$1.06^{+0.28}_{-0.29}$
225	$f_0(1370)^0K^+\dagger$	< 10.7	< 10.7				< 10.7
226	$\rho^0(1450)K^+$	< 11.7	< 11.7				< 11.7
227	$f_0(1500)K^+\dagger$	< 4.4	$0.73 \pm 0.21 \pm 0.47$				0.73 ± 0.52
228	$f_2'(1525)K^+\dagger$	< 3.4	< 3.4	< 4.9			< 3.4
229	ρ^0K^+	4.2 ± 0.5	$3.56 \pm 0.45^{+0.57}_{-0.46}$	$3.89 \pm 0.47^{+0.43}_{-0.41}$	$8.4^{+4.0}_{-3.4} \pm 1.8$		$3.81^{+0.48}_{-0.46}$
230	$K_0^*(1430)^0\pi^+$	47 ± 5	$32.0 \pm 1.2^{+10.8}_{-6.0}$	$51.6 \pm 1.7^{+7.0}_{-7.4}$			$45.2^{+6.2}_{-6.3}$
231	$K_2^*(1430)^0\pi^+$	< 6.9	$5.6 \pm 1.2^{+1.8}_{-0.8}$	< 6.9			$5.6^{+2.2}_{-1.4}$
232	$K^*(1410)^0\pi^+$	< 45		< 45			< 45
233	$K^*(1680)^0\pi^+$	< 12	< 15	< 12			< 12
–	$K_1(1270)^0\pi^+$	New	< 40				< 40
–	$K_1(1400)^0\pi^+$	New	< 39				< 39
–	$f_1(1285)K^+$	New	< 2.0				< 2.0
–	$f_1(1420)K^+\dagger$	New	< 2.9				< 2.9
234	$K^-\pi^+\pi^+$	< 1.8	< 0.95	< 4.5			< 0.95
237	$K^0\pi^+\pi^0$	< 66			< 66		< 66
238	ρ^+K^0	8.0 ± 1.5	$8.0^{+1.4}_{-1.3} \pm 0.6$		< 48		$8.0^{+1.5}_{-1.4}$
239	$K^{*+}\pi^+\pi^-$	75 ± 10	$75.3 \pm 6.0 \pm 8.1$				75.3 ± 10.1

†Product BF - daughter BF taken to be 100%

Table 117: Branching Fractions (BF) of charmless mesonic B^+ decays with kaons - part 2 (in units of 10^{-6}). Upper limits are at 90% CL. Values in red (blue) are new published (preliminary) results since PDG2008 [as of March 12, 2010].

RPP#	Mode	PDG2008 Avg.	BABAR	Belle	CLEO	CDF	New avg.
240	$K^{*+}\rho^0$	< 6.1	< 6.1		< 74		< 6.1
241	$f_0(980)K^{*+} \dagger$	5.2 ± 1.3	$5.2 \pm 1.2 \pm 0.5$				5.2 ± 1.3
242	$a_1^+ K^0$	35 ± 7	$34.9 \pm 5.0 \pm 4.4$				34.9 ± 6.7
243	$K^{*0}\rho^+$	9.2 ± 1.5	$9.6 \pm 1.7 \pm 1.5$	$8.9 \pm 1.7 \pm 1.2$			9.2 ± 1.5
244	$K^{*+}\bar{K}^{*0}$	< 71	$1.2 \pm 0.5 \pm 0.1$		< 71		1.2 ± 0.5
247	$K^+\bar{K}^0$	1.36 ± 0.27	$1.61 \pm 0.44 \pm 0.09$	$1.22^{+0.33+0.13}_{-0.28-0.16}$	< 3.3		$1.36^{+0.29}_{-0.27}$
248	$\bar{K}^0 K^+\pi^0$	< 24			< 24		< 24
249	$K^+K_S K_S$	11.5 ± 1.3	$10.7 \pm 1.2 \pm 1.0$	$13.4 \pm 1.9 \pm 1.5$			11.5 ± 1.3
250	$K_S K_S \pi^+$	< 3.2	< 0.51	< 3.2			< 0.51
251	$K^+K^-\pi^+$	5.0 ± 0.7	$5.0 \pm 0.5 \pm 0.5$	< 13			5.0 ± 0.7
253	$\bar{K}^{*0} K^+$	< 1.1	< 1.1	$0.68 \pm 0.16 \pm 0.10$	< 5.3		0.68 ± 0.19
254	$\bar{K}_0^*(1430)^0 K^+$	< 2.2	< 2.2				< 2.2
–	$\bar{K}_2^*(1430)^0 K^+$	New		< 1.1			< 1.1
255	$K^+K^+\pi^-$	< 1.3	< 0.16	< 2.4			< 0.16
257	$b_1^0 K^+ \dagger$	9.1 ± 2.0	$9.1 \pm 1.7 \pm 1.0$				9.1 ± 2.0
–	$b_1^+ K^0 \dagger$	New	$9.6 \pm 1.7 \pm 0.9$				9.6 ± 1.9
259	$K^{*+}\pi^+K^-$	< 11.8	< 11.8				< 11.8
260	$K^{*+}K^+\pi^-$	< 6.1	< 6.1				< 6.1
261	$K^+K^-K^+$	33.7 ± 2.2	$33.5 \pm 0.9 \pm 1.6$	$30.6 \pm 1.2 \pm 2.3$			32.5 ± 1.5
262	ϕK^+	8.3 ± 0.7	$8.4 \pm 0.7 \pm 0.7$	$9.60 \pm 0.92^{+1.05}_{-0.84}$	$5.5^{+2.1}_{-1.8} \pm 0.6$	$7.6 \pm 1.3 \pm 0.6$	8.30 ± 0.65
264	$a_2(1320)K^+ \dagger$	< 1.1		< 1.1			< 1.1
267	$\phi(1680)K^+ \dagger$	< 0.8		< 0.8			< 0.8
270	$K^{*+}K^+K^-$	36 ± 5	$36.2 \pm 3.3 \pm 3.6$				36.2 ± 4.9
271	ϕK^{*+}	10.5 ± 1.5	$11.2 \pm 1.0 \pm 0.9$	$6.7^{+2.1+0.7}_{-1.9-1.0}$	$10.6^{+6.4+1.8}_{-4.9-1.6}$		10.0 ± 1.1
–	$\phi K_1(1270)^+$	New	$6.1 \pm 1.6 \pm 1.1$				6.1 ± 1.9
272	$\phi K_1(1400)^+$	< 1100	< 3.2				< 3.2
–	$\phi K_0^*(1430)^+$	New	$7.0 \pm 1.3 \pm 0.9$				7.0 ± 1.6
273	$\phi K_2^*(1430)^+$	< 3400	$8.4 \pm 1.8 \pm 1.0$				8.4 ± 2.1
–	$\phi K^*(1410)^+$	New	< 4.3				< 4.3
–	$\phi K_2(1770)^+$	New	< 15				< 15
–	$\phi K_2(1820)^+$	New	< 16				< 16
–	$\phi(1680)K^+ \dagger$	New	< 3.4				< 3.4
–	$a_1^+ K^{*0}$	New	< 3.3				< 3.3
274	$\phi\phi K^+ \S$	$4.9^{+2.4}_{-2.2}$	$7.5 \pm 1.0 \pm 0.7$	$3.2^{+0.6}_{-0.5} \pm 0.3$			4.2 ± 0.6
275	$\eta'\eta'K^+$	< 25	< 25				< 25
–	$K^+\omega\phi$	New		< 1.9			< 1.9
–	$K^+X(1812)\dagger$	New		< 0.32			< 0.32
–	$b_1^0 K^{*+} \dagger$	New	< 6.7				< 6.7
–	$b_1^+ K^{*0} \dagger$	New	< 5.9				< 5.9

\dagger Product BF - daughter BF taken to be 100%; $\S M_{\phi\phi} < 2.85 \text{ GeV}/c^2$

Table 118: Branching Fractions (BF) of charmless mesonic B^+ decays without kaons (in units of 10^{-6}). Upper limits are at 90% CL. Values in red (blue) are new published (preliminary) results since PDG2008 [as of March 12, 2010].

RPP#	Mode	PDG2008 Avg.	BABAR	Belle	CLEO	CDF	New avg.
292	$\pi^+\pi^0$	5.7 ± 0.5	$5.02 \pm 0.46 \pm 0.29$	$6.5 \pm 0.4^{+0.4}_{-0.5}$	$4.6^{+1.8+0.6}_{-1.6-0.7}$		$5.59^{+0.41}_{-0.40}$
293	$\pi^+\pi^+\pi^-$	16.2 ± 1.5	$15.2 \pm 0.6 \pm 1.3$				15.2 ± 1.4
294	$\rho^0\pi^+$	8.7 ± 1.1	$8.1 \pm 0.7^{+1.3}_{-1.6}$	$8.0^{+2.3}_{-2.0} \pm 0.7$	$10.4^{+3.3}_{-3.4} \pm 2.1$		$8.3^{+1.2}_{-1.3}$
295	$f_0(980)\pi^+ \dagger$	< 3.0	< 1.5				< 1.5
296	$f_2(1270)\pi^+$	8.2 ± 2.5	$1.57 \pm 0.42^{+0.55}_{-0.25}$				$1.57^{+0.69}_{-0.49}$
297	$\rho(1450)^0\pi^+ \dagger$	< 2.3	$1.4 \pm 0.4^{+0.5}_{-0.8}$				$1.4^{+0.6}_{-0.9}$
298	$f_0(1370)\pi^+ \dagger$	< 3.0	< 4.0				< 4.0
300	$\pi^+\pi^-\pi^+(NR)$	< 4.6	$5.3 \pm 0.7^{+1.3}_{-0.8}$				$5.3^{+1.5}_{-1.1}$
302	$\rho^+\pi^0$	10.9 ± 1.4	$10.2 \pm 1.4 \pm 0.9$	$13.2 \pm 2.3^{+1.4}_{-1.9}$	< 43		$10.9^{+1.4}_{-1.5}$
304	$\rho^+\rho^0$	18 ± 4	$23.7 \pm 1.4 \pm 1.4$	$31.7 \pm 7.1^{+3.8}_{-6.7}$			$24.0^{+1.9}_{-2.0}$
305	$f_0(980)\rho^+ \dagger$	< 1.9	< 2.0				< 2.0
306	$a_1^+\pi^0$	26 ± 7	$26.4 \pm 5.4 \pm 4.1$				26.4 ± 6.8
307	$a_1^0\pi^+$	20 ± 6	$20.4 \pm 4.7 \pm 3.4$				20.4 ± 5.8
308	$b_1^0\pi^+ \dagger$	6.7 ± 2.0	$6.7 \pm 1.7 \pm 1.0$				6.7 ± 2.0
–	$b_1^+\pi^0 \dagger$	New	< 3.3				< 3.3
309	$\omega\pi^+$	6.9 ± 0.5	$6.7 \pm 0.5 \pm 0.4$	$6.9 \pm 0.6 \pm 0.5$	$11.3^{+3.3}_{-2.9} \pm 1.4$		6.9 ± 0.5
310	$\omega\rho^+$	$10.6^{+2.6}_{-2.3}$	$15.9 \pm 1.6 \pm 1.4$		< 61		15.9 ± 2.1
311	$\eta\pi^+$	4.4 ± 0.4	$4.00 \pm 0.40 \pm 0.24$	$4.2 \pm 0.4 \pm 0.2$	$1.2^{+2.8}_{-1.2}$		4.07 ± 0.32
312	$\eta'\pi^+$	2.7 ± 1.0	$3.5 \pm 0.6 \pm 0.2$	$1.8^{+0.7}_{-0.6} \pm 0.1$	$1.0^{+5.8}_{-1.0}$		$2.7^{+0.5}_{-0.4}$
313	$\eta'\rho^+$	$8.7^{+3.9}_{-3.1}$	$8.7^{+3.1+2.3}_{-2.8-1.3}$	< 5.8	$11.2^{+11.9}_{-7.0}$		$9.1^{+3.7}_{-2.8}$
314	$\eta\rho^+$	5.4 ± 1.9	$9.9 \pm 1.2 \pm 0.8$	$4.1^{+1.4}_{-1.3} \pm 0.4$	$4.8^{+5.2}_{-3.8}$		6.9 ± 1.0
315	$\phi\pi^+$	< 0.24	< 0.24		< 5		< 0.24
316	$\phi\rho^+$	< 16	< 3.0		< 16		< 3.0
317	$a_0(980)^0\pi^+ \dagger$	< 5.8	< 5.8				< 5.8
318	$a_0(980)^+\pi^0 \dagger$	< 1.4	< 1.4				< 1.4
–	$b_1^0\rho^+ \dagger$	New	< 3.3				< 3.3
–	$b_1^+\rho^0 \dagger$	New	< 5.2				< 5.2

†Product BF - daughter BF taken to be 100%;

Table 119: Branching fractions of charmless mesonic B^0 decays with kaons (in units of 10^{-6}). Upper limits are at 90% CL. Values in red (blue) are new published (preliminary) results since PDG2008 [as of March 12, 2010].

RPP#	Mode	PDG2008 Avg.	BABAR	Belle	CLEO	CDF	New avg.
198	$K^+\pi^-$	19.5 ± 0.6	$19.1 \pm 0.6 \pm 0.6$	$19.9 \pm 0.4 \pm 0.8$	$18.0^{+2.3+1.2}_{-2.1-0.9}$		19.4 ± 0.6
199	$K^0\pi^0$	9.8 ± 0.6	$10.1 \pm 0.6 \pm 0.4$	$8.7 \pm 0.5 \pm 0.6$	$12.8^{+4.0+1.7}_{-3.3-1.4}$		9.5 ± 0.5
200	$\eta'K^0$	65 ± 4	$68.5 \pm 2.2 \pm 3.1$	$58.9^{+3.6}_{-3.5} \pm 4.3$	$89^{+13}_{-16} \pm 9$		66.1 ± 3.1
201	$\eta'K^{*0}$	3.8 ± 1.2	$3.8 \pm 1.1 \pm 0.5$	< 2.6	$7.8^{+7.7}_{-5.7}$		3.8 ± 1.2
202	ηK^0	< 1.9	$1.15^{+0.43}_{-0.38} \pm 0.09$	$1.1 \pm 0.4 \pm 0.1$	$0.0^{+3.0}_{-0.0}$		$1.12^{+0.30}_{-0.28}$
203	ηK^{*0}	15.9 ± 1.0	$16.5 \pm 1.1 \pm 0.8$	$15.2 \pm 1.2 \pm 1.0$	$13.8^{+5.5}_{-4.6} \pm 1.6$		15.9 ± 1.0
204	$\eta K_0^*(1430)^0$	11.0 ± 2.2	$9.6 \pm 1.4 \pm 1.3$				9.6 ± 1.9
205	$\eta K_2^*(1430)^0$	9.6 ± 2.1	$9.6 \pm 1.8 \pm 1.1$				9.6 ± 2.1
206	ωK^0	5.0 ± 0.6	$5.4 \pm 0.8 \pm 0.3$	$4.4^{+0.8}_{-0.7} \pm 0.4$	$10.0^{+5.4}_{-4.2} \pm 1.4$		5.0 ± 0.6
207	$a_0(980)^0 K^0 \dagger$	< 7.8	< 7.8				< 7.8
–	$b_1^0 K^0 \dagger$	New	< 7.8				< 7.8
208	$a_0(980)^- K^+ \dagger$	< 1.9	< 1.9				< 1.9
245	$b_1^- K^+ \dagger$	7.4 ± 1.4	$7.4 \pm 1.0 \pm 1.0$				7.4 ± 1.4
209	$a_0(1450)^- K^+ \dagger$	< 3.1	< 3.1				< 3.1
–	$\omega K^+ \pi^- (NR)^1$	New		$5.1 \pm 0.7 \pm 0.7$			5.1 ± 1.0
211	ωK^{*0}	< 4.2	$2.2 \pm 0.6 \pm 0.2$	$1.8 \pm 0.7^{+0.3}_{-0.2}$	< 23		2.0 ± 0.5
–	$\omega K_0^*(1430)^0$	New	$16.0 \pm 1.6 \pm 3.0$				16.0 ± 3.4
–	$\omega K_2^*(1430)^0$	New	$10.1 \pm 2.0 \pm 1.1$				10.1 ± 2.3
212	K^+K^-	< 0.41	$0.04 \pm 0.15 \pm 0.08$	$0.09^{+0.18}_{-0.13} \pm 0.01$	< 0.8	$0.39 \pm 0.16 \pm 0.12 \ddagger$	$0.15^{+0.11}_{-0.10}$
213	$K^0\bar{K}^0$	$0.96^{+0.20}_{-0.18}$	$1.08 \pm 0.28 \pm 0.11$	$0.87^{+0.25}_{-0.20} \pm 0.09$	< 3.3		$0.96^{+0.21}_{-0.19}$
214	$K_S K_S K_S$	$6.2^{+1.2}_{-1.1}$	$6.9^{+0.9}_{-0.8} \pm 0.6$	$4.2^{+1.6}_{-1.3} \pm 0.8$			6.2 ± 0.9
215	$K_S K_S K_L$	< 16	$< 16^2$				$< 16^2$
216	$K^+ \pi^- \pi^0$	37 ± 5	$35.7^{+2.6}_{-1.5} \pm 2.2$	$36.6^{+4.2}_{-4.3} \pm 3.0$	< 40		$35.9^{+2.9}_{-2.4}$
217	$\rho^- K^+$	8.5 ± 2.8	$8.0^{+0.8}_{-1.3} \pm 0.6$	$15.1^{+3.4+2.4}_{-3.3-2.6}$	$16^{+8}_{-6} \pm 3$		$8.6^{+0.9}_{-1.1}$
218	$K^+ \pi^- \pi^0 (NR)$	< 9.4	$4.4 \pm 0.9 \pm 0.5$	< 9.4			4.4 ± 1.0
–	$\rho(1450)^- K^+$	New	< 2.1				< 2.1
–	$\rho(1700)^- K^+$	New	< 1.1				< 1.1
–	$K_0^*(1430)^0 \pi^0$	New	$11.7^{+1.4+4.0}_{-1.3-3.6} \quad 3$				$11.7^{+4.2}_{-3.8}$
–	$K_2^*(1430)^0 \pi^0$	New	< 4.0				< 4.0
–	$K^*(1680)^0 \pi^0$	New	< 7.5				< 7.5
220	$K^0 \pi^+ \pi^-$	44.8 ± 2.6	$50.2 \pm 1.5 \pm 1.8$	$47.5 \pm 2.4 \pm 3.7$	$50^{+10}_{-9} \pm 7$		49.6 ± 2.0
221	$K^0 \pi^+ \pi^- (NR)$	19.9 ± 3.2	$11.1^{+2.5}_{-1.0} \pm 0.9$	$19.9 \pm 2.5^{+1.7}_{-2.0}$			14.7 ± 2.0
222	$\rho^0 K^0$	5.9 ± 0.9	$4.4 \pm 0.7 \pm 0.3$	$6.1 \pm 1.0^{+1.1}_{-1.2}$	< 39		4.7 ± 0.7
224	$K^{*+} \pi^-$	9.8 ± 1.3	$8.3^{+0.9}_{-0.8} \pm 0.8$	$8.4 \pm 1.1^{+1.0}_{-0.9}$	$16^{+6}_{-5} \pm 2$		8.6 ± 0.9
225	$K_0^*(1430)^+ \pi^-$	50^{+8}_{-9}	$29.9^{+2.3}_{-1.7} \pm 3.6$	$49.7 \pm 3.8^{+6.8}_{-8.2}$			$33.5^{+3.9}_{-3.8}$
227	$K^*(1410)^+ \pi^- \dagger$	< 86		< 86			< 86
228	$K^*(1680)^+ \pi^-$	< 10.1	< 25	< 10.1			< 10.1
230	$f_0(980)K^0 \dagger$	$7.6^{+1.9}_{-2.1}$	$6.9 \pm 0.8 \pm 0.6$	$7.6 \pm 1.7^{+0.9}_{-1.3}$			7.0 ± 0.9
231	$f_2(1270)^0 K^0$	< 2.5	$2.7^{+1.0}_{-0.8} \pm 0.9$	$< 2.5 \dagger$			$2.7^{+1.3}_{-1.2}$

\dagger Product BF - daughter BF taken to be 100%, \ddagger Relative BF converted to absolute BF $^{10.755} < M(K\pi) < 1.250 \text{ GeV}/c^2$. 2 Excludes $M(K_S K_S)$ regions [3.400,3.429] and [3.540,3.585] and $M(K_S K_L) < 1.049 \text{ GeV}/c^2$ 3 Includes $K\pi$ S-wave contribution and uncorrected for $K^*(1430)$ BF

Table 120: Branching fractions of charmless mesonic B^0 decays with kaons - part 2 (in units of 10^{-6}). Upper limits are at 90% CL. Values in red (blue) are new published (preliminary) results since PDG2008 [as of March 12, 2010].

RPP#	Mode	PDG2008 Avg.	BABAR	Belle	CLEO	CDF	New avg.
232	$K^{*0}\pi^0$	< 3.5	$3.6 \pm 0.7 \pm 0.4$	$0.4^{+1.9}_{-1.7} \pm 0.1$	$0.0^{+1.3+0.5}_{-0.0-0.0}$		2.4 ± 0.7
233	$K_2^*(1430)^+\pi^-$	< 6.3	< 16.2	< 6.3			< 6.3
–	$K_1(1270)^+\pi^-$	New	17^{+8}_{-11}				17^{+8}_{-11}
–	$K_1(1400)^+\pi^-$	New	17^{+7}_{-9}				17^{+7}_{-9}
234	$K^0K^-\pi^+$	< 18	$6.4 \pm 1.4 \pm 0.6$	< 18	< 21		6.4 ± 1.5
235	$K^{*0}\bar{K}^0$	< 1.9	< 1.9				< 1.9
236	$K^+K^-\pi^0$	< 19			< 19		< 19
–	$K_S K_S \pi^0$	New	< 1.2				< 1.2
–	$K_S K_S \eta$	New	< 1.0				< 1.0
–	$K_S K_S \eta'$	New	< 2.0				< 2.0
237	$K^+K^-K^0$	24.7 ± 2.3	$23.8 \pm 2.0 \pm 1.6$	$28.3 \pm 3.3 \pm 4.0$			24.7 ± 2.3
238	ϕK^0	$8.6^{+1.3}_{-1.1}$	$8.4^{+1.5}_{-1.3} \pm 0.5$	$9.0^{+2.2}_{-1.8} \pm 0.7$	$5.4^{+3.7}_{-2.7} \pm 0.7$		$8.3^{+1.2}_{-1.0}$
239	$K^+\pi^-\pi^+\pi^-$	< 230		< 2.1 †			< 2.1
240	$K^{*0}\pi^+\pi^-$	54 ± 5	$54.5 \pm 2.9 \pm 4.3$	$4.5^{+1.1+0.9}_{-1.0-1.6} \pm 1$			8.0 ± 1.4
241	$K^{*0}\rho^0$	5.6 ± 1.6	$5.6 \pm 0.9 \pm 1.3$	$2.1^{+0.8+0.9}_{-0.7-0.5}$	< 34		3.4 ± 1.0
242	$f_0(980)K^{*0} \dagger$	< 4.3	< 4.3	< 2.2			< 2.2
244	$a_1^- K^+$	16 ± 4	$16.3 \pm 2.9 \pm 2.3$				16.3 ± 3.7
246	$K^{*0}K^+K^-$	27.5 ± 2.6	$27.5 \pm 1.3 \pm 2.2$				27.5 ± 2.6
247	ϕK^{*0}	9.5 ± 0.8	$9.7 \pm 0.5 \pm 0.6$	$10.0^{+1.6+0.7}_{-1.5-0.8}$	$11.5^{+4.5+1.8}_{-3.7-1.7}$		9.8 ± 0.7
248	$K^{*0}\pi^+K^-$	4.6 ± 1.4	$4.6 \pm 1.1 \pm 0.8$	< 31.8			4.6 ± 1.4
249	$K^{*0}\bar{K}^{*0}$	$1.28^{+0.37}_{-0.32}$	$1.28^{+0.35}_{-0.30} \pm 0.11$	$0.26^{+0.33+0.10}_{-0.29-0.08}$	< 22		0.81 ± 0.23
–	$K_0^*(1430)^0\bar{K}_0^*(1430)^0$	New		< 8.4			< 8.4
–	$K_0^*(1430)^0\bar{K}^{*0}$	New		< 3.3			< 3.3
–	$K_0^*(1430)^0\pi^+K^-$	New		< 31.8			< 31.8
–	$K^+\pi^-\pi^+K^-$	New		< 72			< 72
250	$K^{*0}K^+\pi^-$	< 2.2	< 2.2	< 7.6			< 2.2
251	$K^{*0}K^{*0}$	< 0.41	< 0.41	< 0.2	< 37		< 0.2
–	$K_0^*(1430)^0K_0^*(1430)^0$	New		< 4.7			< 4.7
–	$K_0^*(1430)^0K^{*0}$	New		< 1.7			< 1.7
–	$K^+\pi^-K^+\pi^-$	New		< 6.0			< 6.0
252	$K^{*+}\rho^-$	< 12	< 12				< 12
253	$K^{*+}K^{*-}$	< 141	< 2.0		< 141		< 2.0
258	$\phi K_0^*(1430)^0$	4.6 ± 0.9	$3.9 \pm 0.5 \pm 0.5$				3.9 ± 0.7
259	$\phi K^*(1680)^0$	< 3.5	< 3.5				< 3.5
260	$\phi K_3^*(1780)^0$	< 2.7	< 2.7				< 2.7
261	$\phi K_4^*(2045)^0$	< 15.3	< 15.3				< 15.3
263	$\phi K_2^*(1430)^0$	7.8 ± 1.3	$7.5 \pm 0.9 \pm 0.5$				7.5 ± 1.0
264	$\phi\phi K^0 \S$	$4.1^{+1.7}_{-1.4} \pm 0.4$	$4.1^{+1.7}_{-1.4} \pm 0.4$	$2.3^{+1.0}_{-0.7} \pm 0.2$			$2.8^{+0.9}_{-0.7}$
266	$\eta'\eta'K^0$	< 31	< 31				< 31
–	$\rho^0K^+\pi^-$	New		$2.8 \pm 0.5 \pm 0.5$ ²			2.8 ± 0.7
–	$f_0(980)K^+\pi^-$	New		$1.4 \pm 0.4^{+0.3}_{-0.4}$ ²			$1.4^{+0.5}_{-0.6}$
–	$b_1^- K^{*+} \dagger$	New	< 5.0				< 5.0
–	$b_1^0 K^{*0} \dagger$	New	< 8.0				< 8.0

†Product BF - daughter BF taken to be 100%, § $M_{\phi\phi} < 2.85 \text{ GeV}/c^2$ ‡ $0.55 < M(\pi\pi) < 1.42 \text{ GeV}/c^2$ and $0.75 < M(K\pi) < 1.20 \text{ GeV}/c^2$; ¹ $0.55 < M(\pi\pi) < 1.42 \text{ GeV}/c^2$; ² $0.75 < M(K\pi) < 1.20 \text{ GeV}/c^2$

Table 121: Branching fractions of charmless mesonic B^0 decays without kaons (in units of 10^{-6}). Upper limits are at 90% CL. Values in red (blue) are new published (preliminary) results since PDG2008 [as of March 12, 2010].

RPP#	Mode	PDG2008 Avg.	BABAR	Belle	CLEO	CDF	New avg.
284	$\pi^+\pi^-$	5.13 ± 0.24	$5.5 \pm 0.4 \pm 0.3$	$5.1 \pm 0.2 \pm 0.2$	$4.5^{+1.4+0.5}_{-1.2-0.4}$	$5.10 \pm 0.33 \pm 0.36 \ddagger$	5.16 ± 0.22
285	$\pi^0\pi^0$	1.62 ± 0.31	$1.83 \pm 0.21 \pm 0.13$	$1.1 \pm 0.3 \pm 0.1$	< 4.4		1.55 ± 0.19
286	$\eta\pi^0$	< 1.3	< 1.5	< 2.5	< 2.9		< 1.5
287	$\eta\eta$	< 1.8	< 1.0	< 2.0	< 18		< 1.0
288	$\eta'\pi^0$	$1.5^{+1.0}_{-0.8}$	$0.9 \pm 0.4 \pm 0.1$	$2.8 \pm 1.0 \pm 0.3$	$0.0^{+1.8}_{-0.0}$		1.2 ± 0.4
289	$\eta'\eta'$	< 2.4	< 1.7	< 6.5	< 47		< 1.7
290	$\eta'\eta$	< 1.7	< 1.2	< 4.5	< 27		< 1.2
291	$\eta'\rho^0$	< 1.3	< 3.7	< 1.3	< 12		< 1.3
292	$f_0(980)\eta' \dagger$	< 1.5	< 1.5				< 1.5
293	$\eta\rho^0$	< 1.5	< 1.5	< 1.9	< 10		< 1.5
294	$f_0(980)\eta \dagger$	< 1.6	< 0.4				< 0.4
295	$\omega\eta$	< 1.9	< 1.4		< 12		< 1.4
296	$\omega\eta'$	< 2.8	< 1.8	< 2.2	< 60		< 1.8
297	$\omega\rho^0$	< 1.5	< 1.6		< 11		< 1.6
298	$f_0(980)\omega \dagger$	< 1.5	< 1.5				< 1.5
299	$\omega\omega$	< 4.0	< 4.0		< 19		< 4.0
300	$\phi\pi^0$	< 0.28	< 0.28		< 5		< 0.28
301	$\phi\eta$	< 0.6	< 0.5		< 9		< 0.5
302	$\phi\eta'$	< 0.5	< 1.1	< 0.5	< 31		< 0.5
303	$\phi\rho^0$	< 13	< 0.33		< 13		< 0.33
—	$f_0(980)\phi \dagger$	New	< 0.38				< 0.38
304	$\omega\phi$	< 1.2	< 1.2		< 21		< 1.2
305	$\phi\phi$	< 1.5	< 0.2		< 12		< 0.2
306	$a_0^\mp(980)\pi^\pm \dagger$	< 3.1	< 3.1				< 3.1
307	$a_0^\mp(1450)\pi^\pm \dagger$	2.3	< 2.3				< 2.3
309	$\rho^0\pi^0$	1.8 ± 0.5	$1.4 \pm 0.6 \pm 0.3$	$3.0 \pm 0.5 \pm 0.7$	$1.6^{+2.0}_{-1.4} \pm 0.8$		2.0 ± 0.5
310	$\rho^\mp\pi^\pm$	22.8 ± 2.5	$22.6 \pm 1.8 \pm 2.2$	$22.6 \pm 1.1 \pm 4.4$	$27.6^{+8.4}_{-7.4} \pm 4.2$		23.0 ± 2.3
311	$\pi^+\pi^-\pi^+\pi^-$	< 230	< 21.1	< 19.3			< 19.3
312	$\rho^0\rho^0$	1.1 ± 0.4	$0.92 \pm 0.32 \pm 0.14$	$0.4 \pm 0.4^{+0.2}_{-0.3}$	< 18		$0.73^{+0.27}_{-0.28}$
—	$\rho^0\pi^+\pi^-(NR)$	New	< 8.7	< 12			< 8.7
—	$f_0(980)\pi^+\pi^-(NR)$	New		< 3.8			< 3.8
313	$f_0(980)\rho^0 \dagger$	< 0.53	< 0.34	< 0.3			< 0.3
314	$f_0(980)f_0(980) \dagger$	< 0.16	< 0.16	< 0.1			< 0.1
315	$a_1^\mp\pi^\pm$	33 ± 5	$33.2 \pm 3.8 \pm 3.0$	$29.8 \pm 3.2 \pm 4.6$			31.7 ± 3.7
316	$b_1^\mp\pi^\pm \dagger$	10.9 ± 1.5	$10.9 \pm 1.2 \pm 0.9$				10.9 ± 1.5
319	$\rho^+\rho^-$	24.2 ± 3.1	$25.5 \pm 2.1^{+3.6}_{-3.9}$	$22.8 \pm 3.8^{+2.3}_{-2.6}$			$24.2^{+3.1}_{-3.2}$
321	$\omega\pi^0$	< 1.2	< 0.5	< 2.0	< 5.5		< 0.5
323	$a_1^\pm\rho^\mp$	< 61	< 61				< 61
—	$b_1^0\pi^0 \dagger$	New	< 1.9				< 1.9
326	$a_1^\pm a_1^\mp$	< 2800	$47.3 \pm 10.5 \pm 6.3$				47.3 ± 12.2
—	$b_1^\pm\rho^\mp \dagger$	New	< 1.4				< 1.4
—	$b_1^0\rho^0 \dagger$	New	< 3.4				< 3.4

\dagger Product BF - daughter BF taken to be 100%, \ddagger Relative BF converted to absolute BF

Table 122: Relative branching fractions of $B^0 \rightarrow K^+K^-, K^+\pi^-, \pi^+\pi^-$. Values in red (blue) are new published (preliminary) result since PDG2008 [as of March 15, 2007].

RPP#	Mode	PDG2008 Avg.	CDF	DØ	New avg.
179	$\mathcal{B}(B^0 \rightarrow K^+K^-)/\mathcal{B}(B^0 \rightarrow K^+\pi^-)$		$0.020 \pm 0.008 \pm 0.006$		0.020 ± 0.010
229	$\mathcal{B}(B^0 \rightarrow \pi^+\pi^-)/\mathcal{B}(B^0 \rightarrow K^+\pi^-)$		$0.259 \pm 0.017 \pm 0.016$		0.259 ± 0.023

7.2 Radiative and leptonic decays

Table 123: Branching fractions of semileptonic and radiative B^+ decays (in units of 10^{-6}). Upper limits are at 90% CL. Values in red (blue) are new published (preliminary) results since PDG2008 [as of March 12, 2010].

RPP#	Mode	PDG2008 Avg.	BABAR	Belle	CLEO	CDF	New Avg.
276	$K^{*+}\gamma$	40.3 ± 2.6	$42.2 \pm 1.4 \pm 1.6$	$42.5 \pm 3.1 \pm 2.4$	$37.6^{+8.9}_{-8.3} \pm 2.8$		42.1 ± 1.8
277	$K_1^+(1270)\gamma$	43 ± 13		$43 \pm 9 \pm 9$			43 ± 12
278	$K^+\eta\gamma$	9.4 ± 1.1	$7.7 \pm 1.0 \pm 0.4$	$8.4^{+1.5}_{-1.2} \pm 0.9$			7.9 ± 0.9
279	$K^+\eta'\gamma$	< 4.2	$1.9^{+1.5}_{-1.2} \pm 0.1$	$3.6 \pm 1.2 \pm 0.4$			$2.9^{+1.0}_{-0.9}$
280	$K^+\phi\gamma$	3.5 ± 0.6	$3.5 \pm 0.6 \pm 0.4$	$2.34 \pm 0.29 \pm 0.23$			2.58 ± 0.33
281	$K^+\pi^-\pi^+\gamma$	27.6 ± 2.2	$29.5 \pm 1.3 \pm 2.0$ †	$25.0 \pm 1.8 \pm 2.2$ ‡			27.6 ± 1.8
282	$K^{*0}\pi^+\gamma$ §	20^{+7}_{-6}		$20^{+7}_{-6} \pm 2$			20^{+7}_{-6}
283	$K^+\rho^0\gamma$ §	< 20		< 20			< 20
284	$K^+\pi^-\pi^+\gamma$ (N.R.) §	< 9.2		< 9.2			< 9.2
285	$K^0\pi^+\pi^0\gamma$	46 ± 5	$45.6 \pm 4.2 \pm 3.1$ †				45.6 ± 5.2
286	$K_1^+(1400)\gamma$	< 15		< 15			< 15
287	$K_2^*(1430)^+\gamma$	14 ± 4	$14.5 \pm 4.0 \pm 1.5$				14.5 ± 4.3
289	$K_3^*(1780)^+\gamma$	< 39		< 39			< 39
291	$\rho^+\gamma$	$0.98^{+0.25}_{-0.24}$	$1.20^{+0.42}_{-0.37} \pm 0.20$	$0.87^{+0.29+0.09}_{-0.27-0.11}$	< 13		$0.98^{+0.25}_{-0.24}$
338	$p\bar{A}\gamma$	$2.5^{+0.5}_{-0.4}$		$2.45^{+0.44}_{-0.38} \pm 0.22$			$2.45^{+0.49}_{-0.44}$
342	$p\Sigma^0\gamma$	< 4.6		< 4.6			< 4.6
367	$\pi^+\ell^+\ell^-$	< 0.12	< 0.12	< 0.049			< 0.049
368	$\pi^+e^+e^-$	< 0.18	< 0.18	< 0.080			< 0.080
369	$\pi^+\mu^+\mu^-$	< 0.28	< 0.28	< 0.069			< 0.069
370	$\pi^+\nu\bar{\nu}$	< 100	< 100	< 170			< 100
371	$K^+\ell^+\ell^-$	$0.44^{+0.08}_{-0.07}$	$0.48 \pm 0.09 \pm 0.02$	$0.53^{+0.06}_{-0.05} \pm 0.03$			0.51 ± 0.05
372	$K^+e^+e^-$	0.49 ± 0.1	$0.51^{+0.12}_{-0.11} \pm 0.02$	$0.57^{+0.09}_{-0.08} \pm 0.03$	< 2.4		0.55 ± 0.07
373	$K^+\mu^+\mu^-$	$0.39^{+0.10}_{-0.09}$	$0.41^{+0.16}_{-0.15} \pm 0.02$	$0.53 \pm 0.08^{+0.07}_{-0.03}$	< 3.68	$0.38 \pm 0.05 \pm 0.03$	0.43 ± 0.05
374	$K^+\nu\bar{\nu}$	< 14	< 45	< 14	< 240		< 14
375	$\rho^+\nu\bar{\nu}$	< 150		< 150			< 150
376	$K^{*+}\ell^+\ell^-$	0.7 ± 0.5	$1.40^{+0.40}_{-0.37} \pm 0.09$	$1.24^{+0.23}_{-0.21} \pm 0.13$			$1.29^{+0.22}_{-0.21}$
377	$K^{*+}\nu\bar{\nu}$	< 140	< 80	< 140			< 80
378	$K^{*+}e^+e^-$	0.8 ± 0.8	$1.38^{+0.47}_{-0.42} \pm 0.08$	$1.73^{+0.50}_{-0.42} \pm 0.20$			$1.55^{+0.35}_{-0.32}$
379	$K^{*+}\mu^+\mu^-$	$0.8^{+0.6}_{-0.4}$	$1.46^{+0.73}_{-0.75} \pm 0.12$	$1.11^{+0.32}_{-0.27} \pm 0.10$			$1.16^{+0.31}_{-0.27}$
382	$\pi^+e^\pm\mu^\mp$	< 0.17	< 0.17				< 0.17
383	$K^+e^+\mu^-$	< 0.091	< 0.09				< 0.09
384	$K^+e^-\mu^+$	< 0.13	< 0.13				< 0.13
386	$K^+\tau^\pm\mu^\mp$	< 77	< 77				< 77
389	$K^{*+}e^\pm\mu^\mp$	< 1.4	< 1.4				< 1.4
390	$\pi^-e^+e^+$	< 1.6			< 1.6		< 1.6
391	$\pi^-\mu^+\mu^+$	< 1.4			< 1.4		< 1.4
392	$\pi^-e^+\mu^+$	< 1.3			< 1.3		< 1.3
393	$\rho^-e^+e^+$	< 2.6			< 2.6		< 2.6
394	$\rho^-\mu^+\mu^+$	< 5.0			< 5.0		< 5.0
395	$\rho^-e^+\mu^+$	< 3.3			< 3.3		< 3.3
396	$K^-e^+e^+$	< 1.0			< 1.0		< 1.0
397	$K^-\mu^+\mu^+$	< 1.8			< 1.8		< 1.8
398	$K^-e^+\mu^+$	< 2.0			< 2.0		< 2.0
399	$K^{*-}e^+e^+$	< 2.8			< 2.8		< 2.8
400	$K^{*-}\mu^+\mu^+$	< 8.3			< 8.3		< 8.3
401	$K^{*-}e^+\mu^+$	< 4.4			< 4.4		< 4.4

† $M_{K\pi\pi} < 1.8 \text{ GeV}/c^2$; ‡ $1.0 < M_{K\pi\pi} < 2.0 \text{ GeV}/c^2$; § $M_{K\pi\pi} < 2.4 \text{ GeV}/c^2$

Table 124: Branching fractions of semileptonic and radiative B^0 decays (in units of 10^{-6}). Upper limits are at 90% CL. Values in red (blue) are new published (preliminary) results since PDG2008 [as of March 12, 2010].

RPP#	Mode	PDG2008 Avg.	BABAR	Belle	CLEO	CDF	New Avg.
266	$K^{*0}\gamma$	40.1 ± 2.0	$44.7 \pm 1.0 \pm 1.6$	$40.1 \pm 2.1 \pm 1.7$	$45.5^{+7.2}_{-6.8} \pm 3.4$		43.3 ± 1.5
267	$K^0\eta\gamma$	$10.7^{+2.2}_{-1.5}$	$7.1^{+2.1}_{-2.0} \pm 0.4$	$8.7^{+3.1+1.9}_{-2.7-1.6}$			$7.6^{+1.8}_{-1.7}$
268	$K^0\eta'\gamma$	< 6.6	< 6.6	< 6.4			< 6.4
269	$K^0\phi\gamma$	< 2.7	< 2.7	$2.66 \pm 0.60 \pm 0.32$			2.66 ± 0.68
270	$K^+\pi^-\gamma$ §	4.6 ± 1.4		$4.6^{+1.3+0.5}_{-1.2-0.7}$			4.6 ± 1.4
271	$K^*(1410)^0\gamma$	< 130		< 130			< 130
272	$K^+\pi^-\gamma$ (N.R.) §	< 2.6		< 2.6			< 2.6
273	$K^0\pi^+\pi^-\gamma$	19.5 ± 2.2	$18.5 \pm 2.1 \pm 1.2$ †	$24 \pm 4 \pm 3$ ‡			19.5 ± 2.2
274	$K^+\pi^-\pi^0\gamma$	41 ± 4	$40.7 \pm 2.2 \pm 3.1$ †				40.7 ± 3.8
275	$K_1^0(1270)\gamma$	< 58		< 58			< 58
276	$K_1^0(1400)\gamma$	< 12		< 12			< 12
277	$K_2^*(1430)^0\gamma$	12.4 ± 2.4	$12.2 \pm 2.5 \pm 1.0$	$13 \pm 5 \pm 1$			12.4 ± 2.4
279	$K_3^*(1780)^0\gamma$	< 83		< 83			< 83
281	$\rho^0\gamma$	0.93 ± 0.21	$0.97^{+0.24}_{-0.22} \pm 0.06$	$0.78^{+0.17+0.09}_{-0.16-0.10}$	< 17		$0.86^{+0.15}_{-0.14}$
282	$\omega\gamma$	$0.46^{+0.20}_{-0.17}$	$0.50^{+0.27}_{-0.23} \pm 0.09$	$0.40^{+0.19}_{-0.17} \pm 0.13$	< 9.2		$0.44^{+0.18}_{-0.16}$
283	$\phi\gamma$	< 0.85	< 0.85		< 3.3		< 0.85
372	$\pi^0\ell^+\ell^-$	< 0.12	< 0.12	< 0.154			< 0.12
373	$\pi^0\nu\bar{\nu}$	< 220		< 220			< 220
374	$\pi^0e^+e^-$	< 0.14	< 0.14	< 0.227			< 0.14
375	$\pi^0\mu^+\mu^-$	< 0.51	< 0.51	< 0.184			< 0.184
376	$K^0\ell^+\ell^-$	$0.29^{+0.16}_{-0.13}$	$0.21^{+0.15}_{-0.13} \pm 0.02$	$0.34^{+0.09}_{-0.08} \pm 0.02$			$0.31^{+0.08}_{-0.07}$
377	$K^0\nu\bar{\nu}$	< 160		< 160			< 160
378	$\rho^0\nu\bar{\nu}$	< 440		< 440			< 440
379	$K^0e^+e^-$	$0.13^{+0.16}_{-0.11}$	$0.08^{+0.15}_{-0.12} \pm 0.01$	$0.20^{+0.14}_{-0.10} \pm 0.01$	< 8.45		$0.16^{+0.10}_{-0.08}$
380	$K^0\mu^+\mu^-$	$0.57^{+0.22}_{-0.18}$	$0.49^{+0.29}_{-0.25} \pm 0.03$	$0.44^{+0.13}_{-0.10} \pm 0.03$	< 6.64		$0.45^{+0.12}_{-0.10}$
381	$K^{*0}\ell^+\ell^-$	0.95 ± 0.18	$1.03^{+0.22}_{-0.21} \pm 0.07$	$0.97^{+0.13}_{-0.11} \pm 0.07$			$0.99^{+0.13}_{-0.10}$
382	$K^{*0}e^+e^-$	$1.04^{+0.35}_{-0.31}$	$0.86^{+0.26}_{-0.24} \pm 0.05$	$1.18^{+0.27}_{-0.22} \pm 0.09$			$1.03^{+0.11}_{-0.10}$
383	$K^{*0}\mu^+\mu^-$	$1.10^{+0.29}_{-0.26}$	$1.35^{+0.40}_{-0.37} \pm 0.10$	$1.06^{+0.19}_{-0.14} \pm 0.07$		$1.06 \pm 0.14 \pm 0.09$	$1.09^{+0.12}_{-0.11}$
384	$K^{*0}\nu\bar{\nu}$	< 340	< 120	< 340			< 120
385	$\phi\nu\bar{\nu}$	< 58		< 58			< 58
387	$\pi^0e^\pm\mu^\mp$	< 0.14	< 0.14				< 0.14
388	$K^0e^\pm\mu^\pm$	< 0.27	< 0.27				< 0.27
391	$K^{*0}e^\pm\mu^\pm$	< 3.4	< 0.58				< 0.58

† $M_{K\pi\pi} < 1.8 \text{ GeV}/c^2$; ‡ $1.0 < M_{K\pi\pi} < 2.0 \text{ GeV}/c^2$; § $1.25 \text{ GeV}/c^2 < M_{K\pi} < 1.6 \text{ GeV}/c^2$

7.3 $B \rightarrow X_s\gamma$

The decay $b \rightarrow s\gamma$ proceeds through a process of flavor changing neutral current. Since the charged Higgs or SUSY particles may contribute in the penguin loop, the branching fraction is sensitive to physics beyond the Standard Model. Experimentally, the branching fraction is measured using either a semi-inclusive or an inclusive approach. A minimum photon energy requirement is applied in the analysis and the branching fraction is corrected based on the theoretical model for the photon energy spectrum (shape function). Where there are multiple experimental results from an experiment, we use only the ones that are independent for *BABAR* and *Belle* to avoid dealing with correlated errors. Furthermore, the model uncertainties from the shape function should be highly correlated but no proper action was made in our older averages. To perform the average with better precision and good accuracy, it is important to use as many experimental results as possible and to handle the shape function issue in a proper way. In this note, we report the updated average of $b \rightarrow s\gamma$ branching fraction by implementing a common shape function.

Several shape function schemes are commonly used. Usually one is chosen to obtain the

Table 125: Branching fractions of semileptonic and radiative B decays (in units of 10^{-6}). Upper limits are at 90% CL. Values in red (blue) are new published (preliminary) results since PDG2008 [as of March 12, 2010].

RPP#	Mode	PDG2008 Avg.	BABAR	Belle	CLEO	New Avg.
63	$K\eta\gamma$	$8.5^{+1.6}_{-1.5}$		$8.5^{+1.3}_{-1.2} \pm 0.9$		$8.5^{+1.6}_{-1.5}$
65	$K_2^*(1430)\gamma$	$1.7^{+0.6}_{-0.5}$			$1.7 \pm 0.6 \pm 0.1$	1.7 ± 0.6
73	$K_3^*(1780)\gamma$	< 37		< 2.8		< 2.8
74	$s\gamma$	356 ± 25	$327 \pm 18^{+55}_{-41}$	$345 \pm 15 \pm 40$	$321 \pm 43^{+32}_{-29}$	$355 \pm 24 \pm 9$
–	$s\gamma$ with baryons	New			$< 38 \dagger$	$< 38 \dagger$
–	$d\gamma$	New	$14 \pm 5 \pm 4$			14 ± 6
78	$\rho\gamma$	1.36 ± 0.30	$1.73^{+0.34}_{-0.32} \pm 0.17$	$1.21^{+0.24}_{-0.22} \pm 0.12$	< 14	$1.39^{+0.22}_{-0.21}$
79	$\rho/\omega\gamma$	1.28 ± 0.21	$1.63^{+0.30}_{-0.28} \pm 0.16$	$1.14 \pm 0.20^{+0.10}_{-0.12}$	< 14	$1.30^{+0.18}_{-0.19}$
109	$se^+e^- \ddagger$	4.7 ± 1.3	$6.0 \pm 1.7 \pm 1.3$	$4.56 \pm 1.15^{+0.33}_{-0.40}$	< 57	$4.91^{+1.04}_{-1.06}$
110	$s\mu^+\mu^-$	4.3 ± 1.2	$5.0 \pm 2.8 \pm 1.2$	$1.91 \pm 1.02^{+0.16}_{-0.18}$	< 58	$2.23^{+0.97}_{-0.98}$
111	$sl^+\ell^- \ddagger$	4.5 ± 1.0	$5.6 \pm 1.5 \pm 1.3$	$3.33 \pm 0.80^{+0.19}_{-0.24}$	< 42	$3.66^{+0.76}_{-0.77}$
112	$\pi\ell^+\ell^-$	< 0.091	< 0.091	< 0.062		< 0.062
113	Ke^+e^-	$0.38^{+0.08}_{-0.07}$	$0.39^{+0.09}_{-0.08} \pm 0.02$	$0.48^{+0.08}_{-0.07} \pm 0.03$		0.44 ± 0.06
114	$K^*e^+e^-$	1.13 ± 0.27	$0.99^{+0.23}_{-0.21} \pm 0.06$	$1.39^{+0.23}_{-0.20} \pm 0.12$		$1.19^{+0.17}_{-0.16}$
115	$K\mu^+\mu^-$	$0.42^{+0.09}_{-0.08}$	$0.41^{+0.13}_{-0.12} \pm 0.02$	$0.50 \pm 0.06 \pm 0.03$		0.48 ± 0.06
116	$K^*\mu^+\mu^-$	$1.03^{+0.26}_{-0.23}$	$1.35^{+0.35}_{-0.33} \pm 0.10$	$1.10^{+0.16}_{-0.14} \pm 0.08$		$1.15^{+0.16}_{-0.15}$
117	$K\ell^+\ell^-$	0.39 ± 0.07	$0.39 \pm 0.07 \pm 0.02$	$0.48^{+0.05}_{-0.04} \pm 0.03$	< 1.7	0.45 ± 0.04
118	$K^*\ell^+\ell^-$	0.94 ± 0.18	$1.11^{+0.19}_{-0.18} \pm 0.07$	$1.07^{+0.11}_{-0.10} \pm 0.09$	< 3.3	$1.08^{+0.12}_{-0.11}$
–	$K^*\nu\bar{\nu}$	New	< 80			< 80
120	$\pi e^\pm\mu^\mp$	< 0.092	< 0.092		< 1.6	< 0.092
121	$\rho e^\pm\mu^\mp$	< 3.2			< 3.2	< 3.2
122	$Ke^\pm\mu^\mp$	< 0.038	< 0.038		< 1.6	< 0.038
123	$K^*e^\pm\mu^\mp$	< 0.51	< 0.51		< 6.2	< 0.51

$\dagger E_\gamma > 2.0$ GeV; $\ddagger M(\ell^+\ell^-) > 0.2$ GeV/ c^2

Table 126: Branching fractions of inclusive B decays (in units of 10^{-6}). Values in red (blue) are new published (preliminary) results since PDG2008 [as of March 12, 2010].

RPP#	Mode	PDG2008 Avg.	BABAR	Belle	CLEO	New Avg.
–	K^+X	New	$196^{+37+31}_{-34-30} \dagger$			196^{+48}_{-45}
–	K^0X	New	$154^{+55+55}_{-48-41} \dagger$			154^{+77}_{-63}
–	$s\eta$	New		$255 \pm 27^{+41}_{-142} \S$	< 440	255^{+49}_{-144}
–	$s\eta'$	New	$390 \pm 80 \pm 90 \ddagger$		$460 \pm 110 \pm 60 \ddagger$	423 ± 86

$\dagger p^* > 2.34$ GeV; $\S 0.4 < M_{X_s} < 2.6$ GeV; $\ddagger 2.0 < p^* < 2.7$ GeV

extrapolation factor, defined as the ratio of the $b \rightarrow s\gamma$ branching fractions with minimum photon energies above and at 1.6 GeV, and the difference between various schemes are treated as the model uncertainty. O. Buchmüller and H. Flächer have calculated the extrapolation factors [414]. Table 128 lists the extrapolation factors with various photon energy cuts for three different schemes and the average. The appropriate approach to average the experimental results is to first convert them according to the average extrapolation factors and then perform the average, assuming that the errors of the extrapolation factors are 100% correlated.

After surveying all available experimental results, the six shown in Table 129 are selected for the average. They have provided in their papers either the $b \rightarrow s\gamma$ branching fraction at a certain photon energy cut or the extrapolation factor used. Therefore we are able to convert them to the values at $E_{\min} = 1.6$ GeV using the information in Table 128. In the inclusive and

Table 127: Branching fractions of leptonic B decays (in units of 10^{-6}). Upper limits are at 90% CL. Values in red (blue) are new published (preliminary) results since PDG2008 [as of March 12, 2010].

RPP#	Mode	PDG2008 Avg.	BABAR	Belle	CLEO	CDF	DØ	New Avg.
24	$e^+\nu$	< 9.8	< 1.9	< 1.0	< 15			< 1.0
25	$\mu^+\nu$	< 1.7	< 1.0	< 1.7	< 21			< 1.0
26	$\tau^+\nu$	140 ± 40	170 ± 60	165^{+38+35}_{-37-37}	< 840			167 ± 39
27	$e^+\nu_e\gamma$	< 200	< 17		< 200			< 17
28	$\mu^+\nu_\mu\gamma$	< 52	< 26		< 52			< 26
–	$\ell^+\nu_\ell\gamma$	New	< 15.6					< 15.6
366	$\gamma\gamma$	< 0.62	< 1.7	< 0.62				< 0.62
367	e^+e^-	< 0.113	< 0.113	< 0.19	< 0.83	< 0.083		< 0.083
368	$e^+e^-\gamma$	< 0.12	< 0.12					< 0.12
369	$\mu^+\mu^-$	< 0.015	< 0.052	< 0.16	< 0.61	< 0.0060		< 0.0060
370	$\mu^+\mu^-\gamma$	< 0.16	< 0.16					< 0.16
371	$\tau^+\tau^-$	< 4100	< 4100					< 4100
386	$e^\pm\mu^\mp$	< 0.092	< 0.092	< 0.17	< 1.5	< 0.064		< 0.064
392	$e^\pm\tau^\mp$	< 110	< 28		< 110			< 28
393	$\mu^\pm\tau^\mp$	< 38	< 22		< 38			< 22
394	$\nu\bar{\nu}$	< 220	< 220					< 220
395	$\nu\bar{\nu}\gamma$	< 47	< 47					< 47

Table 128: Extrapolation factor in various scheme with various minimum photon energy requirement (in GeV).

Scheme	$E_\gamma < 1.7$	$E_\gamma < 1.8$	$E_\gamma < 1.9$	$E_\gamma < 2.0$	$E_\gamma < 2.242$
Kinetic	0.986 ± 0.001	0.968 ± 0.002	0.939 ± 0.005	0.903 ± 0.009	0.656 ± 0.031
Neubert SF	0.982 ± 0.002	0.962 ± 0.004	0.930 ± 0.008	0.888 ± 0.014	0.665 ± 0.035
Kagan-Neubert	0.988 ± 0.002	0.970 ± 0.005	0.940 ± 0.009	0.892 ± 0.014	0.643 ± 0.033
Average	0.985 ± 0.004	0.967 ± 0.006	0.936 ± 0.010	0.894 ± 0.016	0.655 ± 0.037

full hadronic tag analysis, a possible $B \rightarrow X_d\gamma$ contamination has been considered according to the expectation of $(4.5 \pm 0.3)\%$. The central value is slightly higher than 4.0% used in our 2006 average, and the uncertainty shrinks by a factor of five, due to better understanding of $|V_{td}/V_{ts}|$ from the $B_s\text{-}\bar{B}_s$ mixing and $B \rightarrow \rho/\omega \gamma$ measurements. Compared to the other systematic uncertainties, the error that arises from the $B \rightarrow X_d\gamma$ fraction is too small to be considered. We perform the average assuming that the systematic errors of the shape function and the $d\gamma$ fraction are correlated, and the other systematic errors and the statistical errors are Gaussian and uncorrelated. The obtained average is $\mathcal{B}(B \rightarrow X_s\gamma) = (355 \pm 24 \pm 9) \times 10^{-6}$ with a $\chi^2/\text{DOF} = 0.85/5$, where the errors are combined statistical and systematic, systematic due to the shape function. The second error is estimated to be the difference of the average after simultaneously varying the central value of each experimental result by $\pm 1\sigma$. Although a small fraction of events was used in multiple analyses in the same experiment, we neglect their

statistical correlations. Some other correlated systematic errors, such as photon detection and the background suppression, are not considered in our new average.

Table 129: Reported branching fraction, minimum photon energy, branching fraction at minimum photon energy and converted branching fraction \mathcal{B}^{cnv} for the decay $b \rightarrow s\gamma$. All the branching fractions are in units of 10^{-6} . The errors are, in order, statistical, systematic and theoretical (if exists) for \mathcal{B} , and statistical, systematic and shape-function systematic for \mathcal{B}^{cnv} . Theoretical errors in $\mathcal{B}(\mathcal{E}_\gamma > \mathcal{E}_{\text{min}})$ are merged into the systematic error of \mathcal{B}^{cnv} during conversion. The CLEO measurement on the branching fraction at E_{min} includes $B \rightarrow X_d\gamma$ events.

Mode	Reported \mathcal{B}	E_{min}	\mathcal{B} at E_{min}	Modified \mathcal{B} ($E_{\text{min}} = 1.6$)
CLEO Inc. [369]	$321 \pm 43 \pm 27_{-10}^{+18}$	2.0	$306 \pm 41 \pm 26$	$327 \pm 44 \pm 28 \pm 6$
Belle Semi.[415]	$336 \pm 53 \pm 42_{-54}^{+50}$	2.24	—	$369 \pm 58 \pm 46_{-60}^{+56}$
<i>BABAR</i> Semi.[361]	$335 \pm 19_{-41-9}^{+56+4}$	1.9	$327 \pm 18_{-40-9}^{+55+4}$	$349 \pm 20_{-46-3}^{+59+4}$
<i>BABAR</i> Inc. [362]	—	1.9	$367 \pm 29 \pm 34 \pm 29$	$390 \pm 31 \pm 47 \pm 4$
<i>BABAR</i> Full [416]	$391 \pm 91 \pm 64$	1.9	$366 \pm 85 \pm 60$	$389 \pm 91 \pm 64 \pm 4$
Belle Inc.[417]	—	1.7	$345 \pm 15 \pm 40$	$347 \pm 15 \pm 40 \pm 1$
Average				$355 \pm 24 \pm 9$

7.4 Baryonic decays

Table 130: Branching fractions of baryonic B^+ decays (in units of 10^{-6}). Upper limits are at 90% CL. values in red (blue) are new published (preliminary) results since PDG2008 [as of March 12, 2010].

RPP#	Mode	PDG2008 Avg.	BABAR	Belle	CLEO	New Avg.
327	$p\bar{p}\pi^+$	1.62 ± 0.2	$1.69 \pm 0.29 \pm 0.26$ †	$1.57_{-0.15}^{+0.17} \pm 0.12$ §	< 160	$1.60_{-0.17}^{+0.18}$
330	$p\bar{p}K^+$	5.9 ± 0.5	$6.7 \pm 0.5 \pm 0.4$ †	$5.00_{-0.22}^{+0.24} \pm 0.32$ §		5.48 ± 0.34
331	$\Theta^{++}\bar{p}$ ¹	< 0.091	< 0.09	< 0.091		< 0.09
332	$f_J(2221)K^+$ ²	< 0.41		< 0.41		< 0.41
333	$p\bar{\Lambda}(1520)$	< 1.5	< 1.5			< 1.5
335	$p\bar{p}K^{*+}$	6.6 ± 2.3	$5.3 \pm 1.5 \pm 1.3$ †	$3.38_{-0.60}^{+0.73} \pm 0.39$ ‡		$3.64_{-0.70}^{+0.79}$
336	$f_J(2221)K^{*+}$ ²	< 0.77	< 0.77			< 0.77
337	$p\bar{\Lambda}$	< 0.32		< 0.32	< 1.5	< 0.32
339	$p\bar{\Lambda}\pi^0$	$3.00_{-0.6}^{+0.7}$		$3.00_{-0.53}^{+0.61} \pm 0.33$		$3.00_{-0.62}^{+0.69}$
340	$p\bar{\Sigma}(1385)^0$	< 0.47		< 0.47		< 0.47
341	$\Delta^+\bar{\Lambda}$	< 0.82		< 0.82		< 0.82
344	$\Lambda\bar{\Lambda}\pi^+$	< 2.8		< 0.94 §		< 0.94 §
345	$\Lambda\bar{\Lambda}K^+$	$2.9_{-0.8}^{+1.0}$		$3.38_{-0.36}^{+0.41} \pm 0.41$ ‡		$3.38_{-0.55}^{+0.58}$
—	$\Lambda\bar{\Lambda}K^{*+}$	New		$2.19_{-0.88}^{+1.13} \pm 0.33$ §		$2.19_{-0.94}^{+1.18}$
346	$\bar{\Delta}^0 p$	< 1.38		< 1.38 §	< 380	< 1.38 §
347	$\Delta^{++}\bar{p}$	< 0.14		< 0.14 §	< 150	< 0.14 §
—	$p\bar{\Lambda}\pi^+\pi^-$ (NR)	New		$5.92_{-0.84}^{+0.88} \pm 0.69$		$5.92_{-1.09}^{+1.12}$
—	$p\bar{\Lambda}\rho^0$	New		$4.78_{-0.64}^{+0.67} \pm 0.60$		$4.78_{-0.88}^{+0.90}$
—	$p\bar{\Lambda}f_2(1270)$	New		$2.03_{-0.72}^{+0.77} \pm 0.27$		$2.03_{-0.77}^{+0.82}$

§Di-baryon mass is less than $2.85 \text{ GeV}/c^2$; † Charmonium decays to $p\bar{p}$ have been statistically subtracted;

‡ The charmonium mass region has been vetoed; ¹ $\Theta(1540)^{++} \rightarrow K^+p$ (pentaquark candidate);

² Product BF — daughter BF taken to be 100%

Table 131: Branching fractions of baryonic B^0 decays (in units of 10^{-6}). Upper limits are at 90% CL. values in red (blue) are new published (preliminary) results since PDG2008 [as of March 12, 2010].

RPP#	Mode	PDG2008 Avg.	BABAR	Belle	CLEO	New Avg.
328	$p\bar{p}$	< 0.11	< 0.27	< 0.11	< 1.4	< 0.11
330	$p\bar{p}K^0$	2.7 ± 0.4	$3.0 \pm 0.5 \pm 0.3$ †	$2.51_{-0.29}^{+0.35} \pm 0.21$ ‡		$2.66_{-0.32}^{+0.34}$
331	$\Theta^+\bar{p}$ ¹	< 0.05	< 0.05	< 0.23		< 0.05
332	$f_J(2221)K^0$ ²	< 0.45	< 0.45			< 0.45
333	$p\bar{p}K^{*0}$	1.5 ± 0.6	$1.47 \pm 0.45 \pm 0.40$ †	$1.18_{-0.25}^{+0.29} \pm 0.11$ ‡		$1.24_{-0.25}^{+0.28}$
334	$f_J(2221)K^{*0}$ ²	< 0.15	< 0.15			< 0.15
335	$p\bar{\Lambda}\pi^-$	3.2 ± 0.4	$3.07 \pm 0.31 \pm 0.23$	$3.23_{-0.29}^{+0.33} \pm 0.29$	< 13	$3.14_{-0.28}^{+0.29}$
336	$p\bar{\Sigma}(1385)^-$	< 0.26		< 0.26		< 0.26
337	$\Delta^0\bar{\Lambda}$	< 0.93		< 0.93		< 0.93
338	$p\bar{\Lambda}K^-$	< 0.82		< 0.82		< 0.82
339	$p\bar{\Sigma}^0\pi^-$	< 3.8		< 3.8		< 3.8
340	$\Lambda\bar{\Lambda}$	< 0.32		< 0.32	< 1.2	< 0.32
—	$\Lambda\bar{\Lambda}K^0$	New		$4.76_{-0.68}^{+0.84} \pm 0.61$ ‡		$4.76_{-0.91}^{+1.04}$
—	$\Lambda\bar{\Lambda}K^{*0}$	New		$2.46_{-0.72}^{+0.87} \pm 0.34$ ‡		$2.46_{-0.80}^{+0.93}$

† Charmonium decays to $p\bar{p}$ have been statistically subtracted; ‡ The charmonium mass region has been vetoed;
¹ $\Theta(1540)^+ \rightarrow pK^0$ (pentaquark candidate); ² Product BF — daughter BF taken to be 100%.

7.5 B_s decays

Table 132: B_s branching fractions (in units of 10^{-6}). Upper limits are at 90% CL. Values in red (blue) are new published (preliminary) results since PDG2008 [as of March 12, 2010].

RPP#	Mode	PDG2008 Avg.	Belle	CDF	D0	New Avg.
13	$\pi^+\pi^-$	< 170	< 12	< 1.2		< 1.2
19	$\phi\phi$	14 ± 8		$24.0 \pm 2.1 \pm 8.6 \dagger$		24.0 ± 8.9
20	π^+K^-	< 210	< 26	$5.0 \pm 0.7 \pm 0.8$		5.0 ± 1.1
21	K^+K^-	33 ± 9	$38_{-9}^{+10} \pm 7$	$24.4 \pm 1.4 \pm 4.6$		26.5 ± 4.4
–	$K^0\overline{K}^0$	New	< 33			< 33
26	$\gamma\gamma$	< 5.3	< 8.7			< 8.7
27	$\phi\gamma$	< 120	57_{-15}^{+18+12}			57_{-18}^{+21}
28	$\mu^+\mu^-$	< 0.047		< 0.036	< 0.075	< 0.036
29	e^+e^-	< 54		< 0.28		< 0.28
30	$e^\pm\mu^\mp$	< 6.1		< 0.20		< 0.20
31	$\phi\mu^+\mu^-$	< 3.2		$1.44 \pm 0.33 \pm 0.46$	$< 3.2 \dagger$	1.44 ± 0.57

\dagger Relative BF converted to absolute BF

Table 133: B_s rare relative branching fractions. Values in red (blue) are new published (preliminary) results since PDG2008 [as of March 12, 2010].

RPP#	Mode	PDG2008 Avg.	CDF	D0	New Avg.
9	$f_s\mathcal{B}(B_s^0 \rightarrow \pi^+\pi^-)/f_d\mathcal{B}(B^0 \rightarrow K^+\pi^-)$		$0.007 \pm 0.004 \pm 0.005$		0.007 ± 0.006
15	$\mathcal{B}(B_s^0 \rightarrow \phi\phi)/\mathcal{B}(B_s^0 \rightarrow J/\psi\phi)$		$(1.78 \pm 0.14 \pm 0.20) \times 10^{-2}$		1.78 ± 0.24
16	$f_s\mathcal{B}(B_s^0 \rightarrow K^+\pi^-)/f_d\mathcal{B}(B_d^0 \rightarrow K^+\pi^-)$		$0.071 \pm 0.010 \pm 0.007$		0.071 ± 0.012
17	$f_s\mathcal{B}(B_s^0 \rightarrow K^+K^-)/f_d\mathcal{B}(B_d^0 \rightarrow K^+\pi^-)$		$0.324 \pm 0.019 \pm 0.041$		0.324 ± 0.045
27	$\mathcal{B}(B_s^0 \rightarrow \phi\mu^+\mu^-)/\mathcal{B}(B_s^0 \rightarrow J/\psi\phi)$		$(1.11 \pm 0.25 \pm 0.09) \times 10^{-3}$	$< 3.5 \times 10^{-3}$	1.11 ± 0.27

7.6 Charge asymmetries

Table 134: CP asymmetries for charmless hadronic charged B decays (part I). Values in red (blue) are new published (preliminary) results since PDG2008 [as of March 12, 2010].

RPP#	Mode	PDG2008 Avg.	BABAR	Belle	CLEO	CDF	New Avg.
207	$K^0\pi^+$	0.009 ± 0.029	$-0.029 \pm 0.039 \pm 0.010$	$0.03 \pm 0.03 \pm 0.01$	$0.18 \pm 0.24 \pm 0.02$		0.009 ± 0.025
208	$K^+\pi^0$	0.027 ± 0.032	$0.030 \pm 0.039 \pm 0.010$	$0.07 \pm 0.03 \pm 0.01$	$-0.29 \pm 0.23 \pm 0.02$		0.050 ± 0.025
209	$\eta'K^+$	0.016 ± 0.019	$0.008^{+0.017}_{-0.018} \pm 0.009$	$0.028 \pm 0.028 \pm 0.021$	$0.03 \pm 0.12 \pm 0.02$		$0.013^{+0.016}_{-0.017}$
210	$\eta'K^{*+}$	$-0.30^{+0.33}_{-0.37} \pm 0.02$	$-0.30^{+0.37}_{-0.33} \pm 0.02$				$-0.30^{+0.37}_{-0.33}$
211	ηK^+	-0.27 ± 0.09	$-0.36 \pm 0.11 \pm 0.03$	$-0.39 \pm 0.16 \pm 0.03$			-0.37 ± 0.09
212	ηK^{*+}	0.02 ± 0.06	$0.01 \pm 0.08 \pm 0.02$	$0.03 \pm 0.10 \pm 0.01$			0.02 ± 0.06
213	$\eta K_0^*(1430)^+$	$0.05 \pm 0.13 \pm 0.02$	$0.05 \pm 0.13 \pm 0.02$				0.05 ± 0.13
214	$\eta K_2^*(1430)^+$	$-0.45 \pm 0.30 \pm 0.02$	$-0.45 \pm 0.30 \pm 0.02$				-0.45 ± 0.30
215	ωK^+	0.02 ± 0.05	$-0.01 \pm 0.07 \pm 0.01$	$0.05^{+0.08}_{-0.07} \pm 0.01$			0.02 ± 0.05
216	ωK^{*+}	New	$0.29 \pm 0.35 \pm 0.02$				0.29 ± 0.35
-	$\omega K_0^*(1430)^+$	New	$-0.10 \pm 0.09 \pm 0.02$				-0.10 ± 0.09
-	$\omega K_2^*(1430)^+$	New	$0.14 \pm 0.15 \pm 0.02$				0.14 ± 0.15
219	$K^{*0}\pi^+$	-0.08 ± 0.10	$0.032 \pm 0.052^{+0.016}_{-0.013}$	$-0.149 \pm 0.064 \pm 0.022$			-0.038 ± 0.042
220	$K^{*+}\pi^0$	$0.04 \pm 0.29 \pm 0.05$	$0.04 \pm 0.29 \pm 0.05$				0.04 ± 0.29
221	$K^+\pi^+\pi^-$	0.023 ± 0.031	$0.028 \pm 0.020 \pm 0.023$	$0.049 \pm 0.026 \pm 0.020$			0.038 ± 0.022
223	$f_0(980)K^+$	$-0.04^{+0.08}_{-0.07}$	$-0.106 \pm 0.050^{+0.036}_{-0.015}$	$-0.077 \pm 0.065^{+0.046}_{-0.026}$			$-0.095^{+0.049}_{-0.042}$
224	$f_2(1270)K^+$	$-0.59 \pm 0.22 \pm 0.036$	$-0.85 \pm 0.22^{+0.26}_{-0.13}$	$-0.59 \pm 0.22 \pm 0.04$			$-0.68^{+0.20}_{-0.18}$
227	$f_0(1500)K^+ \dagger$	New	$0.28 \pm 0.26^{+0.15}_{-0.14}$				$0.28^{+0.30}_{-0.29}$
229	$\rho^0 K^+$	$0.31^{+0.11}_{-0.09}$	$0.44 \pm 0.10^{+0.06}_{-0.14}$	$0.30 \pm 0.11^{+0.11}_{-0.05}$			0.37 ± 0.11
230	$K_0^*(1430)^0\pi^+$	0.00 ± 0.07	$0.032 \pm 0.035^{+0.034}_{-0.028}$	$0.076 \pm 0.038^{+0.028}_{-0.022}$			$0.055^{+0.034}_{-0.032}$
231	$K_2^*(1430)^0\pi^+$	New	$0.05 \pm 0.23^{+0.18}_{-0.08}$				$0.05^{+0.29}_{-0.24}$
238	$\rho^+ K^0$	$-0.12 \pm 0.17 \pm 0.02$	$-0.12 \pm 0.17 \pm 0.02$				-0.12 ± 0.17
239	$K^{*+}\pi^+\pi^-$	$0.07 \pm 0.07 \pm 0.04$	$0.07 \pm 0.07 \pm 0.04$				0.07 ± 0.08
240	$K^{*+}\rho^0$	$0.20^{+0.32}_{-0.29} \pm 0.04$	$0.20^{+0.32}_{-0.29} \pm 0.04$				$0.20^{+0.32}_{-0.29}$
241	$f_0(980)K^{*+}$	$-0.34 \pm 0.21 \pm 0.03$	$-0.34 \pm 0.21 \pm 0.03$				-0.34 ± 0.21
242	$a_1^+ K^0$	$0.12 \pm 0.11 \pm 0.02$	$0.12 \pm 0.11 \pm 0.02$				0.12 ± 0.11
243	$K^{*0}\rho^+$	$-0.01 \pm 0.16 \pm 0.02$	$-0.01 \pm 0.16 \pm 0.02$				-0.01 ± 0.16
247	$K^+\bar{K}^0$	$0.12 \pm 0.16 \pm 0.02$	$0.10 \pm 0.26 \pm 0.03$	$0.13^{+0.23}_{-0.24} \pm 0.02$			$0.12^{+0.17}_{-0.18}$
249	$K^+K_S K_S$	$-0.046 \pm 0.20 \pm 0.02$	$-0.04 \pm 0.11 \pm 0.02$				-0.04 ± 0.11
251	$K^+K^-\pi^+$	$0.00 \pm 0.10 \pm 0.03$	$0.00 \pm 0.10 \pm 0.03$				0.00 ± 0.10
257	$b_1^0 K^+$	$-0.46 \pm 0.20 \pm 0.02$	$-0.46 \pm 0.20 \pm 0.02$				-0.46 ± 0.20
-	$b_1^+ K^0$	New	$-0.03 \pm 0.15 \pm 0.02$				-0.03 ± 0.15
261	$K^+K^-K^+$	$-0.017 \pm 0.026 \pm 0.015$	$-0.02 \pm 0.03 \pm 0.02$				-0.02 ± 0.04
262	ϕK^+	0.01 ± 0.06	$0.00 \pm 0.08 \pm 0.02$	$0.01 \pm 0.12 \pm 0.05$		$-0.07 \pm 0.17^{+0.03}_{-0.02}$	-0.01 ± 0.06
270	$K^{*+}K^+K^-$	$0.11 \pm 0.08 \pm 0.03$	$0.11 \pm 0.08 \pm 0.03$				0.11 ± 0.09
271	ϕK^{*+}	-0.01 ± 0.08	$0.00 \pm 0.09 \pm 0.04$	$-0.02 \pm 0.14 \pm 0.03$			-0.01 ± 0.08
-	$\phi K_1(1270)^+$	New	$0.15 \pm 0.19 \pm 0.05$				0.15 ± 0.20
-	$\phi K_0^*(1430)^+$	New	$0.04 \pm 0.15 \pm 0.04$				0.04 ± 0.15
273	$\phi K_2^*(1430)^+$	New	$-0.23 \pm 0.19 \pm 0.06$				-0.23 ± 0.20
274	$\phi\phi K^+$	New		$0.01^{+0.19}_{-0.16} \pm 0.02$			$0.01^{+0.19}_{-0.16}$
276	$K^{*+}\gamma$	New	$0.18 \pm 0.28 \pm 0.07$				0.18 ± 0.29
278	$K^+\eta\gamma$	-0.16 ± 0.10	$-0.09 \pm 0.10 \pm 0.01$	$-0.16 \pm 0.09 \pm 0.06$			-0.12 ± 0.07
280	$K^+\phi\gamma$	$-0.26 \pm 0.14 \pm 0.05$	$-0.26 \pm 0.14 \pm 0.05$				-0.26 ± 0.15

Table 135: CP asymmetries for charmless hadronic charged B decays (part II). Values in red (blue) are new published (preliminary) results since PDG2008 [as of March 12, 2010].

RPP#	Mode	PDG2008 Avg.	BABAR	Belle	CLEO	CDF	New Avg.
291	$\rho^+\gamma$	New		$-0.11 \pm 0.32 \pm 0.09$			-0.11 ± 0.33
292	$\pi^+\pi^0$	0.01 ± 0.06	$0.03 \pm 0.08 \pm 0.01$	$0.07 \pm 0.06 \pm 0.01$			0.06 ± 0.05
293	$\pi^+\pi^-\pi^+$	$-0.007 \pm 0.0077 \pm 0.025$	$0.032 \pm 0.044^{+0.040}_{-0.037}$				$0.032^{+0.059}_{-0.057}$
294	$\rho^0\pi^+$	$-0.074 \pm 0.120^{+0.035}_{-0.055}$	$0.18 \pm 0.07^{+0.05}_{-0.15}$				$0.18^{+0.09}_{-0.17}$
296	$f_2(1270)\pi^+$	$-0.004 \pm 0.247^{+0.28}_{-0.32}$	$0.41 \pm 0.25^{+0.18}_{-0.15}$				$0.41^{+0.31}_{-0.29}$
297	$\rho(1450)^0\pi^+$	New	$-0.06 \pm 0.28^{+0.23}_{-0.32}$				$-0.06^{+0.36}_{-0.42}$
300	$\pi^+\pi^-\pi^+(NR)$	New	$-0.14 \pm 0.14^{+0.18}_{-0.08}$				$-0.14^{+0.23}_{-0.16}$
302	$\rho^+\pi^0$	0.02 ± 0.11	$-0.01 \pm 0.13 \pm 0.02$	$0.06 \pm 0.17^{+0.04}_{-0.05}$			0.02 ± 0.11
304	$\rho^+\rho^0$	-0.08 ± 0.13	$-0.054 \pm 0.055 \pm 0.010$	$0.00 \pm 0.22 \pm 0.03$			-0.051 ± 0.054
308	$b_1^0\pi^+$	$0.05 \pm 0.16 \pm 0.02$	$0.05 \pm 0.16 \pm 0.02$				0.05 ± 0.16
309	$\omega\pi^+$	-0.04 ± 0.06	$-0.02 \pm 0.08 \pm 0.01$	$-0.02 \pm 0.09 \pm 0.01$	$-0.34 \pm 0.25 \pm 0.02$		-0.04 ± 0.06
310	$\omega\rho^+$	$0.04 \pm 0.18 \pm 0.02$	$-0.20 \pm 0.09 \pm 0.02$				-0.20 ± 0.09
311	$\eta\pi^+$	-0.05 ± 0.10	$-0.03 \pm 0.09 \pm 0.03$	$-0.23 \pm 0.09 \pm 0.02$			-0.13 ± 0.07
312	$\eta'\pi^+$	-0.16 ± 0.07	$0.03 \pm 0.17 \pm 0.02$	$0.20^{+0.37}_{-0.36} \pm 0.04$			0.06 ± 0.15
313	$\eta'\rho^+$	$0.04 \pm 0.28 \pm 0.02$	$0.04 \pm 0.28 \pm 0.02$				0.04 ± 0.28
314	$\eta\rho^+$	0.01 ± 0.16	$0.13 \pm 0.11 \pm 0.02$	$-0.04^{+0.34}_{-0.32} \pm 0.01$			0.11 ± 0.11
327	$p\bar{p}\pi^+$	0.00 ± 0.04	$0.04 \pm 0.07 \pm 0.04$	$-0.17 \pm 0.10 \pm 0.02$			-0.04 ± 0.06
330	$p\bar{p}K^+$	-0.16 ± 0.07	$-0.16 \pm 0.08 \pm 0.04$	$-0.02 \pm 0.05 \pm 0.02$			-0.06 ± 0.05
335	$p\bar{p}K^{*+}$	$0.32 \pm 0.13 \pm 0.05$	$0.32 \pm 0.13 \pm 0.05$	$-0.01 \pm 0.19 \pm 0.02$			0.21 ± 0.11
338	$p\bar{A}\gamma$	$0.17 \pm 0.16 \pm 0.05$		$0.17 \pm 0.16 \pm 0.05$			0.17 ± 0.17
339	$p\bar{A}\pi^0$	$0.01 \pm 0.17 \pm 0.04$		$0.01 \pm 0.17 \pm 0.04$			0.01 ± 0.17
371	$K^+\ell\ell$	$-0.07 \pm 0.22 \pm 0.02$	$-0.18 \pm 0.19 \pm 0.01$	$0.04 \pm 0.10 \pm 0.02$			-0.01 ± 0.09
372	$K^+e^+e^-$	New		$0.14 \pm 0.14 \pm 0.03$			0.14 ± 0.14
373	$K^+\mu^+\mu^-$	New		$-0.05 \pm 0.13 \pm 0.03$			-0.05 ± 0.13
376	$K^{*+}\ell\ell$	$0.03 \pm 0.23 \pm 0.03$	$0.01^{+0.26}_{-0.24} \pm 0.02$	$-0.13^{+0.17}_{-0.16} \pm 0.01$			$-0.09^{+0.14}_{-0.13}$
378	$K^{*+}e^+e^-$	New		$-0.14^{+0.23}_{-0.22} \pm 0.02$			$-0.14^{+0.23}_{-0.22}$
379	$K^{*+}\mu^+\mu^-$	New		$-0.12 \pm 0.24 \pm 0.02$			-0.12 ± 0.24

Table 136: CP asymmetries for charmless hadronic neutral B decays. Values in red (blue) are new published (preliminary) results since PDG2008 [as of March 12, 2010].

RPP#	Mode	PDG2008 Avg.	BABAR	Belle	CLEO	CDF	New Avg.
198	$K^+\pi^-$	-0.101 ± 0.015	$-0.107 \pm 0.016^{+0.006}_{-0.004}$	$-0.094 \pm 0.018 \pm 0.008$	$-0.04 \pm 0.16 \pm 0.02$	$-0.086 \pm 0.023 \pm 0.009$	$-0.098^{+0.012}_{-0.011}$
201	$\eta' K^{*0}$	$0.08 \pm 0.25 \pm 0.02$	$0.08 \pm 0.25 \pm 0.02$				0.08 ± 0.25
203	ηK^{*0}	0.19 ± 0.05	$0.21 \pm 0.06 \pm 0.02$	$0.17 \pm 0.08 \pm 0.01$			0.19 ± 0.05
204	$\eta K_0^*(1430)^0$	$0.06 \pm 0.13 \pm 0.02$	$0.06 \pm 0.13 \pm 0.02$				0.06 ± 0.13
205	$\eta K_2^*(1430)^0$	$-0.07 \pm 0.19 \pm 0.02$	$-0.07 \pm 0.19 \pm 0.02$				-0.07 ± 0.19
211	ωK^{*0}	New	$0.45 \pm 0.25 \pm 0.02$				0.45 ± 0.25
–	$\omega K_0^*(1430)^0$	New	$-0.07 \pm 0.09 \pm 0.02$				-0.07 ± 0.09
–	$\omega K_2^*(1430)^0$	New	$0.37 \pm 0.17 \pm 0.02$				0.37 ± 0.17
216	$K^+\pi^-\pi^0$	$0.07 \pm 0.11 \pm 0.01$	$0.030^{+0.045}_{-0.051} \pm 0.055$	$0.07 \pm 0.11 \pm 0.01$			$0.042^{+0.059}_{-0.061}$
217	$\rho^- K^+$	-0.08 ± 0.24	$0.14 \pm 0.06 \pm 0.01$	$0.22^{+0.22+0.06}_{-0.23-0.02}$			0.15 ± 0.06
218	$K^+\pi^-\pi^0(NR)$	New	$0.07 \pm 0.15 \pm 0.04$				0.07 ± 0.15
–	$K_0^*(1430)^0\pi^0$	New	$-0.16 \pm 0.09 \pm 0.04$				-0.16 ± 0.10
224	$K^{*+}\pi^-$	-0.05 ± 0.14	-0.20 ± 0.09	$-0.21 \pm 0.11 \pm 0.07$	$0.26^{+0.33+0.10}_{-0.34-0.08}$		-0.18 ± 0.07
232	$K^{*0}\pi^0$	New	$-0.15 \pm 0.12 \pm 0.02$				-0.15 ± 0.12
233	$K_0^*(1430)^+\pi^-$	New	$0.07 \pm 0.05 \pm 0.01$				0.07 ± 0.05
240	$K^{*0}\pi^+\pi^-$	$0.07 \pm 0.04 \pm 0.03$	$0.07 \pm 0.04 \pm 0.03$				0.07 ± 0.05
241	$K^{*0}\rho^0$	$0.09 \pm 0.19 \pm 0.02$	$0.09 \pm 0.19 \pm 0.02$				0.09 ± 0.19
242	$f_0(980)K^{*0}$	New	$-0.17 \pm 0.28 \pm 0.02$				-0.17 ± 0.28
244	$a_1^+ K^-$	$-0.16 \pm 0.12 \pm 0.01$	$-0.16 \pm 0.12 \pm 0.01$				-0.16 ± 0.12
245	$b_1^- K^+$	$0.07 \pm 0.12 \pm 0.02$	$0.07 \pm 0.12 \pm 0.02$				0.07 ± 0.12
246	$K^{*0}K^+K^-$	$0.01 \pm 0.05 \pm 0.02$	$0.01 \pm 0.05 \pm 0.02$				0.01 ± 0.05
247	ϕK^{*0}	0.01 ± 0.06	$0.01 \pm 0.06 \pm 0.03$	$0.02 \pm 0.09 \pm 0.02$			0.01 ± 0.05
248	$K^{*0}\pi^+K^-$	$0.22 \pm 0.33 \pm 0.20$	$0.22 \pm 0.33 \pm 0.20$				0.22 ± 0.39
258	$\phi K_0^*(1430)^0$	New	$0.20 \pm 0.14 \pm 0.06$				0.20 ± 0.15
263	$\phi K_2^*(1430)^0$	$-0.12 \pm 0.14 \pm 0.04$	$-0.08 \pm 0.12 \pm 0.05$				-0.08 ± 0.13
266	$K^{*0}\gamma$	New	$-0.16 \pm 0.22 \pm 0.07$				-0.16 ± 0.23
285	$\pi^0\pi^0$		$0.43 \pm 0.26 \pm 0.05$	$0.44^{+0.73+0.04}_{-0.62-0.06}$			$0.43^{+0.25}_{-0.24}$
316	$b_{\mp}^{\mp}\pi^{\pm}$	$-0.05 \pm 0.10 \pm 0.02$	$-0.05 \pm 0.10 \pm 0.02$				-0.05 ± 0.10
330	$p\bar{p}K^{*0}$	$0.11 \pm 0.13 \pm 0.06$	$0.11 \pm 0.13 \pm 0.06$	$-0.08 \pm 0.20 \pm 0.02$			0.05 ± 0.12
335	$p\bar{A}\pi^-$	$-0.02 \pm 0.10 \pm 0.03$	$-0.10 \pm 0.10 \pm 0.02$	$-0.02 \pm 0.10 \pm 0.03$			-0.06 ± 0.07
381	$K^{*0}\ell\ell$	New	$0.02 \pm 0.20 \pm 0.02$	$-0.08 \pm 0.12 \pm 0.02$			-0.05 ± 0.10
382	$K^{*0}e^+e^-$	New		$-0.21 \pm 0.19 \pm 0.02$			-0.21 ± 0.19
383	$K^{*0}\mu^+\mu^-$	New		$0.00 \pm 0.15 \pm 0.03$			0.00 ± 0.15

† Measurements of time-dependent CP asymmetries are listed in the section of the Unitarity Triangle.

Table 137: Charmless hadronic CP asymmetries for B^\pm/B^0 admixtures. Values in red (blue) are new published (preliminary) results since PDG2008 [as of March 12, 2010].

RPP#	Mode	PDG2008 Avg.	BABAR	Belle	CLEO	CDF	New Avg.
62	$K^*\gamma$	-0.010 ± 0.028	$-0.003 \pm 0.017 \pm 0.007$	$-0.015 \pm 0.044 \pm 0.012$	$0.08 \pm 0.13 \pm 0.03$		-0.003 ± 0.017
74	$s\gamma$	0.01 ± 0.04	$-0.011 \pm 0.030 \pm 0.014$	$0.002 \pm 0.050 \pm 0.030$	$-0.079 \pm 0.108 \pm 0.022$		-0.012 ± 0.028
-	$(s+d)\gamma$	$-0.110 \pm 0.115 \pm 0.017$	$-0.11 \pm 0.12 \pm 0.02$				-0.11 ± 0.12
111	$s\ell\ell$	$-0.22 \pm 0.26 \pm 0.02$	$-0.22 \pm 0.26 \pm 0.02$				-0.22 ± 0.26
114	$K^*e^+e^-$	New		$-0.18 \pm 0.15 \pm 0.01$			-0.18 ± 0.15
116	$K^*\mu^+\mu^-$	New		$-0.03 \pm 0.13 \pm 0.02$			-0.03 ± 0.13
118	$K^*\ell\ell$	New	$0.01^{+0.16}_{-0.15} \pm 0.01$	$-0.10 \pm 0.10 \pm 0.01$			-0.07 ± 0.08

Table 138: CP asymmetries for charmless hadronic neutral B_S^0 decays. Values in red (blue) are new published (preliminary) results since PDG2008 [as of March 12, 2010].

RPP#	Mode	PDG2008 Avg.	BABAR	Belle	CLEO	CDF	New Avg.
20	$K^+\pi^-$	New				$0.39 \pm 0.15 \pm 0.08$	0.39 ± 0.17

7.7 Polarization measurements

Table 139: Longitudinal polarization fraction f_L for B^+ decays. Values in red (blue) are new published (preliminary) results since PDG2008 [as of March 12, 2010].

RPP#	Mode	PDG2008 Avg.	BABAR	Belle	New Avg.
216	ωK^{*+}	New	$0.41 \pm 0.18 \pm 0.05$		0.41 ± 0.19
–	$\omega K_2^*(1430)^+$	New	$0.56 \pm 0.10 \pm 0.04$		0.56 ± 0.11
243	$K^{*0} \rho^+$	0.48 ± 0.08	$0.52 \pm 0.10 \pm 0.04$	$0.43 \pm 0.11^{+0.05}_{-0.02}$	0.48 ± 0.08
244	$K^{*+} \bar{K}^{*0}$	New	$0.75^{+0.16}_{-0.26} \pm 0.03$		$0.75^{+0.16}_{-0.26}$
271	ϕK^{*+}	0.50 ± 0.07	$0.49 \pm 0.05 \pm 0.03$	$0.52 \pm 0.08 \pm 0.03$	0.50 ± 0.05
–	$\phi K_1^+(1270)$	New	$0.46^{+0.12+0.06}_{-0.13-0.07}$		$0.46^{+0.13}_{-0.15}$
273	$\phi K_2^*(1430)^+$	New	$0.80^{+0.09}_{-0.10} \pm 0.03$		0.80 ± 0.10
304	$\rho^+ \rho^0$	0.91 ± 0.04	$0.950 \pm 0.015 \pm 0.006$	$0.95 \pm 0.11 \pm 0.02$	0.950 ± 0.016
310	$\omega \rho^+$	$0.82 \pm 0.11 \pm 0.02$	$0.90 \pm 0.05 \pm 0.03$		0.90 ± 0.06

Table 140: Full angular analysis of $B^+ \rightarrow \phi K^{*+}$. Values in red (blue) are new published (preliminary) results since PDG2008 [as of March 12, 2010].

Parameter	PDG2008 Avg.	BABAR	Belle	New Avg.
$f_{\perp} = A_{\perp\perp}$	0.20 ± 0.05	$0.21 \pm 0.05 \pm 0.02$	$0.19 \pm 0.08 \pm 0.02$	0.20 ± 0.05
ϕ_{\parallel}	2.34 ± 0.18	$2.47 \pm 0.20 \pm 0.07$	$2.10 \pm 0.28 \pm 0.04$	2.34 ± 0.17
ϕ_{\perp}	2.58 ± 0.17	$2.69 \pm 0.20 \pm 0.03$	$2.31 \pm 0.30 \pm 0.07$	2.58 ± 0.17
δ_0	3.07 ± 0.19	$3.07 \pm 0.18 \pm 0.06$		3.07 ± 0.19
A_{CP}^0	$0.17 \pm 0.11 \pm 0.02$	$0.17 \pm 0.11 \pm 0.02$		0.17 ± 0.11
A_{CP}^{\perp}	$0.22 \pm 0.24 \pm 0.08$	$0.22 \pm 0.24 \pm 0.08$		0.22 ± 0.25
$\Delta\phi_{\parallel}$	$0.07 \pm 0.20 \pm 0.05$	$0.07 \pm 0.20 \pm 0.05$		0.07 ± 0.21
$\Delta\phi_{\perp}$	$0.19 \pm 0.20 \pm 0.07$	$0.19 \pm 0.20 \pm 0.07$		0.19 ± 0.21
$\Delta\delta_0$	0.20 ± 0.18	$0.20 \pm 0.18 \pm 0.03$		0.20 ± 0.18

BR, f_L and A_{CP} are tabulated separately.

Table 141: Longitudinal polarization fraction f_L for B^0 decays. Values in red (blue) are new published (preliminary) results since PDG2008 [as of March 12, 2010].

RPP#	Mode	PDG2008 Avg.	BABAR	Belle	New Avg.
211	ωK^{*0}	New	$0.72 \pm 0.14 \pm 0.02$	$0.56 \pm 0.29^{+0.18}_{-0.08}$	0.70 ± 0.13
–	$\omega K_2^*(1430)^0$	New	$0.45 \pm 0.12 \pm 0.02$		0.45 ± 0.12
241	$K^{*0} \rho^0$	$0.57 \pm 0.09 \pm 0.08$	$0.57 \pm 0.09 \pm 0.08$		0.57 ± 0.12
247	ϕK^{*0}	0.484 ± 0.0033	$0.494 \pm 0.034 \pm 0.013$	$0.45 \pm 0.05 \pm 0.02$	0.480 ± 0.030
249	$K^{*0} \overline{K}^{*0}$	$0.80^{+0.10}_{-0.12} \pm 0.06$	$0.80^{+0.10}_{-0.12} \pm 0.06$		$0.80^{+0.12}_{-0.13}$
263	$\phi K_2^*(1430)^0$	$0.853^{+0.061}_{-0.069} \pm 0.036$	$0.901^{+0.046}_{-0.058} \pm 0.037$		$0.901^{+0.059}_{-0.069}$
312	$\rho^0 \rho^0$	$0.87 \pm 0.13 \pm 0.04$	$0.75^{+0.11}_{-0.14} \pm 0.04$		$0.75^{+0.12}_{-0.15}$
319	$\rho^+ \rho^-$	$0.977^{+0.028}_{-0.024}$	$0.992 \pm 0.024^{+0.026}_{-0.013}$	$0.941^{+0.034}_{-0.040} \pm 0.030$	$0.978^{+0.025}_{-0.022}$
326	$a_1^\pm a_1^\mp$	New	$0.31 \pm 0.22 \pm 0.10$		0.31 ± 0.24

Table 142: Full angular analysis of $B^0 \rightarrow \phi K^{*0}$. Values in red (blue) are new published (preliminary) results since PDG2008 [as of March 12, 2010].

Parameter	PDG2008 Avg.	BABAR	Belle	New Avg.
$f_\perp = A_{\perp\perp}$	0.26 ± 0.04	$0.212 \pm 0.032 \pm 0.013$	$0.31^{+0.06}_{-0.05} \pm 0.02$	0.241 ± 0.029
ϕ_\parallel	2.33 ± 0.14	$2.40 \pm 0.13 \pm 0.08$	$2.40^{+0.28}_{-0.24} \pm 0.07$	$2.40^{+0.14}_{-0.13}$
ϕ_\perp	2.33 ± 0.14	$2.35 \pm 0.13 \pm 0.09$	$2.51 \pm 0.25 \pm 0.06$	2.39 ± 0.13
δ_0	2.78 ± 0.19	$2.82 \pm 0.15 \pm 0.09$		2.82 ± 0.17
A_{CP}^0	0.02 ± 0.07	$0.01 \pm 0.07 \pm 0.02$	$0.13 \pm 0.12 \pm 0.04$	0.04 ± 0.06
A_{CP}^\perp	-0.11 ± 0.12	$-0.04 \pm 0.15 \pm 0.06$	$-0.20 \pm 0.18 \pm 0.04$	-0.11 ± 0.12
$\Delta\phi_\parallel$	0.10 ± 0.24	$0.22 \pm 0.12 \pm 0.08$	$-0.32 \pm 0.27 \pm 0.07$	0.11 ± 0.13
$\Delta\phi_\perp$	0.04 ± 0.23	$0.21 \pm 0.13 \pm 0.08$	$-0.30 \pm 0.25 \pm 0.06$	0.08 ± 0.13
$\Delta\delta_0$	0.21 ± 0.19	$0.27 \pm 0.14 \pm 0.08$		0.27 ± 0.16

BR, f_L and A_{CP} are tabulated separately.

Table 143: Full angular analysis of $B^0 \rightarrow \phi K_2^*(1430)^0$. Values in red (blue) are new published (preliminary) results since PDG2008 [as of March 12, 2010].

Parameter	PDG2008 Avg.	BABAR	Belle	New Avg.
$f_\perp = A_{\perp\perp}$	$0.045^{+0.051}_{-0.042}$	$0.002^{+0.018}_{-0.002} \pm 0.031$		$0.002^{+0.036}_{-0.031}$
ϕ_\parallel	2.90 ± 0.40	$3.96 \pm 0.38 \pm 0.06$		3.96 ± 0.39
δ_0	$3.54^{+0.13}_{-0.15}$	$3.41 \pm 0.13 \pm 0.13$		3.41 ± 0.18
A_{CP}^0	New	$-0.05 \pm 0.06 \pm 0.01$		-0.05 ± 0.06
$\Delta\phi_\parallel$	New	$-1.00 \pm 0.38 \pm 0.09$		-1.00 ± 0.39
$\Delta\delta_0$	New	$0.11 \pm 0.13 \pm 0.06$		0.11 ± 0.14

BR, f_L and A_{CP} are tabulated separately.

8 D decays

8.1 D^0 - \bar{D}^0 Mixing and CP Violation

8.1.1 Introduction

In 2007, Belle [418] and Babar [419] obtained the first evidence for D^0 - \bar{D}^0 mixing, which had been searched for for more than two decades without success. These results were later confirmed by CDF [420]. There are now numerous measurements of D^0 - \bar{D}^0 mixing, with various levels of sensitivity. All the results can be combined to yield world average (WA) values for the mixing parameters $x \equiv (m_1 - m_2)/\Gamma$ and $y \equiv (\Gamma_1 - \Gamma_2)/(2\Gamma)$, where m_1 , m_2 and Γ_1 , Γ_2 are the masses and decay widths for the mass eigenstates $D_1 \equiv p|D^0\rangle - q|\bar{D}^0\rangle$ and $D_2 \equiv p|D^0\rangle + q|\bar{D}^0\rangle$, and $\Gamma = (\Gamma_1 + \Gamma_2)/2$. Here we use the phase convention $CP|D^0\rangle = -|\bar{D}^0\rangle$, $CP|\bar{D}^0\rangle = -|D^0\rangle$; in the absence of CP violation (CPV), $q/p=1$, D_1 is CP -even, and D_2 is CP -odd.

The WA values are calculated by performing a global fit to more than two dozen measured observables. Assuming no CPV , the fit parameters are x , y , δ (the strong phase difference between amplitudes $\mathcal{A}(\bar{D}^0 \rightarrow K^+\pi^-)$ and $\mathcal{A}(D^0 \rightarrow K^+\pi^-)$), a strong phase $\delta_{K\pi\pi}$ entering $D^0 \rightarrow K^+\pi^-\pi^0$ decays, and $R_D \equiv |\mathcal{A}(D^0 \rightarrow K^+\pi^-)/\mathcal{A}(\bar{D}^0 \rightarrow K^+\pi^-)|^2$. To account for possible CPV , three additional parameters are added: $|q/p|$, $\phi \equiv \text{Arg}(q/p)$, and $A_D \equiv (R_D^+ - R_D^-)/(R_D^+ + R_D^-)$, where the $+$ ($-$) superscript corresponds to D^0 (\bar{D}^0) decays.

The observables used are from measurements of $D^0 \rightarrow K^+\ell^-\nu$, $D^0 \rightarrow K^+K^-/\pi^+\pi^-$, $D^0 \rightarrow K^+\pi^-$, $D^0 \rightarrow K^+\pi^-\pi^0$, $D^0 \rightarrow K_S^0\pi^+\pi^-$, and $D^0 \rightarrow K_S^0K^+K^-$ decays; and from double-tagged branching fractions measured at the $\psi(3770)$ resonance. Correlations among observables are accounted for by using covariance matrices provided by the experimental collaborations. Systematic errors among different experiments are assumed uncorrelated as no significant correlations have been identified. We have checked this method with a second method that adds together three-dimensional log-likelihood functions for x , y , and δ obtained from several analyses; this combination accounts for non-Gaussian errors. When both methods are applied to the same set of observables and data, equivalent results are obtained.

Mixing in heavy flavor systems such as those of B^0 and B_s^0 is governed by the short-distance box diagram. In the D^0 system, however, this diagram is doubly-Cabibbo-suppressed relative to amplitudes dominating the decay width, and it is also GIM-suppressed. Thus the short-distance mixing rate is tiny, and D^0 - \bar{D}^0 mixing is expected to be dominated by long-distance processes. These are difficult to calculate reliably, and theoretical estimates for x and y range over two-three orders of magnitude [421, 422, 423, 424, 425].

With the exception of $\psi(3770) \rightarrow DD$ measurements, all methods identify the flavor of the D^0 or \bar{D}^0 when produced by reconstructing the decay $D^{*+} \rightarrow D^0\pi^+$ or $D^{*-} \rightarrow \bar{D}^0\pi^-$; the charge of the pion (which has low momentum and is often referred to as the “soft” pion π_s) identifies the D flavor. For signal decays, $M_{D^*} - M_{D^0} - M_{\pi^+} \equiv Q \approx 6$ MeV, which is close to the threshold; thus analyses typically require that the reconstructed Q be small to suppress backgrounds. For time-dependent measurements, the D^0 decay time is calculated as $(d/p) \times M_{D^0}$, where d is the distance between the D^* and D^0 decay vertices and p is the D^0 momentum. The D^* vertex position is taken to be at the primary vertex for $\bar{p}p$ collider experiments [420], and at the intersection of the D^0 momentum vector with the beamspot profile for e^+e^- experiments.

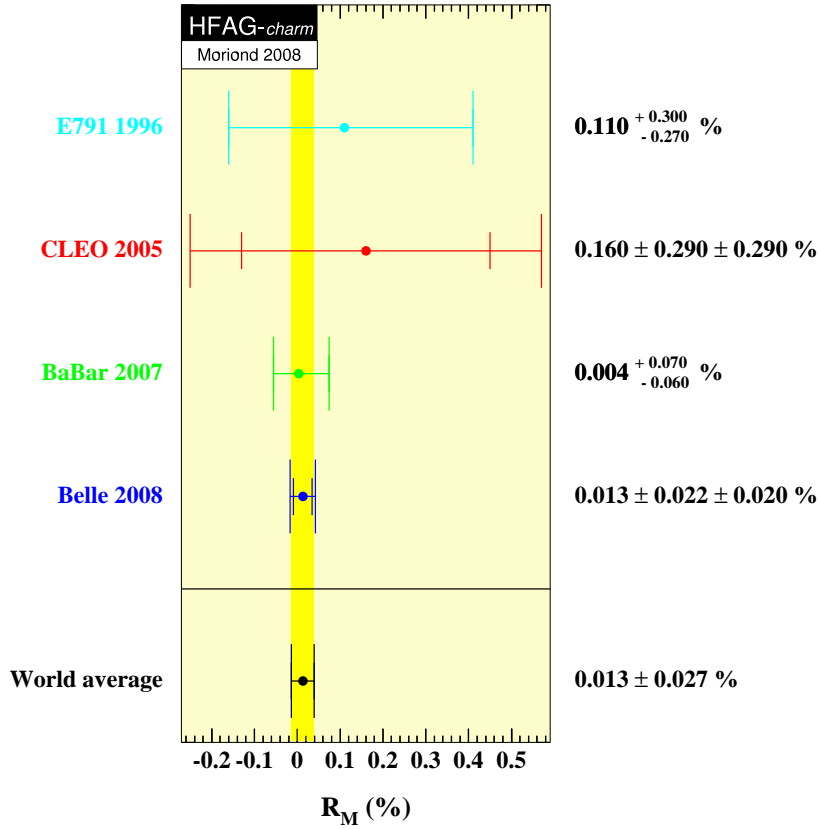


Figure 56: WA value of R_M from Ref. [426], as calculated from $D^0 \rightarrow K^+ \ell^- \nu$ measurements [427, 428, 429, 430].

8.1.2 Input Observables

The global fit determines central values and errors for the underlying parameters using a χ^2 statistic constructed from 30 observables. The parameters are x , y , δ , R_D , A_D , $|q/p|$, ϕ , and $\delta_{K\pi\pi}$. Parameters x and y govern mixing, while A_D , $|q/p|$, and ϕ govern CPV . The parameter δ is the strong phase difference between the amplitudes $\mathcal{A}(\overline{D}^0 \rightarrow K^+ \pi^-)$ and $\mathcal{A}(D^0 \rightarrow K^+ \pi^-)$, and $\delta_{K\pi\pi}$ is the analogous strong phase difference between the amplitudes $\mathcal{A}(\overline{D}^0 \rightarrow K^+ \rho^-)$ and $\mathcal{A}(D^0 \rightarrow K^+ \rho^-)$.³²

All input values are listed in Tables 144 and 145. The observable $R_M = (x^2 + y^2)/2$ calculated from $D^0 \rightarrow K^+ \ell^- \nu$ decays [427, 428, 429, 430] is the WA value calculated by HFAG [426] (see Fig. 56). The observables y_{CP} and A_Γ are also HFAG WA values [426] (see Fig. 57). The $D^0 \rightarrow K^+ \pi^-$ observables used are from Belle [431], Babar [419], and CDF [420]; earlier measurements have much less precision and are not used. The observables from $D^0 \rightarrow K_S^0 \pi^+ \pi^-$ decays for no- CPV are from Belle [432] and BaBar [433], but for the CPV -allowed case only Belle measurements [432] are available. The $D^0 \rightarrow K^+ \pi^- \pi^0$ results are from Babar [434], and the $\psi(3770) \rightarrow \overline{D}D$ results are from CLEOc [319].

The relationships between the observables and the fitted parameters are listed in Table 146.

³²In the $D \rightarrow K^+ \pi^- \pi^0$ Dalitz plot analysis yielding sensitivity to x and y , the $\overline{D}^0 \rightarrow K^+ \pi^- \pi^0$ isobar phases are determined relative to that for $\mathcal{A}(\overline{D}^0 \rightarrow K^+ \rho^-)$, and the $D^0 \rightarrow K^+ \pi^- \pi^0$ isobar phases are determined relative to that for $\mathcal{A}(D^0 \rightarrow K^+ \rho^-)$. As the \overline{D}^0 and D^0 Dalitz plots are fit independently, the phase difference $\delta_{K\pi\pi}$ between the two “normalizing” amplitudes cannot be determined from these fits.

Table 144: All observables except those for $D^0 \rightarrow K^+ \pi^-$ used for the global fit, from Refs. [418, 427, 428, 429, 430, 432, 433, 434, 319, 435, 436, 437, 438].

Mode	Observable	Values	Correlation coefficients
$D^0 \rightarrow K^+ K^- / \pi^+ \pi^-$, ϕK_S^0 [426]	y_{CP}	$(1.107 \pm 0.217)\%$	
	A_Γ	$(0.123 \pm 0.248)\%$	
$D^0 \rightarrow K_S^0 \pi^+ \pi^-$ [433] $K_S^0 K^+ K^-$ (BaBar: no CPV)	x	$(0.16 \pm 0.23 \pm 0.12 \pm 0.08)\%$	0.0615
	y	$(0.57 \pm 0.20 \pm 0.13 \pm 0.07)\%$	
$D^0 \rightarrow K_S^0 \pi^+ \pi^-$ [426] (Belle+CLEO WA: no CPV or no direct CPV)	x	$(0.811 \pm 0.334)\%$	
	y	$(0.309 \pm 0.281)\%$	
	$ q/p $	$0.95 \pm 0.22^{+0.10}_{-0.09}$	
	ϕ	$(-0.035 \pm 0.19 \pm 0.09)$ rad	
$D^0 \rightarrow K_S^0 \pi^+ \pi^-$ [432] (Belle: CPV -allowed)	x	$(0.81 \pm 0.30^{+0.13}_{-0.17})\%$	$\left\{ \begin{array}{cccc} 1 & -0.007 & -0.255\alpha & 0.216 \\ -0.007 & 1 & -0.019\alpha & -0.280 \\ -0.255\alpha & -0.019\alpha & 1 & -0.128\alpha \\ 0.216 & -0.280 & -0.128\alpha & 1 \end{array} \right\}$ $(\alpha = (q/p + 1)^2/2$ is a transformation factor)
	y	$(0.37 \pm 0.25^{+0.10}_{-0.15})\%$	
	$ q/p $	$0.86 \pm 0.30^{+0.10}_{-0.09}$	
	ϕ	$(-0.244 \pm 0.31 \pm 0.09)$ rad	
$D^0 \rightarrow K^+ \ell^- \nu$ [426]	R_M	$(0.0173 \pm 0.0387)\%$	
$D^0 \rightarrow K^+ \pi^- \pi^0$	x''	$(2.61^{+0.57}_{-0.68} \pm 0.39)\%$	-0.75
	y''	$(-0.06^{+0.55}_{-0.64} \pm 0.34)\%$	
$\psi(3770) \rightarrow \bar{D}D$ (CLEOc)	R_M	$(0.199 \pm 0.173 \pm 0.0)\%$	$\left\{ \begin{array}{cccc} 1 & -0.0644 & 0.0072 & 0.0607 \\ -0.0644 & 1 & -0.3172 & -0.8331 \\ 0.0072 & -0.3172 & 1 & 0.3893 \\ 0.0607 & -0.8331 & 0.3893 & 1 \end{array} \right\}$
	y	$(-5.207 \pm 5.571 \pm 2.737)\%$	
	R_D	$(-2.395 \pm 1.739 \pm 0.938)\%$	
	$\sqrt{R_D} \cos \delta$	$(8.878 \pm 3.369 \pm 1.579)\%$	

For each set of correlated observables we construct a difference vector \vec{V} ; e.g., for $D^0 \rightarrow K_S^0 \pi^+ \pi^-$ decays $\vec{V} = (\Delta x, \Delta y, \Delta|q/p|, \Delta\phi)$, where Δ represents the difference between the measured value and the fitted parameter value. The contribution of a set of observables to the χ^2 is calculated as $\vec{V} \cdot (M^{-1}) \cdot \vec{V}^T$, where M^{-1} is the inverse of the covariance matrix for the measurement. All covariance matrices are listed in Tables 144 and 145.

8.1.3 Fit results

The global fit uses MINUIT with the MIGRAD minimizer, and all errors are obtained from MINOS [440]. Three separate fits are performed: (a) assuming CP conservation (A_D and ϕ are fixed to zero, $|q/p|$ is fixed to one); (b) assuming no direct CPV (A_D is fixed to zero); and (c) allowing full CPV (all parameters floated). The results are listed in Table 147. For the CPV -allowed fit, individual contributions to the χ^2 are listed in Table 148. The total χ^2 is 31.9 for $30 - 8 = 22$ degrees of freedom; this corresponds to a confidence level of 0.08, which is small but acceptable given the variety of measurements and systematic uncertainties.

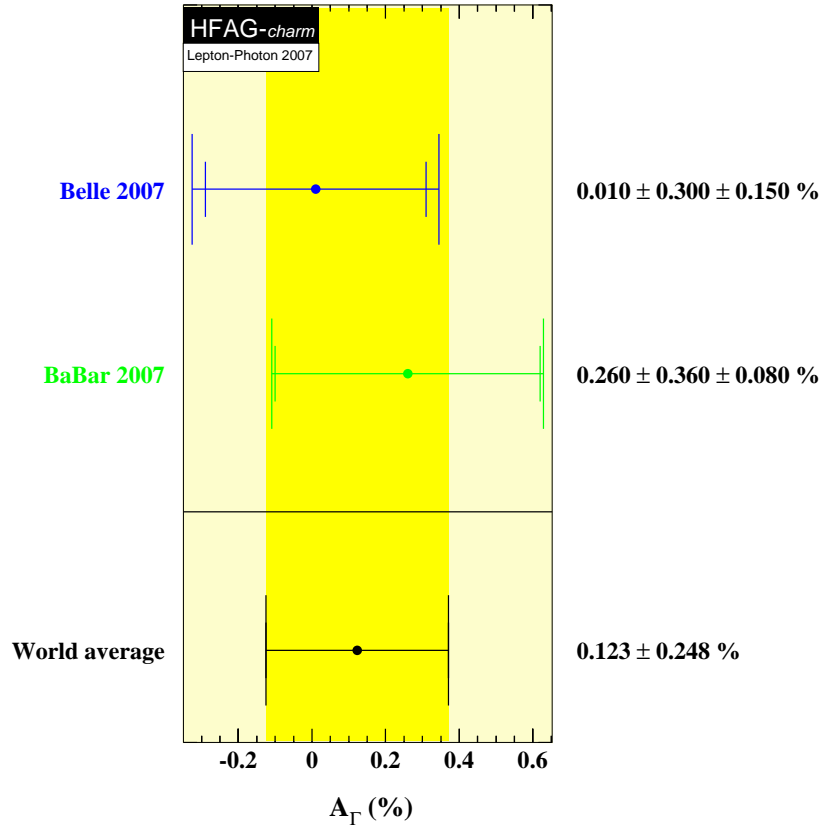
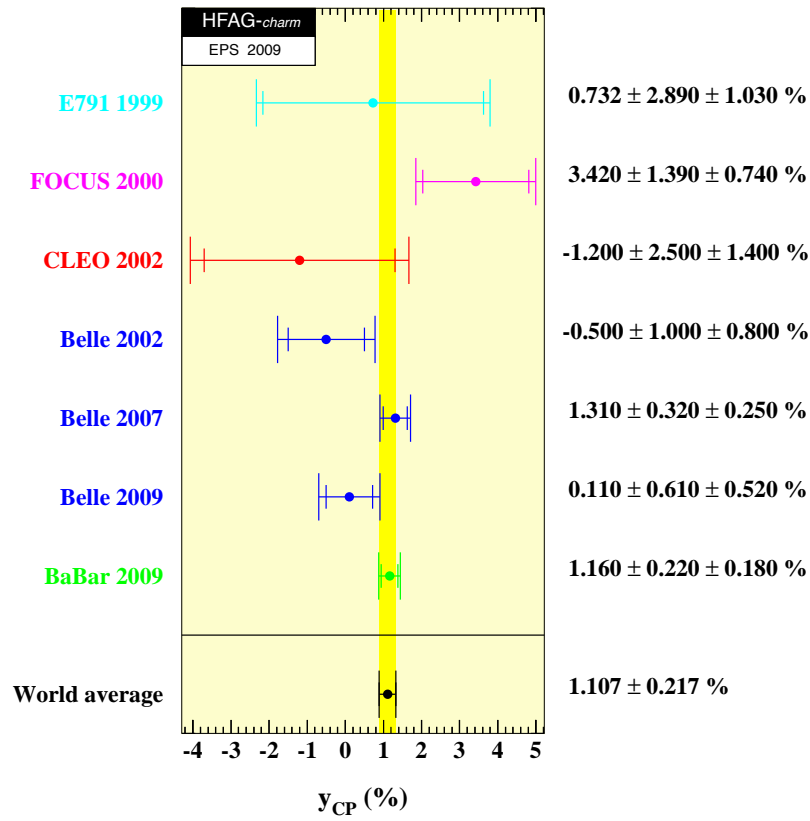


Figure 57: WA values of y_{CP} (top) and A_Γ (bottom) from Ref. [426], as calculated from $D^0 \rightarrow K^+K^-/\pi^+\pi^-$ measurements [418, 435, 436, 437, 438, 439].

Table 145: $D^0 \rightarrow K^+\pi^-$ observables used for the global fit, from Refs. [419, 420, 431].

Mode	Observable	Values	Correlation coefficients
$D^0 \rightarrow K^+\pi^-$ (Babar)	R_D	$(0.303 \pm 0.0189)\%$	$\begin{Bmatrix} 1 & 0.77 & -0.87 \\ 0.77 & 1 & -0.94 \\ -0.87 & -0.94 & 1 \end{Bmatrix}$
	x'^{2+}	$(-0.024 \pm 0.052)\%$	
	y'^+	$(0.98 \pm 0.78)\%$	
$\bar{D}^0 \rightarrow K^-\pi^+$ (Babar)	A_D	$(-2.1 \pm 5.4)\%$	same as above
	x'^{2-}	$(-0.020 \pm 0.050)\%$	
	y'^-	$(0.96 \pm 0.75)\%$	
$D^0 \rightarrow K^+\pi^-$ (Belle)	R_D	$(0.364 \pm 0.018)\%$	$\begin{Bmatrix} 1 & 0.655 & -0.834 \\ 0.655 & 1 & -0.909 \\ -0.834 & -0.909 & 1 \end{Bmatrix}$
	x'^{2+}	$(0.032 \pm 0.037)\%$	
	y'^+	$(-0.12 \pm 0.58)\%$	
$\bar{D}^0 \rightarrow K^-\pi^+$ (Belle)	A_D	$(2.3 \pm 4.7)\%$	same as above
	x'^{2-}	$(0.006 \pm 0.034)\%$	
	y'^-	$(0.20 \pm 0.54)\%$	
$D^0 \rightarrow K^+\pi^-$ + c.c. (CDF)	R_D	$(0.304 \pm 0.055)\%$	$\begin{Bmatrix} 1 & 0.923 & -0.971 \\ 0.923 & 1 & -0.984 \\ -0.971 & -0.984 & 1 \end{Bmatrix}$
	x'^2	$(-0.012 \pm 0.035)\%$	
	y'	$(0.85 \pm 0.76)\%$	

Confidence contours in the two dimensions (x, y) or in $(|q/p|, \phi)$ are obtained by letting, for any point in the two-dimensional plane, all other fitted parameters take their preferred values. The resulting 1σ - 5σ contours are shown in Fig. 58 for the CP -conserving case, and in Fig. 59 for the CPV -allowed case. The contours are determined from the increase of the χ^2 above the minimum value. One observes that the (x, y) contours for the no- CPV fit are almost identical to those for the CPV -allowed fit. In the latter fit, the χ^2 at the no-mixing point $(x, y) = (0, 0)$ is 110 units above the minimum value; for two degrees of freedom this has a confidence level corresponding to 10.2σ . Thus, no mixing is excluded at this high level. In the $(|q/p|, \phi)$ plot, the point $(1, 0)$ is within the 1σ contour; thus the data is consistent with CP conservation.

One-dimensional confidence curves for individual parameters are obtained by letting, for any value of the parameter, all other fitted parameters take their preferred values. The resulting functions $\Delta\chi^2 = \chi^2 - \chi_{\min}^2$ (χ_{\min}^2 is the minimum value) are shown in Fig. 60. The points where $\Delta\chi^2 = 3.84$ determine 95% C.L. intervals for the parameters; these intervals are listed in Table 147.

8.1.4 Conclusions

From the fit results listed in Table 147 and shown in Figs. 59 and 60, we conclude the following:

- the experimental data consistently indicate that D^0 mesons undergo mixing. The no-mixing point $x = y = 0$ is excluded at 10.2σ . The parameter x differs from zero by 2.5σ , and y differs from zero by 5.7σ . This mixing is presumably dominated by long-distance

Table 146: Left: decay modes used to determine fitted parameters x , y , δ , $\delta_{K\pi\pi}$, R_D , A_D , $|q/p|$, and ϕ . Middle: the observables measured for each decay mode. Right: the relationships between the observables measured and the fitted parameters.

Decay Mode	Observables	Relationship
$D^0 \rightarrow K^+ K^- / \pi^+ \pi^-$	y_{CP} A_Γ	$2y_{CP} = (q/p + p/q) y \cos \phi - (q/p - p/q) x \sin \phi$ $2A_\Gamma = (q/p - p/q) y \cos \phi - (q/p + p/q) x \sin \phi$
$D^0 \rightarrow K_S^0 \pi^+ \pi^-$	x y $ q/p $ ϕ	
$D^0 \rightarrow K^+ \ell^- \nu$	R_M	$R_M = (x^2 + y^2)/2$
$D^0 \rightarrow K^+ \pi^- \pi^0$ (Dalitz plot analysis)	x'' y''	$x'' = x \cos \delta_{K\pi\pi} + y \sin \delta_{K\pi\pi}$ $y'' = y \cos \delta_{K\pi\pi} - x \sin \delta_{K\pi\pi}$
“Double-tagged” branching fractions measured in $\psi(3770) \rightarrow DD$ decays	R_M y R_D $\sqrt{R_D} \cos \delta$	$R_M = (x^2 + y^2)/2$
$D^0 \rightarrow K^+ \pi^-$	R_D^+ , R_D^- x'^{2+} , x'^{2-} y'^+ , y'^-	$R_D = (R_D^+ + R_D^-)/2$ $A_D = (R_D^+ - R_D^-)/(R_D^+ + R_D^-)$ $x' = x \cos \delta + y \sin \delta$ $y' = y \cos \delta - x \sin \delta$ $A_M \equiv (q/p ^4 - 1)/(q/p ^4 + 1)$ $x'^{\pm} = [(1 \pm A_M)/(1 \mp A_M)]^{1/4} (x' \cos \phi \pm y' \sin \phi)$ $y'^{\pm} = [(1 \pm A_M)/(1 \mp A_M)]^{1/4} (y' \cos \phi \mp x' \sin \phi)$

Table 147: Results of the global fit for different assumptions concerning CPV .

Parameter	No CPV	No direct CPV	CPV -allowed	CPV -allowed 95% C.L.
x (%)	$0.61^{+0.19}_{-0.20}$	0.59 ± 0.20	0.59 ± 0.20	[0.19, 0.97]
y (%)	0.79 ± 0.13	0.81 ± 0.13	0.80 ± 0.13	[0.54, 1.05]
δ ($^\circ$)	$26.6^{+11.2}_{-12.1}$	$28.3^{+11.3}_{-12.2}$	$27.6^{+11.2}_{-12.2}$	[0.7, 49.5]
R_D (%)	$0.3317^{+0.0080}_{-0.0081}$	$0.3316^{+0.0080}_{-0.0081}$	0.3319 ± 0.0081	[0.316, 0.348]
A_D (%)	—	—	-2.0 ± 2.4	[-6.7, 2.7]
$ q/p $	—	$0.98^{+0.15}_{-0.14}$	$0.91^{+0.19}_{-0.16}$	[0.60, 1.29]
ϕ ($^\circ$)	—	$-2.9^{+6.4}_{-6.6}$	$-10.0^{+9.3}_{-8.7}$	[-26.9, 8.4]
$\delta_{K\pi\pi}$ ($^\circ$)	$21.6^{+22.1}_{-23.2}$	$23.4^{+22.2}_{-23.3}$	$23.2^{+22.3}_{-23.3}$	[-23.2, 66.4]

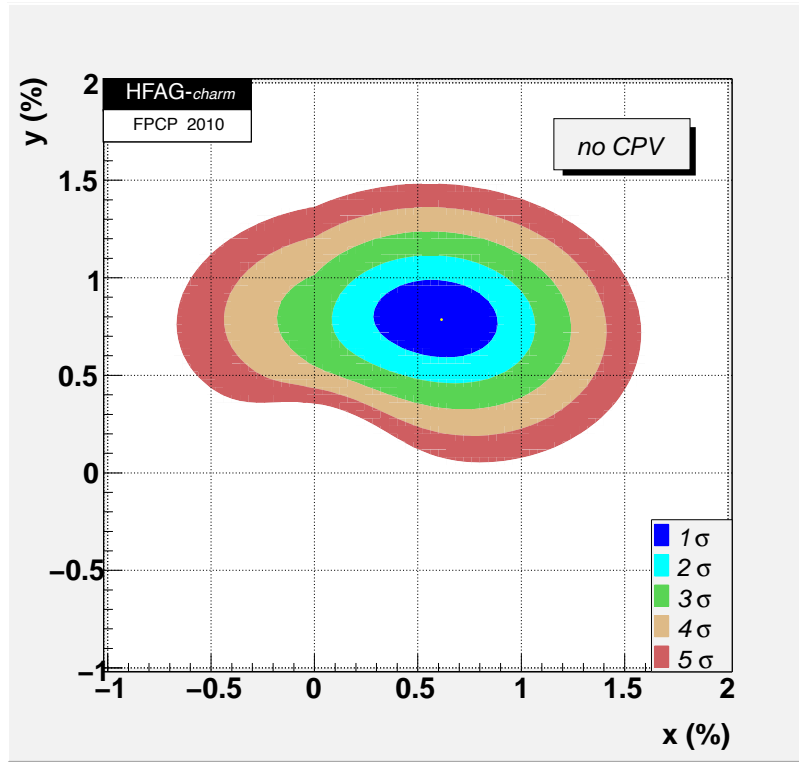


Figure 58: Two-dimensional contours for mixing parameters (x, y) , for no CPV .

processes, which are difficult to calculate. Unless it turns out that $|x| \gg |y|$ [421], which is not indicated, it will probably be difficult to identify new physics from mixing alone.

- Since y_{CP} is positive, the CP -even state is shorter-lived, as in the $K^0-\bar{K}^0$ system. However, since x also appears to be positive, the CP -even state is heavier, unlike in the $K^0-\bar{K}^0$ system.
- There is no evidence (yet) for CPV in the $D^0-\bar{D}^0$ system. Observing CPV at the current level of sensitivity would indicate new physics.

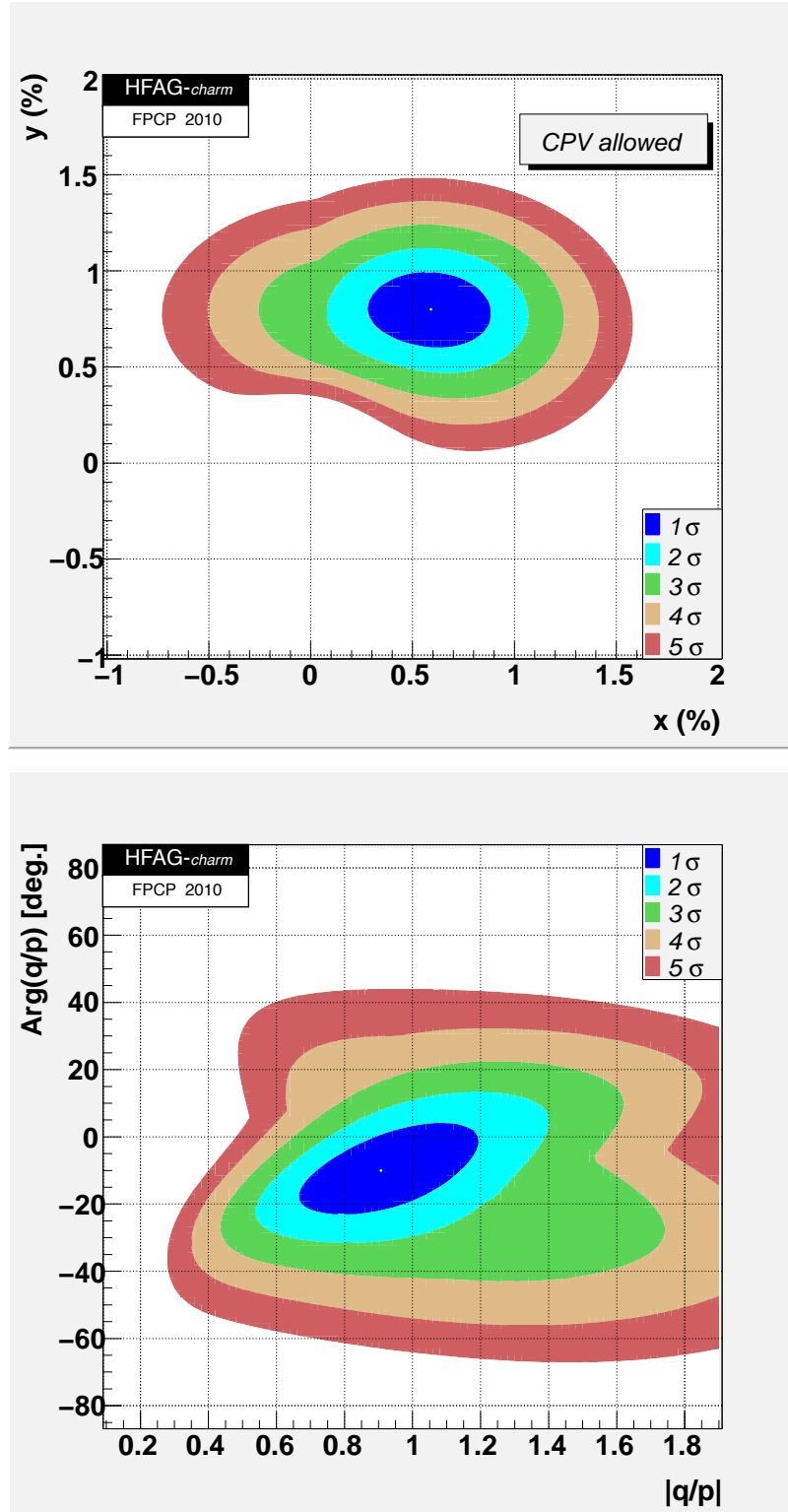


Figure 59: Two-dimensional contours for parameters (x, y) (top) and $(|q/p|, \phi)$ (bottom), allowing for CPV .

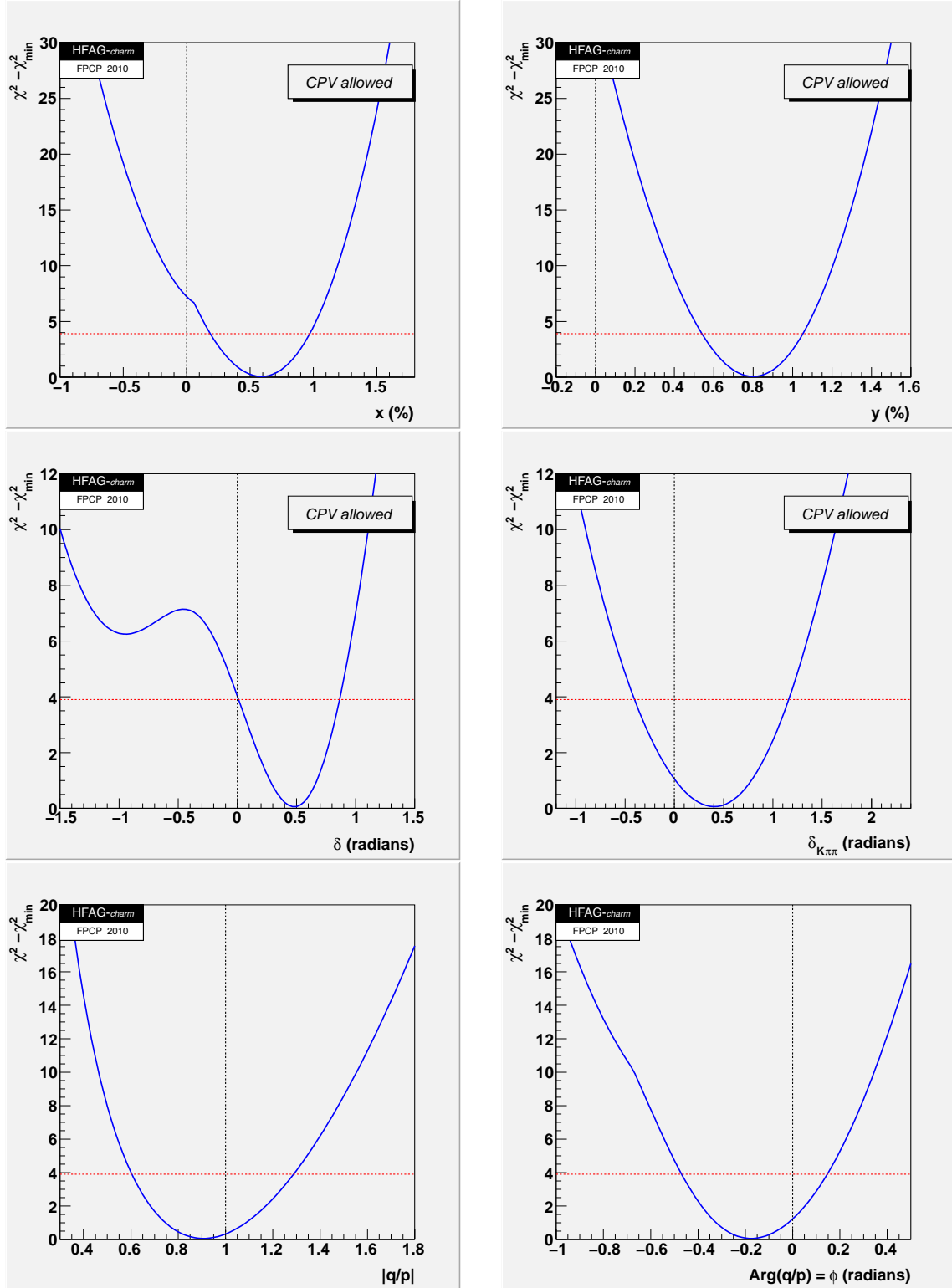


Figure 60: The function $\Delta\chi^2 = \chi^2 - \chi^2_{\min}$ for fitted parameters x , y , δ , $\delta_{K\pi\pi}$, $|q/p|$, and ϕ . The points where $\Delta\chi^2 = 3.84$ (denoted by the dashed horizontal line) determine a 95% C.L. interval.

Table 148: Individual contributions to the χ^2 for the CPV -allowed fit.

Observable	χ^2	$\sum \chi^2$
y_{CP}	2.24	2.24
A_Γ	0.15	2.40
$x_{K^0\pi^+\pi^-}$	0.40	2.80
$y_{K^0\pi^+\pi^-}$	2.15	4.95
$ q/p _{K^0\pi^+\pi^-}$	0.02	4.97
$\phi_{K^0\pi^+\pi^-}$	0.62	5.59
$x_{K^0h^+h^-}$ (BaBar)	2.52	8.11
$y_{K^0h^+h^-}$ (BaBar)	0.69	8.79
$R_M(K^+\ell^-\nu)$	0.09	8.88
$x_{K^+\pi^-\pi^0}$	7.43	16.31
$y_{K^+\pi^-\pi^0}$	0.26	16.57
$R_M/y/R_D/\sqrt{R_D} \cos \delta$ (CLEOc)	5.82	22.39
$R_D^+/x'^{2+}/y'^+$ (Babar)	2.33	24.71
$R_D^-/x'^{2-}/y'^-$ (Babar)	1.55	26.27
$R_D^+/x'^{2+}/y'^+$ (Belle)	4.16	30.43
$R_D^-/x'^{2-}/y'^-$ (Belle)	1.13	31.55
$R_D/x'^2/y'$ (CDF)	0.34	31.89

8.2 Excited $D_{(s)}$ Mesons

Tables 149–151 represent a summary of recent results. For a complete list of related publications, see Ref. [5]. All upper limits (U.L.) correspond to 90% confidence (C.L.) unless otherwise noted. The significances listed are approximate; they are calculated as either $\sqrt{-2\Delta \log \mathcal{L}}$ or $\sqrt{\Delta \chi^2}$, where Δ represents the change in the corresponding minimized function between two hypotheses, e.g., those for different spin states.

The broad charged $J^P = 1^+ c\bar{d}$ state is denoted $D_1(2430)^+$, although it has not yet been observed. The masses and widths of narrow states $D_1(2420)^\pm$, $D_1(2420)^0$, $D_2^*(2460)^0$, $D_2^*(2460)^\pm$ are well-measured, and thus only their averages are given[5]. The same holds for the wide state $D_0^*(2400)^0$. On the other hand for $D_0^*(2400)^\pm$ and $D_1(2430)^0$ the only dedicated measurements available are from [441] and [442], respectively, and hence these measurements are quoted separately. New precise measurements of masses and widths of $D_2^*(2460)^0$ and $D_0^*(2400)^0$ became available recently [443] and are included in the weighted averages³³ shown in Fig. 61. In these averages also the mass of $D_1(2420)^0$ from [445] is used³⁴.

The masses and widths of narrow ($\Gamma \sim 20\text{--}40$ MeV) orbitally excited D mesons (denoted D^{**}), both neutral and charged, are well established. Measurements of broad states ($\Gamma \sim 200\text{--}400$ MeV) are less abundant, as identifying the signal is more challenging. There is a slight discrepancy between the $D_0^*(2400)^0$ masses measured by the Belle[441] and FOCUS[442] experiments. No data exists yet for the $D_1(2430)^\pm$ state. Dalitz plot analyses of $B \rightarrow D^{(*)}\pi\pi$ decays strongly favor the assignments 0^+ and 1^+ for the spin-parity quantum numbers of the $D_0^*(2400)^0/D_0^*(2400)^\pm$ and $D_1(2430)^0$ states, respectively. The measured masses and widths, as well as the J^P values, are in agreement with theoretical predictions based on potential models[446, 447, 448, 449, 450]. The quantitative information on the values of branching fractions for all D^{**} mesons is scarce. In Fig. 61 we include the available measurements from [441, 451] for $D_1(2420)^0$ and from [441, 443] for $D_2^*(2460)^0$. While the branching fractions for B mesons decaying to a narrow D^{**} state and a pion are similar for charged and neutral B initial states, the branching fractions to a broad D^{**} state and π^+ are much larger for B^+ than for B^0 . This may be due to the fact that color-suppressed amplitudes contribute only to the B^+ decay and not to the B^0 decay (for a theoretical discussion, see Ref. [452, 453]).

The first observations of $D_{s1}(2460)^\pm$ and $D_{s0}^*(2317)^\pm$ states are described in Refs. [454] and [455], respectively. The discoveries of the $D_{s0}^*(2317)^\pm$ and $D_{s1}(2460)^\pm$ have triggered increased interest in properties of, and searches for, excited D_s mesons (here generically denoted D_s^{**}). While the masses and widths of $D_{s1}(2536)^\pm$ and $D_{s2}(2573)^\pm$ states are in relatively good agreement with potential model predictions, the masses of $D_{s0}^*(2317)^\pm$ and $D_{s1}(2460)^\pm$ states (and consequently their widths, less than around 5 MeV) are significantly lower than expected (see Ref. [456] for a discussion of $c\bar{s}$ models). Moreover, the mass splitting between these two states greatly exceeds that between the $D_{s1}(2536)^\pm$ and $D_{s2}(2573)^\pm$. These unexpected properties have led to interpretations of the $D_{s0}^*(2317)^\pm$ and $D_{s1}(2460)^\pm$ as exotic four-quark states. Measurements of masses (and the width of $D_{s2}(2573)^\pm$) are averaged by the PDG [5]. In the averages shown in Fig. 62 we include the mass measurement of $D_{s0}^*(2317)^\pm$ and $D_{s1}(2460)^\pm$ from [457]³⁵. Widths of other D_s^{**} mesons are below the current experimental sensitivity and

³³We calculate the weighted average of the PDG [444] and Ref. [443] values.

³⁴PDG does not use values from [445] since they are measured relative to the mass of $D^{(*)\pm}$ mesons.

³⁵We calculate the weighted average of the PDG [444] and Ref. [457] values. The latter are excluded from the PDG average since they are measured relative to the mass of $D_s^{(*)}$ mesons.

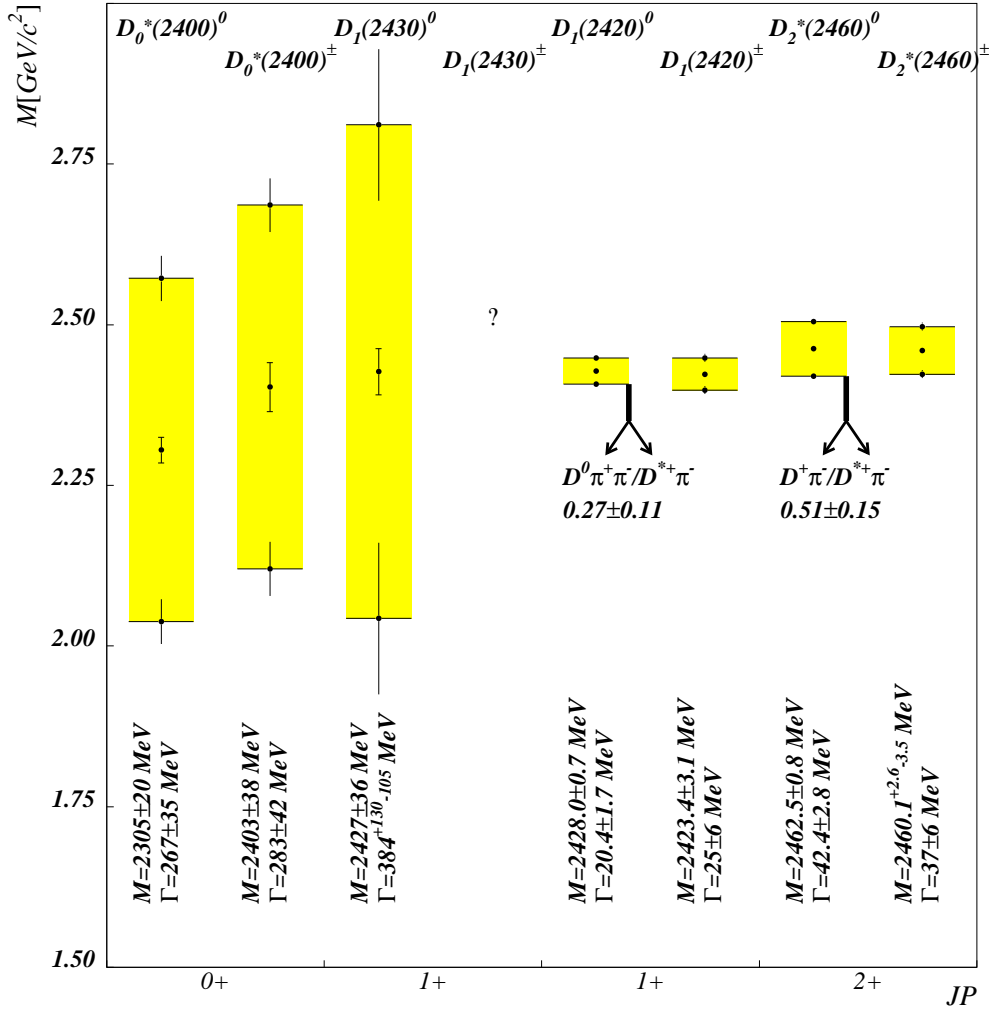


Figure 61: Masses, widths and some branching fractions of orbitally excited D mesons. Shaded regions show the masses and widths of individual states. The central point with error bars denotes the measured mass of each state. Error bars at the edges of the shaded regions denote the uncertainties of the width determination. Divided arrows denote relative branching ratios for the final states marked.

the obtained upper limits are quoted separately.

While there are few measurements with respect to the J^P values of $D_{s0}^*(2317)^\pm$ and $D_{s1}(2460)^\pm$, the available data favors 0^+ and 1^+ , respectively. A molecule-like (DK) interpretation of the $D_{s0}^*(2317)^\pm$ and $D_{s1}(2460)^\pm$ [458, 459] that can account for their low masses and isospin-breaking decay modes is tested by searching for charged and neutral isospin partners of these states; thus far such searches have yielded negative results. Hence the subset of models that predict equal production rates for different charged states is nominally excluded. The molecular picture can also be tested by measuring the rates for the radiative processes $D_{s0}^*(2317)^\pm / D_{s1}(2460)^\pm \rightarrow D_s^{(*)} \gamma$ and comparing to theoretical predictions. The predicted rates, however, are below the sensitivity of current experiments. Another model successful in explaining the total widths

and the $D_{s0}^*(2317)^\pm$ - $D_{s1}(2460)^\pm$ mass splitting is based on the assumption that these states are chiral partners of the ground states D_s^+ and $D_s^{*\pm}$ [460]. While some measured branching fraction ratios agree with predicted values, further experimental tests with better sensitivity are needed to confirm or refute this scenario.

In addition to the $D_{s0}^*(2317)^\pm$ and $D_{s1}(2460)^\pm$ states, other excited D_s states may have been observed. SELEX has reported a $D_{sJ}(2632)^\pm$ candidate [461], but this has not been confirmed by other experiments. Belle and BaBar have observed $D_{sJ}(2700)^\pm$ and $D_{sJ}(2860)^\pm$ states [462, 463], which may be radial excitations of the $D_s^{*\pm}$ and $D_{s0}^*(2317)^\pm$, respectively (see for example [464]). However, the $D_{sJ}(2860)^\pm$ has been searched for in B decays and not observed, which may indicate that this state has higher spin. Recently new precise measurements of $D_{sJ}(2700)^\pm$ and $D_{sJ}(2860)^\pm$ properties were performed by BaBar [465]. The weighted average of the results from [462, 465] is $M(D_{s1}(2700)^\pm) = (2709 \pm 8) \text{ MeV}/c^2$ and $\Gamma(D_{s1}(2700)^\pm) = (126 \pm 31) \text{ MeV}$. In the same paper BaBar observes another state, denoted $D_{sJ}(3040)^\pm$, with a significance of 6 standard deviations. According to calculations of [464] this state is a candidate for the radial excitation of $D_{s1}(2460)^\pm$ or $D_{s1}(2536)^\pm$.

The existing studies of $D_{s1}(2460)^\pm$ provide for sufficient information that the individual branching fractions are calculated by HFAG; they are shown in Fig. 62. Beside this the relative branching ratios of $D_{s1}(2536)^\pm$ are shown [466, 467]. Measurements of individual branching fractions of D_s^{**} are difficult due to the unknown fragmentation of $c\bar{c} \rightarrow D_s^{**}$ (in the studies where D_s^{**} mesons are produced in $c\bar{c}$ fragmentation) or due to the unknown $B \rightarrow D_s^{**} X$ branching fractions (in the studies where D_s^{**} are produced in B meson decays).

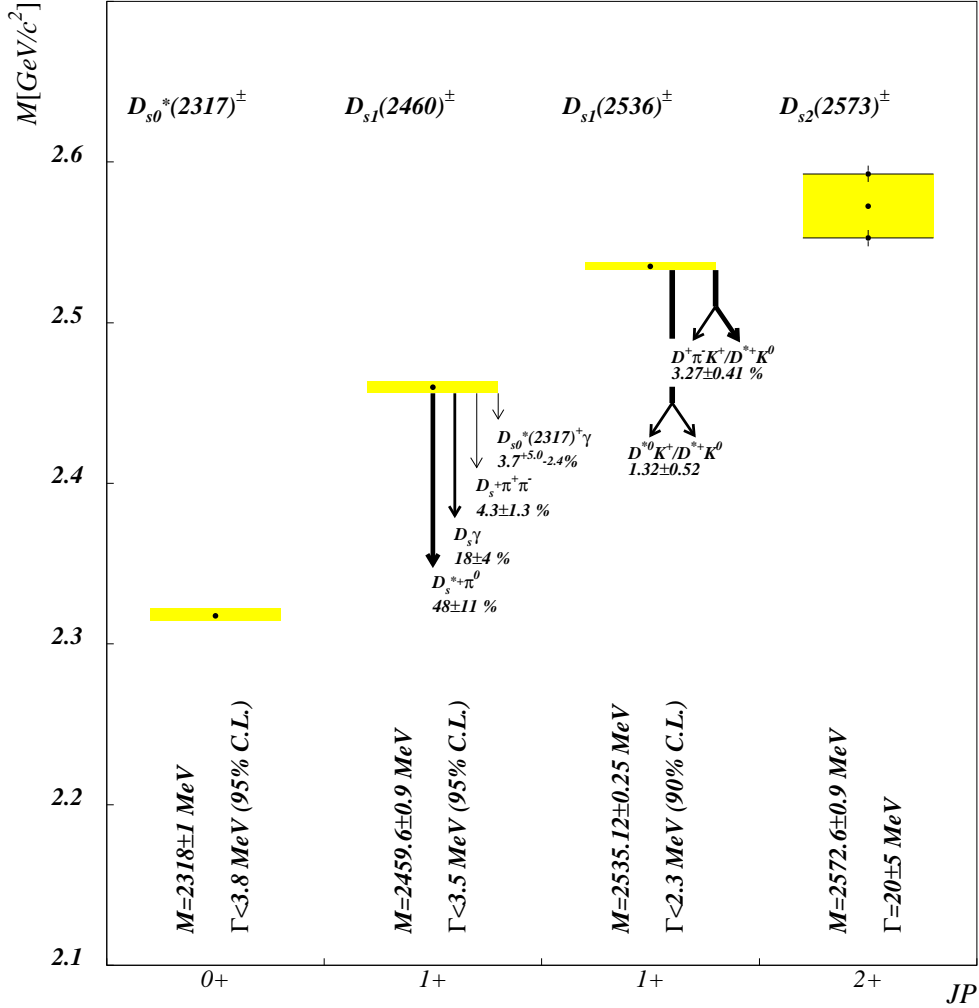


Figure 62: Masses, widths and some branching fractions of orbitally excited D_s mesons. Shaded regions show the masses and widths of individual states (U.L. on the widths in case of $D_{s0}^*(2317)^{\pm}$, $D_{s1}(2460)^{\pm}$, and $D_{s1}(2536)^{\pm}$). The central point with error bars denotes the measured mass of each state. Error bars at the edges of the shaded regions denote the uncertainties of the width determination. Arrows (divided arrows) denote branching fractions (relative branching ratios) for the final states marked.

Table 149: Recent results for properties of D^{**} mesons.

	Main results	Reference	Comments
Masses [MeV/ c^2], widths [MeV]	$M(D_0^*(2400)^0) : 2352 \pm 50$; $\Gamma(D_0^*(2400)^0) : 261 \pm 50$ $M(D_2^*(2460)^0) : 2461.1 \pm 1.6$; $\Gamma(D_2^*(2460)^0) : 43 \pm 4$ $M(D_2^*(2460)^\pm) : 2460.1^{+2.6}_{-3.5}$; $\Gamma(D_2^*(2460)^\pm) : 37 \pm 6$ $M(D_1(2420)^0) : 2422.3 \pm 1.3$; $\Gamma(D_1(2420)^0) : 20.4 \pm 1.7$ $M(D_1(2420)^\pm) : 2423.4 \pm 3.1$; $\Gamma(D_1(2420)^\pm) : 25 \pm 6$	[444]	PDG average; to $M(D_0^*(2400)^0)$ and $\Gamma(D_0^*(2400)^0)$ from [442] also $D_1(2430)^0$ may contribute
	$M(D_1(2430)^0) : 2427 \pm 26 \pm 20 \pm 15$ $\Gamma(D_1(2430)^0) : 384 \pm^{107}_{75} \pm 24 \pm 70$	[441]	last error due to Dalitz model
	$M(D_0^*(2400)^\pm/D_1(2430)^\pm) : 2403 \pm 14 \pm 35$ $\Gamma(D_0^*(2400)^\pm/D_1(2430)^\pm) : 283 \pm 24 \pm 34$	[442]	$D_0^*(2400)^\pm/D_1(2430)^\pm$ may contribute to signal
	$M(D_2^*(2460)^\pm) : 2463.3 \pm 0.6 \pm 0.8$ $M(D_1(2430)^0) : 2421.7 \pm 0.7 \pm 0.6$	[445]	M measured relative to $M^{(*)\pm}$
Branching fractions [10^{-4}]	$B^- \rightarrow D_0^*(2400)^0 \pi^-$, $D_0^*(2400)^0 \rightarrow D^+ \pi^- : 6.1 \pm 0.6 \pm 0.9 \pm 1.6$ $B^- \rightarrow D_2^*(2460)^0 \pi^-$, $D_2^*(2460)^0 \rightarrow D^+ \pi^- : 3.4 \pm 0.3 \pm 0.6 \pm 0.4$ $B^- \rightarrow D_1(2420)^0 \pi^-$, $D_1(2420)^0 \rightarrow D^{*+} \pi^- : 6.8 \pm 0.7 \pm 1.3 \pm 0.3$ $B^- \rightarrow D_2^*(2460)^0 \pi^-$, $D_2^*(2460)^0 \rightarrow D^{*+} \pi^- : 1.8 \pm 0.3 \pm 0.3 \pm 0.2$ $B^- \rightarrow D_1(2430)^0 \pi^-$, $D_1(2430)^0 \rightarrow D^{*+} \pi^- : 5.0 \pm 0.4 \pm 1.0 \pm 0.4$	[441]	
	$\bar{B}^0 \rightarrow D_2^*(2460)^+ \pi^-$, $D_2^*(2460)^+ \rightarrow D^0 \pi^+ : 2.15 \pm 0.17 \pm 0.29 \pm 0.12$ $\bar{B}^0 \rightarrow D_0^*(2400)^+ \pi^-$, $D_0^*(2400)^+ \rightarrow D^0 \pi^+ : 0.60 \pm 0.13 \pm 0.15 \pm 0.22$	[468]	last error due to Dalitz model; $M(D_0^*(2400)^\pm) = M(D_0^*(2400)^0)$, $\Gamma(D_0^*(2400)^\pm) = \Gamma(D_0^*(2400)^0)$ assumed
	$B^- \rightarrow D_1(2420)^0 \pi^-$, $D_1(2420)^0 \rightarrow D^0 \pi^+ \pi^- : 1.85 \pm 0.29 \pm 0.35 \pm^{0.00}_{0.43}$ $\bar{B}^0 \rightarrow D_1(2420)^+ \pi^-$, $D_1(2420)^+ \rightarrow D^+ \pi^+ \pi^- : 0.89 \pm 0.15 \pm 0.17 \pm^{0.00}_{0.27}$	[451]	last error due to possible $D_2^*(2460)^0$, $D_2^*(2460)^\pm$ contr.
	$B^- \rightarrow D_2^*(2460)^0 \pi^-$, $D_2^*(2460)^0 \rightarrow D^+ \pi^- : 3.5 \pm 0.2 \pm 0.2 \pm 0.4$ $B^- \rightarrow D_0^*(2400)^0 \pi^-$, $D_0^*(2400)^0 \rightarrow D^+ \pi^- : 6.8 \pm 0.3 \pm 0.4 \pm 2.0$	[443]	last error due to Blatt-Weisskopf factors and sig./bkg. composition
	$D_0^*(2400)^0 : 0^+$	[441]	0^+ preferred over 1^- , 2^+ with sign. $> 10\sigma$
	$D_1(2430)^0 : 1^+$	[441]	1^+ preferred over 0^- , 1^- , 2^+ with sign. $> 10\sigma$
Quantum numbers (J^P)	$D_0^*(2400)^\pm : 0^+$	[468]	0^+ preferred over 1^- , 2^+ with sign. $\sim 5\sigma$

Table 150: Recent results for masses and branching fractions of excited D_s mesons.

	Main results	Reference	Comments
Masses [MeV/c ²], widths [MeV]	$M(D_{s0}^*(2317)^\pm) : 2318.0 \pm 1.0$ $M(D_{s1}(2460)^\pm) : 2459.6 \pm 0.9$ $M(D_{s1}(2536)^\pm) : 2353.12 \pm 0.25$ $M(D_{s2}(2573)^\pm) : 2572.6 \pm 0.9$ $\Gamma(D_{s2}(2573)^\pm) : 20 \pm 5$	[444]	PDG average
	$M(D_{s0}^*(2317)^\pm) : 2317.2 \pm 0.5 \pm 0.9$ $\Gamma(D_{s0}^*(2317)^\pm) : < 4.6$ $M(D_{s1}(2460)^\pm) : 2459.9 \pm 0.9 \pm 1.6$ $\Gamma(D_{s1}(2460)^\pm) : < 5.5$	[457]	M measured relative to $M(D_s^*)$
	$\Gamma(D_{s0}^*(2317)^\pm) : < 3.8$ $\Gamma(D_{s1}(2460)^\pm) : < 3.5$	[469]	95% C.L. U.L.
	$\Gamma(D_{s1}(2536)^\pm) : < 2.3$	[470]	
	$M(D_{sJ}(2700)^\pm) : 2710 \pm 2 \pm {}^{12}_7$; $\Gamma(D_{sJ}(2700)^\pm) : 149 \pm 7 \pm {}^{39}_{52}$ $M(D_{sJ}(2860)^\pm) : 2862 \pm 2 \pm {}^5_2$; $\Gamma(D_{sJ}(2860)^\pm) : 48 \pm 3 \pm 6$ $M(D_{sJ}(3040)^\pm) : 3044 \pm 8 \pm {}^{30}_5$; $\Gamma(D_{sJ}(3040)^\pm) : 239 \pm 35 \pm {}^{46}_{42}$	[465]	$D_{sJ}(3040)^\pm$ sign. 6σ
	$M(D_{sJ}(2700)^\pm) : 2708 \pm 9 \pm {}^{11}_{10}$; $\Gamma(D_{sJ}(2700)^\pm) : 108 \pm 23 \pm {}^{36}_{31}$	[462]	
	$M(D_{sJ}(2632)^\pm) : 2632.5 \pm 1.7$; $\Gamma(D_{sJ}(2700)^\pm) : < 17$	[461]	not seen by other exp's; sys. err. not given
	$D_{s1}(2460)^\pm \rightarrow D_s^{*+}\pi^0 : (48 \pm 11)\%$ $D_{s1}(2460)^\pm \rightarrow D_s^+\gamma : (18 \pm 4)\%$ $D_{s1}(2460)^\pm \rightarrow D_s^+\pi^+\pi^- : (4.3 \pm 1.3)\%$ $D_{s1}(2460)^\pm \rightarrow D_{s0}^*(2317)^\pm\gamma : (3.7 \pm {}^{5.0}_{2.4})\%$	[444]	
	$B^0 \rightarrow D^- D_{s0}(2317)^+, D_{s0}(2317)^+ \rightarrow D_s^+\pi^0 : 8.6 \pm {}^{3.3}_{2.6} \pm 2.6$ $B^0 \rightarrow D^- D_{s1}(2460)^+, D_{s1}(2460)^+ \rightarrow D_s^{*+}\pi^0 : 22.7 \pm {}^{7.3}_{6.2} \pm 6.8$ $B^0 \rightarrow D^- D_{s1}(2460)^+, D_{s1}(2460)^+ \rightarrow D_s^+\gamma : 8.2 \pm {}^{2.2}_{1.9} \pm 2.5$	[471]	further br. frac. for B^0, B^\pm in paper
	$B^0 \rightarrow D^- D_{s0}(2317)^+, D_{s0}(2317)^+ \rightarrow D_s^+\pi^0 : 18 \pm 4 \pm 3 \pm {}^6_4$ $B^0 \rightarrow D^- D_{s1}(2460)^+, D_{s1}(2460)^+ \rightarrow D_s^{*+}\pi^0 : 28 \pm 8 \pm 5 \pm {}^{10}_6$ $B^0 \rightarrow D^- D_{s1}(2460)^+, D_{s1}(2460)^+ \rightarrow D_s^+\gamma : 8 \pm 2 \pm 1 \pm {}^3_2$	[472]	further br. frac. for B^0, B^\pm in paper; last error from $B(D, D_s^+)$
$\frac{B(D_{s1}(2460)^\pm \rightarrow D_s^+\gamma)}{B(D_{s1}(2460)^\pm \rightarrow D_s^\pm\pi^0)} = 0.55 \pm 0.13 \pm 0.08$ $\frac{B(D_{s1}(2460)^\pm \rightarrow D_s^+\pi^+\pi^-)}{B(D_{s1}(2460)^\pm \rightarrow D_s^\pm\pi^0)} = 0.14 \pm 0.04 \pm 0.02$ $\frac{\sigma(D_{s1}(2536)^\pm)B(D_{s1}(2536)^\pm \rightarrow D_s^+\pi^+\pi^-)}{\sigma(D_{s1}(2460)^\pm)B(D_{s1}(2460)^\pm \rightarrow D_s^\pm\pi^0)} = 1.05 \pm 0.32 \pm 0.06$	[457]		
$B \rightarrow D_{s0}^*(2317)^\pm K^\mp, D_{s0}^*(2317)^\pm \rightarrow D_s^+\pi^0 :$ $0.53 \pm {}^{0.15}_{0.13} \pm 0.07 \pm 0.14$ $B \rightarrow D_{s1}(2460)^\pm K^\mp, D_{s1}(2460)^\pm \rightarrow D_s^+\gamma : < 0.094$	[473]	last error due to $B(D_s^+)$	
$\frac{\sigma(D_{s0}^*(2317)^\pm)B(D_{s0}^*(2317)^\pm \rightarrow D_s^+\pi^0)}{\sigma(D_s^+)}$ $\frac{\sigma(D_{s1}(2460)^\pm)B(D_{s1}(2460)^\pm \rightarrow D_s^\pm\pi^0)}{\sigma(D_s^+)} = (7.9 \pm 1.2 \pm 0.4) \cdot 10^{-2}$ $\frac{\sigma(D_{s1}(2460)^\pm)B(D_{s1}(2460)^\pm \rightarrow D_s^\pm\pi^0)}{\sigma(D_s^+)} = (3.5 \pm 0.9 \pm 0.2) \cdot 10^{-2}$	[455]		
$\frac{B(D_{s1}(2536)^\pm \rightarrow D^\pm\pi^+K^\pm)}{B(D_{s1}(2536)^\pm \rightarrow D^*\pi^+K^0)} = (3.27 \pm 0.18 \pm 0.37)\%$	[466]		
$B \rightarrow D_{s1}(2536)^\pm D^\mp : 1.71 \pm 0.48 \pm 0.32$ $B \rightarrow D_{s1}(2536)^\pm D^{*\mp} : 3.32 \pm 0.88 \pm 0.66$ $B^+ \rightarrow D_{s1}(2536)^+ \bar{D}^0 : 2.16 \pm 0.52 \pm 0.45$ $B^+ \rightarrow D_{s1}(2536)^+ \bar{D}^{*0} : 5.46 \pm 1.17 \pm 1.04$	[474]	$D_{s1}(2536)^+ \rightarrow D^{*0}K^+$ used; br. frac. with $D_{s1}(2536)^+ \rightarrow D^{*+}K^0$ in paper	
$\frac{B(D_{s1}(2536)^+ \rightarrow D^{*0}K^+)}{B(D_{s1}(2536)^+ \rightarrow D^{*+}K^0)} = 1.32 \pm 0.47 \pm 0.23$	[467]		
$B^+ \rightarrow D_{sJ}(2700)^+ \bar{D}^0, D_{sJ}(2700)^+ \rightarrow D^0K^+ : 11.3 \pm 2.2 \pm {}^{1.4}_{2.8}$	[462]		
$\frac{B(D_{s1}(2460)^\pm \rightarrow D_s^+\gamma)}{B(D_{s1}(2460)^\pm \rightarrow D_s^+\pi^0\gamma)} = 0.337 \pm 0.036 \pm 0.038$ $\frac{B(D_{s1}(2460)^\pm \rightarrow D_s^+\pi^+\pi^-)}{B(D_{s1}(2460)^\pm \rightarrow D_s^+\pi^0\gamma)} = 0.077 \pm 0.013 \pm 0.008$	[469]	95% C.L. U.L.	
$B(D_{s1}(2460)^\pm \rightarrow D_s^\pm\pi^0) = (56 \pm 13 \pm 9)\%$ $B(D_{s1}(2460)^\pm \rightarrow D_s^+\gamma) = (16 \pm 4 \pm 3)\%$	[475]		
$\frac{B(D_{sJ}(2632)^+ \rightarrow D^0K^+)}{B(D_{sJ}(2632)^+ \rightarrow D_s^+\eta)} = 0.14 \pm 0.06$	[461]	not seen by other exp's; sys. err. not given	
$\frac{B(D_{sJ}(2700)^\pm \rightarrow D^{*0}K^+)}{D_{sJ}(2700)^\pm \rightarrow D^0K^+} = 0.91 \pm 0.13 \pm 0.12$ $\frac{B(D_{sJ}(2860)^\pm \rightarrow D^{*0}K^+)}{D_{sJ}(2860)^\pm \rightarrow D^0K^+} = 1.10 \pm 0.15 \pm 0.19$	[465]		

Table 151: Recent results for quantum numbers of excited D_s mesons.

Quantum numbers (J^P)	Main results	Reference	Comments
	$\frac{\mathcal{A}_{L=2}(D_{s1}(2536)^\pm \rightarrow D^{*\pm} K_S)}{\mathcal{A}_{L=0}(D_{s1}(2536)^\pm \rightarrow D^{*\pm} K_S)} = (0.63 \pm 0.07 \pm 0.02) \text{Exp}[\pm i(0.76 \pm 0.03 \pm 0.01)]$	[473]	D-/S-wave amp. ratio
	$D_{s0}^*(2317)^\pm : 0^+, 1^-, 2^+, \dots$	[454]	natural J^P based on J^P conserv.
	$D_{s1}(2536)^\pm : 1^+, 1^-$	[474]	1^- preferred over 2^+ with sign. $\sim 4\sigma$; 1^+ preferred over 2^- with sign. $\sim 3\sigma$;
	$D_{sJ}(2700)^\pm : 1^-$	[462]	1^- preferred over $0^+, 2^+$ with sign. $> 10\sigma$
	$D_{sJ}(2700)^\pm, D_{sJ}(2860)^\pm : 1^-, 2^+, \dots$	[465]	natural J^P preferred based on helicity angle distrib.; 0^+ ruled out due to $D_{sJ} \rightarrow D^* K$
	$D_{s1}(2460)^\pm : 1^+$	[471]	1^+ preferred over 2^- with sign. $\sim 6\sigma$
	$D_{s1}(2460)^\pm : J \neq 0$	[469]	0^- disfavored with sign. $\sim 5\sigma$; assuming decay $D_{s1}(2460)^\pm \rightarrow D_s^{*\pm} \pi^0 \rightarrow D_s^+ \gamma \pi^0$

8.3 Semileptonic Decays

8.3.1 Introduction

Semileptonic decays of D mesons involve the interaction of a leptonic current with a hadronic current. The latter is nonperturbative and cannot be calculated from first principles; thus it is usually parameterized in terms of form factors. The transition matrix element is written

$$\mathcal{M} = -i \frac{G_F}{\sqrt{2}} V_{cq} L^\mu H_\mu, \quad (194)$$

where G_F is the Fermi constant and V_{cq} is a CKM matrix element. The leptonic current L_μ is evaluated directly from the lepton spinors and has a simple structure; this allows one to extract information about the form factors (in H_μ) from data on semileptonic decays [476]. Conversely, because there are no final-state interactions between the leptonic and hadronic systems, semileptonic decays for which the form factors can be calculated allow one to determine V_{cq} [2].

8.3.2 $D \rightarrow P\ell\nu$ Decays

When the final state hadron is a pseudoscalar, the hadronic current is given by

$$H_\mu = \langle P(p) | \bar{q} \gamma^\mu c | D(p') \rangle = f_+(q^2) \left[(p' + p)^\mu - \frac{M_D^2 - m_P^2}{q^2} q^\mu \right] + f_0(q^2) \frac{M_D^2 - m_P^2}{q^2} q^\mu, \quad (195)$$

where M_D and p' are the mass and four momentum of the parent D meson, m_P and p are those of the daughter meson, $f_+(q^2)$ and $f_0(q^2)$ are form factors, and $q = p' - p$. Kinematics require that $f_+(0) = f_0(0)$. The contraction $q^\mu L_\mu$ results in terms proportional to m_ℓ [477], and thus for $\ell = e, \mu$ the last two terms in Eq. (195) are negligible. Thus, only the $f_+(q^2)$ form factor is relevant. The differential partial width is

$$\frac{d\Gamma(D \rightarrow P\ell\bar{\nu}_\ell)}{dq^2 d\cos\theta_\ell} = \frac{G_F^2 |V_{cq}|^2}{32\pi^3} p^{*3} |f_+(q^2)|^2 \sin^2\theta_\ell, \quad (196)$$

where p^* is the magnitude of the momentum of the final state hadron in the D rest frame.

The form factor is traditionally parametrized with an explicit pole and a sum of effective poles:

$$f_+(q^2) = \frac{f(0)}{1 - \alpha} \left(\frac{1}{1 - q^2/m_{\text{pole}}^2} \right) + \sum_{k=1}^N \frac{\rho_k}{1 - q^2/(\gamma_k m_{\text{pole}}^2)}, \quad (197)$$

where ρ_k and γ_k are expansion parameters. The parameter m_{pole} is the mass of the lowest-lying $c\bar{q}$ resonance with the appropriate quantum numbers; this is expected to provide the largest contribution to the form factor for the $c \rightarrow q$ transition. For example, for $D \rightarrow \pi$ transitions the dominant resonance is expected to be D^* , and thus $m_{\text{pole}} = m_{D^*}$.

8.3.3 Simple Pole

Equation (197) can be simplified by neglecting the sum over effective poles, leaving only the explicit vector meson pole. This approximation is referred to as “nearest pole dominance” or

“vector-meson dominance.” The resulting parameterization is

$$f_+(q^2) = \frac{f_+(0)}{(1 - q^2/m_{\text{pole}}^2)}. \quad (198)$$

However, values of m_{pole} that give a good fit to the data do not agree with the expected vector meson masses [478]. To address this problem, the “modified pole” or Becirevic-Kaidalov (BK) parameterization [479] was introduced. This parametrization assumes that gluon hard-scattering contributions (δ) are near zero, and scaling violations (β) are near unity [478]:

$$1 + 1/\beta - \delta \equiv \frac{(M_D^2 - m_P^2)}{f_+(0)} \left. \frac{df_+}{dq^2} \right|_{q^2=0} \approx 2. \quad (199)$$

The parameterization takes the form

$$f_+(q^2) = \frac{f_+(0)}{(1 - q^2/m_{\text{pole}}^2)} \left(1 - \alpha_{\text{BK}} \frac{q^2}{m_{\text{pole}}^2} \right). \quad (200)$$

To be consistent with $1 + 1/\beta - \delta \approx 2$, the parameter α_{BK} should be near the value 1.75.

This parameterization has been used by several experiments to determine form factor parameters. Measured values of m_{pole} and α_{BK} are listed Tables 152 and 153 for $D \rightarrow K\ell\nu$ and $D \rightarrow \pi\ell\nu$ decays, respectively. Both tables show α_{BK} to be substantially lower than the expected value of ~ 1.75 .

Table 152: Results for m_{pole} and α_{BK} from various experiments for $D^0 \rightarrow K^-\ell^+\nu$ and $D^+ \rightarrow K_S\ell^+\nu$ decays. The last entry is a lattice QCD prediction.

$D \rightarrow K\ell\nu$ Expt.	Ref.	m_{pole} (GeV/ c^2)	α_{BK}
CLEO III	[480]	$1.89 \pm 0.05^{+0.04}_{-0.03}$	$0.36 \pm 0.10^{+0.03}_{-0.07}$
FOCUS	[481]	$1.93 \pm 0.05 \pm 0.03$	$0.28 \pm 0.08 \pm 0.07$
BELLE	[482]	$1.82 \pm 0.04 \pm 0.03$	$0.52 \pm 0.08 \pm 0.06$
BaBar	[483]	$1.884 \pm 0.012 \pm 0.016$	$0.377 \pm 0.023 \pm 0.031$
CLEO-c ($D^0 \rightarrow K^+$)	[484]	$1.943^{+0.037}_{-0.033} \pm 0.011$	$0.258^{+0.063}_{-0.065} \pm 0.020$
CLEO-c ($D^0 \rightarrow K^+$)	[485]	$1.97 \pm 0.03 \pm 0.01$	$0.21 \pm 0.05 \pm 0.03$
CLEO-c ($D^+ \rightarrow K_S$)	[484]	$2.02^{+0.07}_{-0.06} \pm 0.02$	$0.127^{+0.099}_{-0.104} \pm 0.031$
CLEO-c ($D^+ \rightarrow K_S$)	[485]	$1.96 \pm 0.04 \pm 0.02$	$0.22 \pm 0.08 \pm 0.03$
Fermilab lattice/MILC/HPQCD	[486]	–	0.50 ± 0.04

8.3.4 z Expansion

Several groups have advocated an alternative series expansion around some value $q^2 = t_0$ to parameterize f_+ [487, 488, 489, 476]. This expansion is given in terms of a complex parameter z , which is the analytic continuation of q^2 into the complex plane:

$$z(q^2, t_0) = \frac{\sqrt{t_+ - q^2} - \sqrt{t_+ - t_0}}{\sqrt{t_+ - q^2} + \sqrt{t_+ - t_0}}, \quad (201)$$

Table 153: Results for m_{pole} and α_{BK} from various experiments for $D^0 \rightarrow \pi^- \ell^+ \nu$ and $D^+ \rightarrow \pi^0 \ell^+ \nu$ decays. The last entry is a lattice QCD prediction.

$D \rightarrow \pi \ell \nu$ Expt.	Ref.	m_{pole} (GeV/ c^2)	α_{BK}
CLEO III	[480]	$1.86^{+0.10+0.07}_{-0.06-0.03}$	$0.37^{+0.20}_{-0.31} \pm 0.15$
FOCUS	[481]	$1.91^{+0.30}_{-0.15} \pm 0.07$	–
BELLE	[482]	$1.97 \pm 0.08 \pm 0.04$	$0.10 \pm 0.21 \pm 0.10$
CLEO-c ($D^0 \rightarrow \pi^+$)	[484]	$1.941^{+0.042}_{-0.034} \pm 0.009$	$0.20^{+0.10}_{-0.11} \pm 0.03$
CLEO-c ($D^0 \rightarrow \pi^+$)	[485]	$1.87 \pm 0.03 \pm 0.01$	$0.37 \pm 0.08 \pm 0.03$
CLEO-c ($D^+ \rightarrow \pi^0$)	[484]	$1.99^{+0.11}_{-0.08} \pm 0.06$	$0.05^{+0.19}_{-0.22} \pm 0.13$
CLEO-c ($D^+ \rightarrow \pi^0$)	[485]	$1.97 \pm 0.07 \pm 0.02$	$0.14 \pm 0.16 \pm 0.04$
Fermilab lattice/MILC/HPQCD	[486]	–	0.44 ± 0.04

where $t_{\pm} \equiv (M_D \pm m_h)^2$ and t_0 is the (arbitrary) q^2 value corresponding to $z = 0$. The physical region corresponds to $|z| < 1$.

The form factor is expressed as

$$f_+(q^2) = \frac{1}{P(q^2) \phi(q^2, t_0)} \sum_{k=0}^{\infty} a_k(t_0) [z(q^2, t_0)]^k, \quad (202)$$

where the $P(q^2)$ factor accommodates sub-threshold resonances via

$$P(q^2) \equiv \begin{cases} 1 & (D \rightarrow \pi) \\ z(q^2, M_{D_s^*}^2) & (D \rightarrow K). \end{cases} \quad (203)$$

The “outer” function $\phi(t, t_0)$ can be any analytic function, but a preferred choice (see, *e.g.* Refs. [487, 488, 490]) obtained from the Operator Product Expansion (OPE) is

$$\phi(q^2, t_0) = \alpha \left(\sqrt{t_+ - q^2} + \sqrt{t_+ - t_0} \right) \times \frac{t_+ - q^2}{(t_+ - t_0)^{1/4}} \frac{(\sqrt{t_+ - q^2} + \sqrt{t_+ - t_0})^{3/2}}{(\sqrt{t_+ - q^2} + \sqrt{t_+})^5}, \quad (204)$$

with $\alpha = \sqrt{\pi m_c^2/3}$. The OPE analysis provides a constraint upon the expansion coefficients, $\sum_{k=0}^N a_k^2 \leq 1$. These coefficients receive $1/M$ corrections, and thus the constraint is only approximate. However, the expansion is expected to converge rapidly since $|z| < 0.051$ (0.17) for $D \rightarrow K$ ($D \rightarrow \pi$) over the entire physical q^2 range, and Eq. (202) remains a useful parameterization.

The z -expansion formalism has been used by BaBar [483] and CLEO-c [485]. Their fits used the first three terms of the expansion, and the results for the ratios $r_1 \equiv a_1/a_0$ and $r_2 \equiv a_2/a_0$ are listed in Table 154. The CLEO III[480] results listed are obtained by refitting their data using the full covariance matrix. The BaBar correlation coefficient listed is obtained by refitting their published branching fraction using their published covariance matrix. These measurements correspond to using the standard outer function $\phi(q^2, t_0)$ of Eq. (204) and $t_0 =$

$t_+ \left(1 - \sqrt{1 - t_-/t_+}\right)$. This choice of t_0 constrains $|z|$ to be below a maximum value within the physical region.

Table 154: Results for r_1 and r_2 from various experiments, for $D \rightarrow \pi K \ell \nu$. The correlation coefficient listed is for the total uncertainties (statistical \oplus systematic) on r_1 and r_2 .

Expt.	mode	Ref.	r_1	r_2	ρ
CLEO III	$D^0 \rightarrow K^+$	[480]	$0.2_{-3.0}^{+3.6}$	-89_{-120}^{+104}	-0.99
BaBar		[483]	$-2.5 \pm 0.2 \pm 0.2$	$0.6 \pm 6. \pm 5.$	-0.64
CLEO-c		[485]	$-2.4 \pm 0.4 \pm 0.1$	$21 \pm 11 \pm 2$	-0.81
Average			-2.3 ± 0.23	5.9 ± 6.3	-0.74
CLEO-c	$D^+ \rightarrow K_S$	[485]	$-2.8 \pm 6 \pm 2$	$32 \pm 18 \pm 4$	-0.84
CLEO-c	$D^0 \rightarrow \pi^+$	[485]	$-2.1 \pm 7 \pm 3$	$-1.2 \pm 4.8 \pm 1.7$	-0.96
CLEO-c	$D^+ \rightarrow \pi^0$	[485]	$-0.2 \pm 1.5 \pm 4$	$-9.8 \pm 9.1 \pm 2.1$	-0.97

Table 154 also lists average values for r_1 and r_2 obtained from a simultaneous fit to CLEO III, BaBar, and CLEO-c branching fraction measurements. To account for final-state radiation in the BaBar measurement, we allow a bias shift between the fit parameters for the BaBar data and those for the other measurements (a χ^2 penalty is added to the fit for any deviation from BaBar's central value). Table 154 shows satisfactory agreement between the parameters measured for D^0 and D^+ decays.

8.3.5 $D \rightarrow V \ell \nu$ Decays

When the final state hadron is a vector meson, the decay can proceed through both vector and axial vector currents, and four form factors are needed. The hadronic current is $H_\mu = V_\mu + A_\mu$, where [477]

$$V_\mu = \langle V(p, \varepsilon) | \bar{q} \gamma^\mu c | D(p') \rangle = \frac{2V(q^2)}{M_D + m_h} \varepsilon_{\mu\nu\rho\sigma} \varepsilon^{*\nu} p'^\rho p^\sigma \quad (205)$$

$$\begin{aligned} A_\mu &= \langle V(p, \varepsilon) | -\bar{q} \gamma^\mu \gamma^5 c | D(p') \rangle = -i(M_D + m_h) A_1(q^2) \varepsilon_\mu^* \\ &\quad + i \frac{A_2(q^2)}{M_D + m_h} (\varepsilon^* \cdot q) (p' + p)_\mu \\ &\quad + i \frac{2m_h}{q^2} (A_3(q^2) - A_0(q^2)) [\varepsilon^* \cdot (p' + p)] q_\mu. \end{aligned} \quad (206)$$

In this expression, m_h is the daughter meson mass and

$$A_3(q^2) = \frac{M_D + m_h}{2m_h} A_1(q^2) - \frac{M_D - m_h}{2m_h} A_2(q^2). \quad (207)$$

Kinematics require that $A_3(0) = A_0(0)$. The differential partial width is

$$\begin{aligned} \frac{d\Gamma(D \rightarrow V \ell \bar{\nu}_\ell)}{dq^2 d \cos \theta_\ell} &= \frac{G_F^2 |V_{cq}|^2}{128\pi^3 M_D^2} p^* q^2 \times \\ &\quad \left[\frac{(1 - \cos \theta_\ell)^2}{2} |H_-|^2 + \frac{(1 + \cos \theta_\ell)^2}{2} |H_+|^2 + \sin^2 \theta_\ell |H_0|^2 \right], \end{aligned} \quad (208)$$

where H_{\pm} and H_0 are helicity amplitudes given by

$$H_{\pm} = \frac{1}{M_D + m_h} [(M_B + m_h)^2 A_1(q^2) \mp 2M_D p^* V(q^2)] \quad (209)$$

$$H_0 = \frac{1}{|q|} \frac{M_B^2}{2m_h(M_D + m_h)} \times \left[\left(1 - \frac{m_h^2 - q^2}{M_D^2} \right) (M_D^2 + m_h^2) A_1(q^2) - 4p^{*2} A_2(q^2) \right]. \quad (210)$$

The left-handed nature of the quark current manifests itself as $|H_-| > |H_+|$. The differential decay rate for $D \rightarrow V \ell \nu$ followed by the vector meson decaying into two pseudoscalars is

$$\begin{aligned} \frac{d\Gamma(D \rightarrow V \ell \nu, V \rightarrow P_1 P_2)}{dq^2 d \cos \theta_V d \cos \theta_\ell d\chi} &= \frac{3G_F^2}{2048\pi^4} |V_{cq}|^2 \frac{p^*(q^2) q^2}{M_D^2} \mathcal{B}(V \rightarrow P_1 P_2) \times \\ &\{ (1 + \cos \theta_\ell)^2 \sin^2 \theta_V |H_+(q^2)|^2 \\ &+ (1 - \cos \theta_\ell)^2 \sin^2 \theta_V |H_-(q^2)|^2 \\ &+ 4 \sin^2 \theta_\ell \cos^2 \theta_V |H_0(q^2)|^2 \\ &+ 4 \sin \theta_\ell (1 + \cos \theta_\ell) \sin \theta_V \cos \theta_V \cos \chi H_+(q^2) H_0(q^2) \\ &- 4 \sin \theta_\ell (1 - \cos \theta_\ell) \sin \theta_V \cos \theta_V \cos \chi H_-(q^2) H_0(q^2) \\ &- 2 \sin^2 \theta_\ell \sin^2 \theta_V \cos 2\chi H_+(q^2) H_-(q^2) \}, \quad (211) \end{aligned}$$

where the angles θ_ℓ , θ_V , and χ are defined in Fig. 63.

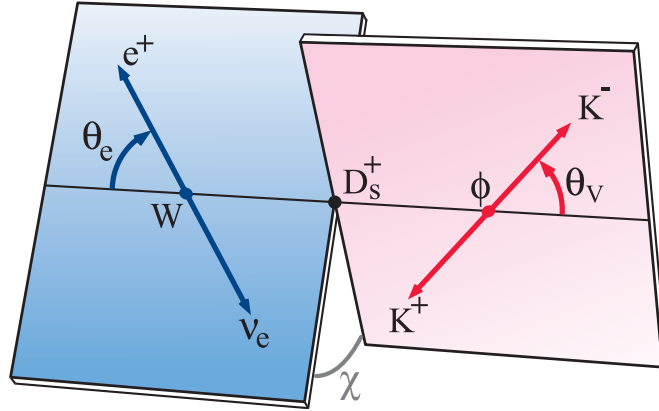


Figure 63: Decay angles θ_V , θ_ℓ and χ . Note that the angle χ between the decay planes is defined in the D -meson reference frame, whereas the angles θ_V and θ_ℓ are defined in the V meson and W reference frames, respectively.

Assuming that the simple pole form of Eq. (198) describes the q^2 -dependence of the form factors, the distribution of Eq. (211) will depend only on the parameters

$$r_V \equiv V(0)/A_1(0), \quad r_2 \equiv A_2(0)/A_1(0). \quad (212)$$

Table 155 lists measurements of r_V and r_2 from several experiments. The average results from $D^+ \rightarrow \bar{K}^{*0} \ell^+ \nu$ decays are also given. The measurements are plotted in Fig. 64 which shows that they are all consistent with one another.

Table 155: Results for r_V and r_2 from various experiments.

Experiment	Ref.	r_V	r_2
$D^+ \rightarrow \bar{K}^{*0} l^+ \nu$			
E691	[491]	$2.0 \pm 0.6 \pm 0.3$	$0.0 \pm 0.5 \pm 0.2$
E653	[492]	$2.00 \pm 0.33 \pm 0.16$	$0.82 \pm 0.22 \pm 0.11$
E687	[493]	$1.74 \pm 0.27 \pm 0.28$	$0.78 \pm 0.18 \pm 0.11$
E791 (e)	[494]	$1.90 \pm 0.11 \pm 0.09$	$0.71 \pm 0.08 \pm 0.09$
E791 (μ)	[495]	$1.84 \pm 0.11 \pm 0.09$	$0.75 \pm 0.08 \pm 0.09$
Beatrice	[496]	$1.45 \pm 0.23 \pm 0.07$	$1.00 \pm 0.15 \pm 0.03$
FOCUS	[497]	$1.504 \pm 0.057 \pm 0.039$	$0.875 \pm 0.049 \pm 0.064$
Average		1.62 ± 0.055	0.83 ± 0.054
$D^0 \rightarrow \bar{K}^0 \pi^- \mu^+ \nu$			
FOCUS	[498]	$1.706 \pm 0.677 \pm 0.342$	$0.912 \pm 0.370 \pm 0.104$
$D_s^+ \rightarrow \phi e^+ \nu$			
BaBar	[499]	$1.636 \pm 0.067 \pm 0.038$	$0.705 \pm 0.056 \pm 0.029$
$D^0, D^+ \rightarrow \rho e \nu$			
CLEO	[500]	$1.40 \pm 0.25 \pm 0.03$	$0.57 \pm 0.18 \pm 0.06$

8.3.6 S -Wave Component

In 2002 FOCUS reported [501] an asymmetry in the observed $\cos(\theta_V)$ distribution. This is interpreted as evidence for an S -wave component in the decay amplitude as follows. Since H_0 typically dominates over H_{\pm} , the distribution given by Eq. (211) is, after integration over χ , roughly proportional to $\cos^2 \theta_V$. Inclusion of a constant S -wave amplitude of the form $A e^{i\delta}$ leads to an interference term proportional to $|AH_0 \sin \theta_{\ell} \cos \theta_V|$; this term causes an asymmetry in $\cos(\theta_V)$. When FOCUS fit their data including this S -wave amplitude, they obtained $A = 0.330 \pm 0.022 \pm 0.015 \text{ GeV}^{-1}$ and $\delta = 0.68 \pm 0.07 \pm 0.05$ [497].

More recently, both BaBar [502] and CLEO-c [503] have also found evidence for an f_0 component in semileptonic D_s decays.

8.3.7 Model-independent Form Factor Measurement

Subsequently the CLEO-c collaboration extracted the form factors $H_+(q^2)$, $H_-(q^2)$, and $H_0(q^2)$ in a model-independent fashion directly as functions of q^2 [504] and also determined the S -wave form factor $h_0(q^2)$ via the interference term, despite the fact that the $K\pi$ mass distribution appears dominated by the vector $K^*(892)$ state. Their results are shown in Figs. 66 and 65. Plots in Fig. 66 clearly show that $H_0(q^2)$ dominates over essentially the full range of q^2 , but especially at low q^2 . They also show that the transverse form factor $H_t(q^2)$ (which can be related to $A_3(q^2)$) is small (compared to Lattice Gauge Theory calculations) and suggest that the form factor ratio $r_3 \equiv A_3(0)/A_1(0)$ is large and negative.

The product $H_0(q^2) \times h_0(q^2)$ is shown in Fig. 65 and clearly indicates the existence of $h_0(q^2)$, although it seems to fall faster with q^2 than $H_0(q^2)$. The other plots in that figure show that D - and F -wave versions of the S -wave $h_0(q^2)$ are not significant.

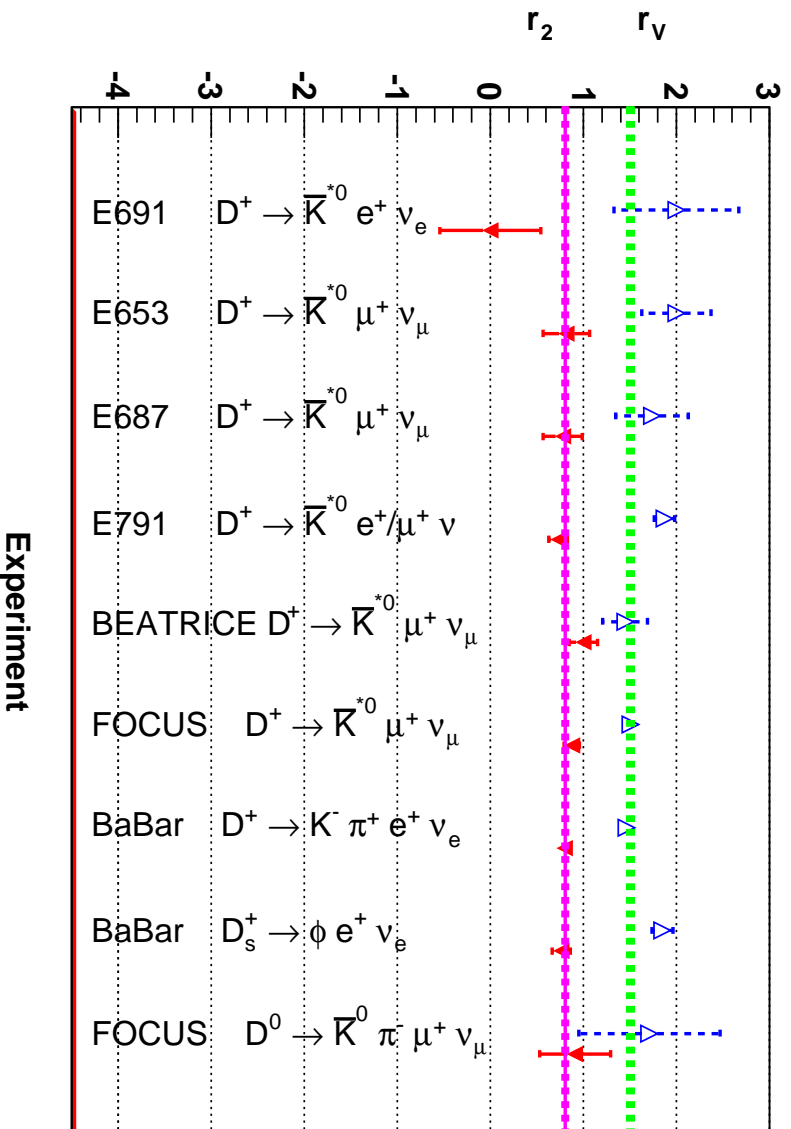


Figure 64: A comparison of r_2 and r_V values from various experiments. The first seven measurements are for $D^+ \rightarrow K^- \pi^+ l^+ \nu_l$ decays. Also shown as a line with $1\text{-}\sigma$ limits is the average of these. The last two points are D_s^+ decays and Cabibbo-suppressed D decays.

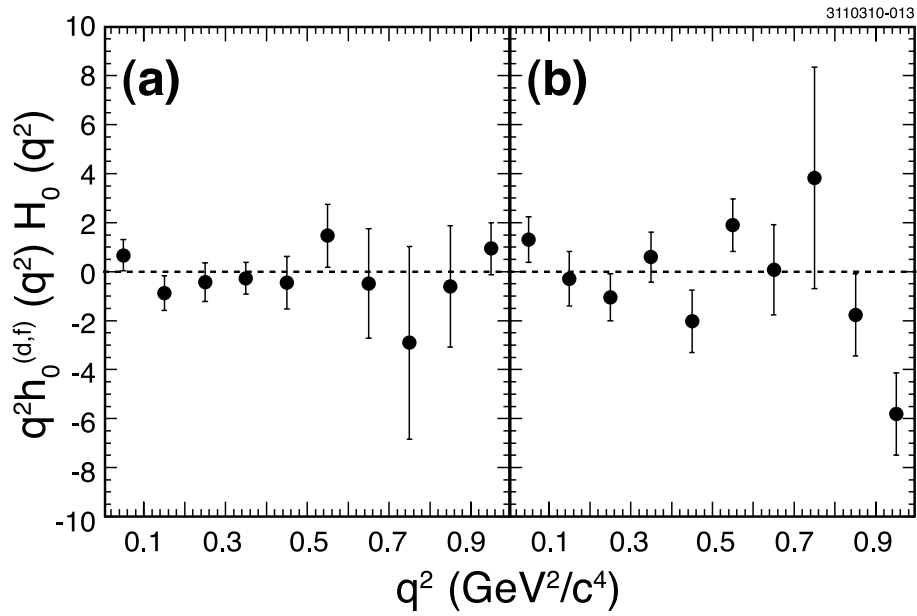
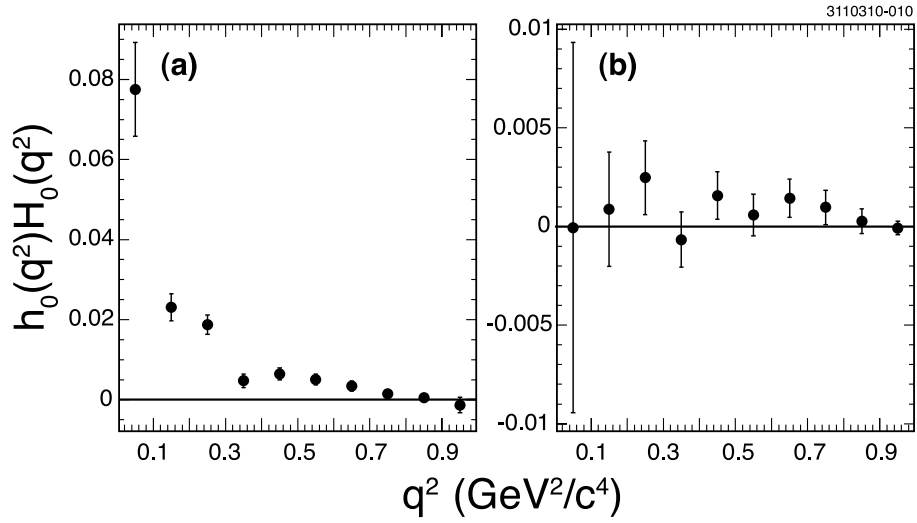


Figure 65: Model-independent form factors $h_0(q^2)$ measured by CLEO-c[504].

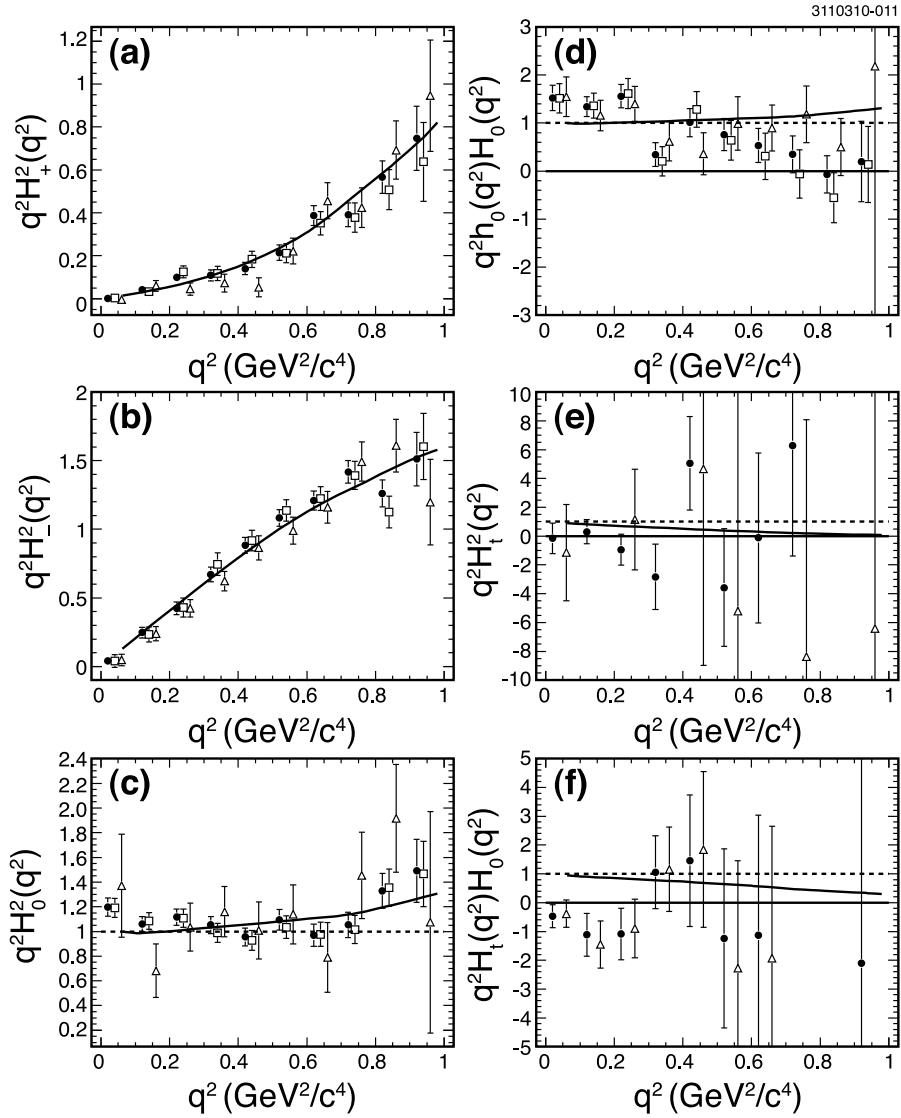


Figure 66: Model-independent form factors $H(q^2)$ measured by CLEO-c[504].

8.4 CP Asymmetries

CP violation occurs if the decay rate for a particle differs from that of its CP -conjugate[505]. In general there are two classes of CP violation, termed *indirect* and *direct*[506]. Indirect CP violation refers to $\Delta C = 2$ processes and arises in D^0 decays due to D^0 - \bar{D}^0 mixing. It can occur as an asymmetry in the mixing itself, or it can result from interference between a decay amplitude arising via mixing and a non-mixed amplitude. Direct CP violation refers to $\Delta C = 1$ processes and occurs in both charged and neutral D decays. It results from interference between two different decay amplitudes (e.g., a penguin and tree amplitude) that have different weak (CKM) and strong phases³⁶. A difference in strong phases typically arises due to final-state interactions (FSI)[507]. A difference in weak phases arises from different CKM vertex couplings, as is often the case for spectator and penguin diagrams.

The CP asymmetry is defined as the difference between D and \bar{D} partial widths divided by their sum:

$$A_{CP} = \frac{\Gamma(D) - \Gamma(\bar{D})}{\Gamma(D) + \Gamma(\bar{D})}. \quad (213)$$

However, to take into account differences in production rates between D and \bar{D} (which would affect the number of respective decays observed), experiments usually normalize to a Cabibbo-favored mode. In this case there is the additional benefit that most corrections due to inefficiencies cancel out, reducing systematic uncertainties. An implicit assumption is that there is no measurable CP violation in the Cabibbo-favored normalizing mode. The CP asymmetry is calculated as

$$A_{CP} = \frac{\eta(D) - \eta(\bar{D})}{\eta(D) + \eta(\bar{D})}, \quad (214)$$

where (considering, for example, $D^0 \rightarrow K^- K^+$)

$$\eta(D) = \frac{N(D^0 \rightarrow K^- K^+)}{N(D^0 \rightarrow K^- \pi^+)}, \quad (215)$$

$$\eta(\bar{D}) = \frac{N(\bar{D}^0 \rightarrow K^- K^+)}{N(\bar{D}^0 \rightarrow K^+ \pi^-)}. \quad (216)$$

In the case of D^+ and D_s^+ decays, A_{CP} measures direct CP violation; in the case of D^0 decays, A_{CP} measures direct and indirect CP violation combined. Values of A_{CP} for D^+ , D^0 and D_s^+ decays are listed in Tables 156, 157 and 158 respectively.

³⁶The weak phase difference will have opposite signs for $D \rightarrow f$ and $\bar{D} \rightarrow \bar{f}$ decays, while the strong phase difference will have the same sign. As a result, squaring the total amplitudes to obtain the decay rates gives interference terms having opposite sign, i.e., non-identical decay rates.

Table 156: CP asymmetries $A_{CP} = [\Gamma(D^+) - \Gamma(D^-)]/[\Gamma(D^+) + \Gamma(D^-)]$ for D^\pm decays.

Mode	Year	Collaboration	A_{CP}
$D^+ \rightarrow \mu^+ \nu$	2008	CLEOc [508]	$+0.08 \pm 0.08$
$D^+ \rightarrow K_s^0 \pi^+$	2010	BELLE [509]	$-0.0071 \pm 0.0019 \pm 0.0020$
	2007	CLEOc [510]	$-0.006 \pm 0.010 \pm 0.003$
	2002	FOCUS [511]	$-0.016 \pm 0.015 \pm 0.009$
		COMBOS average	-0.0072 ± 0.0026
$D^+ \rightarrow K_s^0 K^+$	2010	BELLE [509]	$-0.0016 \pm 0.0058 \pm 0.0025$
	2002	FOCUS [511]	$+0.071 \pm 0.061 \pm 0.012$
		COMBOS average	-0.0009 ± 0.0063
$D^+ \rightarrow \pi^+ \pi^- \pi^+$	1997	E791 [512]	-0.017 ± 0.042 (stat.)
$D^+ \rightarrow K^- \pi^+ \pi^+$	2007	CLEOc [510]	$-0.005 \pm 0.004 \pm 0.009$
$D^+ \rightarrow K_s^0 \pi^+ \pi^0$	2007	CLEO-c [510]	$+0.003 \pm 0.009 \pm 0.003$
$D^+ \rightarrow K^+ K^- \pi^+$	2008	CLEO-c [513]	$-0.0003 \pm 0.0084 \pm 0.0029$
	2005	BABAR [514]	$+0.014 \pm 0.010 \pm 0.008$
	2000	FOCUS [515]	$+0.006 \pm 0.011 \pm 0.005$
	1997	E791 [512]	-0.014 ± 0.029 (stat.)
	1994	E687 [516]	-0.031 ± 0.068 (stat.)
		COMBOS average	$+0.0039 \pm 0.0061$
$D^+ \rightarrow K^- \pi^+ \pi^+ \pi^0$	2007	CLEOc [510]	$+0.010 \pm 0.009 \pm 0.009$
$D^+ \rightarrow K_s^0 \pi^+ \pi^+ \pi^-$	2007	CLEOc [510]	$+0.001 \pm 0.011 \pm 0.006$
$D^+ \rightarrow K_s^0 K^+ \pi^+ \pi^-$	2005	FOCUS [517]	$-0.042 \pm 0.064 \pm 0.022$

Table 157: CP asymmetries $A_{CP} = [\Gamma(D^0) - \Gamma(\bar{D}^0)]/[\Gamma(D^0) + \Gamma(\bar{D}^0)]$ for D^0, \bar{D}^0 decays.

Mode	Year	Collaboration	A_{CP}
$D^0 \rightarrow \pi^+\pi^-$	2008	BELLE [518]	$+0.0043 \pm 0.0052 \pm 0.0012$
	2008	BABAR [519]	$-0.0024 \pm 0.0052 \pm 0.0022$
	2005	CDF [520]	$+0.010 \pm 0.013 \pm 0.006$
	2002	CLEO [437]	$+0.019 \pm 0.032 \pm 0.008$
	2000	FOCUS [515]	$+0.048 \pm 0.039 \pm 0.025$
	1998	E791 [521]	$-0.049 \pm 0.078 \pm 0.030$
		COMBOS average	$+0.0022 \pm 0.0037$
$D^0 \rightarrow \pi^0\pi^0$	2001	CLEO [522]	$+0.001 \pm 0.048$ (stat. and syst. combined)
$D^0 \rightarrow K_s^0\pi^0$	2001	CLEO [522]	$+0.001 \pm 0.013$ (stat. and syst. combined)
$D^0 \rightarrow K^+K^-$	2008	BELLE [518]	$-0.0043 \pm 0.0030 \pm 0.0011$
	2008	BABAR [519]	$+0.0000 \pm 0.0034 \pm 0.0013$
	2005	CDF [520]	$+0.020 \pm 0.012 \pm 0.006$
	2002	CLEO [437]	$+0.000 \pm 0.022 \pm 0.008$
	2000	FOCUS [515]	$-0.001 \pm 0.022 \pm 0.015$
	1998	E791 [521]	$-0.010 \pm 0.049 \pm 0.012$
	1995	CLEO [523]	$+0.080 \pm 0.061$ (stat.)
	1994	E687 [516]	$+0.024 \pm 0.084$ (stat.)
		COMBOS average	$+0.0016 \pm 0.0023$
$D^0 \rightarrow K_s^0K_s^0$	2001	CLEO [522]	-0.23 ± 0.19 (stat. and syst. combined)
$D^0 \rightarrow \pi^+\pi^-\pi^0$	2008	BABAR [524]	$-0.0031 \pm 0.0041 \pm 0.0017$
	2008	BELLE [525]	$+0.0043 \pm 0.0130$
	2005	CLEO [526]	$+0.001_{-0.07}^{+0.09} \pm 0.05$
		COMBOS average	-0.0023 ± 0.0042
$D^0 \rightarrow K^+K^-\pi^0$	2008	BABAR [524]	$0.0100 \pm 0.0167 \pm 0.0025$
$D^0 \rightarrow K^-\pi^+\pi^0$	2007	CLEOc [510]	$+0.002 \pm 0.004 \pm 0.008$
	2001	CLEO [527]	-0.031 ± 0.086 (stat.)
		COMBOS average	$+0.0016 \pm 0.0089$
$D^0 \rightarrow K^+\pi^-\pi^0$	2005	BELLE [528]	-0.006 ± 0.053 (stat.)
	2001	CLEO [529]	$+0.09_{-0.22}^{+0.25}$ (stat.)
		COMBOS average	-0.0014 ± 0.0517
$D^0 \rightarrow K_s^0\pi^+\pi^-$	2004	CLEO [530]	$-0.009 \pm 0.021_{-0.057}^{+0.016}$
$D^0 \rightarrow K^+\pi^-\pi^+\pi^-$	2005	BELLE [528]	-0.018 ± 0.044 (stat.)
$D^0 \rightarrow K^+K^-\pi^+\pi^-$	2005	FOCUS [517]	$-0.082 \pm 0.056 \pm .047$

Table 158: CP asymmetries $A_{CP} = [\Gamma(D_s^+) - \Gamma(D_s^-)]/[\Gamma(D_s^+) + \Gamma(D_s^-)]$ for D_s^\pm decays.

Mode	Year	Collaboration	A_{CP}
$D_s^+ \rightarrow \pi^+\eta$	2008	CLEOc [531]	$-0.082 \pm 0.052 \pm 0.008$
$D_s^+ \rightarrow \pi^+\eta'$	2008	CLEOc [531]	$-0.055 \pm 0.037 \pm 0.012$
$D_s^+ \rightarrow K_s^0\pi^+$	2010	BELLE [509]	$+0.0545 \pm 0.0250 \pm 0.0033$
	2007	CLEOc [532]	$+0.27 \pm 0.11$ (stat.)
		COMBOS average	$+0.0653 \pm 0.0246$
$D_s^+ \rightarrow K^+\pi^0$	2007	CLEOc [532]	$+0.02 \pm 0.29$ (stat.)
$D_s^+ \rightarrow K^+\eta$	2007	CLEOc [532]	-0.20 ± 0.18 (stat.)
$D_s^+ \rightarrow K^+\eta'$	2007	CLEOc [532]	-0.17 ± 0.37 (stat.)
$D_s^+ \rightarrow K^+K_s^0$	2010	BELLE [509]	$+0.0012 \pm 0.0036 \pm 0.0022$
	2008	CLEOc [531]	$+0.049 \pm 0.021 \pm 0.009$
		COMBOS average	$+0.0028 \pm 0.0041$
$D_s^+ \rightarrow \pi^+\pi^+\pi^-$	2008	CLEOc [531]	$+0.020 \pm 0.046 \pm 0.007$
$D_s^+ \rightarrow K^+\pi^+\pi^-$	2008	CLEOc [531]	$+0.112 \pm 0.070 \pm 0.009$
$D_s^+ \rightarrow K^+K^-\pi^+$	2008	CLEOc [531]	$+0.003 \pm 0.011 \pm 0.008$
$D_s^+ \rightarrow K_s^0K^-\pi^+\pi^+$	2008	CLEOc [531]	$-0.007 \pm 0.036 \pm 0.011$
$D_s^+ \rightarrow K^+K^-\pi^+\pi^0$	2008	CLEOc [531]	$-0.059 \pm 0.042 \pm 0.012$

8.5 T -violating Asymmetries

T -violating asymmetries are measured using triple-product correlations and assuming the validity of the CPT theorem. Triple-product correlations of the form $\vec{a} \cdot (\vec{b} \times \vec{c})$, where a , b , and c are spins or momenta, are odd under time reversal (T). For example, for $D^0 \rightarrow K^+K^-\pi^+\pi^-$ decays, $C_T \equiv \vec{p}_{K^+} \cdot (\vec{p}_{\pi^+} \times \vec{p}_{\pi^-})$ changes sign (i.e., is odd) under a T transformation. The corresponding quantity for \bar{D}^0 is $\bar{C}_T \equiv \vec{p}_{K^-} \cdot (\vec{p}_{\pi^-} \times \vec{p}_{\pi^+})$. Defining

$$A_T = \frac{\Gamma(C_T > 0) - \Gamma(C_T < 0)}{\Gamma(C_T > 0) + \Gamma(C_T < 0)} \quad (217)$$

for D^0 decay and

$$\bar{A}_T = \frac{\Gamma(-\bar{C}_T > 0) - \Gamma(-\bar{C}_T < 0)}{\Gamma(-\bar{C}_T > 0) + \Gamma(-\bar{C}_T < 0)} \quad (218)$$

for \bar{D}^0 decay, in the absence of strong phases either $A_T \neq 0$ or $\bar{A}_T \neq 0$ indicates T violation. In these expressions the Γ 's are partial widths. The asymmetry

$$A_{T\text{viol}} \equiv \frac{A_T - \bar{A}_T}{2} \quad (219)$$

tests for T violation even with nonzero strong phases (see Refs. [533, 534, 535, 536, 537]). Values of $A_{T\text{viol}}$ for some D^+ , D_s^+ , and D^0 decay modes are listed in Table 159.

Table 159: T -violating asymmetries $A_{T\text{viol}} = (A_T - \bar{A}_T)/2$.

Mode	Year	Collaboration	$A_{T\text{viol}}$
$D^0 \rightarrow K^+K^-\pi^+\pi^-$	2010	BABAR [538]	$+0.0010 \pm 0.0051 \pm 0.0044$
	2005	FOCUS [517]	$+0.010 \pm 0.057 \pm 0.037$
		COMBOS average	$+0.0010 \pm 0.0067$
$D^+ \rightarrow K_s^0 K^+ \pi^+ \pi^-$	2005	FOCUS [517]	$+0.023 \pm 0.062 \pm 0.022$
$D_s^+ \rightarrow K_s^0 K^+ \pi^+ \pi^-$	2005	FOCUS [517]	$-0.036 \pm 0.067 \pm 0.023$

In summary, Tables 156–159 show that there is no evidence yet for CP or T violation in the charm sector. The most sensitive searches for CP violation have reached a level of sensitivity well below 1%.

8.6 World Average for the D_s^+ Decay Constant f_{D_s}

The Heavy Flavor Averaging Group has used Belle, BaBar, and CLEO measurements of $\mathcal{B}(D_s^+ \rightarrow \mu^+\nu)$ and $\mathcal{B}(D_s^+ \rightarrow \tau^+\nu)$ to calculate a world average (WA) value for the D_s^+ decay constant f_{D_s} . The Belle results are from Ref. [539], the BaBar results are from Refs. [540, 541], and the CLEO results are from Refs. [542, 543, 544].

The value for f_{D_s} is calculated via

$$f_{D_s} = \frac{1}{G_F |V_{cs}| m_\ell \left(1 - \frac{m_\ell^2}{m_{D_s}^2}\right)} \sqrt{\frac{8\pi \mathcal{B}(D_s^+ \rightarrow \ell^+\nu)}{m_{D_s} \tau_{D_s}}}, \quad (220)$$

where, for $\mathcal{B}(D_s^+ \rightarrow \ell^+\nu)$, $\ell^+ = \mu^+$ or $\ell^+ = \tau^+$. The error on f_{D_s} is calculated as follows: values for variables on the right-hand-side of Eq. (220) are sampled from Gaussian distributions having mean values equal to the central values and standard deviations equal to their respective errors. The resulting values of f_{D_s} are plotted, and the r.m.s. of the distribution is taken as the $\pm 1\sigma$ errors. The procedure is done separately for the WA values of $\mathcal{B}(D_s^+ \rightarrow \mu^+\nu)$ and $\mathcal{B}(D_s^+ \rightarrow \tau^+\nu)$, and for the BaBar value [540] of $\mathcal{B}(D_s^+ \rightarrow \mu^+\nu)$.

The BaBar result is treated separately because the signal yield is normalized to $D_s^+ \rightarrow \phi \pi^+$ decays; thus the measurement is

$$\left. \frac{\Gamma(D_s^+ \rightarrow \mu^+\nu)}{\Gamma(D_s^+ \rightarrow \phi \pi^+)} \right|_{\text{BaBar}} = 0.143 \pm 0.018 \text{ (stat.)} \pm 0.006 \text{ (syst.)}. \quad (221)$$

To obtain $\mathcal{B}(D_s^+ \rightarrow \mu^+\nu)$, one must multiply by $\mathcal{B}(D_s^+ \rightarrow \phi \pi^+)$. However, for this analysis the ϕ is reconstructed via $\phi \rightarrow K^+ K^-$ with $|M_{K^+ K^-} - M_\phi| \equiv \Delta M_{KK} < 5.5$ MeV [545]. For the BaBar measurements of $\mathcal{B}(D_s^+ \rightarrow \phi \pi^+)$ [546, 475], a mass window $\Delta M_{KK} < 15$ MeV was used. Because the $D_s^+ \rightarrow \phi \pi^+$ branching fraction depends on ΔM_{KK} (see Table II of Ref. [531]), we do not multiply together the BaBar results for $\Gamma(D_s^+ \rightarrow \mu^+\nu)/\Gamma(D_s^+ \rightarrow \phi \pi^+)$ and $\mathcal{B}(D_s^+ \rightarrow \phi \pi^+)$; instead we use the fact that CLEO has measured the branching fraction $\mathcal{B}(D_s^+ \rightarrow K^+ K^- \pi^+)$ for $\Delta M_{KK} = 5$ MeV. To multiply the BaBar result for $\Gamma(D_s^+ \rightarrow \mu^+\nu)/\Gamma(D_s^+ \rightarrow \phi \pi^+)$ by the CLEO result for $\mathcal{B}(D_s^+ \rightarrow K^+ K^- \pi^+)$ requires dividing Eq. (221) by $\mathcal{B}(\phi \rightarrow K^+ K^-) = 0.491$ (as used in Ref. [540]) and subtracting in quadrature the 1.2% uncertainty in $\mathcal{B}(\phi \rightarrow K^+ K^-)$ from the systematic error. In addition, for the result (221) BaBar subtracted off $D_s^+ \rightarrow f_0(980)(K^+ K^-) \pi^+$ background (48 events); as this process is included in the CLEO measurement, these events must be added back in to BaBar's $\phi \pi^+$ yield. The BaBar result then becomes

$$\left. \frac{\Gamma(D_s^+ \rightarrow \mu^+\nu)}{\Gamma(D_s^+ \rightarrow K^+ K^- \pi^+)} \right|_{\Delta M_{KK}=5.5 \text{ MeV}} = 0.285 \pm 0.035 \text{ (stat.)} \pm 0.011 \text{ (syst.)}. \quad (222)$$

Multiplying this by CLEO's measurement [531]

$$\mathcal{B}(D_s^+ \rightarrow K^+ K^- \pi^+) \Big|_{\Delta M_{KK}=5 \text{ MeV}} = (1.69 \pm 0.08 \pm 0.06)\% \quad (223)$$

gives

$$\mathcal{B}(D_s^+ \rightarrow \mu^+\nu) \Big|_{\text{BaBar adjusted}} = \left(4.81 \pm 0.63 \text{ (stat.)} \pm 0.25 \text{ (syst.)}\right) \times 10^{-3}. \quad (224)$$

In summary, three types of measurements are used to calculate the WA f_{D_s} :

1. the WA $D_s^+ \rightarrow \mu^+ \nu$ branching fraction, which is calculated from Belle and CLEO measurements (see Fig. 67);
2. the WA $D_s^+ \rightarrow \tau^+ \nu$ branching fraction, which is calculated from CLEO and BaBar measurements (see Fig. 68); and
3. the ratio $\Gamma(D_s^+ \rightarrow \mu^+ \nu)/\Gamma(D_s^+ \rightarrow K^+ K^- \pi^+)$ measured by BaBar, adjusted as described above [547].

The WA f_{D_s} value is obtained by averaging the three results, accounting for correlations such as the values of $|V_{cs}|$, m_{D_s} , and τ_{D_s} in Eq. (220). The result is shown in Fig. 69. The WA value is

$$f_{D_s} = 254.6 \pm 5.9 \text{ MeV}, \quad (225)$$

where the statistical and systematic errors are combined. This value can be compared to results from the two most precise lattice QCD calculations: it is 2.1σ higher than that from the HPQCD Collaboration (241 ± 3 MeV [548]), and it is consistent with the less precise result from the Fermilab/MILC Collaboration (249 ± 11 MeV [549]).

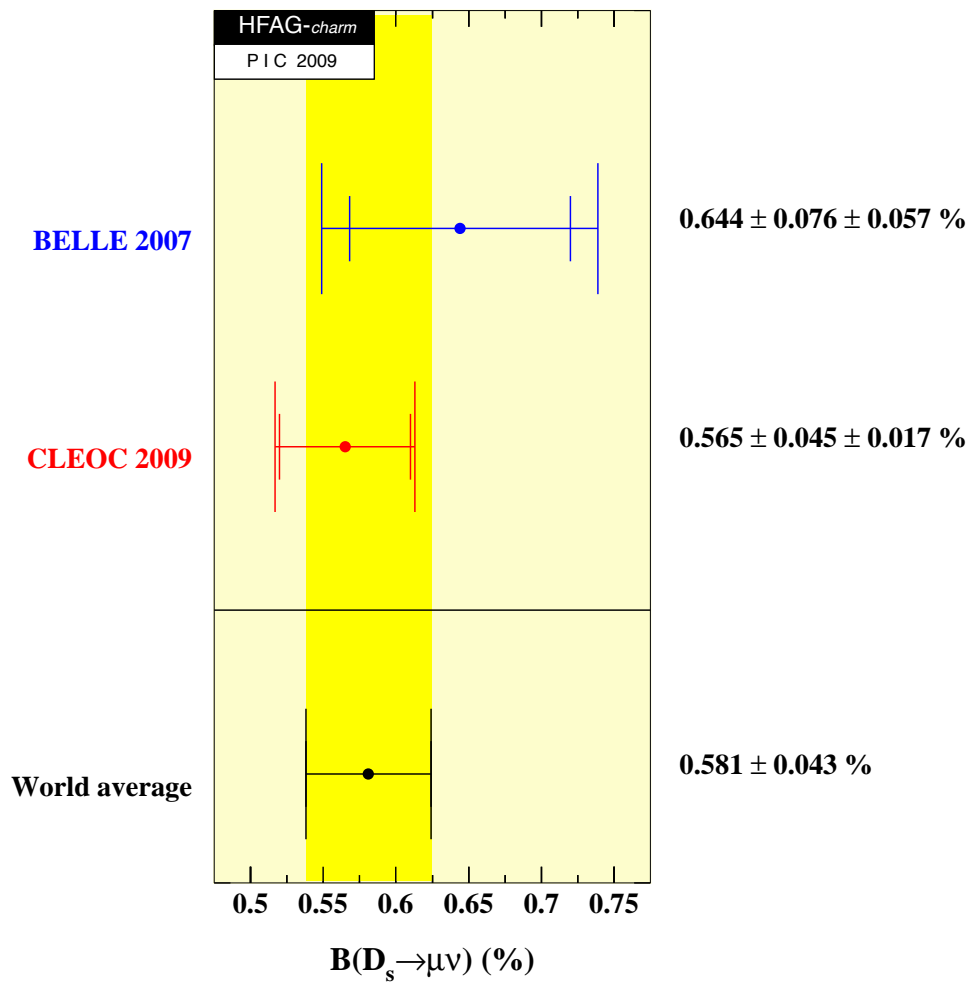


Figure 67: WA value for $\mathcal{B}(D_s^+ \rightarrow \mu^+ \nu)$, as calculated from Refs. [539, 542]. When two errors are listed, the first one is statistical and the second is systematic.

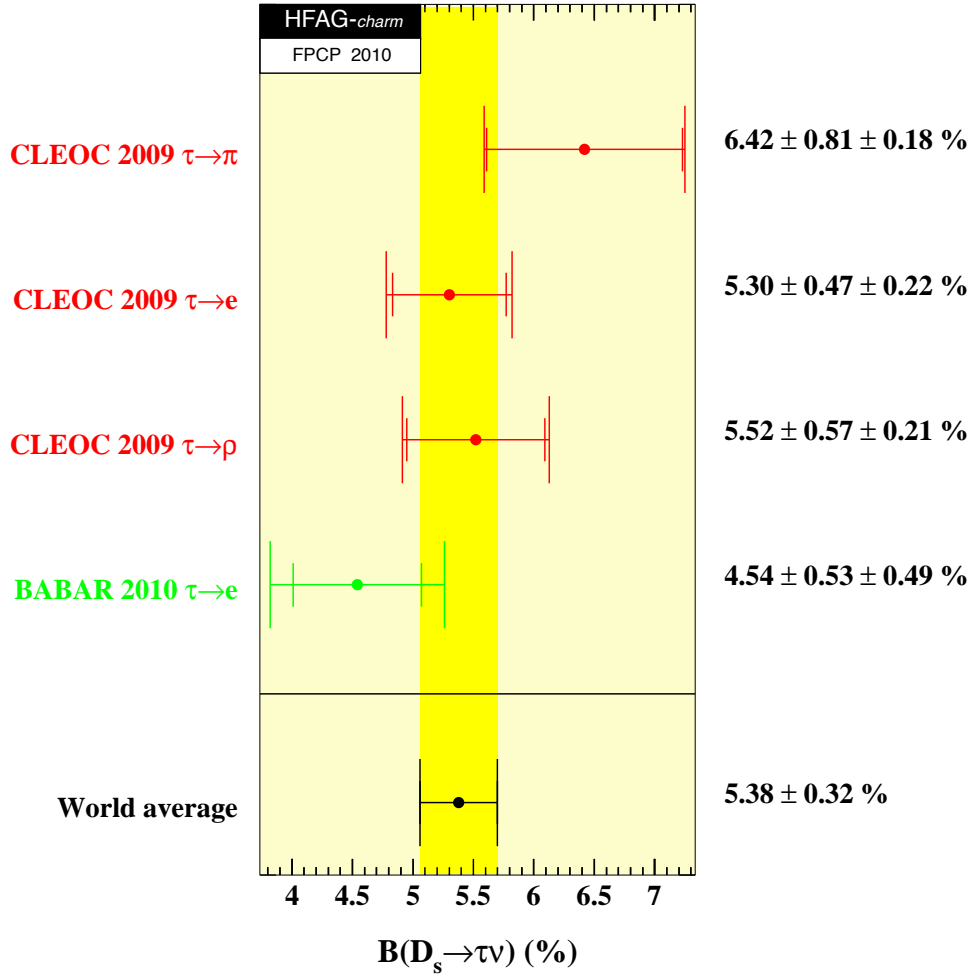


Figure 68: WA value for $\mathcal{B}(D_s^+ \rightarrow \tau^+ \nu)$, as calculated from Refs. [542, 543, 544, 541]. When two errors are listed, the first one is statistical and the second is systematic.

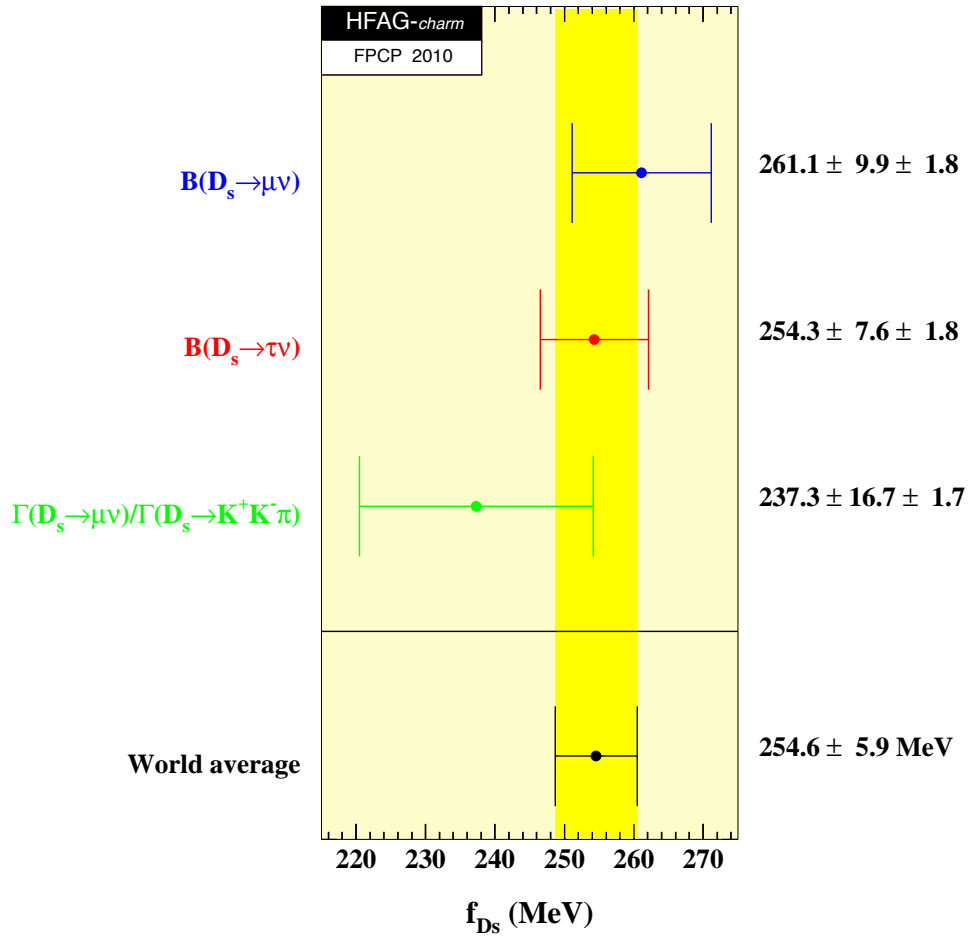


Figure 69: WA value for f_{D_s} . For each measurement, the first error listed is the total uncorrelated error, and the second error is the total correlated error (mostly from τ_{D_s}).

8.7 Two-body Hadronic D^0 Decays and Final State Radiation

Branching fractions measurements for $D^0 \rightarrow K^-\pi^+$, $D^0 \rightarrow \pi^+\pi^-$ and $D^0 \rightarrow K^+K^-$ have reached sufficient precision to allow averages with $\mathcal{O}(1\%)$ relative uncertainties. At these precisions, Final State Radiation (FSR) must be treated correctly and consistently across the input measurements for the accuracy of the averages to match the precision. The sensitivity of measurements to FSR arises because of a tail in the distribution of radiated energy that extends to the kinematic limit. The tail beyond $E_\gamma \approx 30$ MeV causes typical selection variables like the hadronic invariant mass to shift outside the selection range dictated by experimental resolution (see Fig. 70). While the differential rate for the tail is small, the integrated rate amounts to several percent of the total $h^+h^-(n\gamma)$ rate because of the tail's extent. The tail therefore translates directly into a several percent loss in experimental efficiency.

All measurements that include an FSR correction have a correction based on use of PHOTOS [550, 551, 552, 553] within the experiment's Monte Carlo simulation. PHOTOS itself, however, has evolved, over the period spanning the set of measurements. In particular, incorporation of interference between radiation off of the two separate mesons has proceeded in stages: it was first available for particle–antiparticle pairs in version 2.00 (1993), and extended to any two body, all charged, final states in version 2.02 (1999). The effects of interference are clearly visible (Figure 70), and cause a roughly 30% increase in the integrated rate into the high energy photon tail. To evaluate the FSR correction incorporated into a given measurement, we must therefore note whether any correction was made, the version of PHOTOS used in correction, and whether the interference terms in PHOTOS were turned on.

8.7.1 Branching Fraction Corrections

Before averaging the measured branching fractions, the published results are updated, as necessary, to the FSR prediction of PHOTOS 2.15 with interference included. The correction will always shift a branching fraction to a higher value: with no FSR correction or with no interference term in the correction, the experimental efficiency determination will be biased high, and therefore the branching fraction will be biased low.

Most of the branching fraction analyses used the kinematic quantity sensitive to FSR in the candidate selection criteria. For the analyses at the $\psi(3770)$, the variable was ΔE , the difference between the candidate D^0 energy and the beam energy (*e.g.*, $E_K + E_\pi - E_{\text{beam}}$ for $D^0 \rightarrow K^-\pi^+$). In the remainder of the analyses, the relevant quantity was the reconstructed hadronic two-body mass $m_{h^+h^-}$. To correct we need only to evaluate the fraction of decays that FSR moves outside of the range accepted for the analysis.

The corrections were evaluated using an event generator (EvtGen [554]) that incorporates PHOTOS to simulate the portions of the decay process most relevant to the correction. We compared corrections determined both with and without smearing to account for experimental resolution. The differences were negligible, typically of order of a 1% of the correction itself. The immunity of the correction to resolution effects comes about because most of the long FSR-induced tail in, for example, the $m_{h^+h^-}$ distribution resides well away from the selection boundaries. The smearing from resolution, on the other hand, mainly affects the distribution of events right at the boundary.

For measurements incorporating an FSR correction that did not include interference, we update by assessing the FSR-induced efficiency loss for both the PHOTOS version and configuration used in the analysis and our nominal version 2.15 with interference. For measurements

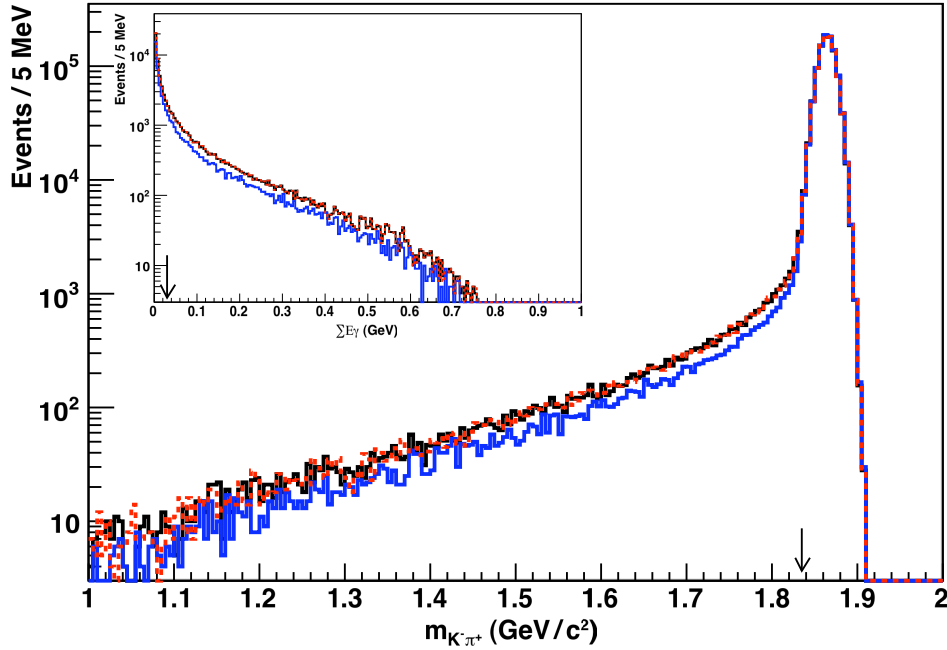


Figure 70: The $K\pi$ invariant mass distribution for $D^0 \rightarrow K^-\pi^+(n\gamma)$ decays. The 3 curves correspond to three different configurations of PHOTOS for modeling FSR: version 2.02 without interference (blue), version 2.02 with interference (red dashed) and version 2.15 with interference (black). The true invariant mass has been smeared with a typical experimental resolution of $10 \text{ MeV}/c^2$. Inset: The corresponding spectrum of total energy radiated per event. The arrow indicates the E_γ value that begins to shift kinematic quantities outside of the range typically accepted in a measurement.

that published their sensitivity to FSR, our generator-level predictions for the original efficiency loss agreed to within a few percent (of the correction). This agreement lends additional credence to the procedure.

Once the event loss from FSR in the most sensitive kinematic quantity is accounted for, the event loss from other quantities is very small. Analyses using D^* tags, for example, showed little sensitivity to FSR in the reconstructed $D^* - D^0$ mass difference: for example, in $m_{K^-\pi^+\pi^+} - m_{K^-\pi^+}$. Because the effect of FSR tends to cancel in the difference of the reconstructed masses, this difference showed a much smaller sensitivity than the two body mass even before a two body mass requirement. In the $\psi(3770)$ analyses, the beam-constrained mass distributions ($\sqrt{E_{\text{beam}}^2 - |\vec{p}_K + \vec{p}_\pi|^2}$) showed little further sensitivity.

The FOCUS [555] analysis of the branching ratios $\mathcal{B}(D^0 \rightarrow \pi^+\pi^-)/\mathcal{B}(D^0 \rightarrow K^-\pi^+)$ and $\mathcal{B}(D^0 \rightarrow K^+K^-)/\mathcal{B}(D^0 \rightarrow K^-\pi^+)$ obtained yields using fits to the two body mass distributions. FSR will both distort the low end of the signal mass peak, and will contribute a signal component to the low side tail used to estimate the background. The fitting procedure is not sensitive to signal events out in the FSR tail, which would be counted as part of the background.

A more complex toy Monte Carlo procedure was required to analyze the effect of FSR on the fitted yields, which were published with no FSR corrections applied. A detailed description of the procedure and results is available at the HFAG site [556], and a brief summary is provided here. Determining the correction involved an iterative procedure in which samples of similar

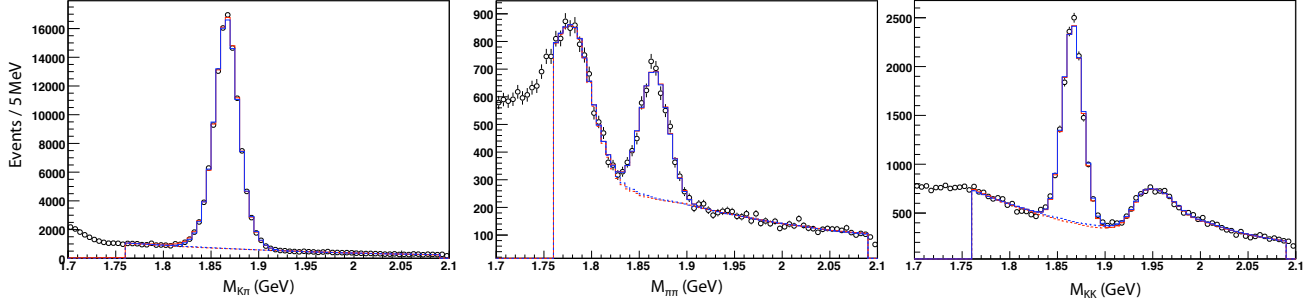


Figure 71: FOCUS data (dots), original fits (blue) and toy MC parameterization (red) for $D^0 \rightarrow K^- \pi^+$ (left) , $D^0 \rightarrow \pi^+ \pi^-$ (center) and $D^0 \rightarrow \pi^+ \pi^-$ (right).

size to the FOCUS sample were generated and then fit using the FOCUS signal and background parameterizations. The MC parameterizations were tuned based on differences between the fits to the toy MC data and the FOCUS fits, and the procedure was repeated. These steps were iterated until the fit parameters matched the original FOCUS parameters.

The toy MC samples for the first iteration were based on the generator-level distribution of $m_{K^- \pi^+}$, $m_{\pi^+ \pi^-}$ and $m_{K^+ K^-}$, including the effects of FSR, smeared according to the original FOCUS resolution function, and on backgrounds thrown using the parameterization from the final FOCUS fits. For each iteration, 400 to 1600 individual data-sized samples were thrown and fit. The means of the parameters from these fits determined the corrections to the generator parameters for the following iteration. The ratio between the number of signal events generated and the final signal yield provides the required FSR correction in the final iteration. Only a few iterations were required in each mode. Figure 71 shows the FOCUS data, the published FOCUS fits, and the final toy MC parameterizations. The toy MC provides an excellent description of the data.

The corrections obtained to the individual FOCUS yields were 1.0298 ± 0.0001 for $K^- \pi^+$, 1.062 ± 0.001 for $\pi^+ \pi^-$, and 1.0183 ± 0.0003 for $K^+ K^-$. These corrections tend to cancel in the branching ratios, leading to corrections of 1.031 to $\mathcal{B}(D^0 \rightarrow \pi^+ \pi^-)/\mathcal{B}(D^0 \rightarrow K^- \pi^+)$, and 0.9888 for $\mathcal{B}(D^0 \rightarrow K^+ K^-)/\mathcal{B}(D^0 \rightarrow K^- \pi^+)$.

Table 160 summarizes the corrected branching fractions. The published FSR-related modeling uncertainties have been replaced by with a new, common, estimate based on the assumption that the dominant uncertainty in the FSR corrections come from the fact that the mesons are treated like structureless particles. No contributions from structure-dependent terms in the decay process (eg. radiation off individual quarks) are included in PHOTOS. Internal studies done by various experiments have indicated that in $K\pi$ decay, the PHOTOS corrections agree with data at the 20-30% level. We therefore attribute a 25 uncertainty to the FSR prediction from potential structure-dependent contributions. For the other two modes, the only difference in structure is the final state valence quark content. While radiative corrections typically come in with a $1/M$ dependence, one would expect the additional contribution from the structure terms to come in on time scales shorter than the hadronization time scale. In this case, you might expect LambdaQCD to be the relevant scale, rather than the quark masses, and therefore that the amplitude is the same for the three modes. In treating the correlations among the measurements this is what we assume. We also assume that the PHOTOS amplitudes

Table 160: The experimental measurements relating to $\mathcal{B}(D^0 \rightarrow K^- \pi^+)$, $\mathcal{B}(D^0 \rightarrow \pi^+ \pi^-)$ and $\mathcal{B}(D^0 \rightarrow K^+ K^-)$ after correcting to the common version and configuration of PHOTOS. The uncertainties are statistical and total systematic, with the FSR-related systematic estimated in this procedure shown in parentheses. Also listed are the percent shifts in the results from the correction, if any, applied here, as well as the original PHOTOS and interference configuration for each publication.

Experiment	result (rescaled)	correction [%]	PHOTOS
$D^0 \rightarrow K^- \pi^+$			
CLEO-c 07 (CC07) [557]	$3.891 \pm 0.035 \pm 0.065(27)\%$	–	2.15/Yes
BaBar 07 (BB07) [558]	$4.035 \pm 0.037 \pm 0.074(24)\%$	0.69	2.02/No
CLEO II 98 (CL98) [559]	$3.920 \pm 0.154 \pm 0.168(32)\%$	2.80	none
ALEPH 97 (AL97) [560]	$3.930 \pm 0.091 \pm 0.125(32)\%$	0.79	2.0/No
ARGUS 94 (AR94) [561]	$3.490 \pm 0.123 \pm 0.288(24)\%$	2.33	none
CLEO II 93 (CL93) [562]	$3.960 \pm 0.080 \pm 0.171(15)\%$	0.38	2.0/No
ALEPH 91 (AL91) [563]	$3.730 \pm 0.351 \pm 0.455(34)\%$	3.12	none
$D^0 \rightarrow \pi^+ \pi^- / D^0 \rightarrow K^- \pi^+$			
CLEO-c 05 (CC05) [564]	$0.0363 \pm 0.0010 \pm 0.0008(01)$	0.25	2.02/No
CDF 05 (CD05) [520]	$0.03594 \pm 0.00054 \pm 0.00043(15)$	–	2.15/Yes
FOCUS 02 (FO02) [555]	$0.0364 \pm 0.0012 \pm 0.0006(02)$	3.10	none
$D^0 \rightarrow K^+ K^- / D^0 \rightarrow K^- \pi^+$			
CDF 05 [520]	$0.0992 \pm 0.0011 \pm 0.0012(01)$	–	2.15/Yes
FOCUS 02 [555]	$0.0982 \pm 0.0014 \pm 0.0014(01)$	-1.12	none
$D^0 \rightarrow K^+ K^-$			
CLEO-c 08 (CC08) [565]	$0.411 \pm 0.008 \pm 0.009\%$	0.64	2.02/No

and any missing structure amplitudes are relatively real with constructive interference. The uncertainties largely cancel in the branching fraction ratios. For the final average branching fractions, the FSR uncertainty on $K\pi$ dominates. Note that because of the relative sizes of FSR in the different modes, the $\pi\pi/K\pi$ branching ratio uncertainty from FSR is positively correlated with that for $K\pi$ branching, while the $KK/K\pi$ branching ratio FSR uncertainty is negatively correlated.

The $\mathcal{B}(D^0 \rightarrow K^- \pi^+)$ measurement of reference [566], the $\mathcal{B}(D^0 \rightarrow \pi^+ \pi^-)/\mathcal{B}(D^0 \rightarrow K^- \pi^+)$ measurements of references [521] and [437] and the $\mathcal{B}(D^0 \rightarrow K^+ K^-)/\mathcal{B}(D^0 \rightarrow K^- \pi^+)$ measurement of reference [437] are excluded from the branching fraction averages presented here. The measurements appear not to have incorporated any FSR corrections, and insufficient information is available to determine the 2-3% corrections that would be required.

8.7.2 Average Branching Fractions

The average branching fractions for $D^0 \rightarrow K^- \pi^+$, $D^0 \rightarrow \pi^+ \pi^-$ and $D^0 \rightarrow K^+ K^-$ are obtained from a single χ^2 minimization procedure, in which the three branching fractions are floating parameters. The central values derive from a fit in which the covariance matrix is the sum of the covariance matrices for the statistical, systematic (excluding FSR) and FSR uncertainties. The statistical uncertainties are obtained from a fit using only the statistical covariance matrix. The systematic uncertainties are obtained from the quadrature uncertainties from a fit with

Table 161: The correlation matrix corresponding to the covariance matrix from the sum of statistical, systematic and FSR covariances.

	CC07	BB07	CL98	AL97	AR94	CL93	AL91	CC05	CD05	FO02	CD05	FO02	CC08
CC07	1.000	0.106	0.043	0.064	0.023	0.025	0.018	0.053	0.078	0.023	-0.015	-0.024	0.416
BB07	0.106	1.000	0.034	0.051	0.019	0.020	0.014	0.042	0.062	0.018	-0.012	-0.019	0.079
CL98	0.043	0.034	1.000	0.021	0.008	0.298	0.006	0.017	0.025	0.007	-0.005	-0.008	0.032
AL97	0.064	0.051	0.021	1.000	0.011	0.012	0.116	0.025	0.038	0.011	-0.007	-0.012	0.048
AR94	0.023	0.019	0.008	0.011	1.000	0.004	0.003	0.009	0.014	0.004	-0.003	-0.004	0.018
CL93	0.025	0.020	0.298	0.012	0.004	1.000	0.003	0.010	0.015	0.004	-0.003	-0.005	0.019
AL91	0.018	0.014	0.006	0.116	0.003	0.003	1.000	0.007	0.010	0.003	-0.002	-0.003	0.013
CC05	0.053	0.042	0.017	0.025	0.009	0.010	0.007	1.000	0.031	0.009	-0.006	-0.010	0.040
CD05	0.078	0.062	0.025	0.038	0.014	0.015	0.010	0.031	1.000	0.013	-0.008	-0.014	0.059
FO02	0.023	0.018	0.007	0.011	0.004	0.004	0.003	0.009	0.013	1.000	-0.002	-0.004	0.017
CD05	-0.015	-0.012	-0.005	-0.007	-0.003	-0.003	-0.002	-0.006	-0.008	-0.002	1.000	0.003	-0.011
FO02	-0.024	-0.019	-0.008	-0.012	-0.004	-0.005	-0.003	-0.010	-0.014	-0.004	0.003	1.000	-0.018
CC08	0.416	0.079	0.032	0.048	0.018	0.019	0.013	0.040	0.059	0.017	-0.011	-0.018	1.000

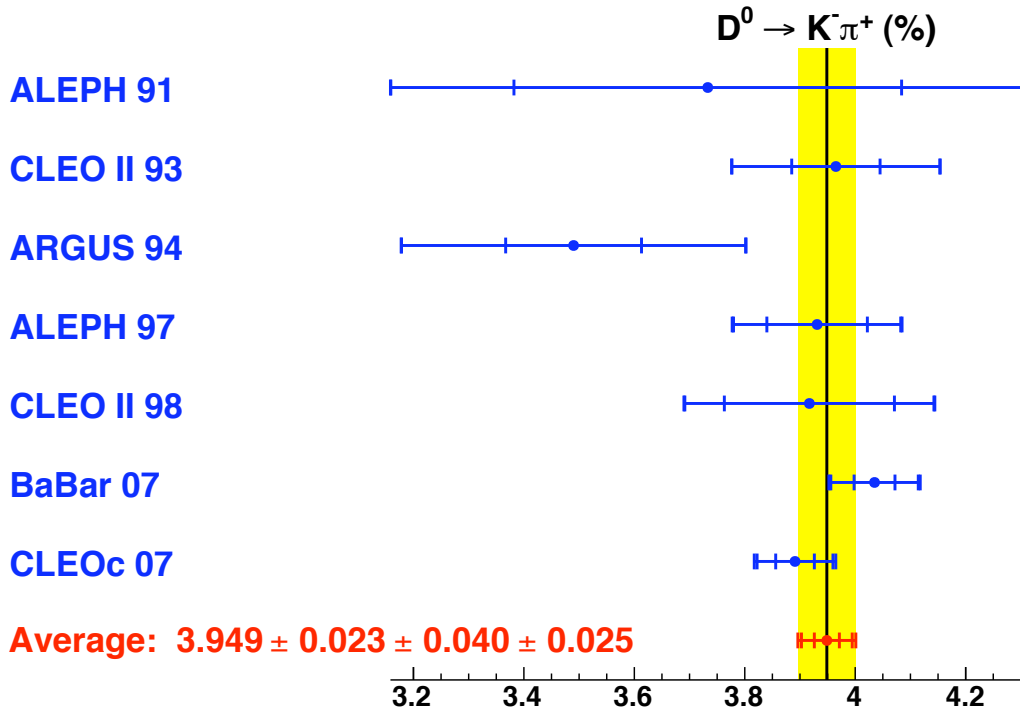


Figure 72: Comparison of measurements of $\mathcal{B}(D^0 \rightarrow K^- \pi^+)$ (blue) with the average branching fraction obtained here (red, and yellow band).

statistical-only and statistical+systematic covariance matrices, and the FSR uncertainties on the averages from the quadrature differences in the uncertainties obtained from the nominal fit and a fit excluding the FSR uncertainties.

In forming the covariance matrix for the FSR uncertainties, the FSR uncertainties are treated as fully correlated (or anti-correlated) as described above. For the systematic covariance matrix, ALEPH's systematic uncertainties in the θ_{D^*} parameter are treated as fully correlated between the ALEPH 97 and ALEPH 91 measurements. Similarly, the tracking efficiency uncertainties in the CLEO II 98 and the CLEO II 93 measurements are treated as fully correlated. Finally, the CLEO-c 07 $D^0 \rightarrow K^- \pi^+$ measurement and the CLEO-c 08 $D^0 \rightarrow K^+ K^-$ measurements have a significant statistical correlation. The 2007 hadronic branching fraction analysis derives the number of $N_{D^0 \bar{D}^0}$ pairs produced in CLEO-c, and that quantity is statistically correlated with the $D^0 \rightarrow K^- \pi^+$ branching fraction in that analysis ($\rho = 0.65$). The 2008 $K^+ K^-$ analysis in turn uses that value of $N_{D^0 \bar{D}^0}$ as the normalization for its branching fraction. Table 161 presents the correlation matrix for the nominal fit (stat.+syst.+FR).

The averaging procedure results in a final χ^2 of 8.5 for 13-3 degrees of freedom. The branching fractions obtained are

$$\begin{aligned}
 \mathcal{B}(D^0 \rightarrow K^- \pi^+) &= 3.949 \pm 0.023 \pm 0.040 \pm 0.025 \\
 \mathcal{B}(D^0 \rightarrow \pi^+ \pi^-) &= 0.143 \pm 0.002 \pm 0.002 \pm 0.001 \\
 \mathcal{B}(D^0 \rightarrow K^+ K^-) &= 0.394 \pm 0.004 \pm 0.005 \pm 0.002.
 \end{aligned}$$

The uncertainties, estimated as described above, are statistical, systematic (excluding FSR),

and FSR modeling. The correlation coefficients from the fit using the total uncertainties are

	$K^-\pi^+$	$\pi^+\pi^-$	K^+K^-
$K^-\pi^+$	1.00	0.72	0.74
$\pi^+\pi^-$	0.72	1.00	0.53
K^+K^-	0.74	0.53	1.00

As the χ^2 would suggest and Fig. 72, the average value for $\mathcal{B}(D^0 \rightarrow K^-\pi^+)$ and the input branching fractions agree very well. With the estimated uncertainty in the FSR modeling used here, the FSR uncertainty dominates the statistical uncertainty in the average, suggesting that experimental work in the near future should focus on verification of FSR with $E_\gamma \gtrsim 100$ MeV.

The $\mathcal{B}(D^0 \rightarrow K^-\pi^+)$ average obtained here is approximately one statistical standard deviation higher than the 2009 PDG update [444]. Table 162 shows the evolution from a fit similar to the PDG's (no FSR corrections or correlations, reference [566] excluded) to the average presented here. There are three main contributions to the difference, which only coincidentally all shift the result upwards. The branching fraction in reference [566] happens to be on the low side, and its exclusion shifts the result by +0.008%. The FSR corrections are expected to shift the result upwards, and indeed contribute a shift of +0.019%. Finally, including the CLEO-c absolute $D^0 \rightarrow K^+K^-$ branching fraction contributes the final shift of +0.009%. As Fig. 73 shows, the K^+K^- branching fractions inferred from the combining the CDF and FOCUS branching ratios and the average $K^-\pi^+$ branching fraction (excluding the CLEO-c K^+K^- result) are both lower than the CLEO-c absolute measurement. The fit, therefore, exerts an upward pressure on the $K^-\pi^+$ result to improve the agreement in the K^+K^- sector.

Table 162: Evolution of the $D^0 \rightarrow K^-\pi^+$ branching fraction from a fit with no FSR corrections or correlations (similar to the average in the PDG 2009 update [444]) to the nominal fit presented here.

Modes	description	$\mathcal{B}(D^0 \rightarrow K^-\pi^+)$ (%)	χ^2 / (d.o.f.)
fit			
$K^-\pi^+$	PDG summer 2009 equivalent	$3.913 \pm 0.022 \pm 0.043$	6.0 / (8-1)
$K^-\pi^+$	drop Ref. [566]	$3.921 \pm 0.023 \pm 0.044$	4.8 / (7-1)
$K^-\pi^+$	add FSR corrections	$3.940 \pm 0.023 \pm 0.041 \pm 0.015$	4.0 / (7-1)
$K^-\pi^+$	add FSR correlations	$3.940 \pm 0.023 \pm 0.041 \pm 0.025$	4.2 / (7-1)
all	CDF + FOCUS only	$3.940 \pm 0.023 \pm 0.041 \pm 0.025$	4.5 / (12-3)
all	add CLEO-c K^+K^-	$3.949 \pm 0.023 \pm 0.040 \pm 0.025$	8.5 / (13-3)

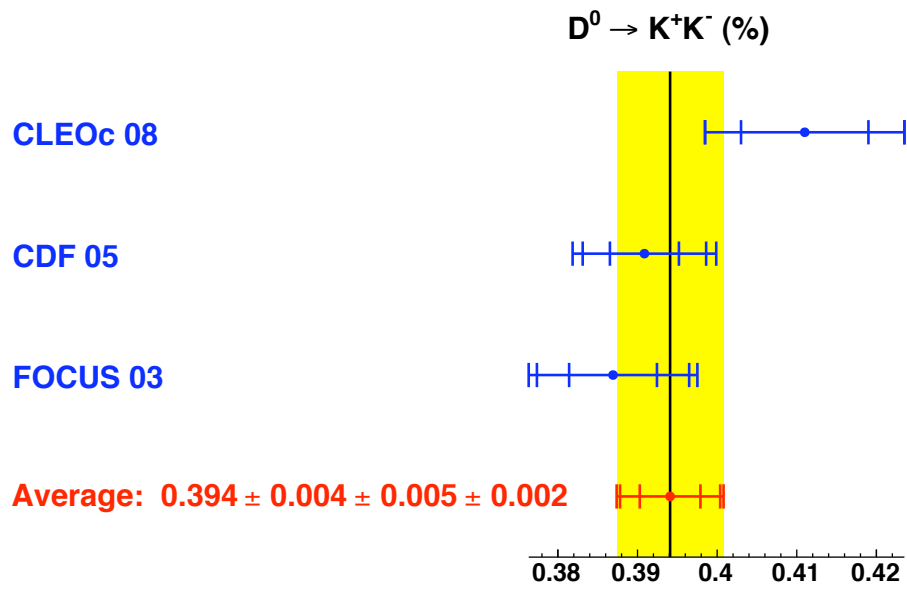


Figure 73: Comparison of the absolute CLEO-c $\mathcal{B}(D^0 \rightarrow K^+K^-)$ measurement, the CDF and FOCUS branching ratio measurements scaled by the $\mathcal{B}(D^0 \rightarrow K^-\pi^+)$ branching fraction, and this average (red point, yellow band).

9 τ lepton Properties

The aim of this chapter is to provide average values of the properties of the τ lepton. The mass of the τ lepton is presented in section 9.1, and the branching fractions of the decay modes are presented in section 9.2. Using these average values, we present tests of charged current lepton universality in section 9.3 and obtain estimates for $|V_{us}|$, the relative weak coupling between up and strange quarks, in section 9.4. We summarize the status of searches for lepton flavor violating decays of the τ lepton in section 9.5.

9.1 Mass of the τ lepton

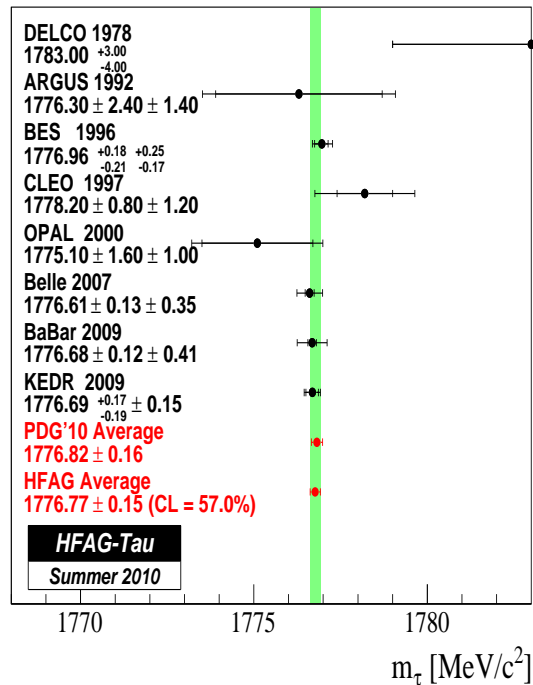


Figure 74: Measurements and average value of m_τ .

The mass of the τ lepton has recently been measured by the BaBar and Belle experiments using the end-point technique from the pseudo-mass distribution in $\tau^- \rightarrow \pi^- \pi^- \pi^+ \nu_\tau$ decays, as well as by the KEDR experiment from a study of the $\tau^+ \tau^-$ cross-section around the production threshold. In Figure 74 we present the measurements and average values of m_τ .

9.2 τ Branching Fractions:

In this section we present the measurements and average values of the τ branching fractions³⁷, including those which have been recently measured by the B-Factories. We take into account correlations between measurements, arising from common dependence on the τ -pair cross-section [567] and the assumed knowledge of the branching fractions for the background modes.

³⁷Charge conjugate τ decays are implied throughout.

For measurements from the same experiment, we treat the dependence on detector-specific systematics as sources of correlated systematic uncertainties.

We report here results from single-quantity averages, which includes correlations between the B-Factories, as well as the results from a global fit, which includes correlations between the different branching fractions. We label results from the former as ‘‘HFAG Average’’, and the latter as ‘‘HFAG Fit’’ in the following figures.

For the ‘‘HFAG Fit’’, we use 131 measurements from non-B-Factory experiments, which includes the set of 124 measurements used in the global fit performed by the PDG [5]. The measurements from non-B-Factories include 37 measurements from ALEPH, 2 measurements from ARGUS, 1 measurement from CELLO, 36 measurements from CLEO, 6 measurements from CLEO3, 14 measurements from DELPHI, 2 measurements from HRS, 11 measurements from L3, 19 measurements from OPAL, and 3 measurements from TPC.

All of these measurements can be expressed as a linear function of the form $\frac{(\sum_i \alpha_i P_i)}{(\sum_j \beta_j P_j)}$ of few selected branching fractions (P_i), which are labelled as base modes. The base modes are chosen such that they sum up to unity.

For the 124 measurements used in the PDG global fit, there are 31 base modes. These results and their corresponding references are listed in Ref. [5]. We first augment this set with 4 additional base modes of $\mathcal{B}(\tau^- \rightarrow K^- \pi^0 \eta \nu_\tau)$, $\mathcal{B}(\tau^- \rightarrow \bar{K}^0 \pi^- \eta \nu_\tau)$, $\mathcal{B}(\tau^- \rightarrow \bar{K}^0 \pi^- 2\pi^0 \nu_\tau)$ and $\mathcal{B}(\tau^- \rightarrow \bar{K}^0 h^- h^- h^+ \nu_\tau)$, because 2 of these modes (containing η) have been recently measured by the B-Factories with significant precision. We also include 2 measurements from CLEO for the modes containing η , 2 measurements from ALEPH for the other modes, and 1 measurement from OPAL of $\mathcal{B}(\tau^- \rightarrow \bar{K}^0 \pi^- \geq 1\pi^0 \nu_\tau)$. We further include 1 measurement of $\mathcal{B}(\tau^- \rightarrow \pi^- \pi^- \pi^+ \eta \nu_\tau)$ from CLEO, 1 measurement of $\mathcal{B}(\tau^- \rightarrow K^- \omega \nu_\tau)$ from CLEO3, and replace 1 base node of $\mathcal{B}(\tau^- \rightarrow h^- \omega \nu_\tau)$ with 2 base nodes containing measurements of $\mathcal{B}(\tau^- \rightarrow \pi^- \omega \nu_\tau)$ and $\mathcal{B}(\tau^- \rightarrow K^- \omega \nu_\tau)$. This leads us to a global fit to a set of 131 measurements with 36 base nodes.

Finally we include the following 22 measurements from the B-Factories:

- 12 measurements from the BaBar collaboration:

$$\begin{aligned}
\mathcal{B}(\tau^- \rightarrow \mu^- \bar{\nu}_\mu \nu_\tau) / \mathcal{B}(\tau^- \rightarrow e^- \bar{\nu}_e \nu_\tau) &= (0.9796 \pm 0.0016 \pm 0.0036) [568], \\
\mathcal{B}(\tau^- \rightarrow \pi^- \nu_\tau) / \mathcal{B}(\tau^- \rightarrow e^- \bar{\nu}_e \nu_\tau) &= (0.5945 \pm 0.0014 \pm 0.0061) [568], \\
\mathcal{B}(\tau^- \rightarrow K^- \nu_\tau) / \mathcal{B}(\tau^- \rightarrow e^- \bar{\nu}_e \nu_\tau) &= (0.03882 \pm 0.00032 \pm 0.00057) [568], \\
\mathcal{B}(\tau^- \rightarrow K^- \pi^0 \nu_\tau) &= (0.416 \pm 0.003 \pm 0.018)\% [569] \\
\mathcal{B}(\tau^- \rightarrow \bar{K}^0 \pi^- \nu_\tau) &= (0.840 \pm 0.004 \pm 0.023)\% [570] \\
\mathcal{B}(\tau^- \rightarrow \bar{K}^0 \pi^- \pi^0 \nu_\tau) &= (0.342 \pm 0.006 \pm 0.015)\% [571] \\
\mathcal{B}(\tau^- \rightarrow \pi^- \pi^- \pi^+ \nu_\tau \text{ (ex. } K^0)) &= (8.834 \pm 0.007 \pm 0.127)\% [572] \\
\mathcal{B}(\tau^- \rightarrow K^- \pi^- \pi^+ \nu_\tau \text{ (ex. } K^0)) &= (0.273 \pm 0.002 \pm 0.009)\% [572] \\
\mathcal{B}(\tau^- \rightarrow K^- \pi^- K^+ \nu_\tau) &= (0.1346 \pm 0.0010 \pm 0.0036)\% [572] \\
\mathcal{B}(\tau^- \rightarrow K^- K^- K^+ \nu_\tau) &= (1.58 \pm 0.13 \pm 0.12) \times 10^{-5} [572] \\
\mathcal{B}(\tau^- \rightarrow 3h^- 2h^+ \nu_\tau \text{ (ex. } K^0)) &= (8.56 \pm 0.05 \pm 0.42) \times 10^{-4} [573] \\
\mathcal{B}(\tau^- \rightarrow 2\pi^- \pi^+ \eta \nu_\tau \text{ (ex. } K^0)) &= (1.60 \pm 0.05 \pm 0.11) \times 10^{-4} [574]
\end{aligned}$$

- 10 measurements from the Belle collaboration:

$$\begin{aligned}
\mathcal{B}(\tau^- \rightarrow h^- \pi^0 \nu_\tau) &= (25.67 \pm 0.01 \pm 0.39)\% [575] \\
\mathcal{B}(\tau^- \rightarrow \bar{K}^0 \pi^- \nu_\tau) &= (0.808 \pm 0.004 \pm 0.026)\% [576] \\
\mathcal{B}(\tau^- \rightarrow \pi^- \pi^- \pi^+ \nu_\tau \text{ (ex. } K^0)) &= (8.420 \pm 0.003 \begin{smallmatrix} +0.260 \\ -0.250 \end{smallmatrix})\% [577] \\
\mathcal{B}(\tau^- \rightarrow K^- \pi^- \pi^+ \nu_\tau \text{ (ex. } K^0)) &= (0.330 \pm 0.001 \begin{smallmatrix} +0.016 \\ -0.017 \end{smallmatrix})\% [577] \\
\mathcal{B}(\tau^- \rightarrow K^- \pi^- K^+ \nu_\tau) &= (0.155 \pm 0.001 \begin{smallmatrix} +0.006 \\ -0.005 \end{smallmatrix})\% [577] \\
\mathcal{B}(\tau^- \rightarrow K^- K^- K^+ \nu_\tau) &= (3.29 \pm 0.17 \begin{smallmatrix} +0.19 \\ -0.20 \end{smallmatrix}) \times 10^{-5} [577] \\
\mathcal{B}(\tau^- \rightarrow \pi^- \pi^0 \eta \nu_\tau) &= (1.35 \pm 0.03 \pm 0.07) \times 10^{-3} [578] \\
\mathcal{B}(\tau^- \rightarrow K^- \eta \nu_\tau) &= (1.58 \pm 0.05 \pm 0.09) \times 10^{-4} [578] \\
\mathcal{B}(\tau^- \rightarrow K^- \pi^0 \eta \nu_\tau) &= (0.46 \pm 0.11 \pm 0.04) \times 10^{-4} [578] \\
\mathcal{B}(\tau^- \rightarrow \bar{K}^0 \pi^- \eta \nu_\tau) &= (0.88 \pm 0.14 \pm 0.04) \times 10^{-4} [578]
\end{aligned}$$

where the uncertainties are statistical and systematic, respectively.

We add to the list of base nodes one additional measurement of $\mathcal{B}(K^- \phi \nu_\tau (\phi \rightarrow KK)) = \mathcal{B}(K^- K^+ K^- \nu_\tau) \times (\mathcal{B}(\phi \rightarrow K^+ K^-) + \mathcal{B}(\phi \rightarrow K_S^0 K_L^0))$, which leads us to a global fit to a set of 153 measurements with 37 base nodes.

We try to take into account the correlations between measurements, and avoid applying the PDG-style scale factors to all our measurements. However, two of the measurements from the B-Factories have significant discrepancy with respect to each other. These are measurements of $\mathcal{B}(\tau^- \rightarrow K^- K^+ K^- \nu_\tau)$ from BaBar and Belle experiments, which are more than 5σ apart. We scale the errors from these measurements by a scale factor of 5.44 obtained from results of single-quantity ‘‘HFAG Average’’, using the same prescription as the PDG collaboration.

As far as possible, we try to include the measurements quoted in the original publications. For example, ALEPH presents results with the correlation matrix between measurements of hadronic modes in Ref. [579]. Their paper also quotes derived measurements for the pionic modes, after subtracting the kaonic contributions as measured by other experiments. PDG interpretes these published correlations between hadronic modes as correlations between the pionic modes, and uses the measurements of pionic modes. Our reasoning is that the B-Factories can measure the kaonic modes with better precision, thanks to the excellent particle-identification system in our respective experiments. Thus the estimates for the kaonic contribution subtracted from the hadronic modes should be revisited based on data from B-Factories.

We interpret the ALEPH data as measurements for the hadronic modes and treat their measured correlation matrix as between the following decay modes : $\tau^- \rightarrow e^- \bar{\nu}_e \nu_\tau$, $\tau^- \rightarrow \mu^- \bar{\nu}_\mu \nu_\tau$, $\tau^- \rightarrow h^- \nu_\tau$, $\tau^- \rightarrow h^- \pi^0 \nu_\tau$, $\tau^- \rightarrow h^- 2\pi^0 \nu_\tau$, $\tau^- \rightarrow h^- 3\pi^0 \nu_\tau$, $\tau^- \rightarrow h^- 4\pi^0 \nu_\tau$, $\tau^- \rightarrow 3h^- \nu_\tau$, $\tau^- \rightarrow 3h^- \pi^0 \nu_\tau$, $\tau^- \rightarrow 3h^- 2\pi^0 \nu_\tau$, $\tau^- \rightarrow 3h^- 3\pi^0 \nu_\tau$, $\tau^- \rightarrow 5h^- \nu_\tau$ and $\tau^- \rightarrow 5h^- \pi^0 \nu_\tau$, where $h^- = \pi^-$ or ^-K , as in the original publication. Since the ALEPH measurements of these branching fractions have been constrained to add up to unity, we exclude the weakest measurement of $\tau^- \rightarrow 3h^- 3\pi^0 \nu_\tau$ in our global fit, as in the PDG global fit.

If the unitarity constraint is dropped from the global fit to 124 measurements, sum of the 31 base modes fall short from unity by 1.0σ (0.9σ) in the scenario when ALEPH correlation matrix is modified (un-modified). From the global fit to 153 measurements including those from B-Factories, sum of the 37 base modes fall short from unity by 1.6σ (1.9σ) when ALEPH correlation matrix is modified (un-modified).

A summary of quality of these global fits are presented in Table 163 for the constrained and unconstrained cases with data from non-B-Factories and including those from B-Factories. The results of the global fit to 131 and 153 measurements are presented in Tables 164 and 165 for the constrained and unconstrained cases, respectively.

	unconstrained fit			constrained fit		
	124	131	153	124	131	153
# of measurements	124	131	153	124	131	153
# of base nodes	31	36	37	31	36	37
χ^2	78.2	83.0	140.9	79.1	83.1	143.4
CL (%)	86.5	80.6	5.8	86.4	82.3	4.9
Deviation from unitarity	-1.0 σ	-0.4 σ	-1.6 σ			

Table 163: Summary of global fits for branching fractions from unconstrained and constrained fits to data from non-B-Factories and including those from B-Factories.

In the following, we present results of branching fractions of modes separated according to one or three or five charged tracks (“prongs”) in the final state, or decays containing K^0 , η , K^{*0} :

- 1-prong decays with 0 or 1 π^0 :

The measurements and average values of $\mathcal{B}(\tau^- \rightarrow \mu^- \bar{\nu}_\mu \nu_\tau)$, $\mathcal{B}(\tau^- \rightarrow \pi^- \nu_\tau)$, $\mathcal{B}(\tau^- \rightarrow K^- \nu_\tau)$, $\mathcal{B}(\tau^- \rightarrow h^- \nu_\tau)$, where $h^- = \pi^-$ or K^- , are presented in Figure 75, and those of $\mathcal{B}(\tau^- \rightarrow \pi^- \pi^0 \nu_\tau)$, $\mathcal{B}(\tau^- \rightarrow K^- \pi^0 \nu_\tau)$ and $\mathcal{B}(\tau^- \rightarrow h^- \pi^0 \nu_\tau)$ decays are presented in Figure 76.

- 3-prong decays with 0 π^0 , 0 K^0 :

The measurements and average values of $\mathcal{B}(\tau^- \rightarrow h^- h^- h^+ \nu_\tau$ (ex. K^0)), $\mathcal{B}(\tau^- \rightarrow \pi^- \pi^- \pi^+ \nu_\tau$ (ex. K^0)), $\mathcal{B}(\tau^- \rightarrow \pi^- K^- \pi^+ \nu_\tau$ (ex. K^0)), $\mathcal{B}(\tau^- \rightarrow \pi^- K^- K^+ \nu_\tau)$ and $\mathcal{B}(\tau^- \rightarrow K^- K^- K^+ \nu_\tau)$, where $h^- = \pi^-$ or K^- , are presented in Figures 77 and 78.

The measurements of $\mathcal{B}(\tau^- \rightarrow K^- \phi \nu_\tau)$ are also presented in Figure 78, along with results from the single-quantity averaging procedure. While the BaBar measurement uses the same data set as in the measurement of $\mathcal{B}(\tau^- \rightarrow K^- K^- K^+ \nu_\tau)$, Belle measurement uses a different data set for $\mathcal{B}(\tau^- \rightarrow K^- \phi \nu_\tau)$ measurement than used for their $\mathcal{B}(\tau^- \rightarrow K^- K^- K^+ \nu_\tau)$ measurement. To avoid redundancy, we do not use measurements of $\mathcal{B}(\tau^- \rightarrow K^- \phi \nu_\tau)$ in the global fit, and no results for this mode from “HFAG Fit” are quoted in Figure 78.

The BaBar experiments also reports $\mathcal{B}(\tau^- \rightarrow \pi^- \phi \nu_\tau) = (3.42 \pm 0.55 \pm 0.25) \times 10^{-5}$ [572]. Since it is the only measurement for this channel, no averaging has been performed.

- 5-prong decays with 0 π^0 , 0 K^0 :

The measurements and average values of $\mathcal{B}(\tau^- \rightarrow h^- h^- h^- h^+ h^+ \nu_\tau$ (ex. K^0)) and $\mathcal{B}(\tau^- \rightarrow \pi^- f_1(1285) \nu_\tau)$ are presented in Figure 79. The $f_1(1285)$ content is determined from $2\pi^- 2\pi^+$ as well as $\pi^- \pi^+ \eta$ final states [574]. The average value of $\mathcal{B}(\tau^- \rightarrow \pi^- f_1(1285) \nu_\tau)$ from the single-quantity averaging procedure is also quoted in Figure 79.

- decays with K^0 :

The measurements and average values of $\mathcal{B}(\tau^- \rightarrow \pi^- \bar{K}^0 \nu_\tau)$ and $\mathcal{B}(\tau^- \rightarrow \pi^- \pi^0 \bar{K}^0 \nu_\tau)$ are presented in Figure 80.

Base modes from τ^- decay	No B-Factory Data	With B-Factory Data
leptonic modes		
$e^- \bar{\nu}_e \nu_\tau$	17.835 ± 0.049	17.818 ± 0.041
$\mu^- \bar{\nu}_\mu \nu_\tau$	17.349 ± 0.047	17.393 ± 0.040
non-strange modes		
$\pi^- \nu_\tau$	10.898 ± 0.066	10.811 ± 0.053
$\pi^- \pi^0 \nu_\tau$	25.489 ± 0.097	25.506 ± 0.092
$\pi^- 2\pi^0 \nu_\tau$ (ex. K^0)	9.227 ± 0.100	9.245 ± 0.100
$\pi^- 3\pi^0 \nu_\tau$ (ex. K^0)	1.029 ± 0.075	1.035 ± 0.075
$h^- 4\pi^0 \nu_\tau$ (ex. K^0, η)	0.098 ± 0.039	0.109 ± 0.039
$K^- K^0 \nu_\tau$	0.152 ± 0.016	0.157 ± 0.016
$K^- \pi^0 K^0 \nu_\tau$	0.154 ± 0.020	0.158 ± 0.020
$\pi^- K_S^0 K_S^0 \nu_\tau$	0.024 ± 0.005	0.024 ± 0.005
$\pi^- K_S^0 K_L^0 \nu_\tau$	0.107 ± 0.025	0.111 ± 0.025
$\pi^- \pi^- \pi^+ \nu_\tau$ (ex. K^0, ω)	8.948 ± 0.062	8.969 ± 0.051
$\pi^- \pi^- \pi^+ \pi^0 \nu_\tau$ (ex. K^0, ω)	2.752 ± 0.070	2.762 ± 0.069
$h^- h^- h^+ 2\pi^0 \nu_\tau$ (ex. K^0, ω, η)	0.085 ± 0.037	0.097 ± 0.036
$h^- h^- h^+ 3\pi^0 \nu_\tau$	0.025 ± 0.005	0.032 ± 0.003
$\pi^- K^- K^+ \nu_\tau$	0.153 ± 0.007	0.143 ± 0.003
$\pi^- K^- K^+ \pi^0 \nu_\tau$	0.006 ± 0.002	0.006 ± 0.002
$3h^- 2h^+ \nu_\tau$ (ex. K^0)	0.081 ± 0.005	0.082 ± 0.003
$3h^- 2h^+ \pi^0 \nu_\tau$ (ex. K^0)	0.019 ± 0.003	0.020 ± 0.002
$\pi^- \pi^0 \eta \nu_\tau$	0.174 ± 0.024	0.139 ± 0.007
$\pi^- \omega \nu_\tau$	1.952 ± 0.064	1.955 ± 0.064
$h^- \pi^0 \omega \nu_\tau$	0.404 ± 0.042	0.406 ± 0.042
strange modes		
$K^- \nu_\tau$	0.686 ± 0.022	0.696 ± 0.010
$K^- \pi^0 \nu_\tau$	0.453 ± 0.027	0.431 ± 0.015
$K^- 2\pi^0 \nu_\tau$ (ex. K^0)	0.057 ± 0.023	0.061 ± 0.022
$K^- 3\pi^0 \nu_\tau$ (ex. K^0, η)	0.037 ± 0.022	0.040 ± 0.022
$\bar{K}^0 \pi^- \nu_\tau$	0.884 ± 0.038	0.826 ± 0.018
$\bar{K}^0 \pi^- \pi^0 \nu_\tau$	0.355 ± 0.036	0.347 ± 0.015
$\bar{K}^0 \pi^- 2\pi^0 \nu_\tau$	0.026 ± 0.023	0.028 ± 0.023
$\bar{K}^0 h^- h^- h^+ \nu_\tau$	0.022 ± 0.020	0.022 ± 0.020
$K^- \pi^- \pi^+ \nu_\tau$ (ex. K^0, ω)	0.334 ± 0.023	0.293 ± 0.007
$K^- \pi^- \pi^+ \pi^0 \nu_\tau$ (ex. K^0, ω, η)	0.039 ± 0.014	0.041 ± 0.014
$K^- \phi \nu_\tau$ ($\phi \rightarrow KK$)		0.004 ± 0.001
$K^- \eta \nu_\tau$	0.027 ± 0.006	0.016 ± 0.001
$K^- \pi^0 \eta \nu_\tau$	0.018 ± 0.009	0.005 ± 0.001
$\bar{K}^0 \pi^- \eta \nu_\tau$	0.022 ± 0.007	0.009 ± 0.001
$K^- \omega \nu_\tau$	0.041 ± 0.009	0.041 ± 0.009
Sum of strange modes	3.0002 ± 0.0764	2.8606 ± 0.0515
Sum of all modes	99.9602 ± 0.1107	99.8389 ± 0.1030

Table 164: Results for branching fractions (in %) from unconstrained fit to data from non-B-Factories and including those from B-Factories.

Base modes from τ^- decay	No B-Factory Data	With B-Factory Data
leptonic modes		
$e^- \bar{\nu}_e \nu_\tau$	17.838 ± 0.048	17.833 ± 0.040
$\mu^- \bar{\nu}_\mu \nu_\tau$	17.352 ± 0.046	17.408 ± 0.038
non-strange modes		
$\pi^- \nu_\tau$	10.903 ± 0.064	10.831 ± 0.051
$\pi^- \pi^0 \nu_\tau$	25.495 ± 0.095	25.531 ± 0.090
$\pi^- 2\pi^0 \nu_\tau$ (ex. K^0)	9.233 ± 0.099	9.278 ± 0.097
$\pi^- 3\pi^0 \nu_\tau$ (ex. K^0)	1.031 ± 0.075	1.046 ± 0.074
$h^- 4\pi^0 \nu_\tau$ (ex. K^0, η)	0.098 ± 0.039	0.107 ± 0.039
$K^- K^0 \nu_\tau$	0.153 ± 0.016	0.160 ± 0.016
$K^- \pi^0 K^0 \nu_\tau$	0.154 ± 0.020	0.162 ± 0.019
$\pi^- K_S^0 K_S^0 \nu_\tau$	0.024 ± 0.005	0.024 ± 0.005
$\pi^- K_S^0 K_L^0 \nu_\tau$	0.108 ± 0.025	0.119 ± 0.024
$\pi^- \pi^- \pi^+ \nu_\tau$ (ex. K^0, ω)	8.952 ± 0.061	8.983 ± 0.050
$\pi^- \pi^- \pi^+ \pi^0 \nu_\tau$ (ex. K^0, ω)	2.749 ± 0.069	2.751 ± 0.069
$h^- h^- h^+ 2\pi^0 \nu_\tau$ (ex. K^0, ω, η)	0.085 ± 0.037	0.097 ± 0.036
$h^- h^- h^+ 3\pi^0 \nu_\tau$	0.026 ± 0.005	0.032 ± 0.003
$\pi^- K^- K^+ \nu_\tau$	0.153 ± 0.007	0.144 ± 0.003
$\pi^- K^- K^+ \pi^0 \nu_\tau$	0.006 ± 0.002	0.006 ± 0.002
$3h^- 2h^+ \nu_\tau$ (ex. K^0)	0.081 ± 0.005	0.082 ± 0.003
$3h^- 2h^+ \pi^0 \nu_\tau$ (ex. K^0)	0.019 ± 0.003	0.020 ± 0.002
$\pi^- \pi^0 \eta \nu_\tau$	0.175 ± 0.024	0.139 ± 0.007
$\pi^- \omega \nu_\tau$	1.953 ± 0.064	1.959 ± 0.064
$h^- \pi^0 \omega \nu_\tau$	0.404 ± 0.042	0.409 ± 0.042
strange modes		
$K^- \nu_\tau$	0.686 ± 0.022	0.697 ± 0.010
$K^- \pi^0 \nu_\tau$	0.453 ± 0.027	0.431 ± 0.015
$K^- 2\pi^0 \nu_\tau$ (ex. K^0)	0.057 ± 0.023	0.060 ± 0.022
$K^- 3\pi^0 \nu_\tau$ (ex. K^0, η)	0.036 ± 0.022	0.039 ± 0.022
$\bar{K}^0 \pi^- \nu_\tau$	0.888 ± 0.037	0.831 ± 0.018
$\bar{K}^0 \pi^- \pi^0 \nu_\tau$	0.358 ± 0.035	0.350 ± 0.015
$\bar{K}^0 \pi^- 2\pi^0 \nu_\tau$	0.027 ± 0.023	0.035 ± 0.023
$\bar{K}^0 h^- h^- h^+ \nu_\tau$	0.023 ± 0.020	0.028 ± 0.020
$K^- \pi^- \pi^+ \nu_\tau$ (ex. K^0, ω)	0.334 ± 0.023	0.293 ± 0.007
$K^- \pi^- \pi^+ \pi^0 \nu_\tau$ (ex. K^0, ω, η)	0.039 ± 0.014	0.041 ± 0.014
$K^- \phi \nu_\tau (\phi \rightarrow KK)$		0.004 ± 0.001
$K^- \eta \nu_\tau$	0.027 ± 0.006	0.016 ± 0.001
$K^- \pi^0 \eta \nu_\tau$	0.018 ± 0.009	0.005 ± 0.001
$\bar{K}^0 \pi^- \eta \nu_\tau$	0.022 ± 0.007	0.009 ± 0.001
$K^- \omega \nu_\tau$	0.041 ± 0.009	0.041 ± 0.009
Sum of strange modes	3.0091 ± 0.0722	2.8796 ± 0.0501
Sum of all modes	100.00	100.00

Table 165: Results for branching fractions (in %) from unitarity constrained fit to data from non-B-Factories and including those from B-Factories.

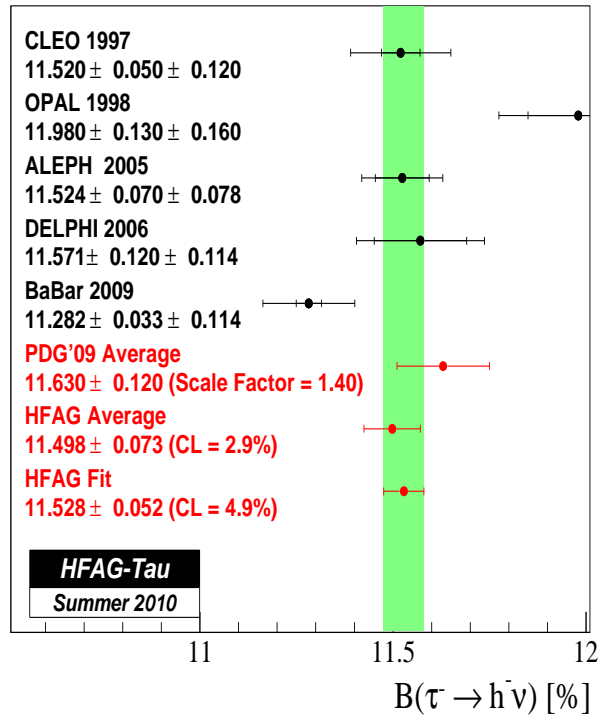
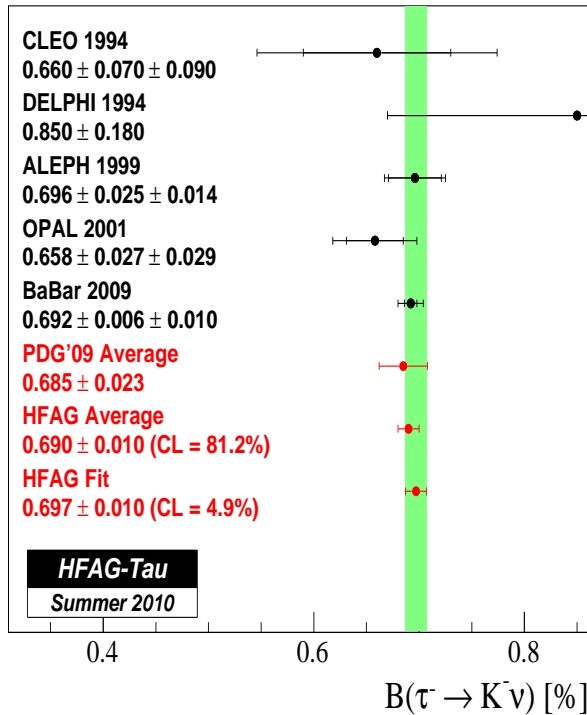
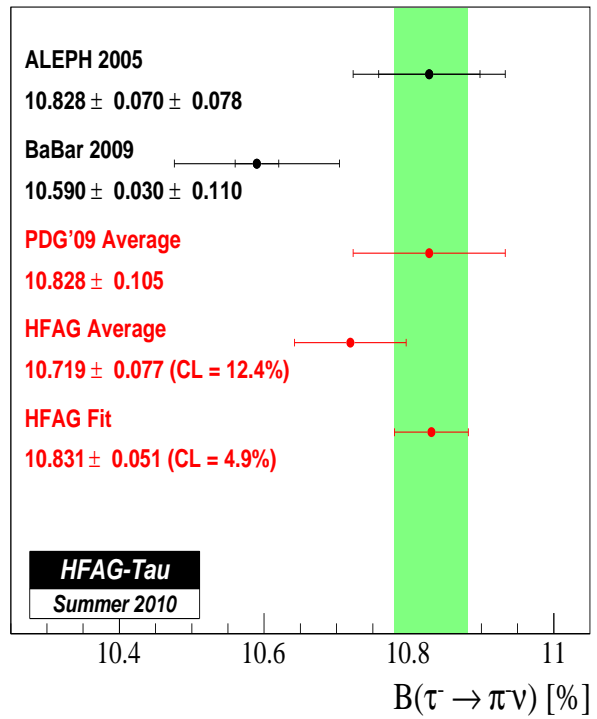
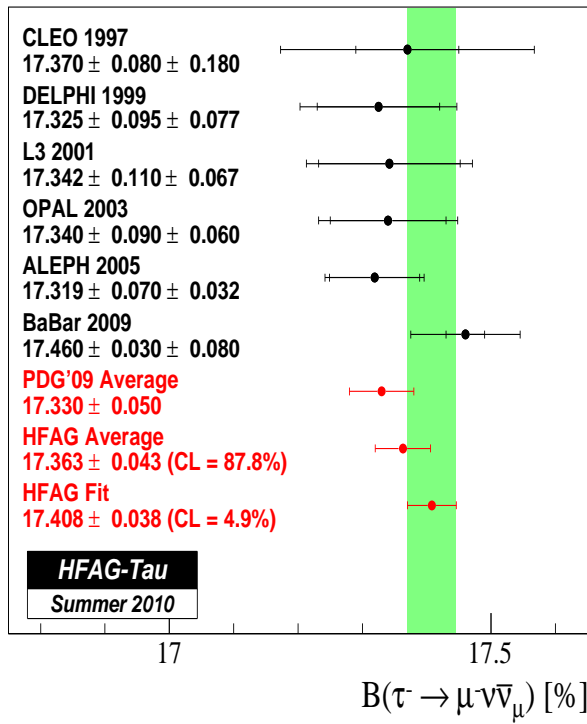


Figure 75: Measurements and average values of 1-prong decays with 0 π^0 .

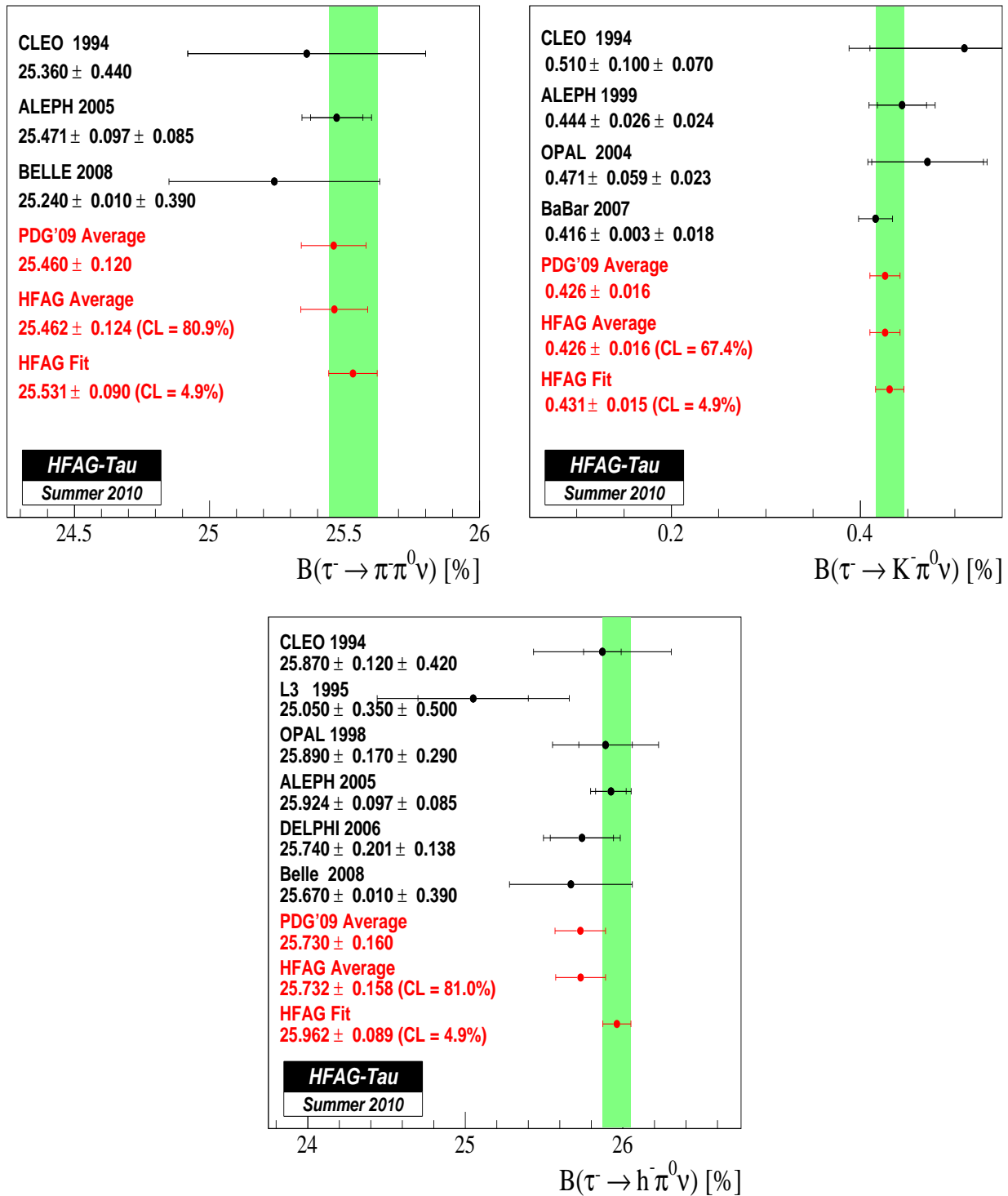


Figure 76: Measurements and average values of 1-prong decays with 1 π^0 .

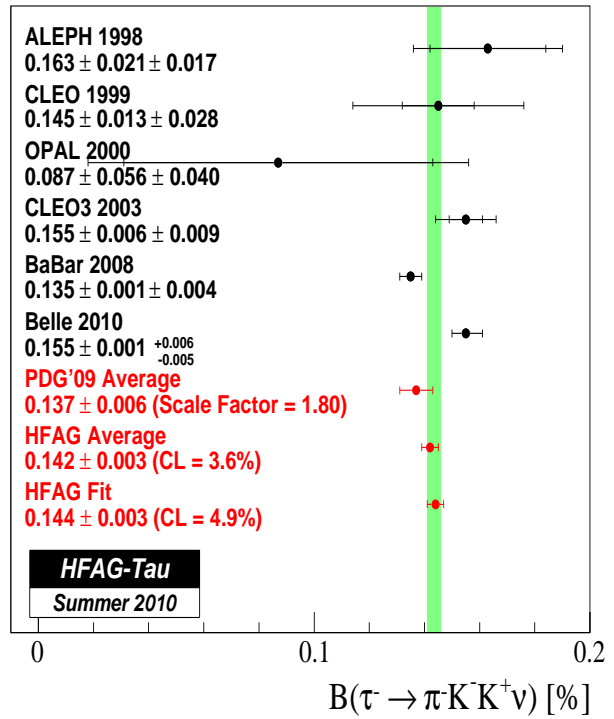
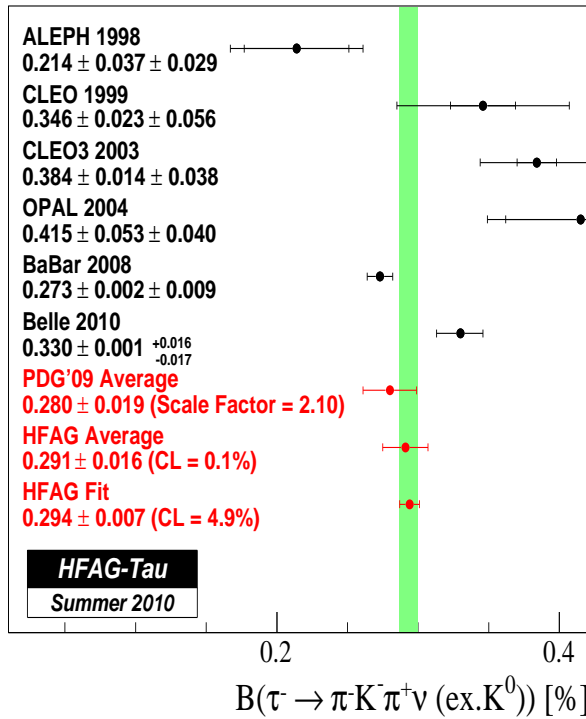
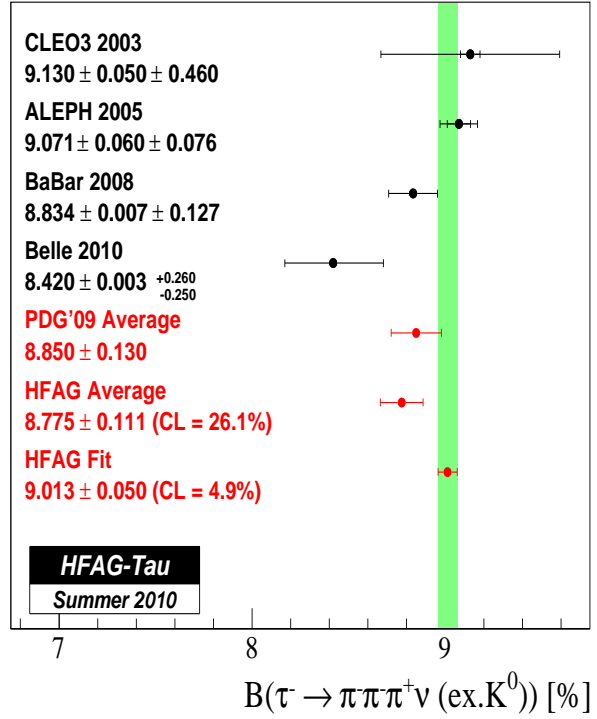
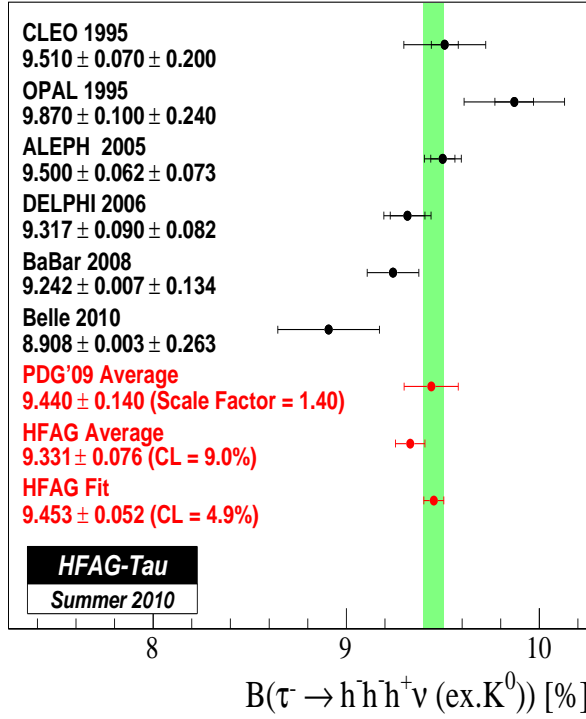


Figure 77: Measurements and average values of 3-prong decays with 0 π^0 , 0 \bar{K}^0 . ALEPH quotes $\mathcal{B}(\tau^- \rightarrow h^- h^- h^+ \nu_\tau)$ (ex. K^0, ω) = $(9.469 \pm 0.062 \pm 0.073)\%$ and $\mathcal{B}(\tau^- \rightarrow \pi^- \pi^- \pi^+ \nu_\tau)$ (ex. K^0, ω) = $(9.041 \pm 0.060 \pm 0.076)\%$. We add $\mathcal{B}(\tau^- \rightarrow h^- \omega \nu_\tau) \times \mathcal{B}(\omega \rightarrow \pi^- \pi^+) = 0.031\%$ and $\mathcal{B}(\tau^- \rightarrow \pi^- \omega \nu_\tau) \times \mathcal{B}(\omega \rightarrow \pi^- \pi^+) = 0.030\%$, respectively, to get the values quoted here.

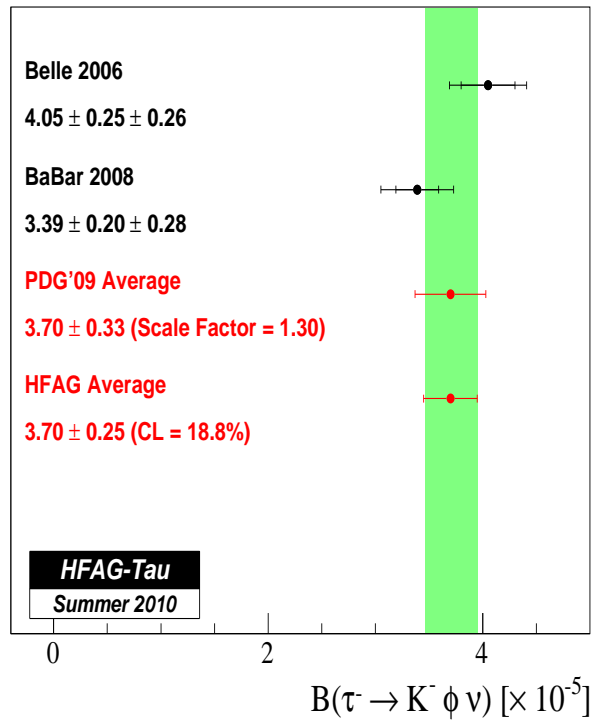
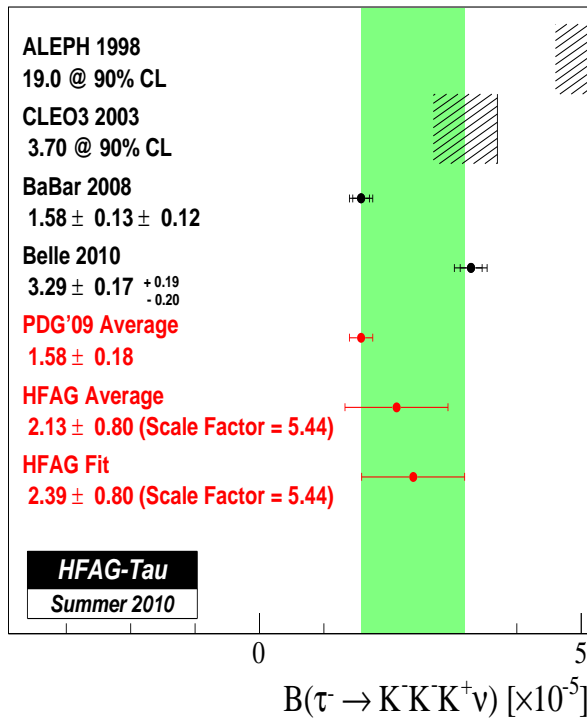


Figure 78: Measurements and average values of $B(\tau^- \rightarrow K^- K^- K^+ \nu_\tau)$ and $B(\tau^- \rightarrow K^- \phi \nu_\tau)$.

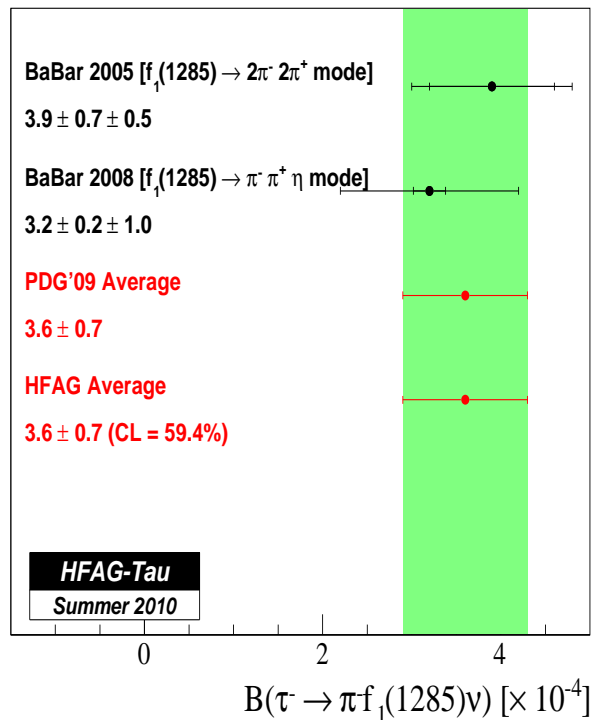
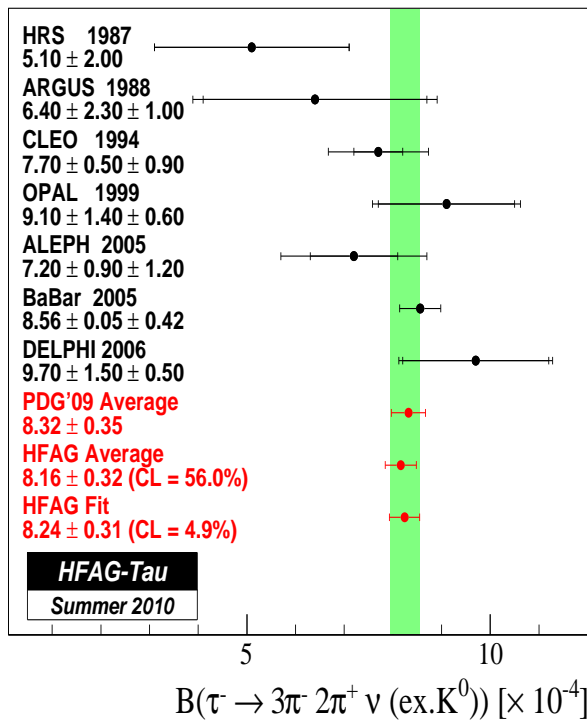


Figure 79: Measurements and average values of $B(\tau^- \rightarrow h^- h^- h^- h^+ h^+ \nu_\tau \text{ (ex. } K^0))$ and $B(\tau^- \rightarrow \pi^- f_1(1285) \nu_\tau)$.

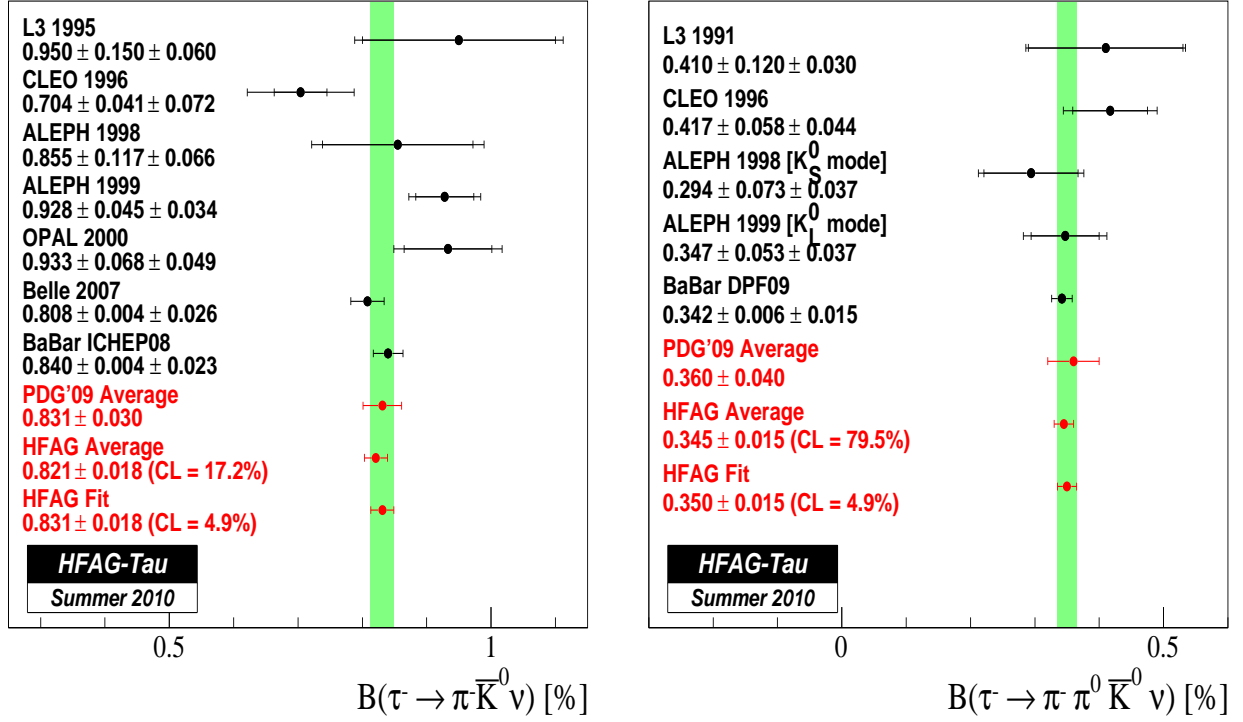


Figure 80: Measurements and average values of $\mathcal{B}(\tau^- \rightarrow \pi^- \bar{K}^0 \nu_\tau)$ and $\mathcal{B}(\tau^- \rightarrow \pi^- \pi^0 \bar{K}^0 \nu_\tau)$.

- decays with η :

The measurements and average values of $\mathcal{B}(\tau^- \rightarrow K^- \eta \nu_\tau)$, $\mathcal{B}(\tau^- \rightarrow \pi^- \bar{K}^0 \eta \nu_\tau)$ and $\mathcal{B}(\tau^- \rightarrow K^- \pi^0 \eta \nu_\tau)$ are presented in Figure 81. The K^{*-} content is determined from $\tau^- \rightarrow \pi^- K_S^0 \eta \nu_\tau$ and $\tau^- \rightarrow K^- \pi^0 \eta \nu_\tau$ decay modes. The measurements and average values for $\mathcal{B}(\tau^- \rightarrow K^{*-} \eta \nu_\tau)$ are also presented in Figure 81.

The measurements and average values of $\mathcal{B}(\tau^- \rightarrow \pi^- \pi^0 \eta \nu_\tau)$ and $\mathcal{B}(\tau^- \rightarrow \pi^- \pi^- \pi^+ \eta \nu_\tau)$ (ex. K^0) are presented in Figure 82.

- decays with K^{*0} :

The measurements and average values for $\mathcal{B}(\tau^- \rightarrow K^- K^{*0} \nu_\tau)$ are presented in Figure 83. The Belle experiments also reports $\mathcal{B}(\tau^- \rightarrow K^- K^{*0} \pi^0 \nu_\tau) = (2.39 \pm 0.46 \pm 0.26) \times 10^{-5}$ [580], which is the first measurement for this mode.

9.3 Tests of Lepton Universality

Tests of $\mu - e$ universality can be expressed as

$$\left(\frac{g_\mu}{g_e}\right)^2 = \frac{\mathcal{B}(\tau^- \rightarrow \mu^- \bar{\nu}_\mu \nu_\tau) f(m_e^2/m_\tau^2)}{\mathcal{B}(\tau^- \rightarrow e^- \bar{\nu}_e \nu_\tau) f(m_\mu^2/m_\tau^2)}, \quad (226)$$

where $f(x) = 1 - 8x + 8x^3 - x^4 - 12x^2 \log x$, assuming that the neutrino masses are negligible [581].

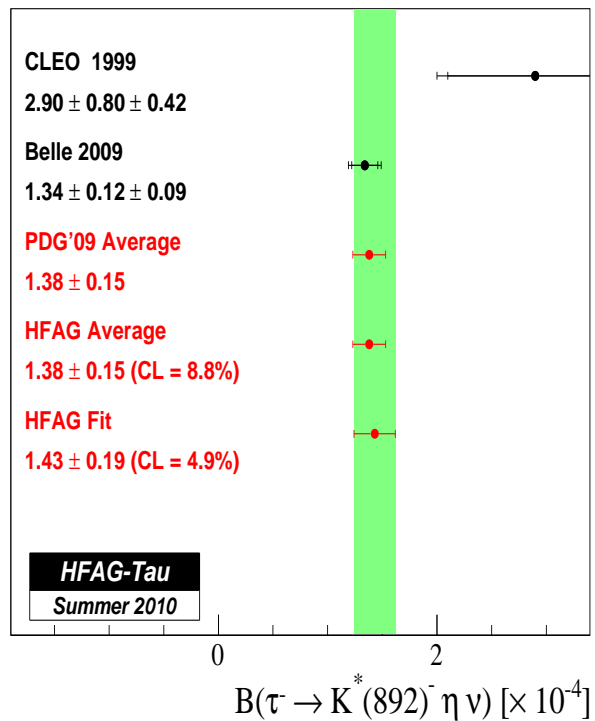
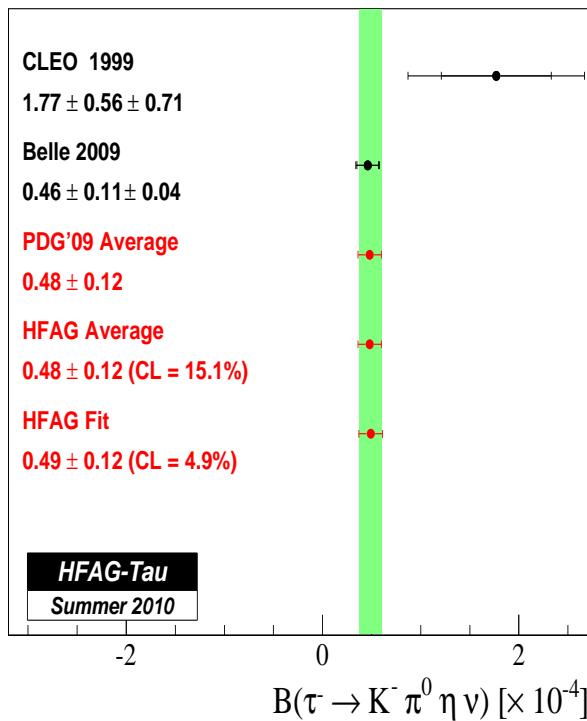
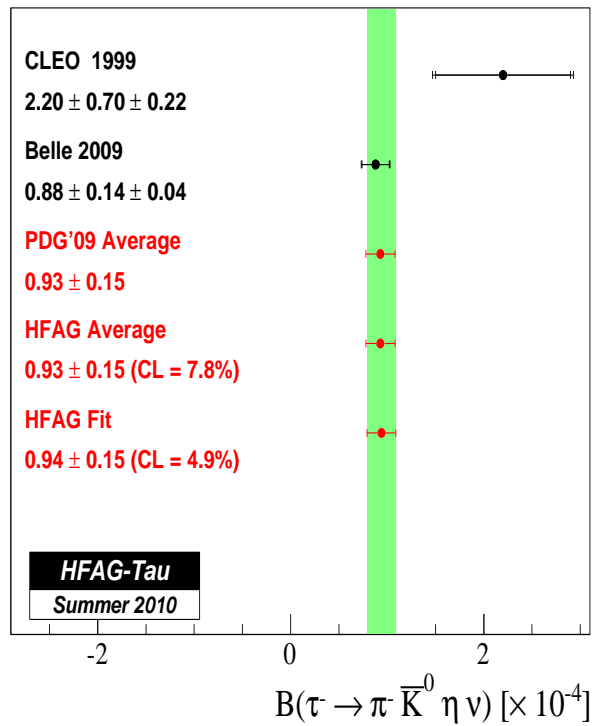
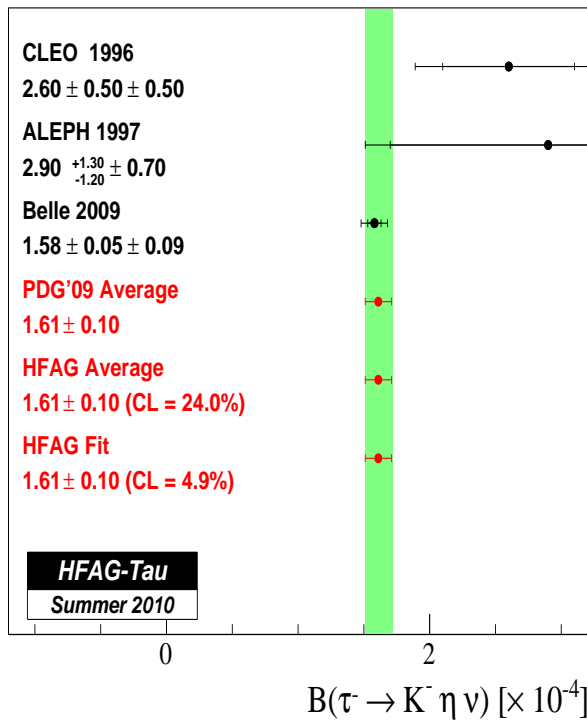


Figure 81: Measurements and average values of $\mathcal{B}(\tau^- \rightarrow K^- \eta \nu_\tau)$, $\mathcal{B}(\tau^- \rightarrow \pi^- \bar{K}^0 \eta \nu_\tau)$, $\mathcal{B}(\tau^- \rightarrow K^- \pi^0 \eta \nu_\tau)$, and $\mathcal{B}(\tau^- \rightarrow K^{*-} \eta \nu_\tau)$.

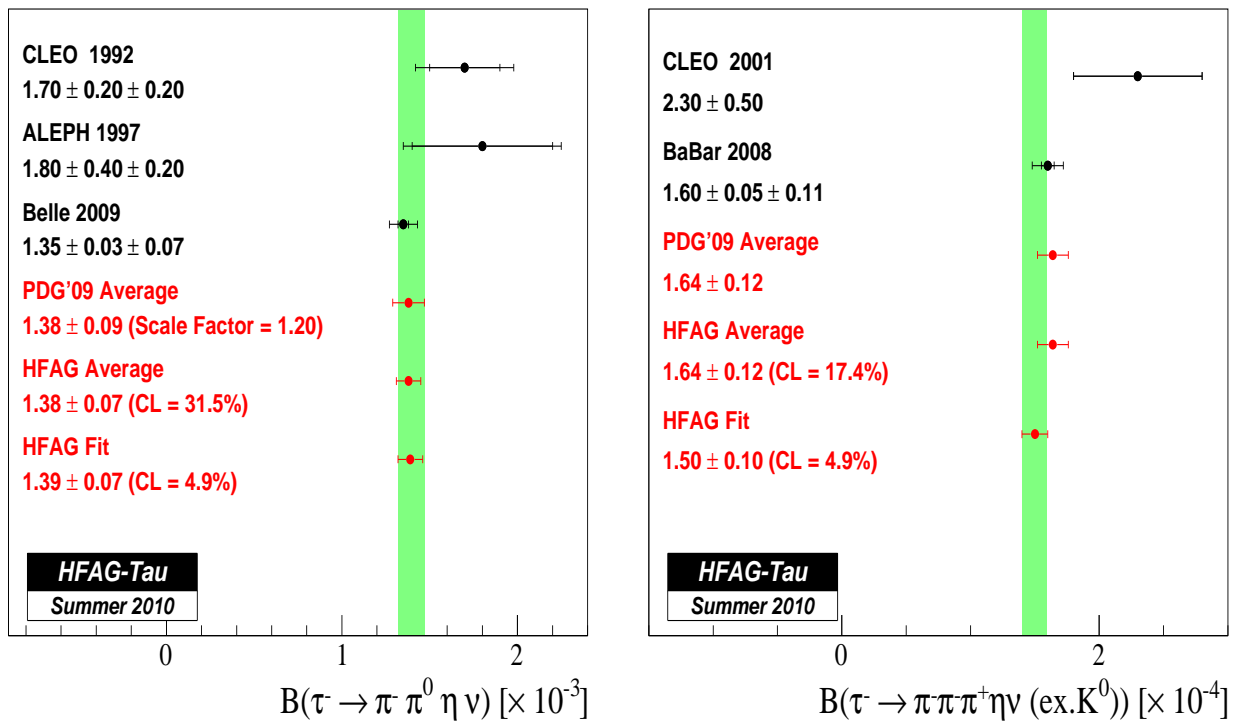


Figure 82: Measurements and average values of $B(\tau^- \rightarrow \pi^- \pi^0 \eta \nu_\tau)$ and $B(\tau^- \rightarrow \pi^- \pi^- \pi^+ \eta \nu_\tau \text{ (ex. } K^0))$.

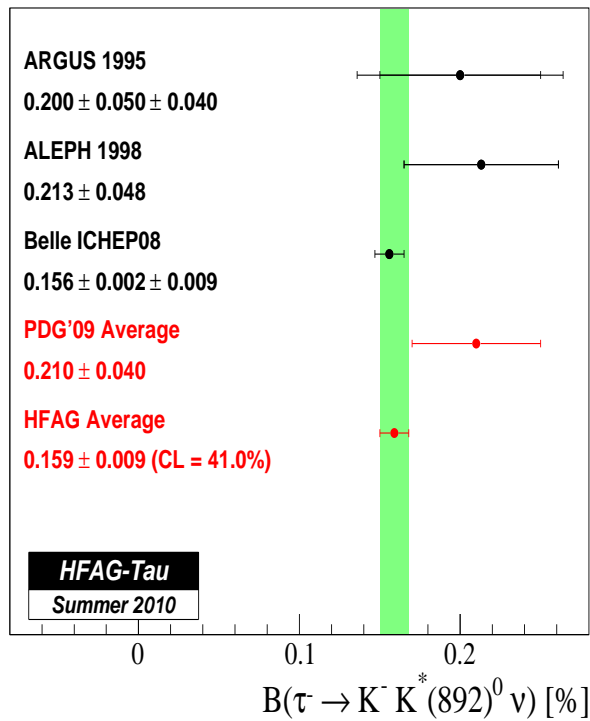


Figure 83: Measurements and average values of $B(\tau^- \rightarrow K^- K^{*0} \nu_\tau)$.

From the unitarity constrained fit, we obtain $\mathcal{B}(\tau^- \rightarrow \mu^- \bar{\nu}_\mu \nu_\tau) / \mathcal{B}(\tau^- \rightarrow e^- \bar{\nu}_e \nu_\tau) = 0.9762 \pm 0.0028$, which includes a correlation co-efficient of 18.33% between the branching fractions. This yields a value of $\left(\frac{g_\mu}{g_e}\right) = 1.0019 \pm 0.0014$, which is consistent with the SM value.

These predictions from τ decays are more precise than the other determinations:

- We average the measurements of $\mathcal{B}(\pi \rightarrow e \nu_e(\gamma)) / \mathcal{B}(\pi \rightarrow \mu \nu_\mu(\gamma)) = (1.2265 \pm 0.0034 \text{ (stat)} \pm 0.0044 \text{ (syst)}) \times 10^{-4}$ from TRIUMF [582] and $= (1.2346 \pm 0.0035 \text{ (stat)} \pm 0.0036 \text{ (syst)}) \times 10^{-4}$ from PSI [583], to obtain a value of $(1.2310 \pm 0.0037) \times 10^{-4}$. Comparing this with the prediction of $(1.2352 \pm 0.0001) \times 10^{-4}$ from recent theoretical calculations [584], we obtain a value of $\left(\frac{g_\mu}{g_e}\right) = 1.0017 \pm 0.0015$.
- The ratio $\mathcal{B}(K \rightarrow e \nu_e(\gamma)) / \mathcal{B}(K \rightarrow \mu \nu_\mu(\gamma))$ has recently been measured very precisely by the KLOE [585] and the NA62 [586] collaborations. Using the new world average value of $(2.487 \pm 0.012) \times 10^{-5}$ from Ref. [587], and the predicted value of $(2.477 \pm 0.001) \times 10^{-5}$ from Ref. [584], we obtain $\left(\frac{g_\mu}{g_e}\right) = 0.9980 \pm 0.0025$.
- From the report of the FlaviaNet Working Group on Kaon Decays [588], we obtain $\left(\frac{g_\mu}{g_e}\right) = 1.0010 \pm 0.0025$ using measurements of $\mathcal{B}(K \rightarrow \pi \mu \bar{\nu}) / \mathcal{B}(K \rightarrow \pi e \bar{\nu})$.
- From the report of the LEP Electroweak Working Group [589], we obtain $\left(\frac{g_\mu}{g_e}\right) = 0.997 \pm 0.010$ using measurements of $\mathcal{B}(W \rightarrow \mu \bar{\nu}_\mu) / \mathcal{B}(W \rightarrow e \bar{\nu}_e)$.

Tau-muon universality is tested with

$$\left(\frac{g_\tau}{g_\mu}\right)^2 = \frac{\mathcal{B}(\tau \rightarrow h \nu_\tau)}{\mathcal{B}(h \rightarrow \mu \bar{\nu}_\mu)} \frac{2m_h m_\mu^2 \tau_h}{(1 + \delta_h) m_\tau^3 \tau_\tau} \left(\frac{1 - m_\mu^2/m_h^2}{1 - m_h^2/m_\tau^2}\right)^2, \quad (227)$$

where $h = \pi$ or K and the radiative corrections are $\delta_\pi = (0.16 \pm 0.14)\%$ and $\delta_K = (0.90 \pm 0.22)\%$ [590, 591, 592]. Using the world averaged mass and lifetime values and meson decay rates [5] and our unitarity constrained fit, we determine $\left(\frac{g_\tau}{g_\mu}\right) = 0.9966 \pm 0.0030$ (0.9860 ± 0.0073) from the pionic and kaonic branching fractions, where the correlation co-efficient between these values are 13.10%. Combining these results, we obtain $\left(\frac{g_\tau}{g_\mu}\right) = 0.9954 \pm 0.0029$, which is 1.6σ below the SM expectation.

We also test lepton universality between τ and μ (e), by comparing the averaged electronic (muonic) branching fractions of the τ lepton with the predicted branching fractions from measurements of the τ and μ lifetimes and their respective masses [5], using known electroweak and radiative corrections [590]. This gives $\left(\frac{g_\tau}{g_\mu}\right) = 1.0011 \pm 0.0021$ and $\left(\frac{g_\tau}{g_e}\right) = 1.0030 \pm 0.0021$. The correlation co-efficient between the determination of $\left(\frac{g_\tau}{g_\mu}\right)$ from electronic branching fraction with the ones obtained from pionic and kaonic branching fractions are 48.16% and 21.82%, respectively. Averaging these three values, we obtain $\left(\frac{g_\tau}{g_\mu}\right) = 1.0001 \pm 0.0020$, which is consistent with the SM value. In Figure 84, we compare these above determinations with each other and with the values obtained from W decays [589].

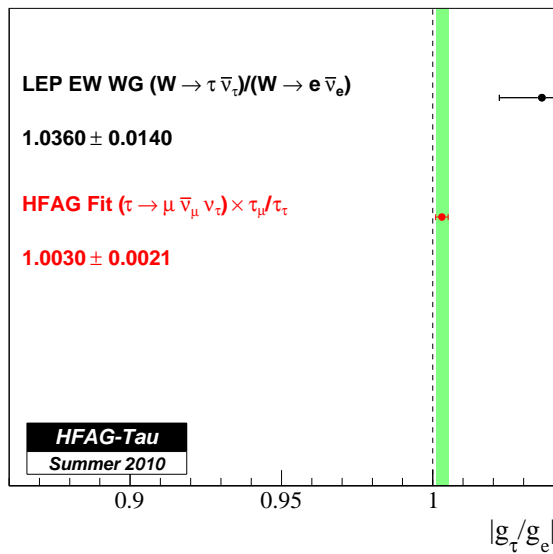
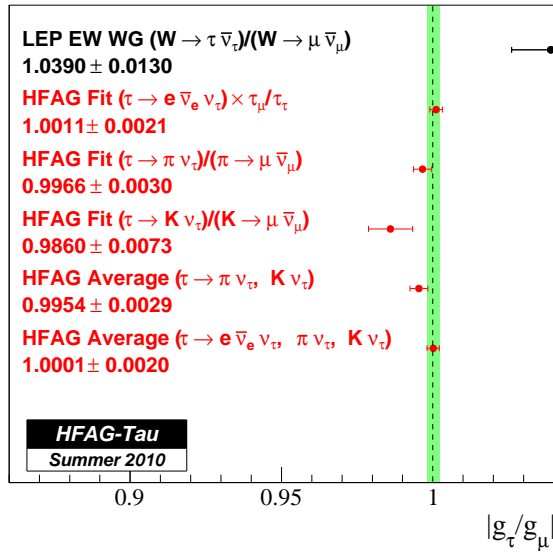
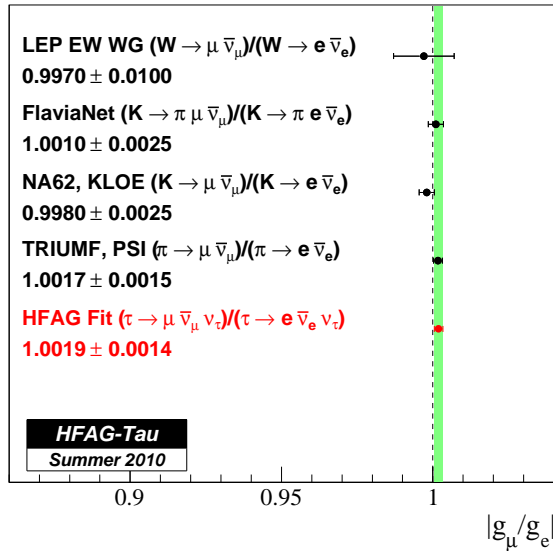


Figure 84: Measurements of lepton universality from W, kaon, pion and tau decays.

9.4 Measurement of $|V_{us}|$

We describe 3 extractions for $|V_{us}|$ using $\mathcal{B}(\tau^- \rightarrow K^- \nu_\tau)$, $\mathcal{B}(\tau^- \rightarrow K^- \nu_\tau)/\mathcal{B}(\tau^- \rightarrow \pi^- \nu_\tau)$, and inclusive sum of τ branching fractions having net strangeness of unity in the final state:

- We use the value of kaon decay constant $f_K = 157 \pm 2 \text{ MeV}$ [548], and our value of

$$\mathcal{B}(\tau^- \rightarrow K^- \nu_\tau) = \frac{G_F^2 f_K^2 |V_{us}|^2 m_\tau^3 \tau_\tau}{16\pi\hbar} \left(1 - \frac{m_K^2}{m_\tau^2}\right)^2 S_{EW},$$

where $S_{EW} = 1.0201 \pm 0.0003$ [593], to determine $|V_{us}| = 0.2204 \pm 0.0032$ from results of the unitarity constrained fit. This value is consistent with the estimate of $|V_{us}| = 0.2255 \pm 0.0010$ obtained using the unitarity constraint on the first row of the CKM matrix.

- We use $f_K/f_\pi = 1.189 \pm 0.007$ [548], $|V_{ud}| = 0.97425 \pm 0.00022$ [594], and the long-distance correction $\delta_{LD} = (0.03 \pm 0.44)\%$, estimated [595] using corrections to $\tau \rightarrow h\nu_\tau$ and $h \rightarrow \mu\nu_\mu$ [590, 591, 592, 596], for the ratio

$$\frac{\mathcal{B}(\tau^- \rightarrow K^- \nu_\tau)}{\mathcal{B}(\tau^- \rightarrow \pi^- \nu_\tau)} = \frac{f_K^2 |V_{us}|^2 \left(1 - \frac{m_K^2}{m_\tau^2}\right)^2}{f_\pi^2 |V_{ud}|^2 \left(1 - \frac{m_\pi^2}{m_\tau^2}\right)^2} (1 + \delta_{LD}),$$

where short-distance electro-weak corrections cancel in this ratio.

From the unitarity constrained fit, we obtain $\mathcal{B}(\tau^- \rightarrow K^- \nu_\tau)/\mathcal{B}(\tau^- \rightarrow \pi^- \nu_\tau) = 0.0644 \pm 0.0009$, which includes a correlation co-efficient of -0.49% between the branching fractions. This yields $|V_{us}| = 0.2238 \pm 0.0022$, which is also consistent with value of $|V_{us}|$ from CKM unitarity prediction.

- The total hadronic width of the τ normalized to the electronic branching fraction, $R_{\text{had}} = \mathcal{B}_{\text{had}}/\mathcal{B}_e$, can be written as $R_{\text{had}} = R_{\text{non-strange}} + R_{\text{strange}}$. We can then measure

$$|V_{us}| = \sqrt{R_{\text{strange}} / \left[\frac{R_{\text{non-strange}}}{|V_{ud}|^2} - \delta R_{\text{theory}} \right]}. \quad (228)$$

Here, we use $|V_{ud}| = 0.97425 \pm 0.00022$ [594], and $\delta R_{\text{theory}} = 0.240 \pm 0.032$ [597] obtained with the updated average value of $m_s(2\text{GeV}) = 94 \pm 6 \text{ MeV}$ [598], which contributes to an error of 0.0010 on $|V_{us}|$. We note that this error is equivalent to half the difference between calculations of $|V_{us}|$ obtained using fixed order perturbation theory (FOPT) and contour improved perturbation theory (CIPT) calculations of δR_{theory} [599], and twice as large as the theoretical error proposed in Ref. [600].

As in Ref. [601], we improve upon the estimate of electronic branching fraction by averaging its direct measurement with its estimates of $(17.899 \pm 0.040)\%$ and $(17.794 \pm 0.062)\%$ obtained from the averaged values of muonic branching fractions and the averaged value of the lifetime of the τ lepton $= (290.6 \pm 1.0) \times 10^{-15} \text{ s}$ [5], assuming lepton universality and taking into account the correlation between the leptonic branching fractions. This gives a more precise estimate for the electronic branching fraction: $\mathcal{B}_e^{\text{uni}} = (17.852 \pm 0.027)\%$.

Assuming lepton universality, the total hadronic branching fraction can be written as: $\mathcal{B}_{\text{had}} = 1 - 1.972558 \mathcal{B}_e^{\text{uni}}$, which gives a value for the total τ hadronic width normalized to the electronic branching fraction as $R_{\text{had}} = 3.6291 \pm 0.0086$.

The non-strange width is $R_{\text{non-strange}} = R_{\text{had}} - R_{\text{strange}}$, where the estimate for the strange width $R_{\text{strange}} = 0.1613 \pm 0.0028$ is obtained from the sum of the strange branching fractions with the unitarity constrained fit as listed in Table 165. This gives a value of $|V_{us}| = 0.2174 \pm 0.0022$, which is 3.3σ lower than the CKM unitarity prediction.

A similar estimation using results from the unconstrained fit to the branching fractions gives $|V_{us}| = 0.2166 \pm 0.0023$, which is 3.6σ lower than the CKM unitarity prediction. Since the sum of base modes from our unconstrained fit is less than unity by 1.6σ , instead of using $\mathcal{B}_{\text{non-strange}} = 1 - \mathcal{B}_{\text{leptonic}} - \mathcal{B}_{\text{strange}}$, we also evaluate $|V_{us}|$ from the sum of the averaged non-strange branching fractions. This gives $|V_{us}| = 0.2169 \pm 0.0023$, which is 3.5σ lower than the CKM unitarity prediction.

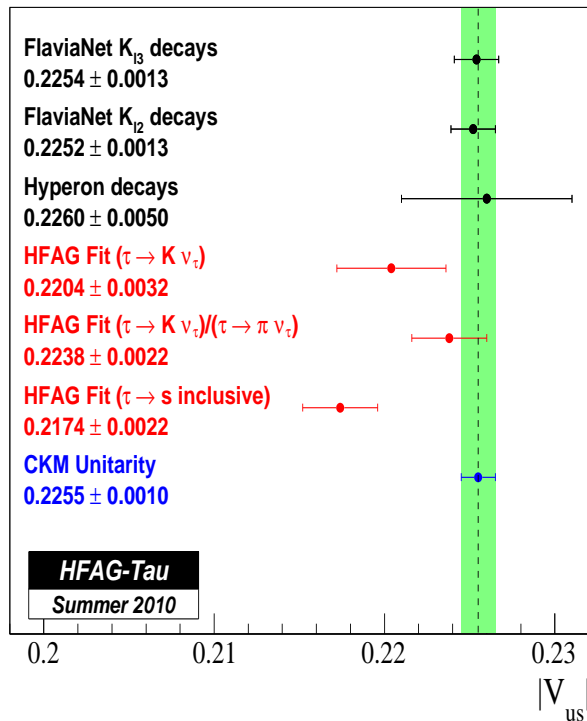


Figure 85: Measurements of $|V_{us}|$ from kaon, hyperon and tau decays.

Summary of these $|V_{us}|$ values are plotted in Figure 85, where we also include values from kaon decays obtained from Ref. [588] and from hyperon decays obtained from Ref. [602].

9.5 Search for lepton flavor violation in τ decays

The status of searches for lepton flavor violation in τ decays is summarized in Figure 86. A table of these results and the corresponding references are provided on the HFAG web site

<http://www.slac.stanford.edu/xorg/hfag/tau/HFAG-TAU-LFV.htm>.

90% C.L. Upper limits for LFV τ decays

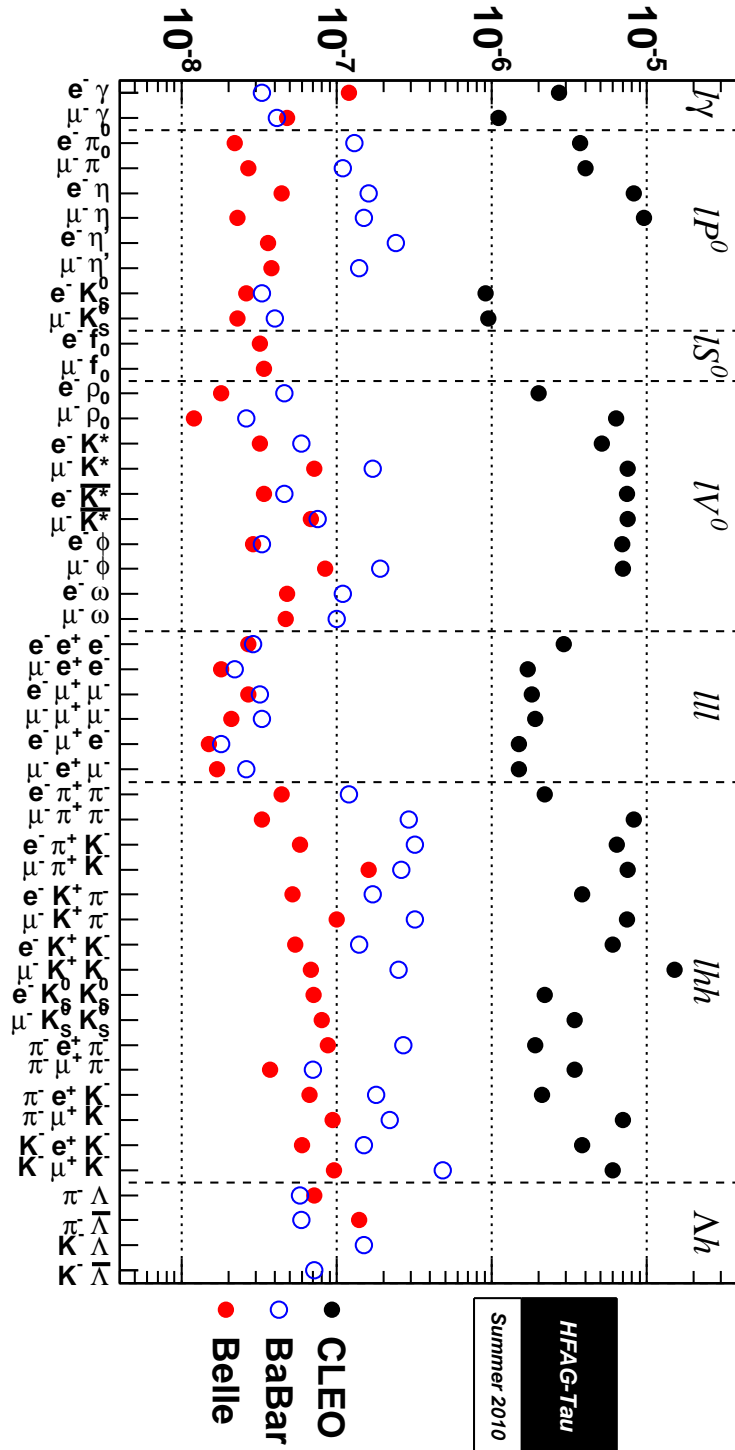


Figure 86: Status of searches for lepton flavor violation in τ decays.

10 Summary

This article provides updated world averages for b -hadron properties at least through the end of 2009. Some results that appeared in the spring of 2010 are also included. A small selection of highlights of the results described in Sections 3-9 is given in Tables 166 and 167.

Concerning lifetime and mixing averages, the most significant changes in the past two years are due to new results from the Tevatron experiments, mainly measurements of b -baryon lifetimes and searches for CP violation in B_s^0 mixing. While DØ has measured a like-sign dimuon asymmetry deviating by 3.2σ from the SM, the latest results on the CP -violation phase in $B_s^0 \rightarrow J/\psi\phi$ no longer show any hint of New Physics. On the other hand, averaging procedures for the b -hadron production fractions have been improved: for the first time we obtain a set of fractions based on Tevatron measurements only, and we also extract the fraction of $\Upsilon(5S)$ decays to B_s^0 pairs taking into account decays without open-bottom mesons.

The measurement of $\sin 2\beta \equiv \sin 2\phi_1$ from $b \rightarrow c\bar{c}s$ transitions such as $B^0 \rightarrow J/\psi K_s^0$ has reached $< 4\%$ precision: $\sin 2\beta \equiv \sin 2\phi_1 = 0.673 \pm 0.023$. Measurements of the same parameter using different quark-level processes provide a consistency test of the Standard Model and allow insight into possible new physics. Recent improvements include the use of time-dependent Dalitz plot analyses of $B^0 \rightarrow K_s^0 K^+ K^-$ and $B^0 \rightarrow K_s^0 \pi^+ \pi^-$ to obtain CP violation parameters for ϕK_s^0 , $f_0(980)K_s^0$ and ρK_s^0 . All results among hadronic $b \rightarrow s$ penguin dominated decays are currently consistent with the Standard Model expectations. Among measurements related to the Unitarity Triangle angle $\alpha \equiv \phi_2$, updates of the parameters of the $\rho\rho$ system now allow constraints at the level of $\approx 6^\circ$. Knowledge of the third angle $\gamma \equiv \phi_3$ also continues to improve. Notwithstanding the well-known statistical issues in extracting the value of the angle itself, the world average values of the parameters in $B \rightarrow DK$ decays now show a significant direct CP violation effect.

Concerning D^0 - \bar{D}^0 mixing, three experiments have now found evidence for this phenomenon: Belle, BABAR, and CDF. These measurements and others (made by Belle, BABAR, CLEO, FNAL E791, FNAL E831) are combined to yield World Average (WA) values for mixing parameters x and y , and for CPV parameters $|q/p|$ and ϕ . From this fit, the no-mixing point $x=y=0$ is excluded at 10.2σ . The parameter x differs from zero by 2.5σ , and y differs from zero by 5.7σ . Mixing at this level is presumably dominated by long-distance processes, which are difficult to calculate. Thus, it may be difficult to identify new physics from mixing alone. The WA value for the observable y_{CP} is positive, which indicates that the CP -even state is shorter-lived as in the K^0 - \bar{K}^0 system. However, x also appears to be positive, which implies that the CP -even state is heavier; this is unlike in the K^0 - \bar{K}^0 system. There is no evidence yet for CPV (either direct or indirect) in the D^0 - \bar{D}^0 system.

11 Acknowledgments

We are grateful for the strong support of the Belle, BABAR, CLEO, CDF, and DØ collaborations, without whom this compilation of results and world averages would not have been possible. The success of these experiments in turn would not have been possible without the excellent operations of the KEKB, PEP-II, CESR, and Tevatron accelerators, and fruitful collaborations between the accelerator groups and the experiments.

Table 166: Selected world averages at the end of 2009 from Chapters 3 and 4.

<i>b</i>-hadron lifetimes	
$\tau(B^0)$	1.518 ± 0.007 ps
$\tau(B^+)$	1.641 ± 0.008 ps
$\bar{\tau}(B_s^0) = 1/\Gamma_s$	$1.477_{-0.022}^{+0.021}$ ps
$\tau(B_c^+)$	0.461 ± 0.036 ps
$\tau(\Lambda_b^0)$	1.425 ± 0.032 ps
$\tau(\Xi_b)$ (mean)	$1.49_{-0.18}^{+0.19}$ ps
$\tau(\Omega_b^-)$	$1.13_{-0.40}^{+0.53}$ ps
<i>b</i>-hadron fractions	
f^{+-}/f^{00} in $\Upsilon(4S)$ decays	1.052 ± 0.028
f_s in $\Upsilon(5S)$ decays	0.202 ± 0.036
f_s, f_{baryon} in Z decays	$0.103 \pm 0.009, 0.090 \pm 0.015$
f_s, f_{baryon} at Tevatron	$0.111 \pm 0.014, 0.211 \pm 0.069$
B^0 and B_s^0 mixing / <i>CPV</i> parameters	
Δm_d	0.508 ± 0.004 ps ⁻¹
$ q/p _d$	1.0024 ± 0.0023
Δm_s	17.78 ± 0.12 ps ⁻¹
$\Delta\Gamma_s = \Gamma_L - \Gamma_H$	$+0.049_{-0.034}^{+0.033}$ ps ⁻¹
$ q/p _s$	1.0044 ± 0.0029
$\phi_s = -2\beta_s$ (90% CL range)	$[-1.20, -0.45] \cup [-2.72, -1.99]$
Measurements related to Unitarity Triangle angles	
$\sin 2\beta \equiv \sin 2\phi_1$	0.673 ± 0.023
$\beta \equiv \phi_1$	$(21.1 \pm 0.9)^\circ$
$-\eta S_{\phi K^0}$	$0.44_{-0.18}^{+0.17}$
$-\eta S_{\eta' K^0}$	0.59 ± 0.07
$-\eta S_{K_S^0 K_S^0 K_S^0}$	0.74 ± 0.17
$S_{K^* \gamma}$	-0.16 ± 0.22
$S_{\pi^+ \pi^-}$	-0.65 ± 0.07
$C_{\pi^+ \pi^-}$	-0.38 ± 0.06
$S_{\rho^+ \rho^-}$	-0.05 ± 0.17
$a(D^{*\pm} \pi^\mp)$	-0.040 ± 0.010
$A_{CP}(B \rightarrow D_{CP^+} K)$	0.24 ± 0.07

Table 167: Selected world averages at the end of 2009 from Chapters 5–9.

Semileptonic B decay parameters	
$\mathcal{B}(\bar{B}^0 \rightarrow D^+ \ell^- \bar{\nu})$	$(2.17 \pm 0.12)\%$
$\mathcal{B}(B^- \rightarrow D^0 \ell^- \bar{\nu})$	$(2.23 \pm 0.11)\%$
$ V_{cb} G(1)$	$(42.3 \pm 1.5) \times 10^{-3}$
$ V_{cb} $ from $\mathcal{B}(\bar{B}^0 \rightarrow D^+ \ell^- \bar{\nu})$	$(39.2 \pm 1.4_{\text{exp}} \pm 0.9_{\text{theo}}) \times 10^{-3}$
Rare B decays	
$\mathcal{B}(\bar{B}^0 \rightarrow D^{*+} \ell^- \bar{\nu})$	$(5.05 \pm 0.12)\%$
$\mathcal{B}(B^- \rightarrow D^{*0} \ell^- \bar{\nu})$	$(5.63 \pm 0.18)\%$
$ V_{cb} F(1)$	$(36.04 \pm 0.52) \times 10^{-3}$
$ V_{cb} $ from $\mathcal{B}(\bar{B}^0 \rightarrow D^{*+} \ell^- \bar{\nu})$	$(38.9 \pm 0.6_{\text{exp}} \pm 1.0_{\text{theo}}) \times 10^{-3}$
$\mathcal{B}(\bar{B} \rightarrow \pi \ell \bar{\nu})$	$(1.36 \pm 0.05 \pm 0.05) \times 10^{-4}$
$ V_{ub} $ from $\mathcal{B}(\bar{B} \rightarrow \pi \ell \bar{\nu})$	$(3.05\text{-}3.73) \times 10^{-3}$
Rare B decays	
$A_{CP}(B^0 \rightarrow K^+ \pi^-) - A_{CP}(B^+ \rightarrow K^+ \pi^0)$	$-0.148^{+0.028}_{-0.027} (5.3\sigma)$
$\mathcal{B}(B^+ \rightarrow \tau^+ \nu)$	$(1.67 \pm 0.39) \times 10^{-4}$
D^0 mixing and CPV parameters	
x	$(0.59 \pm 0.20)\%$
y	$(0.80 \pm 0.13)\%$
A_D	$(-2.0 \pm 2.4)\%$
$ q/p $	$0.91^{+0.19}_{-0.16}$
ϕ	$(-10.0^{+9.3}_{-8.7})^\circ$
τ parameters, Lepton Universality, and V_{us}	
m_τ (MeV/ c^2)	1776.77 ± 0.15
g_μ/g_e	1.0019 ± 0.0014
g_τ/g_μ	1.0001 ± 0.0020
g_τ/g_e	1.0030 ± 0.0021
$ V_{us} $ from $\mathcal{B}(\tau^- \rightarrow K^- \nu_\tau)$	0.2204 ± 0.0032
$ V_{us} $ from $\mathcal{B}(\tau^- \rightarrow K^- \nu_\tau)/\mathcal{B}(\tau^- \rightarrow \pi^- \nu_\tau)$	0.2238 ± 0.0022
$ V_{us} $ from inclusive sum of strange branching fractions	0.2174 ± 0.0022

References

- [1] N. Cabibbo, Phys. Rev. Lett. **10**, 531–533 (1963).
- [2] M. Kobayashi and T. Maskawa, Prog. Theor. Phys. **49**, 652–657 (1973).
- [3] D. Abbaneo *et al.*, ALEPH, CDF, DELPHI, L3, OPAL, and SLD collaborations, arXiv:hep-ex/0009052 (2000), CERN-EP-2000-096; arXiv:hep-ex/0112028 (2001), CERN-EP-2001-050.
- [4] E. Barberio *et al.* (Heavy Flavor Averaging Group) (2008), arXiv:0808.1297 [hep-ex].
- [5] K. Nakamura *et al.* (Particle Data Group), J. Phys. **G37**, 075021 (2010).
- [6] B. Aubert *et al.* (BABAR collaboration), Phys. Rev. Lett. **94**, 141801 (2005), arXiv:hep-ex/0412062.
- [7] B. Aubert *et al.* (BABAR collaboration), Phys. Rev. **D65**, 032001 (2002), arXiv:hep-ex/0107025.
- [8] B. Aubert *et al.* (BABAR collaboration), Phys. Rev. **D69**, 071101 (2004), arXiv:hep-ex/0401028.
- [9] J. P. Alexander *et al.* (CLEO collaboration), Phys. Rev. Lett. **86**, 2737–2741 (2001), arXiv:hep-ex/0006002.
- [10] S. B. Athar *et al.* (CLEO collaboration), Phys. Rev. **D66**, 052003 (2002), arXiv:hep-ex/0202033.
- [11] N. C. Hastings *et al.* (Belle collaboration), Phys. Rev. **D67**, 052004 (2003), arXiv:hep-ex/0212033.
- [12] B. Aubert *et al.* (BABAR collaboration), Phys. Rev. Lett. **95**, 042001 (2005), arXiv:hep-ex/0504001.
- [13] B. Aubert *et al.* (BABAR collaboration), Phys. Rev. Lett. **96**, 232001 (2006), arXiv:hep-ex/0604031; A. Sokolov *et al.* (Belle collaboration), Phys. Rev. **D75**, 071103 (2007), arXiv:hep-ex/0611026; B. Aubert *et al.* (BABAR collaboration), Phys. Rev. **D78**, 112002 (2008), arXiv:0807.2014 [hep-ex].
- [14] B. Barish *et al.* (CLEO collaboration), Phys. Rev. Lett. **76**, 1570–1574 (1996).
- [15] A. Drutskoy *et al.* (Belle collaboration), Phys. Rev. **D81**, 112003 (2010), arXiv:1003.5885 [hep-ex].
- [16] G. S. Huang *et al.* (CLEO collaboration), Phys. Rev. **D75**, 012002 (2007), arXiv:hep-ex/0610035; this supersedes the results of Ref. [18].
- [17] A. Drutskoy *et al.* (Belle collaboration), Phys. Rev. Lett. **98**, 052001 (2007), arXiv:hep-ex/0608015.

- [18] M. Artuso *et al.* (CLEO collaboration), Phys. Rev. Lett. **95**, 261801 (2005),
arXiv:hep-ex/0508047.
- [19] K. F. Chen *et al.* (Belle collaboration), Phys. Rev. Lett. **100**, 112001 (2008),
arXiv:0710.2577 [hep-ex].
- [20] R. Louvot *et al.* (Belle collaboration), Phys. Rev. Lett. **102**, 021801 (2009),
arXiv:0809.2526 [hep-ex].
- [21] P. Abreu *et al.* (DELPHI collaboration), Phys. Lett. **B289**, 199–210 (1992); P. D.
Acton *et al.* (OPAL collaboration), Phys. Lett. **B295**, 357–370 (1992); D. Buskulic *et al.*
(ALEPH collaboration), Phys. Lett. **B361**, 221–233 (1995).
- [22] P. Abreu *et al.* (DELPHI collaboration), Z. Phys. **C68**, 375–390 (1995).
- [23] R. Barate *et al.* (ALEPH collaboration), Eur. Phys. J. **C2**, 197–211 (1998).
- [24] D. Buskulic *et al.* (ALEPH collaboration), Phys. Lett. **B384**, 449–460 (1996).
- [25] J. Abdallah *et al.* (DELPHI collaboration), Eur. Phys. J. **C44**, 299–309 (2005),
arXiv:hep-ex/0510023.
- [26] P. Abreu *et al.* (DELPHI collaboration), Z. Phys. **C68**, 541–554 (1995).
- [27] R. Barate *et al.* (ALEPH collaboration), Eur. Phys. J. **C5**, 205–227 (1998).
- [28] J. Abdallah *et al.* (DELPHI collaboration), Phys. Lett. **B576**, 29–42 (2003),
arXiv:hep-ex/0311005.
- [29] T. Affolder *et al.* (CDF collaboration), Phys. Rev. Lett. **84**, 1663–1668 (2000),
arXiv:hep-ex/9909011.
- [30] T. Aaltonen *et al.* (CDF collaboration), Phys. Rev. **D77**, 072003 (2008),
arXiv:0801.4375 [hep-ex].
- [31] T. Aaltonen *et al.* (CDF collaboration), Phys. Rev. **D79**, 032001 (2009),
arXiv:0810.3213 [hep-ex].
- [32] F. Abe *et al.* (CDF collaboration), Phys. Rev. **D60**, 092005 (1999).
- [33] V. M. Abazov *et al.* (DØ collaboration), Phys. Rev. Lett. **99**, 052001 (2007),
arXiv:0706.1690 [hep-ex].
- [34] V. M. Abazov *et al.* (DØ collaboration), Phys. Rev. Lett. **101**, 232002 (2008),
arXiv:0808.4142 [hep-ex].
- [35] T. Aaltonen *et al.* (CDF collaboration), Phys. Rev. **D80**, 072003 (2009),
arXiv:0905.3123 [hep-ex].

- [36] S. Schael *et al.*, ALEPH, CDF, DELPHI, L3, OPAL, and SLD collaborations, LEP Electroweak Working Group, SLD Electroweak and Heavy Flavour Working Groups, Phys. Rept. **427**, 257 (2006), [arXiv:hep-ex/0509008](#); we use the average given in Eq. 5.39 of this paper, obtained from a 10-parameter global fit of all electroweak data where the asymmetry measurements have been excluded.
- [37] D. Acosta *et al.* (CDF collaboration), Phys. Rev. **D69**, 012002 (2004), [arXiv:hep-ex/0309030](#); this supersedes the $\bar{\chi}$ value of Ref. [117].
- [38] V. M. Abazov *et al.* (DØ collaboration), Phys. Rev. **D74**, 092001 (2006), [arXiv:hep-ex/0609014](#).
- [39] M. A. Shifman and M. B. Voloshin, Sov. Phys. JETP **64**, 698 (1986); J. Chay, H. Georgi, and B. Grinstein, Phys. Lett. **B247**, 399–405 (1990); I. I. Bigi, N. G. Uraltsev, and A. I. Vainshtein, Phys. Lett. **B293**, 430–436 (1992), [arXiv:hep-ph/9207214](#); erratum Phys. Lett. **B297**, 477 (1992).
- [40] I. I. Bigi, [arXiv:hep-ph/9508408](#) (1995); G. Bellini, I. I. Bigi, and P. J. Dornan, Phys. Rept. **289**, 1–155 (1997).
- [41] M. Ciuchini, E. Franco, V. Lubicz, and F. Mescia, Nucl. Phys. **B625**, 211–238 (2002), [arXiv:hep-ph/0110375](#); M. Beneke, G. Buchalla, C. Greub, A. Lenz, and U. Nierste, Nucl. Phys. **B639**, 389–407 (2002), [arXiv:hep-ph/0202106](#); E. Franco, V. Lubicz, F. Mescia, and C. Tarantino, Nucl. Phys. **B633**, 212–236 (2002), [arXiv:hep-ph/0203089](#).
- [42] C. Tarantino, Eur. Phys. J. **C33**, s895–s899 (2004), [arXiv:hep-ph/0310241](#); F. Gabbiani, A. I. Onishchenko, and A. A. Petrov, Phys. Rev. **D68**, 114006 (2003), [arXiv:hep-ph/0303235](#).
- [43] F. Gabbiani, A. I. Onishchenko, and A. A. Petrov, Phys. Rev. **D70**, 094031 (2004), [arXiv:hep-ph/0407004](#).
- [44] L. Di Ciaccio *et al.* (1996), internal note by former B lifetime working group, http://lepbosec.web.cern.ch/LEPBOSC/lifetimes/ps/final_blife.ps.
- [45] D. Buskulic *et al.* (ALEPH collaboration), Phys. Lett. **B314**, 459–470 (1993).
- [46] P. Abreu *et al.* (DELPHI collaboration), Z. Phys. **C63**, 3–16 (1994).
- [47] P. Abreu *et al.* (DELPHI collaboration), Phys. Lett. **B377**, 195–204 (1996).
- [48] J. Abdallah *et al.* (DELPHI collaboration), Eur. Phys. J. **C33**, 307–324 (2004), [arXiv:hep-ex/0401025](#).
- [49] M. Acciarri *et al.* (L3 collaboration), Phys. Lett. **B416**, 220–232 (1998).
- [50] K. Ackerstaff *et al.* (OPAL collaboration), Z. Phys. **C73**, 397–408 (1997).
- [51] K. Abe *et al.* (SLD collaboration), Phys. Rev. Lett. **75**, 3624–3628 (1995), [arXiv:hep-ex/9511005](#).

- [52] D. Buskulic *et al.* (ALEPH collaboration), Phys. Lett. **B369**, 151–162 (1996).
- [53] P. D. Acton *et al.* (OPAL collaboration), Z. Phys. **C60**, 217–228 (1993).
- [54] F. Abe *et al.* (CDF collaboration), Phys. Rev. **D57**, 5382–5401 (1998).
- [55] R. Barate *et al.* (ALEPH collaboration), Phys. Lett. **B492**, 275–287 (2000), [arXiv:hep-ex/0008016](#).
- [56] D. Buskulic *et al.* (ALEPH collaboration), Z. Phys. **C71**, 31–44 (1996).
- [57] P. Abreu *et al.* (DELPHI collaboration), Z. Phys. **C68**, 13–24 (1995).
- [58] W. Adam *et al.* (DELPHI collaboration), Z. Phys. **C68**, 363–374 (1995).
- [59] P. Abreu *et al.* (DELPHI collaboration), Z. Phys. **C74**, 19–32 (1997).
- [60] M. Acciarri *et al.* (L3 collaboration), Phys. Lett. **B438**, 417–429 (1998).
- [61] R. Akers *et al.* (OPAL collaboration), Z. Phys. **C67**, 379–388 (1995).
- [62] G. Abbiendi *et al.* (OPAL collaboration), Eur. Phys. J. **C12**, 609–626 (2000), [arXiv:hep-ex/9901017](#).
- [63] G. Abbiendi *et al.* (OPAL collaboration), Phys. Lett. **B493**, 266–280 (2000), [arXiv:hep-ex/0010013](#).
- [64] K. Abe *et al.* (SLD collaboration), Phys. Rev. Lett. **79**, 590–596 (1997).
- [65] F. Abe *et al.* (CDF collaboration), Phys. Rev. **D58**, 092002 (1998), [arXiv:hep-ex/9806018](#).
- [66] D. E. Acosta *et al.* (CDF collaboration), Phys. Rev. **D65**, 092009 (2002).
- [67] CDF collaboration, CDF note 7514, 1 March 2005, <http://www-cdf.fnal.gov/physics/new/bottom/050224.blessed-bsemi-life/>.
- [68] CDF collaboration, CDF note 7386, 23 March 2005, <http://www-cdf.fnal.gov/physics/new/bottom/050303.blessed-bhadlife/>.
- [69] CDF collaboration, CDF note 10071, 23 February 2010, <http://www-cdf.fnal.gov/physics/new/bottom/091217.blessed-JpsiX4.3/jpsix.html>; these preliminary results replace the $\Lambda_b \rightarrow J/\psi \Lambda$ and $B^0 \rightarrow J/\psi K_S$ lifetime measurements of A. Abulencia *et al.* (CDF collaboration), Phys. Rev. Lett. **98**, 122001 (2007), [arXiv:hep-ex/0609021](#); as well as the $B^0 \rightarrow J/\psi K^{*0}$ lifetime measurement of D. E. Acosta *et al.* (CDF collaboration), Phys. Rev. Lett. **94**, 101803 (2005), [arXiv:hep-ex/0412057](#).
- [70] V. M. Abazov *et al.* (DØ collaboration), Phys. Rev. Lett. **102**, 032001 (2009), [arXiv:0810.0037 \[hep-ex\]](#); this replaces V. M. Abazov *et al.* (DØ collaboration), Phys. Rev. Lett. **95**, 171801 (2005), [arXiv:hep-ex/0507084](#).

- [71] V. M. Abazov *et al.* (DØ collaboration), Phys. Rev. Lett. **99**, 142001 (2007), arXiv:0704.3909 [hep-ex]; this replaces V. M. Abazov *et al.* (DØ collaboration), Phys. Rev. Lett. **94**, 102001 (2005), arXiv:hep-ex/0410054.
- [72] B. Aubert *et al.* (BABAR collaboration), Phys. Rev. Lett. **87**, 201803 (2001), arXiv:hep-ex/0107019.
- [73] B. Aubert *et al.* (BABAR collaboration), Phys. Rev. Lett. **89**, 011802 (2002), arXiv:hep-ex/0202005; erratum Phys. Rev. Lett. **89**, 169903 (2002).
- [74] B. Aubert *et al.* (BABAR collaboration), Phys. Rev. **D67**, 072002 (2003), arXiv:hep-ex/0212017.
- [75] B. Aubert *et al.* (BABAR collaboration), Phys. Rev. **D67**, 091101 (2003), arXiv:hep-ex/0212012.
- [76] B. Aubert *et al.* (BABAR collaboration), Phys. Rev. **D73**, 012004 (2006), arXiv:hep-ex/0507054.
- [77] K. Abe *et al.* (BELLE collaboration), Phys. Rev. **D71**, 072003 (2005), arXiv:hep-ex/0408111.
- [78] CDF collaboration, CDF note 9370, 25 June 2008, http://www-cdf.fnal.gov/physics/new/bottom/080612.blessed-MCfree_Blifetime/.
- [79] V. M. Abazov *et al.* (DØ collaboration), Phys. Rev. Lett. **94**, 182001 (2005), arXiv:hep-ex/0410052.
- [80] A. Lenz and U. Nierste, JHEP **06**, 072 (2007), arXiv:hep-ph/0612167.
- [81] M. Beneke, G. Buchalla, C. Greub, A. Lenz, and U. Nierste, Phys. Lett. **B459**, 631–640 (1999), arXiv:hep-ph/9808385.
- [82] K. Hartkorn and H. G. Moser, Eur. Phys. J. **C8**, 381–383 (1999).
- [83] D. Buskulic *et al.* (ALEPH collaboration), Phys. Lett. **B377**, 205–221 (1996).
- [84] F. Abe *et al.* (CDF collaboration), Phys. Rev. **D59**, 032004 (1999), arXiv:hep-ex/9808003.
- [85] P. Abreu *et al.* (DELPHI collaboration), Eur. Phys. J. **C16**, 555 (2000), arXiv:hep-ex/0107077.
- [86] K. Ackerstaff *et al.* (OPAL collaboration), Phys. Lett. **B426**, 161–179 (1998), arXiv:hep-ex/9802002.
- [87] V. M. Abazov *et al.* (DØ collaboration), Phys. Rev. Lett. **97**, 241801 (2006), arXiv:hep-ex/0604046.

- [88] CDF collaboration, CDF note 9203 v2, 23 October 2008,
<http://www-cdf.fnal.gov/physics/new/bottom/080207.blessed-bs-lifetime/>;
 we consider that these new results supersede the ones from the 3-year old CDF note 7386 [68], although the lifetime analysis of one of the modes ($B_s \rightarrow D_s \pi \pi \pi$) has not been updated.
- [89] CDF collaboration, CDF note 7757, 13 August 2005,
http://www-cdf.fnal.gov/physics/new/bottom/050707.blessed-bs-semi_life/.
- [90] R. Barate *et al.* (ALEPH collaboration), Eur. Phys. J. **C4**, 367–385 (1998).
- [91] P. Abreu *et al.* (DELPHI collaboration), Eur. Phys. J. **C18**, 229–252 (2000),
 arXiv:hep-ex/0105077.
- [92] K. Ackerstaff *et al.* (OPAL collaboration), Eur. Phys. J. **C2**, 407–416 (1998),
 arXiv:hep-ex/9708023.
- [93] CDF collaboration, CDF note 8524, 7 March 2007,
http://www-cdf.fnal.gov/physics/new/bottom/061130.blessed-bh-lifetime_v2/;
 all these preliminary results are superseded by Ref. [69] except those on $B_s^0 \rightarrow J/\psi \phi$.
- [94] V. M. Abazov *et al.* (DØ collaboration), Phys. Rev. Lett. **94**, 042001 (2005),
 arXiv:hep-ex/0409043.
- [95] R. Barate *et al.* (ALEPH collaboration), Phys. Lett. **B486**, 286–299 (2000).
- [96] D. Tonelli (for the CDF collaboration), arXiv:hep-ex/0605038 (2006).
- [97] CDF collaboration, CDF note 10206, 18 July 2010,
http://www-cdf.fnal.gov/physics/new/bottom/100513.blessed-BsJpsiPhi_5.2fb/.
- [98] F. Abe *et al.* (CDF collaboration), Phys. Rev. Lett. **81**, 2432–2437 (1998),
 arXiv:hep-ex/9805034.
- [99] CDF collaboration, CDF note 9294, 28 April 2008,
http://www-cdf.fnal.gov/physics/new/bottom/080327.blessed-BC_LT_SemiLeptonic/;
 this replaces A. Abulencia *et al.* (CDF collaboration), Phys. Rev. Lett. **97**, 012002 (2006), arXiv:hep-ex/0603027.
- [100] V. M. Abazov *et al.* (DØ collaboration), Phys. Rev. Lett. **102**, 092001 (2009),
 arXiv:0805.2614 [hep-ex].
- [101] A. Abulencia *et al.* (CDF collaboration), Phys. Rev. Lett. **96**, 082002 (2006),
 arXiv:hep-ex/0505076.
- [102] T. Aaltonen *et al.* (CDF collaboration), Phys. Rev. Lett. **100**, 182002 (2008),
 arXiv:0712.1506 [hep-ex].
- [103] D. E. Acosta *et al.* (CDF collaboration), Phys. Rev. Lett. **96**, 202001 (2006),
 arXiv:hep-ex/0508022.

- [104] D. Buskulic *et al.* (ALEPH collaboration), Phys. Lett. **B365**, 437–447 (1996).
- [105] F. Abe *et al.* (CDF collaboration), Phys. Rev. Lett. **77**, 1439–1443 (1996).
- [106] T. Aaltonen *et al.* (CDF collaboration), Phys. Rev. Lett. **104**, 102002 (2010), [arXiv:0912.3566 \[hep-ex\]](#).
- [107] V. M. Abazov *et al.* (DØ collaboration), Phys. Rev. Lett. **99**, 182001 (2007), [arXiv:0706.2358 \[hep-ex\]](#).
- [108] P. Abreu *et al.* (DELPHI collaboration), Eur. Phys. J. **C10**, 185–199 (1999).
- [109] P. Abreu *et al.* (DELPHI collaboration), Z. Phys. **C71**, 199–210 (1996).
- [110] R. Akers *et al.* (OPAL collaboration), Z. Phys. **C69**, 195–214 (1996).
- [111] M. Beneke, G. Buchalla, and I. Dunietz, Phys. Rev. **D54**, 4419–4431 (1996), [arXiv:hep-ph/9605259](#); Y.-Y. Keum and U. Nierste, Phys. Rev. **D57**, 4282–4289 (1998), [arXiv:hep-ph/9710512](#).
- [112] M. B. Voloshin, Phys. Rept. **320**, 275–285 (1999), [arXiv:hep-ph/9901445](#); B. Guberina, B. Melic, and H. Stefancic, Phys. Lett. **B469**, 253–258 (1999), [arXiv:hep-ph/9907468](#); M. Neubert and C. T. Sachrajda, Nucl. Phys. **B483**, 339–370 (1997), [arXiv:hep-ph/9603202](#).
- [113] N. G. Uraltsev, Phys. Lett. **B376**, 303–308 (1996), [arXiv:hep-ph/9602324](#); D. Pirjol and N. Uraltsev, Phys. Rev. **D59**, 034012 (1999), [arXiv:hep-ph/9805488](#); P. Colangelo and F. De Fazio, Phys. Lett. **B387**, 371–378 (1996), [arXiv:hep-ph/9604425](#); M. Di Pierro, C. T. Sachrajda, and C. Michael (UKQCD collaboration), Phys. Lett. **B468**, 143 (1999), [arXiv:hep-lat/9906031](#).
- [114] J. E. Bartelt *et al.* (CLEO collaboration), Phys. Rev. Lett. **71**, 1680–1684 (1993).
- [115] B. H. Behrens *et al.* (CLEO collaboration), Phys. Lett. **B490**, 36–44 (2000), [arXiv:hep-ex/0005013](#).
- [116] D. E. Jaffe *et al.* (CLEO collaboration), Phys. Rev. Lett. **86**, 5000–5003 (2001), [arXiv:hep-ex/0101006](#).
- [117] F. Abe *et al.* (CDF collaboration), Phys. Rev. **D55**, 2546–2558 (1997).
- [118] CDF collaboration, CDF note 9015, 16 October 2007, <http://www-cdf.fnal.gov/physics/new/bottom/070816.blessed-acp-bsemil/>.
- [119] K. Ackerstaff *et al.* (OPAL collaboration), Z. Phys. **C76**, 401–415 (1997), [arXiv:hep-ex/9707009](#).
- [120] R. Barate *et al.* (ALEPH collaboration), Eur. Phys. J. **C20**, 431–443 (2001).
- [121] B. Aubert *et al.* (BABAR collaboration), Phys. Rev. Lett. **92**, 181801 (2004), [arXiv:hep-ex/0311037](#); and Phys. Rev. **D70**, 012007 (2004), [arXiv:hep-ex/0403002](#).

- [122] B. Aubert *et al.* (BABAR collaboration), Phys. Rev. Lett. **88**, 231801 (2002), arXiv:hep-ex/0202041.
- [123] B. Aubert *et al.* (BABAR collaboration), Phys. Rev. Lett. **96**, 251802 (2006), arXiv:hep-ex/0603053.
- [124] B. Aubert *et al.* (BABAR collaboration) (2006), arXiv:hep-ex/0607091.
- [125] E. Nakano *et al.* (Belle collaboration), Phys. Rev. **D73**, 112002 (2006), arXiv:hep-ex/0505017.
- [126] M. Beneke, G. Buchalla, and I. Dunietz, Phys. Lett. **B393**, 132–142 (1997), arXiv:hep-ph/9609357; I. Dunietz, Eur. Phys. J. **C7**, 197–203 (1999), arXiv:hep-ph/9806521.
- [127] V. M. Abazov *et al.* (DØ collaboration), Phys. Rev. **D82**, 032001 (2010), arXiv:1005.2757 [hep-ex]; V. M. Abazov *et al.* (DØ collaboration), Phys. Rev. Lett. **105**, 081801 (2010), arXiv:1007.0395 [hep-ex].
- [128] D. Buskulic *et al.* (ALEPH collaboration), Z. Phys. **C75**, 397–407 (1997).
- [129] P. Abreu *et al.* (DELPHI collaboration), Z. Phys. **C76**, 579–598 (1997).
- [130] J. Abdallah *et al.* (DELPHI collaboration), Eur. Phys. J. **C28**, 155 (2003), arXiv:hep-ex/0303032.
- [131] M. Acciarri *et al.* (L3 collaboration), Eur. Phys. J. **C5**, 195–203 (1998).
- [132] K. Ackerstaff *et al.* (OPAL collaboration), Z. Phys. **C76**, 417–423 (1997), arXiv:hep-ex/9707010.
- [133] G. Alexander *et al.* (OPAL collaboration), Z. Phys. **C72**, 377–388 (1996).
- [134] F. Abe *et al.* (CDF collaboration), Phys. Rev. Lett. **80**, 2057–2062 (1998), arXiv:hep-ex/9712004; and Phys. Rev. **D59**, 032001 (1999), arXiv:hep-ex/9806026.
- [135] F. Abe *et al.* (CDF collaboration), Phys. Rev. **D60**, 051101 (1999).
- [136] F. Abe *et al.* (CDF collaboration), Phys. Rev. **D60**, 072003 (1999), arXiv:hep-ex/9903011.
- [137] T. Affolder *et al.* (CDF collaboration), Phys. Rev. **D60**, 112004 (1999), arXiv:hep-ex/9907053.
- [138] CDF collaboration, CDF note 8235, 26 April 2006, http://www-cdf.fnal.gov/physics/new/bottom/060406.blessed-semi_B0mix/.
- [139] CDF collaboration, CDF note 7920, 15 November 2005, http://www-cdf.fnal.gov/physics/new/bottom/050804.hadr_B0mix/.
- [140] V. M. Abazov *et al.* (DØ collaboration), Phys. Rev. **D74**, 112002 (2006), arXiv:hep-ex/0609034.

- [141] B. Aubert *et al.* (BABAR collaboration), Phys. Rev. Lett. **88**, 221802 (2002), arXiv:hep-ex/0112044; B. Aubert *et al.* (BABAR collaboration), Phys. Rev. **D66**, 032003 (2002), arXiv:hep-ex/0201020.
- [142] B. Aubert *et al.* (BABAR collaboration), Phys. Rev. Lett. **88**, 221803 (2002), arXiv:hep-ex/0112045.
- [143] Y. Zheng *et al.* (Belle collaboration), Phys. Rev. **D67**, 092004 (2003), arXiv:hep-ex/0211065.
- [144] H. Albrecht *et al.* (ARGUS collaboration), Z. Phys. **C55**, 357–364 (1992); H. Albrecht *et al.* (ARGUS collaboration), Phys. Lett. **B324**, 249–254 (1994).
- [145] V. M. Abazov *et al.* (DØ collaboration), Phys. Rev. **D76**, 057101 (2007), arXiv:hep-ex/0702030.
- [146] V. M. Abazov *et al.* (DØ collaboration), Phys. Rev. **D82**, 012003 (2010), arXiv:0904.3907 [hep-ex]; this replaces V. M. Abazov *et al.* (DØ collaboration), Phys. Rev. Lett. **98**, 151801 (2007), arXiv:hep-ex/0701007.
- [147] R. Aleksan, A. Le Yaouanc, L. Oliver, O. Pene, and J. C. Raynal, Phys. Lett. **B316**, 567–577 (1993).
- [148] CDF collaboration, CDF note 9458, 7 August 2008, http://www-cdf.fnal.gov/physics/new/bottom/080724.blessed-tagged_BsJpsiPhi_update_prelim/; this replaces T. Aaltonen *et al.* (CDF collaboration), Phys. Rev. Lett. **100**, 121803 (2008), arXiv:0712.2348 [hep-ex]; as well as T. Aaltonen *et al.* (CDF collaboration), Phys. Rev. Lett. **100**, 161802 (2008), arXiv:0712.2397 [hep-ex].
- [149] V. M. Abazov *et al.* (DØ collaboration), Phys. Rev. Lett. **101**, 241801 (2008), arXiv:0802.2255 [hep-ex]; this replaces V. M. Abazov *et al.* (DØ collaboration), Phys. Rev. Lett. **98**, 121801 (2007), arXiv:hep-ex/0701012.
- [150] I. Dunietz, R. Fleischer, and U. Nierste, Phys. Rev. **D63**, 114015 (2001), arXiv:hep-ph/0012219.
- [151] U. Nierste, private communication, September 2006.
- [152] V. M. Abazov *et al.* (DØ collaboration), Phys. Rev. Lett. **102**, 091801 (2009), arXiv:0811.2173 [hep-ex]; this replaces V. M. Abazov *et al.* (DØ collaboration), Phys. Rev. Lett. **99**, 241801 (2007), arXiv:hep-ex/0702049.
- [153] S. Esen *et al.* (Belle collaboration), arXiv:1005.5177 [hep-ex] (2010), to appear in Phys. Rev. Lett.
- [154] T. Aaltonen *et al.* (CDF collaboration), Phys. Rev. Lett. **100**, 021803 (2008).
- [155] As determined before direct experimental inputs of $2\beta_s^{J/\psi\phi} = -\phi_s^{J/\psi\phi}$; J. Charles *et al.* (CKMfitter collaboration), Eur. Phys. J. **C41**, 1–131 (2005), arXiv:hep-ph/0406184, with updated results and plots available at <http://ckmfitter.in2p3.fr>; M. Bona *et al.* (UTfit collaboration), JHEP **10**, 081 (2006), arXiv:hep-ph/0606167.

- [156] M. Bona *et al.* (UTfit collaboration), *PMC Phys.* **A3**, 6 (2009), [arXiv:0803.0659 \[hep-ph\]](#).
- [157] DØ collaboration, additional online information with Ref. [149], likelihood scans for fits with floating strong constraints δ_i available at , <http://www-d0.fnal.gov/Run2Physics/WWW/results/final/B/B08A/>.
- [158] CDF collaboration, CDF note 9787, 22 July 2009, http://www-cdf.fnal.gov/physics/new/bottom/090721.blessed-betas_combination2.8/.
- [159] DØ collaboration, DØ note 5928-CONF, 22 July 2009, <http://www-d0.fnal.gov/Run2Physics/WWW/results/prelim/B/B59/>.
- [160] M. Beneke, G. Buchalla, A. Lenz, and U. Nierste, *Phys. Lett.* **B576**, 173–183 (2003), [arXiv:hep-ph/0307344](#).
- [161] A. Abulencia *et al.* (CDF collaboration), *Phys. Rev. Lett.* **97**, 242003 (2006), [arXiv:hep-ex/0609040](#); this supersedes A. Abulencia *et al.* (CDF - Run II collaboration), *Phys. Rev. Lett.* **97**, 062003 (2006), [arXiv:hep-ex/0606027](#).
- [162] DØ collaboration, DØ note 5474-CONF, 21 August 2007, <http://www-d0.fnal.gov/Run2Physics/WWW/results/prelim/B/B51/>; DØ collaboration, DØ note 5254-CONF, 24 October 2006, <http://www-d0.fnal.gov/Run2Physics/WWW/results/prelim/B/B46/>; these two notes supersede any previous preliminary results from DØ and replace V. M. Abazov *et al.* (DØ collaboration), *Phys. Rev. Lett.* **97**, 021802 (2006), [arXiv:hep-ex/0603029](#).
- [163] DØ collaboration, DØ note 5618-CONF v1.2, 2 May 2008, <http://www-d0.fnal.gov/Run2Physics/WWW/results/prelim/B/B54/>.
- [164] M. Okamoto, *PoS LAT2005*, 013 (2006), [arXiv:hep-lat/0510113](#); this estimate is obtained by combining the unquenched lattice QCD calculations from A. Gray *et al.* (HPQCD collaboration), *Phys. Rev. Lett.* **95**, 212001 (2005), [arXiv:hep-lat/0507015](#); and S. Aoki *et al.* (JLQCD collaboration), *Phys. Rev. Lett.* **91**, 212001 (2003), [arXiv:hep-ph/0307039](#).
- [165] H. G. Moser and A. Roussarie, *Nucl. Instrum. Meth.* **A384**, 491–505 (1997).
- [166] A. Heister *et al.* (ALEPH collaboration), *Eur. Phys. J.* **C29**, 143–170 (2003).
- [167] J. Abdallah *et al.* (DELPHI collaboration), *Eur. Phys. J.* **C35**, 35–52 (2004), [arXiv:hep-ex/0404013](#).
- [168] G. Abbiendi *et al.* (OPAL collaboration), *Eur. Phys. J.* **C11**, 587–598 (1999), [arXiv:hep-ex/9907061](#).
- [169] G. Abbiendi *et al.* (OPAL collaboration), *Eur. Phys. J.* **C19**, 241–256 (2001), [arXiv:hep-ex/0011052](#).
- [170] K. Abe *et al.* (SLD collaboration), *Phys. Rev.* **D67**, 012006 (2003), [arXiv:hep-ex/0209002](#).

- [171] K. Abe *et al.* (SLD collaboration), Phys. Rev. **D66**, 032009 (2002),
arXiv:hep-ex/0207048.
- [172] F. Abe *et al.* (CDF collaboration), Phys. Rev. Lett. **82**, 3576–3580 (1999).
- [173] K. Abe *et al.* (SLD collaboration), arXiv:hep-ex/0012043 (2000).
- [174] L.-L. Chau and W.-Y. Keung, Phys. Rev. Lett. **53**, 1802 (1984).
- [175] L. Wolfenstein, Phys. Rev. Lett. **51**, 1945 (1983).
- [176] A. J. Buras, M. E. Lautenbacher, and G. Ostermaier, Phys. Rev. **D50**, 3433–3446 (1994), arXiv:hep-ph/9403384.
- [177] C. Jarlskog, Phys. Rev. Lett. **55**, 1039 (1985).
- [178] C. Jarlskog, Phys. Lett. **B615**, 207–212 (2005), arXiv:hep-ph/0503199.
- [179] J. D. Bjorken, P. F. Harrison, and W. G. Scott, Phys. Rev. **D74**, 073012 (2006),
arXiv:hep-ph/0511201.
- [180] P. F. Harrison, S. Dallison, and W. G. Scott, Phys. Lett. **B680**, 328–333 (2009),
arXiv:0904.3077 [hep-ph].
- [181] B. Aubert *et al.* (BABAR collaboration), Phys. Rev. Lett. **86**, 2515–2522 (2001),
arXiv:hep-ex/0102030.
- [182] K. Abe *et al.* (Belle collaboration), Phys. Rev. Lett. **87**, 091802 (2001),
arXiv:hep-ex/0107061.
- [183] A. B. Carter and A. I. Sanda, Phys. Rev. **D23**, 1567 (1981).
- [184] I. I. Y. Bigi and A. I. Sanda, Nucl. Phys. **B193**, 85 (1981).
- [185] B. Aubert *et al.* (BABAR collaboration), Phys. Rev. **D79**, 032002 (2009),
arXiv:0808.1866 [hep-ex].
- [186] P. Krokovny *et al.* (Belle collaboration), Phys. Rev. Lett. **97**, 081801 (2006),
arXiv:hep-ex/0605023.
- [187] B. Aubert *et al.* (BABAR collaboration), Phys. Rev. Lett. **99**, 231802 (2007),
arXiv:0708.1544 [hep-ex].
- [188] T. E. Browder, A. Datta, P. J. O’Donnell, and S. Pakvasa, Phys. Rev. **D61**, 054009 (2000), arXiv:hep-ph/9905425.
- [189] B. Aubert *et al.* (BABAR collaboration), Phys. Rev. **D74**, 091101 (2006),
arXiv:hep-ex/0608016.
- [190] J. Dalseno *et al.* (Belle collaboration), Phys. Rev. **D76**, 072004 (2007),
arXiv:0706.2045 [hep-ex].

- [191] B. Aubert *et al.* (*BABAR* collaboration), Phys. Rev. Lett. **99**, 161802 (2007), arXiv:0706.3885 [hep-ex].
- [192] B. Aubert *et al.* (*BABAR* collaboration), arXiv:0808.0700 [hep-ex] (2008).
- [193] J. Dalseno, Belle collaboration, Preliminary results presented at ICHEP2008, http://www.hep.upenn.edu/ichep08/talks/misc/download_slides?Talk_id=163.
- [194] A. Garmash *et al.* (Belle collaboration), Phys. Rev. **D71**, 092003 (2005), arXiv:hep-ex/0412066.
- [195] B. Aubert *et al.* (*BABAR* collaboration), Phys. Rev. **D74**, 032003 (2006), arXiv:hep-ex/0605003.
- [196] B. Aubert *et al.* (*BABAR* collaboration), Phys. Rev. **D80**, 112001 (2009), arXiv:0905.3615 [hep-ex].
- [197] J. Dalseno *et al.* (Belle collaboration), Phys. Rev. **D79**, 072004 (2009), arXiv:0811.3665 [hep-ex].
- [198] A. Garmash *et al.* (Belle collaboration), Phys. Rev. Lett. **96**, 251803 (2006), arXiv:hep-ex/0512066.
- [199] B. Aubert *et al.* (*BABAR* collaboration), Phys. Rev. **D72**, 072003 (2005), arXiv:hep-ex/0507004.
- [200] B. Aubert *et al.* (*BABAR* collaboration), Phys. Rev. **D78**, 012004 (2008), arXiv:0803.4451 [hep-ex].
- [201] A. E. Snyder and H. R. Quinn, Phys. Rev. **D48**, 2139–2144 (1993).
- [202] H. R. Quinn and J. P. Silva, Phys. Rev. **D62**, 054002 (2000), arXiv:hep-ph/0001290.
- [203] B. Aubert *et al.* (*BABAR* collaboration), Phys. Rev. **D76**, 012004 (2007), arXiv:hep-ex/0703008.
- [204] A. Kusaka *et al.* (Belle collaboration), Phys. Rev. Lett. **98**, 221602 (2007), arXiv:hep-ex/0701015.
- [205] A. Kusaka *et al.* (Belle collaboration), Phys. Rev. **D77**, 072001 (2008), arXiv:0710.4974 [hep-ex].
- [206] J. Charles *et al.*, CKMfitter Group, Eur. Phys. J. **C41**, 1–131 (2005), arXiv:hep-ph/0406184, see also online updates, <http://ckmfitter.in2p3.fr/>.
- [207] T. Aushev *et al.* (Belle collaboration), Phys. Rev. Lett. **93**, 201802 (2004), arXiv:hep-ex/0408051.
- [208] B. Aubert *et al.* (*BABAR* collaboration), Phys. Rev. Lett. **91**, 201802 (2003), arXiv:hep-ex/0306030.

- [209] C. C. Wang *et al.* (Belle collaboration), Phys. Rev. Lett. **94**, 121801 (2005),
arXiv:hep-ex/0408003.
- [210] B. Aubert *et al.* (BABAR collaboration), Phys. Rev. **D73**, 111101 (2006),
arXiv:hep-ex/0602049.
- [211] B. Aubert *et al.* (BABAR collaboration), Phys. Rev. **D71**, 112003 (2005),
arXiv:hep-ex/0504035.
- [212] O. Long, M. Baak, R. N. Cahn, and D. Kirkby, Phys. Rev. **D68**, 034010 (2003),
arXiv:hep-ex/0303030.
- [213] I. Adachi *et al.* (Belle collaboration), arXiv:0809.3203 [hep-ex] (2008).
- [214] F. J. Ronga *et al.* (Belle collaboration), Phys. Rev. **D73**, 092003 (2006),
arXiv:hep-ex/0604013.
- [215] R. Fleischer, Nucl. Phys. **B671**, 459–482 (2003), arXiv:hep-ph/0304027.
- [216] D. Atwood, M. Gronau, and A. Soni, Phys. Rev. Lett. **79**, 185–188 (1997),
arXiv:hep-ph/9704272.
- [217] D. Atwood, T. Gershon, M. Hazumi, and A. Soni, Phys. Rev. **D71**, 076003 (2005),
arXiv:hep-ph/0410036.
- [218] B. Grinstein, Y. Grossman, Z. Ligeti, and D. Pirjol, Phys. Rev. **D71**, 011504 (2005),
arXiv:hep-ph/0412019.
- [219] B. Grinstein and D. Pirjol, Phys. Rev. **D73**, 014013 (2006), arXiv:hep-ph/0510104.
- [220] M. Matsumori and A. I. Sanda, Phys. Rev. **D73**, 114022 (2006),
arXiv:hep-ph/0512175.
- [221] P. Ball and R. Zwicky, Phys. Lett. **B642**, 478–486 (2006), arXiv:hep-ph/0609037.
- [222] I. I. Y. Bigi and A. I. Sanda, Phys. Lett. **B211**, 213 (1988).
- [223] M. Gronau and D. London., Phys. Lett. **B253**, 483–488 (1991).
- [224] M. Gronau and D. Wyler, Phys. Lett. **B265**, 172–176 (1991).
- [225] D. Atwood, I. Dunietz, and A. Soni, Phys. Rev. Lett. **78**, 3257–3260 (1997),
arXiv:hep-ph/9612433.
- [226] D. Atwood, I. Dunietz, and A. Soni, Phys. Rev. **D63**, 036005 (2001),
arXiv:hep-ph/0008090.
- [227] A. Giri, Y. Grossman, A. Soffer, and J. Zupan, Phys. Rev. **D68**, 054018 (2003),
arXiv:hep-ph/0303187.
- [228] A. Poluektov *et al.* (Belle collaboration), Phys. Rev. **D70**, 072003 (2004),
arXiv:hep-ex/0406067.

- [229] A. Bondar and A. Poluektov, Eur. Phys. J. **C47**, 347–353 (2006),
arXiv:hep-ph/0510246.
- [230] A. Bondar and A. Poluektov, Eur. Phys. J. **C55**, 51 (2008),
arXiv:0801.0840 [hep-ex].
- [231] D. Atwood and A. Soni, Phys. Rev. **D68**, 033003 (2003), arXiv:hep-ph/0304085.
- [232] B. Aubert *et al.* (BABAR collaboration), Phys. Rev. Lett. **99**, 251801 (2007),
arXiv:hep-ex/0703037.
- [233] B. Aubert *et al.* (BABAR collaboration), Phys. Rev. **D76**, 031102 (2007),
arXiv:0704.0522 [hep-ex].
- [234] R. Itoh *et al.* (Belle collaboration), Phys. Rev. Lett. **95**, 091601 (2005),
arXiv:hep-ex/0504030.
- [235] K. F. Chen *et al.* (Belle collaboration), Phys. Rev. Lett. **98**, 031802 (2007),
arXiv:hep-ex/0608039.
- [236] H. Sahoo *et al.* (Belle collaboration), Phys. Rev. **D77**, 091103 (2008),
arXiv:0708.2604 [hep-ex].
- [237] B. Aubert *et al.* (BABAR collaboration), Phys. Rev. **D79**, 072009 (2009),
arXiv:0902.1708 [hep-ex].
- [238] B. Aubert *et al.* (BABAR collaboration), Phys. Rev. **D69**, 052001 (2004),
arXiv:hep-ex/0309039.
- [239] R. Barate *et al.* (ALEPH collaboration), Phys. Lett. **B492**, 259–274 (2000),
arXiv:hep-ex/0009058.
- [240] K. Ackerstaff *et al.* (OPAL collaboration), Eur. Phys. J. **C5**, 379–388 (1998),
arXiv:hep-ex/9801022.
- [241] A. A. Affolder *et al.* (CDF collaboration), Phys. Rev. **D61**, 072005 (2000),
arXiv:hep-ex/9909003.
- [242] M. Bona *et al.* (UTfit collaboration), JHEP **07**, 028 (2005), arXiv:hep-ph/0501199,
see also online updates, <http://www.utfit.org/>.
- [243] I. Dunietz, H. R. Quinn, A. Snyder, W. Toki, and H. J. Lipkin,
Phys. Rev. **D43**, 2193–2208 (1991).
- [244] D. Aston *et al.*, Nucl. Phys. **B296**, 493 (1988).
- [245] M. Suzuki, Phys. Rev. **D64**, 117503 (2001), arXiv:hep-ph/0106354.
- [246] B. Aubert *et al.* (BABAR collaboration), Phys. Rev. **D71**, 032005 (2005),
arXiv:hep-ex/0411016.

- [247] T. Aaltonen *et al.* (CDF collaboration), Phys. Rev. Lett. **100**, 161802 (2008), arXiv:0712.2397 [hep-ex].
- [248] CDF and D0 collaborations, CDF note 9787 and D0 note 5928, 2009, http://tevbwg.fnal.gov/results/Summer2009_betas/.
- [249] V. M. Abazov *et al.* (D0 collaboration), Phys. Rev. Lett. **101**, 241801 (2008), arXiv:0802.2255 [hep-ex].
- [250] Y. Grossman and M. P. Worah, Phys. Lett. **B395**, 241–249 (1997), arXiv:hep-ph/9612269.
- [251] R. Fleischer, Phys. Lett. **B562**, 234–244 (2003), arXiv:hep-ph/0301255.
- [252] R. Fleischer, Nucl. Phys. **B659**, 321–355 (2003), arXiv:hep-ph/0301256.
- [253] B. Aubert *et al.* (BABAR collaboration), Phys. Rev. Lett. **99**, 081801 (2007), arXiv:hep-ex/0703019.
- [254] A. Bondar, T. Gershon, and P. Krokovny, Phys. Lett. **B624**, 1–10 (2005), arXiv:hep-ph/0503174.
- [255] R. Fleischer, Int. J. Mod. Phys. **A12**, 2459–2522 (1997), arXiv:hep-ph/9612446.
- [256] D. London and A. Soni, Phys. Lett. **B407**, 61–65 (1997), arXiv:hep-ph/9704277.
- [257] M. Ciuchini, E. Franco, G. Martinelli, A. Masiero, and L. Silvestrini, Phys. Rev. Lett. **79**, 978–981 (1997), arXiv:hep-ph/9704274.
- [258] T. Gershon and M. Hazumi, Phys. Lett. **B596**, 163–172 (2004), arXiv:hep-ph/0402097.
- [259] Y. Grossman, Z. Ligeti, Y. Nir, and H. Quinn, Phys. Rev. **D68**, 015004 (2003), arXiv:hep-ph/0303171.
- [260] M. Gronau and J. L. Rosner, Phys. Lett. **B564**, 90–96 (2003), arXiv:hep-ph/0304178.
- [261] M. Gronau, Y. Grossman, and J. L. Rosner, Phys. Lett. **B579**, 331–339 (2004), arXiv:hep-ph/0310020.
- [262] M. Gronau, J. L. Rosner, and J. Zupan, Phys. Lett. **B596**, 107–115 (2004), arXiv:hep-ph/0403287.
- [263] H.-Y. Cheng, C.-K. Chua, and A. Soni, Phys. Rev. **D72**, 014006 (2005), arXiv:hep-ph/0502235.
- [264] M. Gronau and J. L. Rosner, Phys. Rev. **D71**, 074019 (2005), arXiv:hep-ph/0503131.
- [265] G. Buchalla, G. Hiller, Y. Nir, and G. Raz, JHEP **09**, 074 (2005), arXiv:hep-ph/0503151.
- [266] M. Beneke, Phys. Lett. **B620**, 143–150 (2005), arXiv:hep-ph/0505075.

- [267] G. Engelhard, Y. Nir, and G. Raz, Phys. Rev. **D72**, 075013 (2005),
arXiv:hep-ph/0505194.
- [268] H.-Y. Cheng, C.-K. Chua, and A. Soni, Phys. Rev. **D72**, 094003 (2005),
arXiv:hep-ph/0506268.
- [269] G. Engelhard and G. Raz, Phys. Rev. **D72**, 114017 (2005), arXiv:hep-ph/0508046.
- [270] M. Gronau, J. L. Rosner, and J. Zupan, Phys. Rev. **D74**, 093003 (2006),
arXiv:hep-ph/0608085.
- [271] L. Silvestrini, Ann. Rev. Nucl. Part. Sci. **57**, 405–440 (2007),
arXiv:0705.1624 [hep-ph].
- [272] R. Dutta and S. Gardner, Phys. Rev. **D78**, 034021 (2008),
arXiv:0805.1963 [hep-ph].
- [273] M. Fujikawa *et al.* (Belle collaboration), Phys. Rev. **D81**, 011101 (2010),
arXiv:0809.4366 [hep-ex].
- [274] K. Abe *et al.* (Belle collaboration), arXiv:0708.1845 [hep-ex] (2007).
- [275] B. Aubert *et al.* (BABAR collaboration), Phys. Rev. **D79**, 052003 (2009),
arXiv:0809.1174 [hep-ex].
- [276] M. Fujikawa, Belle collaboration, Preliminary results presented at CKM2008,
<http://agenda.infn.it/materialDisplay.py?contribId=34&sessionId=8&materialId=slides&confId=1066>.
- [277] K. Abe *et al.* (Belle collaboration), Phys. Rev. **D76**, 091103 (2007),
arXiv:hep-ex/0609006.
- [278] B. Aubert *et al.* (BABAR collaboration), Phys. Rev. **D76**, 071101 (2007),
arXiv:hep-ex/0702010.
- [279] B. Aubert *et al.* (BABAR collaboration), Phys. Rev. **D78**, 092008 (2008),
arXiv:0808.3586 [hep-ex].
- [280] B. Aubert *et al.* (BABAR collaboration), Phys. Rev. **D71**, 091102 (2005),
arXiv:hep-ex/0502019.
- [281] K. Vervink *et al.* (Belle collaboration), Phys. Rev. **D80**, 111104 (2009),
arXiv:0901.4057 [hep-ex].
- [282] B. Aubert *et al.* (BABAR collaboration), Phys. Rev. Lett. **101**, 021801 (2008),
arXiv:0804.0896 [hep-ex].
- [283] S. E. Lee *et al.* (Belle collaboration), Phys. Rev. **D77**, 071101 (2008),
arXiv:0708.0304 [hep-ex].
- [284] S. Fratina *et al.* (Belle collaboration), Phys. Rev. Lett. **98**, 221802 (2007),
arXiv:hep-ex/0702031.

- [285] B. Aubert *et al.* (*BABAR* collaboration), Phys. Rev. Lett. **97**, 171805 (2006),
arXiv:hep-ex/0608036.
- [286] Y. Nakahama *et al.* (Belle collaboration), Phys. Rev. Lett. **100**, 121601 (2008),
arXiv:0712.4234 [hep-ex].
- [287] B. Aubert *et al.* (*BABAR* collaboration), Phys. Rev. **D78**, 071102 (2008),
arXiv:0807.3103 [hep-ex].
- [288] Y. Ushiroda *et al.* (Belle collaboration), Phys. Rev. **D74**, 111104 (2006),
arXiv:hep-ex/0608017.
- [289] B. Aubert *et al.* (*BABAR* collaboration), Phys. Rev. **D79**, 011102 (2009),
arXiv:0805.1317 [hep-ex].
- [290] J. Li *et al.* (Belle collaboration), Phys. Rev. Lett. **101**, 251601 (2008),
arXiv:0806.1980 [hep-ex].
- [291] Y. Ushiroda *et al.* (Belle collaboration), Phys. Rev. Lett. **100**, 021602 (2008),
arXiv:0709.2769 [hep-ex].
- [292] B. Aubert *et al.* (*BABAR* collaboration), Phys. Rev. **D76**, 052007 (2007),
arXiv:0705.2157 [hep-ex].
- [293] A. Somov *et al.* (Belle collaboration), Phys. Rev. Lett. **96**, 171801 (2006),
arXiv:hep-ex/0601024.
- [294] B. Aubert *et al.* (*BABAR* collaboration), Phys. Rev. **D78**, 071104 (2008),
arXiv:0807.4977 [hep-ex].
- [295] C. C. Chiang *et al.* (Belle collaboration), Phys. Rev. **D78**, 111102 (2008),
arXiv:0808.2576 [hep-ex].
- [296] B. Aubert *et al.* (*BABAR* collaboration), Phys. Rev. Lett. **98**, 181803 (2007),
arXiv:hep-ex/0612050.
- [297] B. Aubert *et al.* (*BABAR* collaboration), Phys. Rev. **D81**, 052009 (2010),
arXiv:0909.2171 [hep-ex].
- [298] B. Aubert *et al.* (*BABAR* collaboration), arXiv:0807.4226 [hep-ex] (2008).
- [299] H. Ishino *et al.* (Belle collaboration), Phys. Rev. Lett. **98**, 211801 (2007),
arXiv:hep-ex/0608035.
- [300] A. Somov *et al.* (Belle collaboration), Phys. Rev. **D76**, 011104 (2007),
arXiv:hep-ex/0702009.
- [301] M. Gronau and D. London, Phys. Rev. Lett. **65**, 3381–3384 (1990).
- [302] B. Aubert *et al.* (*BABAR* collaboration), Phys. Rev. **D76**, 091102 (2007),
arXiv:0707.2798 [hep-ex].

- [303] B. Aubert *et al.* (*BABAR* collaboration), Phys. Rev. Lett. **102**, 141802 (2009), arXiv:0901.3522 [hep-ex].
- [304] H. J. Lipkin, Y. Nir, H. R. Quinn, and A. Snyder, Phys. Rev. **D44**, 1454–1460 (1991).
- [305] M. Gronau and J. Zupan, Phys. Rev. **D73**, 057502 (2006), arXiv:hep-ph/0512148.
- [306] B. Aubert *et al.* (*BABAR* collaboration), Phys. Rev. **D77**, 071102 (2008), arXiv:0712.3469 [hep-ex].
- [307] K. Abe *et al.* (Belle collaboration), arXiv:hep-ex/0307074 (2003).
- [308] B. Aubert *et al.* (*BABAR* collaboration), Phys. Rev. **D77**, 111102 (2008), arXiv:0802.4052 [hep-ex].
- [309] K. Abe *et al.* (Belle collaboration), Phys. Rev. **D73**, 051106 (2006), arXiv:hep-ex/0601032.
- [310] T. Aaltonen *et al.* (CDF collaboration), Phys. Rev. **D81**, 031105 (2010), arXiv:0911.0425 [hep-ex].
- [311] B. Aubert *et al.* (*BABAR* collaboration), Phys. Rev. **D78**, 092002 (2008), arXiv:0807.2408 [hep-ex].
- [312] B. Aubert *et al.* (*BABAR* collaboration), Phys. Rev. **D80**, 092001 (2009), arXiv:0909.3981 [hep-ex].
- [313] A. Bondar and T. Gershon, Phys. Rev. **D70**, 091503 (2004), arXiv:hep-ph/0409281.
- [314] N. Lopez March, *BABAR* collaboration, Preliminary results presented at EPS2009, <http://indico.ifj.edu.pl/MaKaC/materialDisplay.py?contribId=863&sessionId=0&materialId=slides&confId=11>.
- [315] Y. Horii *et al.* (Belle collaboration), Phys. Rev. **D78**, 071901 (2008), arXiv:0804.2063 [hep-ex].
- [316] B. Aubert *et al.* (*BABAR* collaboration), Phys. Rev. **D76**, 111101 (2007), arXiv:0708.0182 [hep-ex].
- [317] B. Aubert *et al.* (*BABAR* collaboration), Phys. Rev. **D80**, 031102 (2009), arXiv:0904.2112 [hep-ex].
- [318] M. Gronau, Phys. Lett. **B557**, 198–206 (2003), arXiv:hep-ph/0211282.
- [319] D. M. Asner *et al.* (CLEO collaboration), Phys. Rev. **D78**, 012001 (2008), arXiv:0802.2268 [hep-ex].
- [320] N. Lowrey *et al.* (CLEO collaboration), Phys. Rev. **D80**, 031105 (2009), arXiv:0903.4853 [hep-ex].
- [321] P. Krokovny *et al.* (Belle collaboration), Phys. Rev. Lett. **90**, 141802 (2003), arXiv:hep-ex/0212066.

- [322] B. Aubert *et al.* (BABAR collaboration), Phys. Rev. **D78**, 034023 (2008), arXiv:0804.2089 [hep-ex].
- [323] A. Poluektov *et al.* (Belle collaboration), arXiv:1003.3360 [hep-ex] (2010).
- [324] A. Poluektov *et al.* (Belle collaboration), Phys. Rev. **D73**, 112009 (2006), arXiv:hep-ex/0604054.
- [325] B. Aubert *et al.* (BABAR collaboration), Phys. Rev. **D79**, 072003 (2009), arXiv:0805.2001 [hep-ex].
- [326] B semileptonic decays common input parameters, www.slac.stanford.edu/xorg/hfag/semi/EndOfYear09/common/common.param.
- [327] D. Buskulic *et al.* (ALEPH collaboration), Phys. Lett. **B395**, 373–387 (1997).
- [328] J. E. Bartelt *et al.* (CLEO collaboration), Phys. Rev. Lett. **82**, 3746 (1999), arXiv:hep-ex/9811042.
- [329] K. Abe *et al.* (Belle collaboration), Phys. Lett. **B526**, 258–268 (2002), arXiv:hep-ex/0111082.
- [330] B. Aubert *et al.* (BABAR collaboration), Phys. Rev. Lett. **100**, 151802 (2008), arXiv:0712.3503 [hep-ex].
- [331] R. Fulton *et al.* (CLEO collaboration), Phys. Rev. **D43**, 651–663 (1991).
- [332] B. Aubert *et al.* (BABAR collaboration), Phys. Rev. **D79**, 012002 (2009), arXiv:0809.0828 [hep-ex].
- [333] B. Aubert *et al.* (BABAR collaboration), Phys. Rev. Lett. **104**, 011802 (2010), arXiv:0904.4063 [hep-ex].
- [334] M. Okamoto *et al.*, Nucl. Phys. Proc. Suppl. **140**, 461–463 (2005), arXiv:hep-lat/0409116.
- [335] G. M. de Divitiis, E. Molinaro, R. Petronzio, and N. Tantalo, Phys. Lett. **B655**, 45–49 (2007), arXiv:0707.0582 [hep-lat].
- [336] G. Abbiendi *et al.* (OPAL collaboration), Phys. Lett. **B482**, 15–30 (2000), arXiv:hep-ex/0003013.
- [337] P. Abreu *et al.* (DELPHI collaboration), Phys. Lett. **B510**, 55–74 (2001), arXiv:hep-ex/0104026.
- [338] I. Adachi *et al.* (Belle collaboration) (2008), arXiv:0810.1657 [hep-ex].
- [339] N. E. Adam *et al.* (CLEO collaboration), Phys. Rev. **D67**, 032001 (2003), arXiv:hep-ex/0210040.
- [340] J. Abdallah *et al.* (DELPHI collaboration), Eur. Phys. J. **C33**, 213–232 (2004), arXiv:hep-ex/0401023.

- [341] B. Aubert *et al.* (BABAR collaboration), Phys. Rev. **D77**, 032002 (2008), arXiv:0705.4008 [hep-ex].
- [342] H. Albrecht *et al.* (ARGUS collaboration), Phys. Lett. **B275**, 195–201 (1992).
- [343] B. Aubert *et al.* (BABAR collaboration), Phys. Rev. Lett. **100**, 231803 (2008), arXiv:0712.3493 [hep-ex].
- [344] I. Adachi *et al.* (Belle collaboration) (2009), arXiv:0910.3534 [hep-ex].
- [345] I. Caprini, L. Lellouch, and M. Neubert, Nucl. Phys. **B530**, 153–181 (1998), arXiv:hep-ph/9712417.
- [346] C. Bernard *et al.*, Phys. Rev. **D79**, 014506 (2009), arXiv:0808.2519 [hep-lat].
- [347] D. Liventsev *et al.* (Belle collaboration), Phys. Rev. **D77**, 091503 (2008), arXiv:0711.3252 [hep-ex].
- [348] N. Isgur and M. B. Wise, Phys. Rev. Lett. **66**, 1130–1133 (1991).
- [349] D. Buskulic *et al.* (ALEPH collaboration), Z. Phys. **C73**, 601–612 (1997).
- [350] G. Abbiendi *et al.* (OPAL collaboration), Eur. Phys. J. **C30**, 467–475 (2003), arXiv:hep-ex/0301018.
- [351] A. Anastassov *et al.* (CLEO collaboration), Phys. Rev. Lett. **80**, 4127–4131 (1998), arXiv:hep-ex/9708035.
- [352] V. M. Abazov *et al.* (D0 collaboration), Phys. Rev. Lett. **95**, 171803 (2005), arXiv:hep-ex/0507046.
- [353] B. Aubert *et al.* (BABAR collaboration), Phys. Rev. Lett. **101**, 261802 (2008), arXiv:0808.0528 [hep-ex].
- [354] B. Aubert *et al.* (BABAR collaboration), Phys. Rev. Lett. **103**, 051803 (2009), arXiv:0808.0333 [hep-ex].
- [355] J. Abdallah *et al.* (DELPHI collaboration), Eur. Phys. J. **C45**, 35–59 (2006), arXiv:hep-ex/0510024.
- [356] D. Benson, I. I. Bigi, T. Mannel, and N. Uraltsev, Nucl. Phys. **B665**, 367–401 (2003), arXiv:hep-ph/0302262.
- [357] C. W. Bauer, Z. Ligeti, M. Luke, A. V. Manohar, and M. Trott, Phys. Rev. **D70**, 094017 (2004), arXiv:hep-ph/0408002.
- [358] P. Gambino and N. Uraltsev, Eur. Phys. J. **C34**, 181–189 (2004), arXiv:hep-ph/0401063.
- [359] D. Benson, I. I. Bigi, and N. Uraltsev, Nucl. Phys. **B710**, 371–401 (2005), arXiv:hep-ph/0410080.

- [360] C. Schwanda *et al.* (Belle collaboration), Phys. Rev. **D78**, 032016 (2008), arXiv:0803.2158 [hep-ex].
- [361] B. Aubert *et al.* (BABAR collaboration), Phys. Rev. **D72**, 052004 (2005), arXiv:hep-ex/0508004.
- [362] B. Aubert *et al.* (BaBar collaboration), Phys. Rev. Lett. **97**, 171803 (2006), arXiv:hep-ex/0607071.
- [363] B. Aubert *et al.* (BABAR collaboration), Phys. Rev. **D81**, 032003 (2010), arXiv:0908.0415 [hep-ex].
- [364] B. Aubert *et al.* (BABAR collaboration), Phys. Rev. **D69**, 111104 (2004), arXiv:hep-ex/0403030.
- [365] C. Schwanda *et al.* (BELLE collaboration), Phys. Rev. **D75**, 032005 (2007), arXiv:hep-ex/0611044.
- [366] A. Limosani *et al.* (Belle collaboration), Phys. Rev. Lett. **103**, 241801 (2009), arXiv:0907.1384 [hep-ex].
- [367] P. Urquijo *et al.* (Belle collaboration), Phys. Rev. **D75**, 032001 (2007), arXiv:hep-ex/0610012.
- [368] D. E. Acosta *et al.* (CDF collaboration), Phys. Rev. **D71**, 051103 (2005), arXiv:hep-ex/0502003.
- [369] S. Chen *et al.* (CLEO collaboration), Phys. Rev. Lett. **87**, 251807 (2001), arXiv:hep-ex/0108032.
- [370] S. E. Csorna *et al.* (CLEO collaboration), Phys. Rev. **D70**, 032002 (2004), arXiv:hep-ex/0403052.
- [371] J. Abdallah *et al.* (DELPHI collaboration), Eur. Phys. J. **C45**, 35–59 (2006), arXiv:hep-ex/0510024.
- [372] N. E. Adam *et al.* (CLEO collaboration), Phys. Rev. Lett. **99**, 041802 (2007), arXiv:hep-ex/0703041.
- [373] B. Aubert *et al.* (BABAR collaboration), Phys. Rev. Lett. **98**, 091801 (2007), arXiv:hep-ex/0612020.
- [374] T. Hokuue *et al.* (Belle collaboration), Phys. Lett. **B648**, 139–148 (2007), arXiv:hep-ex/0604024.
- [375] B. Aubert *et al.* (BABAR collaboration), Phys. Rev. Lett. **101**, 081801 (2008), arXiv:0805.2408 [hep-ex].
- [376] B. Aubert *et al.* (BABAR collaboration), Phys. Rev. Lett. **97**, 211801 (2006), arXiv:hep-ex/0607089.
- [377] I. Adachi *et al.* (Belle collaboration) (2008), arXiv:0812.1414 [hep-ex].

- [378] P. Ball and R. Zwicky, Phys. Rev. **D71**, 014015 (2005), [arXiv:hep-ph/0406232](#).
- [379] E. Dalgic *et al.*, Phys. Rev. **D73**, 074502 (2006), [arXiv:hep-lat/0601021](#).
- [380] A. Abada *et al.*, Nucl. Phys. **B619**, 565–587 (2001), [arXiv:hep-lat/0011065](#).
- [381] B. H. Behrens *et al.* (CLEO collaboration), Phys. Rev. **D61**, 052001 (2000), [arXiv:hep-ex/9905056](#).
- [382] B. Aubert *et al.* (BABAR collaboration), Phys. Rev. **D72**, 051102 (2005), [arXiv:hep-ex/0507003](#).
- [383] B. Aubert *et al.* (BABAR collaboration), Phys. Rev. **D79**, 052011 (2009), [arXiv:0808.3524 \[hep-ex\]](#).
- [384] R. Gray *et al.* (CLEO collaboration), Phys. Rev. **D76**, 012007 (2007), [arXiv:hep-ex/0703042](#).
- [385] S. B. Athar *et al.* (CLEO collaboration), Phys. Rev. **D68**, 072003 (2003), [arXiv:hep-ex/0304019](#).
- [386] B. Aubert *et al.* (BABAR collaboration) (2006), [arXiv:hep-ex/0607066](#).
- [387] P. Urquijo *et al.* (Belle collaboration), Phys. Rev. Lett. **104**, 021801 (2010), [arXiv:0907.0379 \[hep-ex\]](#).
- [388] I. Bizjak *et al.* (Belle collaboration), Phys. Rev. Lett. **95**, 241801 (2005), [arXiv:hep-ex/0505088](#).
- [389] B. Aubert *et al.* (BABAR collaboration), Phys. Rev. Lett. **100**, 171802 (2008), [arXiv:0708.3702 \[hep-ex\]](#).
- [390] C. W. Bauer, Z. Ligeti, and M. E. Luke, Phys. Rev. **D64**, 113004 (2001), [arXiv:hep-ph/0107074](#).
- [391] M. Neubert, Phys. Rev. **D49**, 4623–4633 (1994), [arXiv:hep-ph/9312311](#).
- [392] A. K. Leibovich, I. Low, and I. Z. Rothstein, Phys. Rev. **D61**, 053006 (2000), [arXiv:hep-ph/9909404](#).
- [393] B. O. Lange, M. Neubert, and G. Paz, JHEP **10**, 084 (2005), [arXiv:hep-ph/0508178](#).
- [394] B. Aubert *et al.* (BABAR collaboration), Phys. Rev. Lett. **96**, 221801 (2006), [arXiv:hep-ex/0601046](#).
- [395] V. B. Golubev, Y. I. Skovpen, and V. G. Luth, Phys. Rev. **D76**, 114003 (2007), [arXiv:hep-ph/0702072](#).
- [396] B. Aubert *et al.* (BABAR collaboration), Phys. Rev. **D73**, 012006 (2006), [arXiv:hep-ex/0509040](#).
- [397] B. Aubert *et al.* (BABAR collaboration), Phys. Rev. **D72**, 052004 (2005), [arXiv:hep-ex/0508004](#).

- [398] R. V. Kowalewski and S. Menke, Phys. Lett. **B541**, 29–34 (2002),
arXiv:hep-ex/0205038.
- [399] B. Aubert *et al.* (BABAR collaboration), Phys. Rev. Lett. **95**, 111801 (2005),
arXiv:hep-ex/0506036.
- [400] A. Bornheim *et al.* (CLEO collaboration), Phys. Rev. Lett. **88**, 231803 (2002),
arXiv:hep-ex/0202019.
- [401] A. Limosani *et al.* (Belle collaboration), Phys. Lett. **B621**, 28–40 (2005),
arXiv:hep-ex/0504046.
- [402] H. Kakuno *et al.* (BELLE collaboration), Phys. Rev. Lett. **92**, 101801 (2004),
arXiv:hep-ex/0311048.
- [403] B. O. Lange, M. Neubert, and G. Paz, Phys. Rev. **D72**, 073006 (2005),
arXiv:hep-ph/0504071.
- [404] S. W. Bosch, B. O. Lange, M. Neubert, and G. Paz, Nucl. Phys. **B699**, 335–386 (2004),
arXiv:hep-ph/0402094.
- [405] S. W. Bosch, M. Neubert, and G. Paz, JHEP **11**, 073 (2004), arXiv:hep-ph/0409115.
- [406] M. Neubert, Eur. Phys. J. **C44**, 205–209 (2005), arXiv:hep-ph/0411027.
- [407] J. R. Andersen and E. Gardi, JHEP **01**, 097 (2006), arXiv:hep-ph/0509360.
- [408] P. Gambino, P. Giordano, G. Ossola, and N. Uraltsev, JHEP **10**, 058 (2007),
arXiv:0707.2493 [hep-ph].
- [409] U. Aglietti, F. Di Lodovico, G. Ferrera, and G. Ricciardi, Eur. Phys. J. **C59**, 831–840
(2009), arXiv:0711.0860 [hep-ph].
- [410] U. Aglietti, G. Ferrera, and G. Ricciardi, Nucl. Phys. **B768**, 85–115 (2007),
arXiv:hep-ph/0608047.
- [411] U. Aglietti, G. Ricciardi, and G. Ferrera, Phys. Rev. **D74**, 034004 (2006),
arXiv:hep-ph/0507285.
- [412] U. Aglietti, G. Ricciardi, and G. Ferrera, Phys. Rev. **D74**, 034005 (2006),
arXiv:hep-ph/0509095.
- [413] U. Aglietti, G. Ricciardi, and G. Ferrera, Phys. Rev. **D74**, 034006 (2006),
arXiv:hep-ph/0509271.
- [414] O. Buchmüller and H. Flächer, Phys. Rev. **D73**, 073008 (2006),
arXiv:hep-ph/0507253.
- [415] K. Abe *et al.* (Belle collaboration), Phys. Lett. **B511**, 151–158 (2001),
arXiv:hep-ex/0103042.

- [416] B. Aubert *et al.* (BABAR collaboration), Phys. Rev. **D77**, 051103 (2008),
arXiv:0711.4889 [hep-ex].
- [417] A. Limosani *et al.* (Belle collaboration), Phys. Rev. Lett. **103**, 241801 (2009),
arXiv:0907.1384 [hep-ex].
- [418] M. Staric *et al.* (Belle collaboration), Phys. Rev. Lett. **98**, 211803 (2007),
arXiv:hep-ex/0703036.
- [419] B. Aubert *et al.* (BABAR collaboration), Phys. Rev. Lett. **98**, 211802 (2007),
arXiv:hep-ex/0703020.
- [420] T. Aaltonen *et al.* (CDF collaboration), Phys. Rev. Lett. **100**, 121802 (2008),
arXiv:0712.1567 [hep-ex].
- [421] I. I. Y. Bigi and N. G. Uraltsev, Nucl. Phys. **B592**, 92–106 (2001),
arXiv:hep-ph/0005089.
- [422] A. A. Petrov (2003), arXiv:hep-ph/0311371.
- [423] A. A. Petrov, Nucl. Phys. Proc. Suppl. **142**, 333–339 (2005), arXiv:hep-ph/0409130.
- [424] A. F. Falk, Y. Grossman, Z. Ligeti, Y. Nir, and A. A. Petrov, Phys. Rev. **D69**, 114021
(2004), arXiv:hep-ph/0402204.
- [425] M. Bobrowski, A. Lenz, J. Riedl, and J. Rohrwild, JHEP **03**, 009 (2010),
arXiv:1002.4794 [hep-ph].
- [426] Charm physics results,
<http://www.slac.stanford.edu/xorg/hfag/charm/index.html>.
- [427] E. M. Aitala *et al.* (E791 collaboration), Phys. Rev. Lett. **77**, 2384–2387 (1996),
arXiv:hep-ex/9606016.
- [428] C. Cawthfield *et al.* (CLEO collaboration), Phys. Rev. **D71**, 077101 (2005),
arXiv:hep-ex/0502012.
- [429] B. Aubert *et al.* (BABAR collaboration), Phys. Rev. **D76**, 014018 (2007),
arXiv:0705.0704 [hep-ex].
- [430] U. Bitenc *et al.* (BELLE collaboration), Phys. Rev. **D77**, 112003 (2008),
arXiv:0802.2952 [hep-ex].
- [431] L. M. Zhang *et al.* (BELLE collaboration), Phys. Rev. Lett. **96**, 151801 (2006),
arXiv:hep-ex/0601029.
- [432] L. M. Zhang *et al.* (BELLE collaboration), Phys. Rev. Lett. **99**, 131803 (2007),
arXiv:0704.1000 [hep-ex].
- [433] P. del Amo Sanchez *et al.* (BABAR collaboration) (2010), arXiv:1004.5053 [hep-ex].

- [434] B. Aubert *et al.* (BABAR collaboration), Phys. Rev. Lett. **103**, 211801 (2009), arXiv:0807.4544 [hep-ex].
- [435] E. M. Aitala *et al.* (E791 collaboration), Phys. Rev. Lett. **83**, 32–36 (1999), arXiv:hep-ex/9903012.
- [436] J. M. Link *et al.* (FOCUS collaboration), Phys. Lett. **B485**, 62–70 (2000), arXiv:hep-ex/0004034.
- [437] S. E. Csorna *et al.* (CLEO collaboration), Phys. Rev. **D65**, 092001 (2002), arXiv:hep-ex/0111024.
- [438] B. Aubert *et al.* (BABAR collaboration), Phys. Rev. **D78**, 011105 (2008), arXiv:0712.2249 [hep-ex].
- [439] A. Zupanc *et al.* (Belle collaboration), Phys. Rev. **D80**, 052006 (2009), arXiv:0905.4185 [hep-ex].
- [440] MINUIT reference manual, <http://wwwasdoc.web.cern.ch/wwwasdoc/minuit/minmain.html>.
- [441] K. Abe *et al.* (Belle collaboration), Phys. Rev. **D69**, 112002 (2004), arXiv:hep-ex/0307021.
- [442] J. M. Link *et al.* (FOCUS collaboration), Phys. Lett. **B586**, 11–20 (2004), arXiv:hep-ex/0312060.
- [443] B. Aubert *et al.* (BABAR collaboration), Phys. Rev. **D79**, 112004 (2009), arXiv:0901.1291 [hep-ex].
- [444] C. Amsler *et al.* (Particle Data Group), Phys. Lett. **B667**, 1 (2008).
- [445] A. Abulencia *et al.* (CDF collaboration), Phys. Rev. **D73**, 051104 (2006), arXiv:hep-ex/0512069.
- [446] S. Godfrey and N. Isgur, Phys. Rev. **D32**, 189–231 (1985).
- [447] J. L. Rosner, Comments Nucl. Part. Phys. **16**, 109 (1986).
- [448] S. Godfrey and R. Kokoski, Phys. Rev. **D43**, 1679–1687 (1991).
- [449] N. Isgur and M. B. Wise, Phys. Rev. Lett. **66**, 1130–1133 (1991).
- [450] M. Di Pierro and E. Eichten, Phys. Rev. **D64**, 114004 (2001), arXiv:hep-ph/0104208.
- [451] K. Abe *et al.* (Belle collaboration), Phys. Rev. Lett. **94**, 221805 (2005), arXiv:hep-ex/0410091.
- [452] P. Colangelo, F. De Fazio, and R. Ferrandes, Mod. Phys. Lett. **A19**, 2083–2102 (2004), arXiv:hep-ph/0407137.
- [453] F. Jugeau, A. Le Yaouanc, L. Oliver, and J. C. Raynal, Phys. Rev. **D72**, 094010 (2005), arXiv:hep-ph/0504206.

- [454] B. Aubert *et al.* (BABAR collaboration), Phys. Rev. Lett. **90**, 242001 (2003),
arXiv:hep-ex/0304021.
- [455] D. Besson *et al.* (CLEO collaboration), Phys. Rev. **D68**, 032002 (2003),
arXiv:hep-ex/0305100.
- [456] R. N. Cahn and J. D. Jackson, Phys. Rev. **D68**, 037502 (2003),
arXiv:hep-ph/0305012.
- [457] K. Abe *et al.* (Belle collaboration), Phys. Rev. Lett. **92**, 012002 (2004),
arXiv:hep-ex/0307052.
- [458] T. Barnes, F. E. Close, and H. J. Lipkin, Phys. Rev. **D68**, 054006 (2003),
arXiv:hep-ph/0305025.
- [459] H. J. Lipkin, Phys. Lett. **B580**, 50–53 (2004), arXiv:hep-ph/0306204.
- [460] W. A. Bardeen, E. J. Eichten, and C. T. Hill, Phys. Rev. **D68**, 054024 (2003),
arXiv:hep-ph/0305049.
- [461] A. V. Evdokimov *et al.* (SELEX collaboration), Phys. Rev. Lett. **93**, 242001 (2004),
arXiv:hep-ex/0406045.
- [462] J. Brodzicka *et al.* (Belle collaboration), Phys. Rev. Lett. **100**, 092001 (2008),
arXiv:0707.3491 [hep-ex].
- [463] B. Aubert *et al.* (BABAR collaboration), Phys. Rev. Lett. **97**, 222001 (2006),
arXiv:hep-ex/0607082.
- [464] T. Matsuki, T. Morii, and K. Sudoh, Eur. Phys. J. **A31**, 701–704 (2007),
arXiv:hep-ph/0610186.
- [465] B. Aubert *et al.* (BABAR collaboration), Phys. Rev. **D80**, 092003 (2009),
arXiv:0908.0806 [hep-ex].
- [466] V. Balagura *et al.* (Belle collaboration), Phys. Rev. **D77**, 032001 (2008),
arXiv:0709.4184 [hep-ex].
- [467] A. Heister *et al.* (ALEPH collaboration), Phys. Lett. **B526**, 34–49 (2002),
arXiv:hep-ex/0112010.
- [468] A. Kuzmin *et al.* (Belle collaboration), Phys. Rev. **D76**, 012006 (2007),
arXiv:hep-ex/0611054.
- [469] B. Aubert *et al.* (BABAR collaboration), Phys. Rev. **D74**, 032007 (2006),
arXiv:hep-ex/0604030.
- [470] J. P. Alexander *et al.* (CLEO collaboration), Phys. Lett. **B303**, 377–384 (1993).
- [471] P. Krokovny *et al.* (Belle collaboration), Phys. Rev. Lett. **91**, 262002 (2003),
arXiv:hep-ex/0308019.

- [472] B. Aubert *et al.* (BABAR collaboration), Phys. Rev. Lett. **93**, 181801 (2004), arXiv:hep-ex/0408041.
- [473] A. Drutskoy *et al.* (Belle collaboration), Phys. Rev. Lett. **94**, 061802 (2005), arXiv:hep-ex/0409026.
- [474] B. Aubert *et al.* (BABAR collaboration), Phys. Rev. **D77**, 011102 (2008), arXiv:0708.1565 [hep-ex].
- [475] B. Aubert *et al.* (BABAR collaboration), Phys. Rev. **D74**, 031103 (2006), arXiv:hep-ex/0605036.
- [476] T. Becher and R. J. Hill, Phys. Lett. **B633**, 61–69 (2006), arXiv:hep-ph/0509090.
- [477] F. J. Gilman and R. L. Singleton, Phys. Rev. **D41**, 142 (1990).
- [478] R. J. Hill (2006), arXiv:hep-ph/0606023.
- [479] D. Becirevic and A. B. Kaidalov, Phys. Lett. **B478**, 417–423 (2000), arXiv:hep-ph/9904490.
- [480] G. S. Huang *et al.* (CLEO collaboration), Phys. Rev. Lett. **94**, 011802 (2005), arXiv:hep-ex/0407035.
- [481] J. M. Link *et al.* (FOCUS collaboration), Phys. Lett. **B607**, 233–242 (2005), arXiv:hep-ex/0410037.
- [482] L. Widhalm *et al.* (Belle collaboration), Phys. Rev. Lett. **97**, 061804 (2006), arXiv:hep-ex/0604049.
- [483] B. Aubert *et al.* (BABAR collaboration) (2006), arXiv:hep-ex/0607077.
- [484] Y. Gao, CLEO collaboration, Preliminary results presented at ICHEP2006, http://ichep06.jinr.ru/reports/192_10s3_10p40_gao.pdf.
- [485] S. Dobbs *et al.* (CLEO collaboration), Phys. Rev. **D77**, 112005 (2008), arXiv:0712.1020 [hep-ex].
- [486] C. Aubin *et al.* (Fermilab Lattice collaboration), Phys. Rev. Lett. **94**, 011601 (2005), arXiv:hep-ph/0408306.
- [487] C. G. Boyd, B. Grinstein, and R. F. Lebed, Phys. Rev. Lett. **74**, 4603–4606 (1995), arXiv:hep-ph/9412324.
- [488] C. G. Boyd and M. J. Savage, Phys. Rev. **D56**, 303–311 (1997), arXiv:hep-ph/9702300.
- [489] M. C. Arnesen, B. Grinstein, I. Z. Rothstein, and I. W. Stewart, Phys. Rev. Lett. **95**, 071802 (2005), arXiv:hep-ph/0504209.
- [490] C. Bourrely, B. Machet, and E. de Rafael, Nucl. Phys. **B189**, 157 (1981).

- [491] J. C. Anjos *et al.*, Phys. Rev. Lett. **65**, 2630–2633 (1990).
- [492] K. Kodama *et al.* (Fermilab E653 collaboration), Phys. Lett. **B274**, 246–252 (1992).
- [493] P. L. Frabetti *et al.* (E687 collaboration), Phys. Lett. **B307**, 262–268 (1993).
- [494] E. M. Aitala *et al.* (E791 collaboration), Phys. Rev. Lett. **80**, 1393–1397 (1998),
arXiv:hep-ph/9710216.
- [495] E. M. Aitala *et al.* (E791 collaboration), Phys. Lett. **B440**, 435–441 (1998),
arXiv:hep-ex/9809026.
- [496] M. Adamovich *et al.* (BEATRICE collaboration), Eur. Phys. J. **C6**, 35–41 (1999).
- [497] J. M. Link *et al.* (FOCUS collaboration), Phys. Lett. **B544**, 89–96 (2002),
arXiv:hep-ex/0207049.
- [498] J. M. Link *et al.* (FOCUS collaboration), Phys. Lett. **B607**, 67–77 (2005),
arXiv:hep-ex/0410067.
- [499] B. Aubert *et al.* (BABAR collaboration) (2006), arXiv:hep-ex/0607085.
- [500] H. Mahlke (2007), arXiv:hep-ex/0702014.
- [501] J. M. Link *et al.* (FOCUS collaboration), Phys. Lett. **B535**, 43–51 (2002),
arXiv:hep-ex/0203031.
- [502] B. Aubert *et al.* (BABAR collaboration), Phys. Rev. **D78**, 051101 (2008),
arXiv:0807.1599 [hep-ex].
- [503] K. M. Ecklund *et al.* (CLEO collaboration), Phys. Rev. **D80**, 052009 (2009),
arXiv:0907.3201 [hep-ex].
- [504] R. A. Briere *et al.* (CLEO collaboration), Phys. Rev. **D81**, 112001 (2010),
arXiv:1004.1954 [hep-ex].
- [505] I. I. Y. Bigi and A. I. Sanda, Camb. Monogr. Part. Phys. Nucl. Phys. Cosmol. **9**, 1–382
(2000).
- [506] Y. Nir (1999), arXiv:hep-ph/9911321.
- [507] F. Buccella, M. Lusignoli, G. Miele, A. Pugliese, and P. Santorelli,
Phys. Rev. **D51**, 3478–3486 (1995), arXiv:hep-ph/9411286.
- [508] B. I. Eisenstein *et al.* (CLEO collaboration), Phys. Rev. **D78**, 052003 (2008),
arXiv:0806.2112 [hep-ex].
- [509] B. R. Ko *et al.* (Belle collaboration), Phys. Rev. Lett. **104**, 181602 (2010),
arXiv:1001.3202 [hep-ex].
- [510] S. Dobbs *et al.* (CLEO collaboration), Phys. Rev. **D76**, 112001 (2007),
arXiv:0709.3783 [hep-ex].

- [511] J. M. Link *et al.* (FOCUS collaboration), Phys. Rev. Lett. **88**, 041602; 159903(E) (2002), arXiv:hep-ex/0109022.
- [512] E. M. Aitala *et al.* (E791 collaboration), Phys. Lett. **B403**, 377–382 (1997), arXiv:hep-ex/9612005.
- [513] P. Rubin *et al.* (CLEO collaboration), Phys. Rev. **D78**, 072003 (2008), arXiv:0807.4545 [hep-ex].
- [514] B. Aubert *et al.* (BABAR collaboration), Phys. Rev. **D71**, 091101 (2005), arXiv:hep-ex/0501075.
- [515] J. M. Link *et al.* (FOCUS collaboration), Phys. Lett. **B491**, 232–239 (2000), arXiv:hep-ex/0005037.
- [516] P. L. Frabetti *et al.* (E687 collaboration), Phys. Rev. **D50**, 2953–2956 (1994).
- [517] J. M. Link *et al.* (FOCUS collaboration), Phys. Lett. **B622**, 239–248 (2005), arXiv:hep-ex/0506012.
- [518] M. Staric *et al.* (Belle collaboration), Phys. Lett. **B670**, 190–195 (2008), arXiv:0807.0148 [hep-ex].
- [519] B. Aubert *et al.* (BaBar collaboration), Phys. Rev. Lett. **100**, 061803 (2008), arXiv:0709.2715 [hep-ex].
- [520] D. E. Acosta *et al.* (CDF collaboration), Phys. Rev. Lett. **94**, 122001 (2005), arXiv:hep-ex/0504006.
- [521] E. M. Aitala *et al.* (E791 collaboration), Phys. Lett. **B421**, 405–411 (1998), arXiv:hep-ex/9711003.
- [522] G. Bonvicini *et al.* (CLEO collaboration), Phys. Rev. **D63**, 071101 (2001), arXiv:hep-ex/0012054.
- [523] J. E. Bartelt *et al.* (CLEO collaboration), Phys. Rev. **D52**, 4860–4867 (1995).
- [524] B. Aubert *et al.* (BABAR collaboration), Phys. Rev. **D78**, 051102 (2008), arXiv:0802.4035 [hep-ex].
- [525] K. Arinstein (Belle collaboration), Phys. Lett. **B662**, 102–110 (2008), arXiv:0801.2439 [hep-ex].
- [526] D. Cronin-Hennessy *et al.* (CLEO collaboration), Phys. Rev. **D72**, 031102 (2005), arXiv:hep-ex/0503052.
- [527] S. Kopp *et al.* (CLEO collaboration), Phys. Rev. **D63**, 092001 (2001), arXiv:hep-ex/0011065.
- [528] X. C. Tian *et al.* (Belle collaboration), Phys. Rev. Lett. **95**, 231801 (2005), arXiv:hep-ex/0507071.

- [529] G. Brandenburg *et al.* (CLEO collaboration), Phys. Rev. Lett. **87**, 071802 (2001), arXiv:hep-ex/0105002.
- [530] D. M. Asner *et al.* (CLEO collaboration), Phys. Rev. **D70**, 091101 (2004), arXiv:hep-ex/0311033.
- [531] J. P. Alexander *et al.* (CLEO collaboration), Phys. Rev. Lett. **100**, 161804 (2008), arXiv:0801.0680 [hep-ex].
- [532] G. S. Adams *et al.* (CLEO collaboration), Phys. Rev. Lett. **99**, 191805 (2007), arXiv:0708.0139 [hep-ex].
- [533] E. Golowich and G. Valencia, Phys. Rev. **D40**, 112 (1989).
- [534] I. I. Y. Bigi (2001), arXiv:hep-ph/0107102.
- [535] W. Bensalem, A. Datta, and D. London, Phys. Rev. **D66**, 094004 (2002), arXiv:hep-ph/0208054.
- [536] W. Bensalem and D. London, Phys. Rev. **D64**, 116003 (2001), arXiv:hep-ph/0005018.
- [537] W. Bensalem, A. Datta, and D. London, Phys. Lett. **B538**, 309–320 (2002), arXiv:hep-ph/0205009.
- [538] P. del Amo Sanchez *et al.* (BABAR collaboration) (2010), arXiv:1003.3397 [hep-ex].
- [539] K. Abe *et al.* (Belle collaboration), Phys. Rev. Lett. **100**, 241801 (2008), arXiv:0709.1340 [hep-ex].
- [540] B. Aubert *et al.* (BABAR collaboration), Phys. Rev. Lett. **98**, 141801 (2007), arXiv:hep-ex/0607094.
- [541] J. P. Lees *et al.* (BABAR collaboration) (2010), arXiv:1003.3063 [hep-ex].
- [542] J. P. Alexander *et al.* (CLEO collaboration), Phys. Rev. **D79**, 052001 (2009), arXiv:0901.1216 [hep-ex].
- [543] P. U. E. Onyisi *et al.* (CLEO collaboration), Phys. Rev. **D79**, 052002 (2009), arXiv:0901.1147 [hep-ex].
- [544] P. Naik *et al.* (CLEO collaboration), Phys. Rev. **D80**, 112004 (2009), arXiv:0910.3602 [hep-ex].
- [545] J. Coleman (BaBar collaboration), private communication.
- [546] B. Aubert *et al.* (BaBar collaboration), Phys. Rev. **D71**, 091104 (2005), arXiv:hep-ex/0502041.
- [547] We do not use a less precise CLEO measurement of $\Gamma(D_s^+ \rightarrow \mu^+ \nu) / \Gamma(D_s^+ \rightarrow \phi \pi^+)$ [from M. Chadha *et al.* (CLEO collaboration), Phys. Rev. D **58** 032002 (1998)], as ΔM_{KK} is not documented.

- [548] E. Follana, C. T. H. Davies, G. P. Lepage, and J. Shigemitsu (HPQCD collaboration), Phys. Rev. Lett. **100**, 062002 (2008), arXiv:0706.1726 [hep-lat].
- [549] C. Bernard *et al.*, PoS **LATTICE2008**, 278 (2008), arXiv:0904.1895 [hep-lat].
- [550] E. Barberio, B. van Eijk, and Z. Was, Comput. Phys. Commun. **66**, 115–128 (1991).
- [551] E. Barberio and Z. Was, Comput. Phys. Commun. **79**, 291–308 (1994).
- [552] P. Golonka and Z. Was, Eur. Phys. J. **C45**, 97–107 (2006), arXiv:hep-ph/0506026.
- [553] P. Golonka and Z. Was, Eur. Phys. J. **C50**, 53–62 (2007), arXiv:hep-ph/0604232.
- [554] A. Ryd *et al.*, EVTGEN-V00-11-07.
- [555] J. M. Link *et al.* (FOCUS collaboration), Phys. Lett. **B555**, 167–173 (2003), arXiv:hep-ex/0212058.
- [556] D hadronic branching fractions and final state radiation, http://www.slac.stanford.edu/xorg/hfag/charm/hadronic/dhad_15sep09.html.
- [557] S. Dobbs *et al.* (CLEO collaboration), Phys. Rev. **D76**, 112001 (2007), arXiv:0709.3783 [hep-ex].
- [558] B. Aubert *et al.* (BABAR collaboration), Phys. Rev. Lett. **100**, 051802 (2008), arXiv:0704.2080 [hep-ex].
- [559] M. Artuso *et al.* (CLEO collaboration), Phys. Rev. Lett. **80**, 3193–3197 (1998), arXiv:hep-ex/9712023.
- [560] R. Barate *et al.* (ALEPH collaboration), Phys. Lett. **B403**, 367–376 (1997).
- [561] H. Albrecht *et al.* (ARGUS collaboration), Phys. Lett. **B340**, 125–128 (1994).
- [562] D. S. Akerib *et al.* (CLEO collaboration), Phys. Rev. Lett. **71**, 3070–3074 (1993).
- [563] D. Decamp *et al.* (ALEPH collaboration), Phys. Lett. **B266**, 218–230 (1991).
- [564] P. Rubin *et al.* (CLEO collaboration), Phys. Rev. Lett. **96**, 081802 (2006), arXiv:hep-ex/0512063.
- [565] G. Bonvicini *et al.* (CLEO collaboration), Phys. Rev. **D77**, 091106 (2008), arXiv:0803.0793 [hep-ex].
- [566] T. E. Coan *et al.* (CLEO collaboration), Phys. Rev. Lett. **80**, 1150–1155 (1998), arXiv:hep-ex/9710028.
- [567] S. Banerjee, B. Pietrzyk, J. M. Roney, and Z. Was, Phys. Rev. **D77**, 054012 (2008), arXiv:0706.3235 [hep-ph].
- [568] B. Aubert *et al.* (BABAR collaboration), Phys. Rev. Lett. **105**, 051602 (2010), arXiv:0912.0242 [hep-ex].

- [569] B. Aubert *et al.* (BABAR collaboration), Phys. Rev. **D76**, 051104 (2007), [arXiv:0707.2922 \[hep-ex\]](#).
- [570] B. Aubert *et al.* (BABAR collaboration), Nucl. Phys. Proc. Suppl. **189**, 193–198 (2009), [arXiv:0808.1121 \[hep-ex\]](#).
- [571] S. Paramesvaran (BaBar collaboration) (2009), [arXiv:0910.2884 \[hep-ex\]](#).
- [572] B. Aubert *et al.* (BABAR collaboration), Phys. Rev. Lett. **100**, 011801 (2008), [arXiv:0707.2981 \[hep-ex\]](#).
- [573] B. Aubert *et al.* (the BABAR collaboration), Phys. Rev. **D72**, 072001 (2005), [arXiv:hep-ex/0505004](#).
- [574] B. Aubert *et al.* (BaBar collaboration), Phys. Rev. **D77**, 112002 (2008), [arXiv:0803.0772 \[hep-ex\]](#).
- [575] M. Fujikawa *et al.* (Belle collaboration), Phys. Rev. **D78**, 072006 (2008), [arXiv:0805.3773 \[hep-ex\]](#).
- [576] D. Epifanov *et al.* (Belle collaboration), Phys. Lett. **B654**, 65–73 (2007), [arXiv:0706.2231 \[hep-ex\]](#).
- [577] M. J. Lee *et al.* (Belle collaboration), Phys. Rev. **D81**, 113007 (2010), [arXiv:1001.0083 \[hep-ex\]](#).
- [578] K. Inami *et al.* (Belle collaboration), Phys. Lett. **B672**, 209–218 (2009), [arXiv:0811.0088 \[hep-ex\]](#).
- [579] S. Schael *et al.* (ALEPH collaboration), Phys. Rept. **421**, 191–284 (2005), [arXiv:hep-ex/0506072](#).
- [580] I. Adachi *et al.* (Belle collaboration) (2008), [arXiv:0808.1059 \[hep-ex\]](#).
- [581] Y.-S. Tsai, Phys. Rev. **D4**, 2821 (1971).
- [582] D. I. Britton *et al.*, Phys. Rev. Lett. **68**, 3000–3003 (1992).
- [583] G. Czapek *et al.*, Phys. Rev. Lett. **70**, 17–20 (1993).
- [584] V. Cirigliano and I. Rosell, JHEP **10**, 005 (2007), [arXiv:0707.4464 \[hep-ph\]](#).
- [585] F. Ambrosino *et al.* (KLOE collaboration), Eur. Phys. J. **C64**, 627–636 (2009), [arXiv:0907.3594 \[hep-ex\]](#).
- [586] E. Goudzovski (NA62 collaboration) (2010), [arXiv:1008.1219 \[hep-ex\]](#).
- [587] E. Goudzovski Presented at BEACH, Perugia, Italy (June 2010), <http://agenda.infn.it/getFile.py/access?contribId=145&sessionId=20&resId=0&materialId=slides&confId=1963>.
- [588] M. Antonelli *et al.* (2010), [arXiv:1005.2323 \[hep-ph\]](#).
- [589] J. Alcaraz *et al.* (ALEPH collaboration) (2006), [arXiv:hep-ex/0612034](#).

- [590] W. J. Marciano and A. Sirlin, Phys. Rev. Lett. **71**, 3629–3632 (1993).
- [591] R. Decker and M. Finkemeier, Nucl. Phys. **B438**, 17–53 (1995),
arXiv:hep-ph/9403385.
- [592] R. Decker and M. Finkemeier, Phys. Lett. **B334**, 199–202 (1994).
- [593] J. Erler, Rev. Mex. Fis. **50**, 200–202 (2004), arXiv:hep-ph/0211345.
- [594] J. C. Hardy and I. S. Towner, Phys. Rev. **C79**, 055502 (2009),
arXiv:0812.1202 [nucl-ex].
- [595] S. Banerjee (BaBar collaboration) (2008), arXiv:0811.1429 [hep-ex].
- [596] W. J. Marciano, Phys. Rev. Lett. **93**, 231803 (2004), arXiv:hep-ph/0402299.
- [597] E. Gamiz, M. Jamin, A. Pich, J. Prades, and F. Schwab,
Nucl. Phys. Proc. Suppl. **169**, 85–89 (2007), arXiv:hep-ph/0612154.
- [598] M. Jamin, J. A. Oller, and A. Pich, Phys. Rev. **D74**, 074009 (2006),
arXiv:hep-ph/0605095.
- [599] K. Maltman (2010), arXiv:1011.6391 [hep-ph].
- [600] E. Gamiz, M. Jamin, A. Pich, J. Prades, and F. Schwab, PoS **KAON**, 008 (2008),
arXiv:0709.0282 [hep-ph].
- [601] M. Davier, A. Hocker, and Z. Zhang, Rev. Mod. Phys. **78**, 1043–1109 (2006),
arXiv:hep-ph/0507078.
- [602] M. Jamin Presented at the Electroweak session of Rencontres de Moriond (March 2007),
<http://indico.in2p3.fr/getFile.py/access?contribId=38&sessionId=4&resId=0&materialId=slides&confId=151>.